A Sheffield Hallam University thesis

ProQuest Number: 10697209

ProQuest 10697209

ProQuest LLC.
789 East Eisenhower Parkway
P.O. Box 1346
Ann Arbor, MI 48106 – 1346

Investigation of the mechanisms underlying the development of atherosclerosis

Daniel Marcus Kelly

A Thesis submitted in partial fulfilment of the requirements of Sheffield Hallam University for the degree of Doctor of Philosophy

October 2010

Abstract

It has become increasingly evident that low serum levels of testosterone experienced by aging males are associated with cardiovascular disease. Clinical trials have shown that testosterone replacement therapy (TRT) can improve symptoms of cardiovascular disease and reduce the inflammatory burden, evident in the early stages of atherosclerosis. Thus, a potential role of testosterone as an anti-inflammatory agent has emerged. The over-recruitment and activation of leukocytes characteristic of early atherosclerosis is considered the driving force behind atheroma development and is regulated by the concerted activities of several cytokines, chemokines and adhesion molecules, expressed by vascular endothelial and smooth muscle cells. The chemokines CCL2 and CX_3CL1, which influence the migration of these leukocytes to sites of inflammation, have been implicated in disease progression. Whether testosterone has a modulatory effect on these orchestrating inflammatory molecules remains largely unknown.

The aim of this thesis was to determine whether testosterone influences vascular inflammation as part of its beneficial effects on atherosclerosis, using a combined *in vitro* and *in vivo* approach. Primary human aortic endothelial and smooth muscle cells *in vitro* were investigated for CX_3CL1 and CCL2 expression under pro-inflammatory conditions, as a model of vascular inflammation. Androgen treatment of these vascular cells, with or without AR blockade, was studied to determine potential anti-inflammatory effects. In addition, the testicular feminised (Tfm) mouse, which expresses low endogenous testosterone and a non-functional androgen receptor (AR), was used to assess the *in vivo* effect of androgen status upon atheroma formation, serum lipids and inflammatory mediators, to identify actions of testosterone on these pathways.

Findings from this thesis confirmed that CX_3CL1 and CCL2 are involved in vascular inflammation associated with atherosclerosis evident by the *in vitro* up-regulation by pro-inflammatory cytokines, and also that CX_3CL1 was present, along with CX_3CR1, in early fatty streaks in the aortic root of Tfm mice. A high-cholesterol diet was associated with increased fatty streak formation in the aortic root of wildtype mice, an effect that was significantly amplified by the low endogenous testosterone and a non-functional AR (in the Tfm mouse). Physiological TRT reduced fatty streak formation in the Tfm mouse but did not have significant effects on circulating cytokines. No significant modulation of CX_3CL1 or CCL2 expression by testosterone treatment *in vitro* was observed, although further work is required to definitively confirm this finding.

This thesis has demonstrated that physiological concentrations of testosterone can inhibit fatty streak formation, via an AR-independent mechanism in Tfm mice, although not through systemic or local anti-inflammatory actions. The mechanisms by which TRT may confer cardiovascular benefits to men with hypotestosteronemia and cardiovascular risk requires further investigation.

Contents

List of figures

List of Tables

Abbreviations

AAA	Abdominal aortic aneurysm
ADAM	A disintegrin and metalloproteinase
ADT	Androgen deprivation therapy
ANOVA	Analysis of variance
APC	Antigen presenting cell
Apo	Apolipoprotein
AR	Androgen receptor
ARE	Androgen response elements
BCA	Bicinchoninic acid
bFGF	Basic fibroblast growth factor
BrdU	Bromodeoxyuridine
BSA	Bovine serum albumin
CAD	Coronary artery disease
CD	Cluster of differentiation
cDNA	Complimentary DNA
CHD	Coronary heart disease
CLSM	Confocal laser scanning microscopy
CRP	C-reactive protein
CSF	Colony stimulating factor
Ct	Cycle threshold
CVD	Cardiovascular disease
DAPI	4',6-diamidino-2-phenylindole
DEPC	Diethylpyrocarbonate
DHEA	Dehydroepiandrosterone
DHT	Dihydrotestosterone
ECM	Extracellular matrix
EDTA	Ethylenediaminetetraacetic acid
EGF	Epidermal growth factor
ELISA	Enzyme linked immunosorbant assay
eNOS	Endothelial nitric oxide synthase
ER	Oestrogen receptor
ERE	Oestrogen receptor element
FBS	Foetal bovine serum
FCS	Foetal calf serum
FRET	Fluorescence resonance energy transfer
GAG	Glycosaminoglycans
GAS	Gamma-activated sequence
GnRH	Gonadotropin releasing hormone
HAEC	Human aortic endothelial cells

HASMC	Human aortic smooth muscle cells
HDL	High density lipoprotein
HEK	Human embryonic kidney
HUVEC	Human umbilical vein endothelial cells
HSP	Heat shock protein
ICAM	Intercellular adhesion molecule
ICC	Immunocytochemistry
IDL	Intermediate density lipoprotein
IFN	Interferon
Ig	Immunoglobulin
IL-	Interleukin
IMT	Intima-media thickness
iNOS	Inducible nitric oxide synthase
LDL	Low density lipoprotein
LH	Luteinizing hormone
LPS	Lipopolysaccharide
MCP1	Monocyte chemoattraction protein 1
M-CSF	Macrophage colony stimulating factor
MFI	Mean fluorescence index
MHC	Major histocompatability complex
MI	Myocardial infarction
MMP	Matrix metalloproteinase
mRNA	Messenger RNA
NFκB	Nuclear factor kappa B
NK	Natural killer
NO	Nitric oxide
NOS	Nitric oxide synthase
ORO	Oil red O
oxLDL	Oxidised low density lipoprotein
PBMC	Peripheral blood mononuclear cells
PBS	Phosphate buffered saline
PCR	Polymerase chain reaction
PDGF	Platelet derived growth factor
PE	Phycoerytherin
PFA	Paraformaldehyde
PI	Propidium iodide
POD	Peroxidase
PSGL-1	P-selectin glycoprotein-1
qRT-PCR	Quantitative reverse transcription polymerase chain reaction
RANTES	Regulated upon activation, normal T cell expressed and secreted
ROS	Reactive oxygen species
SEM	Standard error of the mean

SHBG	Sex hormone binding globulin
SMC	Smooth muscle cell
SOD	Superoxide dismutase
STAT	Signal transducer and activator of transcription
TC	Total cholesterol
Tfm	Testicular feminised mouse
TGF	Transforming growth factor
TIMP	Tissue inhibitor of metalloproteinase
TLR	Toll-like receptor
TMB	Tetramethyl-benzidine
TNF	Tumour necrosis factor
Treg	Regulatory T cell
TRT	Testosterone replacement therapy
VCAM	Vascular cell adhesion molecule
VLDL	Very low density lipoprotein
VSMC	Vascular smooth muscle cells
vWF	Von Willebrand Factor

Published Abstracts

Kelly DM, Channer KS, Woodroofe MN & Sellers DJ. Immunomodulatory effects of testosterone on fractalkine expression in human aortic endothelial and smooth muscle cells. *Proc Life Sciences*, PC352 Poster Communications. July 2007. Life Sciences. Glasgow, UK.

Kelly D, Channer K, Woodroofe N, and Sellers D. Investigating the immunomodulatory effects of testosterone on cell type-specific expression of CX3CL1 in human aortic vascular cells. *Fundamental and Clinical Pharmacology* 22: 73-74 Suppl. 2 August 2008. Manchester, UK.

Kelly DM, Channer KS, Woodroofe MN and Sellers DJ. Investigating the role of testosterone and inflammation in atherosclerosis. *Immunology* 125: 116-117 Suppl. 1 December 2008. Glasgow, UK.

Kelly D, Sellers D, Woodroofe MN, & Channer K. Investigating anti-inflammatory effects of testosterone in atherosclerosis. *Atherosclerosis Supplements* 10 (2):P667 June 2009. Boston, MA., USA.

Kelly DM Sellers DJ, Woodroofe, Jones TH & Channer KS. Effect of Testosterone on Inflammatory Markers in Development of Early Atherogenesis in the Testicular Feminised Mouse (Tfm) Model. *Endocrinology Reviews* 31 (3): S593 Suppl. 1 June 2010. San Diego CA., USA.

Acknowledgements

I would firstly and most importantly like to thank my supervisors Professor Nicola Woodroofe and Dr Donna Sellers, whose support and guidance through the entirety of my PhD have been invaluable, and without which I would not have reached where I am. In addition, I am most grateful to Professor Kevin Channer for his extended support.

Thanks to Prof. Jones for input throughout various stages of my PhD. Your support is much appreciated. A special thanks to Joanne Nettleship for her support, encouragement and invaluable advice when things got tough. Thanks to Murali for your wisdom and friendship.

I would like to thank my friends and colleagues of the BMRC for their help, technical advice and friendship, especially Claire Bradford, Robert Widdowson and Helen Denny. An enormous thank you to my family and "non-science" friends who have helped me in more ways than they realise.

A special thanks to Dr Karen Thethi and Dr Mark Cobain who inspired and encouraged me down the research path. It was you who planted the idea in my head all those years ago which, try as I might, I could not make it go away.

Chapter 1

General Introduction

1.1 Cardiovascular Disease

Cardiovascular disease (CVD) remains the major cause of mortality in the western world, accounting for nearly half of all deaths in Europe (48%) and the European Union (42%), and is the UK's biggest killer (Rayner *et al.* 2009). CVD comprises all diseases of the heart and circulatory system, but primarily includes coronary heart disease (myocardial infarction, angina, heart failure and coronary death), cerebrovascular diseases (stroke, transient ischaemic attacks) and peripheral vascular diseases (intermittent claudication, gangrene) (Glaudemans *et al.* 2010). The major underlying cause of CVD is atherosclerosis. In order to improve prognosis and provide better therapies for cardiovascular disease, it is critical to develop a greater understanding of the basic pathophysiological processes of atherosclerosis.

1.2 Atherosclerosis

Atherosclerosis is a complex disease of the large and medium sized arteries that has a lengthy asymptomatic phase of development. Beginning in the first decade of life, although early vascular changes are minor, atherosclerosis can progress over time and typically manifests clinically in middle and late adulthood or, more often than not, it may regress and disappear with time (Hansson and Libby 2006, Hong 2010).

This disease is characterised by the over recruitment of leukocytes and lipid accumulation in the vessel wall, leading to a loss of normal vascular function and stenosis, narrowing of the arteries. Stenosis interrupts the normal blood flow through the vessel, which can manifest as specific clinical complications depending upon the location of the affected vessel (Figure 1.1b). Over time, as the accumulation of lipid and immune cells continues, these lesions, known as atherosclerotic plaques, mature and take on new characteristics, often becoming vulnerable to rupture as a result of aggressive immunological activity. Although clinical complications of stenosis occur, the most severe clinical manifestations of

1

A

Tunica intima (mainly endothelial cells)

Tunica media (mainly smooth muscle cells)

Tunica adventitia (mainly connective tissue)

B

reduced blood flow

plaque

C

clot

Heart	Brain	Periphery
Coronary artery disease (CAD)	Carotid artery disease	Peripheral artery disease (PAD)
•Angina	•Asympotmatic •Transient ischemic attack	•Intermittent claudication •Abdominal aortic aneurysm (AAA)

Heart	Brain	Periphery
Mycocardial Infaction (MI)	Stroke	Gangrene

Figure 1.1; Illustration of an artery showing stenosis and blockage with associated clinical complications. Arteries are made up of multiple distinctive layers which results in a dynamic responsive tissue (a). As leukocytes and lipid accumulates in the vessel wall during atherosclerosis, there is a narrowing of the lumen restricting blood flow. Dependent upon the vascular territory of the atherosclerotic lesion, clinical complications occur as a result of restricted blood flow (b). If the artery becomes totally occluded by clot formation at the lesion site, severe and sometimes fatal consequences can ensue (c).

atherosclerosis arise from plaque rupture, which exposes the thrombotic plaque contents to the blood and sudden thrombotic occlusion may ensue (figure 1.2). Depending upon the vascular location of the blockage, severe and often fatal clinical complications transpire, such as myocardial infarction (MI) and stroke (figure 1.1c). The precise mechanisms that underlie this plaque development remain disputed. However, over the past three decades our understanding has evolved from early hypotheses based on lipid deposition within the vessel wall, to a more complex interplay between the conventional risk factors (obesity, smoking, family history, hypertension), inflammation and dysfunction of the vasculature. These pan-vascular processes are now focussed on immunological involvement and have established atherosclerosis as an inflammatory lipid pathology.

1.2.1 Initiation of inflammatory atherosclerotic events

As excessive atherogenic lipids in the vascular wall influence inflammation, which subsequently affects vascular permeability to lipids creating a circular and perpetuating situation, the debate over the triggers of atherosclerosis continues.

It is plausible that distal events that alter systemic inflammatory status have the potential to modify and activate local inflammatory actions in the artery at the site of atheroma formation. Such events may include; increases in circulating lipoprotein particles acting locally on the vasculature to affect oxidative status (see following sections), extravascular infection that elevates systemic cytokine production and immune activation, hyperglycaemic modification of macromolecules associated with diabetes that subsequently cause endothelial activation, hypertension-induced alterations of oxidative and inflammatory status, as well as physical damage from shear stress in extreme cases, and increases in circulating inflammatory cytokines from adipose tissue due to obesity (see Libby 2006 for review). In addition, local intravascular infection might also provide a local inflammatory stimulus, as seen with microbial agents such as Chlamydia pneumoniae (Kol *et al*. 1999).

Regardless of which of these preceding events may initiate the inflammation in atherosclerosis, the role of lipids and their transformation to immunogenic species by oxidative reactions remains central to early athero-inflammatory events.

A

Normal Artery

Endothelial cell · Smooth muscle cell · Monocyte · T-cell · Cholesterol · Adhesion molecule

B Fatty Streak Lesion

Endothelial cell · Smooth muscle cell · Monocyte · Macrophage · Foam cell · T-cell · Cholesterol

C Mature Atherosclerotic Plaque

Endothelial cell · Smooth muscle cell · Monocyte · Macrophage · Foam cell · T-cell · Dendritic cell · Dead cell · Cholesterol

4
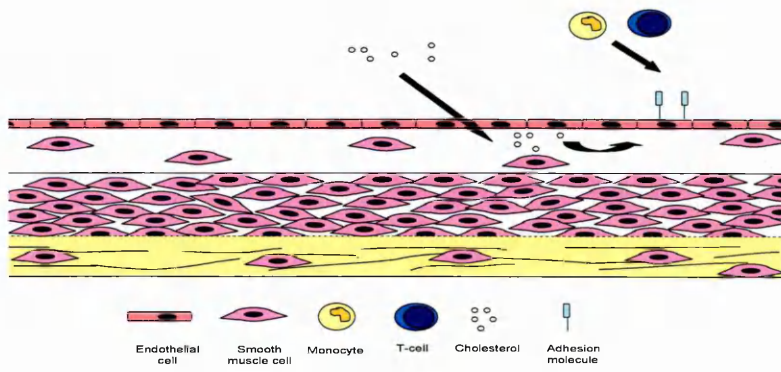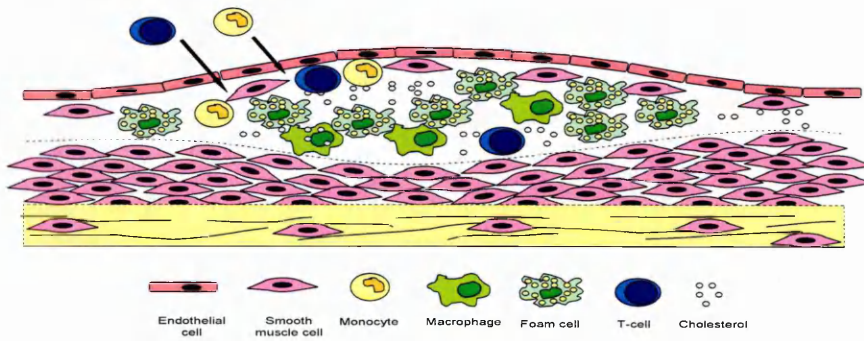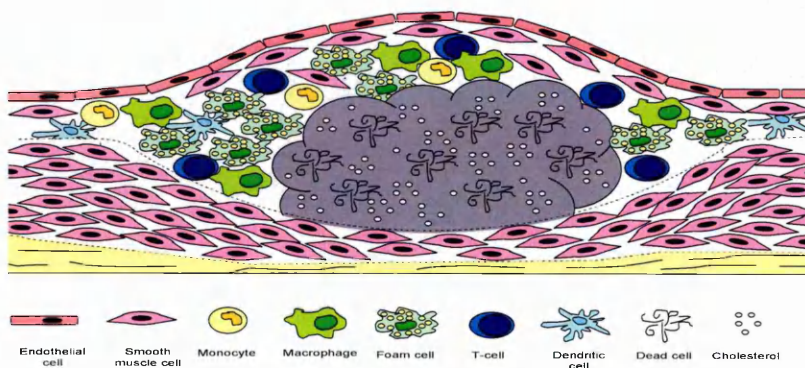
D Plaque Rupture and Thrombosis

| Endothelial cell | Smooth muscle cell | Monocyte | Macrophage | Foam cell | T-cell | Dendritic cell | Dead cell | Cholesterol |

Erythrocyte | Platelet | Fibrin
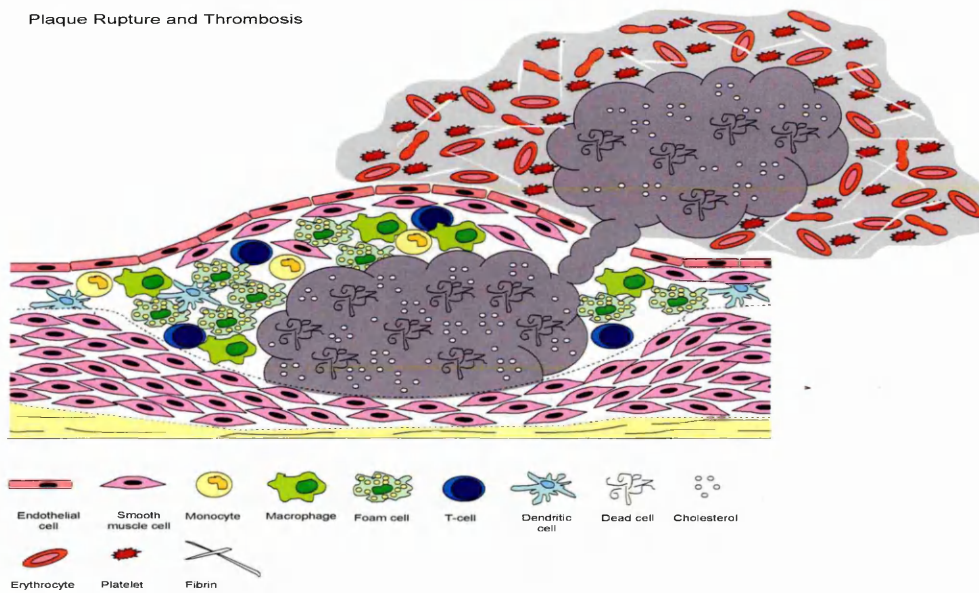
Figure 1.2; The stages of atherosclerosis. A) Leukocyte recruitment (predominantly monocytes and T cells) to the nascent atherosclerotic lesion at sites of endothelial activations due to lipid accumulation. Pro-inflammatory mediators expressed within the activated vascular wall promote leukocyte maturation and subsequent release of inflammatory mediators such as cytokines, chemokines and adhesion molecules. Additional leukocytes are attracted to the lesion and the fatty streak develops (B). Fatty streaks develop into mature atherosclerotic plaques as a central necrotic core of lipid and dead cells develops as a result of inflammation-induced apoptosis (C). Additionally, smooth muscle cells migrate from the tunica media to form a protective cap over the plaque through deposition of strength-giving collagen. When this protective fibrous cap thins, due to continued aggressive inflammation, the plaque is prone to rupture exposing its contents to the circulating blood. Coagulants in the blood are activated and form a thrombus that causes most of the acute complications of atherosclerosis (D). Adapted from Hansson and Libby (2006).

1.2.1.1   *The role of lipids*

Although our knowledge of atherosclerosis has developed beyond early theories that suggested only a primary hyperlipidemia, the role of lipids, and particularly cholesterol, cannot be ignored as they are implicated in the initiation, development and progression of the disease. Abnormalities in lipoprotein profiles are still recognised as the most important cause of premature atherosclerosis (Knopp 1999).

1.2.1.1.1   Cholesterol

Cholesterol is a biologically important molecule within the body, acting as a structural component in cell membranes and as a precursor to steroid hormones, vitamin D and bile acids (Daniels *et al*. 2009). The majority of the cholesterol needed to maintain a healthy status is biosynthesised in the liver. Hence a much smaller proportion is required from dietary intake of foods high in saturated fatty acids. This balance is altered with dietary intake, with biosynthesis reduced when intake is high and increased when it is low (Jones 1997). This tight regulatory balance is essential for maintaining health. However, the homeostatic mechanisms can be inadequate when dietary cholesterol intake is excessive or in pathologies that alter lipid processing.

As cholesterol is water insoluble it is not found free in the blood. Instead it is esterified to fatty acids and packaged into lipoprotein particles. There are five main classes of lipoproteins, based on size and protein-to-lipid ratio density (the more protein the higher the density) (Daniels *et al*. 2009) (figure 1.3). Dietary cholesterol is packaged into chylomicrons in the intestine through the esterification of free cholesterol and the synthesis of triglycerides from free fatty acids, amalgamated together with apolipoprotein B (apoB) (Daniels *et al*. 2009). These particles pass into the circulation where they are targeted by lipase enzymes which break down chylomicron components to allow the redistribution of fatty acids. Very low density lipoproteins (VLDL) are produced by the liver from chylomicron remnants and function to distribute triglycerides and cholesterol esters to the rest of the body. As they circulate, high density lipoprotein (HDL) and lipoprotein lipase enzymes in the capillaries remove triglycerides and alter the VLDL particles to an intermediate density lipoprotein (IDL), which is either removed from the plasma by the liver or further transformed to a low density lipoprotein (LDL) by continued reduction of fatty acids and apolipoproteins (Gunston *et al*. 2007). LDLs are the main source of cholesterol
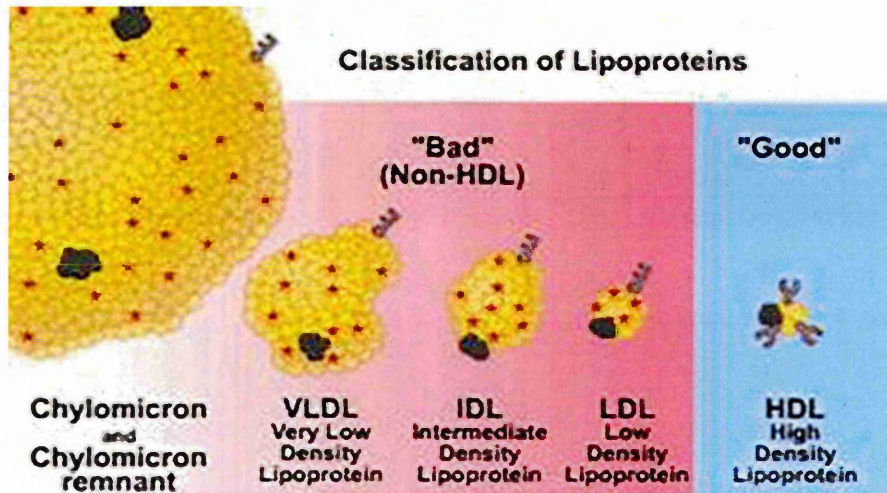
Figure 1.3; Classification of lipoproteins. The five main classes of lipoproteins, based on size and protein-to-lipid ratio density. Dietary cholesterol is packaged into chylomicrons in the intestine. Lipase activity frees some of the fatty acid content, thus increasing the density of the particle and forming VLDL. Further lipase activity occurs at different locations, sequentially reducing the lipid content of the particles to form IDL, LDL then HDL. *Cholesterol (red stars), apolipoprotein B (keys), apolipoprotein A (y shapes), and membrane proteins (blue dots).*
From http://cme.medscape.com/viewarticle/416521_3

transport in the circulation and are considered atherogenic due to their propensity to bind to connective tissue in the intima of arteries (Mourao and Bracamonte 1984). Conversely, HDL presents anti-atherogenic properties due to its ability to negate cholesterol accumulation in tissues. HDL is continuously manufactured in the liver and circulates in the blood, acting as a scavenger for free cholesterol and cholesteryl esters from chylomicrons and VLDL. HDL can also acquire cholesterol from LDL particles in the circulation or tissues, before returning to the liver, where reverse cholesterol transport removes cholesterol and it is used to synthesise bile acids or it is excreted (Daniels *et al.* 2009).

LDLs and other lipoproteins can freely enter the artery wall from the plasma, and can be taken up by vascular cells via receptor-mediated endocytosis or lipase activity, or can remain free in the intima (Goldstein and Brown 1977, Dabagh *et al.* 2009). Equally, they can return to the circulation from the tissues, dependent upon circulating concentrations. When plasma levels are high (hyperlipidaemia) entry can be greater than exit, and lipoproteins accumulate in the vascular wall (Barter 2005). Therefore, the lipid profile of an individual may greatly influence susceptibility to atherosclerosis, with particular emphasis on the balance between circulating cholesterol-rich LDLs and cholesterol-clearing HDLs. This is demonstrated by many cross-sectional and epidemiological studies implicating atherogenic dyslipidemia (low HDL-cholesterol, increased triglycerides and non-HDL cholesterol, and elevated small dense LDL particle concentrations) with CVD (See Musunuru 2010).

1.2.1.2 The role of shear stress and oxidative status

Remarkably, atherosclerotic lesions tend to develop in predisposed areas of the vasculature that are associated with specific haemodynamic conditions. Physiological laminar shear stress is created by the dragging force generated by blood flow over the luminal surface of the vascular endothelium (Patel *et al.* 2000). It is of particular importance for protecting the endothelium from abnormal activation and the promotion of atherogenesis. The protective effect of laminar shear stress is thought to be due to the release and activity of nitric oxide (NO) (Tao *et al.* 2006, Pan 2009). NO is a potent endogenous vasodilator contributing to the maintenance of tone, reactivity and homeostasis of the vasculature, and influences local and regional blood flow (Naploi and Ignarro 2001, Förstermann 2010). Importantly, NO also

decreases endothelial permeability and reduces the flux of lipoproteins into the vessel wall (Cardona-Sanclemente and Born 1995).

Synthesis of NO occurs via endothelial nitric oxide synthase (eNOS) or inducible nitric oxide synthase (iNOS) which can be regulated by elevations in calcium ion concentration, as a result of vascular mechano-chemical sensitive responses to haemodynamics (Jagnandan *et al*. 2005, Napoli *et al*. 2006). Physiological laminar shear stress increases the abundance of eNOS in the vasculature, thus maintaining NO and vascular function (De Nigris *et al*. 2003). However, at locations subjected to oscillating or prolonged low or high shear forces, such as near arterial branches, bifurcations and curvatures, NO activity is reduced (Napoli *et al*. 2006). A reduction in NO synthesis is a major contributing factor to endothelial dysfunction (Wever *et al*. 1998) and reduced eNOS expression has been demonstrated in human atherosclerotic lesions (Oemar *et al*. 1998).

Focal and regional haemodynamic parameters influence endothelial gene expression with an increase in pro-inflammatory gene expression in areas of disturbed flow, compared to anti-inflammatory gene expression in areas of healthy high shear stress (Davies *et al*. 2009, Boon and Horrevoets 2009). This may be mediated via NO activity, through the regulation of transcription factors associated with inflammatory genes and suppression of the expression of atherogenic molecules (De Caterina *et al*. 1995, Shin *et al*. 1996). Loss of NO and subsequent upregulation of these pro-inflammatory genes may result in activation of the endothelium. Cultured endothelial cells exposed to oscillatory shear stress mimicking arterial blood flow display increased expression of several leukocyte adhesion molecules (Dai *et al*. 2004). Hastings *et al*. (2007) observed that cultured endothelial cells exposed to disturbed flow patterns show increased expression and secretion of the inflammatory cytokine IL-8. Disturbed haemodynamics also increase vascular expression of endothelin-1 (ET-1), a potent vasoactive peptide, which in turn induces the appearance of adhesion molecules and promotes excessive oxidative stress (Grover-Paez and Zavalza-Gomez 2009). In addition vascular wall shear stress has the capability to act beyond the endothelium, with turbulent flow leading to an increased production of proteoglycan molecules by smooth muscle cells (Grover-Paez *et al*. 2009). Proteoglycans can bind and retain lipoprotein particles, facilitating their oxidative modification and subsequent inflammatory events (Skalen *et al*. 2002). The mechanisms by which these inflammatory characteristics evolve

are not fully understood, but may be caused indirectly due to NO depletion and subsequent inflammatory signal pathway activation.

1.2.1.3   Oxidation of LDL

The cause and effect relationship between endothelial dysfunction and vascular dyslipidemia, and therefore the first step that initiates endothelial activation, has not yet been identified. The infiltration of LDL, however, is considered a fundamental juncture. Once LDL has penetrated the endothelium it is susceptible to modifications by reactive molecules present in the vascular wall as a result of normal and pathologically altered metabolic function.

Reactive oxygen species (ROS) are naturally occuring oxidants produced through normal eukaryotic metabolism. These free and non-free radicals possess potent oxidative ability, capable of damaging cellular components including lipids and membranes (Madamanchi *et al.* 2005). Oxygen radicals also possess the capacity to modify unsaturated fatty acid residues of triglycerides and phospholipids of LDL, resulting in highly reactive oxidised-LDL (oxLDL). The mechanisms by which LDL is oxidised remains unknown, and the modified structures of oxLDL are also not yet clear, in part due to the heterogeneous nature of the composite mixture of modified particles (Itabe 2009). However transformation of residues on LDL molecules are known to alter its structure to form atherogenic neoepitopes, with properties that can be recognised by scavenger receptors on macrophages that are capable of initiating an immune response (Hörkkö *et al.* 2000). As oxLDL is a self-protein, altered in a way that is capable of immune interactions and initiation of inflammation, atherosclerosis may be considered an autoimmune disease (See Mandal *et al.* 2005, Blasi 2008). In addition, LDL and oxLDL have been shown to increase ROS generation through eNOS uncoupling, whereby synthesis of this enzyme is increased but function is altered as a result of decreased L-arginine uptake (the eNOS substrate for NO production), and disruption of the transcription of NOS ultimately decreases the production of NO (Pritchard *et al.* 1995, Jessup 1996, Vergnani *et al.* 2000). Cells have evolved a protective mechanism by which these oxidants can be enzymatically "mopped-up" by superoxide dismutases (SOD), catalase and glutathione peroxidase, which break down oxidised lipid and neutralise their proinflammatory effects (Heistad *et al.* 2008). This homeostatic balance usually sees a compensatory increase in levels of SOD in response to heightened metabolic activities and

oxidative stress (Heistad *et al.* 2008). However, in pathophysiological conditions, excess oxidants can overwhelm the scavenging capacity of these cellular antioxidant systems resulting in oxidative damage (Madamanchi *et al.* 2005).

Alterations in oxidative status, as a result of increased ROS accumulation and subsequent oxidative damage, can activate nuclear transcription factors that increase the expression of cytokines, chemokines and adhesion molecules involved in atherogenesis within cells of the vasculature (Reape and Groot 1999). Vascular cell adhesion molecule-1 (VCAM-1), intra-cellular adhesion molecule-1 (ICAM-1), E-selectin, and P-selectin are expressed on endothelial cells at locations considered to be reflective of disturbed haemodynamics and are also upregulated by oxLDL (Reape and Groot 1999, Galkina and Ley 2007). Immune recruitment to activated endothelium may primarily be a protective response for oxLDL clearance, yet could ultimately initiate inflammation typical of atherosclerosis. Again, this vascular activation affects endothelial permeability to macromolecules, and in hypercholesterolemia, LDL can diffuse into the intima (Ogunrinade *et al.* 2002). In addition, elevated levels of ROS can induce oxidative damage of DNA leading to arrest of cell growth and apoptosis, which in turn is capable of initiating immune responses (Bennett 2001). The target of ROS-induced DNA damage in atherosclerotic lesions is unclear. However, ROS is capable of provoking toxicity in vascular cells (Li *et al.* 1997) and macrophage apoptosis (Martinet *et al.* 2001).

ROS are generated in atherosclerotic plaques, particularly by macrophages (Kojda *et al.* 1999). Therefore, vascular oxidative stress is exacerbated by elevated atherogenic lipid profiles and the activity of recruited immune cells, leading to excessive ROS formation and vascular injury/activation. In the presence of hypercholesterolemia this, in turn increases LDL influx into the vessel wall, subsequent LDL oxidation and leads to NO inactivation, which further accelerates superoxide generation and LDL oxidation, perpetuating endothelial dysfunction (Arimura *et al.* 2001, Chen *et al.* 2006). The initial cause of endothelial injury/activation, lipid accumulation and oxidative damage-modification remains unclear. However, it is clear that the combination of these events is capable of promoting immune responses.

1.3 Immune response in atherosclerosis

The initiating events that trigger the arterial inflammation associated with atherosclerosis are not completely known. However, as seen above, elevated atherogenic lipids in the vessel wall, endothelial dysfunction and modified lipids and proteins due to increased oxidative activity, can all result in immunogenic epitopes that can activate and injure the endothelium.

1.3.1   Early vascular changes

Activated vascular cells at arterial sites prone to atheroma promote early inflammatory cell recruitment, a process that is orchestrated by cytokines, chemokines and adhesion molecules.

1.3.1.1   Cytokines

Cytokines are pleiotropic signalling proteins, important for regulating inflammatory and immune responses through autocrine, paracrine and juxtocrine activity. They are regulators of innate and adaptive immune responses and can generally be divided into several classes; interleukins (IL), tumour necrosis factors (TNF), interferons (IFN), colony stimulating factors (CSF), transforming growth factors (TGF) and chemokines (Tedgui and Mallat 2006). Many cytokines have the ability to act synergistically in their immunological function and can be both pro- and anti-inflammatory.

1.3.1.2   Chemokines

Chemokines are a family of low molecular weight soluble chemoattractant proteins, released at the site of inflammation that act on immune cells and vascular cells in a localised manner to regulate several processes involved in inflammation, including leukocyte trafficking, apoptosis, proliferation and further cytokine and chemokine synthesis (Taub and Oppenheim, Rollins 1997). There are approximately 42 human chemokines that can be subdivided into four families (C, CC, CXC and CX_3C) based on the number and spacing of the first two cysteine residues in a conserved cysteine motif (Bazan et al. 1997, Zlotnik and Yoshie 2000). With 20 known chemokine receptors and extensive overlap of ligand-receptor recognition, the chemokine system has the capacity to be very specific yet very

complex (Surmi *et al.* 2009) (Table 1.1). The orchestration of this chemokine system in atherosclerosis is, as yet, not clearly defined. However, many chemokines have been identified in human atherosclerotic lesions demonstrating their involvement in the pathogenesis of the disease (Reape and Groote 1999, Abi-Younes *et al.* 2000, Greaves and Gordon 2001, Wong *et al.* 2002a).

As circulating leukocytes come into contact with inflammatory chemokines, released from the activated endothelium, receptor-ligand binding occurs and the cells become active. This occurs through actin rearrangement and a change in cell shape, enabling movement to the inflammatory site via concentration gradient-induced migration (Charo and Taubman 2004). The consequence of this receptor activation is not limited to locomotion, as gene transcription can take place, leading to other functions such as increased adhesive characteristics through the modulation of integrins, selectins and other adhesion molecules (Thelen 2001).

In addition, chemokines secreted at sites of inflammation can be immobilised and concentrated on the surface of immune and vascular cells via binding to proteoglycans (Kuschert *et al.* 1999). This creates an endothelial milieu favourable to leukocyte adhesion and transmigration into the vascular wall, whereby inflammation is perpetuated.

1.3.1.3   Adhesion molecules

Adhesion molecules aid cell-cell communication and are involved in the recruitment of immune cells, in conjunction with chemoattractant molecules, which are often co-expressed. Endothelial cells, under normal circumstances, have a low adhesive capacity for leukocytes and platelets. However, in atherosclerosis-prone sites, increased adhesion molecule expression occurs with immunological consequence. As an initial response to inflammatory stimuli, vascular endothelial cells increase expression of leukocyte adhesion molecules such as VCAM-1, ICAM-1, E-selectin, P-selectin and integrins, which are considered to be involved in atherogenesis (Sima *et al.* 2009).

Circulating leukocytes initially tether to the luminal surface of the endothelium via integrin- and selectin-mediated binding, either directly or through platelet interactions. This binding is transient and not sufficient to firmly capture leukocytes, but can slow their progression

Chemokine Family	Chemokine Nomenclature	Common Synonyms	Chemokine Receptor
C chemokines	XCL1	Lymphotactinα/SCMα	XCR1
	XCL2	Lymphotactinβ/SCMβ	XCR1
CC chemokines	CCL1	I-309	CCR8
	CCL2	MCP-1	CCR2
	CCL3	MIP-1α	CCR1, CCR5
	CCL4	MIP-1β	CCR5
	CCL5	RANTES	CCR6
	CCL7	MCP-3	CCR1, CCR2, CCR5
	CCL8	MCP-2	CCR3
	CCL11	Eotaxin	CCR3
	CCL13	MCP-4	CCR2, CCR3
	CCL14	HCC-1	CCR1
	CCL15	HCC-2	CCR1, CCR4
	CCL16	HCC-4	CCR1
	CCL17	TARC	CCR4
	CCL18	PARC	Unknown
	CCL19	MIP-3β/ELC	CCR7
	CCL20	MIP-3α/LARC	CCR6
	CCL21	SLC/6Ckine	CCR7
	CCL22	MDC/STCP-1	CCR4
	CCL23	MPIF-1	CCR1
	CCL24	MPIF-2	CCR3
	CCL25	TECK	CCR9
	CCL26	Eotaxin-3	CCR3
	CCL27	CTACK/ILC	CCR10
	CCL28	MEC	CCR10
CXC chemokines	CXCL1	GROα	CXCR1, CXCR2
	CXCL2	GROβ	CXCR2
	CXCL3	GROγ	CXCR2
	CXCL4	PF4	CXCR3B
	CXCL5	ENA-78	CXCR2
	CXCL6	GCP-2	CXCR1, CXCR2
	CXCL7	NAP-2	CXCR2
	CXCL8	IL-8	CXCR1, CXCR2
	CXCL9	MIG	CXCR3
	CXCL10	IP-10	CXCR3
	CXCL11	ITAC	CXCR3
	CXCL12	SDF-1α/β	CXCR4
	CXCL13	BCA-1/BLC	CXCR5
	CXCL14	BRAK	Unknown
	CXCL16	-	CXCR6
CX$_3$C chemokines	CX$_3$CL1	Fractalkine	CX$_3$CR1

Table 1.1; Human chemokine families. There are approximately 42 human chemokines that are subdivided into four families based on the number and spacing of the first two cysteine residues in a conserved cysteine motif. 20 known chemokine receptors allow extensive overlap of ligand-receptor recognition. See Mantovani *et al.* (2006).

allowing for further tethering to additional adhesion molecules. This creates a 'rolling' effect of the leukocyte along the endothelium and maximises cell-cell communication (Figure 1.4). Under normal conditions selectin and integrin interactions are reversible and are not sufficient to bind rolling leukocytes. Cytokines and chemokines released from endothelial sites of inflammation activate integrins and selectins and result in the firm capture of leukocytes (Campbell *et al.* 1998, Weber 2003). The binding of other up-regulated adhesion molecules, due to the close contact of leukocyte rolling, may mediate integrin activation or may independently instigate cell arrest. Firm adhesion of leukocytes to the endothelium propagates intra-cellular signaling in both leukocytes and endothelial cells to facilitate diapedesis of immune cells into the sub-endothelial space (vascular intima), independently or via further chemokine signalling (Weber 2003, Ley *et al* 2007).

1.3.2 Cell types involved in atherosclerosis

The accumulation of inflammatory cells within the artery wall, predominantly monocytes and T cells in early plaques, leads to increased local production of cytokines, growth factors and chemokines from vascular cells and immune cells. These factors enhance and amplify the cascade of inflammatory events that attract and activate further leukocytes to the intima, such as mast cells, neutrophils, natural killer cells and rarely B-cells (figure 1.5) (Libby *et al.* 2002a).

1.3.2.1 Monocytes/macrophages

Monocytes have been identified as the 'crucial force' in driving atherogenesis, and are present at all stages of plaque development (Weber *et al.* 2008). In early plaques, macrophages are the predominant inflammatory cells and represent the effector cells of the innate immune response (Hansson and Libby 2006).

Circulating monocytes are recruited to sites of inflammation predominantly by chemokines. Monocyte chemoattractant protein-1 (MCP1, or CCL2) (Gu *et al.* 1998, Boring *et al.* 1998), fractalkine (CX_3CL1) (Bazan *et al.* 1997, Guo *et al.* 2003), and CCL5 (Tacke *et al.* 2007, Combadiere *et al.* 2008) are considered to act as chemoattractants for monocytes, initiating their migration towards the inflammatory site down a concentration gradient and assisting in extravasation into the vessel. Monocyte differentiation into macrophages in the vascular intima results from stimulation with macrophage colony-stimulating factor (M-CSF),
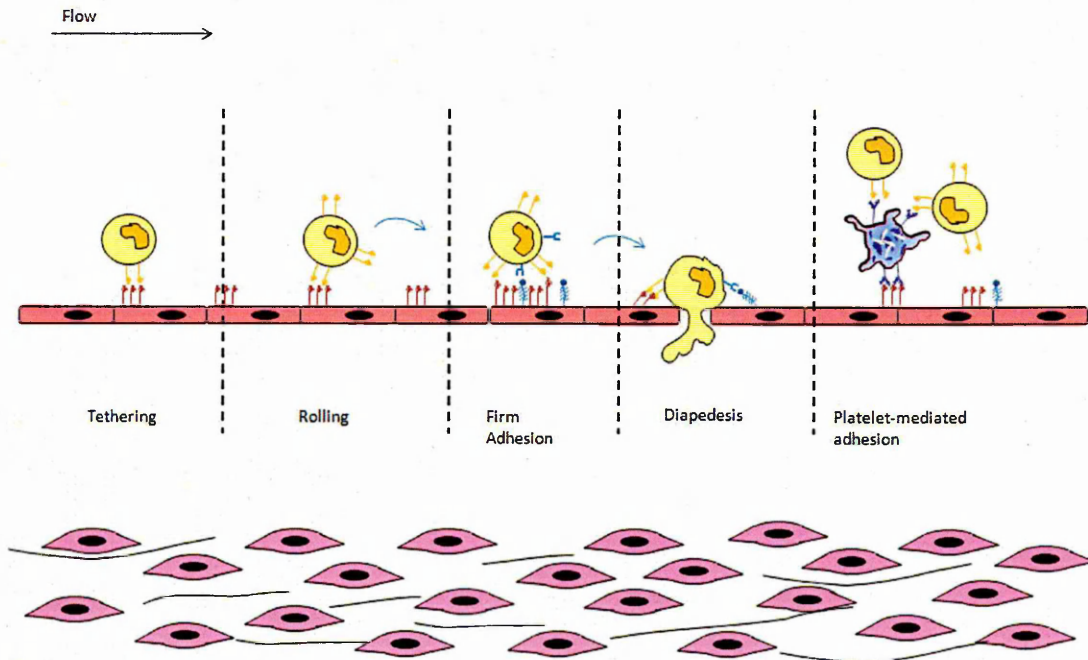
Figure 1.4; Leukocyte migration into the vascular wall. Circulating leukocytes initially tether to the luminal surface of the endothelium via reversible integrin- and selectin-mediated binding, either directly or through platelet interactions. Leukocytes roll over the endothelium maximising cell-cell communication which leads to firm adhesion to activated integrins and selectins or additional adhesion molecules. Intra-cellular signalling in both leukocytes and endothelial cells facilitates diapedesis of immune cells into the sub-endothelial space. See Weber (2003)

INNATE

Macrophage	Neutrophil	Mast cell	Natural Killer Cell	Dendritic cell	Platelet

ROS Proteases TNFα IL-1, IL-12, IL-18	ROS Cytokines Proteases	Cytokines Growth factors	Cytokines Growth factors	Cytokines Proteases TNFα, IFNγ	IL-1β Growth factors ROS

↓DL accumulation
Oxidative damage and LDL oxidation
Smooth muscle cell proliferation
Adverse arterial remodelling and intimal thickening
Additional inflammatory cell activation

ADAPTIVE

Th1 T cell	Th2 T cell	Treg	B cell

IFNγ, TNFα IL-12, IL-15, IL-18	IL-4 IL-10	IL-10 TGFβ	Antibodies

Proatherogenic ↑ Leukocyte activation ↑ Proliferation	Anti-atherogenic ↓Foam cell production ↓Proliferation	Anti-atherogenic ↓Th1 activation ↓Proliferation	Mixed data

Figure 1.5; Immune cells involved in atherosclerosis. Summary of some of the functions ascribed to various cell types in atherosclerosis. Many of these innate and adaptive cells of the immune response interact and regulate activation and function of other immune and vascular cells through the secretion of inflammatory mediators such as cytokines, chemokines and growth factors and proteases which are involved in plaque destabilisation. In addition, cells are capable of altering oxidative status through reactive oxygen species (ROS) generation.

produced by activated endothelial and smooth muscle cells (Rajavashisth *et al*. 1990b). In addition, M-CSF can induce scavenger receptor expression on macrophages (Clinton *et al*. 1992). Scavenger receptors are a family of pattern-recognition receptors, including CD36, CD68, CXCR16, lectin-type oxidised low-density lipoprotein receptor-1 (LOX1), scavenger receptor-A (SR-A) and SR-B1, which bind proteins recognised as foreign, including modified LDL, and internalise them for proteolytic degradation (See Hansson and Libby 2006). These receptors may have evolved as a means of recognising oxidised self-antigens to mediate their degradation and clearance to avoid autoimmunity (Greaves and Gordon 2008). In atherosclerosis, these protective mechanisms may become overwhelmed, leading to pathological outcomes. Also implicated in the initial events of immune recognition and recruitment are toll-like receptors (TLR), which have a similar function to scavenger receptors, but can directly elicit inflammatory responses (Libby *et al*. 2009).

Macrophages bind, via their scavenger receptors, engulf and degrade oxLDL particles to generate free cholesterol for efflux. However, during hypercholesterolemia and heightened vascular activation associated with atherosclerosis, the clearing of cholesterol is inhibited and lipid accumulates within the macrophages forming so-called 'foam cells' due to their foamy appearance under the microscope (Galis *et al*. 1995). Additionally, at sites of inflammation, macrophages and monocytes are capable of phagocytosis of lipid-laden platelets, also causing foam cell formation, and the conversion of monocytes to foam cells is inducible by platelet-derived factors (Reviewed in Seigel-Axel *et al*. 2008). Foam cells are the characteristic cells of early 'fatty streak' atherosclerosis (Montecucco and Mach 2009).

Monocytes exhibit heterogeneity, falling into two distinct subsets relating to high and low immunological activity, potentially identified by expression of cell adhesion ligands and chemokine receptors which determine their subsequent role in inflammation (Tacke *et al*. 2007, Libby *et al*. 2008). Inflammatory monocytes are $CCR2^+$ and CX_3CR1^{lo} and are thought to adhere preferentially to activated endothelium, moving rapidly from the blood to sites of inflammation and giving rise to classically activated (M1) macrophages (Geissmann *et al*. 2003, Swirski *et al*. 2007). In addition, these monocytes express high levels of P-selectin glycoprotein-1 (PSGL-1) that contributes to homing and rolling on the arterial endothelium by demonstrating a high capacity for binding the selectin adhesion molecules (An *et al*. 2008, Shimada 2009). In contrast, the second subset of 'non-classical' monocytes express high CX_3CR1 levels but are CCR2 negative. These monocytes, with distinct adhesive

capabilities, are considered to 'patrol' the luminal side of the endothelium (Woolard and Geissman 2010) and are destined to become less inflammatory resident M2 macrophages (Geissmann *et al.* 2003) or dendritic cells (Tacke *et al.* 2007), potentially involved in atherosclerosis. Whether this subset patrols the entire vascular tree, however, is yet to be explored (Woolard and Geissman 2010).

Also, circulating monocyte subsets show plasticity and are capable of converting to the alternate phenotype depending upon the activating stimuli (Swirski *et al.* 2007). Proatherogenic stimuli, such as dyslipidemia, leads to a profound increase in the expression of proinflammatory subsets of monocytes, which mature into M1 macrophages in the intima and exhibit heightened proinflammatory activity (Geissmann *et al.* 2003, Schlitt *et al.* 2004, Swirski *et al.* 2007, Tacke *et al.* 2007). The specific contributions of monocyte and macrophage subsets remain largely unknown, however, their presence in early lesions is clear.

Pro-atherogenic M1 macrophages predominate in athero-development and secrete pro-inflammatory cytokine mediators such as IL-1, TNFα and ROS, thereby promoting continued immune cell recruitment and accumulation of lipid within the artery wall (Hansson 2005). Several lines of investigation suggest that the initiation of cytokine production from macrophages in atherosclerotic sites is most likely elicited by oxLDL (Tedgui 2005). TNFα and IL-1β are also secreted by activated and lipid-laden macrophages provoking multiple cellular effects within the vasculature that promote atheroma formation (Packard *et al.* 2009). In addition, TLR activation leads to the production of cytokines by macrophages. In particular, TNFα and IFNγ are secreted in high levels from TLR-activated dendritic cells (Krutzik *et al.* 2005). The less inflammatory M2 macrophages may function to modulate athero-progression by dampening the inflammatory response through secretion of anti-inflammatory mediators such as IL-10 and TGFβ (Gordon 2003) promoting resolution of inflammation (Martinez *et al.* 2009).

Macrophages, foam cells and dendritic cells act as antigen presenting cells (APC) to leukocytes of the adaptive immune response. OxLDL is ingested and processed by lysosomal degradation resulting in oxLDL-derived epitope delivery and display on the cell membrane by major histocompatibility complex (MHC) class I and II molecules (van

Puijvelde *et al.* 2006). This presentation allows for interaction with cells of the adaptive immune response (See section 1.3.2.2).

1.3.2.2   T cells

The significant presence of T cells and their production of cytokines and other inflammatory modulators in atherosclerotic plaques implicate a regulatory role for these adaptive immune cells in instructing the more abundant effector cells of the innate immune response (Hansson *et al.* 2000), and thus demonstrate a link between pathways of innate and adaptive immunity in early atherosclerosis. Circulating T cells enter the arterial intima in the early stages of atherosclerosis in response to adhesion molecule expression on the activated endothelium and local release of chemokines, in a manner similar to monocytes. Activated vascular cells and macrophages in the developing plaque produce the T cell chemoattractant CCL5 (also known as RANTES (regulated on activation, normal T-cell expressed and secreted)) (Mach *et al.* 1999). In addition, T cells respond to the IFNγ-inducible chemokines IFNγ-inducible protein-10 (IP-10, CXCL10), monokine induced by IFNγ (MIG, CXCL9) and CXCL11 (also known as IFNγ-inducible T cell α-chemoattractant (I-TAC)) and adhere to VCAM-1 at sites of atheroma (Libby 2009).

Most T cells in atherosclerotic lesions are CD4$^+$ T cells, but there are also a small proportion of CD8$^+$ cells (Paulsson *et al.* 2000). Local CD4$^+$ T cell activation occurs due to interaction with antigen presenting cells. Naive T cells, with specific oxLDL receptors, bind the MHC class II-oxLDL antigen complex on APCs resulting in the proliferation and clonal expansion of oxLDL specific T-cells (Stemme *et al.* 1995). During this T cell-APC interaction, additional membrane proteins aid communication between T cells and macrophages, significantly CD40-CD40 ligand (CD40L) interactions, which activate both cell types (Libby 2006). Upon oxLDL recognition, T cells undergo antigen-dependent activation in which they synthesise CD40L. CD40L interacts with CD40 on the macrophage surface activating its effector mechanisms, including enhanced cytokine production (IL-1, IL-12, TNF-α) (Phipps 2000). In addition, CD40-CD40L interactions are critical for the development of T cell effector functions of proliferation, differentiation and cytokine production (Laman *et al.* 1996). T cell cytokines include TNF-α, IFN-γ, IL-4, IL-6, IL-12, IL-2, (Phipps 2000, Hansson and Libby 2006, van Puijvelde *et al.* 2006). These cytokines, in turn, control further macrophage activation including scavenger receptor expression, MHC expression and cytokine production, in

addition to their effects on the vascular wall. This perpetuating active "cross talk" through the Th1 cytokine repertoire accelerates atherosclerosis (Hörkkö *et al.* 2000).

Upon activation, T lymphocytes differentiate into particular subsets, dependent on co-stimulation from cytokines, growth factors and specific cell-cell interactions, and are therefore controlled by the local inflammatory milieu. Most oxLDL reactive CD4+ T cells have a T helper 1 (Th1) phenotype (Stemme *et al.* 1995, Zhou *et al.* 2001), and consequently CD4+ Th1 cells are the predominant T cell in lesions, with CD8+ cytotoxic T cells detected to a lesser extent (Hosono *et al.* 2003). The differentiation of CD4+ T cells into Th1, Th2 or regulatory T cell (Treg) subsets is driven by the influence of cytokines. Th1 cell differentiation is driven by the proinflammatory cytokines IL-18 and IL-12 synergistically (Packard *et al.* 2009), whereas IL-4 induces the Th2 subset (Weirda *et al.* 2010) and IL-10 and TGFβ provoke regulatory T cells (Tregs) whilst also down-regulating Th1 cell production (Ait-Oufella *et al.* 2009).

Th1 cells are the predominant T cell in atherosclerotic plaques and are the primary source of IFNγ, although NK cells, and to a lesser extent macrophages, can also produce IFNγ (Andersson *et al.* 2010). IFNγ potentiates the production of proinflammatory Th1-promoting cytokines IL-12 and IL-18 by macrophages and smooth muscle cells, in addition to MHC-II expression, increased lipid uptake and increased APC activation (Leon and Zuckerman 2005, Hansson and Libby 2006). IFNγ may influence foam cell formation through the inhibition of scavenger receptor expression, as demonstrated in the THP-1 macrophage cell line (Li *et al.* 1995, Grewal *et al.* 2001, Wuttge *et al.* 2004, Wagsater *et al.* 2004) and subsequent decrease of modified LDL uptake (Reiss *et al.* 2004).

The role of Th2 cells in atherosclerosis is poorly understood though it is generally considered that they are anti-atherogenic as they oppose pro-atherogenic Th1 differentiation and cell response, and produce the anti-inflammatory cytokines IL-4, IL-5, IL-10 and IL-13 (Andersson *et al.* 2010). Mice predisposed to a Th2 response are found to be resistant to diet-induced atherosclerosis (Paigen *et al.* 1985) and elimination of the Th2 response gives rise to atherosclerosis susceptibility (Huber *et al.* 2001). Th2 cells, however, are rarely detected in mouse atherosclerotic lesions (Mallat *et al.* 2009).

Tregs are considered to influence the inflammatory progression of atherosclerosis through the release of anti-inflammatory cytokines, such as IL-10 and TGFβ, and their presence in all

developmental stages of human plaque formation could explain the smouldering chronic inflammatory process that occurs throughout the longstanding course of the disease (de Boer *et al.* 2007).

1.3.2.3   *Platelets*

There is accumulating evidence for the involvement of platelets in early and late atherosclerosis through their contribution to endothelial activation, modulation of inflammatory responses leading to lesion formation, and subsequent thrombotic complications.

Platelets are influenced by circulating lipids. LDL, VLDL and particularly oxLDL can bind to specific receptors on platelets, including scavenger receptors SR-B1, CD36 and LOX-1, mediating lipoprotein-platelet interactions (Badimon *et al.* 2009). The specificity and detailed function of these receptors is a matter of debate (Seigel-Axel *et al.* 2008). Platelet interactions with native LDL may function as a mechanism of lipoprotein exchange between the tissues and the circulation, delivering vital cellular components or facilitating lipid clearance. In contrast, oxLDL binding to platelets induces activation, morphological changes and promotes hyperaggregation (Tandon *et al.* 1989, Surya and Akkerman 1993, Elisaf *et al.* 1999). Whether lipoproteins are simply bound to the platelet surface or endocytosed is not fully understood.

Activated platelets are prone to adhere to the endothelium, particularly at sites of endothelial dysfunction or activation, where adhesion molecule expression is increased or the extracellular matrix is exposed. These mechanisms may initially serve to protect the endothelium, by initiating vascular repair through the release of growth factors and the attraction of progenitor cells (reviewed in Badimon *et al.* 2009). There is also evidence that platelets adhere to intact endothelium, possibly due to their sensitisation by pro-inflammatory stimuli and lipoprotein status (Seigel-Axel *et al.* 2008). Platelets adhere following the well-controlled mechanism of tethering and rolling, initiated by P-selectin-PSGL-1 interactions. Tethering further activates platelets, increasing cell-cell communication with the endothelium via increased production of cytokines, chemokines and adhesion molecules, and ultimately promotes platelet arrest (Lindemann *et al.* 2007). Firm platelet adhesion causes maximal platelet activation, leading to increased inflammatory mediator secretion (Lindemann *et al.* 2007). For example, endothelial CD40

interactions with CD40L on platelets induces the secretion of the chemokines CCL2 and IL-8 (CXCL8) from endothelial cells, thereby generating chemotactic signals that recruit leukocytes (Henn *et al.* 1998). Additionally, activated platelets secrete IL-1β, a potent inflammatory cytokine (see Lindemann *et al.* 2007). Consequently, these cytokines are able to further activate endothelial expression of adhesion molecules ICAM-1, VCAM-1 and P-selectin (Lindemann *et al.* 2007). Therefore, platelets can activate, and be activated by, dysfunctional endothelium either directly or indirectly as a consequence of lipoprotein interactions (see figure 1.6).

In addition, there is evidence that both resting and activated platelets are capable of generating ROS. Due to their interactions with lipoproteins, this may augment oxLDL formation (See Seigel-Axel *et al.* 2008). Therefore, although most evidence indicates a fundamental role in endothelial activation and leukocyte adhesion, platelets may have multiple influences on atheroma development.

1.3.2.4   Additional leukocytes

As the early fatty streak develops, further cell types, such as mast cells, neutrophils, natural killer cells and rare reports of B cells appear in the plaques as they progress into the mature atherosclerotic state, although they remain relatively minor constituents and relatively poorly understood with regard to plaque development (Libby and Aikawa 2002). Each of these immune cells is capable of exacerbating the inflammatory environment through the balance of pro- and anti-infammatory mediators that regulate the magnitude of the inflammation in the lesion, though their specific contributions and interactions are not definitively established (See Packard *et al.* 2009 for review) (Figure 1.5).

1.3.3   Atherosclerotic plaque progression

The inflammatory events orchestrating the development and progression of atherosclerosis are tightly regulated by the balance between pro- and anti-inflammatory activities. These mechanisms originally arise to provide vascular protection, clearing the vessel wall of toxic lipids as well as healing the damaged endothelium, and many of the key immune events in early lesions function normally, with the objective of resolving the inflammation (Tabas 2009). Many cytokines and cells have both pro- and anti-inflammatory functions, depending upon the local inflammatory milieu.
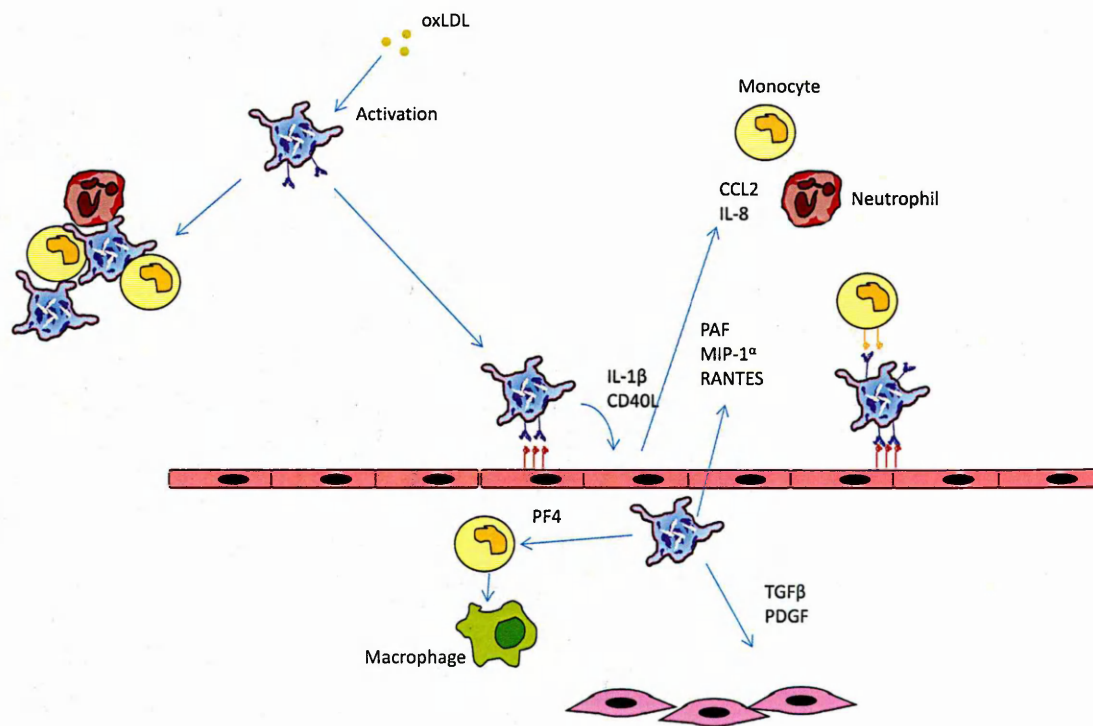
Figure 1.6; Platelet activation and adhesion to the endothelium. Platelets are influenced by circulating lipids which can promote hyperaggregation. Activated platelets adhere to the endothelium via tethering and rolling, initiated by P-selectin-PSGL-1 interactions. Tethering and adhesion increases the production of cytokines (IL-1β), chemokines (PAF, MIP-1, RANTES), additional adhesion molecules (CD40L) which ultimately promote platelet arrest and diapedesis. Consequently, these inflammatory mechanisms are able to further activate endothelial expression of adhesion molecules ICAM-1, VCAM-1 and P-selectin, and IL-8 and CCL2 secretion. This in turn attracts further leukocytes to the endothelium where they can bind attached platelets or directly to endothelial adhesion molecules (Lindemann *et al.* 2007). *PAF, platelet activating factor; TGFβ, transforming growth factor-β; PDGF, platelet derived growth factor; RANTES, regulated upon activation normal T cell expressed and secreted; MIP-1, macrophage inflammatory protein-1; PF4, platelet factor-4.*

When anti-inflammatory mechanisms are overwhelmed and atheroma formation continues, the vascular wall can remodel to compensate and reduce the detriment of growing inflammation. The continuous influx of cells into the arterial intima and the mediators secreted by activated leukocytes and vascular cells leads to changes in the structure of the vessel converting the early fatty streak into a more complex and advanced lesion. SMC proliferate and migrate from the tunica media producing strength-giving collagen which adds structural quality to the plaque by creating a fibrous cap over the lesion and decreases vulnerability to rupture (Figure 1.2b). This remodelling of the vascular wall, from leukocyte entry to SMC functioning, is thought to be directed by the activity of endogenous proteases, matrix metalloproteinases (MMPs), that are capable of degrading all components of the blood vessel wall (Ikeda and Shimada 2003) and are involved in physiological and pathological reorganisation of the vasculature (Galis *et al.* 2002). The human MMP family contains at least 23 members that are classified into subgroups (e.g. collagenases, gelatinases, stromelysins and others) based on their substrate specificity, although many MMPs have overlapping substrate specificities (Johnson 2007). MMPs are produced by vascular cells and macrophages as a result of stimulation by growth factors (epidermal growth factor (EGF), platelet-derived growth factor (PDGF) and basic fibroblast growth factor (bFGF)) (Dollery *et al.* 1995, George 2000), cytokines (IL-1, IL-6, TNF-α) (Galis *et al.* 1994b), contact with inflammatory cell ligands (such as CD40L) (Schonbeck *et al.* 1997) and oxLDL (Rajagopalan *et al.* 1996). Normal human arteries do not express active collagenases, yet macrophages in human plaque areas demonstrate expression of interstitial collagenases MMP-1 and gelatinases MMP-2 and -9 by immunohistochemistry (Galis *et al.* 1994a, Nikkari *et al.* 1995).

The close contact of VSMC with adjacent cells and their surrounding basement membrane are considered to inhibit proliferation (Johnson 2007). In atherosclerosis as MMPs free VSMC from these tight physical barriers via extracellular matrix (ECM) decomposition and proliferation signals are intensified in addition to the cells ability to traverse through the weakened basement membrane to remodel the vasculature. SMC migrate and proliferate in response to this ECM liberation and in response to chemokines down concentration gradients, to give strength to the expanding vascular wall through the formation of a fibrous cap over the lesion (Johnson 2007). In addition, the proteolytic activity of MMPs can release the active form of TGFβ from inactive complexes, thus promoting anti-inflammatory actions in addition to smooth muscle cell survival and collagen synthesis (Karsdal *et al.* 2002,

Maeda *et al.*2002, Yu *et al.* 2000). Studies on MMP knockout mice reveal that their role in atherosclerosis is complex as some MMPs support lesion growth and destabilisation while others suppress growth and promote lesion stability, partly due to their overlapping substrates and differential control of enzymatic activity by cytokines and growth factors (Johnson *et al.* 2005, Johnson *et al.* 2006). Therefore, the nature of MMP activity is influenced by the stage of lesion development and its associated inflammatory environment, as well as the vascular location (Johnson *et al.* 2006).

The proteolytic activity of MMPs is regulated by tissue inhibitors of metalloproteinases (TIMPs), which reversibly inhibit enzymatic activity by binding to the catalytic domain of the enzyme to form inactive complexes (Fassina *et al.* 2000). Four mammalian TIMPs (TIMP-1, -2, -3, and -4) have been characterised which can be synthesised by vascular cells and immune cells, often in conjunction with MMP production, thus maintaining the balance between matrix synthesis and degradation, under normal physiological conditions (Johnson 2007). Gene transcription of TIMP-1 and -3 can be upregulated by several growth factors and the cytokines IL-1 and TNFα (see Johnson 2007). Conversely, TIMP-2 is considered to be unregulated (Fassina *et al.* 2000), although TGFβ and TNFα have been shown to down-regulate TIMP-2 levels (Stetler-Stevenson *et al.* 1989). Thus inflammatory mediators involved in atherosclerosis can influence MMP activity and expression of their tissue inhibitors to influence the structure of the plaque.

Vascular remodelling can create stenosis, often with clinical complications of restricted blood flow. Although it is not considered fatal and is not necessarily related to negative CVD outcomes, luminal stenosis can further alter laminar blood flow, leading to the complications of oxidative stress and endothelial dysfunction, thus potentiating atherosclerosis (Kinlay *et al.* 2002). More recently it has been demonstrated that atherosclerotic arteries compensate by outward enlargement (diffuse atherosclerosis) to maintain lumen diameter, rather than as previously suggested by distension on the luminal side of the artery, which may obstruct the blood flow (focal atherosclerosis) (Galis and Khatri 2002). This 'positive remodelling', whereby lumen size is not affected by plaque growth due to the expansion of the external elastic membrane, often has no clinical symptoms. With this recent knowledge it has become apparent that relatively small plaques, identified by ultrasound, may only be the tip of the atherosclerotic 'iceburg' (Libby and Theroux 2005).

In addition to remodelling, prolonged exposure to pro-inflammatory cytokines along with increased lipids and an elevated oxidative status in plaque regions contribute to apoptosis of lesion cells including macrophages (Seimon and Tabas 2008), SMC (Stoneman and Bennett 2004) and endothelial cells (Choy et al. 2001). This increased cell death can result in the build up of a necrotic core within the plaque (Figure 1.2c). Increased cell death within the lesion, particularly of SMC, significantly weakens the plaque and consequently susceptibility to rupture is increased (Chandrasekar et al. 2006, Mallat et al. 2001c).

1.3.4 Plaque rupture

As the plaque develops and fatty streaks are converted to more advanced lesions, the inflammatory milieu alters and the immune response progresses leading to a change in the structure and vulnerability of the plaque due to continued leukocyte influx and retarded inflammatory cell egress.

Failure of macrophage egress leads to prolonged production of MMPs by foam cells in the lesion (Tabas et al. 2009). The activity of MMPs can evade normal control without alteration in regulatory TIMPs expression and can lead to detrimental vascular modifications resulting in excessive ECM destruction (Galis et al. 2002, Ikeda et al. 2003, Cho and Reidy 2002). This deprives VSMC from matrix-dependent and cell-cell and cell-matrix survival signals, leading to apoptosis and the formation of a necrotic core in the developing lesion (Ilic et al. 1998, Almeida et al. 2000). In addition, the processing of pro-TNFα to its active form from the surface of TNFα-expressing cells by numerous MMPs, may lead to apoptosis of neighbouring cells, as TNFα can act as a death ligand signal dependent upon coregulatory stimulation from other inflammatory pathways (see Johnson 2007 and Van Herreweghe et al. 2010).

The switch to a selective recruitment of Th1 cells represents an important point towards disruptive events destabilising the plaque, including increased cytokine-mediated cell death and decreased proliferation (Glaudemans et al. 2010). IFNγ strongly inhibits the production of interstitial collagens by VSMC (Amento et al. 1991). IFNγ can also inhibit the proliferation of SMC, thereby reducing the stability of the plaque (Hansson et al. 1989a). Through paracrine and autocrine mechanisms, TNFα can induce apoptosis of SMC (Boyle et al. 2003) and it is proposed that endothelial cell apoptosis might be a major determinant of plaque rupture (Durand et al. 2004). Thus, the aggressive inflammatory profile within vulnerable

plaque sites promotes increased breakdown and decreased synthesis of collagen, yielding a doubly negative consequence for plaque stability. Coupled with increased cell death, degradation of the protective structural components of the lesion results in plaque rupture and the exposure of thrombotic factors to reactive clotting agents in the blood. Thrombus ensues, with the potential to totally occlude the vessel with detrimental consequence (Figure 1.2d).

The most vulnerable plaques are those with low positive remodelling, increased concentration of inflammatory cells and relatively large necrotic core thickness (Bui 2009). The thinning of the fibrous cap renders the plaque susceptible to physical disruption. These lesions are often less advanced rapidly growing lesions with only a moderate stenosis. In fact, angiographic studies reveal that the majority of acute myocardial infarcts occur in vessels with stenosis of less than 70% (Falk *et al.* 1995), and a relatively small amount of stenosis in an artery, which may appear normal, may still give rise to acute fatal thrombosis (Libby 2001a). Thus, vascular remodelling may initially be protective and compensate for the inflammation at the plaque site, maintaining integrity of the blood vessel wall even when stenosis occurs. It is when this remodelling does not occur, is no longer effective, or has developed beyond protective-compensatory processes, that rupture or acute coronary consequences manifest. It may therefore be concluded that the quality rather than quantity of the plaque is paramount and stability has a greater importance for acute thrombotic pathologies.

Although not fully elucidated, it is clear that plaque composition is critical to future clinical events and that immunological mediators, namely cytokines, chemokines and adhesion molecules, orchestrate and define this composition through multiple functions. The presence of immune cells in the atherosclerotic plaque has been demonstrated as a major contributing factor for lesion progression at all stages of atheroma development through to plaque rupture (See Yilmaz *et al.* 2007). Therefore, mediators that promote leukocyte recruitment and accumulation at atherosclerotic lesion sites are central to all stages of disease progression.

1.4 Role of the monocyte chemoattractant CCL2 in atherosclerosis

CCL2 has been strongly linked with atherosclerosis as its target specificity makes it a key candidate for the signal that attracts monocytes to the activated artery wall in lesion development (Coll *et al.* 2007).

CCL2 is a low molecular weight C-C or β-chemokine that is secreted by endothelial cells (Rollins *et al.* 1990), SMC (Valente *et al.* 1988), monocyte/macrophages (Yoshimura *et al.* 1989a), and fibroblasts (Strieter *et al.* 1999b) in response to inflammatory stimuli. Pro-inflammatory cytokines IL-1β, TNFα, IFNγ and altered haemodynamic forces have been shown to induce endothelial CCL2 expression and secretion (Rollins *et al.* 1990, Sica *et al.* 1990, Shyy *et al.* 1994, Cybulsky and Gimbrone 1991, Gimbrone *et al.* 1997), and PDGF and IL-1β can induce CCL2 expression in VSMC (Taubman *et al.* 1992, Lim *et al.* 2009). Walch *et al.* (2006) demonstrated that IL-4 was capable of inducing the genes encoding CCL2 in the vascular endothelium, through *in vitro* experiments using HUVEC. Chen and colleagues (2004a) have demonstrated that TNFα enhances ROS-mediated CCL2 expression in human aortic endothelial cells (HAEC) and human dermal microvascular endothelial cells (HMEC). Additionally, oxLDL and oxVLDL induced significant increases in CCL2 mRNA and protein in aortic endothelial cells (Yu *et al.* 1998) and vascular endothelial and SMC exposed to minimally modified lipids express elevated levels of CCL2 in culture (Cushing *et al.* 1990). Rollins *et al.* (1990) have demonstrated that human vascular endothelial cells express little CCL2 under normal culture conditions, although this expression is markedly induced by pro-inflammatory cytokines. These data therefore suggest that CCL2 is upregulated in pro-atherogenic conditions.

1.4.1 CCR2

The actions of CCL2 are mediated through cell surface receptors and although it binds to CCR2, CCR1 and CCR9, signal transduction only appears to occur via CCR2 at physiological concentrations of the ligand (Charo *et al.* 1994, Nibbs *et al.* 1997, Neote *et al.* 1993). CCR2 is a 7 transmembrane-spanning GTP-binding protein-coupled receptor (Charo *et al.* 1994)

and exists in two highly homologous isoforms in humans, CCR2A and CCR2B (Wong *et al.* 1997).

CCR2 is expressed on circulating leukocytes, primarily monocytes but also basophils, NK cells, dendritic cells and certain subsets of T cells (Charo *et al.* 1994, Mackay 1996, Sozzani *et al.* 1997, Nieto *et al.* 1998, Ochensberger *et al.* 1999, Sica *et al.* 1997). The recruitment of monocytes and their migration to sites of inflammation may be regulated by a number of different signalling molecules, but CCL2 is considered the most important and appears to be responsible for their migration into the intima at sites of lesion formation in early atherosclerosis (Gu *et al.* 1998, Boring *et al.* 1998, Coll *et al.* 2007). Han *et al* (1998) demonstrated that THP-1 monocytes displayed chemotactic activity toward CCL2, with chemotactic activities increasing in correlation with CCR2 expression level. Similarly, Tangirala *et al.* (1997) showed decreased chemotactic activity of THP-1 monocytes following down-regulation of CCL2 gene expression. Weber *et al.* (1999) also reported that Mono Mac 6 cells migrated across a HUVEC layer towards CCL2, and that these monocytes demonstrated a 45% higher surface expression of CCR2 than non-migrating cells.

In addition to chemotaxis, CCL2-CCR2 binding promotes monocyte adhesion to the inflamed endothelium under conditions of physiological shear stress by increasing the activation of β2-integrin (Gerszten *et al.* 1999, Luscinskas *et al.* 2000, Maus *et al.* 2002). Similarly, CCL2 stimulation of CCR2$^+$ THP-1 and isolated human monocytes leads to an increased expression of CX$_3$CR1 protein on the cell surface and subsequently increased their adhesion to immobilised CX$_3$CL1 (Green *et al.* 2006).

In addition, experimental evidence from HUVEC indicates that endothelial cells are capable of CCR2 expression, although at lower levels than monocytes, responding to CCL2 through chemotaxis, which suggests a potential role in revascularisation and angiogenesis associated with advanced plaque development (Salcedo *et al.* 2000, Weber *et al.* 1999a). Furthermore, CCR2 has been identified on human VSMC where it may influence proliferation and migration associated with atherosclerotic vascular remodelling (Hayes *et al.* 1998, Viedt *et al.* 2002).

A finely tuned network of cytokines, chemokines and cell-cell communication regulates CCR2 expression in distinct cellular systems. Han *et al.* (1998) discovered that isolated human monocytes and THP-1 cells treated with oxLDL decreased their expression of CCR2

whereas native LDL induces rapid expression of CCR2 mRNA and protein. This suggests that CCL2 may primarily be involved in monocyte extravasation into the intima and only plays a minor role in subsequent events within the lesion where oxLDL would be at higher concentrations. However, Weber *et al.* (1999b) also noted that oxLDL counteracts a TNFα-induced down-regulation of CCR2 in monocytes and actually increases CCR2 mRNA and protein expression, contradictory to earlier findings, suggesting that the down-regulatory actions of cytokines may be modified by a pro-atherogenic milieu. The transformation of monocytes to a less CCL2-responsive state via down-regulation of CCR2 expression is regulated by certain pro-inflammatory cytokines such as TNFα (Rollins *et al.* 1990, Tangirala *et al.* 1997, Weber *et al.* 1999a). Therefore, any subsequent egress from the intima, as monocyte/macrophages traverse the endothelium from basal to apical direction, is considered to be regulated by chemokines or soluble factors other than CCL2, as CCR2 expression is reduced by the growing pro-inflammatory conditions in the lesion (Randolph *et al.* 1996).

1.4.2   Role of CCL2 in atherosclerosis

Experimental and clinical data provide evidence that CCL2 and CCR2 play a pivotal role in early stages of atherosclerosis.

1.4.2.1   Evidence from animal studies

There are numerous animal studies that implicate the involvement of CCL2 in atherosclerosis. Atherosclerosis-prone LDL receptor knockout mice deficient in CCL2 display 83% less lipid deposition throughout their aortas, with lesions of a reduced size and with less macrophage infiltration when compared to wildtype CCR2 genotype controls (Gu *et al.* 1998). Comparable results were observed in ApoE-/- mice genetically manipulated to be CCR2 deficient (Boring *et al.* 1998, Dawson *et al.* 1999)

Indeed, CCR2 knock-out mice display a phenotype similar to that of CCL2 deficient mice whereby significant defects in the recruitment of monocytes to sites of inflammation occur (Boring *et al.* 1997, Kurihara *et al.* 1997, Kuzeil *et al.* 1997). Furthermore, Gosling *et al.* (1999) showed that CCL2 deficiency reduced susceptibility to atherosclerosis in mice overexpressing apoB, the primary apolipoprotein in LDL. Furthermore, the overexpression of CCL2 in apoE deficient trangenic mice accelerates atherosclerosis by increasing the

number of macrophages in artery lesions (Aiello *et al.* 1999). In addition, blockade of CCL2-CCR2 interaction, through gene therapy, in atherosclerosis-prone mice was seen to inhibit the formation of fatty streak lesions and limit the progression of pre-existing plaques, without affecting serum lipid concentrations (see Coll *et al.* 2007). Although, Schecter *et al.* (2004) demonstrated CCL2 activation of SMC isolated from CCR2-/- animals, suggesting that a different receptor may be important in mediating some of the CCL2 effects.

1.4.2.2   *Evidence from clinical studies*

Evidence for the role of CCL2 in CVD is accumulating. CCL2 has been shown to be associated with acute coronary syndromes (Kervinen *et al.* 2004), subclinical atherosclerosis as measured by coronary risk factors (Deo *et al.* 2004), and obesity (Ohman and Eitzman 2009, Kim *et al.* 2006a). Additionally, CAD patients assessed for circulating CCL2 levels showed significantly higher concentrations than those of controls (Martinovic *et al.* 2005, Herder *et al.* 2006), and in CAD patients with the additional presence of PAD (Hoogeveen *et al.* 2005). Plasma CCL2 is elevated in patients after severe acute MI (Parissis *et al.* 2002, Kobusiak-Prokopowicz *et al.* 2007) and was positively associated with frequency of its occurrence (de Lemos *et al.* 20073). Higher CCL2 concentrations in the serum and/or plasma of HIV and renal insufficiency patients were associated with increased carotid IMT measures (Alonzo-Villaverde *et al.* 2004, Coll *et al.* 2006, Iwai *et al.* 2006, Pawlak *et al.* 2006). Furthermore, higher CCL2 values were seen in the serum of stroke patients compared to healthy controls (Arakelyan *et al.* 2005). These data on circulating CCL2 levels correlate with findings showing that CCL2 is upregulated in human atherosclerotic plaques (Nelken *et al.* 1991, Yla-Herttualla *et al.* 1991), a potentially more reliable measure of localised CCL2 activity.

In addition, peripheral blood mononuclear cells (PBMCs) from patients with CAD spontaneously secrete more CCL2 than PBMCs from healthy controls, and release greater amounts when stimulated with oxLDL (Breland *et al.* 2008, Oliveira *et al.* 2009). Okumoto *et al.* (2009) showed a positive correlation between CCR2 expression on circulating monocytes and serum CCL2 with carotid intima-media thickness and cardio-ankle vascular index, as measures of atherosclerotic indices, in chronic haemodialysis patients.

In contrast, a recent study failed to demonstrate a relationship between serum CCL2 and acute coronary syndrome outcomes in patients recovering from MI (Korybalska *et al.* 2010). A similar lack of correlation has also been documented between circulating CCL2 and

coronary heart disease (CHD) atherosclerotic burden assessed with the Framingham risk score (Mosedale et al. 2005), and for MI following a multivariate analysis of a large cohort from the Framingham study (McDermott et al. 2005).

These contrasting data reveal the difficulty of clinical studies and in the comparison of results from different investigations where different spectrums of the same disease are assessed. However, the majority of the evidence suggests a role for CCL2 in the progression of atherosclerosis. It is not yet clearly established whether it may be an independent risk factor for athero-development.

1.5 Role of the novel chemokine fractalkine in atherosclerosis

The importance of chemokines and adhesion molecules as the orchestrating inflammatory mediators in atherosclerosis has also led to a significant amount of focus on the novel chemokine, fractalkine (CX_3CL1). This is due to its proposed dual structure and function as both an adhesion molecule and chemoattractant.

Synthesised as a 50-70kDa precursor, CX_3CL1 is processed and glycosylated to a mature 100kDa species (Garton et al. 2001). The extracellular chemokine domain of CX_3CL1 comprises a novel arrangement of cysteine residues (CysXaaXaaXaaCys), classifying it as the only member of its chemokine subfamily (CX_3C) (Bazan et al. 1997). Extending from the CX_3C motif is a mucin-like stalk which acts as an efficient presentation molecule for the bio-effector chemokine domain situated on the distal end of the molecule (Imai et al. 1997). A transmembrane domain and an intracellular domain follow to anchor CX_3CL1 to the cell membrane (Figure 1.7). CX_3CL1 is expressed by vascular endothelial and SMC, with expression amplified by pro-inflammatory cytokines TNFα (Ahn et al. 2004, Ollivier et al. 2003, Lesnik et al. 2003), IFNγ (Bazan et al. 1997, Imaizumi et al. 2000, Ollivier et al. 2003, Lesnik et al. 2003), IL-1, IL-6 (Bazan et al. 1997, Garcia et al. 2000) as well as oxLDL (Barlic et al. 2007), whilst anti-inflammatory cytokines IL-4 and IL-13 inhibit CX_3CL1 expression (Fraticelli et al. 2001). In addition, CX_3CL1 expression has been detected in dendritic cells (Papadopoulos et al. 1999) and macrophages (Greaves and Gordon 2001), although to a lesser extent.

CXXXC

-24 1   77   318 337 373

■ Signal peptide
■ Chemokine domain
■ Mucin-like stalk
■ Transmembrane domain
■ Cytoplasmic domain
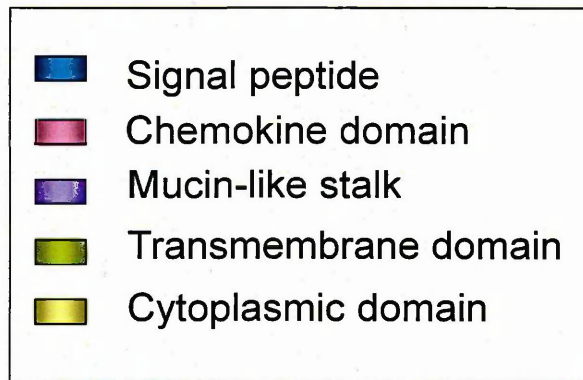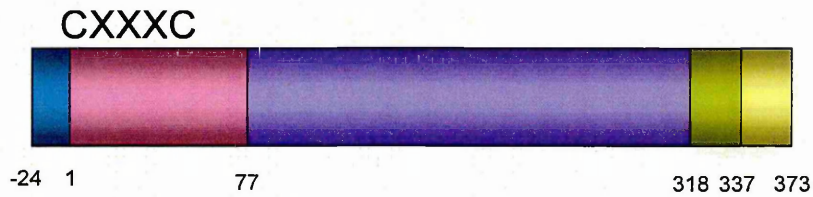
Figure 1.7; Schematic structure of CX₃CL1. CX₃CL1 is a large protein of 373 amino acids containing multiple domains and is structurally different from other chemokines. Beginning with the predicted signal peptide, it contains an N-terminal chemokine domain (residues 1-76) with the unique 3-residue insertion between cysteines (CX₃C), mucin-like stalk (residues 77-317), transmembrane domain (residues 318-336) and intracellular domain (residues 337-373). Adapted from Umehara *et al.* (2004)

The chemokine region of CX_3CL1 can be enzymatically cleaved from its membrane anchor to release the bio-effector domain as a soluble 85-95kDa fragment. This enables processes beyond the cell surface to occur and establishes a dual existence of CX_3CL1 as a cell-associated molecule and a shed protein. A Disintigrin and Metalloprotease-17 (ADAM-17) is a member of a family of multidomain, type I transmembrane proteins containing a zinc-dependent catalytic domain, a disintegrin domain, a transmembrane domain and a cytoplasmic tail (Tsou *et al.* 2001). ADAM-17 is synthesised as an inactive pro-form, or zymogen, that is cleaved intracellularly by the proteolytic enzyme furin, or a furin-type pro-protein convertase, to yield a mature active enzyme that is translocated to the membrane surface (Moss *et al.* 1997, Schlondorff *et al.* 2000). It is only this mature active form of ADAM-17 that is expressed on the cell surface (Doedens and Black 2000, Schlondorff *et al.* 2000) and its enzymatic activities act only on substrates expressed on the same cell (Itai *et al.* 2001). Rapid inducible cleavage of CX_3CL1 is considered to be via ADAM-17 (Garton *et al.* 2001, Hundhausen *et al.* 2003, Tsou *et al.* 2001). Previous studies have demonstrated that ADAM-17 mediates this inducible cleavage of CX_3CL1 following phorbol 12-myristate 13-acetate (PMA) stimulation, an effect that was not observed in cells isolated from ADAM-17 knockout mice or when MMP activity was blocked (Chapman *et al.* 2000b, Garton *et al.* 2001, Tsou *et al.* 2001). In cells deficient of ADAM-17, unstimulated CX_3CL1 cleavage remained, suggesting that an alternate protein was responsible for constitutive shedding (Tsou *et al.* 2001). Constitutive CX_3CL1 cleavage at proximal membrane regions is thought to be mediated by ADAM-10, which has high sequence homology to ADAM-17. Hundhausen *et al.* (2003) have reported an enhanced constitutive cleavage of CX_3CL1 in a primate fibroblast cell line (COS-7) overexpressing ADAM-10. Additionally, murine ADAM-10-deficient fibroblasts display markedly reduced constitutive cleavage of CX_3CL1 (Hundhausen *et al.* 2003). Inhibiting the activity of ADAM-10 in HUVEC and a human endothelial cell line, EVC304, led to an increased adhesion of a CX_3CR1-expressing murine pre-B cell line (Schwarz *et al.* 2010).

The catalytic activity of ADAM enzymes is regulated by endogenous TIMPs. TIMPs are a family of proteins made up of four structurally similar members, TIMP-1, -2, -3, and -4, which bind with varying affinity to MMPs and inhibit their activity via noncovalent interactions (Crocker *et al.* 2004, Gomis-Ruth *et al.* 1997). The expression of TIMPs has been shown to be down-regulated by pro-inflammatory cytokines TNFα and IL-1β in cardiac and endothelial cells, suggesting that the activity of ADAMs may be enhanced during

inflammation (Singh *et al.* 2005, Li *et al.* 2004, Bugno *et al.* 1999). TIMP-3 has been found to be the endogenous inhibitor of ADAM-17 (Amour *et al.* 1998). ADAM-10 activity has been shown, *in vitro*, to be inhibited by TIMP-1 and TIMP-3 (Amour *et al.* 2000).

Proteomic and functional investigations have recently revealed that MMP2 and cathepsin S are also capable of cleaving CX_3CL1 (Dean 2007, Clark *et al.* 2007). However, as broad spectrum metalloproteinase inhibitors are capable of blocking constitutive and inducible CX_3CL1 shedding (Chapman *et al.* 2000b, Garton *et al.* 2001, Hundhausen *et al.* 2003), the role of cathepsin S may be limited.

Remarkably, Schulte *et al.* (2007) illustrated further cleavage of CX_3CL1 after initial chemokine domain shedding, by ADAM proteases, although the function of the resulting liberated intracellular fragment was not determined. A potential role as an intracellular signal molecule was proposed, due to its comparable activity with the type-1 surface molecules Notch and E-cadherin (Reiss *et al.* 2006). However rapid enzymatic degradation may more likely occur in the cytoplasm.

In the basal state, approximately half of the CX_3CL1 is located on the membrane of endothelial cells and human embryonic kidney (HEK) cells, with the majority remaining in a separate punctuate juxtanuclear compartment (Liu *et al.* 2005, Hermand *et al.* 2008). The latter was suggested to act as an internal storage site for CX_3CL1, allowing recycling of the protein to the membrane upon pro-inflammatory stimuli or down-regulating surface expression via stimulation of endocytosis. This permits an additional level of functional regulation beyond transcription and translation, whereby the CX_3CL1 could be rapidly mobilised to increase surface expression upon stimulation. Huang *et al.* (2009) suggest that the endocytosis of CX_3CL1 is a protective mechanism against proteolytic cleavage from the plasma membrane by endogenous sheddases, since inhibition of this intracellular trafficking resulted in extensive cleavage and release of soluble chemokine. This idea is consistent with the cell surface expression pattern of active ADAM-17 and ADAM-10 (Doedens and Black 2000, Schlondorff *et al.* 2000). Taken together, these findings suggest that the equilibrium of CX_3CL1 between the membrane-bound molecule and its cleaved soluble form will greatly influence its function, either in adhesion or chemoattraction.

1.5.1 CX$_3$CR1

Unlike other chemokines, CX$_3$CL1 interacts exclusively with a single receptor and therefore cells expressing the CX$_3$CL1 receptor (CX$_3$CR1) are indisputably targets for CX$_3$CL1 (Imai *et al.* 1997, Bazan *et al.* 1997). CX$_3$CL1 exerts both its chemotactic and adhesive effects through the CX$_3$CL1 receptor (CX$_3$CR1) (Combadiere *et al.* 1998). As a seven transmembrane spanning structure, CX$_3$CR1 binds the signal peptide domain of CX$_3$CL1 with high affinity, activating intracellular pathways of inflammation and directly mediating cell adhesion, when the chemokine is anchored to the cell membrane, or cell migration, when the chemokine is shed (Imai *et al.* 1997).

CX$_3$CR1 expression has been demonstrated on many different cell types associated with atherosclerosis both *in vivo* and *in vitro*, including monocytes, macrophages, T cells, NK cells, dendritic cells, and vascular smooth muscle cells. CX$_3$CR1 activation leads to distinct functions within these cells dependent upon cell type, location and ligand position (e.g. cell-bound or shed) (Imai *et al.* 1997, Combadiere *et al.* 1998).

1.5.2 Functions of soluble CX$_3$CL1

Following its shedding from the cell surface, soluble CX$_3$CL1 is free to recruit cells expressing CX$_3$CR1, enabling them to migrate along concentration gradients to the site of inflammation, where they can exert their effects. Previous studies have demonstrated that soluble CX$_3$CL1 exhibits chemotactic activity for monocytes, NK cells, T-cells and dendritic cells expressing CX$_3$CR1 (Bazan *et al.* 1997, Guo *et al.* 2003).

Similar to other chemotactic factors, soluble CX$_3$CL1 can also adhere to glycosaminoglycans (GAGs) on the luminal surface of endothelial cells creating a stationary and localised chemoattractant gradient drawing leukocytes to inflammatory sites (Surmi *et al.* 2009). HEK293 cells transfected to express high concentrations of CX$_3$CR1 demonstrate chemotactic responses to soluble CX$_3$CL1, migrating across concentration gradients (Combadiere *et al.* 1998). Similarly, Imai *et al.* (1997) revealed the chemotactic activity of subsets of isolated lymphocytes (particularly CD4+) and, although to a lesser extent, monocytes in response to soluble CX$_3$CL1. Moreover, human monocyte-derived macrophages and murine bone marrow-derived macrophages displayed effective chemotaxis towards apoptotic CX$_3$CL1-secreting B cells in culture, with CX$_3$CR1 deficiency

reducing this migration (Truman *et al.* 2008). Almost all NK cells express CX_3CR1 and particular subsets demonstrate migratory responses to soluble CX_3CL1 and enhanced cytolytic function against target cells, contributing to the endothelial injury (Fong *et al.* 2000, Yoneda *et al.* 2000).

The expression of CX_3CR1, however, does not always determine the migratory activity of leukocytes to CX_3CL1, as only a percentage of the cell types identified with the receptor respond to soluble CX_3CL1 (Imai *et al.* 1997). CX_3CL1 acts as a potent chemoattractant for NK cells, T-cells and dendritic cells, but exerts a poor effect on monocyte migration *in vitro* (Vitale *et al.* 2004). Rather, the chemoattraction of monocytes is considered to be largely due to CCL2, with CX_3CL1 functioning primarily as an adhesion molecule (Umehara *et al.* 2001).

Chapman *et al.* (2000a) argued that CX_3CL1 cleavage from the cell membrane represents a terminating event to down-regulate the adhesive properties of the molecule rather than liberate a chemotactic molecule. This was supported by blocking the activity of ADAM-17 and ADAM-10 which led to increased adhesion, but blocked transmigration (Schwarz *et al.* 2010). In addition, soluble CX_3CL1 has been found to prevent the chemoattractant effects of CCL2 on monocyte trafficking (Vitale *et al.* 2004), block the adhesion of NK cells to the endothelium (see McDermott *et al.* 2001) and reduce the adhesive properties of CX_3CR1-expressing cells to the endothelium and aortic SMC *in vitro* by blocking the receptor (Imai *et al.* 1997, Chapman *et al.* 2000b, Ollivier *et al.* 2003).

In addition to CX_3CR1-dependent leukocyte recruitment, VSMC express the receptor and may also function through CX_3CL1 to influence lesion development. SMC CX_3CR1 expression is considered to be involved in vascular remodelling and a ligand-induced proliferation and migration in response to CX_3CL1 has been demonstrated (Perros *et al.* 2007, Lucas *et al.* 2003, Chandrasekar *et al.* 2003).

Thus, the cleavage of CX_3CL1 from the cell membrane plays a role in atherosclerosis acting on cells which express CX_3CR1. However, the mechanisms are not fully elucidated and may depend on other influencing factors at the site of atherogenesis.

1.5.3 Adhesive functions of CX₃CL1

Bazan and colleagues (1997) first demonstrated that monocytes and T cells which express CX_3CR1 adhere to monolayers of CX_3CL1-expressing HEK293 cells under static conditions in culture. THP-1 cells have also been shown to adhere to CX_3CL1-expressing ECV304 cells in culture (Hundhausen *et al.* 2003). This adhesive interaction of CX_3CL1-CX_3CR1 has been shown to be independent of additional cell-cell adhesion molecule contact. Transfected HEK293 cells expressing CX_3CR1 adhered to CX_3CL1-coated slides and endothelial cells under flow conditions, with no effect of inhibiting receptor intracellular signals and therefore upregulation of alternate adhesion molecules (Haskell *et al.* 1999). Also, K562 myelogenous leukaemia cells, which do not express selectins, adhered to immobilised CX_3CL1 under flow conditions (Fong *et al.* 1998).

Recently, Hermand *et al.* (2008) reported that clustering of CX_3CL1 on the cell membrane is essential for adhesive potency, similar to integrin adhesion requirements and comparable to PSGL-1 dimerisation (Wehrle-Haller and Imhof 2003, Snapp *et al.* 1998). This molecular aggregation is critically dependent upon the transmembrane domain of the protein.

Cell bound or soluble CX_3CL1 may also upregulate additional cell adhesion molecules, as G-protein coupled CX_3CR1 signalling has been demonstrated (Charo *et al.* 2004, Cambien *et al.* 2001, Thelen *et al.* 2001) and ligand-stimulation of CX_3CR1-expressing endothelial cells results in an upregulation of ICAM-1 (Yang *et al.* 2007). Furthermore, G-protein mediated mechanisms of CX_3CR1 enhance integrin binding avidity for its ligand and further facilitate adhesion and prolonged cell arrest at the endothelium, as well as activating cell signal cascades that facilitate diapedesis (Goda *et al.* 2000). In addition, cell adhesion is enhanced by co-immobilisation of CX_3CL1 with integrin ligands allowing for multiple concurrent binding interactions (Umehara *et al.* 2001).

Membrane-bound CX_3CL1 has been shown to enhance activation, degranulation and adhesive properties of platelets (Schafer *et al.* 2004). Platelets expressing CX_3CR1 accumulate at the inflamed endothelium as an essential mechanism of CX_3CL1-induced leukocyte adhesion under arterial shear conditions. This interaction leads to platelet activation and upregulation of P-selectin, further creating an inflammatory site capable of slowing and adhering leukocytes to the luminal surface of the vessel (Schulz *et al.* 2007). Pre-treatment of platelets from rats with CX_3CL1 heightened their adhesive properties,

increasing P-selectin surface expression and enhancing adhesion to collagen and fibrinogen (Schafer *et al.* 2004).

SMC expression of CX_3CL1 may serve to retain CX_3CR1+ leukocytes in the subendothelial space of arteries in a similar manner suggested for ICAM-1 and VCAM-1 (Doran *et al.* 2008). This allows the infiltration and anchoring of leukocytes beyond the endothelium and into smooth muscle layers of the vasculature, typical of vascular remodelling in plaque development.

1.5.4   Additional properties of CX_3CL1

In addition to the functions documented above, CX_3CL1 may have a number of other properties. CX_3CL1 has been demonstrated to have anti-apoptotic and proliferative effects on SMC (White *et al.* 2009, Perros *et al.* 2007). Both these mechanisms may contribute to the morphology of the atherosclerotic plaque, ultimately influencing stability and/or vulnerability to rupture. Therefore, CX_3CL1 appears to act beyond the recruitment of inflammatory cells at the endothelium. VSMC express CX_3CR1 in addition to CX_3CL1 production, allowing a potential self-regulatory signalling loop for the control of SMC function at sites of atherosclerosis.

CX_3CR1 is expressed on both CD8+ and CD4+ subsets of T lymphocytes and preferentially in Th1 compared to Th2 cells (Foussat *et al.* 2000, Fraticelli *et al.* 2001). As CX_3CL1 is induced in endothelial cells by cytokines produced by Th1 cells, such as IFNγ and TNFα, and Th1 cells express CX_3CR1, an amplifying inflammatory circuit exists to perpetuate pro-inflammatory cytokine and chemokine release in athero-development. Additionally, a dose-dependent differential regulation of cytokine secretion was observed in macrophages stimulated with CX_3CL1 (Mizutani *et al.* 2007).

Landsman *et al* (2009) suggest a role for CX_3CL1-CX_3CR1 interactions in the transmission of essential survival signals in monocytes and foam cells, preventing induced cell death and therefore maintaining the presence of activated immune cells continuing the pro-inflammatory milieu. Also, foam cell death in early disease stages has been shown to correlate with decreased atherogenesis (Tabas 2005). CX_3CL1-induced monocyte survival may also be potentially atheroprotective as macrophage apoptosis in late stages of

atherosclerosis contributes to the destabilising lipid-rich necrotic core within advanced plaques (Jaffer *et al.* 2006).

Taken together, this functional data supports a role for CX_3CL1 in the vascular inflammation associated with atherosclerosis, although the underlying mechanisms remain unclear.

1.5.5 Role of CX_3CL1 in atherosclerosis

Experimental and clinical data provide evidence that the novel chemokine CX_3CL1 and its receptor CX_3CR1 play an important role in the inflammation associated with early stages of atherosclerosis.

1.5.5.1 Evidence from animal studies

Compelling evidence for a role of CX_3CL1 in atherosclerosis has arisen from experimental animal models of atherosclerosis. Significant reductions in atherosclerotic lesion formation of high-cholesterol diet-fed apoE-/- mice, where the gene encoding CX_3CR1 was lacking (Lesnik *et al.* 2003). Similar results were reported by Combadiere *et al.* (2003). Teupser *et al.* (2004) found a reduction in brachiocephalic artery atherosclerosis in apoE-/- CX_3CL1-/- mice compared to controls, although no difference was apparent in aortic root lesions. In addition, when combined with CCR2 deficiency, CX_3CL1-/- apoE-/- mice displayed dramatically reduced macrophage accumulation in the artery wall and the subsequent development of atherosclerosis (Saedrup *et al.* 2007). These mechanisms may function through the proposed survival signal induction by CX_3CL1-CX_3CR1 interactions in foam cells, plaque macrophages and monocytes, a mechanism not observed in CX_3CR1 deficient mice (Landsman *et al.* 2009).

1.5.5.2 Evidence from clinical studies

Evidence for the role of CX_3CL1 in atherosclerosis, and its *in vivo* significance in plaque progression and clinical CVD consequences, has only recently become a focus of interest. Expressional, functional and epidemiological data has revealed a significant, yet undefined, role for CX_3CL1 and its receptor in atherosclerosis (Greaves and Gordon 2001, Fong *et al.* 1998, Harrison *et al.* 2001, McDermott *et al.* 2001, Moatti *et al.* 2001, Lesnik *et al.* 2003).

Clinical evidence for a role for CX_3CL1 in atherosclerosis is apparent from human genetic investigations of non-functional CX_3CL1-CX_3CR1 systems. Two naturally occurring single nucleotide polymorphisms have been detected in the region encoding the CX_3CR1, resulting in a dysfunctional receptor directly affecting ligand recognition and significantly decreasing CX_3CL1 binding capacity (Faure *et al*. 2000, Moatti *et al*. 2001, McDermott *et al*. 2003, Daoudi *et al*. 2004). The majority of data from these population-based retrospective studies identify an associated decreased risk of atherosclerosis when the mutated non-functional CX_3CR1 allele is present. The prevalence of CX_3CR1 polymorphisms was of a lower frequency in CAD patients diagnosed via angiography (Apostolakis *et al*. 2007a), and within similar patient cohorts, a mutated allele resulted in a protective effect on the occurrence of acute coronary events (Niessner *et al*. 2005, Moatti *et al*. 2001). These results were supported by a recent study in a Chinese population assessed for carotid atherosclerosis (Zhao *et al*. 2010). McDermott *et al*. (2001) also conclude that patients expressing a CX_3CR1 polymorphism have a reduced risk of atherosclerosis as a consequence of improved endothelial function, a finding that was independent of established CAD risk factors (McDermott *et al*. 2003, Hattori *et al*. 2005).

However, no replicable associations were observed between CX_3CR1 polymorphisms and carotid artery IMT (Debette *et al*. 2009), ischaemic cerebrovascular disease (Hattori *et al*. 2005), CAD (Niessner *et al*. 2005) and acute coronary syndrome (Apostolakis *et al*. 2007a, Niessner *et al*. 2005). These disparities may depend on the specific polymorphic mutation and subsequent receptor functioning, in addition to the distinct clinical manifestations of the CVD investigated. The exact functional effect of the mutated alleles is unclear (Apostolakis *et al*. 2009). Also, the power needed in particular investigations to predict negative correlation may reduce the sensitivity to detect subtle differences between disease and control groups. In addition, the concept of redundancy is well recognised in chemokine and chemokine receptor systems, therefore alternative chemokines or receptors may substitute for the mutation in particular situations, abrogating any decrease in inflammation (Umehara 2001).

Immunohistochemical studies demonstrate CX_3CL1 expression in human atherosclerotic coronary arteries but not in normal arteries, whereas its receptor, CX_3CR1, is expressed throughout the vessel (Wong *et al*. 2002a). Patel *et al*. (2008) also detected CX_3CR1+ cells in the abdominal aortas of patients with AAA where there was a thickening of the vessels.

Lucas and colleagues (2003) also demonstrated receptor and ligand presence in human coronary artery atherosclerotic plaques, with a positive correlation between the number of CX_3CL1-expressing cells and CX_3CR1+ cells in the lesion. In addition, high levels of CX_3CL1 mRNA have been observed in some human vessels with advanced atherosclerotic lesions, emphasising the upregulated expression of CX_3CL1 in atherogenesis (Wong *et al.* 2002a, Greaves and Gordon 2001).

Also, when comparing peripheral blood mononuclear cells (PBMC) of angiographically evaluated CAD patients with healthy counterparts, a higher number of CX_3CR1+ monocytic cells were observed (Apostolakis *et al.* 2009). This finding was similar to an earlier study in which isolated PBMC from patients with AAA demonstrated higher percentages of CX_3CR1+ NK cells and T cells (Patel *et al.* 2008). The fact that atherosclerotic patients express increased vascular CX_3CL1 and more CX_3CR1 on peripheral blood monocytes supports the proposed importance of CX_3CL1 in atherogenesis.

Thus, CX_3CL1 unequivocally has a role in inflammatory processes typical of atherosclerosis, yet to date it is still uncertain at what stage of pathogenesis this chemokine is involved and the mechanisms underlying its activation, its subsequent activity and clinical relevance all remain uncertain.

1.6 CCL2 and CX₃CL1 interactions

The complex array of chemokines involved in atherosclerosis have the potential to interact with each other through multiple mechanisms that influence disease progression. Therefore, the relationship between CCL2 and CX_3CL1, two of the major inflammatory mediators in athero-development, is considered.

Classical monocytes ($CCR2^+$ and CX_3CR1^{lo}) are dependent upon both CCR2 and CX_3CL1 for trafficking and entry into plaques, and combined inhibition of these pathways markedly reduced monocyte/macrophage accumulation in the atherosclerotic lesions of apoE knockout mice (Combadiere *et al.* 2008). The trafficking mechanisms of $CCR2^-$ CX_3CR1^{hi} monocytes are so far unknown.

Saedrup *et al.* (2007) provide evidence for CX_3CL1 in the direct recruitment and/or capture of CCR2-deficient monocytes, suggesting independent roles for CCR2 and CX_3CL1. Tacke *et*

al. (2007), however, demonstrated that CCR2⁻ CX_3CR1^{hi} monocytes enter plaques in a CCR2- and CX_3CR1-independent manner and instead use CCR5, albeit less efficiently and less frequently than classical monocyte trafficking. In addition, CCR2⁺ CX_3CR1^{lo} monocytes were also shown to express and utilise CCR5 for trafficking, suggesting that multiple chemokines act in concert to control the migration of specific leukocyte populations, though the extent to which each individually contributes *in vivo* remains elusive. The combined inhibition of CCL2, CX_3CR1 and CCR5 resulted in a 90% reduction in lesion size in atherosclerosis-prone mice (Combadiere *et al.* 2008). This reduction was associated with fewer circulating monocytes and this was considered to be at least partly due to a decrease in monocytosis from the bone marrow, and therefore a potential systemic anti-inflammatory effect upstream from plaque formation. Whether these receptors function independently, sequentially or synergistically remains to be fully understood.

The importance of CCL2 activity in CX_3CL1-mediated adhesion of PBMCs to the endothelium was supported by Green *et al.* (2006) who demonstrated that CCL2 upregulates CX_3CR1 expression by PBMCs and THP-1 monocytes via a CCR2-mediated p38 MAP kinase pathway, thus increasing adhesion to immobilised CX_3CL1. The authors suggested that *in vivo* CX_3CL1 and CCL2 act concurrently and sequentially and highlighted the possibility that CCL2 potentiates the functional inflammatory activities of CX_3CL1. CCL2 enhancement of monocyte adhesion to CX_3CL1 may act to retain monocytes in the vascular wall on activated SMC and different monocytes may thus be recruited to different locations (Barlic *et al.* 2006).

These data suggest a complex interplay between CCL2, CX_3CL1 and their receptors in the chemoattraction, adhesion and transendothelial migration of monocytes into the vasculature, which can be independent of classic adhesion cascades, but are often cooperative and complementary. Although the mechanisms are not completely elucidated, the expression of CCL2 and CX_3CL1 at sites of inflammation, such as atherosclerotic plaques, may differentially regulate the migration of monocyte subsets into the vascular wall. As monocytes/macrophages are considered the most abundant inflammatory cells in atherosclerotic lesions that participate in all stages of pathology, therapeutic mechanisms that target the disruption of their recruitment may be of clinical benefit.

1.7   Testosterone

Testosterone is the predominant sex hormone in males and is an anabolic steroid hormone belonging to the androgen group. Derived from cholesterol as its starting material, testosterone is synthesised from the precursatory substances dehydroepiandrosterone (DHEA) and androstenodione (see figure 1.8). This takes place primarily in Leydig cells in the testes of males, and to a lesser extent in the ovaries of females, with a small amount also produced in the adrenal glands (Rang *et al*. 1999). This process is regulated by the hypothalamic-adrenal-gonadal axis, with luteinizing hormone (LH) released from the pituitary following gonadotropin releasing hormone (GnRH) stimulation, stimulating the synthesis and release of testosterone from the testes (Rang *et al*. 1999). Most circulating testosterone is transported to target tissues via the circulation, either as free testosterone or bound to specific plasma proteins (sex hormone binding globulin (SHBG)) (68%) or weakly bound to albumin (30%). Only 1-2% of testosterone is free/unbound (Vermeulen and Verdonck 1968, Dunn *et al*. 1981), with SHBG holding much of the body's circulating testosterone inactive in the blood until target tissue activities lead to its release. The primary role of androgens is in the development of primary and secondary sexual characteristics, directing sexual differentiation, development and maintenance of the male phenotype (Silverthorn 1998).

Testosterone can act via four possible pathways (figure 1.9). The direct pathway involves the binding of testosterone to cytoplasmic androgen receptors (AR), following free diffusion across the target cell membrane. The AR is held in an inactive state in the cytoplasm by chaperone proteins, (heat shock proteins (HSP)) (Pratt and Toft 1997, Defranco 2000). Upon testosterone binding, ARs dissociate from their HSP and undergo a conformational change that results in tight homodimer formation with a neighbouring activated AR and the exposure of their nuclear targeting signal domains and DNA binding sites. This active homodimer traffics to the nucleus where it binds to specific androgen response elements (ARE) located in the DNA of target genes and acts directly as a transcription factor (see Liu *et al*. 2003 for review). The second pathway is termed the amplification pathway, due to the conversion of testosterone to its more potent metabolite dihydrotestosterone (DHT). Testosterone is converted to DHT in the cytoplasm by two enzymes, type 1 and type 2 5α-reductase (Rommerts 2004). DHT potentiates the effects of testosterone action as it binds
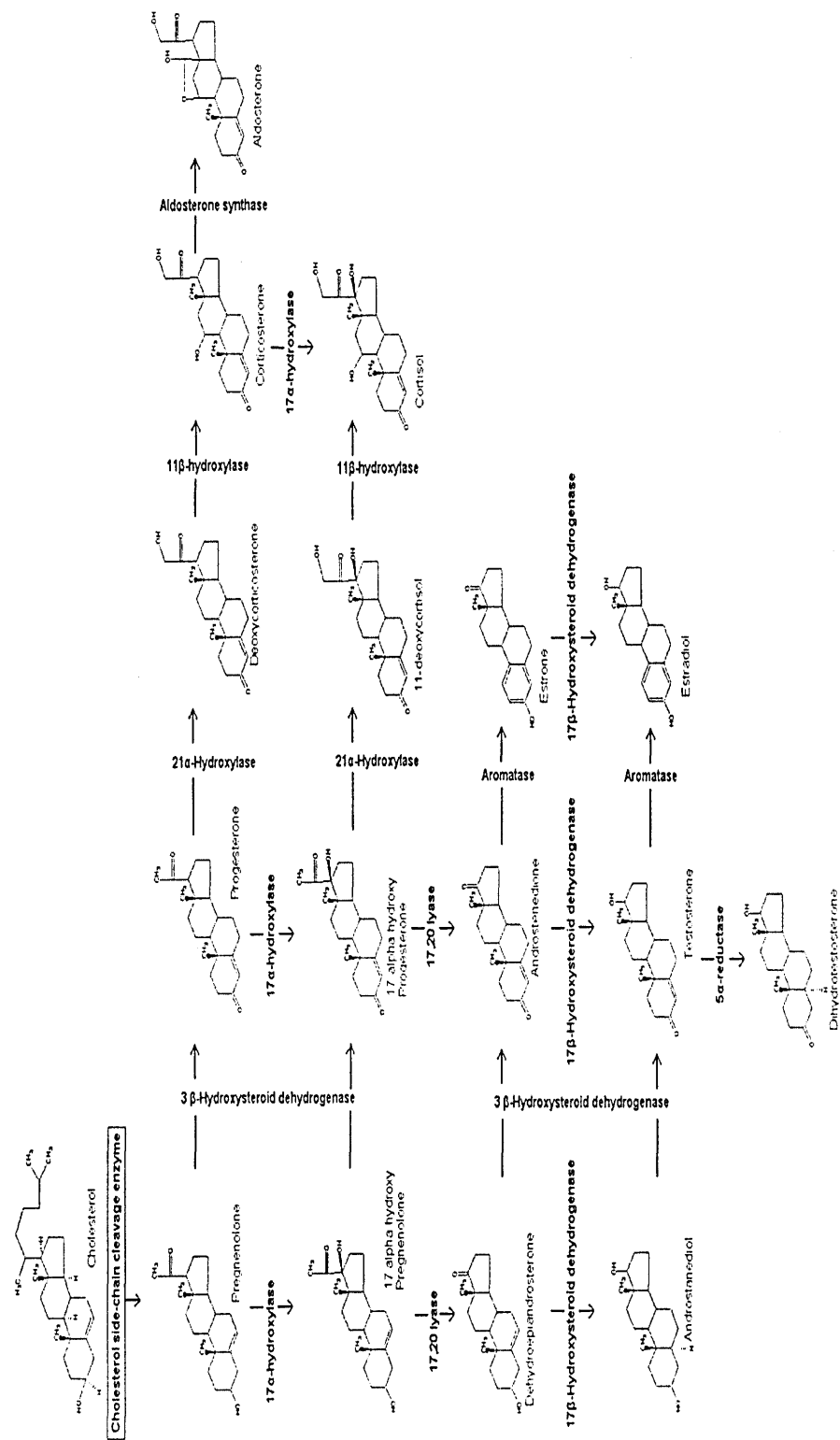
Figure 1.8; The steroidogenesis pathway. The steroidogenesis pathway for some of the major steroids such as glucocorticoids (cortisol), mineralocorticoids (aldosterone), progestins (progesterone), oestrogens (estrone, estradiol) and androgens (androstenedione, testosterone, dehydroepiandrosterone). Steroid hormones originate from cholesterol and are converted by a highly regulated and complex pathway of multiple enzymes which determine the end product. From http://commons.wikimedia.org/wiki/File:Steroidogenesis.gif

46
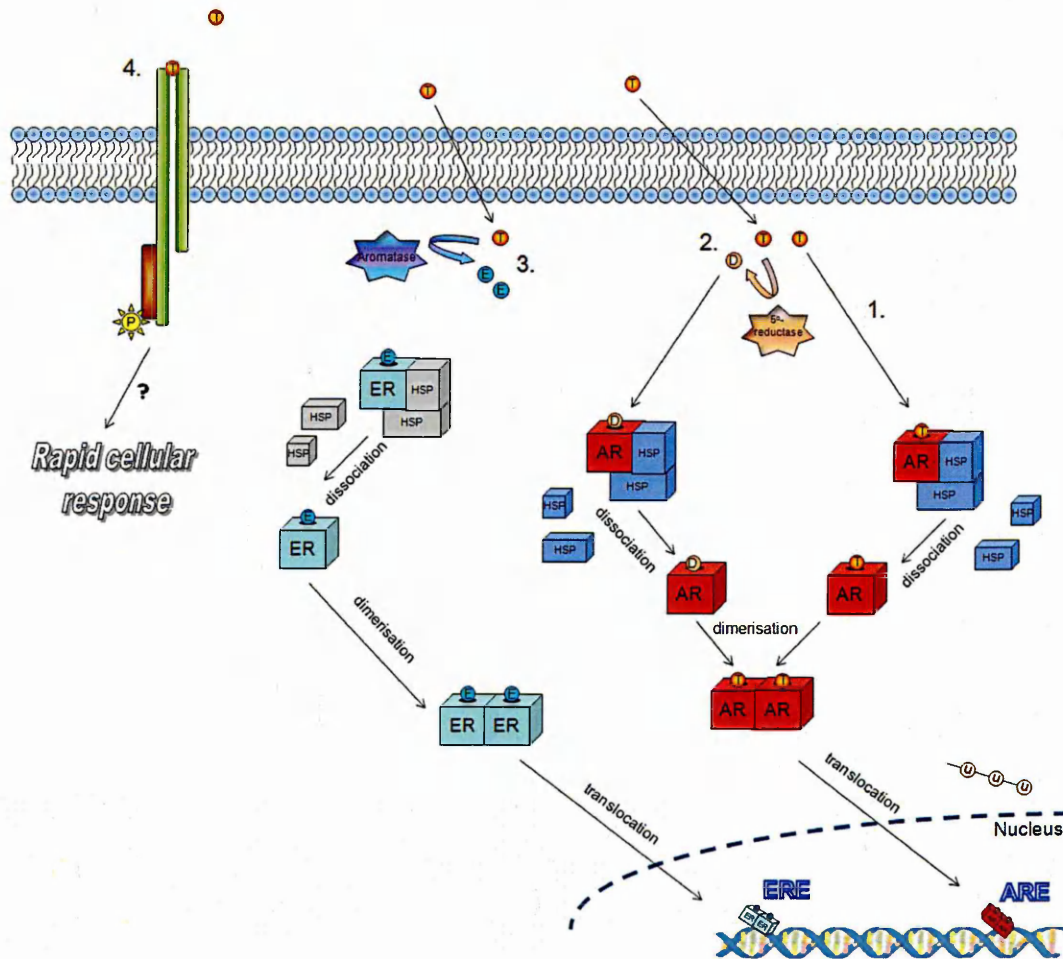
Figure 1.9; Testosterone signalling pathways. Testosterone (T) can freely diffuse across the target cell membrane 1) The direct pathway involves the binding of testosterone to cytoplasmic androgen receptors (AR). 2) The amplification pathway sees the conversion of testosterone to its more potent metabolite DHT (D) by 5α-reductase. The AR is held in an inactive state in the cytoplasm by heat shock proteins (HSP). Active AR homodimers traffic to the nucleus where they bind to androgen response elements (ARE). 3) The diversification pathway sees the conversion of testosterone to estradiol (E) by aromatase. Oestrogen binds to the oestrogen receptor (ER) which targets oestrogen response elements (ERE) in DNA. 4) Testosterone may also act via nongenomic pathways through the involvement of a hypothetical non-classical membrane-associated steroid receptor.

to the AR with higher affinity and has a slower dissociation rate from the receptor complex, amplifying the effects of testosterone more than two-fold. The third pathway of action is called the diversification pathway as testosterone is converted and acts upon oestrogen receptors, often producing different outcomes to those of the AR. Testosterone is converted to 17β-estradiol by the enzymatic activity of aromatase located in the cytoplasm of cells (Rommerts 2004).

In addition to these genomic pathways, there is evidence to suggest that a forth pathway exists whereby testosterone may also act via nongenomic mechanisms through the involvement of a hypothetical non-classical membrane-associated steroid receptor. These actions are mainly characterised by only a short delay of action and lack of susceptibility to inhibitors of transcription and protein synthesis (Heinlein and Chang 2002). Testosterone may exert these nongenomic effects in part by binding to a G-protein coupled receptor specific for the SHBG-testosterone complex, which, in turn, initiates a cAMP-mediated non-transcriptional pathway rapidly affecting intracellular calcium concentrations (Rosner *et al.* 1992, Benten *et al.* 1999). Calcium fluctuations are subsequently involved in the activation of intracellular signalling, ultimately influencing specific target proteins and cellular responses (Alberts *et al.* 1994).

1.7.1 Role of Androgens in CVD

Gender differences in mortality and morbidity relating to CVD have long been apparent, with men being more than twice as likely to suffer from coronary heart disease as women of a similar age (Lerner *et al.* 1986, Rayner *et al.* 1998), a fact that remains consistent across various ethnic and social groups (Malkin *et al.* 2003a). The differences in gender-related risk are thought to be associated with sex hormones (Malkin *et al.* 2003a). It was originally proposed that oestrogens have protective mechanisms in the development of atherosclerosis. This was supported by evidence that post-menopausal women demonstrate an increased risk of atherosclerosis, similar to that of age-related males, after a post-menopausal catch-up time of around 10 years when the female steroid declines (Malkin *et al.* 2003b). Further to this, androgens were considered to be detrimental to cardiovascular health, due to the adverse effects seen in cases of anabolic steroid over-use and abuse (See van Amsterdam *et al.* 2010 for review).

However, the marked gender difference observed in CVD risk is no longer thought to be due to testosterone or male gender *per se*. In fact it is more likely that low testosterone levels associated with aging and related comorbidities are directly linked with cardiovascular pathology and atherosclerosis. The age-related decline in testosterone observed in males is complex, surpassing a simple decrease in synthesis in the Leydig cells (Midzak *et al.* 2009). Stimulated to produce testosterone by luteinizing hormone, the Leydig cells in the testis may develop reduced responsiveness to this hormonal feedback circuit over time as a result of accumulatory intrinsic and extrinsic factors, not completely elucidated, resulting in lower circulating testosterone levels (For review see Midzak *et al.* 2009). It is becoming increasingly evident, however, that this age-related androgen decline is associated with emerging pathophysiologies of multiple diseases, in particular diseases of cardiovascular and metabolic consequence (Lunenfeld and Nieschlag 2007).

Several epidemiological studies have found a negative association between testosterone levels and CVD outcomes (Mäkinen *et al.* 2005, English *et al.* 2000c, Vikan *et al.* 2009). In the Rotterdam study, elderly men in the highest tertile of endogenous testosterone levels had a risk reduction of 60-80% of severe aortic atherosclerosis after adjusting for age and cardiovascular risk factors (Hak *et al.* 2002). Akishita *et al.* (2009) has recently replicated such findings in a Japanese population of 171 middle-aged men. Carotid IMT, as an indicator of general atherosclerosis, was also found to be associated with low total testosterone measures in large elderly male populations (Svartberg *et al.* 2006, Muller *et al.* 2004). This correlation was also shown in men with obesity and type 2 diabetes (De Pergola *et al.* 2003, Fukui *et al.* 2003). Another recent population-based study in a cohort of 1954 men advocated an association between low serum testosterone levels and increased mortality during a 7.2 year follow-up, after controlling for cardiovascular risk factors (Haring *et al.* 2010). This study did not adjust associations for age however, which may be indicative of testosterone levels and other compounding influences rather than a direct testosterone association. Male CAD patients have lower testosterone levels than men with normal coronary angiograms of the same age, although this correlation was with free and bioavailable testosterone but not total testosterone (English *et al.* 2000c). Furthermore, Pugh *et al.* (2000) reported that in a cohort of 831 male CAD patients, hypogonadism had a prevalence of greater than 20 percent. In contrast, two recent studies found no association between testosterone and abdominal aortic calcification as a measure of sub-clinical atherosclerosis, highlighting the complexity of potential endocrine influences on CVD

(Michos *et al.* 2008, Post *et al.* 2007). These investigations highlight that differences in reports may be attributed to the large divergence in study design, the array of associated risk factors used to adjust the results, differences in patient populations, and disparity in the vascular location of clinical measurement.

Androgen deprivation therapy (ADT), often used for the treatment of prostate cancer, has revealed further evidence for the protective role of testosterone in maintaining cardiovascular health. Men suffering from prostate cancer and receiving ADT experience shorter time to MI compared to age matched controls (D'Amico *et al.* 2007), express 20% higher risk of serious cardiovascular morbidity than similar men not receiving ADT (Saigal *et al.* 2007), and demonstrate increased risk of death from CVD (Keating *et al.* 2006, Tsai *et al.* 2007). A recent meta-analysis of studies over the last 20 years found an overall increase in risk for cardiovascular pathologies in male prostate cancer patients undergoing ADT, supporting the negative implications of low testosterone (Shahani *et al.* 2008).

It is also now becoming apparent that testosterone replacement can potentially improve cardiovascular symptoms and health outcomes dependent upon the physiological setting (See Jones and Saad 2009, Bain 2010 for review). The administration of testosterone has long since been shown to alleviate symptoms of angina in men and women (Lesser *et al.* 1946, English *et al.* 2000b), improve cardiac output (Pugh *et al.* 2003), and has been demonstrated to be useful for treating chronic heart failure (Malkin *et al.* 2006b, Pugh *et al.* 2004). TRT in hypogonadal men with ischaemic heart disease led to a delay in time to ischaemia and reduced cholesterol and TNFα levels (Malkin *et al.* 2004b), with male CAD patients demonstrating similar ischaemic improvements following TRT (Rosano *et al.* 1999, Webb *et al.* 1999). Additionally, a direct link has been made between long-term testosterone treatment and a significant reduction in carotid IMT as an indicator of vascular damage in overweight middle-aged men (Zitzmann *et al.* 2008).

Aromatase gene expression has been detected in the endothelium and smooth muscle of vascular tissue (Harada *et al.* 1999, Murakami *et al.* 2001) and the protective effects of testosterone have been suggested to be due to its localised conversion to estradiol by aromatase (Nathan *et al.* 2001). The presence of oestrogen receptors in vascular cells supports this notion, with expression in atherosclerotic vessels being reduced relative to normal arteries (Kim-Schulze *et al.* 1996). Additionally, both type 1 and type 2 5α-reductase

have been identified in vascular tissue suggesting a potential modulatory role of vascular tissues in the conversion of testosterone to DHT as a further potential mechanism of androgen action (Eicheler *et al.* 1994, Fujimoto *et al.* 1994).

The relationship between androgens and CVD risk factors is therefore now well established, with the general consensus that low testosterone bestows negative outcomes. Low testosterone has recently been regarded as an independent risk factor for CVD (Maggio *et al.* 2009). However, the underlying mechanisms by which testosterone exerts these observed cardiovascular benefits is complex and has not been completely delineated.

1.7.1.1   *Effects of androgens on lipids*

Androgens have extensive anabolic actions in many tissues and organs, and, of particular relevance, on lipid metabolism. Although not completely elucidated, testosterone has effects on circulating lipid profiles that may influence atherosclerotic risk (Jones and Saad 2009).

Many epidemiological studies have confirmed a direct correlation between obesity (more accurately visceral obesity) and CVD (Maison *et al.* 2001, Casaneuva *et al.* 2009, and See Després *et al.* 2009 for review) with the role of low testosterone as a concomitant factor (Goncharov *et al.* 2009, and see Stanworth *et al.* 2009 for review). Zumoff *et al.* (1990) found that free testosterone and non-SHBG-bound testosterone are decreased in obese men in proportion to the degree of obesity. More recently, decreased levels of total and free testosterone were associated with obesity in the Massachusetts Male Aging Study (Derby *et al.* 2006).

As previously mentioned (section 1.2.1.1), the balance of circulating lipids contributes to the risk of atherosclerosis, with a disruption of this balance associated with plaque development. Low levels of testosterone have been associated with an atherogenic lipoprotein profile, characterised by high LDL and triglyceride levels (Wu and von Eckardstein 2003), and a negative correlation between serum levels of testosterone and total and LDL-cholesterol has been observed in cross-sectional studies (Barrett-Conner *et al.* 1988, Barrett-Conner *et al.* 1992, Haffner *et al.* 1993, Simon *et al.* 1997, Barud *et al.* 2002). In contrast to this, Khaw *et al.* (2007) reported that LDL levels were increased in patients in the upper quartile of endogenous testosterone levels compared to the lower quartile. The

authors also reported a positive association of HDL with testosterone level, an observation demonstrated in other observational and cross-sectional studies (Simon *et al* 1997, van Pottelbergh *et al*. 2003). A few cross-sectional studies, however, have found no association between serum lipid measurements and endogenous testosterone (Kiel *et al*. 1989, Denti *et al*. 2000).

Patients undergoing ADT demonstrate increased total cholesterol and LDL cholesterol (Dockery *et al*. 2003, Nishiyama *et al*. 2005, Braga-basaria *et al*. 2006, Yannucci *et al*. 2006, Smith *et al*. 2008), elevated triglycerides and reduced HDL cholesterol (Haffner *et al*. 1993), or all of these indicators of atherogenic lipid profiles (Haidar *et al*. 2007) when compared to baseline or controls.

In contrast, the majority of data from studies investigating TRT in hypogonadal and eugonadal men show improvements in lipid and lipoprotein profiles (Table 1.2). However, discrepancies and conflicts in the data indicate the complexity of the relationships and underlying interactions. The dose of androgen administration may play a central role in the efficacy of cardiovascular benefits. Specifically, supraphysiologiccal doses of exogenous androgen administered to healthy eugonadal men generally results in significant reductions in HDL and elevations in LDL (Hurley *et al*. 1984, Thompson *et al*. 1989, Bhasin *et al*. 1996, Singh *et al*. 2003). Alternatively, physiological replacement in men with low endogenous testosterone yields favourable, or neutral, lipid profiles. Differences in study design, doses and formulations of androgens used, route of administration, duration of treatment and follow-up, and/or methods of analysis may explain the variability in the results.

Dyslipidaemia, altered body fat distribution to visceral areas and resulting obesity can, in turn, also influence androgen levels, making it difficult to invoke a cause-and-effect relationship between low levels of testosterone and negative metabolic outcomes. For instance, it has been demonstrated that adipose tissue exhibits high concentrations of aromatase capable of converting testosterone to estradiol, not only reducing bioavailable testosterone, but also shifting the androgen-oestrogen balance in males (Hammoud *et al*. 2006). An increased conversion of androstenedione to oestrone by aromatase in body fat and muscle supports this (Schneider *et al*. 1979). To further exacerbate this sex hormone imbalance, an oestrogen-mediated reduction in luteinizing hormone represses stimulation

Authors	Patients (age)	Test substance (dose)	Triglycerides	Total Cholesterol	LDL-C	HDL-C
Agledahl et al 2008	26 hypogonadal men	TE (100mg i.m./week for 12 months)	↔	↔	↔	↔
Allan et al. 2008	60 healthy but symptomatic of androgen deficiency (≥75 years)	TT (5mg/day for 52 weeks)	↔	↔	↔	↔
Bagatell et al. 1994	19 eugonadal men ()	TE (200mg i.m./week for 20 weeks)	↔	↓	↔	↓*
Dobs et al. 2001	29 hypogonadal men (21-65)	TT (1 year following prior treatment with TE)	↑*	↓NS	↓NS	↓*
Emmelot-Vonk et al. 2008	237 low normal testosterone levels (60-80 years)	TU (160mg oral/day for 6 months)	↔	↓*	↔	↓*
Howell et al. 2001	35 hypogonadal men (40.9 mean age)	TT (2.5-5mg/day for 12 months)	↔	↔	↓*	↔
Kapoor et al. 2006	24 hypogonadal men with type 2 diabetes (>30 years)	TES (200mg i.m./2 weeks for 3 months)	↔	↓NS	↔	↔
Ly et al. 2001	18 hypogonadal men (≥60 years)	DHT (70mg/day transdermal for 3 months)	↔	↓*	↓*	↔
Malkin et al. 2004	27 hypogonadal men (26-78)	TES (100mg i.m./2 weeks for 1 month)	↓*	↓*	↓*	↔
Malkin et al. 2004	10 hypogonadal men with ischaemic heart disease (60 mean age)	TES (100mg i.m./2 weeks for 1 month)	↔	↓*	↔	↔
Page et al. 2005	70 hypogonadal men (71 mean age)	TES (200mg i.m./2 weeks for 3 years)	↓*	↓*	↓*	↓NS
Saad et al. 2007	Men with sexual dysfunction and metabolic syndrome (54-76)	TU (1000mg i.m. at weeks 0 and 6 and thereafter every 12 weeks for 12 months)	ND	↔	↔	↑
Saad et al. 2008	27 male late onset hypogonadism (60 mean age)	TT (50mg/day for 9 months)	↓*	↓*	↓*	↑*
Saad et al 2008	28 male late onset hypogonadism (61 mean age)	TU (1000mg i.m. at weeks 0 and 6 and thereafter every 12 weeks for 9 months)	↓*	↓*	↓*	↓*
Tenover 1992	13 aged men (57-76 years)	TE (100mg i.m./week for 3 months)	ND	↓	↓	↓
Thompson et al 1989	11 eugonadal men (ND)	TE (200mg i.m./week for 6 weeks)	ND	ND	↓	ND
Tripathy et al. 1998	10 hypogonadal men (ND)	'testosterone replacement therapy'	↔	↓*	↓*	↔
Uyanik et al. 1997	37 eugonadal men (53-89)	TU (120mg oral/day for 2 months)	↔	↓*	↓*	↔
Zgliczynski et al 1996	22 hypogonadal men (18-77)	TE (200mg i.m./2 weeks for 12 months)	↔	↓*	↓*	↔
Zitzmann and Nieschlag 2007	66 hypogonadal men (38 mean age)	TU (1000mg i.m. at weeks 0 and 6 and thereafter every 12 weeks for 44 weeks)	ND	ND	↓*	↑*

Table 1.2: Summary of studies investigating the relationship between testosterone replacement therapy and plasma lipid parameters. **Arrows indicate change in measurement:** ↑(increase), ↓(decrease), ↔(no change); NS, non-significant change; ND, not determined; i.m., intramuscular injection; TE, testosterone enthanoate; TU, testosterone undecanoate; TT, transdermal testosterone; TES, testosterone esters; DHT, dihydrotestosterone. Adapted from Traish *et al.* (2009), Jones and Saad (2009).

53

of the testis to produce testosterone (Vermeulen *et al.* 1993). In addition, adipose tissue has been shown to express several steroidogenic and steroid-inactivating enzymes (Blouin *et al.* 2008). This circular relationship further demonstrates a link between lipids, testosterone and atherosclerosis, although the causality of the relationship is not yet known and cannot be unravelled by epidemiological studies.

Therefore, it may be concluded that androgen deficiency is associated with negative lipid profiles and that this detrimental alteration can be somewhat ameliorated by replacing testosterone to physiological levels in men.

1.7.1.2   *Effects of Androgens on vascular function*

The AR is expressed ubiquitously in cells of the vasculature. Testosterone exhibits direct vasodilatory effects on vascular smooth muscle (Jones *et al.* 2003) with the mechanism of action thought to be androgen receptor-independent via calcium channel blockade and/or potassium channel opening (Ding and Stallone 2001, Jones *et al.* 2003), or increased release of endothelium-derived NO (See Miller and Mulvagh 2007). This is supported by the fact that acute vasodilatory actions of testosterone in rat coronary arteries and thoracic aortae of mice were not abolished by the androgen receptor blocker flutamide, suggesting a non-classical AR-mediated mechanism (Jones *et al.* 2004, Channer and Jones 2003). The maintenance of vascular tone is important in atheroprotection, where reduced vasodilatory responses and enhanced vasoconstriction further restrict haemodynamic flow through atherosclerotic vessels with stenosis, exacerbating clinical symptoms and perpetuating atherogenesis through vascular dysfunction. As previously described (section 1.2.1.2), dysfunctional vascular reactivity that influences vessel shear stress, can significantly alter metabolic processes in cells of the vessel wall leading to elevated oxidative status. Testosterone may, therefore, alleviate haemodynamic symptoms of atherosclerosis and improve atherosclerotic outcomes associated with disturbed flow patterns.

Recent evidence showed that low levels of testosterone are related to increased oxidative stress and a reduced antioxidant capacity in men, potentially as a mechanism of disturbed flow due to loss of vascular reactivity, and that TRT was capable of reversing this status (Mancini *et al.* 2008). The negative correlation between testosterone and hypertension has also been demonstrated (Barrett-connor *et al.* 1988, Phillips *et al.* 1993, Simon *et al.* 1997,). This is further supported by the evidence that patients with prostate cancer undergoing

ADT experience arterial stiffness, as measured by pulse-wave analysis in the radial artery (Smith *et al.* 2001).

The vascular system is a target for direct androgen action and beneficial effects of TRT on symptoms of angina (Maggio *et al.* 2009), blood pressure (Khaw *et al.* 1988), and erectile dysfunction (Corona *et al.* 2008a) may be due to vasodilatory actions of testosterone. Men with CHD show enhanced vasoreactivity following testosterone treatment (Webb *et al.* 1999, Kang *et al.* 2002). Low testosterone levels in men are associated with erectile dysfunction possibly as a result of impaired penile blood flow due to diminished vasoreactivity (Yassin *et al.* 2008, Corona *et al.* 2009) and it is suggested that erectile dysfunction and atherosclerosis are often closely related pathologies. In concordance with this, testosterone has been reported to display both acute and chronic vasodilatory effects upon various vascular beds (Manolakou *et al.* 2009), and testosterone improves cardiac output in patients with angina after exercise (Jaffe 1977) and myocardial ischemia in CAD patients (Webb *et al.* 1999, Rosano *et al.* 1999). Both chronic exposure to physiological testosterone therapy (Kang *et al.* 2002) and acute exposure to supraphysiological doses of testosterone (Ong *et al.* 2000) are reported to increase flow-mediated brachial artery vasodilation, and occurs as a result of increased NO release from the endothelium in responses to changes in shear stress in men with CAD.

However, studies regarding the vasoreactive effects of testosterone are contradictory, with several reports assigning vasoconstrictive properties to testosterone. These actions have been proposed to be mediated via direct ion channel inhibition or activation, or indirectly by stimulating various vasoconstriction pathways (Kumai *et al.* 1995, Reckelhoff *et al.* 2000) or inhibiting other vasodilators (Masuda *et al.* 1991, Ceballos *et al.* 1999) from studies performed in rats. Kienitz and Quinkler (2008) attribute these discordant findings to the mode of administration of androgens, suggesting that a decrease in vascular tone seems to follow acute exposure to supraphysiological doses, whereas the long-term net effect of physiological androgens appears to be vasoconstrictive, with some dependence on prior exposure, or pre-treatment, of the vascular cells. The importance of age, as a factor leading to diminished vasoreactivity is also emphasised, although is not thought to be mediated through a decline in endothelial or VSMC function (English *et al.* 2000a).

1.7.1.3 Effects of Androgens on inflammation

With the reported benefits of testosterone in CVD and the inflammatory nature of atherosclerosis, several clinical studies investigating the association between androgen levels and immune function/inflammation have emerged.

1.7.1.3.1 Effects of androgens on cytokines

The potential benefit of testosterone in reducing inflammatory cytokines has been demonstrated in several observational clinical studies. It has been suggested that plasma cytokine levels correlate negatively with androgen levels in men (Yesilova *et al.* 2000) and women (Christodoulakos *et al.* 2007). Yang *et al.* (2005) confirmed a significant inverse correlation between serum testosterone levels and IL-6, sICAM-1 and C-reactive protein (CRP, a non-specific acute-phase reactant and marker of inflammation). Indeed, elderly hypogonadal men also exhibit raised serum levels of TNFα and IL-6 (Khosla *et al.* 2002). An inverse relationship was seen between serum IL-1β and endogenous testosterone in CAD patients, with the increase in IL-1β significantly related to disease severity in a stepwise manner (Pugh *et al.* 2003, Nettleship *et al.* 2007b). No association was observed for TNFα, IL-6 and IL-10, although IL-10 was implicated in disease progression. Such observations suggest that the underlying testosterone status may modulate cytokine production in men with CAD.

TRT studies have further implicated immunomodulatory actions of androgens in hypogonadal men with cardiovascular symptoms, showing a significant reduction in TNFα and an elevation of circulating anti-inflammatory IL-10 (Malkin *et al.* 2004a, Malkin *et al.* 2004b). Additionally, PBMC isolated from androgen deficient men with type II diabetes showed a reduction or complete abrogation of *ex vivo* IL-6, IL-1β and TNFα production when treated with testosterone (Corrales *et al.* 2006). Testosterone also inhibits the production of proinflammatory cytokines such as IL-6, IL-1β and TNF-α in a range of cell types including human endothelial cells (Hatakeyama *et al.* 2002) and human monocytes (Kanda *et al.* 1996) and testosterone can stimulate the production of anti-inflammatory cytokines such as IL-10 from lymphocytes (Liva and Voskuhl 2001).

Testosterone may influence circulating cytokine profiles and consequential inflammation indirectly through its proposed action on lipids, as adipose tissue is considered to act as an endocrine organ secreting numerous inflammatory factors (see Traish *et al.* 2009). As

androgens play a critical role in regulating body fat distribution via mechanisms influencing adipogenesis, fatty acid synthesis and lipolysis (Blouin *et al.* 2005, Blouin *et al.* 2008), the shift towards increased visceral obesity, and therefore increased adipose tissue body content, seen with aging, may result from this age related testosterone decline in men. This, in turn, may increase inflammatory reactivity through adipose cytokine secretion and the promotion of favourable conditions for the development of atherosclerosis, diabetes, and metabolic syndrome. TNFα is expressed by adipocytes and stromovascular cells within adipose tissue (Fain *et al.* 2004), although this may result in localised effects rather than systemic inflammatory actions as circulating levels are low and TNFα receptors are expressed by adipocytes (Ruan and Lodish 2003). Additionally, IL-6 and IL-6 receptors are expressed in adipocytes and adipose tissue matrix (Fain *et al.* 2004), with high levels detectable in the circulation allowing for a potential systemic inflammatory influence. In fact, plasma IL-6 concentrations are considered to predict diabetes and CVD (Fernandez-Real *et al.* 2003).

In addition, atherogenic circulating lipids contribute to oxidative stress and endothelial dysfunction, promoting increased local cytokines, chemokines and adhesion molecules indicative of early inflammatory atherogenesis. By influencing lipid metabolism, testosterone may indirectly ameliorate vascular inflammation through local and systemic cytokine modulation. Furthermore, the antioxidant properties of testosterone are thought to be due to its conversion to oestrogen by aromatase and its ability to increase the activity of antioxidant enzymes (such as SOD) in the vascular wall, although the exact mechanisms remain unknown (Massafra *et al.* 2000).

1.7.1.3.2   Effects of androgens on leukocytes

Anti-inflammatory mechanisms of androgens have been long recognised with the majority of the evidence suggesting that their actions are mediated, at least in part, by a suppressive effect on pro-inflammatory cytokine activation and corresponding up-regulation of anti-inflammatory cytokines (Pugh et al. 2002).To a lesser extent and only more recently, androgenic effects on immune cell behaviour are becoming apparent with particular reference to the predominant plaque leukocytes, macrophages and T cells.

Corcoran and colleagues (2010) have recently shown that both physiological and supraphysiological concentrations of testosterone reduced the expression and secretion of

TNFα and IL-1β in monocyte-derived macrophages obtained from a CHD age-relevant population. No effects were observed on IL-6 and CRP expression. In addition, androgen deprivation increases T cell levels and enhances stimulatory proliferative response suggesting that testosterone may have a suppressive effect on T cell inflammatory response and therefore reduce the prominent Th1 cytokines relevant to plaque development (Roden et al. 2004). Moreover, isolated mouse CD4+ T cells increased anti-inflammatory IL-10 production following treatment with DHT (Liva and Voskuhl. 2001). In contrast, through the study of AR knockout mice (ARKO), Lai et al. (2009) demonstrated that signalling through the AR enhanced TNFα and CCR2 expression in isolated macrophages. This elevated inflammatory response, however, was related to cutaneous wound healing and may be a condition and tissue specific response.

The accumulation of cholesterol in macrophages and the subsequent formation of foam cells as a prominent early feature of fatty streak formation is influenced by androgens. A recent report by Qui and colleagues (2010) demonstrated that DHT significantly reduced high-cholesterol diet-induced foam cell formation in the proximal descending aorta of male New Zealand white rabbits. This was accompanied by a decreased expression of lectin-like oxLDL receptor-1 (LOX-1) in these cells. The same group also showed that in cultured macrophages the induction of foam cell formation by oxLDL was inhibited by DHT, an effect that was only observed in macrophages isolated from male wild-type mice but not in male AR-null mice (Qui et al. 2010). Primary human monocyte-derived macrophages treated with testosterone displayed a dose-dependent upregulation of SR-BI (Langer at al. 2002). Due to the SR-BI role in association of ApoA containing lipid molecules, primarily HDL, to the macrophage membrane and assists in the transfer of cholesterol to the lipoprotein molecule, upregulation of SR-BI consequently, increased cholesterol efflux (Langer at al. 2002). Similarly, Orekhov et al. (2009) demonstrated that DHT inhibited cholesterol accumulation in both male and female primary cultured monocyte-derived macrophages and suggested the mechanism was via stimulation of cholesterol efflux rather than inhibition of LDL uptake, although SR-BI was not investigated.

In summary, it is clear that androgens modulate vessel wall function and that a loss of vasoreactivity may result in negative vascular changes and endothelial damage, precursory and contributory to the inflammatory development of atherosclerotic lesion formation. Specific actions of testosterone on inflammation as a key factor of athero-development are

apparent yet complex and not completely understood. Further investigations are required to explian the nature and underlying mechanisms of this influence on immunomodulation and its potential actions on atherogenesis.

1.1.8 Hypothesis and aims of this thesis

The overall aim of the study was to investigate the inflammatory response seen in early atherosclerosis to address the hypothesis that testosterone has beneficial effects on atherosclerosis through anti-inflammatory actions. In particular, determining the effect of testosterone on two key immunological mediators implicated in atherosclerosis, CCL2 and CX_3CL1, and investigating the role of the androgen receptor in potential testosterone-mediated effects.

A combined *in vitro* and *in vivo* approach was taken with the following objectives:

- To optimise a cell culture model of CX_3CL1 and CCL2 pro-inflammatory vascular upregulation, and determine the effects of testosterone on the modulation of these inflammatory mediators.
    - To investigate the role of the AR in *in vitro* vascular cell inflammation

- To determine the role of TRT on fatty streak formation in an animal model of low testosterone and diet-induced atherosclerosis.
    - To investigate the role of the AR in lipid streak development and atherosclerotic risk factors and inflammatory mediators

CHAPTER 2

In vitro investigation of the role of testosterone on pro-inflammatory chemokine upregulation in aortic vascular cells

2.1 Introduction

The inflammatory process of leukocyte migration into the vascular wall of arteries in the development of atherosclerotic lesions directly involves endothelial and smooth muscle cells. These vascular cells are both the source and the target of many of the inflammatory mediators whose concerted activities orchestrate the pathology of the disease.

2.1.1 Cytokine regulation of inflammatory mediators

The recruited cells in vascular inflammation at atherosclerotic sites are predominantly monocyte/macrophages and T cells, which initiate and co-ordinate early inflammatory events through the release of multiple cytokines. Two of the major cytokines secreted by activated T cells and macrophages are TNFα and IFNγ, which have been repeatedly implicated in atherosclerosis (Hansson *et al.* 1989b, Barath *et al.* 1990, Rus *et al* 1991, Tipping and Hancock 1993, Ridker *et al.* 2000a, 2005, Skoog *et al.* 2002). In addition, these cytokines have been shown to alter endothelial permeability to favour leukocyte transmigration (Wojciak-Stothard *et al.* 1998). Therefore, TNFα and IFNγ have pivotal roles in promoting the atherosclerotic process. Mice lacking TNFα have been shown to have reduced atherosclerosis (Branen *et al.* 2004;), and mice deficient in IFNγ or its receptor also demonstrate retarded atheroma formation (Gupta *et al.* 1997, Buono *et al.* 2003).

2.1.1.1   TNFα

The pro-inflammatory cytokine TNFα is secreted by activated and lipid-laden macrophages and exists in two forms; a transmembrane protein and a mature soluble protein (Packard *et al.* 2009). Cleaved from the cell membrane by ADAM-17, TNFα signals through either of its two receptors (TNFR1, TNFR2) to mediate numerous inflammatory processes depending on the cell

type and stimuli. TNF binding to its receptor (TNFR) recruits associated proteins; TNF Receptor Associated Death Domain (TRADD), TNF Receptor Associated Factors (TRAFs), and Receptor Interacting Protein (RIP1), to converge at the cytoplasmic tail of TNFR and form an activated complex which represents the molecular link between several possible signalling pathways (Hauer *et al*. 2005). Once TRAFs are activated, they in turn interact with specific members of other second messenger signal pathways, of particular interest, the mitogen-activated protein kinase kinase kinase (MAPKKK or MAP3K) group. Specific MAPKKKs have the ability to activate inhibitory-κB kinase complexes (IKKs) which in turn phosphorylate inhibitory-kappa-B (IκB) proteins targeting them for proteolytic degradation. The degradation of IκB proteins, which hold NFκB inactive in the cytoplasm, exposes nuclear localisation signals and allows NFκB activation and translocation to the nucleus, where it is known to upregulate many proinflammatory molecules (Ghosh and Baltimore 1990, Van der Heiden *et al*. 2010)(Figure 2.1).

2.1.1.2   *IFNγ*

IFN-γ is a type-II class of interferon involved in inflammatory processes and is considered to have a key role in the progression of atherosclerosis. Secreted by T-cells and NK cells following synergistic activation by IL-12 and IL-18, IFNγ becomes biologically active as a homodimer and acts upon cells of the immune system and vasculature that express the IFNγ receptor (IFN-γR) (Umehara *et al*. 2004). The binding of IFNγ to IFN-γR1 and IFN-γR2 subunits results in receptor clustering at the cell membrane to form an active intracellular receptor complex. IFN-γR1 is constitutively associated with Janus Kinase-1 (JAK1) and IFN-γR2 with JAK2. On ligand-induced dimerisation, JAK2 rapidly phosphorylates itself and the corresponding JAK1 on intracellular regions of IFN-γR1, which further activates both kinases (Kohlhuber *et al*. 1997). JAK1 phosphorylates the specific tyrosine residue 440 on IFN-γR1 to reveal a docking site for the subsequent kinase in this signalling pathway, signal transducer and activator of transcription-1 (STAT1) (Mahboubi and Pober 2002). Inactive cytoplasmic STAT1 is recruited to IFN-γR1 upon activation of the receptor kinase complex and binds temporarily to its docking site where it is phosphorylated by JAK2 on tyrosine residues. Adjacent phosphorylated STAT1 molecules homo- or hetero-dimerise to become active and disassociate from the receptor complex. Translocation to the nucleus follows, where STAT1 binds to specific γ-activated sequence (GAS) elements to induce gene transcription (See Kotenko and Pestka 2000 for review)(Figure 2.2). Several IFNγ-inducible chemokines have been observed in human atherosclerotic coronary arteries (Ranjbaran *et al*. 2007) and IFNγ stimulation of vascular cells has been shown to enhance adhesion molecule expression (Couffinhal *et al*. 1994, Kota *et al*. 2005).

1. IKK assembly

Multiple signalling pathways
(MAPKKK)

NEMO
(IKK-γ)

IKK-α   IKK-β

NFκB
P50 Rel A   IκB

NFκB held inactive in
cytoplasm

IKK-α   NEMO   IKK-β
(IKK-γ)

2. Phosphorylation

IKK

NFκB
P60 Rel A   IκB   P

3. Poly-ubiquitination

Ubiquitin ligase
E3 complex

NFκB
P60 Rel A   IκB   P
U U U

4. Degradation

NFκB
P60 Rel A

U   U
U

Proteasome

5. Translocation

NFκB
P60 Rel A

nucleus

κB binding sites
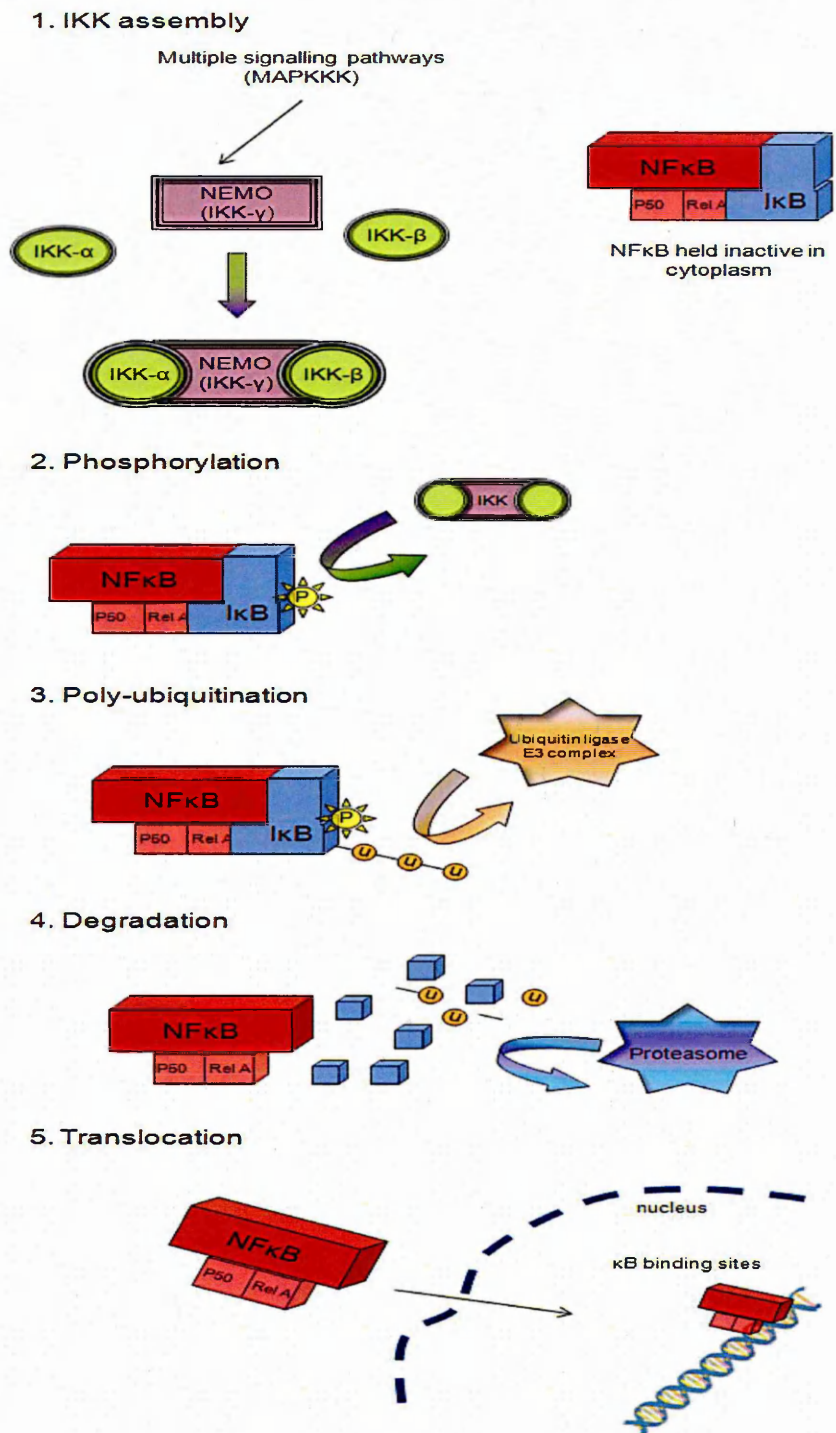
Figure 2.1; Schematic representation of NFκB signalling. 1) Specific MAPKKKs have the ability to interact and stimulate inhibitory-kappa-B kinase complexes (IKKs) leading to their assembly as an activating complex. Made up of two catalytic subunits, IKKα and IKKβ, and a structural component, NEMO/IKKγ/IKKAP, IKKs exist in the cytoplasm. NFκB is held inactive in the cytoplasm by inhibitory-kappa-B (IκB). 2) Activated IKKs phosphorylate IκB on two conserved serine residues in the N-terminal domain. 3) This leads to the polyubiquitination of IκB proteins by a ubiquitin ligase E3 complex, subsequently targeting them for degradation by the 26S proteasome (4). 5) Degradation of the IκB protein exposes NFκB nuclear localization signal on the NFκB molecule thus allowing its translocation to the nucleus and subsequent association with κB binding sites in the promoter regions of specific genes.

62
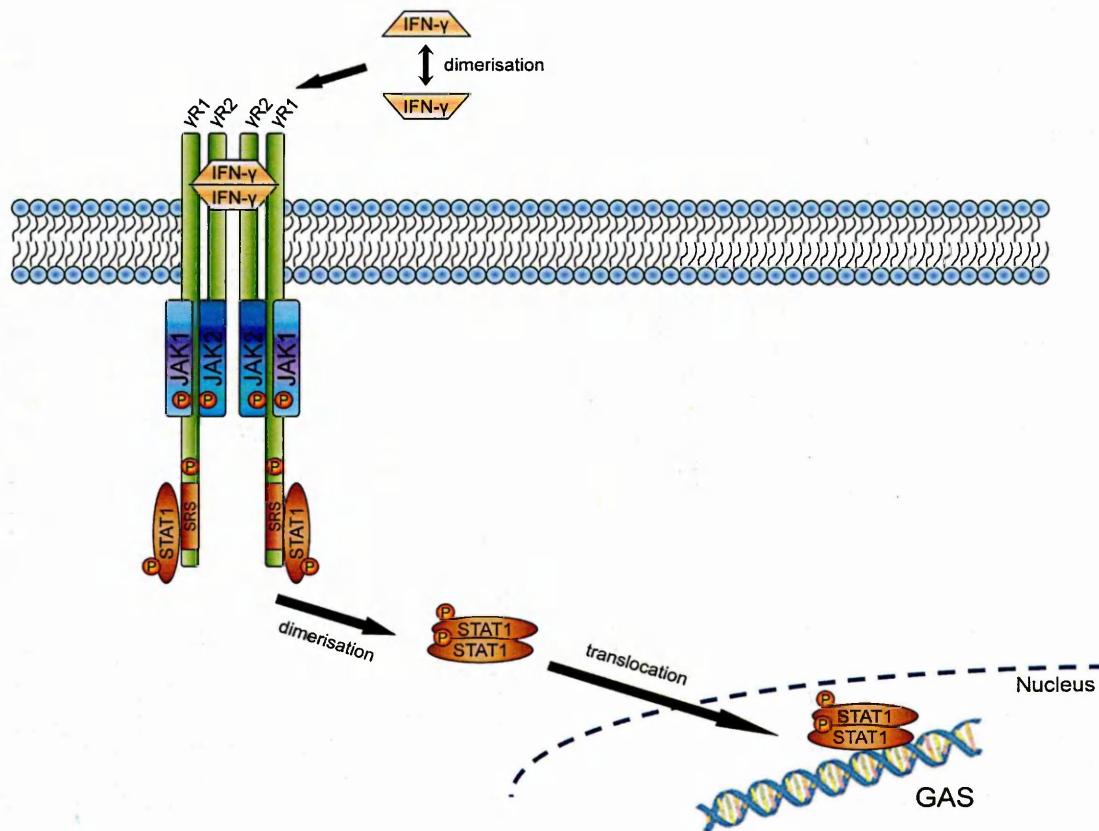
Figure 2.2; Schematic representation of JAK/STAT signalling. The binding of IFN-γ to IFN-γR1 and IFN-γR2 subunits results in receptor clustering at the cell membrane to form an active intracellular receptor complex. IFN-γR1 is constitutively associated with Janus Kinase-1 (JAK1) and IFN-γR2 with JAK2. On ligand-induced dimerisation, JAK2 rapidly phosphorylates itself and the corresponding JAK1 on intracellular regions of IFN-γR1 which further activates both kinases. JAK1 further phosphorylates the specific tyrosine residue 440 on IFN-γR1 to reveal a docking site for the subsequent kinase in this signalling pathway, signal transducer and activator of transcription-1 (STAT1). Inactive cytoplasmic STAT1 is recruited to IFN-γR1 upon activation of the receptor kinase complex and binds temporarily to its docking site where it is phosphorylated by JAK2 on tyrosine residues. Adjacent phosphorylated STAT molecules homo- or hetero-dimerise to become active and disassociate from the receptor complex. Translocation to the nucleus follows where STAT moleculess bind to specific γ-activated sequence (GAS) elements to induce gene transcription (See Kotenko *et al*. 2000 for review).

2.1.1.3   IL-18

IL-18 is a pleiotropic proinflammatory cytokine whose role in atherogenesis is only recently starting to be uncovered. MI patients have notably higher levels of IL-18 than patients with stable angina or healthy controls (Seta *et al.* 2000, Mallat *et al.*2001a, Mallat *et al.* 2002, Narins *et al.* 2004), and IL-18 has been shown to be elevated in heart failure patients (Naito *et al.* 2002), suggesting a role in plaque instability. IL-18 was demonstrated as an independent risk factor for cardiovascular death in a cohort of CAD patients (Blankenberg *et al.* 2002).

Produced as a biologically inactive precursor protein (Pro-IL-18) primarily by activated monocyte/macrophage cells, IL-18 is cleaved from its 24kD precursor to an 18kD active molecule by caspase-1 (Mallat *et al.* 2001a). Also known as Interferon-gamma inducing factor (IGIF), IL-18 induces the production of IFNγ in T cells. NK cells, subsets of macrophages, and more recently VSMC and endothelial cells have been identified as possessing the heterodimeric IL-18 receptor (IL-18R) complex and express IFNγ when stimulated with recombinant IL-18 *in vitro* (Sahar *et al.* 2005). IL-18 augments the production of various other mediators involved in atherosclerosis in cells expressing its receptor. IL-1β, IL-8, IL-6, CCL2, TNFα and several adhesion molecules are induced directly by IL-18 (Puren *et al.* 1998, Vidal-Vanaclocha *et al.* 2000, Gerdes *et al.* 2002). Additionally, IL-18 has been directly linked to vascular remodelling through its possible activation of tyrosine kinase pathways and transcription factors implicated in SMC proliferation and migration (Sahar *et al.* 2005). Therefore, IL-18 is a relatively new mediator in the atherosclerosis story, with potential inflammatory actions in atherogenesis which warrant further investigation.

Upon IL-18 binding to IL-18Rα, IL-18Rβ is recruited to form a high-affinity complex at the cell membrane which induces second messenger signalling pathways similar to those of other cytokines (Gracie *et al.* 2003). Initially, IL-1R-associated kinase (IRAK) is recruited to the complex and is subsequently activated and autophosphorylated leading to its dissociation from the receptor (Wesche *et al.* 1997, Adachi *et al.* 1998, Kanakaraj *et al.* 1999). IRAK can then interact with TRAF6 and once activated, as with TNFα signalling, can in turn interact with specific members of other second messenger signalling pathways ultimately leading to IκB degradation and NFκB activation (See Gracie *et al.* 2003).

2.1.2   Chemokines

Activated vascular cells express a number of chemokines that influence the recruitment of leukocytes to the vessel wall. However, several lines of evidence support the notion that CCL2-

CCR2 and CX_3CL1-CX_3CR1 are the primary chemokine-receptor pairs that drive atherosclerotic lesion formation (See section 1.6).

2.1.2.1 *CX₃CL1*

The expression of fractalkine has been repeatedly shown in vascular endothelial cells *in vitro*, and can be amplified upon stimulation with inflammatory cytokines; TNFα (Ahn *et al.* 2004), IFNγ (Bazan *et al.* 1997, Imaizumi *et al.* 2000), IL-1, IL-6 (Bazan *et al.* 1997, Garcia *et al.* 2000) and oxLDL (Barlic *et al.* 2007). Endothelial cells express little CX_3CL1 mRNA constitutively but a marked increase is observed following activation with inflammatory stimuli, TNFα or IL-1β (Bazan *et al.* 1997). Anti-inflammatory cytokines IL-4 and IL-13 inhibit induction of CX_3CL1 by TNFα and IFNγ, lending support to the role of CX_3CL1 in inflammatory processes (Fraticelli *et al.* 2001). In addition to endothelial expression of CX_3CL1, VSMC synthesise and release CX_3CL1 in response to pro-inflammatory cytokines (Ollivier *et al.* 2003). Aortic SMC grown in culture synthesise and express CX_3CL1 in response to proinflammatory cytokines, leading to increased adhesion and chemoattraction of CX_3CR1+ leukocytes (Ollivier *et al.* 2003, Lesnik *et al.* 2003). Patel *et al.* (2008) also demonstrated a TNFα-induced upregulation of CX_3CL1 expression in human saphenous vein endothelial and SMC in relation to AAA.

The intracellular signal transduction preceding the upregulation of CX_3CL1 is a lot less clear, but is considered to be mainly via NFκB signalling pathways (Ahn *et al.* 2004). Garcia *et al.* (2000) demonstrated a central role for NFκB pathways in the activation of endothelial cells by inflammatory molecules or vascular injury. The human CX_3CL1 gene is located on chromosome 16 and there are binding sites for both NFκB and STAT in the promoter region of the gene (Nomiyama *et al.* 1998). Therefore, inflammatory molecules known to activate NFκB, such as TNFα, and STAT, such as IFNγ, may therefore lead to increased expression of chemokines such as CX_3CL1.

2.1.2.2 *CCL2*

Rollins *et al* (1990) demonstrated that human vascular endothelial cells express little CCL2 under normal culture conditions, and that expression is markedly induced by pro-inflammatory cytokines IL-1β and TNFα, and to a lesser extent by IFNγ. Another study reported that TNFα induced CCL2 expression in human pulmonary artery endothelial cells (HPAEC) and that this expression was essential for firm adhesion of monocytes under conditions of physiological flow (Maus *et al.* 2002). This was in agreement with an earlier study (Kukreti *et al.* 1997), in which the mechanisms of firm adhesion were considered to be mediated via CCL2 activation of integrins on monocytes. In HUVEC, CCL2 has been demonstrated to be up-regulated by TNFα,

IL-1β, (Strieter *et al.* 1989a, Sica *et al.* 1990, Cybulsky *et al.* 1991). Taubman *et al.* (1992) and Lim *et al* (2009) have also described the upregulation of CCL2 mRNA and secreted protein in IL-1β- and platelet derived growth factor (PDGF)-stimulated HASMC respectively.

The underlying signalling pathways leading to CCL2 gene transcription are complex and not fully understood. However, it appears that two NFκB binding sites, located near the transcription initiation site, are critical elements in CCL2 induction, in response to proinflammatory cytokines such as IL-1β and TNFα (Ueda *et al.* 1994; Ping *et al.* 1996; Ueda *et al.* 1997). Furthermore, Chen *et al.* (2004) indicated that TNFα-stimulated CCL2 production is dually regulated by activator protein-1 (AP-1) and NFκB pathways in rat VSMC. Alternate pathways are also implicated, that do not require NFκB activation (Lim *et al.* 2009). Valente *et al.* (1998) identified GAS elements at the promoter site of CCL2 that resemble the binding site for STAT transcription factors, and demonstrated that STAT1 was primarily involved in IFNγ up-regulation of CCL2. The authors also noted that this gene induction was influenced by other complex regulatory factors, adding a multifaceted level of control to CCL2 transcription.

2.1.3 Testosterone as an anti-inflammatory agent

Testosterone is considered to be immunosuppressive and there are several *in vitro* studies to support this. Testosterone inhibits the production of proinflammatory cytokines such as IL-6, IL-1β and TNFα in a range of human, mouse and rat monocytes (Li *et al.* 1993, Kanda *et al.* 1996, D'Agostino *et al.* 1999), fibroblasts (Gornstein *et al.* 1999) and osteoblasts (Hofbauer *et al.* 1999). In addition, testosterone can stimulate the production of anti-inflammatory cytokines such as IL-10 in lymphocytes (Liva and Voskuhl 2001), and murine macrophages (D'Agostino *et al.* 1999). Also, activation of the AR influences the expression of chemokine receptors CXCR4 and CCR1, and subsequent chemokine responses, in prostate cancer cells (Akashi *et al.* 2006). Conversely, testosterone has also been seen to increase TNFα expression in a monocytic cell line (Zhu *et al.* 2009).

Testosterone is thought to modulate SMC through the upregulation of proliferation-associated genes and through possible inhibition of pro-inflammatory cytokines, decreasing apoptosis and promoting proliferation (Williams *et al.* 2002, Nakamura *et al.* 2006). Proliferation of SMC has been suggested to be a result of conversion of testosterone to DHT (Fujimoto *et al.* 1994). While this proliferation adds to the vascular remodelling associated with atherosclerosis, potential athero-protective effects are plausible, since SMC impart strength to the vascular wall and promote fibrous cap formation, reducing the likelihood of thrombotic episodes. However, testosterone enhances human vascular endothelial cell apoptosis when

administrated at physiological levels in culture (Ling *et al.* 2002), whereas oestrogen inhibits TNFα- and oxLDL-induced apoptosis (Florian *et al.* 2007).

This data, along with the previously discussed anti-inflammatory effects of TRT in clinical studies (see section 1.7.1.3), supports the proposed role of testosterone in the modulation of inflammatory mediators, although the underlying mechanisms remain relatively unknown. Sex steroid hormones have specifically been shown to demonstrate the ability to modulate the expression of adhesion molecules (Table 2.1), and to a lesser extent chemokines (Table 2.2), on vascular cells allowing a direct involvement in early atherogenesis. The results from such studies are, however, inconsistent.

2.1.3.1 Effects of testosterone on adhesion molecules

TNFα induced VCAM-1 expression in HAEC was inhibited by testosterone treatment suggesting that the male androgen plays an important role in the prevention of atherogenesis (Hatakeyama *et al.* 2002). This study additionally described an inhibition of NFκB activation, not only as a potential mechanism for decreased VCAM-1 expression, but also as a prospective modulator of several other inflammatory gene targets known to be activated by NFκB. The promoter regions of the genes encoding ICAM-1, VCAM-1 and E-selectin all contain at least one κB site required for cytokine gene activation (Neish *et al.* 1992, Kaszubska *et al.* 1993, Hou *et al.* 1994, Read *et al.* 1994). It is suggested that the influence of androgens on NFκB may be via inhibition of NFκB nuclear translocation, as a result of decreased IKK and consequent IκB activity, rather than a direct action on NFκB (Death *et al.* 2004). Norata *et al.* (2006) furthered this notion by elegantly demonstrating a decreased inflammatory response to TNFα and LPS in human endothelial cells when treated with DHT. This included a reduction in adhesion molecule VCAM-1 and ICAM-1 expression and cytokines IL-6, CCL2, and TNFα release, amongst other inflammatory markers. Again, the mode of action was proposed to be via inhibition of NFκB activity. Although this study was performed in HUVEC, and therefore may not be reflective of the behaviour of other endothelial cell types, the inhibition of VCAM-1 expression supports the findings of the previous investigation using HAEC (Hatakeyama *et al.* 2002). In addition to testosterone's interaction with NFκB, preliminary data has proposed that DHT and IFNγ can modulate each other's signalling via an interaction at the transcriptional level, suggesting that androgens may down-regulate IFN-induced genes (Bettoun *et al.* 2005).

Contradictory to the proposed athero-protective role of testosterone, several studies have demonstrated that cytokine-stimulated upregulation of adhesion molecules is increased in

Study	Vascular Cells (origin)	Hormone Treatment	Cytokine Treatment	Result	Mechanism
Mukherjee et al. (2002)	HUVEC (female)	Testosterone (48h; 1nM – 1uM)	TNFα (10ng/ml; 4hr following hormone treatment)	↓ VCAM-1	ER via aromatisation
		17-β-estradiol (48h; 20nM)	TNFα (10ng/ml; 4hr following hormone treatment)	↓ VCAM-1	ER
		DHT (48h; 1nM – 1uM)	TNFα (10ng/ml; 4hr following hormone treatment)	↔ VCAM-1	
Zhang et al. (2002)	HUVEC (unspecified)	Testosterone (1-6h; 10nM)	TNFα (100U/ml; 1-6hr co-incubation)	↑ VCAM-1 ↑ E-selectin ↔ ICAM-1	AR
		17-β-estradiol (1-6h; 10nM)	TNFα (100U/ml; 1-6hr co-incubation)	↑ VCAM-1 ↑ E-selectin ↔ ICAM-1	ER
Death et al. (2004)	HUVEC (male)	DHT (48h; 400nM)	IL-1β (10U/ml; final 24hrs)	↑ VCAM-1	AR
	HUVEC (female)	DHT (48h; 400nM)	IL-1β (10U/ml; final 24hrs)	↔ VCAM-1	
McCrohon et al. (1999)	HUVEC (male & female)	DHT (48h; 40 + 400nM	IL-1β (50U/ml; final 24 hrs)	↑ VCAM-1 ↔ ICAM-1 ↔ E-selectin	AR
		DHT (48h; 40 + 400nM)	TNFα (500U/ml; final 24 hrs)	↑ VCAM-1 ↔ ICAM-1 ↔ E-selectin	AR
Caulin-Glaser et al. (1996)	HUVEC (female)	17-β-estradiol (48h; 1000ng/ml)	IL-1 (20U/ml; 4hr following hormone treatment)	↓VCAM-1 ↓ICAM-1 ↓ E-selectin	ER
Hatakeyama et al. (2002)	HAEC (unspecified)	Testosterone (24h; 1-1000nM)	TNFα (20ng/ml; 4hr following hormone treatment)	↓ VCAM	AR
Nakagami et al. (2010)	BAEC (unspecified)	17-β-estradiol (24h; 0.01, 1 +50 ng/ml)	Lp(a) (5ug/ml; 6hr following hormone treatment)	↓VCAM-1 ↓ICAM-1 ↓ E-selectin	NI
Norata et al. (2006)	HUVEC (unspecified)	DHT (1h; 1µM)	TNFα (10ng/ml; 4hr following hormone treatment)	↓ICAM-1 ↓VCAM-1 ↔PECAM-1 ↔E-selectin	AR
Aziz & Wakefield (1996)	HUVEC (unspecified)	17-β-estradiol (6h;5+100ng/ml)	TNFα (250U/ml; 6hr co-incubation)	↑ E-selectin ↔ ICAM-1 ↔VCAM-1	NI
		17-β-estradiol (6h; 5 + 100ng/ml)	IL-1 (250U/ml; 6h co-incubation)	↔ ICAM-1 ↔ VCAM-1 ↔ E-selectin	NI
		17-β-estradiol (6h; 5 + 100ng/ml)	TNFα (250U/ml; 23hr co-incubation)	↑ ICAM-1 ↔ VCAM-1 ↔ E-selectin	NI
		17-β-estradiol (6h; 5 + 100ng/ml)	IL-1 (250U/ml; 23hr co-incubation)	↑ ICAM-1 ↔ VCAM-1 ↔ E-selectin	NI

Xing _et al._ (2007)	RASMC (female)	17-β-estradiol (24h; 5 + 1µM)	TNFα (0.1-2.5ng/ml; 6hr following hormone treatment)	↓ICAM-1 ↓VCAM-1 ↓P-selectin	ER(β)
Simoncini _et al._ (2000)	HSVEC (male and female)	17-β-estradiol (48h; 10µM/L)	LPS (100ng/ml; 18h following hormone treatment)	↓VCAM-1	NI
		17-β-estradiol (48h; 10µM/L)	IL-1α (1ng/ml; 18h following hormone treatment)	↓VCAM-1	NI
		17-β-estradiol (48h; 10µM/L)	TNFα (1ng/ml; 18h following hormone treatment)	↓VCAM-1	NI

**Table 2.1; Summary of in vitro studies investigating hormone modulation of vascular cell adhesion molecule expression under pro-inflammatory conditions.** Expression was either up-regulated (↑), down-regulated (↓), or not altered (↔) as a result of hormone treatment. BAEC, bovine aortic endothelial cells; HAEC, human aortic endothelial cells; HUVEC, human umbilical vein endothelial cells; HSVEC, human saphenous vein endothelial cells; RASMC, rat aortic smooth muscle cells; AR, androgen receptor; ER, Oestrogen receptor; LPS, lipopolysaccharide; NI, not investigated.

Study	Vascular Cells (origin)	Hormone Treatment	Cytokine Treatment	Result	Mechanism
Norata et al. (2006)	HUVEC (unspecified)	DHT (1h; 1µM)	TNFα (10ng/ml; 4h following hormone treatment)	↓CCL2	nonAR
Norata et al. (2010)	HUVEC (unspecified)	3β-Adiol (1h; 10nM)	TNFα (10ng/ml; 4h following hormone treatment)	↓CCL2	ERβ
		17β-estradiol (1h; 10nM)	TNFα (10ng/ml; 4h following hormone treatment)	↔CCL2	
Jiang et al. (2010)	RASMC (female)	17β-estradiol (24h; 10nM-10µM)	LPS (0.1µg/ml; 24h following hormone treatment)	↓CCL2	
Xing et al. (2007)	RASMC (female)	17β-estradiol (24h; 5 + 1µM)	TNFα (0.1-2.5ng/ml; 6h following hormone treatment)	↓CCL2	ER(β)

Table2.2; Summary of in vitro studies investigating hormone modulation of vascular cell chemokine expression under pro-inflammatory conditions. Expression was either up-regulated (↑), down- regulated (↓), or not altered (↔) as a result of hormone treatment. BAEC, bovine aortic endothelial cells; HAEC, human aortic endothelial cells; HUVEC, human umbilical vein endothelial cells; HSVEC, human saphenous vein endothelial cells; RASMC, rat aortic smooth muscle cells; AR, androgen receptor; ER, Oestrogen receptor; LPS, lipopolysaccharide; NI, not investigated.

cultured endothelial cells upon treatment with androgens (McCrohon *et al.* 1999, Zhang *et al.* 2002; Death *et al.* 2004). Through direct AR antagonism, Zhang *et al.* (2002) completely abrogated the androgen enhancement of TNFα-induced E-selectin and VCAM-1 up-regulation, indicating that testosterone functions through the AR to modulate adhesion molecule expression. In support of this, McCrohon *et al.* (1999) reported that DHT increased the expression of VCAM-1 in HUVEC without cytokine influence, and that this effect was antagonised by blockade of AR. Zhang *et al.* (2002), however, observed no effect of testosterone. This may be due to the higher affinity binding of DHT to the AR. There is no direct evidence for existence of androgen response elements on VCAM-1 gene promoter regions, and the enhanced expression observed was not believed to be due to an up-regulation of cytokine receptors, suggesting other signalling pathways that may direct these pro-atherogenic actions of androgens. Death and colleagues (2004) support the role of the AR in the enhancement of pro-inflammatory cytokine-stimulated expression of adhesion molecules. Treatment of HUVEC with DHT and IL-1β, significantly increased VCAM-1 expression, and this was blocked by AR antagonism with hydroxyflutamide. The authors further demonstrated that DHT increased VCAM-1 promoter activity via NFκB activation, although not via direct interactions between AR and NFκB. Instead, DHT was demonstrated to decrease the level of IκB protein through heightened degradation, thus activating NFκB and subsequent VCAM-1 expression. In addition, 27 genes related to atherosclerotic functions, including adhesion and inflammation, have been found to be up-regulated in monocytes isolated from males treated with DHT (Ng *et al.* 2003). The same genes were not altered in female donors following the same treatment, indicating that androgen actions may be gender specific.

The attenuating effects of testosterone on adhesion molecule up-regulation in cultured vascular endothelial cells have been proposed to be due to conversion of testosterone to estradiol and to act via the ER rather than the AR (Mukherjee *et al.* 2002). Mukherjee *et al.* (2002) showed that testosterone could attenuate TNFα-induced VCAM-1 upregulation in HUVEC, an action that was abolished by both ER antagonism and aromatase inhibition. This study utilised HUVEC of female origin and may not be directly comparable to investigations with male endothelial cells. In parallel, another study has reported that 17β-estradiol can inhibit IL-1-induced ICAM-1, VCAM-1 and E-selectin expression in HUVEC isolated from a female foetus (Caulin-Glaser *et al.* 1996;). Xing *et al.* (2007) reported that 17β-estradiol inhibits mRNA expression of ICAM-1, VCAM-1, P-selectin and CCL2 in rat aortic SMC, and further described that this effect was attenuated by ERβ blockade. Additionally, Nakagami *et al.* (2010) have recently demonstrated that 17β-estradiol inhibits lipoprotein-a (Lp-a; an atherogenic

lipoprotein) induced expression of VCAM-1, ICAM-1, and E-selectin in bovine aortic endothelial cells; and IL-1β, TNFα and CCL2 in macrophages differentiated from THP-1 cells. Simoncini *et al.* (2000) also showed that 17β-estradiol inhibited expression of VCAM-1 when induced by LPS, IL-1α or TNFα. The authors considered this effect to be due to 17β-estradiol influence on NFκB. Furthermore, ER has also been shown to inhibit NFκB activity in several cell lines (see Kalaitzidis and Gilmore 2005). The ER is considered to directly bind subunits of NFκB *in vitro* and inhibit transcriptional activity, possibly by preventing DNA binding or by inhibiting essential coactivator protein association (Stein and Yang 1995). However ER-NFκB complexes have not been reported. 17β-estradiol has been suggested to influence NFκB activities indirectly through the stabilisation of IκB, via inhibition of IKK (Simoncini *et al.* 2000).

Contradictory to these reports, Aziz *et al.* (1996) demonstrated that 17β-estradiol enhanced the expression of E-selectin after TNFα stimulation, and supported similar findings from a previous study where VCAM-1 and ICAM-1 were additionally upregulated, promoting leukocyte adherence (Cid *et al.* 1994;). Both these investigations reported a lack of oestrogen modulation on adhesion molecule expression following IL-1β stimulation, whereas Zhang *et al.* (2002) reported that estradiol enhanced TNFα-induced mRNA and surface expression of E-selectin and VCAM-1. The effect was completely abrogated by pre-incubating the cells with the oestrogen antagonist tamoxifen.

Therefore, it is apparent that sex hormones are capable of inducing both pro- and anti-inflammatory effects. The mechanisms underlying these effects remain to be clarified, but may be via the co-regulation of inflammatory genes by either direct androgen or oestrogen response element activation or by "cross-talking" to other signalling molecules. The outcome of such signalling may rely on multiple other concurrent pathways dependent upon present cellular status and may be influenced by cell phenotype. This level of complexity in regulation may account for conflicting reports in the data, and demonstrate that further research in this area is required (see Kalaitzidis and Gilmore 2005).

2.1.3.2   *Effects of testosterone on chemokines*

Testosterone has been shown to increase CCL2 expression in a monocyte cell line and this was thought to be a result of NFκB activation (Zhu *et al.* 2009). Yamada *et al.* (1996) found no effect of testosterone on monocyte migration *in vitro*. Norata *et al.* (2006) demonstrated that DHT could inhibit a LPS-induced upregulation of CCL2 in HUVEC, an effect that was abolished by AR antagonism. The authors additionally reported that the upregulatory effects of TNFα on CCL2 expression were partially, but significantly, inhibited by DHT treatment, an effect that

was not significantly altered by AR blockade. This may suggest that the observed anti-inflammatory effects of DHT occur via AR and non-AR mediated pathways, depending on the inflammatory stimuli. Moreover, Norata *et al.* (2010) recently extended this theory by demonstrating that DHT can reduce TNFα-induced CCL2 expression in HUVEC via conversion to 5α-androstane-3β,17β-diol (3β-adiol) and subsequent activation of ER. While DHT is non-aromatisable, 3β-adiol is a product of DHT metabolism by 3-hydroxysteroid dehydrogenase enzymes, present in endothelial cells, and is a molecule unable to bind to the AR, but has high affinity for ER (Weilhua *et al.* 2002, Guerini *et al.* 2005). This supports the idea that androgenic anti-inflammatory actions are mediated via ER activation. Indeed, 17β-estradiol inhibits CCL2 expression in VSMC (Jiang *et al.* 2010) and fibroblasts (Kovacs *et al.* 1996), and inhibits monocyte migration towards CCL2 (Yamada *et al.* 1996). Xing *et al.* (2007) have shown a direct inhibitory effect of 17β-estradiol on TNFα-induced expression of CCL2 in rat aortic SMC. Through subsequent receptor antagonism, the authors demonstrate that the mechanisms controlling this chemokine suppression are directed through ERβ. In addition, this study also described the down-regulation of cytokine-induced neutrophil chemoattractant (CINC)-2β, a member of the CXC chemokine family. In rats, this chemokine is considered to act in a similar manner to human IL-8 in the potent chemoattraction of neutrophils. Moreover, blocking CINC-2 activity reduced the chemotactic activity of differentiated myeloid leukaemia HL-60 cells to the same extent as 17β-estradiol, but did not completely ablate the activity, partially inhibiting the migration of neutrophils (Xing *et al.* 2007). Data from this study, therefore, implicates a role for oestrogens, and potentially testosterone via aromatisation to 17β-estradiol, in the recruitment of inflammatory immune cells to the vascular wall. In contrast, however, Norata *et al* (2010) found no effect of 17β-estradiol on TNFα-induced CCL2 expression.

2.1.3.3 Molecular mechanisms underlying the anti-inflammatory actions of testosterone

NFκB and AR both act at the transcriptional level and have been experimentally found to be antagonistic to one another (McKay and Cidlowski 1999), limiting gene expression to relative nuclear presence of either factor. Keller *et al.* (1996) showed that DHT repressed activation of the IL-6 promotor via the AR partly by elevating IκB and consequently inhibiting NFκB translocation. As the AR and NFκB are mutual antagonists their interaction and influence on function can be bidirectional, with inflammatory agents that activate NFκB interfering with normal androgen signalling as well as AR interrupting NFκB inflammatory transcription. If this is the case, prolonged exposure of vascular cells to the inflammatory activation of NFκB associated with atherosclerosis may reduce or alter the protective effects of testosterone. In

addition, physical interactions of NFκB subunits and promoter regions of the AR gene have been observed (Supakar *et al.* 1995), suggesting a possible feedback loop whereby inflammatory activities in cells promote increased androgen sensitivity through increased receptor synthesis, and thereby possible anti-inflammatory regulatory consequences. The *in vivo* significance of these interactions, however, remains to be established.

2.1.4   Summary

Androgens are capable of modulating the inflammatory response associated with atherosclerosis through specific affects on chemokines and adhesion molecules, and this is demonstrable in cell culture models. The extent of this modulation and the supposed pro- or anti-inflammatory actions present differently in different cell types, at different concentrations, for different treatment periods, when used in combination with different inflammatory stimulants and dependent upon the target investigated. Also, it is not clear whether testosterone functions through the AR (either directly or following conversion to DHT), or through the ER (following aromatization to estradiol or conversion to 3β-adiol), or via non-classical receptor-mediated mechanisms. This highlights the complexity of interactions between sex hormones and inflammation. Though the mode of action may be via multiple divergent signalling pathways that are not yet completely understood, the role of NFκB and STAT may be important, as these transcription factors are activated by pro-atherogenic cytokines, such as TNFα and IFNγ, and show potential interaction with AR and ER. Experimental observations regarding the role of testosterone in adhesion molecule and chemokine expression suggest that testosterone may influence the recruitment of inflammatory cells to the vascular wall in atherosclerosis. The conflicting data from these studies, however, highlights the requirement for further investigations to elucidate the precise underlying cellular mechanisms. Whether testosterone has a modulatory effect on chemokine expression, and in particular the central chemokines CX_3CL1 and CCL2, in human aortic vascular cells has not previously been investigated.

2.1.5 Hypothesis and aims of the *in vitro* study

The aim of the *in vitro* study was to use a primary vascular cell culture model to address the hypothesis that testosterone down-regulates the proinflammatory upregulation of the key chemokines CX_3CL1 and CCL2 in aortic vascular cells.

Aims

1. To characterise and establish a cell culture model of CX_3CL1 and CCL2 pro-inflammatory vascular upregulation in primary human aortic endothelial and smooth muscle cells.

2. To identify the effect of pro-inflammatory cytokine treatment on the expression and shedding of the novel chemokine CX_3CL1 in HASMC and HAEC, and to investigate the underlying control mechanisms of CX_3CL1 shedding.

3. To identify the effect of pro-inflammatory cytokine treatment on the expression of CCL2 in HASMC and HAEC.

4. To investigate the effects of androgen treatment on the expression of CX_3CL1 and CCL2 in HASMC and HAEC under normal and pro-inflammatory conditions, and investigate the role of the androgen receptor in potential testosterone-mediated effects.

2.2 Methods

2.2.1 Cell culture

All cell culture procedures were carried out under sterile conditions in a laminar flow hood using sterile equipment.

2.2.1.1 Human aortic vascular cells

Human aortic smooth muscle cells (HASMC) and human aortic endothelial cells (HAEC) were obtained from Cascade Biologics™, UK. Cells were in the tertiary stage of culture after isolation from a 16 year old and a 15 year old male donor respectively. These adherent primary cell cultures were grown at 37°C in a 5% CO_2/95% air atmosphere in low serum medium in cell culture flasks (Fisher Scientific, UK). HAECs were cultured in Medium-200 (Cascade Biologics, UK), a basal culture medium, supplemented with low serum growth supplement (LSGS; containing 2% v/v foetal bovine serum (FBS); hydrocortisone 1μg/ml; human epidermal growth factor 10ng/ml; basic fibroblast growth factor 3ng/ml; and heparin 10μg/ml; Cascade Biologics, UK). HASMCs were cultured in Medium-231 (Cascade Biologics, UK) supplemented with smooth muscle growth supplement (SMGS; containing 5% v/v FBS; recombinant human basic fibroblast growth factor 3ng/ml, recombinant human epidermal growth factor 10ng/ml, and insulin 5μg/ml). Media were changed approximately every 48 hours and all vascular cell culture experiments were performed using cells up to a maximum passage number of 10 to avoid dedifferentiation.

2.2.1.2 THP-1 cells

THP-1 cells are a human monocytic leukaemia cell line derived from the peripheral blood of a 1 year old male with acute monocytic leukaemia. THP-1 cells are widely used as an appropriate model of human blood monocytes, as they express many distinct monocytic markers and characteristics, which are maintained over time in culture (Tsuchiya *et al*. 1980). These cells were used in the study as a positive control for specific gene and protein targets.

THP-1 cells, originally obtained from the European collection of cell cultures (ECACC, UK), were cultured in RPMI 1640 (GIBCO®) media with 2mM glutamine, 10% foetal calf serum (FCS) and 2mM penicillin/streptomycin (GIBCO®). Media were changed approximately every 48 hours. The passage number of this cell line was unknown.

2.2.1.3   DuCaP cells

DuCaP (dura mater cancer of the prostate) cells are an adherent prostate cancer cell line, established from a dura mater metastasis xenograft in severe combined immunodeficient mice (SCID) originating from a patient with castration resistant prostate cancer (Lee *et al.* 2001). DuCaPs express elevated levels of the wild type AR gene and are often deemed appropriate for testing agents targeting AR or androgen metabolism (Pfeiffer *et al.* 2010).

The DuCaP cell line was a kind donation from Dr. Ken Pienta (University of Michigan, MI, USA). These cells were included in the study to test the delivery of androgens to cells in culture. DuCaP cells were cultured in RPMI 1640 (GIBCO®) media with 2mM glutamine, 5% FCS and 2mM penicillin/streptomycin (GIBCO®). Media were changed approximately every 48 hours. The passage number of this cell line was unknown. Prior to experimental investigation, cells were transferred to charcoal-stripped media for a period of 48 hours.

2.2.1.3.1   Preparation of charcoal-stripped media

Treatment of FCS with charcoal stripping removes any unknown lipid-related elements in the sera, such as hormones, without affecting the amino acid, glucose and salt content. In brief, FCS was incubated with dextran-coated charcoal (Sigma-Aldich, UK) for 30 min in a water bath at 55°C with periodical shaking. After centrifugation (20,000 x g for 20 min) the supernatant was treated with sulphatase (Sigma-Aldrich, UK) (2 U/ml of serum) for 2 hours at 37°C in a water bath. Incubation with dextran-coated charcoal and centrifugation was repeated, and the resulting supernatant was filtered through a 0.2μm filter (Fisher, UK) and added to RPMI media in place of untreated FCS.

2.2.2 Subculture of cells

At 70-90% confluence medium was removed from the culture flasks and cells were washed twice with phosphate buffered saline (PBS (GIBCO®)). 1ml/25cm^2 of trypsin/EDTA solution (0.5% trypsin and 0.53nM EDTA (GIBCO®, UK) was applied to the cells (HAEC, HASMC and DuCaPs) and incubated at room temperature for 3 minutes. The flask was tapped gently to dislodge cells from the surface and an equal amount of complete (serum-containing) medium added to neutralise the trypsin/EDTA. The cell suspension was removed to sterile tubes and centrifuged for 5 minutes at 200 x g. After removing the supernatant the cells were resuspended in 1ml of fresh medium, 20μl of this cell suspension was added to 20μl of trypan blue solution (0.4% trypan blue prepared in 0.81% sodium chloride and 0.06% potassium phosphate (Sigma-Aldrich, UK)) and incubated for 5 minutes. Using a haemocytometer, cell

viability was determined by counting cells that excluded the blue stain (i.e. dead, non-viable cells stain blue). By calculating the ratio of blue to normal cells, the percentage viability was obtained. Viable cells were then further diluted to working densities and used in the experimental procedures, subcultured or cryopreserved. For THP-1 cell subculture, the same procedure was followed with the omission of the trypsinisation step.

2.2.3 Cryopreservation of cells

Cells were removed from the culture flasks as in section 2.2.2, and resuspended in 1ml of FCS (GIBCO®, UK). Using a haemocytometer, cells were counted, then further diluted within the range of 2×10^6-10×10^6 cells/ml with freezing medium (final concentration of 10% DMSO (Sigma-Aldrich, UK), 90% FBS). 1ml of cell suspension was aliquoted per cryovial (NALGENE®, UK) and stored at -80°C in a Cryo 1°C freezing container (NALGENE®, UK) for 4 hours or overnight in order to gradually lower the temperature by 1°C/minute for maximal cell preservation. Frozen cell suspensions were then transferred to liquid nitrogen storage.

2.2.3.1 Initiation of cryopreserved cells

A cryovial of cells was removed from liquid nitrogen storage and thawed at 37°C for approximately 5 minutes or until contents thawed. The vial was wiped with 70% ethanol and the cell suspension was pipetted up and down to disperse the cells. Cells were then transferred to an appropriate number of culture flasks in order to obtain an optimal seeding density of approximately 1.25×10^4, estimated from previous freezing densities assuming near maximal preservation, in a volume of medium equivalent to $1ml/5cm^2$. Following inoculation, the flasks were swirled to distribute the cells evenly and then cultured for a minimum of 24 hours before media change or subculture.

2.2.4 Testing for the presence of mycoplasma in cell cultures

Mycoplasma is a genus of bacteria that is commonly recognised as a contaminant of mammalian cell cultures. Due to their extremely small size the contamination is not readily apparent and infection may not kill or stop cells from dividing, but their effects can be wide ranging and can potentially invalidate experimental procedures. Mycoplasmal infection can extensively influence cell growth, morphology, metabolism and the functional activity of the cell, ultimately decreasing viability (Hay *et al.* 1989, Rottem and Yogev 2000). The importance of routine testing for mycoplasma in cell culture procedures is therefore paramount for experimental validity.

The EZ-PCR mycoplasma test kit (Geneflow, UK) was used in the present study. This kit uses PCR to specifically amplify a conserved, mycoplasma-specific ribosomal RNA gene region using optimised primers. The primer set allows for sensitive and specific detection of various mycoplasma species in cell culture supernatants. PCR-amplified DNA fragments are verified by electrophoresis to confirm the presence or absence of mycoplasmal infection.

Method

1ml of cell culture supernatant was transferred to a 1.5ml Eppendorf tube and centrifuged at 250 x g for 5 minutes to pellet the cellular debris. The supernatant was then transferred to a sterile tube and further centrifuged at 20,000 x g for 10 minutes to pellet any mycoplasma. The supernatant was carefully aspirated and the pellet was resuspended in 50μl of buffer solution (Geneflow, UK) and mixed thoroughly by pipetting. The sample was heated to 95°C for 3 minutes on a heating block and then allowed to cool. 5μl of the sample was added to a PCR tube and mixed with 35μl of nuclease-free water (Sigma-Aldrich, UK) and 10μl of reaction mix (Geneflow, UK). A positive control test reaction was also prepared by adding 1μl of positive template control to 39μl of nuclease-free water and 10μl of reaction mix. Tubes were placed into a thermal cycler (MWG Biotech, UK) and subjected to the following conditions;

94°C	30 seconds	
94°C	30 seconds	
60°C	120 seconds	35 cycles
72°C	60 seconds	
94°C	30 seconds	
60°C	120 seconds	
72°C	5 minutes	

20μl of the resulting PCR product was placed on a 2% agarose gel pre-stained with ethidium bromide (Sigma-Aldrich, UK). To form the agarose gel, 1g of agarose (Bioline, UK) was dissolved in 50ml TBE buffer (89mM Tris-HCl pH 7.8, 89mM borate and 2mM EDTA) with 2μl ethidium bromide. Loading dye (Promega, UK) was diluted 1:1 with each sample and 8μl of the sample was loaded onto the gel. A 100bp ladder (VWR International Ltd., UK) was also loaded onto the gel to allow for DNA band sizing. Using TBE as the buffer, the gel was run at 100V for 30 minutes. Mycoplasma primer sets produce a PCR product of 270bp, where mycoplasma DNA is present. Gels were visualised using a UVP Bioimaging system (Bio-Rad, UK) and images obtained with Labworks 4 software.

2.2.5 Experimental conditions for testing the effects of cytokines on CX₃CL1 and CCL2 expression in human aortic vascular cells

Cells were seeded into 6 well plates, 96 well plates and chamber slides (NUNC™), at an initial density of 1×10^5 cells/ml in complete medium, equivalent to $1ml/5cm^2$. Cells were cultured at 37°C for 24h prior to treatment, then washed twice with PBS and incubated for a further 24 hours in serum free media.

Cells were treated with recombinant human cytokines TNFα, IFNγ and IL-18, alone or in combination. TNFα and IFNγ (Peprotech, UK) were initially reconstituted in sterile water and PBS respectively, to working aliquots of 100μg/ml and stored at -20°C. Recombinant human IL-18 (R&D Systems, UK) was directly aliquoted at 50μg/ml and stored at -80°C. All cytokines were further diluted in serum-free medium to working concentrations of 1, 10, and 100ng/ml alone or in combination. Cells were incubated for 2-4h for gene expression analysis, 2-48h for protein expression analysis, with the cytokines alone or in combination and then the supernatant and cell lysates collected. Serum-free medium was used as a control and all treatments were performed in duplicate with experiments repeated at least three times for each condition.

2.2.6 Experimental conditions for testing the effects of androgens on CX₃CL1 and CCL2 expression in human aortic vascular cells

Testosterone or DHT (Sigma-Aldrich, UK) was dissolved in ethanol (Fisher Scientific, UK) at an initial dilution of 100mg/ml and stored at 4°C until used. The androgen solution was further diluted in serum-free medium to working concentrations, via an intermediary 1:1000 dilution in ethanol. Cells were seeded as above and were cultured for 24h prior to treatment, then washed twice with PBS and incubated for a further 24h in serum free media. Cells were then incubated with the androgen at working concentrations of 1, 10, 100 and 1000nM for 2-48h, either prior to cytokine treatment or with the cytokines. Ethanol, at a volume equal to that of the diluted working solution of testosterone or DHT, was used as the vehicle control.

2.2.6.1   Experimental conditions for testing the effects of androgen receptor blockade

Flutamide is a non-steroidal anti-androgen that inhibits the actions of testosterone and DHT by binding to and blocking the AR (Illiescu *et al.* 2003). Flutamide (Sigma-Aldrich, UK) was dissolved in ethanol (Fisher Scientific, UK) at an initial concentration of 100mg/ml and stored at 4°C until used. The solution was further diluted in serum-free medium to working concentrations, via an intermediary 1:1000 dilution in ethanol. Cells were incubated with flutamide at working concentrations of 1, 10, 100 and 1000nM for 2-48h along with the androgen treatments. Ethanol, at a volume equal to that of the diluted working solution of flutamide, was used as the vehicle control.

2.2.7   Investigating the effects of cell treatments on cell proliferation

2.2.7.1   Bromodeoxyuridine (BrdU) assay

To determine and quantify the effects of various mediators on cell proliferation, ELISAs that target markers of proliferative activity can be employed. BrdU is a pyrimidine analogue that is incorporated into newly synthesised cellular DNA of proliferating cells in place of the nucleoside thymidine as they replicate and divide (Gratzner 1982; Alison 1995). BrdU can then be measured by antibody detection. An anti-BrdU antibody, which specifically binds BrdU that has been incorporated into the DNA of proliferating cells, conjugated to a peroxidase (POD) enzyme, which converts the substrate tetramethylbenzidine (TMB) to a coloured product, was utilised. Resulting colour change is directly correlated to the amount of BrdU present and thus the amount of DNA synthesised in proliferating cells.

Method

Cells were seeded onto 96-well plates at known densities (0.5×10^4 – 1×10^5 cells/ml) and cultured in 200µl of serum-containing media for 24h. After this period the media were removed and replaced with serum-free media, and cells were incubated for a further 24h. Cells were finally incubated in the presence or absence of the cytokines/androgens, in triplicate, as outlined above. The BrdU cell proliferation ELISA kit (Roche, UK) contained all solutions other than the stop solution (1M H_2SO_4 ; Fisher Scientific, UK). BrdU labelling solution was added directly to the test wells at a dilution of 1:10 (e.g. 20µl added to 180µl of medium) and incubated for 4h at 37°C in 5% CO_2/95% air atmosphere. The labelling medium was removed by aspiration and wells were left to air dry for 5-10min. 200µl of FixDenat solution was added

to the wells for 30 minutes at room temperature to fix the cells and denature the DNA. FixDenat solution was removed by aspiration and blotting onto a clean paper towel. 100μl of mouse anti-BrdU-POD antibody working solution was added to the cells and left to incubate for 90min at room temperature. Antibody conjugate was then removed by aspiration and blotting, followed by 3 washes with 300μl/well of wash solution. The plate was blotted again after the final wash step to ensure complete removal of liquid. 100μl of TMB substrate solution was added to the wells and incubated at room temperature for approximately 30min or until sufficient colour developed. Stop solution (1M H_2SO_4) was added at 25μl/well, the plate tapped to mix thoroughly and the optical density determined at 450nm within 5min of the stop solution being added using a Labsystems Victor II Wallac MULTISKAN-MS plate reader (Perkin Elmer, UK). Blank controls were performed in duplicate to provide information about the non-specific binding of BrdU and the anti-BrdU-POD conjugate to the plate. These control wells contained no cells but underwent the same assay procedure as the test wells. Optical density readings for blank control wells were subtracted from those for all test wells. In addition, a background control was performed in duplicate, to account for non-specific binding of the anti-BrdU-POD conjugate to the cells, and underwent the same procedure but with the omission of the BrdU label.

2.2.7.2   *Quantification of cell protein using the bicinchoninic acid assay (BCA)*

The BCA assay is a method for determining the total protein content in a solution. Cu^{2+} ions from cupric sulphate can be reduced to Cu^+ by the peptide bonds in protein. The amount of Cu^{2+} reduced is proportional to the amount of protein present in a solution. Molecules of bicinchoninic acid then chelate with each Cu^+ ion, forming a purple-coloured product that can absorb light at a wavelength of 570nm. Samples can be quantified by comparing them to standard protein solutions of known concentrations (Walker *et al.* 1994). Total protein was measured to account for potential differences in cell number that may result from different treatments.

Method

Bovine serum albumin (BSA) fraction V (Fisher Scientific, UK) was serially diluted from a 50mg/ml stock solution in PBS (GIBCO°) over a range of 0μg/ml - 5000μg/ml to obtain a standard curve. 20μl of standards were pipetted in triplicate along with 20μl of samples in duplicate onto a 96-well plate. This was immediately followed by the addition of 200μl of BCA working solution (4% Copper sulphate solution (Sigma-Aldrich, UK) diluted 1:50 in BCA solution (Sigma-Aldrich, UK)) to all the wells, and incubation at room temperature for 30min.

82

Absorbance was read at 570nm using a Labsystems Victor II Wallac MULTISKAN-MS plate reader (Perkin Elmer, UK) and sample protein concentrations were calculated from the standard curve using Microsoft Office Excel (Microsoft, USA).

2.2.8 Investigation of protein expression in human aortic vascular cells by immunocytochemistry

Immunocytochemistry is a sensitive and versatile technique which uses antibody affinity and selectivity to detect a single epitope, mainly proteins, in its cellular location. The architecture of the cell, and therefore the target proteins (antigens), require fixation before detection. This is accomplished by use of a fixative which cross-links protein molecules and changes the chemical properties of the tissue or cell constituents to preserve morphology. This process, however, can impact on the ability of antibodies to specifically bind to their target, as the three-dimensional protein conformation can be altered and proteins can even be cleaved from the cell (Fritschy 2008). Fixatives can also be used to permeablise the cells to allow the detection of intracellular antigens. Antibodies raised against specific antigens are incubated with the cells to allow antigen-antibody binding to occur. Unbound antibody is removed by washing and the bound antibody is detected either directly, if the primary antibody is labelled, or indirectly, using labelled secondary antibodies directed against the primary antibody (Figure 2.3). Indirect immuno-labelling has the ability to amplify the signal, as multiple secondary antibody molecules can bind to a single epitope-bound primary antibody. Antibodies can be enzyme-labelled, requiring the addition of a substrate for local colour change, or fluorophor-labelled, requiring specific wavelength excitation for fluorescence emission. To reduce background and non-specific staining, and to minimise conformational protein alterations and epitope masking, the immunocytochemical conditions need to be optimised for each specific cell type and antibody.

In this thesis, indirect immunofluorescence was used for immunocytochemical analysis, whereby epifluorescence microscopy detects the light signal emitted by a fluorochrome bound to the secondary antibody.

Method
The methods of fixation, blocking, antibody dilution, incubation period and counterstaining were optimised to provide the strongest specific antigen staining with the lowest non-specific binding for each cell type and antibody. Once this was established, the procedure was utilised for all immunostaining (See Table 2.3).

83
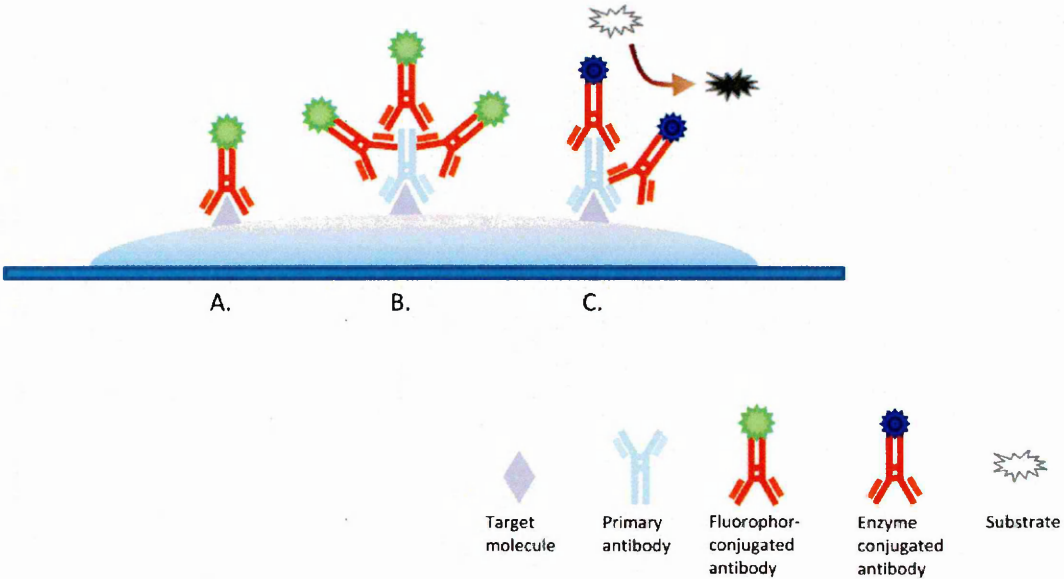
Figure 2.3; Schematic representation of immunocytochemical detection of antigens on cells or tissue. Antigens can be detected directly (A) with the use of a conjugated antibody directed against the target antigen, or indirectly (B and C) with the use of a second conjugated antibody directed against the primary antibody. Antibodies can be conjugated to fluorescent molecules (A and B) or enzymes (C) that react with a substrate to create a colour change. The use of a secondary antibody amplifies the signal generated due to the binding of multiple conjugated antibodies to a single primary antibody.

Primary Antibody Target	Supplier	Isotype/ species	Fixative	Block	Dilution	Secondary Antibody
CX$_3$CL1	R&D (MAB3651)	IgG$_1$ (ms, monoclonal)	Acetone	-	(1:25-1:400) **1:100**	**Rb x Ms 488** (1:400-1:800) **1:400**
CX$_3$CR1	Santa Cruz (sc-30030)	IgG (rb, polyclonal)	Acetone	5% BSA	(1:25-1:400) **1:50**	**Gt x Rb 568** (1:400-1:800) **1:400**
ADAM-17	Santa-Cruz (sc-25782)	IgG (rb, polyclonal)	Acetone 4%PFA	5% Serum	(1:25-1:400) **1:50**	**Gt x Rb 568** (1:400-1:800) **1:800**
ADAM-10	abCam (ab1997)	IgG (rb, polyclonal)	Acetone 4%PFA	5% Serum	(1:25-1:400) **1:50**	**Gt x Rb 568** (1:400-1:800) **1:800**
AR	abCam (ab2742)	IgG (rt, monoclonal)	Acetone	5% BSA	(1:25-1:400) **1:25**	**Gt x Rt FITC** (1:200-1:400) **1:400**
α-Actin	Sigma-Aldrich (A2547)	IgG$_{2A}$ (ms, monoclonal)	Acetone	-	(1:25-1:400) **1:200**	**Rb x Ms 488** (1:400-1:800) **1:800**
vWF	Dako (M0616)	IgG$_1$ (ms, monoclonal)	Acetone	-	(1:25-1:400) **1:400**	**Rb x Ms 488** (1:800-1:1000) **1:800**
α-Tubulin	Sigma-Aldrich (T5168)	IgG$_1$ (ms, monoclonal)	Acetone	-	(1:25-1:400) **1:400**	**Rb x Ms 488** (1:800-1:1000) **1:800**

Table 2.3; Antibodies used for immunocytochemistry. Summary of the antibodies used for target protein detection in human aortic vascular cells following optimisation of methods. The fixative, block and dilutions of primary and secondary antibodies were selected to produce the highest amount of specific staining whilst reducing, or preferentially eliminating, non-specific binding. The range of antibody dilutions tested is shown, with the selected optimum dilution in bold. *AR, androgen receptor; vWF, von Willebrand Factor; ms, mouse; rb, rabbit; rt, rat; gt, goat; x, anti (e.g. rabbit anti-mouse).*

Cells were seeded onto chamber slides at a density of 1×10^5 cells/ml in a volume of medium equivalent to $1ml/5cm^2$ and cultured with or without test reagents as appropriate. Media was aspirated carefully and cells were washed twice in PBS before fixation. For THP-1 cells, the suspended cell line was centrifuged (200 x g for 5 mins) to pellet the cells, washed by resuspending in 5ml of PBS and the centrifugation repeated. The cell pellet was resuspended in 1ml of PBS and cells counted using a haemocytometer. Cell concentration was adjusted, ranging from 1×10^3 - 1×10^5 cells/ml, and 200µl of cell suspension was loaded into a cytospin tunnel assembled with a microscope slide. The cytospin assembly was then spun at 200 x g for 3 minutes in a Shandon cytospin centrifuge (Thermo Scientific, UK) to propel the cells onto the slide, the slide removed from the assembly and cells fixed by the appropriate optimised method.

Potential non-specific binding of the antibody was blocked using the appropriate optimised blocking method (See Table 2.3). Primary antibodies specific to the cellular targets were used for detection at the optimised dilutions in PBS. The primary antibody was applied to the cells and incubated overnight at 4°C. Cells were then washed 3 times for 5 minutes with PBS containing 0.05% Tween 20 (PBS-T) (Sigma-Aldrich, UK). Primary antibody binding was visualized by incubation with a secondary antibody reactive to the species of the primary antibody, at the optimised dilutions in PBS, for 1 hour at room temperature whilst protected from light. Cells were subsequently washed with PBS-T, as before, to remove any unbound antibody. Nuclei were stained using Vectashield mounting medium containing 4',6-Diamidino-2-phenyindole (DAPI) (Vector Labs Inc, UK) and covered with coverslips which were sealed at the edges with nail varnish to prevent cell drying. Negative controls, lacking the primary antibody, were included to determine non-specific binding of the secondary antibodies. The exclusion of both primary and secondary antibodies was initially used to determine cellular autofluorescence and establish whether Sudan black blocking was necessary. Cells were examined and images captured using a Zeiss 510 laser scanning confocal microscope (Carl Zeiss Ltd, UK).

2.2.8.1   *Confocal laser scanning microscopy (CLSM).*

Confocal laser scanning microscopy (CLSM) is a valuable technique in biomedical science for imaging tissues or cells which have been labelled with one or more fluorescent probes. Samples are excited or illuminated by a multi-wavelength laser or multiple lasers capable of excitation at several wavelengths. Due to a series of mirrors and filters only light emitted from a specific focal plane reaches the detector and all other signal is filtered out (Figure 2.4). With such specific focus, image information is maximally resolute with reduced background
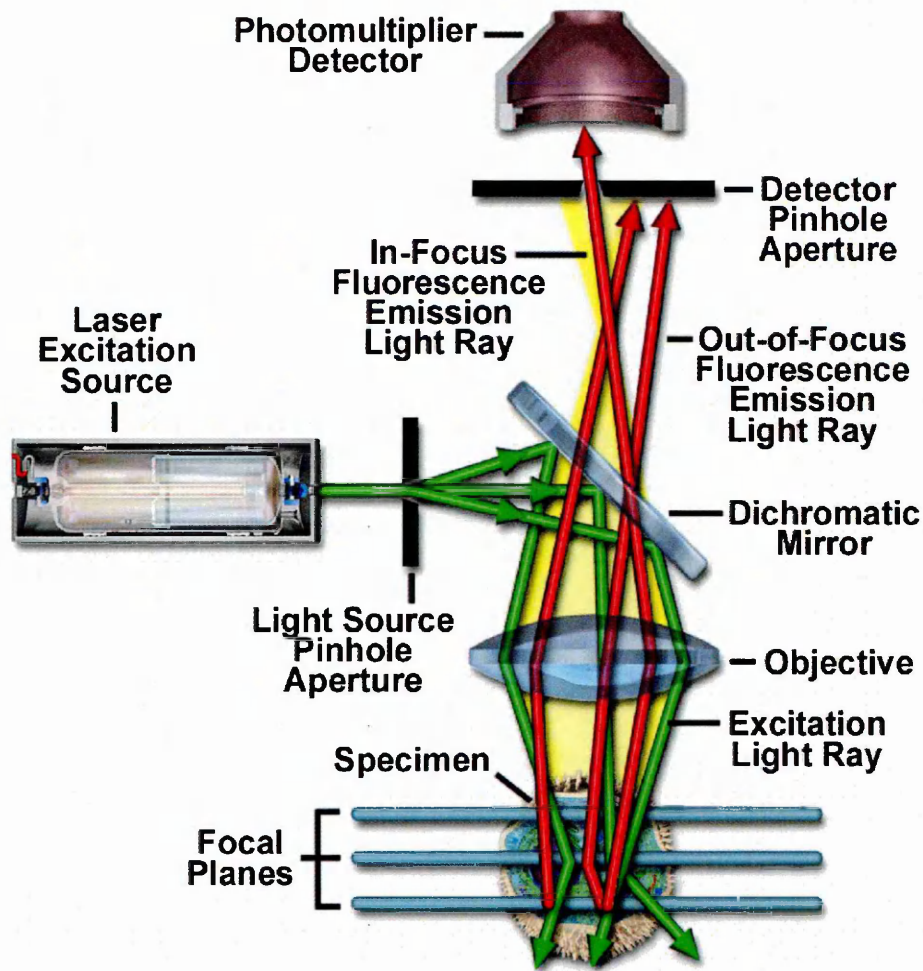
Figure 2.4; Schematic diagram of the optical pathway and principal components in a confocal laser scanning microscope. The laser beam passes through a light source pinhole aperture and is reflected by a dichromatic mirror towards the microscope objective. The objective focuses the laser beam to a chosen focal plane within the specimen that becomes confocal with the pinhole apertures of the light source and detector (Claxton 2005). By re-focussing the objective, an alternate focal plane can be investigated. Light emitted from focal planes above or below the region of interest (or objective focal plane), that would normally interfere with the resolution of structures in focus, is obstructed and excluded from detection as it is unable to pass through the detector pinhole aperture. Focussed light that passes through the detector pinhole aperture is collected by a photomultiplier detector, which produces a signal that is directly proportional to the brightness of the light. This signal is finally converted to create an image directly processed by the associated computer and displayed as a high-resolution image representative of the objective focal slice.
From www.olympusconfocal.com/theory/LSCMIntro.pdf

fluorescence and improved signal-to-noise at the chosen depth (Sandison and Webb 1994). This scanned fluorescence detection at specific depths throughout the tissue allows for an optical sectioning, which uses light rather than physical means to serially section the specimen further with sequential image acquisition at each step, or slice (Paddock 2000). By acquiring, collating and processing these multiple scanned images of focal sections throughout the specimen at known intervals, a three-dimensional representation of the sample can be constructed to provide detailed structural information.

Method

Processed cells mounted on chamber slides were stored at 4°C in the dark until image analysis on the confocal microscope. Microscope settings were optimised for each target antibody to maximise fluorescence detection while minimising background and maintaining image resolution. Once these parameters were established the settings were re-applied to all samples and negative controls to ensure consistent and reliable image reproduction.

2.2.9 Investigation of CX$_3$CL1 and CCL2 expression in human aortic vascular cells using Enzyme-Linked Immuno-Sorbant Assay (ELISA)

Enzyme-Linked Immuno-Sorbant Assay (ELISA) is a technique used to detect a specific antigen or antibody in a sample. Sandwich ELISAs employ two antibodies specific to different epitopes of the antigen, with the first capturing and immobilising the antigen (capture antibody), and the second forming a complex by binding multiple different epitope of the same antigen (detection antibody) and thus amplifying the reaction and increasing the sensitivity of the assay. The detection antibody is biotinylated and when streptavidin-horseraddish peroxidise (HRP) is added, it binds to biotin on the detection antibody. Finally, a peroxidase substrate is added allowing enzymatic conversion to take place which results in a colour change proportional to the amount of starting antigen in the sample. This colour change is detectable by spectrophotometry and can be quantified using a standard curve of known antigen concentrations. All steps are followed by a thorough washing process to remove any proteins or antibodies that are not specifically bound (Figure 2.5). The major advantages of a sandwich ELISA is specificity, allowing the use of crude or impure samples with relative precision, and it's quantitative capacity.
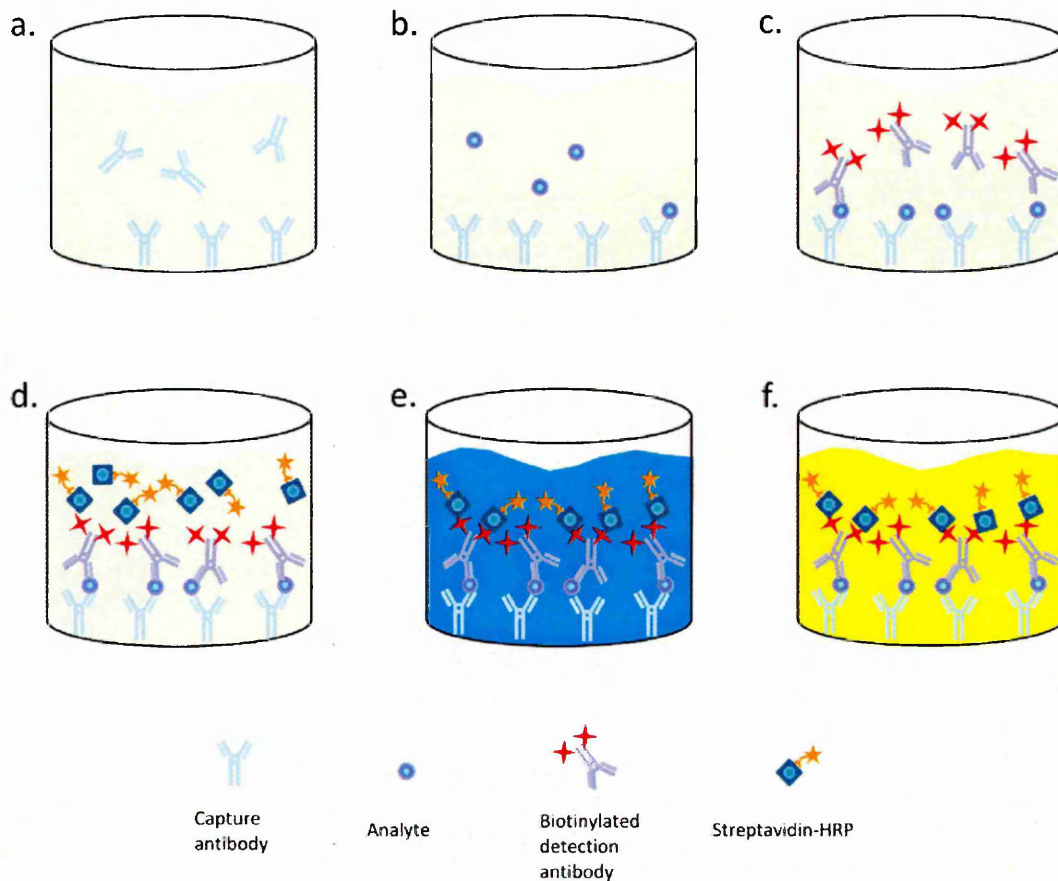
Figure 2.5; Schematic representation of the principles of an enzyme-linked immunosorbant assay (ELISA). a) Initially an analyte-specific primary antibody is coated onto the wells of a 96-well plate, followed by washing and blocking. b) Standards, samples and controls are added and incubated on the plate to allow the target molecule to bind to the immobilised capture antibody. Aspiration and wash steps follow. c) A biotinylated detection antibody is added which binds to a second epitope on the analyte. This forms a capture antibody-analyte-detection antibody 'sandwich' complex. Unbound antibody is removed by washing. d) Streptavidin-HRP is added, which binds to biotin on the detection antibody, and this is followed by washing. e) TMB, a peroxidase substrate, is added to the wells and is converted to a blue coloured reaction product by HRP in proportion to the amount of bound analyte. f) Finally, H_2SO_4 is added to stop the reaction and turn the reaction product yellow. The product is quantified by spectrophotometry.

2.2.9.1 Preparation of cell samples for ELISA

Cells were seeded onto 6 well plates as described in 2.2.5 and subjected to cytokine and/or androgen treatments. The supernatants were collected, centrifuged to pellet debris, removed to a fresh tube and stored at -80°C until analysis. Cells were lysed and the protein extracted using 500µl/well of CelLytic-m buffer (Sigma-Aldrich, UK) containing 10% protease inhibitor cocktail (Sigma-Aldrich, UK) at 4°C for 15min with gentle agitation. All cellular material was removed from the plate surface by cell scraping and then mixed into a homogenous solution by repeated pipetting. The lysates were centrifuged at 12,000 x g to pellet cellular debris and the resulting protein-containing supernatants were then stored at -80°C until analysis.

2.2.9.2 Investigation of CX₃CL1 expression in human aortic vascular cells by ELISA

A DuoSet® ELISA development kit (R&D Systems, UK) specific for the CX$_3$CL1 chemokine domain was used, according to the manufacturer's instructions, to determine the concentration of human CX$_3$CL1 concentrations in the cell supernatants and lysates. In brief, mouse anti-human CX$_3$CL1 capture antibody was diluted to a working concentration of 4µg/ml in PBS (137mM NaCl, 2.7mM KCl, 8.1mM Na$_2$HPO$_4$, 1.5mM KH$_2$PO$_4$, pH 7.2-7.4, 0.2µm filtered) and a 96 well plate was coated with 100µl/well, sealed and incubated overnight at room temperature. Each well was then aspirated and washed 3 times with 300µl/well wash buffer (PBS + 0.05% Tween® 20 (Sigma-Aldrich, UK)). After the last wash, any remaining liquid was removed by blotting against a clean paper towel. Plates were blocked by the addition of 300µl/well of reagent diluent (1% BSA (Fisher Scientific, UK) in PBS) and incubated at room temperature for a minimum of 1h. The aspiration and wash step was repeated. CX$_3$CL1 standards were prepared by dilution of the recombinant human CX$_3$CL1 stock solution (240ng/ml) in reagent diluent, to produce a range of 0-20ng/ml. This was after initially testing for CX$_3$CL1 recovery from standards diluted in celLytic or culture medium as appropriate. 100µl/well of sample or standard was added to the plate in duplicate, sealed and incubated for 2h at room temperature. The wells were aspirated and washed before 100µl/well of detection antibody (biotinylated mouse anti-human CX$_3$CL1), diluted to a working concentration of 500ng/ml in reagent diluent, was added to each well and incubated for 2h at room temperature. Subsequently, the aspiration and wash steps were repeated, followed by the addition of 100µl/well of streptavidin-HRP diluted in reagent diluent 1:100. The plate was then covered and incubated in the dark for 20min. The aspiration/wash step was repeated and 100µl/well of substrate solution (1:1 mixture of colour reagent A (H$_2$O$_2$) and colour reagent B (tetramethylbenzidine; TMB)) were added to the plate and incubated for 20min at room

temperature in the dark. 50μl of stop solution (1M H_2SO_4) was subsequently added to all wells and the optical density of each well was determined immediately using a Labsystems Victor II Wallac MULTISKAN-MS plate reader (Perkin Elmer, UK) at 450nm. Wavelength correction was applied at 570nm to correct for optical imperfections in the plate. Unknown CX_3CL1 concentrations were calculated from a standard curve of known CX_3CL1 concentrations using Microsoft Office Excel.

2.2.9.3   *Investigation of CCL2 expression in human aortic vascular cells by ELISA*

The human CCL2 ELISA development kit (R&D Systems, UK) employs the same methods and principles as the human CX_3CL1 ELISA (see above), but utilises mouse anti-human CCL2 and biotinylated goat anti-human CCL2 as the capture and detection antibody pair respectively. This was used to detect CCL2 in cell supernatants and lysates of human aortic vascular cells following the same procedures as in 2.2.9.2.

2.2.10   Investigation of surface protein expression in human aortic smooth muscle cells using flow cytometry

Flow cytometry is a laser-based technology that allows the rapid measurement of individual particles based on their light-scattering, fluorescent and other optical properties. Scattering and emission data can be used to simultaneously examine a variety of biochemical, biophysical and molecular aspects of a particle (Jaroszeski and Radcliff 1999). Most often the particles analysed are individual cells. The flow cytometer is composed of four closely related systems. The fluidics system orders the sample into a stream of single particles by creating a drag effect from faster flowing sheaf fluid surrounding the sample, which passes through a narrowing central chamber. This hydrodynamically focuses the sample suspension into a very thin sample stream (Nolan and Yang 2007) (Figure 2.6a). Once in single cell flow, the sample passes through an illumination system, where each individual particle is interrogated by one or more beams of light. The resulting light-scattering and fluorescence is directed by multiple optical filters to the appropriate photomultiplier detector tubes and then converted to electrical signal by the optical and electronics system (Figure 2.6c). These electronic signals can be processed and stored by the computer control system and provide information about the particles properties (Radcliff and Jaroszeski 1998). Partially diffracted light is collected by the forward scatter detector (FSC) as a measure of relative cell size. Light that is reflected or refracted is collected by the side scatter detector (SSC) and relates to the complexity of the cell. FCS and SSC are unique for every cell type and the combination of these parameters can
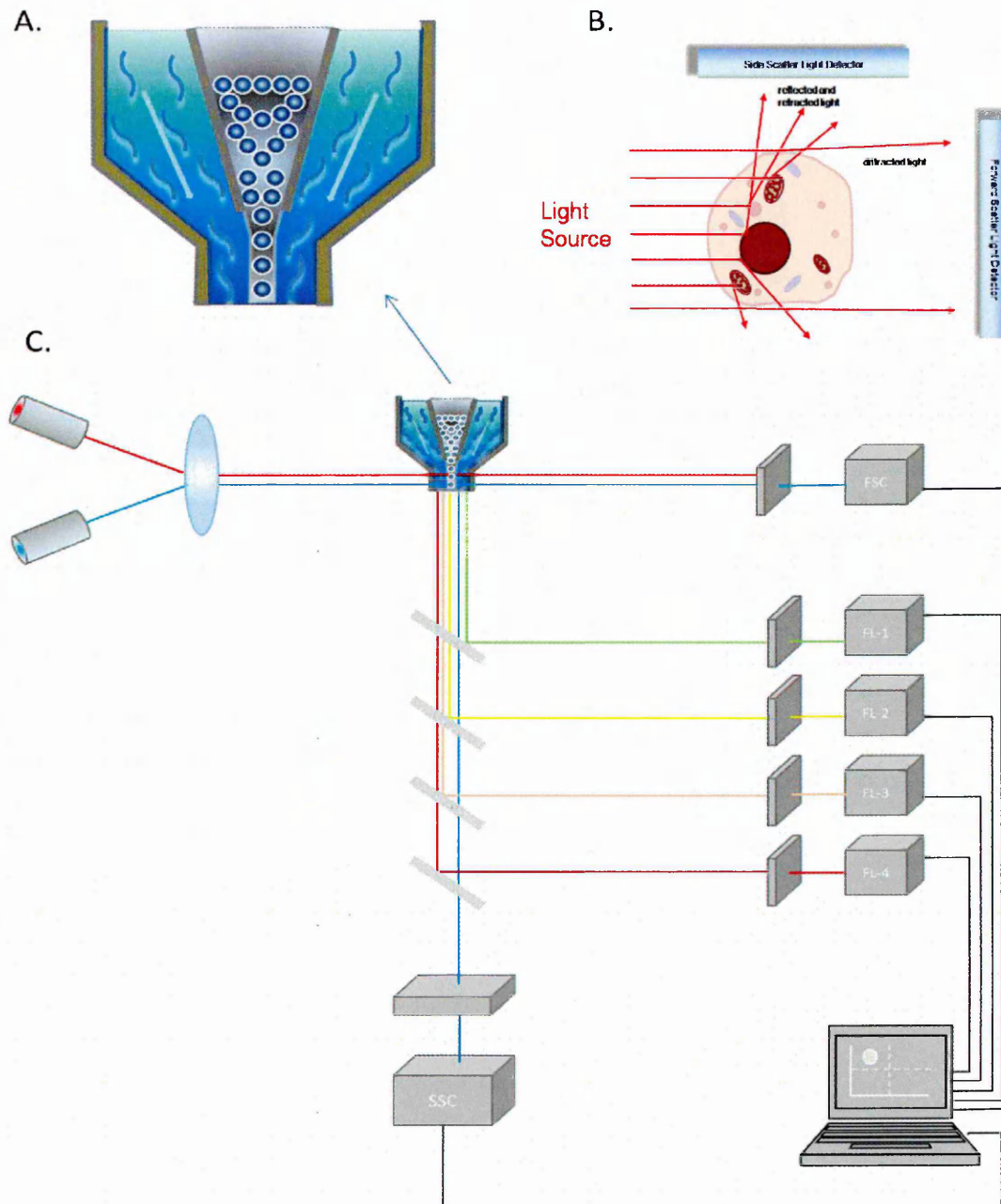
Figure 2.6; Schematic representation of flow cytometry analysis. Samples of cell suspensions are drawn into the flow cytometer and the drag effect of the fast flowing sheath fluid surrounding the samples creates a single stream of cells (A). Light that is scattered in the forward direction (FSC) is diffracted light related to surface area and provides information of the cell or particle size. Light scattered at approximately 90° to the excitation light beam is reflected and refracted light, known as the side scatter (SSC) and provides information related to granular content and complexity of the cell or particle (B). Samples are interrogated by light and lasers to ascertain cellular information. The different signals emitted are filtered and reflected to appropriate detectors (FL1-4) which relay the signal to a computer where data is analysed (C). Adapted from
http://www.abdserotec.com/support/introduction_to_flow_cytometry-685.html

be used to differentiate cell types and distinguish between live cells and cellular debris. Fluorescence measurements at different wavelengths, dependent on the fluorochrome selected, are distinguished by separate detectors and provide information about specific cellular molecules typically identified by fluorescent conjugated antibodies.

The resulting flow cytometry data is graphically presented with interpretation reliant on processing the data within histograms and dot plots. The technique of gating or drawing regions around populations on dual parameter plots allows the exclusion of particles that may interfere with analysis and the focussed examination of populations of interest. This increases the specificity but also increases the extent of user-defined parameters and requires stringent standardisation between experiments for reliable and comparable results (Herzenberg *et al.* 2006).

2.2.10.1   *Optimisation of cell retrieval from culture for flow cytometry*

To maximise cell viability and minimise cell surface disruptions, the method of cell removal of adherent cells from culture flasks to produce a single cell suspension for flow cytometry was investigated.

Method

Cells were seeded at an initial density of 1×10^5 cells/ml into culture flasks ($25 cm^2$) in complete medium equivalent to $1 ml/5 cm^2$. Cells were incubated for 24h prior to treatment, then washed twice with PBS and incubated for a further 24h in serum-free media containing 10ng/ml TNFα plus IFNγ to induce CX_3CL1 expression. Four different methods were used to remove cells from culture flasks; addition of 3ml 0.5% trypsin/0.2% EDTA (GIBCO®) for 5min at room temperature, 3ml non-enzymatic cell dissociation solution (Sigma-Aldrich, UK) at room temperature until cells were dislodged, 3ml non-enzymatic cell dissociation solution at 37°C until cells were dislodged, or cell scraping. Samples were then analysed for CX_3CL1 expression by flow cytometry and the suitability of each removal method was assessed based upon cell viability and the preservation of cell surface CX_3CL1 expression.

2.2.10.2   *Flow cytometry method*

3ml of complete media was added to cells removed from culture flasks enzymatically or cells were gently scraped from the flask surface whilst still in growth medium. The resulting cell suspension was dispensed into a sterile tube and centrifuged at 208 x g for 5min to pellet the cells. The cells were resuspended in 1ml of PBS containing 1% FCS (GIBCO®, UK) and cells were

counted using a haemocytometer. The cell suspension was divided into appropriate tubes at a concentration of 1 x 10^6 cells per tube and 1ml of PBS/FBS was added to each tube. Cells were centrifuged for 5min at 208 x g and the resulting supernatant discarded. Cell pellets were resuspended in 50µl of PBS/FCS and 5µl of previously titrated conjugated antibody (anti-human CX$_3$CL$_1$ Phycoerythrin MAb IgG$_1$, anti-human ADAM17 Fluorescein MAb IgG$_1$; R&D Systems, UK) or isotype control (Mouse IgG$_1$ Phycoerythrin Isotype Control, Mouse IgG$_1$ Fluorescein Isotype Control; R&D Systems, UK) was added. Samples were mixed thoroughly and incubated at 4°C for 1h. To remove any unbound antibody, 1ml of PBS/FBS was added to each tube, mixed and centrifuged at 208 x g for 5min. Supernatant was removed and the resulting pellet was resuspended in 300µl of PBS/FBS. Directly before samples were analysed, 25µl of propidium iodide (100µg/ml in PBS; Sigma-Aldrich, UK) was added to the cell suspension and mixed thoroughly. All samples were analysed on a FACS Calibur flow cytometer and data processed using Cell Quest Pro software (Becton Dickinson, UK). 10,000 events were measured per sample and the mean fluorescence index (MFI) was calculated by subtracting the geometric mean fluorescence of isotype controls from geometric mean fluorescence of samples.

2.2.11 Molecular investigation of gene expression in human aortic vascular cells using semi-quantitative real-time reverse transcription polymerase chain reaction (qRT-PCR)

Reverse transcription polymerase chain reaction (RT-PCR) is an improvement on the classical PCR reaction, in which specific sequences of DNA are amplified through thermocycling. If the gene of interest is present in a sample, then the primers anneal to their corresponding sequence and amplification takes place in an exponential manner as the thermocycling conditions, or cycle, are repeated to allow millions of copies of the target DNA to be synthesised (Templeton 1992). RT-PCR measures target gene expression in mRNA samples and first requires the reverse transcription of mRNA to a complementary DNA (cDNA) sequence. This is achieved by the enzyme reverse transcriptase which elongates and copies the single-strand RNA using deoxynucleotide triphosphates (dNTPs), at primer initiated sites, to make long single-stranded cDNA sequences of the entire length of RNA. Once cDNA templates have been synthesised the conventional PCR reaction can be utilised, whereby primers designed to sit at 3' and 5' ends of a specific DNA sequence initiate DNA polymerase activity to copy the target sequence into double-stranded DNA. The double-stranded DNA product from this reaction undergoes many repeats (cycles) of the thermocycling conditions; heating to denature the hydrogen bonds of the alpha-DNA helix thus separating the strands, and cooling

to anneal primers and encourage polymerisation, allowing millions of copies of target DNA to be synthesised exponentially. The amplified product of known length (amplicon), denoted by the distance between the primers on the target sequence of the gene, is produced and can be measured and semi-quantified by agarose gel electrophoresis. This analysis is subject to considerable variability due to the precision of the agarose gel in resolving band size and the quantification of ethidium bromide fluorescence imaging. In addition, the end-point data collection allows inclusion of variations in enzyme kinetics between each reaction, or tube (http://www.appliedbiosystems.com/absite/us/en/home/applicationstechnolo gies/real-time-pcr/real-time-pcr-vs-traditional-pcr.printable.html). These differences begin to appear in the linear phase of amplification and present most clearly at the plateaux phase towards the end of the repeated cyclings (or run) as reagents are being consumed and kinetics vary. Replicates of the same sample will behave differently and express variable end-point results due to these factors (Figure 2.7).

Real-time RT-PCR, as the name suggests, measures amplification cycle by cycle in real-time. By quantifying PCR product while the reaction is in the exponential phase of amplification and where there is an exact doubling of product every cycle, the precision of the analysis is greatly enhanced. The real-time RT-PCR assay measures fluorescent signal produced during each cycle of the PCR reaction by either intercalation of a fluorogenic dye into double-stranded DNA (SYBR Green), or the separation of a fluorescent molecule from its adjacent signal quenching molecule (TaqMan®, Molecular beacons, Scorpions®) (Wong et al. 2005). As more of the amplicon is produced the fluorescence intensifies. Individual reactions are characterised by the PCR cycle at which the fluorescence first increases above a background or threshold level (Cycle threshold; Ct), which is usually ten times the standard deviation of the baseline measurement (Wong et al. 2005). The increase in fluorescent signal and the point at which it crosses the specified threshold is proportional to the amount of starting DNA target, thus allowing quantification of target molecules. As real-time PCR collects data during the exponential phase, which is the most constant and reproducible phase of PCR amplification, increased accuracy in the calculation of relative abundance of the target molecules is permitted and the high degree of variability generated by measuring the PCR end product is eliminated (Figure 2.7).

2.2.11.1 RNA Extraction

Total RNA can be isolated from cells or tissue directly and rapidly through the use of organic and aqueous solvent separation. TRI® reagent (Sigma-Aldrich, UK) combines phenol and guanidine thiocyanate in a monophasic solution to rapidly inhibit RNase activity, slowing and
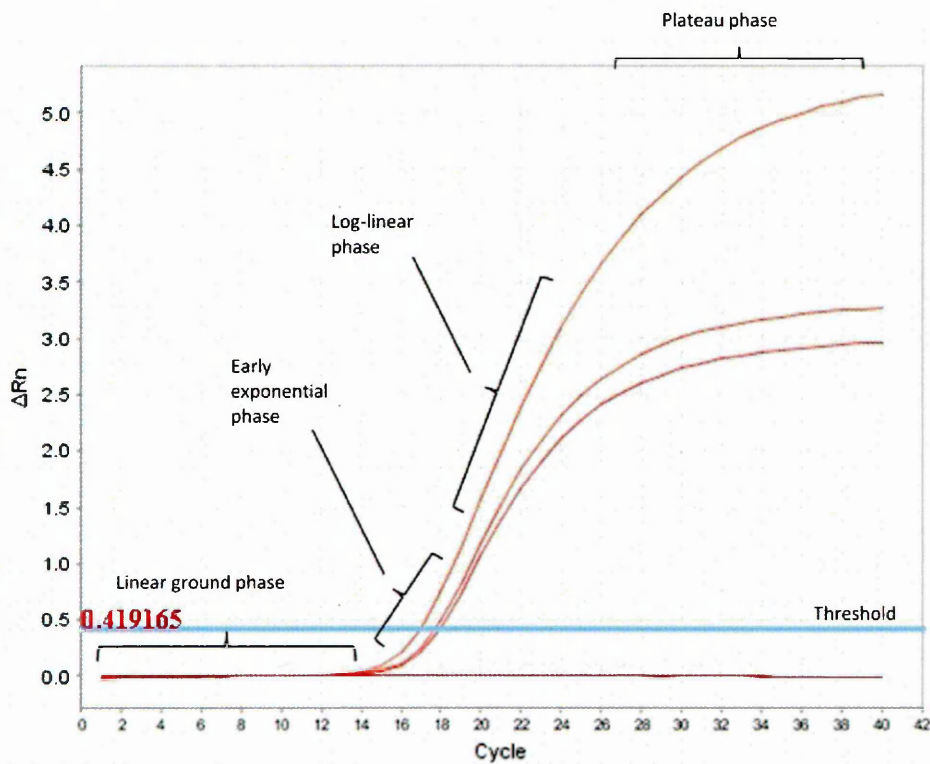
Figure 2.7; qRT-PCR amplification plot. Real-time PCR measures fluorescence at the exponential phase of amplification, increasing accuracy and reliability and reducing the inter-reaction variability of end-point measurement. Repeats of the same sample possess only a small amount of variability at the exponential phase, but this presents as large differences by the end of the amplification.

preventing RNA degradation. The addition of chloroform enables the phasic separation of protein, DNA and RNA simultaneously into aqueous and organic layers. Once separated, RNA can be precipitated and washed to yield RNA suitable for downstream applications such as qRT-PCR.

Method

RNA was extracted from cultured cells using TRI® reagent according to the manufacturer's instructions. In brief, 200μl or 400μl of TRI® reagent was added directly onto 24-well and 6-well culture plates respectively to lyse the cells, disrupting and solubilising cellular components. The resulting solution was repeatedly pipetted, transferred to a tube and vortexed to ensure complete cellular disruption. Chloroform (Sigma-Aldrich, UK) was added, equivalent to 100μl per 1ml of TRI® reagent, and samples were vortex mixed then allowed to stand for 5 minutes at room temperature. Samples were centrifuged at 12,000 x g for 15min at 4°C to separate protein, DNA and RNA into three layers. The upper aqueous layer containing RNA was removed to a clean 1.5ml tube, then 500μl of isopropanol per ml of TRI® reagent added, vortex mixed briefly, left to stand at room temperature for 5min and centrifuged at 12,000 x g for 10min at 4°C. The supernatant was discarded and the precipitated RNA pellet was washed by adding 1ml of 75% ethanol, vortex mixed and centrifuged at 12,000 x g for 5min at 4°C. The supernatant was discarded and the resulting RNA pellet was briefly air dried and solubilised in 10-50μl of diethylpyrocarbonate (DEPC)-treated water (Sigma-Aldrich, UK).

2.2.11.2   *Quantification of RNA*

It is advantageous to use approximately the same amount of RNA when comparing different samples to minimise variations in reverse transcription kinetics and ultimately cDNA product; therefore, accurate RNA quantification is beneficial.

The NanoDrop® ND1000 (Labtech International Ltd, UK) is a full-spectrum UV/VIS spectrophotometer capable of measuring nucleic acid concentrations and sample purity in small sample volumes (as low as 1μl). Using surface tension, an aqueous sample forms a column between the two fibre optic-containing pedestals. Light is passed through the sample and absorbance measured at difference wavelengths for the appropriate concentration and purity analysis (Gallagher 2008). Measured at 260 and 280nm, the nucleic acid concentration is calculated using a slightly modified Beer-Lambert equation;

$$c=(A*e)/b$$

c, is nucleic acid concentration
A, is absorbance in AU
e, is wavelength-dependent extinction coefficient in ng-cm/μl
b, is pathlength in cm

This predicts a linear change in absorbance with concentration. Sample concentrations are calculated automatically with the NanoDrop® software and are represented as ng/μl. The ratio of sample absorbance at 260 and 280nm provides an indication of the RNA purity (acceptable at approximately ~2.0±0.4). Acceptable ranges may be established for individual studies. The ratio of sample absorbance at 260 and 230nm is a secondary measure of nucleic acid purity and may indicate the presence of co-purified contaminantes (accepted as 'pure' at approximately ~1.8-2.2) (http://www.bio. davidson.edu/projects/gcat/protocols/ NanoDrop_tip.pdf).

Method

1μl of sample or blank was pipetted onto the lower measurement pedestal. The upper measurement pedestal was lowered and brought into contact with the sample, which was analysed as described above. Samples were wiped clear from the measurement pedestals between each analysis. DEPC-treated water was used as a blank control measurement to calibrate the NanoDrop.

2.2.11.3   *Determination of RNA Integrity*

Assessment of RNA integrity is an additional control to minimise non-specific sample variations and unrepresentative expression profiles of target genes. Where moderately degraded RNA samples may still result in reasonable and comparable RT-PCR when normalised to reference genes, the use of high quality RNA will provide the most accurate and reliable down-stream analysis reflective of a sample's natural state (Fleige and Pfaffl 2006) and reduce any potential gene-specific differential degradation of individual mRNAs, that would ultimately affect analysis (Bustin *et al*. 2005).

RNA integrity can be assessed by agarose gel electrophoresis. The gel is stained with ethidium bromide, and the presence of two sharp bands denoting 28S and 18S rRNA components in the gel are used as an indicator of RNA integrity. The brightness of the 28S and 18S bands under UV light should possess an intensity ratio of approximately 2:1 respectively (Sambrook and Russel 2001).

Method

2μl of the extracted RNA sample was mixed with 2μl loading buffer (Promega, UK) and loaded onto a 1% agarose gel pre-stained with ethidium bromide. To form the agarose gel, 1g of agarose (Bioline, UK) was dissolved in 50ml TBE buffer (89mM Tris-HCl pH 7.8, 89mM borate and 2mM EDTA) with 2μl ethiduim bromide (10mg/ml). Using TBE as the buffer, the gel was

run for 30 minutes at 100v and the resulting gel was visualised on a UVP Bioimaging system using LabWorks 4 software (Bio-Rad, UK).

2.2.11.4   cDNA Synthesis

Accurate and precise quantification of RNA targets relies on the performance of the reverse transcription reaction and subsequent conversion to cDNA. The priming method for cDNA synthesis can vary dependent upon the characteristics of the sample and down-stream application, with advantages and disadvantages to each that have to be considered before selection (Bustin and Mueller 2005, Bustin *et al*. 2009).

Random primers (or random hexamers) anneal to the RNA template at multiple locations and produce more than one cDNA target per original mRNA template. Random hexamers transcribe the entire RNA sequence producing cDNA that covers the whole transcript and is a useful priming method, when several different amplicons need to be analysed from a small amount of RNA. Based on this, random primers were selected as the priming method for cDNA synthesis in this study.

RNA is reverse transcribed into cDNA by the enzyme reverse transcriptase (RT). Initiated by the binding of the primer, RT elongates the sequence using dNTPs to produce a complementary sequence.

Method

RNA was diluted in DEPC-treated water (Sigma-Aldrich) to give a concentration of 1μg in 10μl in a PCR tube. To each tube the reaction components from the high capacity cDNA synthesis kit (Applied Biosystems, UK) were added (2μl reverse transcription buffer, 0.8μl dNTPs mix, 2μl random primers, 1μl RT enzyme, and 4.2μl nuclease-free water) to give a final volume of 20μl. The samples were then loaded into a thermocycler and run on the following single cycle;

	STEP 1	STEP 2	STEP 3	STEP 4
Temperature(°C)	25	37	85	4
Time	10min	120min	5sec	Hold

A minus RT control reaction was utilised to investigate genomic DNA contamination for each cell type or experimental procedure used. In this reaction all components were included other

than the RT enzyme. The lack of amplification in these samples in the subsequent qRT-PCR analysis indicated no contamination from genomic DNA.

2.2.11.5 *qRT-PCR using TaqMan® methodology*

TaqMan sequence detection chemistry has three levels of specificity for targeting a gene of interest. In addition to forward and reverse primers, an oligonucleotide probe designed to target a specific sequence that lies within the amplified target sequence, or amplicon, of the primers provides an extra level of specificity compared to standard PCR and non-specific dye intercalation methodologies (Bustin *et al.* 2005). This greatly reduces the chance of mis-priming events leading to the amplification of alternate sequences to the target, and eliminates the possibility of primer-dimer formation (where primers bind with themselves) resulting in fluorescence emission.

The oligonucleotide probe contains a high-energy fluorescent reporter dye on the 5' end and a subsequent low-energy quencher dye on the 3' end. The fluorescence of the reporter dye is greatly reduced by the proximity of the quencher through a process known as fluorescence resonance energy transfer (FRET) through space (Livak *et al.* 1995). If the target sequence is present in the DNA sample, then the probe anneals downstream from one of the primer binding sites. As amplification takes place, the nuclease activity at the 5' end of the Taq DNA polymerase cleaves the probe as the primers extend. This separates the reporter dye from the quencher, and fluorescence signal is emitted when excited. The probe is eventually removed from the target strand and the full amplicon sequence synthesised (Figure 2.8). This process continues with each cycle resulting in an increase in fluorescence intensity relative to the amount of amplicon produced as increasing amounts of probe are cleaved. The cycle at which the fluorescence intensity increases above the threshold (Ct) is proportional to the initial abundance of the target sequence (or gene) (Bustin *et al.* 2005).

Method

TaqMan primer probes (see Appendix 1 for product detail) were purchased as pre-designed, pre-optimised assays intended to cross exon-exon boundaries in the target gene sequence to ensure that only DNA transcribed from mRNA was amplified (Sandhu and Acharya 2005).

For each gene target 1μl of sample or controls (no RT controls and no template controls) were carefully pipetted in triplicate into 384-well or 46-well PCR plates (Applied Biosystems, UK) on ice. This was followed by 4.2μl of DEPC-treated water (Sigma-Aldrich, UK), 4μl of TaqMan® Universal PCR mastermix (Applied Biosystems, UK) and 1μl of the target-specific primer-probe mix (Applied Biosystems, UK). Plates were covered with an adhesive film, centrifuged to
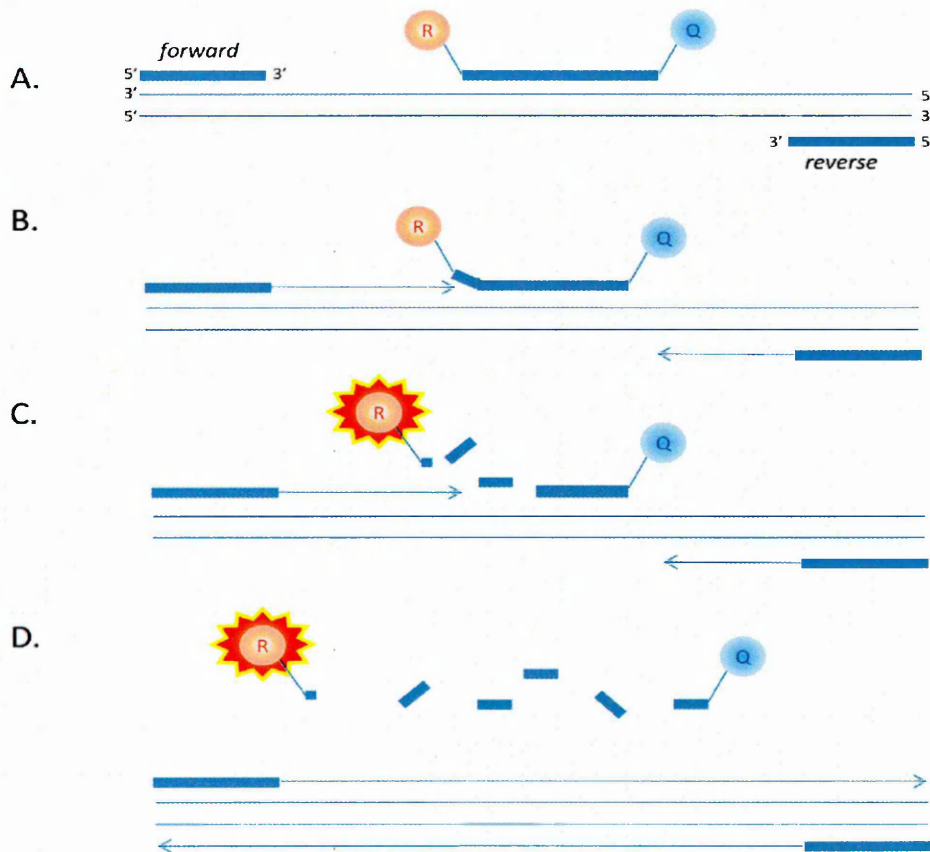
Figure 2.8; Schematic representation of the qRT-PCR TaqMan chemistry. A) Sequence-specific forward and reverse primers and oligonucleotide probe hybridise to the target DNA template. As amplification takes place, the nuclease activity at the 5' end of the Taq DNA polymerase cleaves the probe as the primers extend (B and C). This separates the reporter dye (R) from the quencher (Q), and fluorescence signal is increased. D) The probe is eventually removed from the target strand and the full amplicon sequence synthesised.
Adapted from; www3.appliedbiosystems.com/AB_Home/applications technologies/Real-TimePCR/TaqManvsSYBRGreenChemistries/index.htm

ensure that all solutions were collected at the bottom of the wells then analysed using either the 7900HT PCR system or StepOne™ real-time PCR system (Applied Biosystems, UK) for 384-well and 46-well plates respectively using the following cycle;
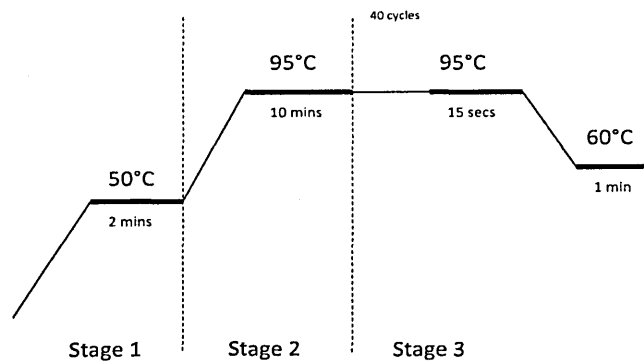
The universal PCR mastermix contained a passive reference fluorescence dye, ROX™, which the reporter dye is normalised to during analysis to control for fluctuations in reaction concentrations or volumes caused by pipetting errors. No template controls (NTC) were included for each target on each plate to detect PCR contamination or determine any unintended amplification.

2.2.11.6 Selection of endogenous control reference genes

Accurate normalisation of gene expression is essential for the reliable quantification and comparison of gene expression studies. In order to measure variations in the levels of a target gene's mRNA across a range of samples, expression values must be represented relative to the expression of endogenous control genes, or reference genes (often referred to as housekeeping genes) (Vandesomple *et al.* 2002). Reference genes are presumed to be continually expressed as they produce proteins necessary for basal cellular function. Ideally this expression should not only be continuous but also unaffected by experimental conditions, creating an internally stable reference. By normalising to an endogenously consistent reference gene expression, variations in total RNA quantity and quality, enzymatic efficiencies and differences between cells or tissues can be accounted for and controlled for in order to identify real gene-specific variation (Vandesomple *et al.* 2002, Bustin *et al.* 2005, Fleige and Pfaffl 2006). However, all genes are regulated to some extent and are not all expressed independently of experimental conditions (Bustin *et al.* 2005). It is therefore necessary to thoroughly validate the use of reference genes for each tissue or cell type and for all experimental treatments as the selection of appropriate controls affects the validity of the results (Thellin *et al.* 1999).

To validate the presumed stability of a particular reference gene, it is necessary to normalise its own expression, to control for the previously mentioned nonspecific variations, creating a circular problem (Vandesomple *et al.* 2002). GeNorm (Primer Design Ltd, UK) is an algorithm-based computer program that uses a pair-wise comparison to rank the expression profile of each reference gene against that of all other reference genes to elicit an expression ratio across experimental conditions. Stepwise exclusion of the lowest ranked genes reveals candidate reference genes demonstrating the most stable expression ratio relative to each other and identifies them as appropriate reference genes suitable for the experimental procedure (Vandesomple *et al.* 2002). It has been suggested that between three and five reference genes should be used for qRT-PCR investigation (Vandesomple *et al.* 2002). However this is impractical and costly for high throughput, low budget investigations (Barber *et al.* 2005). Therefore, GeNorm suggests the number of reference genes needed for accurate normalisation, based upon the relative stability of the highest ranked expression ratio combinations at an acceptable degree of variation which can be user-specified.

An additional consideration when selecting suitable reference genes is the relative abundance of that gene. Genes of low abundance, and therefore high Ct values, unavoidably give rise to poorer precision and decrease the capabilities of qRT-PCR to detect small-fold changes. By selecting reference genes that are stable and suitably abundant, accuracies of normalisation are improved (Thellin *et al.* 1999, Bustin *et al.* 2005).

Method

Six commonly used reference genes (RPL13A, β-actin, β-2 microglobulin, GAPDH, HRPT1 and SDHA) were tested for their stability across the experimental conditions in the investigation. To avoid co-regulation biases during reference gene selection, genes with unrelated functions were chosen (Table 2.4). Following qRT-PCR, reference genes with high Ct values or no amplification were excluded as unsuitable. The remaining reference genes were analysed using GeNorm software (Primer Design Ltd, UK) to determine the most stable genes within each experimental condition. Prior to input into the geNorm program, Ct values for each target were transformed to quantities relative to the highest expression of that target gene across the investigated sample conditions. This was achieved by subtracting the lowest Ct value from all Ct values for the given reference gene. The quantities were then converted to linear form to account for the logarithmic nature of the PCR reaction (Livak *et al.* 2001);

$$2^{-(\text{sample Ct - lowest Ct sample})}$$

Gene Symbol	Accession number	Gene name	Function	Aliases
GAPDH	NM_002046	Glyceraldehyde-3-phosphate dehydrogenase	Enzyme involved in glycolysis and gluconeogenesis	G3PD GAPD MGC88685
RPL13A	NM_012423	Ribosomal protein L13a	Structural component of the large 60S ribosomal subunit	
ACTB	NM_001101	Beta-actin (β-actin)	Cytoskeletal structural protein	PS1TP5BP1 BACTIN
B2M	NM_004048	Beta-2-microglobulin	Beta-chain of major histocompatibility complex class I molecules	
HPRT1	NM_000194	Hypoxanthine guanine phosphoribosyl transferase I	Involved in metabolic salvage of purines in mammals	HGPRT HPRT
SDHA	NM_004168	Succinate dehydrogenase complex, subunit A	Electron transporter in the citric acid cycle in mitochondria	FP SDH2 SDHF

Table 2.4; Summary of reference genes tested for qRT-PCR analysis. Six genes were investigated for suitability as endogenous controls for subsequent qRT-PCR analysis. The reference genes investigated were selected to have unrelated functions to minimise co-regulation biases.

The highest relative quantities for each gene were therefore set to one. These raw reference gene quantities were then inserted into the geNorm software, which calculates the relatively 'most stable' gene expression and suggests a potential number of reference genes required for accurate normalisation.

2.2.11.7   Determination of Primer Efficiencies

With optimal amplification efficiency (100%) there is a doubling of PCR product with every cycle during the exponential phase of PCR amplification (Livak *et al.* 2001). The relative quantification method relies on the efficiencies of the primers used to be approximately equal and optimally as close to 100% as possible.

A two-fold serial dilution of the template cDNA ranging from 1:1 to 1:32 in DEPC-treated water was created to assess primer efficiencies. A plot of Ct values for all target and reference genes against log dilution factor was constructed. A linear trendline was applied, with the slope of the line used to calculate the percentage efficiency of each primer.

$$Efficiency_x = 10^{(-1/slope)} - 1$$

Linear correlation with R^2 values >0.95 were demonstrated, indicating that the Ct values acceptably matched the trendline fitted. Exponential primer efficiencies between the ranges of 90-110% were accepted and considered to demonstrate acceptable comparability of amplification kinetics efficiency for investigated genes.

2.2.11.8   Validation of primer targets by electrophoresis

Products amplified by TaqMan primers in the real-time RT-PCR analysis for each target were further validated by visualisation on an agarose gel. Products should yield a single band, indicating that only one specific sequence has been amplified, at a known size

Method
8µl of real-time RT-PCR product for each target was mixed with 2µl of 5x loading dye (Promega, UK) and run on a 2.5% agarose gel at 100V for 30min. Bands were visualised using a UVP bioimaging system (BioRad, UK) and compared to expected band sizes as indicated from primer probe assays (Applied Biosystems, UK).

2.2.11.9   *Relative quantification analysis of qRT-PCR data*

Triplicate Ct values from the same sample were averaged to give a representative value and account for inter-assay variability. Mean Ct values of all sample targets were first normalised to the expression of the appropriate reference gene Ct to determine the ΔCt value;

$$\Delta Ct = Ct\ target - Ct\ reference$$

For semi-quantitative analysis of mRNA expression, the Ct values for target genes in experimental conditions were represented relative to their expression in control conditions. The control conditions, or calibrator sample, would therefore be the 'normal', 'untreated' or 'zero' sample. An average ΔCt of control samples from each repeat of the experiment was taken as the ΔCt calibrator value for which all other individual ΔCt values were normalised, including individual control ΔCts. This allowed for between-experiment variation to be accounted for in control samples. Test samples were presented as relative fold-change from control. This relative quantification was calculated as $\Delta\Delta$Ct;

$$\Delta\Delta Ct = \Delta Ct\ sample - \Delta Ct\ calibrator$$

This data was then converted to linear form to account for the exponential nature of the PCR reaction;

$$2^{-\Delta\Delta Ct}$$

The $2^{-\Delta\Delta Ct}$ value for calibrator control samples is approximately 1, and data is represented as fold-change from this calibrator control value (Livak *et al.* 2001).

$2^{-\Delta\Delta Ct}$ values of repeated experiments were presented as mean $\pm$ SEM and statistical differences between experimental groups were determined using the non-parametric Kruskal-Wallis test followed by Dunn's post hoc test.

2.2.12   Statistical Analysis

Data is presented as mean $\pm$ SEM unless otherwise stated. Experimental groups were assessed for normality by D'Agostino and Pearson omnibus normality test where eight or more individual values were applicable for each group. Where sample numbers were below eight, a Kolmogorov-Smirnov (KS) was applied to test goodness-of-fit of the sample population to a theoretical normal distribution that represents the typical 'bell-shaped' curve. Where sample numbers were too small (<6) to be graphically represented as the 'bell-shaped' curve on a

frequency distribution plot and subsequent KS test, non-parametric tests were employed (Zar 2010).

In addition, normally distributed samples were tested for equal variance within the groups as parametric tests assume this attribute within the data. Bartlett's test of homogeneity of variance was used to assess this. Data of unequal variance or non-normal distribution was transformed by logarithm, square root, or negative reciprocal and data retested for normality and variance. If the transformed data then met these requirements, parametric tests were applied to assess significant differences between sample means. Where three or more samples were compared a one-way ANOVA followed by Tukey's post hoc was used to establish the significance of any differences. For two group comparisons a student's t test was used. If the transformed data remained non-normal, of unequal variance, or sample size was considered too small for parametric analyses, a non-parametric Kruskal-Wallis test was applied to the original data for multiple groups, followed by Dunn's post hoc test. For two group comparisons a Mann Whitney U test was used. Significance was accepted at P≤0.05 (Zar 2010).

2.3 Results

2.3.1 Cell culture characterisation

Primary HASMC and HAEC proliferated at differential rates, with endothelial cells exhibiting a much longer doubling time (approx 48h and 96h respectively)(Figure 2.9). In addition, while SMC were relatively robust with regard to the stresses of subculture, recovering within hours of trypsin dislodgement and splitting, endothelial cells required a longer period of time to return to a steady proliferative state (approximately overnight). Endothelial cells continued to proliferate for only 3-4 passages after removal from liquid nitrogen and after two freeze-thaw cycles. HASMC, in contrast, retained a steady state of proliferation after many passages and withstood multiple freeze-thaw cycles, maintaining comparable doubling times beyond passage 12. Cells were used experimentally below passage 10, for both cell types, to ensure phenotypic consistency. The growth patterns of the cells restricted the number of experiments, due to the difficulty in obtaining sufficient numbers of endothelial cells for experimental procedures. For this reason, most of the preliminary investigations were carried out on HASMC, with endothelial cells utilised for the principal experiments where possible, dependent on cell numbers.

Within the cell passage limits, cell morphology remained consistent for both cell types, with characteristic phenotype markers diffusely expressed when investigated by immunocytochemistry at early and late passages. HASMC expressed smooth muscle α-actin, but were negative for von Willebrand Factor (vWF), an exclusive endothelial protein, while tubulin staining demonstrated the cytoskeletal substructure of the cells (Figure 2.10). HAEC, as expected, were positive for vWF and negative for α-actin, although a low level of non-specific staining could be seen (Figure 2.10). This may be the result of potential cross-reactivity between alternate and common actin isoforms of the cytoskeleton, which share a high percentage of sequence homology, even at the variable N-terminus region where the antibody was directed (Skalli et al. 1986). Again, tubulin staining highlighted the cytoskeletal structure of endothelial cells comparable with that of smooth muscle cells (Figure 2.10).

Analysis of cell culture supernatants for mycoplasma infection demonstrated negative results for all cells used in this investigation. HASMC and HAEC were tested routinely at intervals throughout the duration of the investigation. THP-1 cells and DuCAPs were tested once prior to experimentation, due to the short time-frame of use in the project, but also showed no mycoplasma was present in the cultures. Figure 2.11 shows a representative agarose gel of
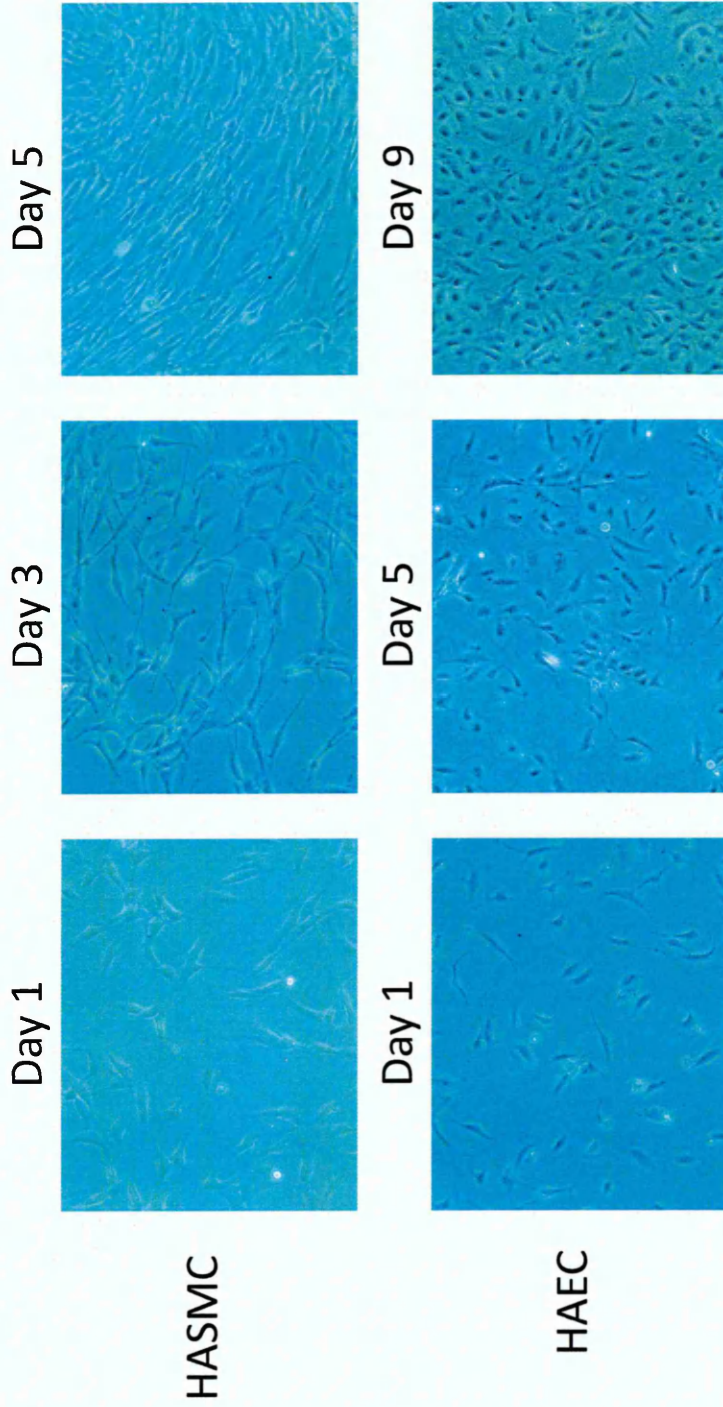
Figure 2.9: Cell proliferation of human aortic smooth muscle cells (HASMC) and human aortic endothelial cells (HAEC) in culture over time. Both primary cell types have an elongated shape, HASMC being much more elongated. HAEC proliferate at a slower rate and form a tight monolayer when confluent with typical cobblestone appearance. HASMC form a tight striated monolayer when confluent *Magnification x100.*
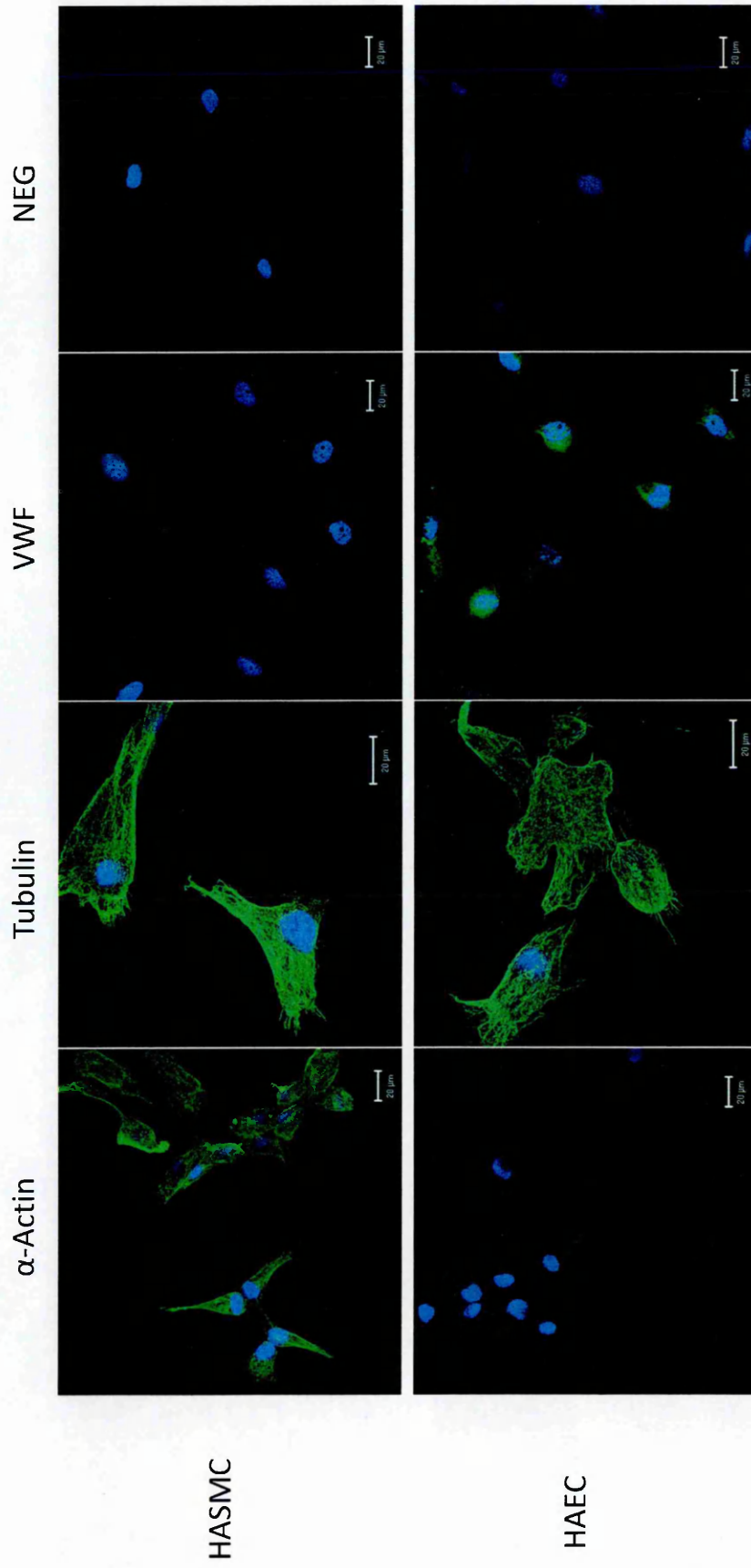
Figure 2.10; Human aortic vascular cell expression of characteristic cell markers detected by immunocytochemistry. HASMC stain positive for α-actin (Alexafluor 488; green) and negative for vWF. HAEC display positive staining for vWF (Alexafluor 488; green) but negative for α-actin. Tubulin (Alexafluor 488; green) displays cytoskeletal structure in both cell types. Negative controls, omitting the primary antibody demonstrated no non-specific binding of secondary antibody. Cells are counterstained with DAPI (Blue).

resulting PCR products from the mycoplasma test.

2.3.2 Optimisation of cytokine treatments

HASMC were treated with TNFα, IFNγ or IL-18, either alone or in combination, and at a range of concentrations from 0-100ng/ml. ELISA of the cell culture supernatants, as a measure of cleaved CX_3CL1, demonstrated that combination of TNFα with IFNγ produced the largest effect on CX_3CL1 upregulation (Figure 2.12). TNFα alone had no significant effect on cleaved CX_3CL1 expression, and a similar finding was seen with IL-18. IFNγ alone increased CX_3CL1 expression in a dose-dependent manner, reaching significance at 100ng/ml. When SMC were co-treated with TNFα and IFNγ, expression of CX_3CL1 was significantly upregulated, in a dose-dependent manner. These two cytokines seemed to act synergistically, as the magnitude of CX_3CL1 expression was more than additive compared to the effect of these factors alone. When IL-18 was combined with either IFNγ or TNFα plus IFNγ, no additional increase in CX_3CL1 expression was observed, (Figure 2.12). The combination of TNFα with IFNγ was therefore selected as an appropriate cytokine treatment to induce detectable and significant CX_3CL1 upregulation.

A time course of expression of cleaved (measured in supernatants) and cell-bound (measured in cell lysates) CX_3CL1 was measured by ELISA. Cleaved CX_3CL1 expression increased with time in response to TNFα plus IFNγ treatment of cells, at both 10ng/ml and 100ng/ml, with the largest effect seen at 24 and 48h (Figure 2.13). Increased expression of cleaved CX_3CL1 was first detected at the 16h time point, indicating a lag between cytokine-induced upregulation and subsequent enzymatic cleavage. Cell-bound CX_3CL1 expression was increased more rapidly in response to these cytokines, with detectable increases observed as early as 2h post-treatment. Expression peaked at between 8 and 16h then steadily started to decrease from 24h, in a dose-dependent manner, returning almost to basal expression levels by 48h at both concentrations of cytokine stimulations (Figure 2.13b). Controls, in which there was no cytokine treatment, showed very little cleaved and cell-bound CX_3CL1 expression over time. Taking into consideration the increases in both cleaved and cell-bound CX_3CL1 expression, an incubation time of 24h was chosen for the cytokine stimulations for all subsequent experiments.

2.3.3 Optimisation of Flow Cytometry

In this study flow cytometry was used to measure protein expression in live cells. Therefore, the methods for removal of adherent cells from the culture surface were compared to ascertain the optimal procedure for maximal cell viability, whilst maintaining the cells'
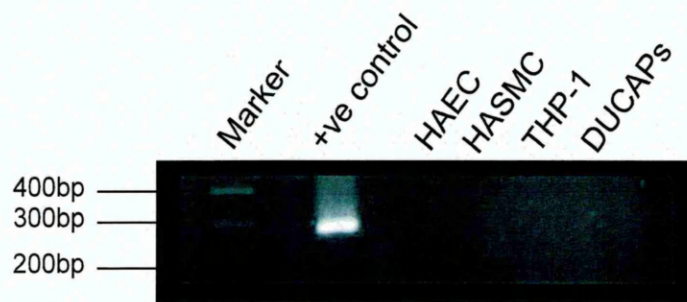
Figure 2.11: Agarose gel electrophoresis of mycoplasma PCR products. Cells were tested for mycoplasma contamination. Following PCR and 1% agarose gel electrophoresis, the absence of a band at 285bp in cell culture supernatants indicated that all cell cultures were negative for the presence of mycoplasma.
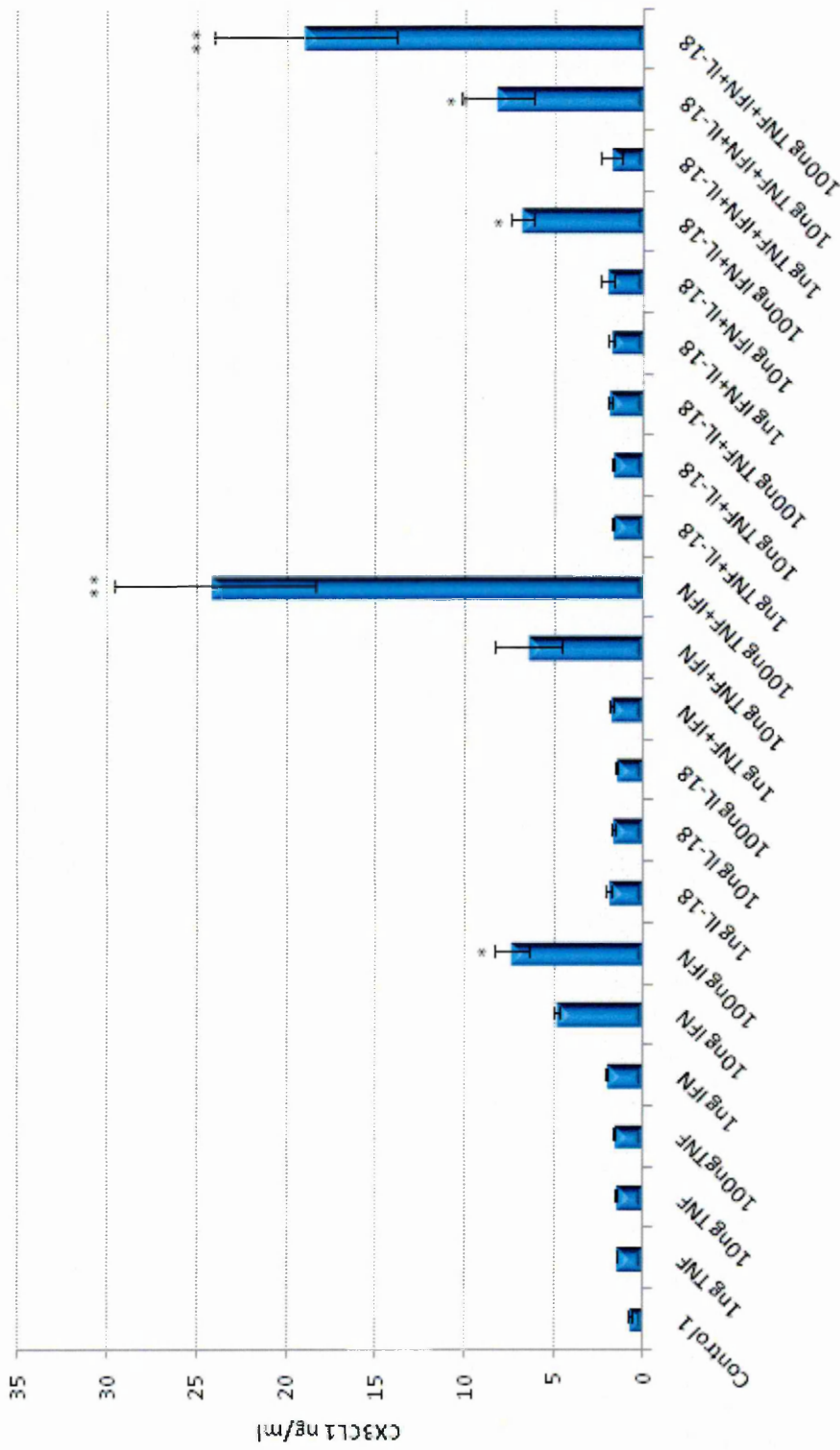
Figure 2.12: ELISA determination of CX₃CL1 protein expression in HASMC culture supernatants following cytokine treatment. A significant increase in cleaved CX$_3$CL1 expression was observed for several cytokine treatments, with the largest effect demonstrated for TNFα + IFNγ in combination. n=3 *P<0.05, **P<0.01.

A. Cell Supernatants
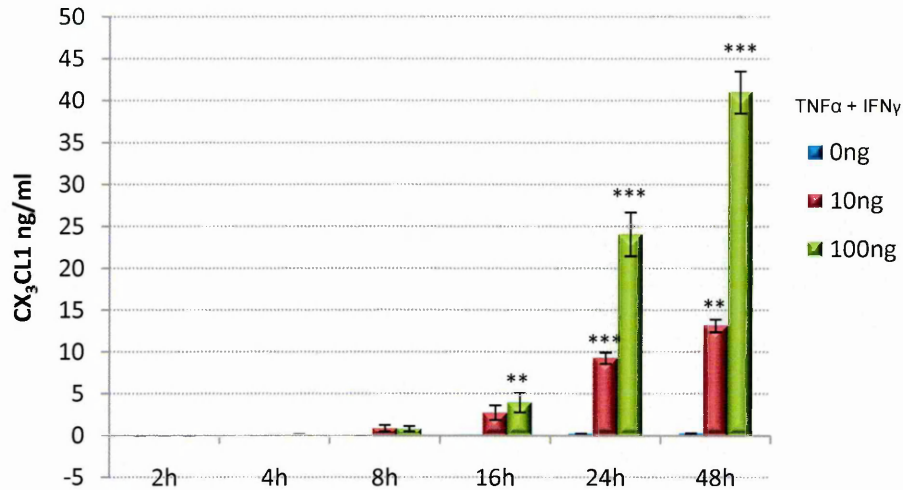
B. Cell Lysates
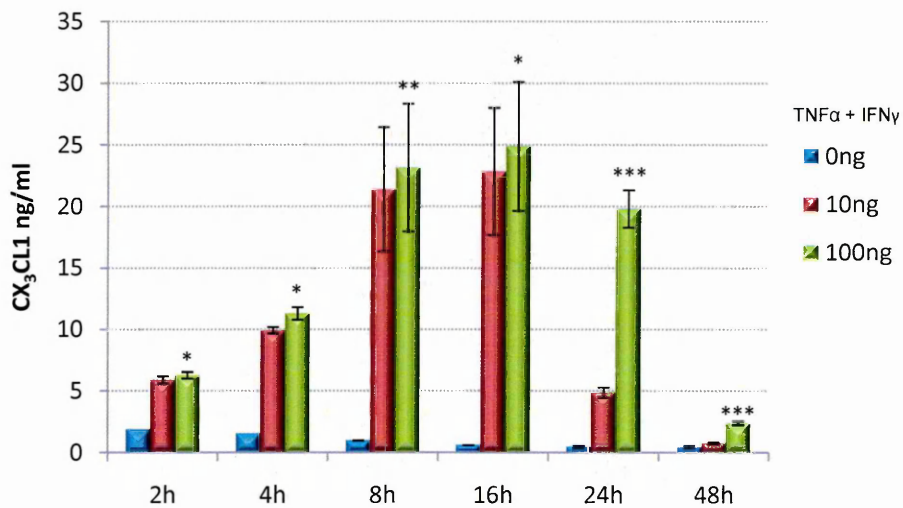
Figure 2.13 Investigation of CX₃CL1 protein expression over time in HASMC following cytokine treatment measured by ELISA. Cleaved (supernatant) CX₃CL1 expression increased significantly from 16h compared to control (A). Cell bound (lysate) CX₃CL1 expression increased more rapidly following cytokine treatment, peaking at 16h before falling back to basal levels by 48h (B). n=3 *P<0.05, **P<0.01, ***P<0.001 vs control (0ng) Kruskal-Wallis n=3.

structural integrity. Cell viability was maintained above 90% when cells were removed by trypsin or 37°C cell dissociation solution methods, with trypsin displaying slightly superior viability (94.97% and 93.75% respectively). Removal of cells by room temperature cell dissociation solution resulted in a lower cell viability, potentially due to the extended period required for complete removal from the surface which was approximately 45 minutes. Cell scraping produced the lowest cell viability most likely due to the severe physical detachment of this method (Figure 2.14). CX_3CL1 expression was induced by 10ng/ml TNFα plus IFNγ treatment for 24 hours and then cell-surface expression was measured in cells removed by all methods. Although trypsin removal maintained cell viability, it appeared to cleave CX_3CL1 from the cell surface, and low expression was observed (Figure 2.15). This was also apparent for the few viable cells analysed following removal by cell scraping. Removal of cells by the cell dissociation solution at room temperature resulted in a retention of slightly more CX_3CL1 on the cell surface, but this was still greatly reduced compared to cells removed by the 37°C cell dissociation solution method (Figure 2.15). Thus, the latter method was selected as the removal method for all cells in subsequent experimental procedures.

2.3.4 Optimisation of qRT-PCR

Integrity of the RNA isolated from the cells was assessed by agarose gel electrophoresis. The presence of two sharp bands, denoting 28S and 18S rRNA components, with an intensity ratio of approximately 2:1 respectively (Fleige and Pfaffl 2006) was observed, indicating acceptable RNA integrity for the majority of samples (Figure 2.16). Where no bands, a single band, blurred bands or bands of the wrong size were detected, the final wash steps of the RNA extraction process were repeated and samples analysed again, otherwise these samples were not included in subsequent analysis.

2.3.4.1   Selection of endogenous reference gene controls

Six reference genes (RPL13A, β-actin, β-2 microglobulin, GAPDH, HRPT1 and SDHA) were tested for their stability across the experimental conditions and suitability for the qRT-PCR investigation. HRPT1 and SDHA were excluded from further analysis, due to low expression or unexpected product characteristics upon agarose gel analysis (data not shown). The remaining reference genes were tested under all experimental conditions. GeNorm established RPL13A and GAPDH to be the most relatively stable genes expressed in HASMC and HAEC. For all subsequent qRT-PCR experiments target gene expression was normalised to these two reference genes.
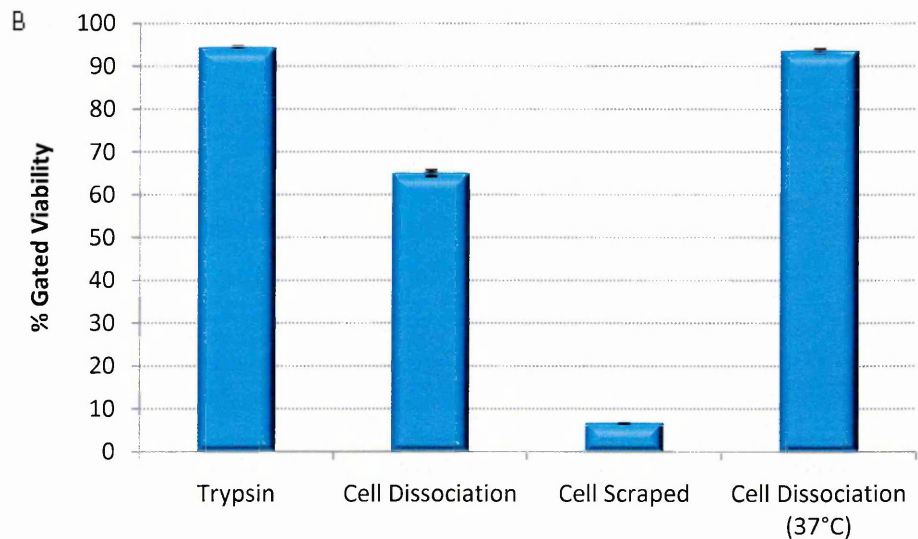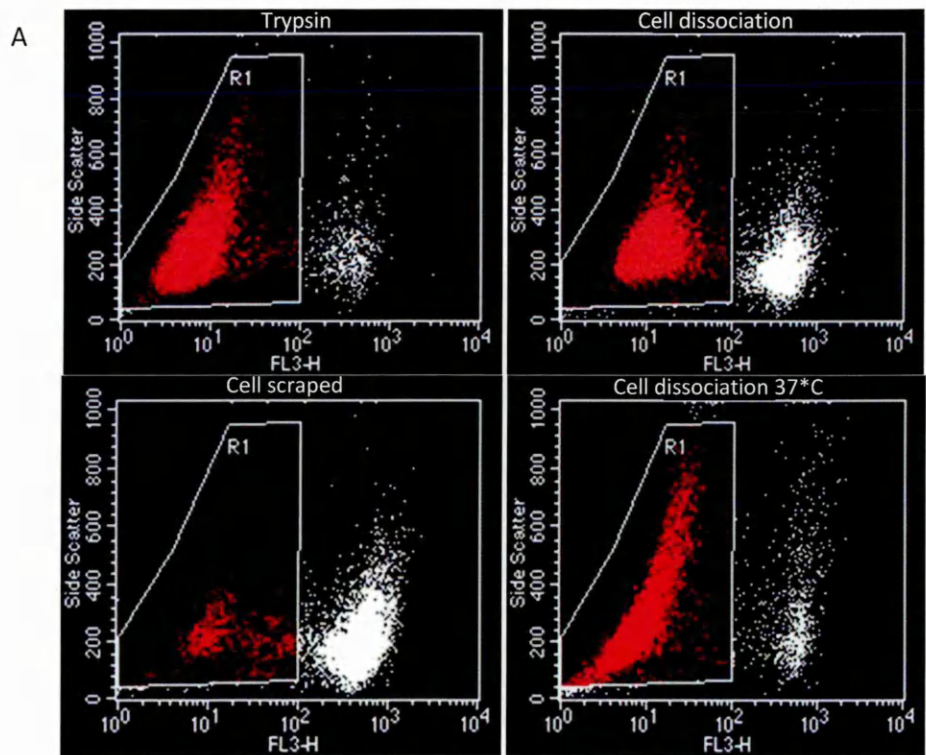
Figure 2.14; Flow cytometry analysis of HASMC viability following different methods of cell retrieval from culture. A) The gated area marked R1 in the dot plots indicates cells that are negative for propidium iodide (PI), measured on the X axis, and therefore corresponds to viable cells. The percentage of gated cells shifts considerably with the method of removal. B) The histograms correspond to the percentage of the total cells gated in the PI negative region. n=2

A

B
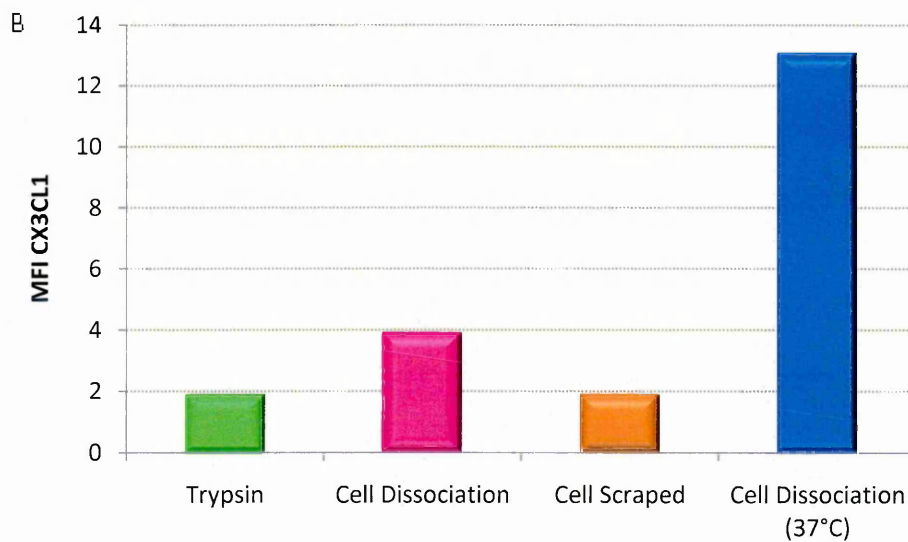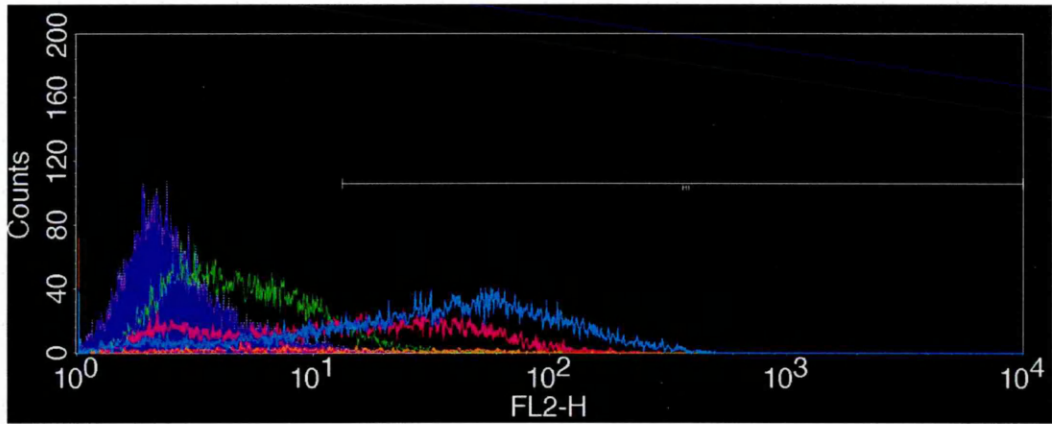
Figure 2.15; Flow cytometry analysis of HASMC expression of CX₃CL1 following different methods of cell retrieval. (A) Histogram plot demonstrating the difference in fluorescence (measured on FL2-H), corresponding to anti-CX$_3$CL1 PE conjugated antibody binding, for the different methods of cell removal. (B) The mean fluorescence index (MFI) of CX$_3$CL1 staining demonstrates the effects of the different removal methods on cell surface expression. CX$_3$CL1 appears to be cleaved from cells during the cell removal process. Removal of cells by the cell dissociation solution at 37°C retains the most cell surface CX$_3$CL1 staining. n=1.
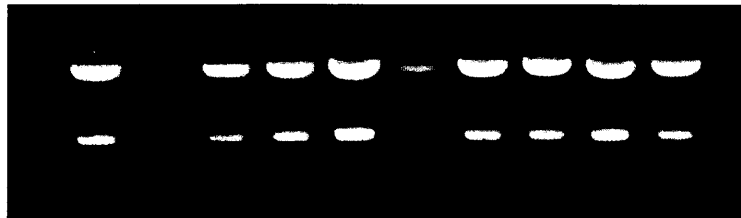
Figure 2.16; Representative agarose gel electrophoresis of RNA samples extracted from HASMC. Each lane represents a separate sample, with good quality RNA indicated by two clear bands (denoting 28S and 18S rRNA components) at an approximate ratio of 2:1.

2.3.4.2   Primer efficiencies

Primer efficiencies of all target genes and reference control genes were considered acceptable, as they were within the 100±10% range (Figure 2.17 and 2.18), apart from the CX_3CR1 gene, which was undetectable. Primer products were in the expected range of their predicted amplicon sizes, and demonstrated a single product when analysed by agarose gel electrophoresis (Figure 2.19).

2.3.5 Analysis of CX_3CL1 expression following cytokine treatment of human aortic vascular cells

2.3.5.1   Analysis of CX_3CL1 expression by ELISA

Both HASMC and HAEC demonstrated a dose-dependent increase in cleaved (measured in cultured supernatants) and cell-bound (measured in cell lysates) CX_3CL1 expression following cytokine treatment, when measured by ELISA. All increases were significant at both 10ng/ml and 100ng/ml TNFα plus IFNγ treatments ($P<0.05$ ANOVA, n=6), and were similar in magnitude in SMC (Figure 2.20) and endothelial cells (Figure 2.21). This upregulation of CX_3CL1 expression upon cytokine treatment was not due to effects on cell proliferation, as no significant differences were observed in DNA synthesis (BrdU ELISA) and total protein content (BCA assay) respectively following cytokine treatment (Figure 2.22 and 2.23 respectively).

2.3.5.2   Analysis of CX_3CL1 expression by flow cytometry

The dose-dependent increase in expression of cell-bound CX_3CL1 following cytokine treatment observed by ELISA, was replicated by flow cytometry analysis of HASMC. Cell-bound CX_3CL1 was increased at 1, 10 and 100ng/ml TNFα + IFNγ in these cells and significantly increased at 100ng/ml ($P<0.05$ Kruskal Wallis, n=3) (Figure 2.24). Though a substantial difference was observed, significance was not demonstrated at the 10ng/ml treatment. Concurrent measurement of cell viability by propidium iodide uptake revealed no significant differences between the treatment conditions (Data not shown).

2.3.5.3   Analysis of CX_3CL1 expression by immunocytochemistry

The increase in CX_3CL1 expression following cytokine treatment was demonstrated visually in HASMC and HAEC by immunocytochemistry. Under basal conditions, with no cytokine treatment, CX_3CL1 was found to be located diffusely in the cytoplasm and on the cell membrane in a similar manner in both cell types (Figure 2.25). The intensity of CX_3CL1 staining increased in cells treated with 100ng/ml TNFα plus IFNγ for 24 hours, with cellular location

GAPDH $y = -3.1058x + 22.251$, $R^2 = 0.9909$

RPL13A $y = -3.4054x + 22.434$, $R^2 = 0.9981$

B2M $y = -3.5627x + 21.51$, $R^2 = 0.9932$

CX$_3$CL1 $y = -3.1694x + 24.582$, $R^2 = 0.9977$

CCL2 $y = -3.4492x + 22.702$, $R^2 = 0.985$

ADAM17 $y = -3.4153x + 29.486$, $R^2 = 0.9916$

ADAM10 $y = -3.2997x + 26.584$, $R^2 = 0.9948$

AR $y = -3.4322x + 32.599$, $R^2 = 0.9969$

TIMP1 $y = -3.4349x + 23.605$, $R^2 = 0.9982$

TIMP3 $y = -3.1884x + 26.764$, $R^2 = 0.9992$
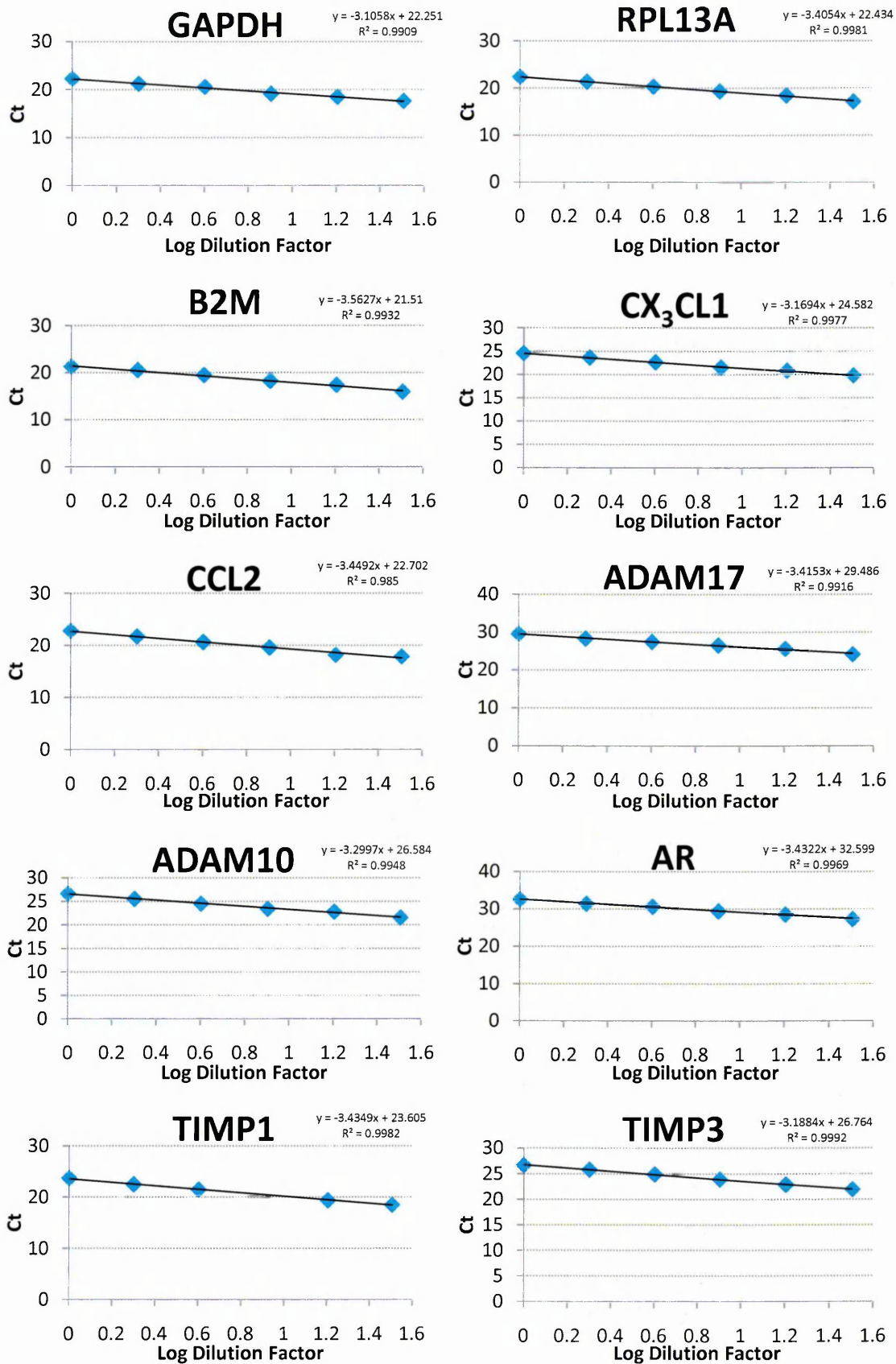
Figure 2.17; Primer efficiency plots for TaqMan qRT-PCR targets. As the template starting quantity is reduced by half through serial dilution, approximately one cycle difference is observed. When this is plotted against Log dilution factor a linear slope of the Ct values is approximately -3.32, where this value equals 100% efficiency.

Gene Target	% Efficiency
GAPDH	109.88
RPL13A	96.63
B2M	90.85
CX$_3$CL1	106.78
CCL2	94.95
ADAM17	96.25
ADAM10	100.94
AR	95.59
TIMP1	95.49
TIMP3	105.89

Figure 2.18; Calculated primer efficiencies for TaqMan qRT-PCR targets. Calculated primer efficiencies from slope values fall in the range of 100 ± 10%.
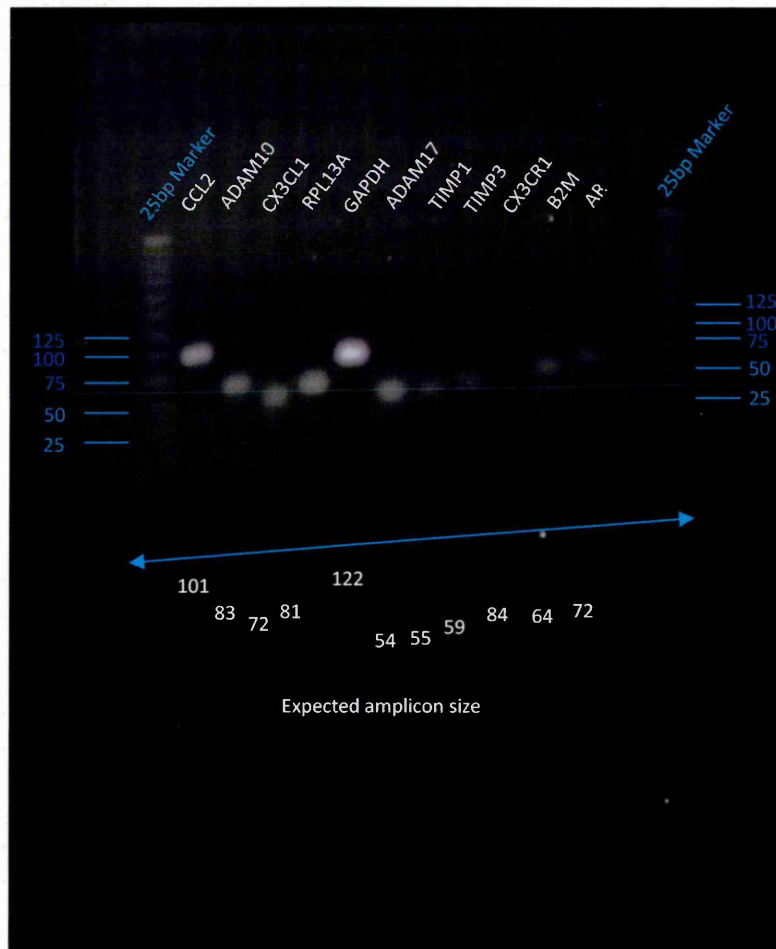
Figure 2.19; Agarose gel electrophoresis of primer products from qRT-PCR amplification. HASMC samples were run on a 2.5% agarose gel following qRT-PCR amplification and amplicon sizes were compared to a 25bp marker. A single product was detectable for all targets, other than CX$_3$CR1 where no product was observed. The arrowed line indicates the resulting migration angle due to imperfections in the gel, or equipment. Band size comparisons were used to account for this.
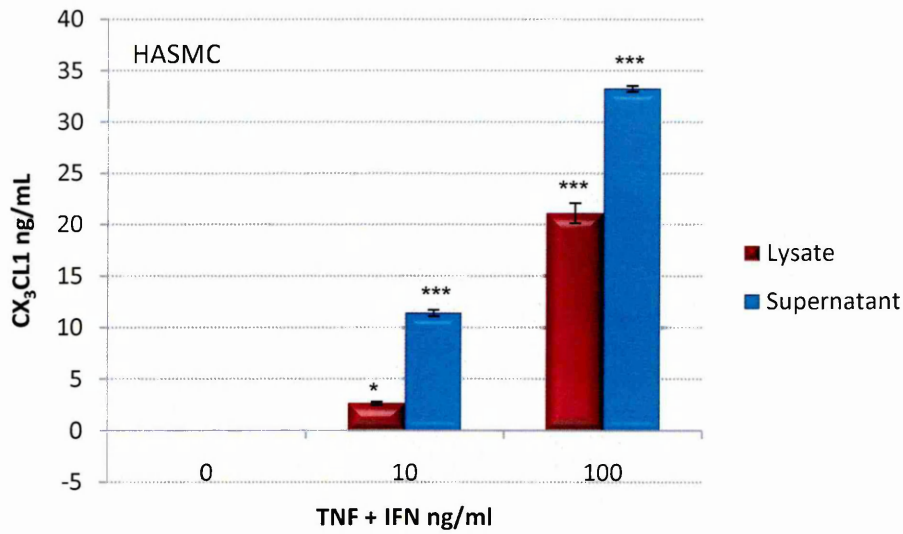
Figure 2.20; CX₃CL1 expression in HASMC determined by ELISA. A dose-dependent increase in cleaved (supernatant) and cell-associated (lysate) CX_3CL1 protein was seen after a 24h incubation with TNFα + IFNγ. *P<0.05, **P<0.01, ***P<0.001vs 0ng/ml ANOVA n=6.
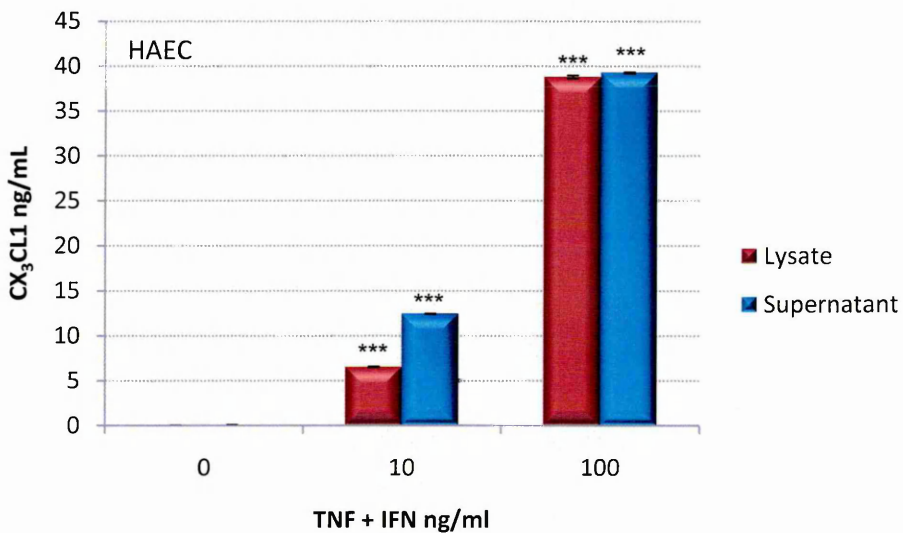
Figure 2.21; CX₃CL1 expression in HAEC determined by ELISA. A dose-dependent increase in cleaved (supernatant) and cell-associated (lysate) CX_3CL1 protein was seen after a 24h incubation with TNFα + IFNγ. *P<0.05, **P<0.01, ***P<0.001 vs 0ng/ml ANOVA n=6.

122
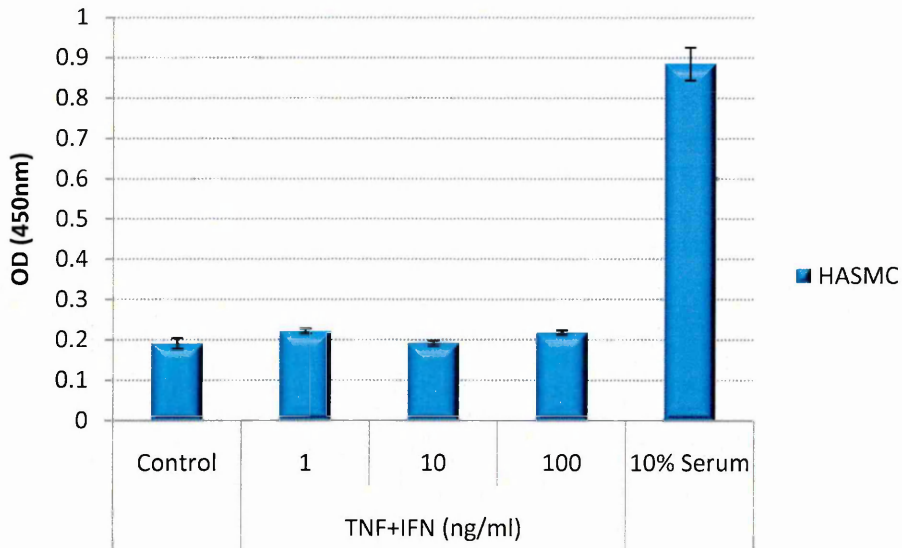
Figure 2.22; DNA synthesis in HASMC as measured by BrdU proliferation ELISA following cytokine treatments. No significant effects were observed for all treatments in serum-free media. 10% serum media was used as a positive control. *****P<0.001 vs Control, ANOVA, n=6*
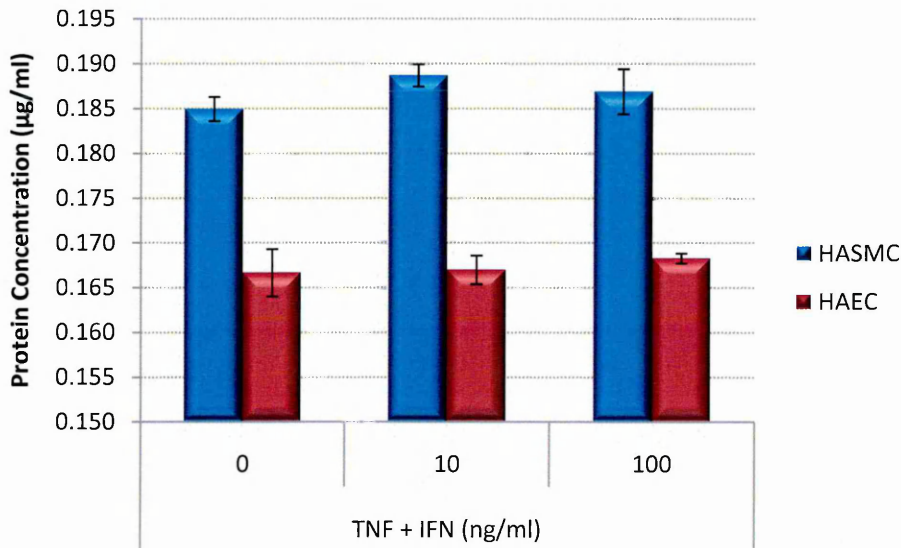
Figure 2.23; Total protein content of HASMC and HAEC as measured by BCA following cytokine treatments. No significant changes were observed following experimental treatments when compared to untreated control (0ng). *Kruskal-Wallis n=3.*
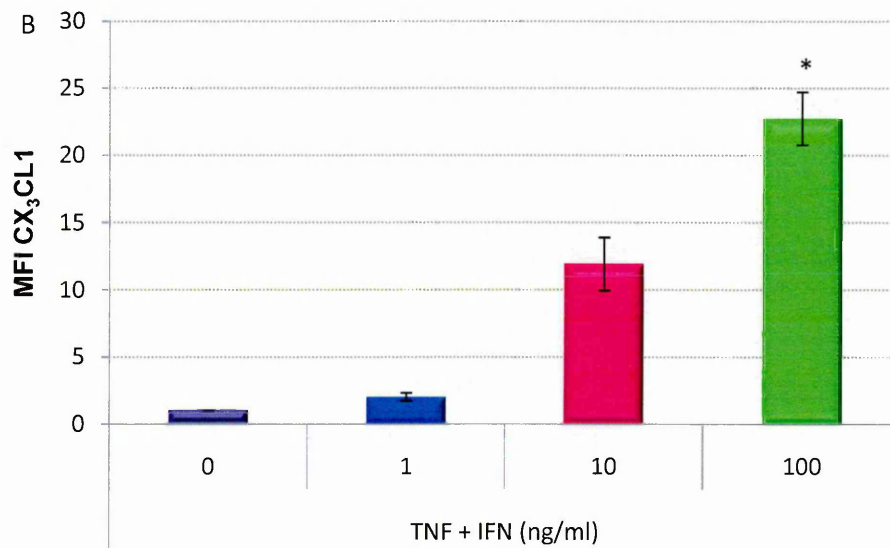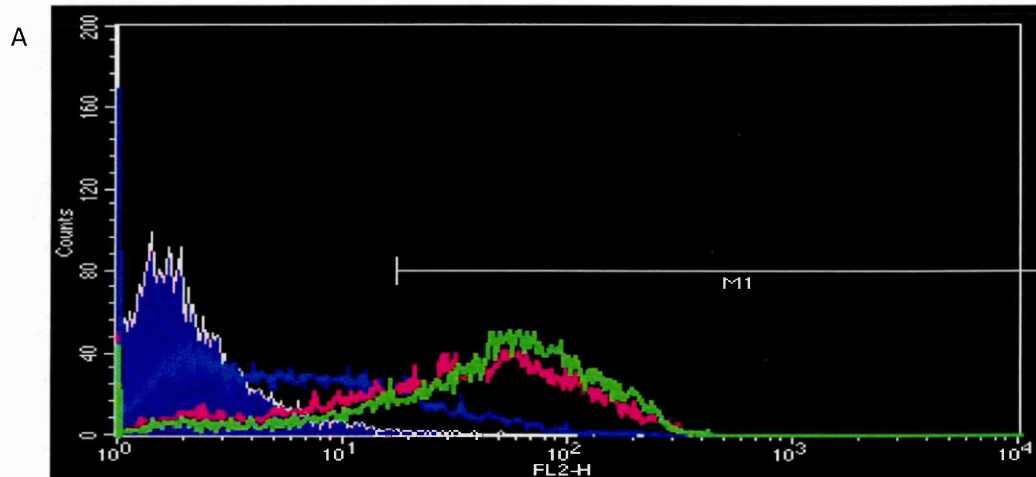
Figure 2.24; Flow cytometry analysis of cell surface CX₃CL1 expression in HASMC following cytokine treatment. Cells demonstrated a dose-dependent response to TNFα + IFNγ treatment. (A). As cytokine concentration increased, the histogram traces shifted to the right on the x-axis (FL2-H) indicating increased fluorescence due to antibody binding (B). The mean fluorescence index (MFI) represents the amount of positive staining normalised to isotype control. Colours in bar chart (B) correspond to lines in histogram (A). *P<0.05 vs 0ng/ml, Kruskal-Wallis, n=3.
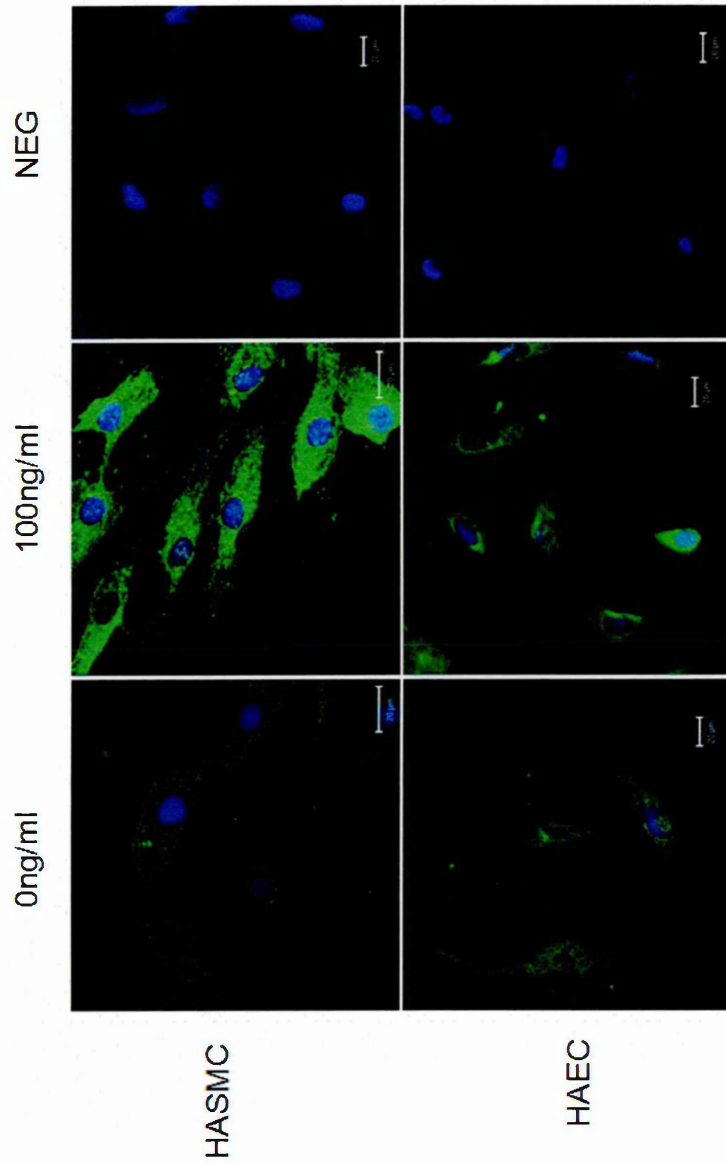
Figure 2.25; Immunocytochemical analysis of CX₃CL1 expression in human aortic vascular cells following cytokine treatment. Cells were treated with 100ng/ml TNFα + IFNγ for 24hrs prior to analysis. CX₃CL1 staining appears brighter following cytokine treatment. Negative controls with the omission of the primary antibody revealed no non-specific binding of the secondary antibody. Nuclei were counterstained with DAPI (Blue).

remaining consistent. Intensity of staining was not quantified, and was used only as a visual representation. The intensity of smooth muscle cell CX_3CL1 staining appeared greater than that of endothelial cells, in contrast to the expression detected by ELISA.

2.3.5.4   *Analysis of CX₃CL1 mRNA expression by qRT-PCR*

Expression of CX_3CL1 mRNA increased following cytokine treatment in both HASMC and HAEC, in a dose-dependent manner (Figure 2.26). Fold changes were of a large magnitude, but due to the variability of the data and the small sample sizes (n=3), significance was only demonstrated at 100ng/ml TNFα plus IFNγ for SMC and endothelial cells alike ($p < 0.05$, $p < 0.01$ respectively, Kruskal Wallis). The cytokine induced increase in mRNA expression was substantially greater in HASMC compared to HAEC, with fold change in expression demonstrated as thousand-fold opposed to hundred-fold, indicating a 10x greater magnitude in HASMC.

In summary, CX_3CL1 expression was significantly and dose-dependently increased in HASMC and HAEC by treatment with TNFα + IFNγ, at both the protein and mRNA level. The magnitude of increase in expression was different between the different cell types, although this was technique dependent (Table 2.5).

2.3.6 Expression of ADAM-10 and -17 in human vascular cells

Since experiments indicated a significant increase in shedding of CX_3CL1 into the supernatant following cytokine treatment of vascular cells, the expression of ADAM-10 and ADAM-17, known sheddases for CX_3CL1 (Garton *et al.* 2001, Tsou *et al.* 2001, Hundhausen *et al.* 2003), were investigated.

2.3.6.1   *Analysis of ADAM-10 and -17 expression by immunocytochemistry*

Immunocytochemical investigation demonstrated that ADAM-10 and ADAM-17 were constitutively expressed on the cell membrane and in the cytoplasm of HASMC (Figure 2.27). When fixed with 4% PFA, the staining patterns of both ADAM-17 and ADAM-10 was membraneous and represented the cell-bound, and therefore active, fraction of these enzymes. Following acetone fixation and permeablisation, both ADAM-17 and ADAM-10 were also found to localise in perinuclear compartments (Figure 2.27).
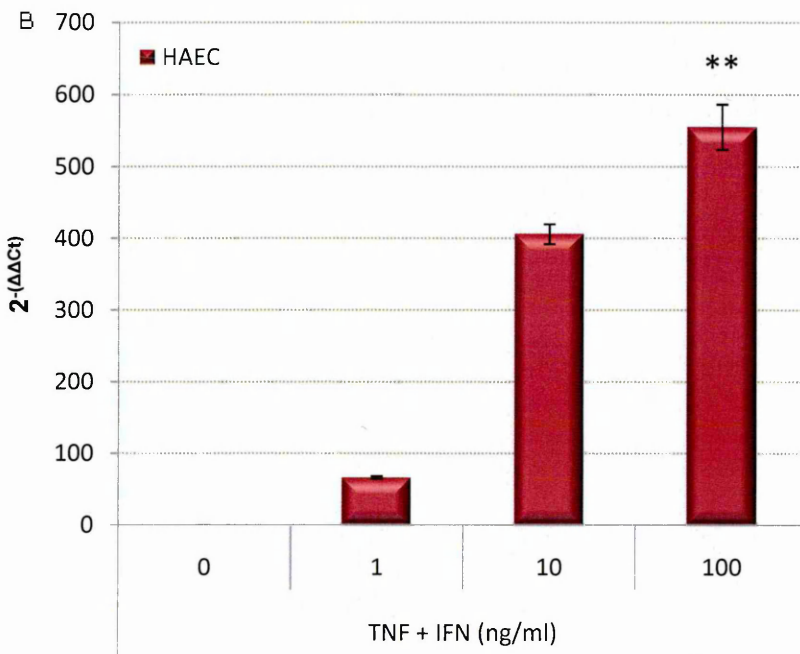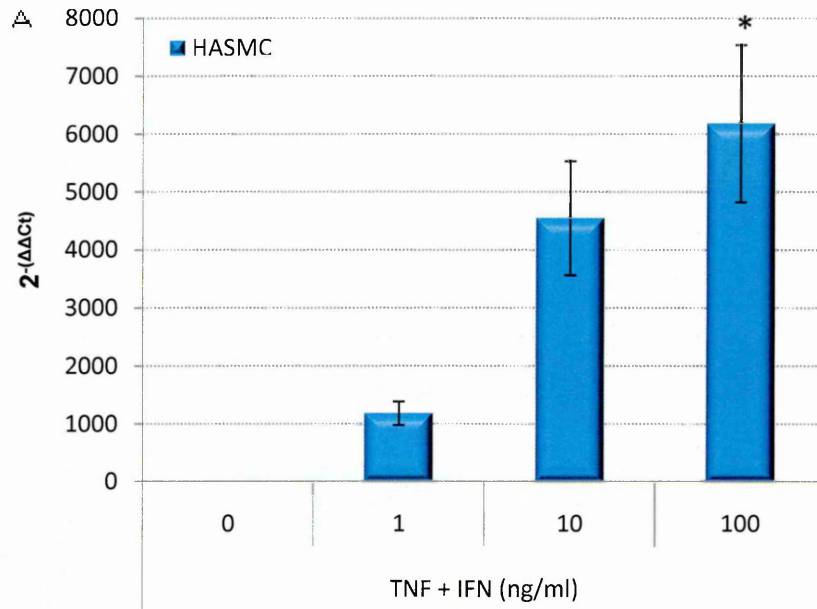
Figure 2.26; qRT-PCR analysis of CX₃CL1 mRNA expression in human aortic vascular cells following cytokine treatment. Both HASMC (A) and HAEC (B) demonstrated a dose-dependent increase in CX₃CL1 mRNA expression following TNFα + IFNγ treatments relative to control. HASMC showed a 10-fold greater upregulation than HAEC. $2^{-\Delta\Delta Ct}$ is representative of fold-change from control. *P<0.05, **P<0.01 vs 0ng/ml, Kruskal-Wallis, n=3.

Cytokines TNFα+IFNγ (ng/ml)		HASMC			HAEC		
		1	10	100	1	10	100
ELISA	Supernatant	NI	↑***	↑***	NI	↑***	↑***
	Lysate	NI	↑*	↑***	NI	↑***	↑***
ICC		NI	NI	↑	NI	NI	↑
qRT-PCR		↑	↑	↑*	↑	↑	↑**
Flow Cytometry		↑	↑	↑*	NI	NI	NI

Table 2.5; Summary of cytokine-induced CX₃CL1 expression in human aortic vascular cells. CX$_3$CL1 was consistently upregulated by proinflammatory cytokines TNFα and IFNγ in both HASMC and HAEC. *P<0.05, **P<0.01, ***P<0.001; NI=not investigated
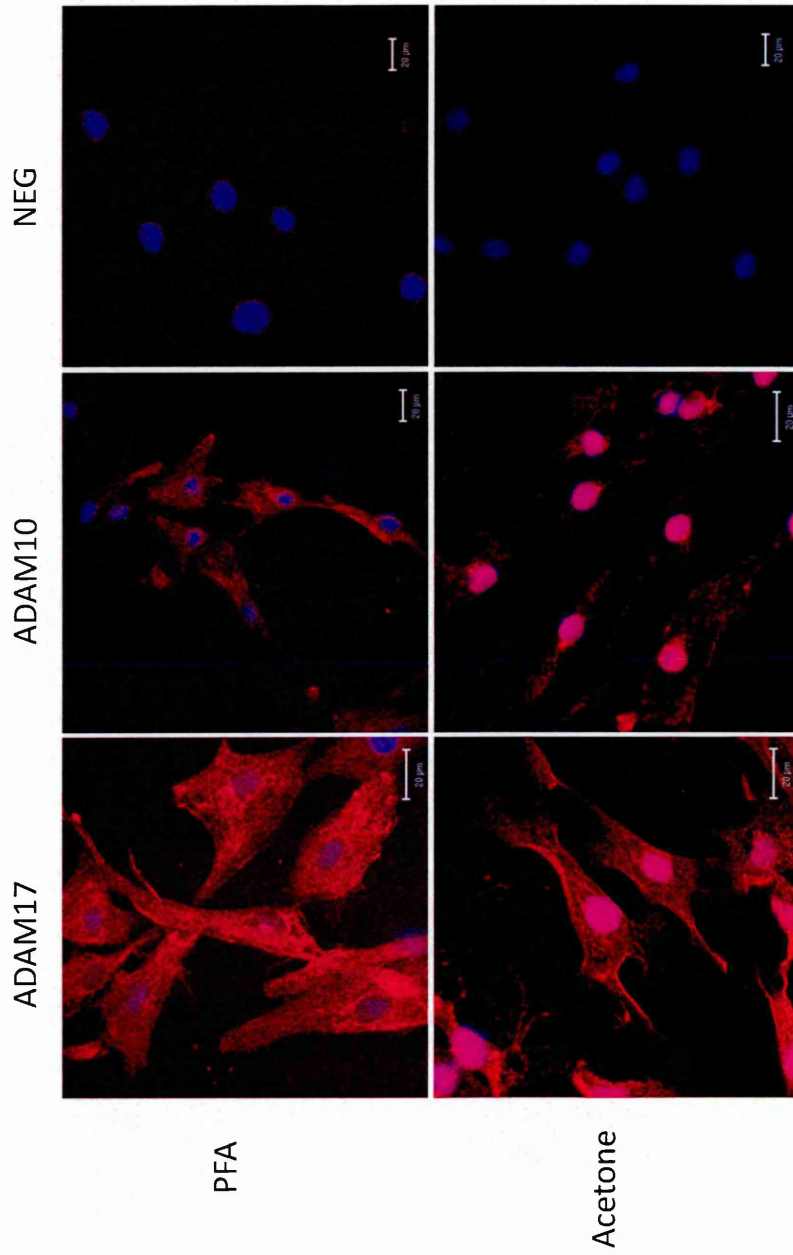
Figure 2.27; Immunocytochemical analysis of ADAM-17 and ADAM-10 expression in HASMC. **Fixation with 4% PFA reveals positive staining for ADAM-17 and ADAM-10 on the cell surface of HASMC. Acetone fixation and permeablisation revealed perinuclear localisation of both ADAM-17 and ADAM-10. Negative controls with the omission of the primary antibody revealed no non-specific binding of the secondary antibody. Nuclei were counterstained with DAPI (Blue).**

2.3.6.2   Analysis of ADAM17 expression by flow cytometry

The expression of cell-surface ADAM-17 appeared to be marginally, but not significantly, upregulated in a dose-dependent manner by treatment of HASMC with TNFα plus IFNγ , when assessed by flow cytometry and MFI analysed(Figure 2.28b). Histogram plots revealed no significant modulation of ADAM-17 surface expression by cytokine treatment (Figure 2.28a).

2.3.6.3   Analysis of ADAM-10 and -17 expression by qRT-PCR

Expression of ADAM-10 and ADAM-17 mRNA was not significantly altered by cytokine treatment in vascular endothelial or SMC (Figure 2.29). Some fluctuations did occur, with slight increases for ADAM-17 expression in HASMC at 10 and 100ng/ml, but these did not reach significance. The endogenous inhibitors of ADAM-17 and ADAM-10, TIMP-3 and TIMP-1, were also not significantly modulated at the mRNA level in HAEC and HASMC when these cells were treated with the pro-inflammatory cytokines TNFα plus IFNγ. A slight decrease in TIMP-3 mRNA expression was observed but this did not reach significance (Figure 2.29).

In summary, ADAM-17 and ADAM-10 (the enzymes responsible for CX_3CL1 shedding) are expressed by aortic vascular cells, along with their tissue inhibitors TIMP-3 and TIMP-1. Although ADAM-17 expression appeared to be slightly increased by TNFα + IFNγ, significance was not demonstrated and the magnitude of the increases was small. In addition, no changes in TIMP-3 or TIMP-1 expression were observed following cytokine treatment.

2.3.7 Expression of CX_3CR1 in human aortic vascular cells

To determine whether CX_3CL1 can act in an autocrine manner on aortic vascular cells, the expression of its receptor was investigated.

2.3.7.1   Analysis of CX_3CR1 mRNA expression by qRT-PCR

CX_3CR1 mRNA was undetectable by qRT-PCR in both HASMC and HAEC under basal conditions and following treatment with inflammatory cytokine (0-100ng/ml TNFα + IFNγ). To determine the specificity of the primer-probe used, THP-1 cells were assessed for CX_3CR1 expression as a positive control. CX_3CR1 mRNA was expressed in this cell line, confirming the specificity of the primers (Figure 2.30b). In addition, CX_3CR1 mRNA expression in THP-1 cells was down-regulated following treatment with 10 and 100ng/ml TNFα plus IFNγ for 2 hours (Figure 2.30c).

A

B
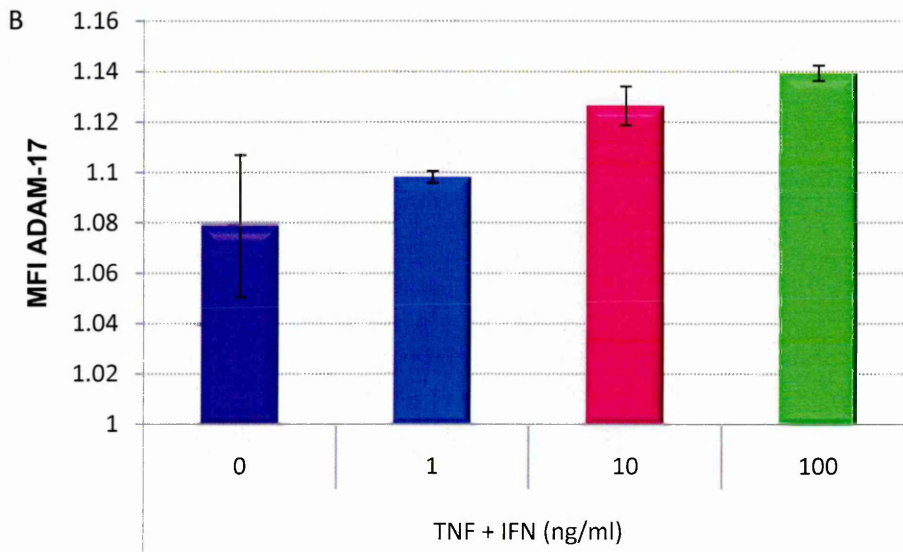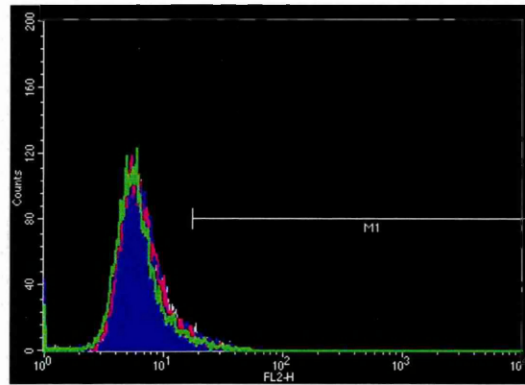
Figure 2.28; Flow cytometry analysis of cell surface ADAM-17 expression in HASMC following cytokine treatment. A dose-dependent increase in ADAM-17 is apparent following TNFα + IFNγ treatment, although changes were not significantly different from control, which can be seen from the small magnitude of the Y axis scale (B) and the lack of movement in cell traces on the histogram (A). Colours in bar chart (B) correspond to lines in histogram (A). *Kruskal-Wallis n=3.*
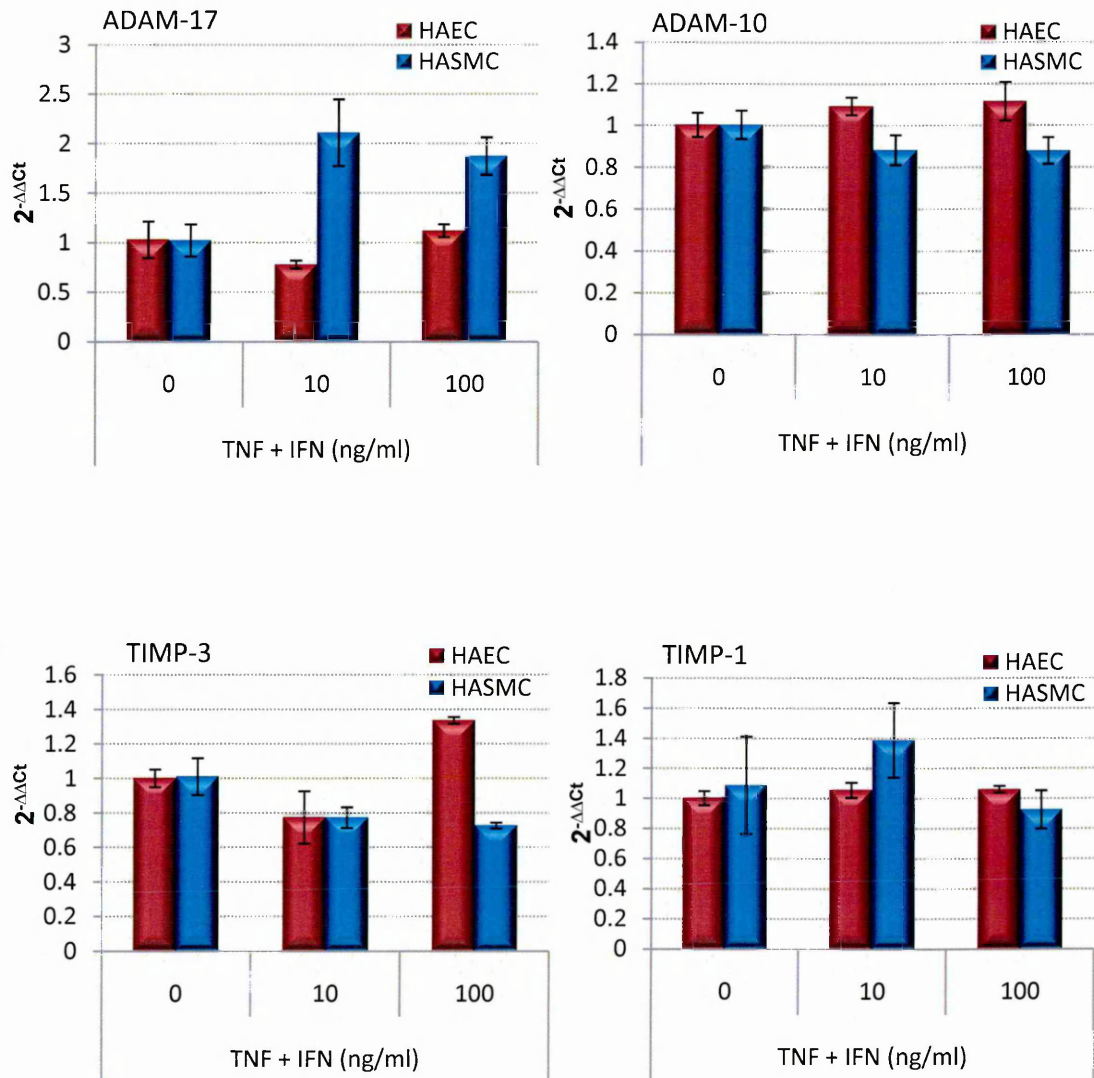
Figure 2.29 qRT-PCR analysis of ADAM-17, -10 and their corresponding tissue inhibitors, TIMP-1 and TIMP-3, in aortic vascular cells following cytokine treatment. No significant changes in mRNA expression occurred following 2h TNFα + IFNγ treatment. *Kruskal-Wallis n=3.*
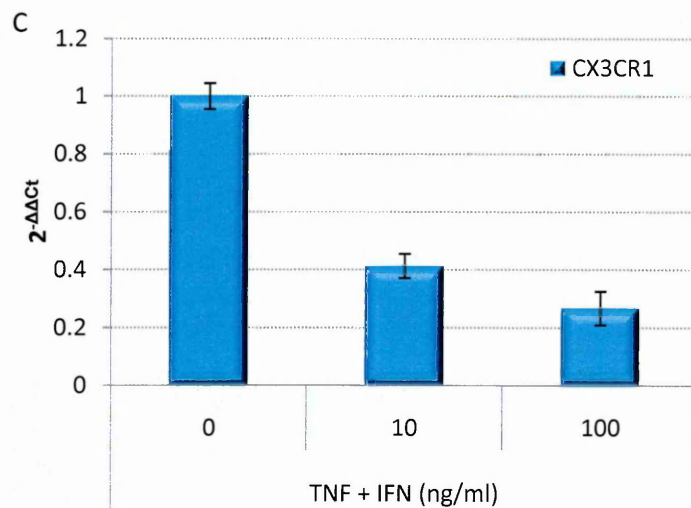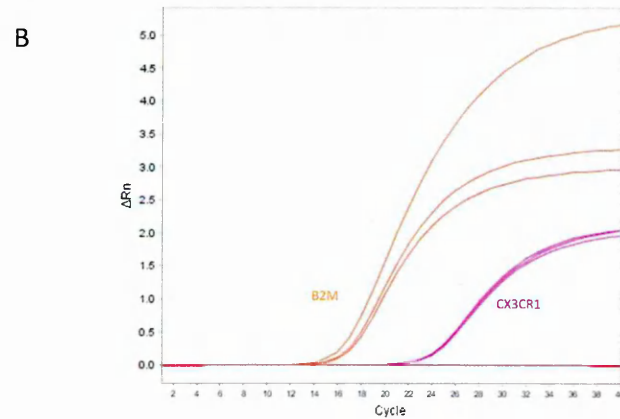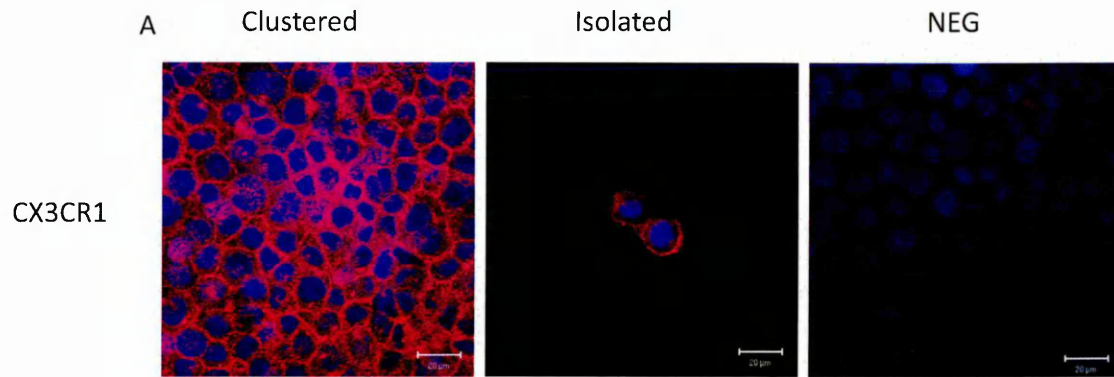
Figure 2.30; CX₃CR1 expression in THP-1 cells. (A) CX₃CR1 protein expression was confirmed by immunocytochemistry in THP-1 cells when aggregated as a result of cytospinning, and when isolated (n=1). Staining appeared to be localised to the cell membrane. A negative control with the omission of the primary antibody revealed no non-specific binding of the secondary antibody. Nuclei were counterstained with DAPI (Blue). (B) CX₃CR1 mRNA was detected in THP-1 cells by qRT-PCR as demonstrated by triplicate amplification curves. B2M was used as the reference gene. CX₃CR1 mRNA expression was down regulated following treatment of cells with TNFα + IFNγ (C). *n=2.*

2.3.7.2 Analysis of CX3CR1 expression by immunocytochemistry

Contrary to qRT-PCR findings, the CX$_3$CR1 protein was detected in HASMC and HAEC by immunocytochemistry (Figure 2.31). The receptor appeared punctuate throughout the cell in HASMC, and clustered in a perinuclear location in HAEC.

THP-1 cells were used as a positive control for CX$_3$CR1 immunofluorescent staining. As these cells were a suspension cell line, a small volume of cells was cytospun onto glass slides before immunostaining. This was performed at high and low cell density, to rule out non-specific binding to aggregated cells, and to demonstrate universal cell staining. THP-1 cells appeared immuno-positive for CX$_3$CR1 staining, which was localised on the cell membrane of both clustered and isolated cells, suggesting specificity of the antibodies (Figure 2.30a).

In summary, CX$_3$CR1 protein was expressed on the surface of aortic vascular cells, but the mRNA was not detected by qRT-PCR. This disparity did not appear to be due to non-specific activity of the antibodies used in immunocytochemistry or lack of specificity of primer-probes used in qRT-PCR.

2.3.8 CCL2 expression in human aortic vascular cells

Since CCL2 has been implicated in monocyte recruitment to atherosclerotic lesions, its expression was investigated in the cell model used in this project.

2.3.8.1 Analysis of CCL2 expression by ELISA

The CCL2 protein was expressed in both HASMC and HAEC as measured by ELISA. HAEC-associated and secreted CCL2 was increased following 24h cytokine treatment, in a dose-dependent manner, as was cell-associated CCL2 in HASMC. This upregulation was significant at 10 and 100ng/ml TNFα + IFNγ ($P<0.001$, ANOVA, n=3). No significant changes were observed for secreted CCL2 in HASMC. A similar magnitude of expression was exhibited for both cell types (Figure 2.32).

2.3.8.2 Analysis of CCL2 mRNA expression by qRT-PCR

qRT-PCR demonstrated a dose-dependent upregulation of CCL2 mRNA expression in vascular cells following cytokine treatment (Figure 2.33). The increase was similar between the two cell types, and appeared to plateau at 10ng/ml. Increases were significant for HAEC at 10 and 100ng/ml ($P<0.05$, Kruskal Wallis, n=3) and at 100ng/ml for HASMC ($P<0.05$, Kruskal Wallis, n=3). In summary, vascular aortic endothelial and smooth muscle cells express CCL2 at the protein and mRNA level, and this expression is upregulated by proinflammatory cytokines.

CX3CR1 NEG
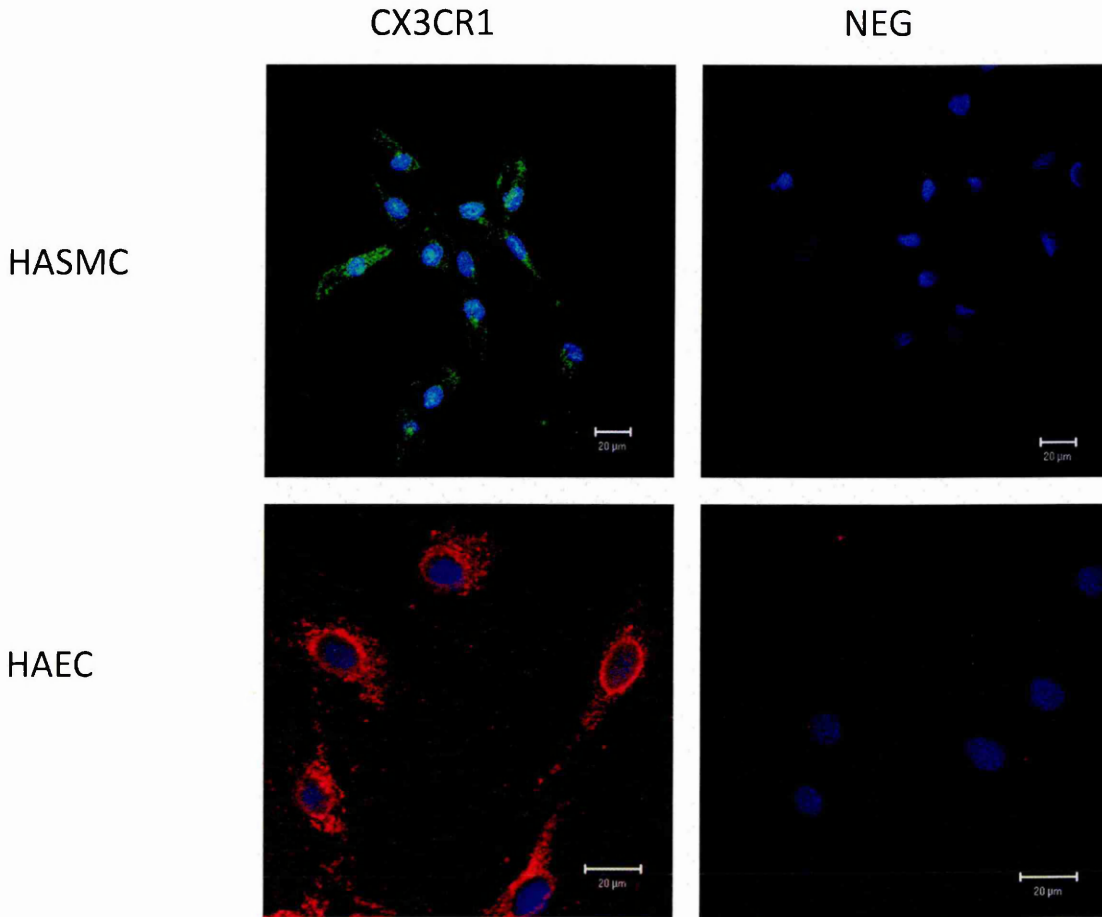
HASMC

HAEC

Figure 2.31; Immunocytochemical analysis of CX$_3$CR1 expression in human aortic vascular cells. Both HASMC and HAEC demonstrate immuno-positive staining for CX$_3$CR1. The receptor expression appeared punctuate through the cytoplasm of HASMC and partially clustered around the nucleus of HAEC following actetone fixation and permeablisation. Negative controls with the omission of the primary antibody revealed no non-specific binding of the secondary antibody. Nuclei were counterstained with DAPI (Blue).
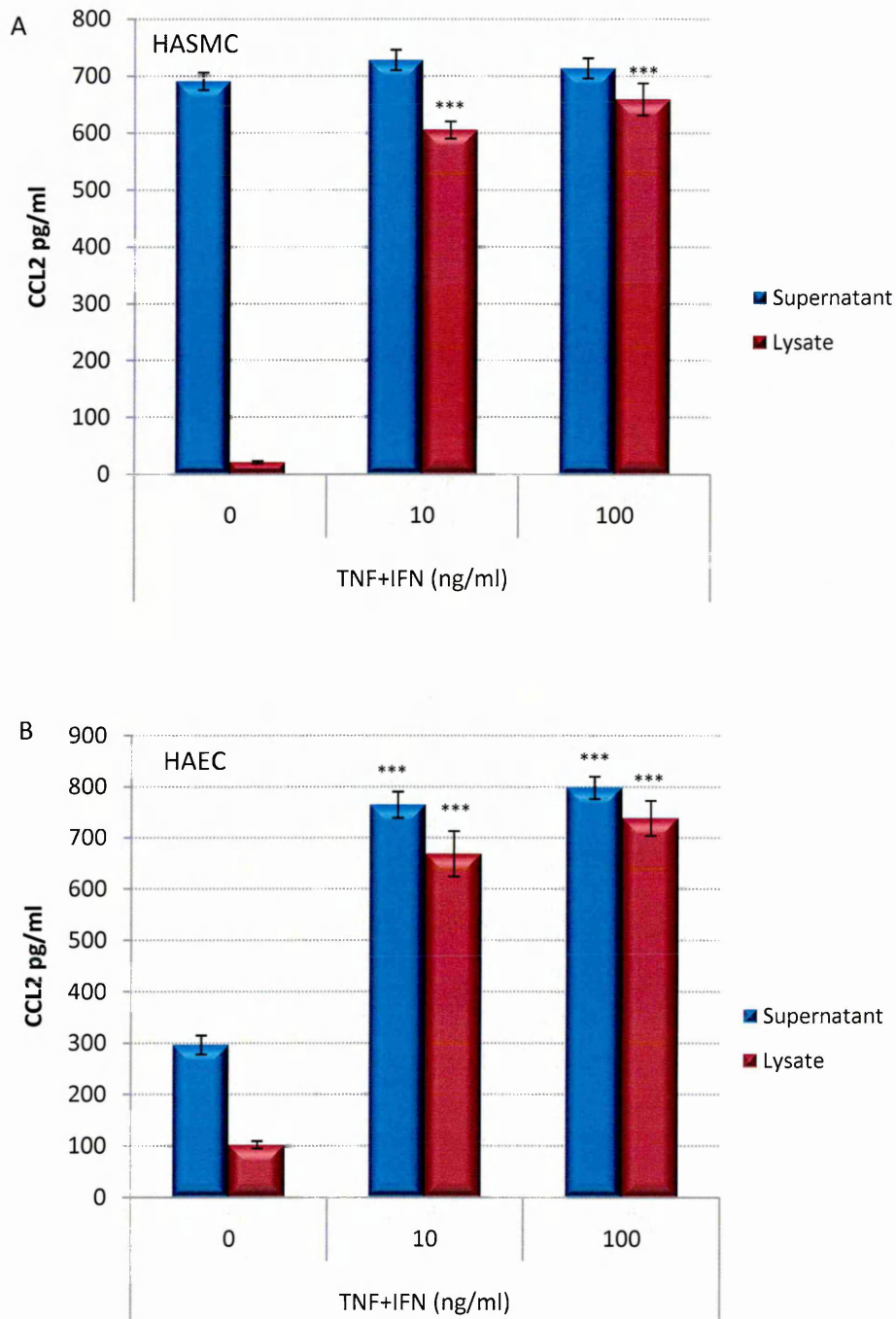
Figure 2.32; ELISA analysis of CCL2 expression in human aortic vascular cells following cytokine treatment. Cellular (lysate) CCL2 was upregulated in HASMC. Secreted (supernatant) HASMC CCL2 was not significantly altered due to high basal expression (A). Cellular and secreted CCL2 were significantly upregulated following TNFα + IFNγ treatment in HAEC (B). ***P<0.001, ANOVA, n=6

136
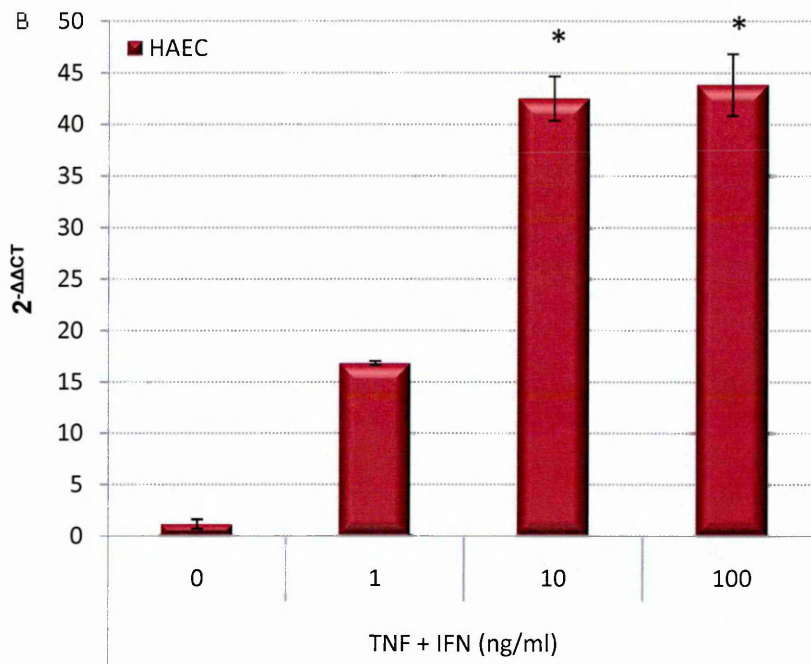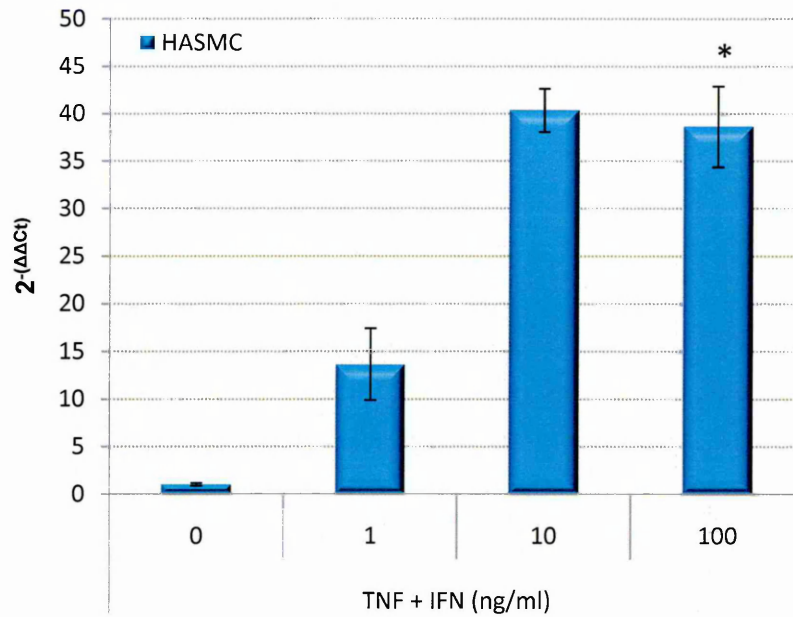
Figure 2.33; qRT-PCR analysis of CCL2 mRNA expression in human aortic vascular cells following cytokine treatment. Both HASMC (A) and HAEC (B) demonstrated a dose-dependent upregulation of CCL2 mRNA following 2h TNFα + IFNγ treatment. *P<0.05, Kruskal-Wallis n=3.

137

2.3.9 Investigation of androgen modulation of cytokine-induced CX₃CL1 expression in vascular cells

In order to determine any potential modulatory effect of androgens in inflammation, the effect of testosterone and DHT on cytokine-induced CX$_3$CL1 expression was investigated.

2.3.9.1 *Effect of androgens on CX₃CL1 expression: analysis by ELISA*

Testosterone and DHT showed no significant or reproducible modulation of CX$_3$CL1 expression induced by 10 or 100ng TNFα plus IFNγ stimulation in HASMC, as measured by ELISA. No effects were seen when the androgens were applied for either 2h (data not shown, n=3), 24h prior to the 24h cytokine treatment, or concurrently with the cytokines for 8h (n=6 and n=2 respectively; see figure 2.34 and 2.35). Similarly in HAEC there was a lack of androgen modulation of CX$_3$CL1 expression in supernatants and lysates, after 24h DHT treatment followed by the addition of 10ng/ml TNFα plus IFNγ for 24h (n=6; figure 2.36). Androgens did not affect cell proliferation, as no significant differences were observed in DNA synthesis (measured by BrdU ELISA) or total protein content (measured by BCA assay) respectively, following testosterone or DHT treatment (Figure 2.37 and 2.28 respectively).

2.3.9.2 *Effect of androgens on CX₃CL1 expression: analysis by qRT-PCR*

Androgens, similarly, did not affect the cytokine-induced CX$_3$CL1 mRNA expression, as measured by qRT-PCR. Expression of CX$_3$CL1 mRNA was not significantly modulated in HASMC following 24h of 10nM androgen treatment and 2h of 10ng/ml cytokine stimulation, although testosterone did appear to slightly down-regulate cytokine-induced CX$_3$CL1 mRNA expression (n=3; see figure 2.39).

Androgen modulation was investigated further in vascular cells cultured in complete medium (containing serum), to test whether the presence of growth factors is needed for androgens to exert a modulatory action on inflammation, as suggested by Orio (2002) and Bakin (2003). To exclude the possibility of androgens present in the serum causing an effect, experiments were performed in the presence and absence of the antiandrogen flutamide alone, or in combination with either testosterone or DHT. As measured by qRT-PCR, no significant effects or trends were seen in the expression of CX$_3$CL1 in vascular cells following 24h treatment with testosterone or DHT, with or without flutamide (n=3; see figures 2.40 and 2.41). When a subsequent 2h 10ng/ml cytokine stimulation was applied after the 24h androgen treatment,
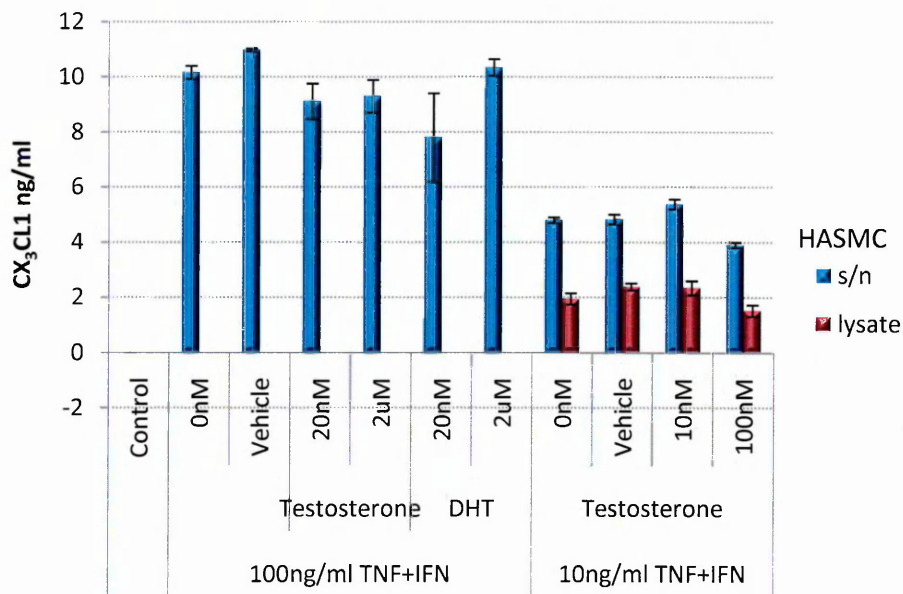
Figure 2.34; ELISA analysis of CX₃CL1 expression in HASMC following cytokine and 24h androgen treatment. Cell-associated (lysate) and secreted (supernatant) 24h 10 or 100ng/ml cytokine-induced CX₃CL1 expression was not altered by 24h pre-treatment with testosterone or DHT. *Kruskal-Wallis n=6*
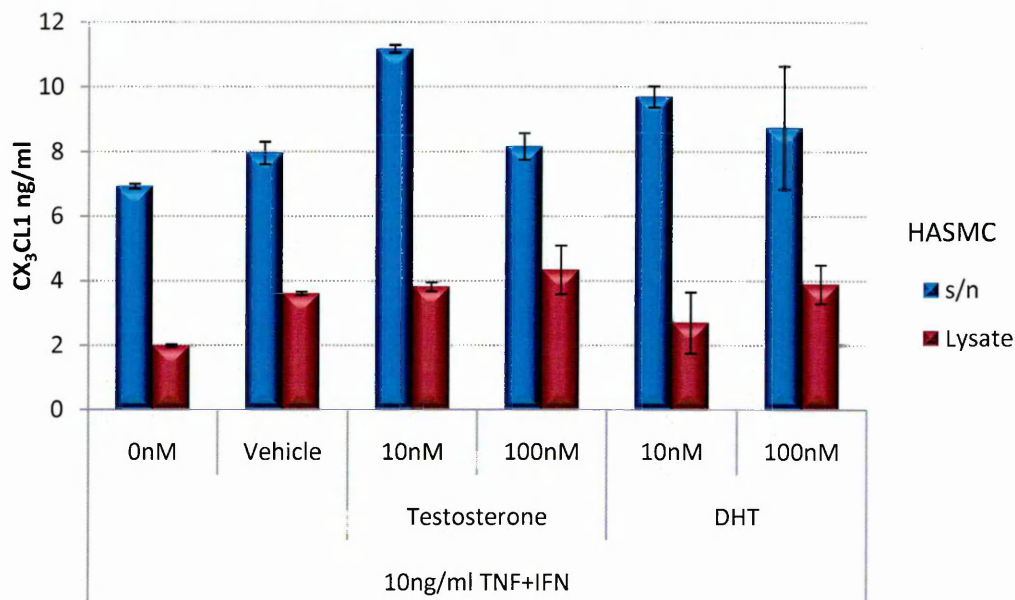
Figure 2.35; ELISA analysis of CX₃CL1 expression in HASMC following 8h cytokine and androgen co-treatment. Cell-associated (lysate) and secreted (supernatant) 8h 10ng/ml cytokine-induced CX₃CL1 expression was not altered by 8h co-treatment with testosterone or DHT. *Kruskal-Wallis n=2*

139
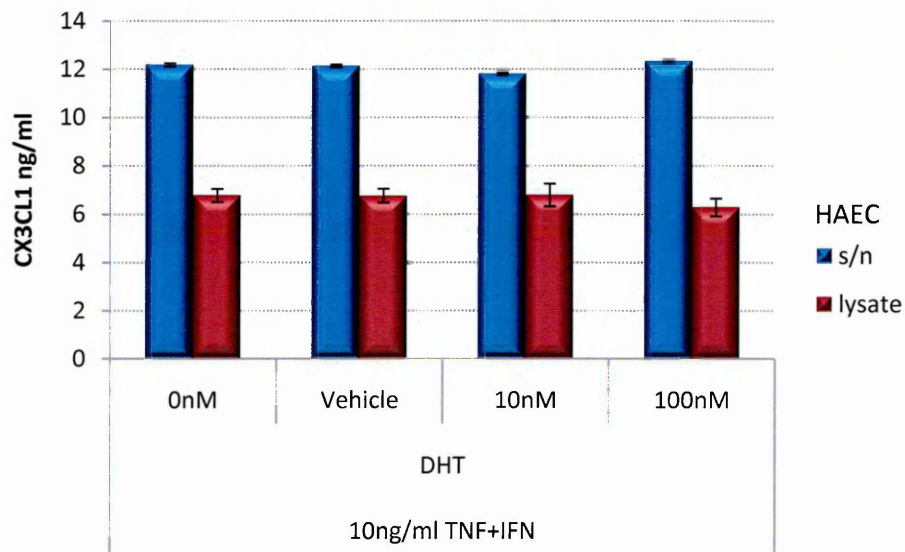
Figure 2.36; ELISA analysis of CX₃CL1 expression in HAEC following cytokine and 24h androgen treatment. Cell-associated (lysate) and secreted (supernatant, s/n) 24h cytokine-induced CX_3CL1 expression was not altered by 24h pre-treatment with DHT. *Kruskal-Wallis n=6*
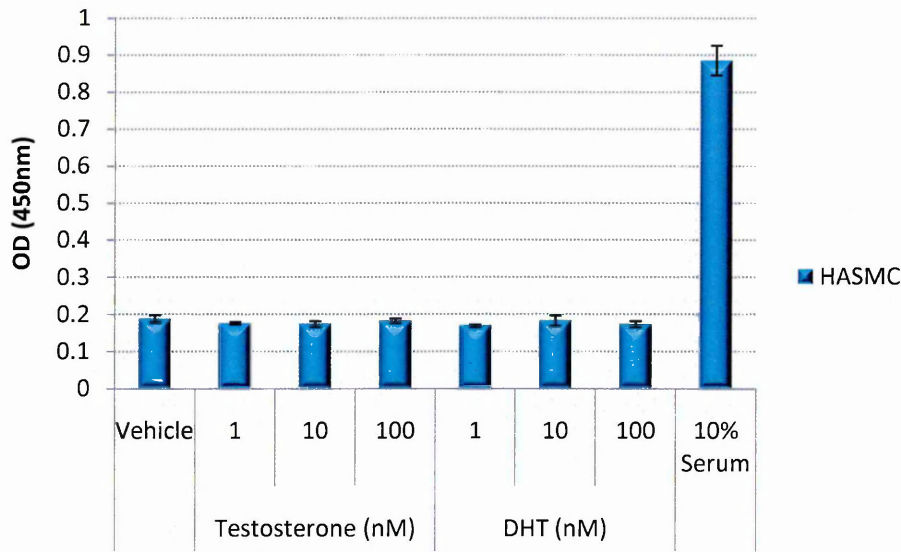
Figure 2.37; DNA synthesis in HASMC as measured by BrdU proliferation ELISA following androgen treatments. No significant effects were observed for all treatments in serum-free media. 10% serum media was used as a positive control. ***P<0.001 vs vehicle, ANOVA, n=6
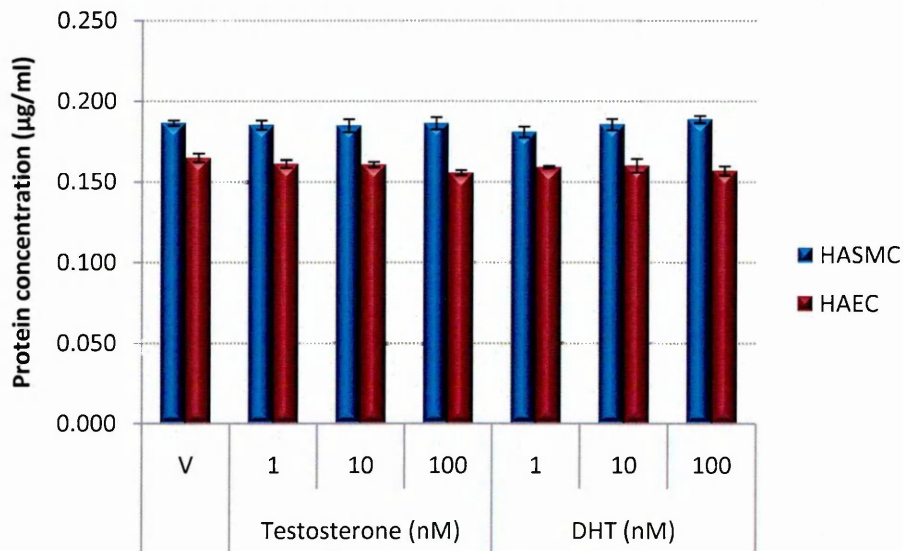
Figure 2.38; Total protein content of HASMC and HAEC samples as measured by BCA following androgen treatments. No significant changes were observed following experimental treatments when compared to untreated vehicle (0ng). *Kruskal-Wallis n=3.*

141
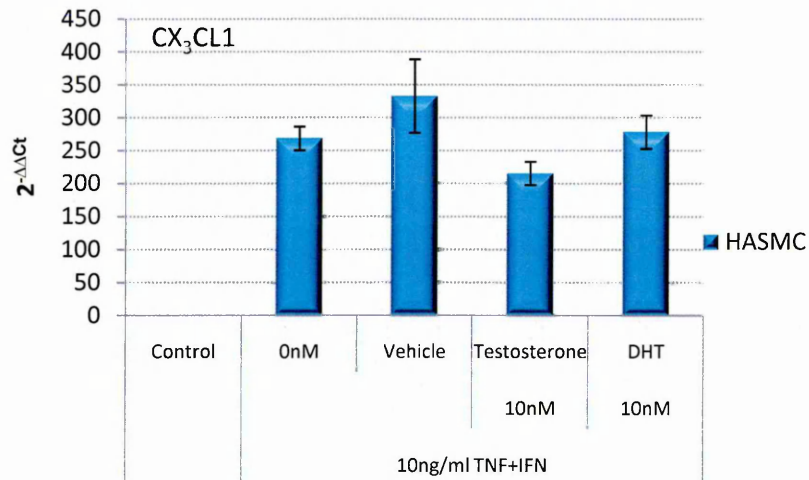
Figure 2.39; qRT-PCR analysis of CX₃CL1 mRNA expression in HASMC following cytokine and androgen treatment. 24hr androgen and 2hr cytokine treatment demonstrated CX₃CL1 expression appeared marginally but not significantly reduced by testosterone treatment. No effect was of DHT was observed. *Kruskal-Wallis n=3.*
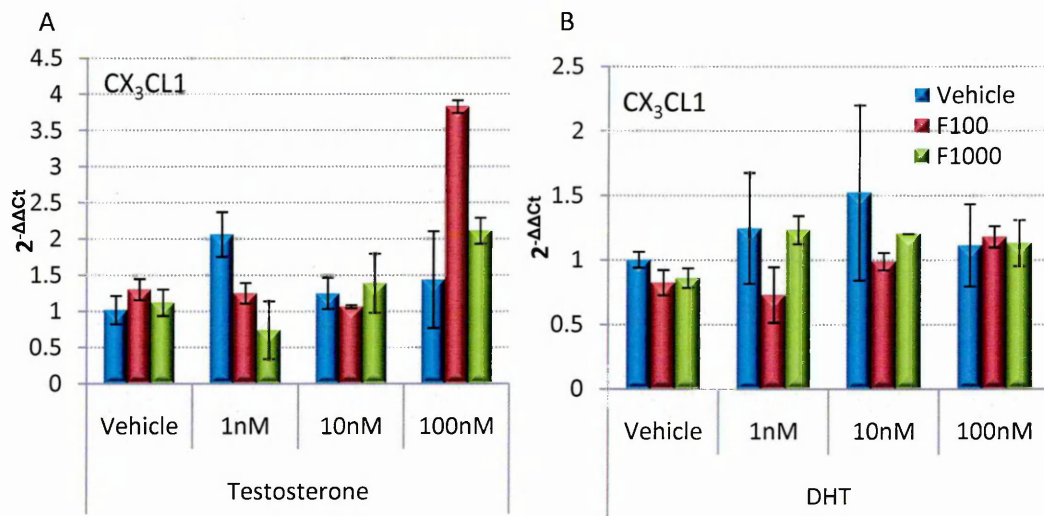
Figure 2.40; qRT-PCR analysis of CX₃CL1 mRNA expression in HASMC following androgen treatment and AR blockade. No significant effects or trends were seen in the expression of CX₃CL1 in vascular cells following 24h treatment with testosterone (A) or DHT (B), with or without flutamide (F100=Flutamide 100nM, F1000=Flutamide 1000nM). *Kruskal-Wallis n=3.*
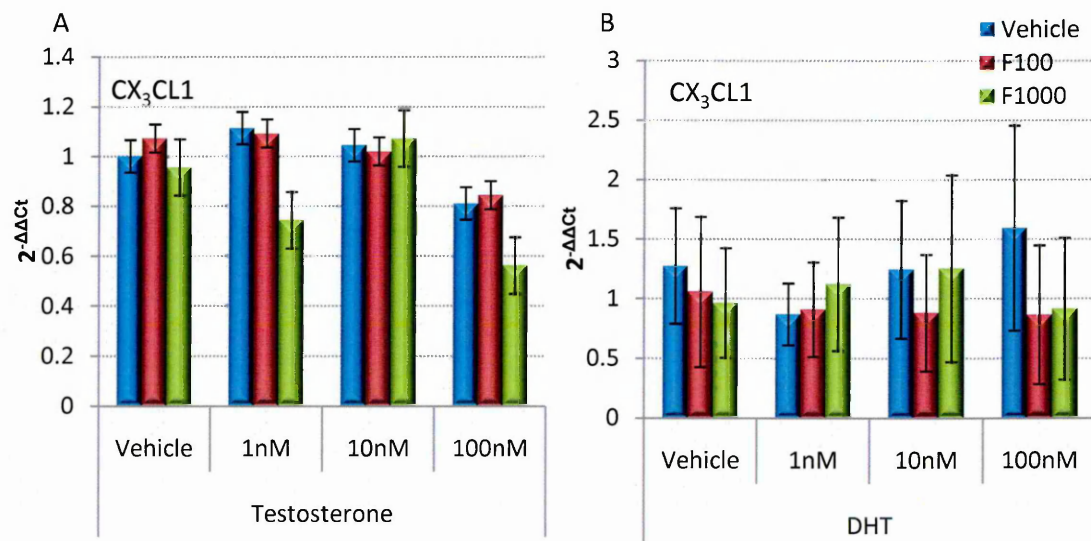
Figure 2.41; qRT-PCR analysis of CX$_3$CL1 mRNA expression in HAEC following androgen treatment and AR blockade. No significant effects or trends were seen in the expression of CX$_3$CL1 in vascular cells following 24h treatment with testosterone (h) or DHT (i), with or without flutamide (F100=Flutamide 100nM, F1000=Flutamide 1000nM). *Kruskal-Wallis n=3.*

CX$_3$CL1 mRNA expression in HASMC appeared to be physiologically, although not statistically, down-regulated in a dose-dependent manner by testosterone. This trend was not altered by AR antagonism (n=3; figure 2.42). However, no effect was seen with DHT treatment under the same experimental conditions (n=3; figure 2.42). In agreement with this, in HAEC DHT did not modulate cytokine-induced CX$_3$CL1 upregulation (n=3; figure 2.43), whereas a slight physiological, but not statistically significant, reduction due to testosterone was observed, particularly at the higher concentration of 100ng/ml TNFα plus IFNγ (n=3; figure 2.43). This down-regulation was abolished by co-treatment with 1000nM flutamide, suggesting an AR-mediated response.

2.3.10 Investigation of androgen modulation of cytokine-induced CCL2 expression in vascular cells

In order to further study a potential modulatory effect of androgens in inflammation, the effect of testosterone and DHT on cytokine-induced CCL2 expression was investigated.

2.3.10.1 *Effect of androgens on CCL2 expression: analysis by ELISA*

As cytokine-induced CX$_3$CL1 protein expression in vascular cells was not modulated by androgens when cells were incubated in 10nM to 2μM for 24h prior to 24h TNFα plus IFNγ treatment, in this experiment only supraphysiological doses of testosterone were used to test for an effect on CCL2 expression in HASMC. Pre-treatment with 0.1 and 10μM testosterone produced no significant effect on cytokine-induced CCL2 expression, measured in both the cell supernatants and lysates (n=2; see figure 2.44).

2.3.10.2 *Effect of androgens on CCL2 expression: analysis by qRT-PCR*

Expression of CCL2 mRNA in vascular cells was similarly not significantly modulated by 24h treatment with testosterone or DHT, either with or without flutamide in serum containing media. However, 100nM testosterone treatment did appear to reduce CCL2 mRNA expression in HAEC, both with and without AR antagonism (n=3; see figures 2.45 and 2.46). As with CX$_3$CL1 mRNA expression, when a subsequent 2h 10ng/ml cytokine stimulation was applied after the 24h androgen treatments, expression of CCL2 mRNA in HAEC appeared physiologically, although not statistically, down-regulated by testosterone, particularly at 10nM concentrations. Again this trend was abrogated by AR antagonism, suggesting an AR-mediated response (n=3; figure 2.47). However, no effect was seen with DHT treatment under
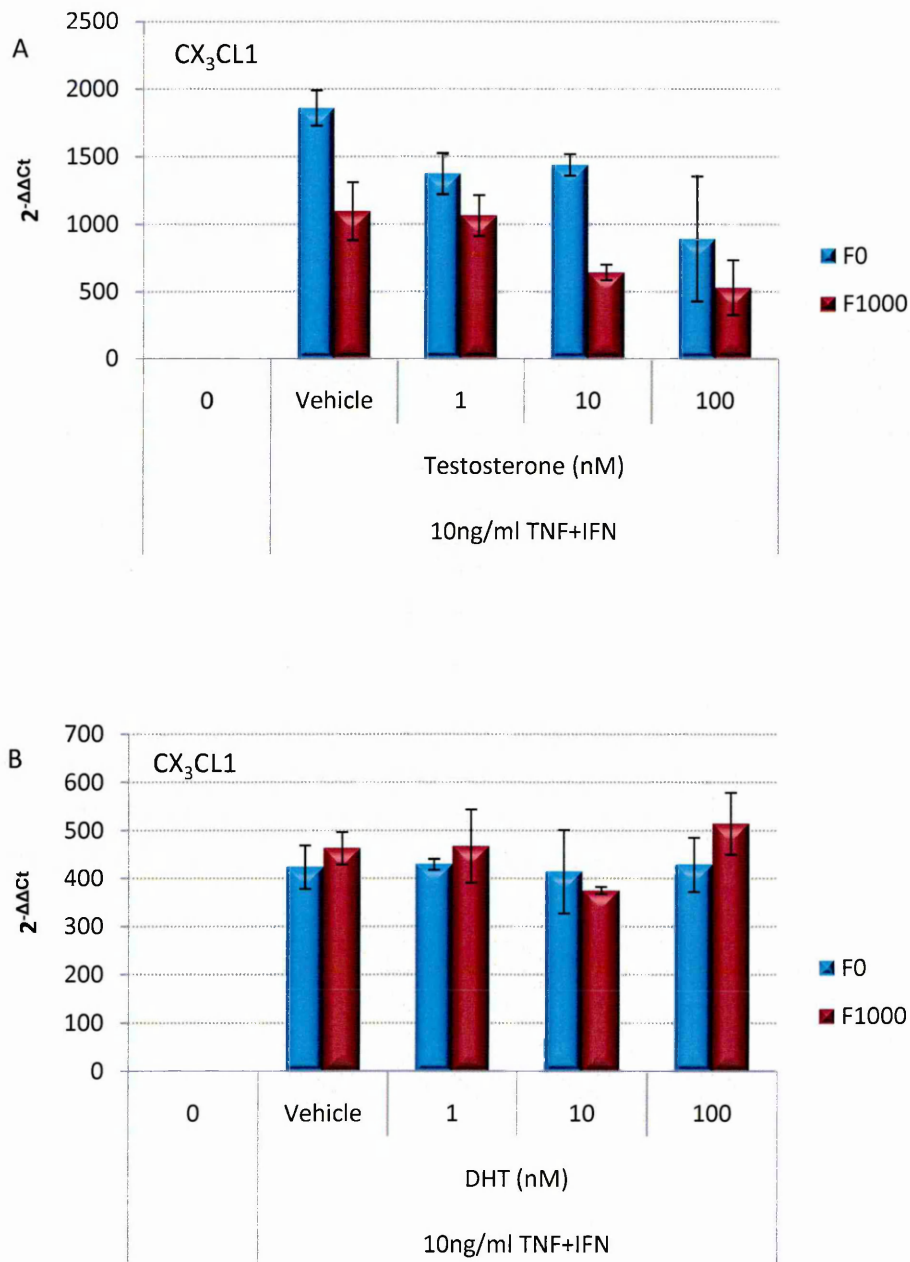
Figure 2.42; qRT-PCR analysis of CX₃CL1 mRNA expression in HASMC following cytokine and androgen treatment with AR blockade. TNFα plus IFNγ-induced CX₃CL1 expression appeared marginally but not significantly reduced by testosterone treatment, an effect that was not altered by blocking the AR with 1000nM flutamide (F1000) (A). No effect was observed with DHT treatment (B). *Kruskal-Wallis n=3.*
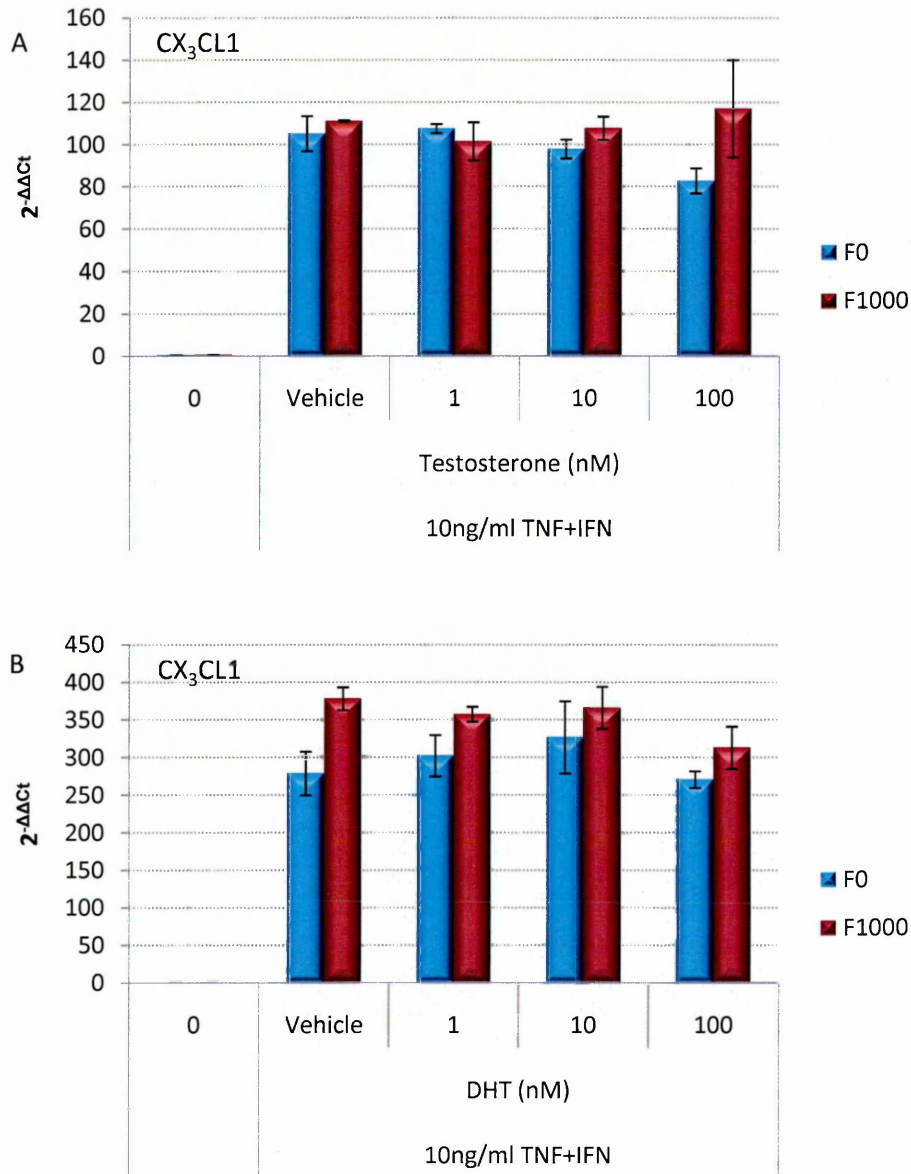
Figure 2.43; qRT-PCR analysis of CX₃CL1 mRNA expression in HAEC following cytokine and androgen treatment with AR blockade. TNFα plus IFNγ-induced CX₃CL1 expression appeared marginally but not significantly reduced by testosterone treatment, an effect that was abrogated by blocking the AR with 1000nM flutamide (F1000) (A). No effect was observed with DHT treatment (B). *Kruskal-Wallis n=3.*
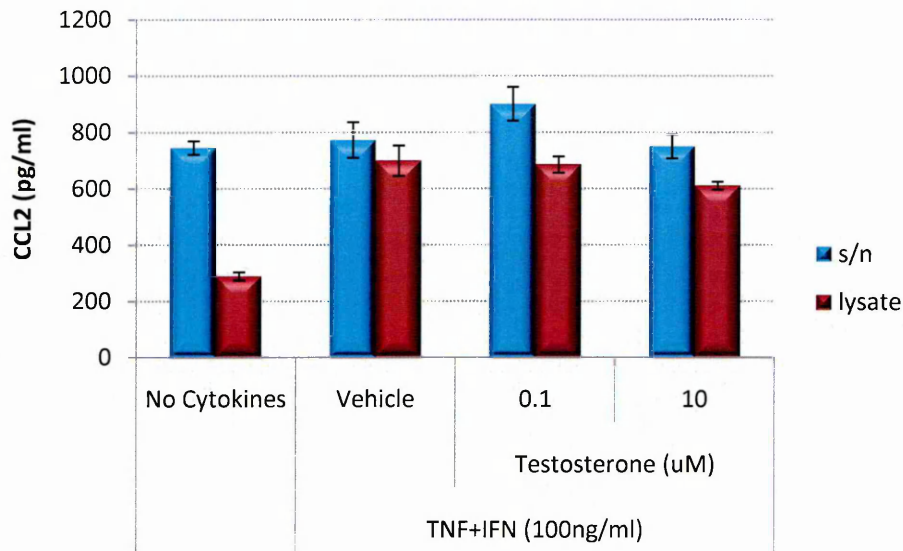
Figure 2.44; ELISA analysis of CCL2 expression in HASMC following cytokine and androgen treatment. Cell-associated (lysate) and secreted (supernatant, s/n) 24h cytokine-induced CCL2 expression was not altered by 24h pre-treatment with DHT. *Kruskal-Wallis n=2*
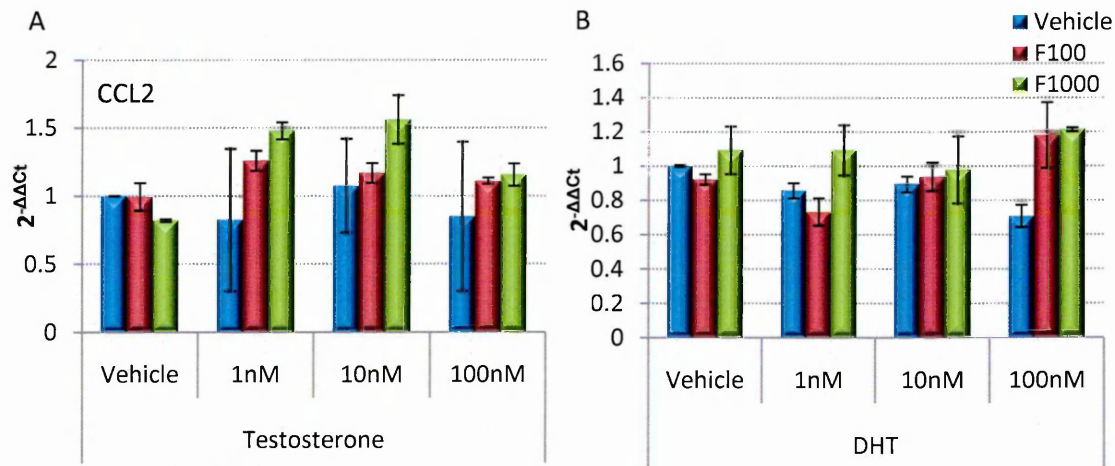
Figure 2.45; qRT-PCR analysis of CCL2 mRNA expression in HASMC following androgen treatment and AR blockade. No significant effects or trends were seen in the expression of CCL2 in vascular cells following 24h treatment with testosterone (A) or DHT (B), with or without flutamide (F100=Flutamide 100nM, F1000=Flutamide 1000nM). *Kruskal-Wallis n=3.*

147
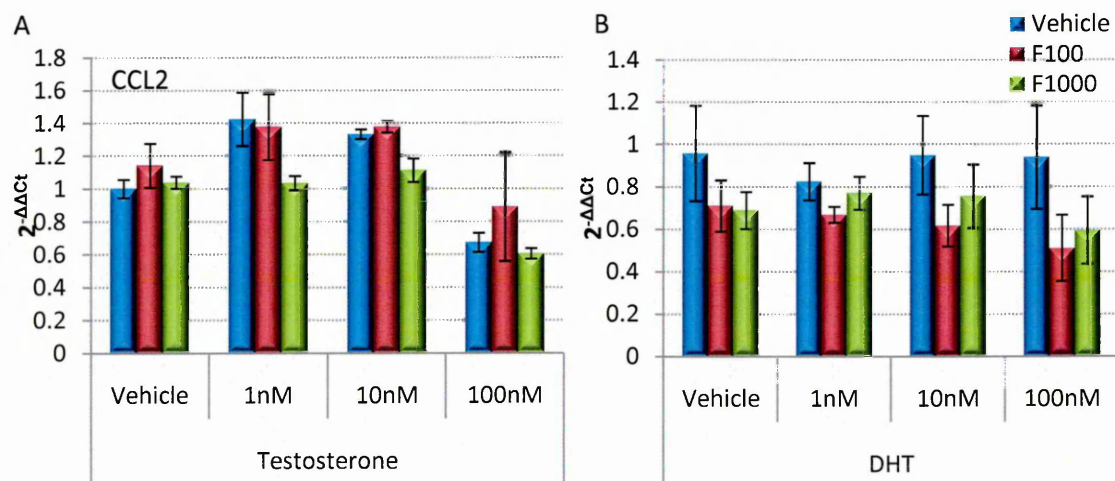
Figure 2.46; qRT-PCR analysis of CCL2 mRNA expression in HAEC following androgen treatment and AR blockade. No significant effects or trends were seen in the expression of CCL2 in HAEC following 24h treatment with testosterone (m) or DHT (n), with or without flutamide. *Kruskal-Wallis n=3.*

the same experimental conditions (n=3; figure 2.47), and there was no effect of testosterone or DHT on HASMC cytokine-induced CCL2 upregulation (n=3; see figure 2.48).

2.3.11   Androgen delivery test

To test androgen action on vascular cells, AR mRNA was assessed in HASMC and HAEC following testosterone or DHT treatment. No modulation was observed and only low copy numbers of the AR gene were expressed (n=3; see figure 2.49).

AR expression was confirmed in the human vascular cells by immunocytochemistry. AR staining was demonstrated at low levels in the cytoplasm and the perinuclear regions of HASMC. HAEC displayed a similar pattern of staining, but with increased AR staining in the perinuclear region. Negative controls, with the omission of the primary antibody, showed no staining, ruling out potential non-specific binding of the secondary antibody (Figure 2.50).

To investigate whether this lack of effect on vascular cells was due to a failure to deliver the androgens to the cells, the prostate cancer cell line DuCAPs (Figure 2.51) was utilised, since these cells are known for their androgenic response due to amplified AR expression (Saramaki *et al.* 2008). DHT (n=3) and testosterone (n=1) were shown to down-regulate AR expression in DuCAPs in a dose-dependent manner following 24h treatment (Figure 2.51). This down-regulation was not statistically significant, due to the variability of data and lack of power associated with qRT-PCR experiments. However, the physiological effect was clearly evident. This confirmed that androgens were being delivered to the cells in this experimental system. The pronounced effect of androgens seen in DuCAPs compared to the vascular cells maybe due to the greatly increased copy number of AR mRNA observed relative to GAPDH in these cells, potentially translating to an increased AR protein expression and activity relative to the vascular cells (Figure 2.52).

2.3.12   Summary

The cytokine (TNFα + IFNγ)-induced upregulation of CX$_3$CL1 in aortic vascular cells in this model was not significantly modulated by testosterone or DHT treatment. Slight modulations in expression were observed, particularly following testosterone treatment, and mostly showed a down-regulation with AR antagonism differentially regulating any such modulations dependent upon cell type, treatment duration and whether testosterone or DHT was used. However, the majority of the different culture conditions investigated demonstrated no androgenic effects and where slight trends were apparent significance was lacking. Similar inconsistent results were seen for the modulation of cytokine-induced CCL2 upregulation.
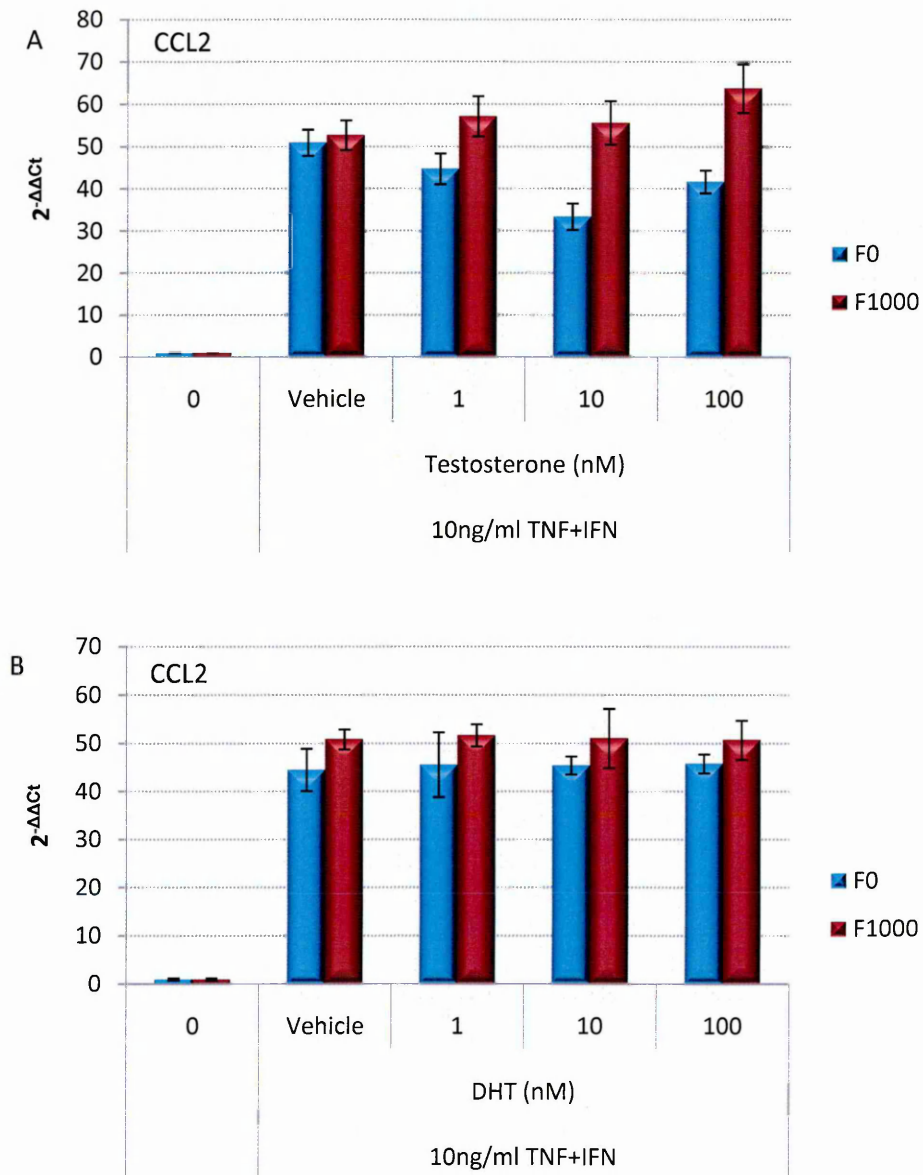
Figure 2.47; qRT-PCR analysis of CCL2 mRNA expression in HAEC following cytokine and androgen treatment wityh AR blockade. TNFα plus IFNγ-induced CCL2 expression appeared marginally but not significantly reduced by testosterone treatment, an effect that was abrogated by blocking the AR with 1000nM flutamide (F1000) (A). No effect was seen with DHT treatment (B). *Kruskal-Wallis n=3.*
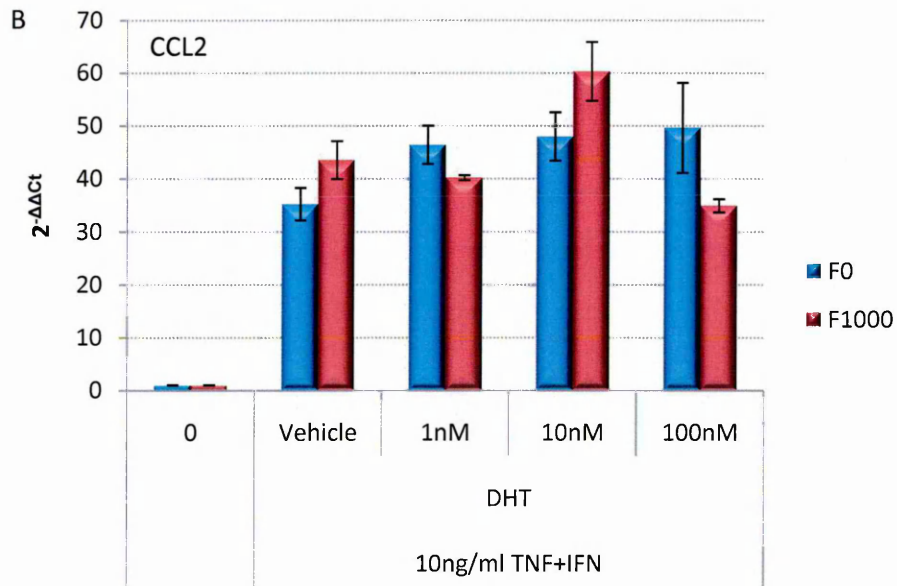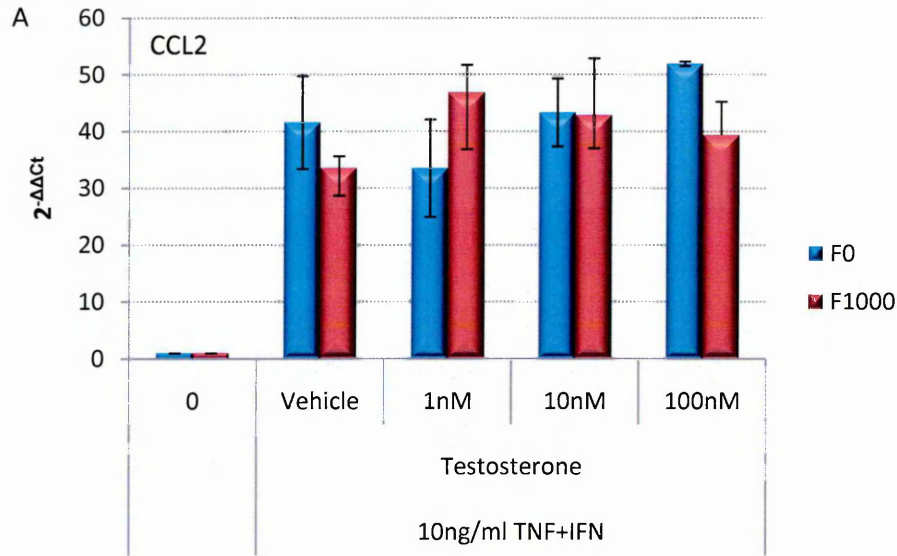
Figure 2.48; qRT-PCR analysis of CCL2 mRNA expression in HASMC following cytokine and androgen treatment with AR blockade. 2hr cytokine-induced CCL2 expression was not significantly altered by 24hr pre-treatment with testosterone (A) or DHT (B) treatment, with or without AR blockade (1000nM flutamide; F1000). *Kruskal-Wallis n=3.*
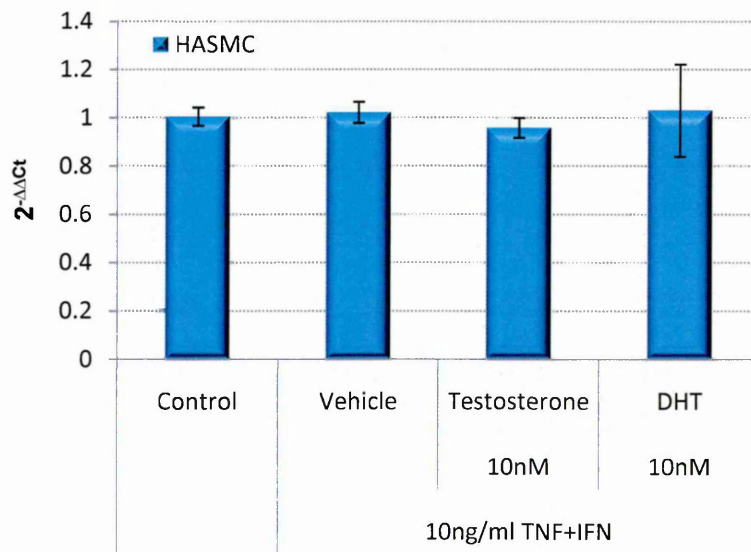
Figure 2.49; qRT-PCR analysis of AR mRNA expression in HASMC following cytokine and androgen treatment. 24hr androgen treatment followed by 2hr cytokine stimulation demonstrated no effect on AR expression. *Kruskal-Wallis n=3.*
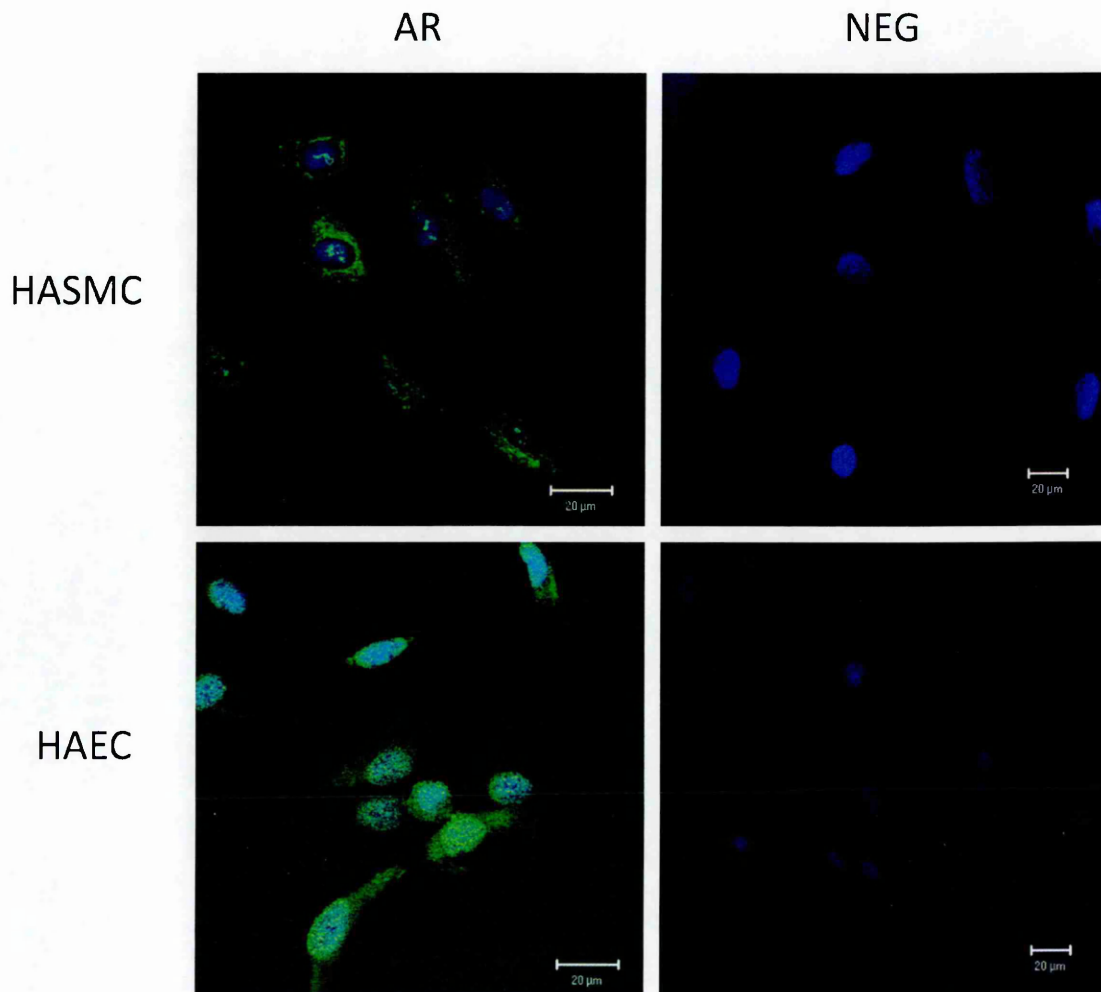
Figure 2.50; Immunocytochemical analysis of androgen receptor expression in human aortic vascular cells. Both HASMC and HAEC display positive immunofluorescent staining for the AR. The AR appears to be located in the cytoplasm and the nuclear regions of the cells following acetone fixation and permeablisation. Negative controls with the omission of the primary antibody revealed no non-specific binding of the secondary antibody. Nuclei were counterstained with DAPI (Blue).

153
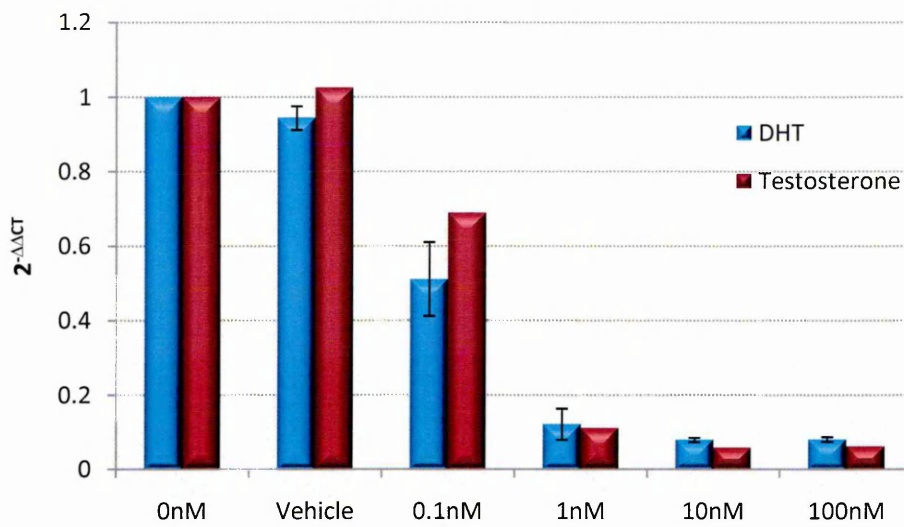
Figure 2.51; qRT-PCR analysis of androgen receptor mRNA expression in DuCaP cells following androgen treatment. DHT dose-dependently decreases AR expression in DuCAP cells (n=3). The same pattern is seen with testosterone treatment (n=1).

AR	DUCAPs	HASMC	HAEC
	2.973909151	0.002041509	0.000631
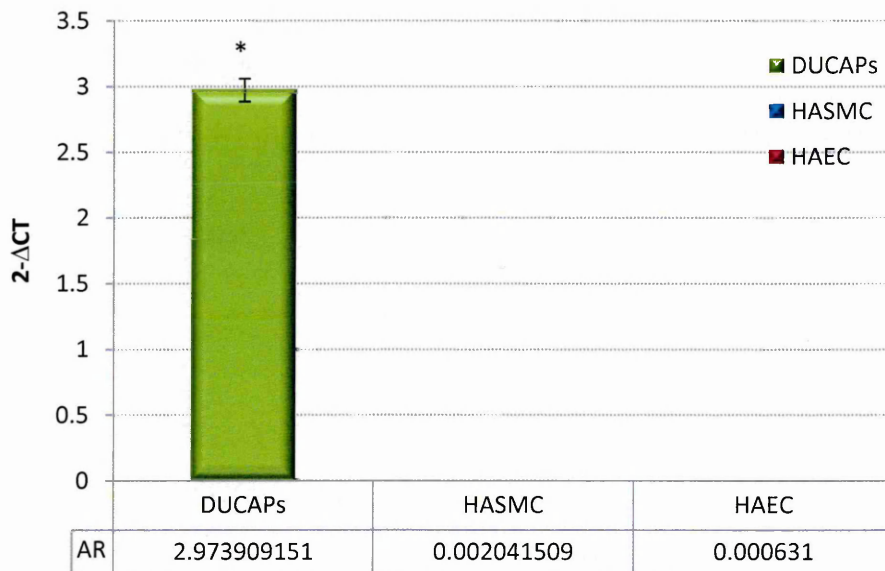
Figure 2.52; qRT-PCR relative expression of androgen receptor mRNA in DuCaP cells and human aortic vascular cells. The relative copy number of AR mRNA normalised to GAPDH, as measured by $2^{-\Delta Ct}$, was greater in the DuCaPs. *P<0.05vs DuCaPs, n=3, Kruskal-Wallis.*

2.4 Discussion

2.4.1 Optimisation of cytokine treatments

The main aim of the *in vitro* studies was to establish an inducible pro-inflammatory cell culture environment for both HAEC and HASMC as a model of vascular CX_3CL1 and CCL2 upregulation, whereby expression could be reliably measured and the impact of testosterone on the inflammatory response assessed.

In this study, IFNγ treatment of HASMC brought about an increase in CX_3CL1 protein expression in the cell culture supernatants, whereas TNFα and IL-18 had no effect. This is in contrast to previous research which has demonstrated on several occasions that TNFα stimulation of vascular cells leads to the upregulation and expression of CX_3CL1 (Chapman *et al.* 2000, Garcia *et al.* 2000, Ludwig *et al.* 2002, Lesnik *et al.* 2003, Ollivier *et al.* 2003, Ahn *et al.* 2004). In particular, Ollivier *et al.* (2003) investigated the expression of CX_3CL1 in HASMC following TNFα stimulation. Following 4 hours exposure to TNFα (0.1-20ng/ml), added to the culture medium, CX_3CL1 cell protein (measured via ELISA and flow cytometry) and mRNA (measured via qRT-PCR) was significantly upregulated. It is possible that the different results found in the present study are a result of measuring just cleaved CX_3CL1 in the culture supernatant. In the study by Ollivier *et al.* (2003) it was reported that CX_3CL1 released into the culture supernatant made up a maximum of just 30% of the CX_3CL1 expressed, and taken with the proposition that cell-bound CX_3CL1 can be recycled from the membrane to regulate surface expression (Huang *et al.* 2009, Liu *et al.* 2004), measurement of shed CX_3CL1 alone may not be an adequate measure. The detection of CX_3CL1 in culture supernatants may be more reflective of the activity of its endogenous sheddases rather than CX_3CL1 expression *per se*.

The present study does however support previous findings where IFNγ increased CX_3CL1 expression in vascular endothelial cells (Bazan *et al.* 1997, Imaizumi *et al.* 2000) and in vascular SMC (Ludwig *et al* 2002, Ollivier *et al.* 2003, Lesnik *et al.* 2003) in a dose dependent manner. Again, the measurement of cleaved CX_3CL1 may represent sheddase function, as well as an increase in CX_3CL1 expression.

IL-18 had no effect on CX_3CL1 expression in HASMC in the present study, when applied alone or in combination with TNFα, IFNγ or TNFα and IFNγ together. As IL-18 augments the production of various other mediators, such as IFNγ, IL-1β, IL-8, IL-6, MCP-1, TNFα, and several adhesion molecules (Puren *et al.* 1998, Vidal-Vanaclocha *et al.* 2000, Gerdes *et al.* 2002), as

well as playing a role in SMC proliferation and migration (Sahar *et al.* 2005), it is possible that this cytokine may produce it's proatherogenic effects via interaction with, and regulation of, other mediators rather than having a direct action on CX_3CL1 expression.

The combination of TNFα and IFNγ dose-dependently upregulated shed CX_3CL1 expression in HASMC in a manner that was more than additive compared to the effects observed from single cytokine treatments. This would suggest that TNFα and IFNγ act in synergy to increase CX_3CL1 expression. TNFα and IFNγ are known to cooperate with each other in the upregulation of various genes (Paludan 2000). The synergistic induction of CX_3CL1 by TNFα and IFNγ has been reported previously in vascular endothelial cells (Matsumiya *et al.* 2010), and in cultured astrocytes (Yoshida *et al.* 2001). Matsumiya *et al.* (2010) recently attempted to characterise these mechanisms. The authors reported regulation at a post-transcriptional level, with TNFα stabilising the CX_3CL1 mRNA expressed in response to IFNγ. This would allow for increased translation and protein assembly of CX_3CL1, therefore elevating the levels of expression. This theory is supported by the findings of the present study, as TNFα stimulation alone resulted in no increase in CX_3CL1 expression, whereas IFNγ generated a modest upregulation, which was enhanced by combined stimulation with TNFα. Additionally, a combined stimulation with TNFα and IFNγ has previously been shown to increase *in vitro* CX_3CL1 expression in HASMC, measured by ELISA, flow cytometry and qRT-PCR (Ludwig *et al.* 2002, Ollivier *et al.* 2003, Lesnik *et al.* 2003).

Investigation of this TNFα and IFNγ-induced CX_3CL1 upregulation over time revealed that cleaved CX_3CL1 increased with the duration of cytokine stimulation, first detected at 8 hours post-stimulation and then rising to maximal levels by 48 hours. Cell-associated CX_3CL1 was increased rapidly, as early as 2 hours post-stimulation, and displayed maximal expression between 8 and 24 hours post-stimulation, before returning almost to basal levels by 48 hours. This time-course of cell-associated CX_3CL1 expression in HASMC is reflective of the expression seen in HUVEC, whereby detection of full-length CX_3CL1 is observed at 6 hours post TNFα treatment (25ng/ml), reaching maximal concentrations at 12 hours, before returning towards basal levels by 24 hours (Chapman *et al.* 2000). These authors additionally reported a TNFα-induced increase in expression of CX_3CL1 mRNA at 2 hours, peaking between 6 and 12 hours, before falling at 24 hours post stimulation. Therefore, the decline in cell-associated CX_3CL1 described may be due to down-regulation of the cytokine-induced gene expression and surface shedding. This is possible as soluble CX_3CL1 in culture supernatants rose correspondingly. Chapman *et al.* (2000) also demonstrated a time-dependent increase of soluble CX_3CL1 in the culture media beginning at 12 hours post stimulation and increasing at 24 hours. As with the present study, this may not be reflective of increased production and

cleavage of CX_3CL1, but may result from CX_3CL1 accumulation in the cell culture supernatants over the time course of the experiment. Ollivier *et al.* (2003) also demonstrated an increase in CX_3CL1 mRNA expression in HASMC following TNFα plus IFNγ treatment, detectable at 2 hours post stimulation, peaking at 8h and falling by 16h. Additionally, Yoshida *et al.* (2001) demonstrated an almost identical time course profile of CX_3CL1 expression in the cell lysates and culture medium of astrocytes following a combined stimulation with TNFα and IFNγ, as seen in the present investigation. Thus, the response does not appear to be cell type-specific and the mechanism may be common to a number of cell types.

The time course of detection of both cell-associated and soluble CX_3CL1 in the present study supports the previous hypothesis that full-length CX_3CL1 is produced by vascular cells and directed to the membrane before it's release by a cleavage event (Bazan *et al.* 1997). Whether this cleavage *in vivo* serves to release CX_3CL1 as a chemoattractant, or whether it represents a terminating event to cellular expression remains controversial, and may depend on cell type, vascular location and additional inflammatory influences (Chapman *et al.* 2000, Ludwig *et al.* 2007).

In the present study there was a rapid induction (<2 hours) of CX_3CL1 protein expression in HASMC lysates which may indicate liberation from intracellular pools, as *de novo* protein synthesis characteristically requires a longer time period (Liu *et al.* 2005). Similar rapid protein detection has been observed in human fibroblasts and endothelial cells for the expression of CCL2 (Streiter *et al.* 1989b) and CX_3CR1 in monocytes (Green *et al.* 2006). However, the majority of CX_3CL1 protein measured in the cell lysates by ELISA in the present study was observed between 8 and 24 hours post cytokine treatment, which is more likely to be representative of gene upregulation and subsequent protein synthesis.

2.4.2 Analysis of CX₃CL1 expression following cytokine treatment of human aortic vascular cells

In the present study the dose-dependent increase in expression of cell-bound CX_3CL1 following pro-inflammatory cytokine treatment observed by ELISA and qRT-PCR in HASMC and HAEC, and flow cytometric analysis of HASMC, clearly indicate a role for this novel chemokine in vascular inflammation. Although substantial increases in expression were observed, indicating a physiological relevance, statistical significance was not always demonstrated, possibly due to low sample numbers and the subsequent use of non-parametric statistical analysis. In contrast to the expression of CX_3CL1 detected by ELISA, but in parallel with qRT-PCR data, the intensity of smooth muscle cell CX_3CL1 staining appeared greater than that of endothelial cells, as

157

analysed by immunocytochemistry. The fluorescence intensity was not quantified, however, so definitive conclusions cannot be drawn. Mixed reports exist as to the expression patterns of CX_3CL1 in vascular cells. Hansson and Libby (2006) describe that CX_3CL1 is preferentially expressed by smooth muscle cells, however, the major source of CX_3CL1 production in the arteries of CVD risk vessels has been considered to be from the endothelial cells (Perros et al. 2007). CX_3CL1 may have differential expression and function in cells dependent upon vascular location and current inflammatory status.

As stated in the previous section, the dose-dependent increases in CX_3CL1 expression seen in the present study have been reported previously in HASMC following TNFα and IFNγ stimulation (Ludwig et al. 2002, Ollivier et al. 2003, Lesnik et al. 2003). The mechanism by which this upregulation occurs is not fully elucidated, however NFκB and STAT signalling pathways may be involved. The human CX_3CL1 gene is located on chromosome 16 and there are binding sites for both NFκB and STAT in the promoter region of the gene (Nomiyama et al. 1998). TNFα and IFNγ receptor activation results in NFκB and STAT activity respectively, and is therefore capable of promoting CX_3CL1 gene transcription (Kotenko et al. 2000, Van der Heiden et al. 2010).

To control for potential effects of cytokine treatments on proliferation and cell number, which might affect the interpretation of the expressional results comparative to control conditions, BrdU and BCA assays were employed. The upregulation of CX_3CL1 protein and mRNA expression resulting from cytokine treatment was not considered to be a result of increased proliferation or cell number and was therefore a true reflection of CX_3CL1 synthesis. There was no significant effect of cytokine treatments on cell proliferation in HASMC as measured by BrdU assay. In parallel, the measurement of cell viability by propidium iodide uptake and subsequent flow cytometric analysis, revealed no significant differences between the cytokine treatment conditions in HASMC. Total protein from HASMC and HAEC samples was not altered between experimental conditions, as measured by BCA assay, supporting the proliferation and viability data. Therefore the samples were able to be directly compared. In contrast to this data, previous research has demonstrated both proliferative and apoptotic actions of TNFα and IFNγ in vascular cells. Yu et al (2009) reported a TNFα-induced apoptosis in bovine carotid artery endothelial cells, a mechanism that was also observed in human vascular endothelial cells (Chandra et al. 2003, Ramana et al. 2004). Dimmeler et al. (1999) provided evidence that apoptosis of vascular endothelial cells is due to the post translational modification of anti-apoptotic proteins sensitising the cells to cell death signals. Opposing results were observed for the effects of TNFα signalling in VSMC isolated from rat aorta (OuYang et al. 2002) and human vessels (Lee et al. 2005, Rajesh et al. 2008), as cell proliferation was reported post-

stimulation. These data suggest a cell type-specific action of TNFα. In contrast to these actions of TNFα, IFNγ has been reported to elicit pro-apoptotic effects in VSMC (Rosner *et al*. 2006, Bai *et al*. 2008). However, taken out of context of the atherosclerotic milieu at any given time in lesion development, isolated cytokine stimulations may not be fully representative of *in vivo* mechanisms, as additional apoptotic and/or survival signals may influence the fate of the vascular cells. These previous studies investigated the effects of single cytokine treatments, to elucidate the mechanisms of cell proliferation and apoptosis, as opposed to the combined stimulation used in the present study. It is plausible that in HASMC proliferation signals induced by TNFα (OuYang *et al*. 2002, Lee *et al*. 2005, Rajesh *et al*. 2008) are combined with apoptotic signals induced by IFNγ (Rosner *et al*. 2006, Bai *et al*. 2008) resulting in signal suppression and ultimately no overall effect on cell survival or growth. For the purpose of this study it was important to consider the effects of cytokine treatments on cell proliferation or apoptosis, as this may have biased the analysis. Since no effect was observed, it was considered that any subsequent effects of cytokine treatment were due to direct effects on target expression.

In summary, human aortic vascular cell expression of CX_3CL1 is significantly, and reproducibly, upregulated by the combination of proinflammatory cytokines TNFα and IFNγ in a dose-dependent manner. Thus, in the present study these experimental conditions were used as a suitable *in vitro* model of chemokine upregulation in aortic vascular cells.

2.4.3 Expression of ADAM-10 and ADAM-17 in human vascular cells

ADAM-10 and ADAM-17, and their tissue inhibitors TIMP-1 and TIMP-3, regulate the cleavage of CX_3CL1 from the surface of cells and therefore direct the functioning of this chemokine. Expression of these mediators was assessed in relation to the demonstrated cytokine-induced CX_3CL1 upregulation.

In the present study qRT-PCR and flow cytometry data suggest that the cytokine-induced increase in cleaved CX_3CL1 in aortic vascular cells is not a result of increased expression of ADAM-17 or ADAM-10, or decreased expression of their tissue inhibitors TIMP-1 and TIMP-3. As ADAM-10 is involved in the constitutive cleavage of CX_3CL1 (Hundhausen *et al*. 2003), it may be expected that the expression of this enzyme would not alter following stimulation. Previous studies have demonstrated that ADAM-17 mediates the inducible cleavage of CX_3CL1 following PMA stimulation (Chapman *et al*. 2000a, Garton *et al*. 2001, Tsou *et al*. 2001). These studies demonstrated increased ADAM-17 activity via increased concentrations of soluble CX_3CL1 in

culture supernatant, but did not investigate expression of the ADAM enzymes, or their tissue inhibitors, or, therefore, the mechanisms by which increased cleavage occurs. Doedens and Black (2000) demonstrated a down-regulation of PMA-induced ADAM-17 cell surface expression on monocytes in culture. This was partially due to internalisation of the enzyme, followed by degradation. ADAM-17 has also been reported to be associated with cholesterol-rich subcellular membrane microdomains, termed lipid rafts (Tellier *et al.* 2006). It is possible that this pool of ADAM-17 may cycle to the membrane to increase catalytic activity, rather than increasing gene transcription and subsequent protein expression. Comparable to the present study and supporting this idea, Schlondorff *et al.* (2000) reported that endogenous ADAM-17 localises predominantly in a perinuclear location, with at least some detected on the cell surface in COS-7 cells, an SV40 transformed kidney cell line from the African green monkey. Additionally, this distribution was not detectably altered by PMA stimulation. However, Huang *et al.* (2009) showed ADAM-17 and ADAM-10 expression predominantly on the cell surface in ECV-304 cells, a cell line originating from HUVEC. ADAM-17 expression was maintained on the surface of neutrophils following activation and induction of apoptosis (Walcheck *et al.* 2006). These differences may exist as functional disparities between different cell types in the regulation of cell surface cleavage of substrates. Additionally, the specificity of the antibodies used to localise the ADAM-17 protein may influence the findings, as specific targeting of the mature form of ADAM-17 may provide alternative staining patterns to antibodies directed against the pro-form or both. The antibody used in the present study however, mapped within an extracellular domain and would therefore bind both mature and pro-forms. However, no effect of cytokine stimulation on surface expression of ADAM-17 was demonstrated in the current study by flow cytometry, suggesting that translocation between subcellular compartments and the cell surface does not regulate the shedding of CX_3CL1 in HASMC.

ADAM-17 is additionally involved in the cleavage of some 50 transmembrane proteins including TNFα, TGFα, p75 TNF receptor, L-selectin and β-amyloid precursor protein (see Schlondorff *et al.* 2000). Similarly, ADAM-10 has high sequence homology to ADAM-17 and is implicated in the cleavage of many of the same substrate molecules (Hundhausen *et al.* 2003). Multiple substrate targets for these enzymes means that control of CX_3CL1 shedding at a level other than ADAM-17 or ADAM-10 expression would bestow greater specificity to the shedding of this substrate and the consequential cellular effects.

A down-regulation of TIMP-3 mRNA and protein has been reported in cardiac endothelial cells following TNFα and IL-1β treatment, suggesting that pro-inflammatory cytokines may increase ADAMs activity, and thus CX_3CL1 shedding, by decreasing endogenous inhibitors of catalytic

activity (Singh *et al.* 2005). The present study, however, demonstrated no modulation of either TIMP-3 or TIMP-1 mRNA expression, implicating that increased CX_3CL1 shedding as a result of $TNF\alpha$ and $IFN\gamma$ stimulation acts via an alternate mechanism.

A lack of cytokine regulation of ADAM-10, ADAM-17 and their tissue inhibitors in the presence of increased CX_3CL1 shedding may imply that additional enzymes could be responsible for ectodomain cleavage. Proteomic and functional investigations have recently revealed that MMP2 and cathepsin S are capable of cleaving CX_3CL1 (Dean *et al.* 2007, Clark *et al.* 2007). However, as broad spectrum metalloproteinase inhibitors are capable of blocking constitutive and inducible CX_3CL1 shedding (Chapman *et al.* 2000a, Garton *et al.* 2001, Hundhausen *et al.* 2003), the role of cathepsin S may be limited. Indeed, Bourd-Boittin *et al.* (2009) have also demonstrated that CX_3CL1 shedding in hepatic stellate cells is primarily due to the activity of MMP-2, whereas ADAM-10 and ADAM-17 only partially contribute to this cleavage. Whether the mechanisms of CX_3CL1 shedding are universal, or are differentially regulated in different tissues or cells, has not been investigated. Further investigation into the expression of these potential CX_3CL1 sheddases, in correspondence with cytokine-induced soluble CX_3CL1 expression by the vascular cells, would be useful to elaborate the mechanisms influencing the cleavage of this novel chemokine in atherosclerosis.

2.4.4 Expression of CX_3CR1 in human aortic vascular cells

While the functional roles remain relatively unexplored, CX_3CR1 expression on SMC is becoming apparent and may play a part in atherogenesis.

Contrary to the qRT-PCR findings in the present study, where no CX_3CR1 mRNA was identified, the CX_3CR1 protein was found to be expressed in HASMC and HAEC by immunocytochemistry. CX_3CR1 expression has been demonstrated on SMC in atherosclerotic plaque regions of human coronary arteries (Lucas 2003) and pulmonary arteries of rats (Perros *et al.* 2007). Additionally, it has been shown that primary rat pulmonary artery SMC (Perros *et al.* 2007) and rat aortic SMC (Chandrasekar *et al.* 2003) proliferate in response to CX_3CL1 in culture, while White *et al.* (2010) report a similar anti-apoptotic and proliferative effect of CX_3CL1 on primary human coronary artery SMC. Neither of these studies reported a migratory effect of CX_3CL1 on SMC, although this was demonstrated in the earlier study by Lucas *et al.* (2003). This suggests that CX_3CR1 is present on vascular SMC and that CX_3CL1 has a role in atherosclerosis beyond leukocyte attraction and adhesion. The critical balance of SMC apoptosis and proliferation that determines both plaque stability and vessel stenosis, and potentially the migration of SMC from the tunica media, may be mediated through CX_3CR1 interactions.

Previous research on endothelial cell expression of CX_3CR1 is limited. Crola Da Silva et al. (2009) investigated a range of endothelial cell lines for the expression of CX_3CR1, including two microvascular endothelial types. Human microvascular skin and brain endothelial cells displayed mRNA for CX_3CR1. A subset of vascular endothelial cells isolated from rat synovial tissue in a model of arthritis (Ruth et al. 2001) and human dermal microvascular cells (Volin et al. 2001) have additionally been shown to express CX_3CR1. Of particular relevance, Ryu et al. (2008) support the hypothesis that vascular endothelial cells express CX_3CR1. The authors reported that HAEC constitutively express CX_3CR1 and that mRNA expression is upregulated following CX_3CL1 stimulation. This allows for an autocrine action of CX_3CL1 on endothelial cells and is thought to influence angiogenic activities (Ryu et al. 2008).

In the present study, the conflicting data from qRT-PCR and immunocytochemical studies does not allow for clear conclusions to be drawn as to whether CX_3CR1 is expressed on HASMC and HAEC. The immunostaining results may need to be treated with caution, especially since high background staining and slight staining in the negative control wells occurred, as this may result from non-specific binding of the secondary antibody, which in turn may limit the reliability of the positive staining. Isotype controls would further validate the specificity of the primary antibody. The pitfalls of immunostaining techniques are reviewed extensively elsewhere (Lorincz and Nusser 2008, Fritschy 2008). The technique relies heavily on the specificity of the antibodies used to recognise the target antigens. In practice however, IgGs often unpredictably bind with low affinity to numerous, mostly undefined, cell and tissue constituents, giving rise to non-specific signals (Fritschy 2008). Therefore, setting the threshold between background and specific staining is vital, yet principally arbitrary. THP-1 monocytic cells were used as a positive control to validate antibody specificity and aid the determination of background staining, in an attempt to reduce the technical limitations. The use of isotype control antibodies and/or blocking the primary antibody prior to staining with soluble peptide, would also have been useful, and would be important controls for future studies.

In terms of the reliability of the qRT-PCR data, validation of the CX_3CR1 primer-probes used via target detection in THP-1 monocytes confirmed the reliability of the procedure. The correlation between mRNA and protein expression is not always invariant, and Gygi et al. (1999) described how mRNA is an insufficient predictor of protein expression. Post-transcriptional mechanisms controlling the translation rate of the proteins, the half lives of specific mRNAs or proteins, and the intracellular location and molecular association of the protein products may all contribute to the disparity between mRNA and protein quantification (See Gygi et al. 1999). Intracellular storage of CX_3CR1 has been proposed in monocytes, with rapidly induced translocation to the membrane allowing a post-transcriptional level of control

162

of CX_3CR1 expression and potentially negating the need for steady-state or inducible mRNA activity (See Green *et al.* 2006). Immunocytochemical analysis in the present study may support this theory, as CX_3CR1 appeared punctuate through the cytoplasm of HASMC and predominantly in a perinuclear location in HAEC. Additional investigations using flow cytometry or western blotting analysis would add the necessary extra data to determine and validate the expression pattern of this receptor in, and on, vascular cells.

CX_3CR1 expression in THP-1 cells was down-regulated by cytokine stimulation, suggesting a negative inflammatory feedback loop. Similarly, Weber *et al.* (1999b) induced a down-regulation of CCR2 mRNA and surface expression in isolated blood monocytes and Mono Mac 6 cells through $TNF\alpha$ stimulation, suggesting that proinflammatory cytokines can reduce chemokine receptor expression. This down-regulation of CX_3CR1 may represent a switch in monocyte subset to the more inflammatory $CCL2^+$ CX_3CR1^{lo} type (Swirski *et al.* 2007). Alternately, a reduction in CX_3CR1 expression may limit the binding of monocytes to CX_3CL1-expressing vascular cells, allowing for movement into, within and out of the vessel as these innate leukocytes patrol the inflamed vasculature. THP-1 cells are an immortalised cancer cell line and are therefore limited in their relation to typical human monocytes. Further studies using isolated PBMCs would be advantageous for future investigations.

2.4.5 CCL2 expression in human aortic vascular cells

As with CX_3CL1 expression, CCL2 was constitutively expressed in HASMC and HAEC. Expression was dose-dependently increased at the mRNA and protein level, following treatment with $TNF\alpha$ plus $IFN\gamma$, indicating a role for CCL2 in vascular inflammation. The lack of statistical significance of the data, for what appeared physiological alterations in mRNA expression, may be due to the low sample numbers and the conservative nature of the non-parametric statistics used to assess the differences.

Rollins *et al.* (1990) reported that HUVEC express little CCL2 under standard culture conditions, and that significantly higher levels can be induced by treatment of the cells with $TNF\alpha$ and, to a lesser extent, $IFN\gamma$. $TNF\alpha$ treatment increased the expression of CCL2 in primary human pulmonary artery endothelial cells (Maus *et al.* 2002) and in HUVEC there was an increased expression in response to injury (Weber *et al.* 1999a), lending further support for a role of CCL2 in vascular injury and inflammation. Additionally, Norata *et al.* (2010) have recently published that CCL2 mRNA is expressed basally in HUVEC and upregulated following incubation with $TNF\alpha$, supporting earlier work by the same group (Norata *et al.* 2006). CCL2 released from the endothelium acts as a chemoattractant, locally recruiting circulating monocytes and also

promoting monocytosis from bone marrow. Thus, CCL2 has local and distant effects on inflammatory mechanisms, many of which are typical of atheroma formation (see Combadiere *et al.* 2008).

CCL2 expression has been demonstrated in VSMC, with expression increased by LPS (Jiang *et al.* 2010) and IL-1β stimulation (Lim *et al.* 2009), indicating a role in pro-inflammatory processes in the vessel wall. SMC expression of CCL2 may facilitate the gradient-assisted diapedesis and migration of monocytes into the subendothelial space. Additionally, SMC also express CCR2 and can modulate their own function through autocrine mechanisms that promote proliferation and migration (Hayes *et al.* 1998). Within the vessel wall, SMC CCL2 secretion may act in a paracrine manner to further promote SMC migration to particular plaque areas, enabling the vascular remodelling characteristic of athero-development (Hayes *et al.* 1998).

High basal expression of CCL2 in the culture supernatant of HASMC could potentially be due to a lack of cell-cell contact communication between cells in culture, creating a cellular environment conducive to inflammation. Therefore, survival signals from cell-cell integrin signalling, which can activate intracellular kinases, and extracellular fibronectin signals may be reduced as a result of non-confluent cultures (Ilic *et al.* 1998, Stoneman and Bennett 2004). However, as both cell-associated and secreted CCL2 data displayed comparable expression patterns in HAEC, and were similar to the upregulation demonstrated for CX$_3$CL1 expression, the high basal levels may simply be an erroneous result. The dose-dependent increases in CCL2 mRNA were reflected at the protein level in HAEC and in the previous CX$_3$CL1 expression data, thus supporting this idea. Secreted CCL2 in culture supernatants may be expected to follow the same pattern, as CX$_3$CL1 and CCL2 appear co-ordinately regulated in response to TNFα and IFNγ. Increasing the sample numbers of this investigation may clarify this ambiguity.

It has been suggested that multiple chemokines operate in concert to control the migration of inflammatory subsets of monocytes in inflammation (Tacke *et al.* 2007). The present study supports this notion, as inflammatory cytokines upregulate CX$_3$CL1 and CCL2 in similar concentration-dependent patterns in HASMC and HAEC. The higher expression of CX$_3$CL1 may be representative of the low receptor expression on inflammatory monocyte subsets, considered to actively infiltrate inflamed tissue such as at sites of atheroma development, therefore requiring higher CX$_3$CL1 concentrations to induce migration (Geissmann *et al.* 2003, Combadiere *et al.* 2008). The specific contributions of individual chemokines and their cognate receptors are not completely understood.

2.4.6 Investigation of androgen modulation of cytokine-induced CX₃CL1 and CCL2 expression in vascular cells

No significant effects of testosterone or DHT treatment on CX_3CL1 and CCL2 expression were observed in the present study, suggesting that androgens do not modulate the expression of these chemokines in this *in vitro* model of chemokine regulation. To ensure that this was not a result of inactive androgens or due to lack of ARs, control experiments were performed.

AR expression was investigated in HASMC as a positive control to confirm that androgen delivery was successful in the treatment conditions. AR mRNA expression has been previously demonstrated to be upregulated by 24 hour testosterone treatment in VSMC, with protein expression only partially inhibited by androgen antagonism (Ma *et al*. 2005a, Ma *et al*. 2005b). However, a 10 minute exposure of vascular SMC to testosterone resulted in a transient down-regulation of AR protein (Ma *et al*. 2005a). These studies highlight the role of androgens in modulating their own receptor expression. In the present study, no effect on constitutive AR mRNA was observed, making it difficult to establish conclusive evidence that the lack of androgen modulation on CX_3CL1 and CCL2 was a physiological phenomenon and not simply a result of lack of androgen delivery to the cells. The further investigation of DuCaP AR mRNA expression following identical androgen treatment procedures revealed a dose-dependent decrease with both DHT and testosterone, indicating successful androgen delivery to the cells. Although not definitively investigated, the effect may have been due to the greatly enhanced AR expression in the prostatic cancer cell line compared to vascular cells, whereby the effect on AR expression is mediated through the AR. This, therefore, suggests that the lack of significant effects of androgens on CX_3CL1 and CCL2 expression in the present study are not due to a lack of androgen exposure.

Norata *et al*. (2006) have previously shown a significant decline in TNFα-induced and IL-6-induced CCL2 mRNA expression in HUVEC following a 1h pre-treatment with DHT. This decline was partially reduced by AR antagonism. The same group later demonstrated that the same pro-inflammatory upregulation was not significantly altered by 17β-estradiol, although it appeared physiologically reduced (Norata *et al*. 2010). This would suggest that potential anti-inflammatory effects of testosterone on CCL2 expression may function through both AR and ER actions. While the present study demonstrated a slight, but non-significant, decrease in TNFα plus IFNγ-induced CCL2 upregulation in HASMC following testosterone treatment, this effect was abrogated by blockade of the AR. Similar effects were seen in the mRNA expression data obtained for testosterone modulation of cytokine induced-CX_3CL1 regulation in HAEC in the

current investigation. This supports the study by Hatakeyama *et al.* (2002), who have shown, with qRT-PCR analysis in HAEC, that a testosterone reduction of TNFα-upregulated VCAM-1 mRNA expression was dependent on AR function, as co-incubation with cyproterone acetate, a steroidal antiandrogen, abolished the effect.

Mukherjee *et al.* (2001) also demonstrated that TNFα-induced VCAM-1 mRNA and protein expression was reduced by testosterone, but not by DHT, suggesting that testosterone may act through an AR-independent mechanism. Although the study did not look at the effects of blocking the AR, inhibition of aromatase completely abrogated the testosterone reduction of VCAM-1 expression, thus indicating that conversion to estradiol and subsequent ER activation may be the mode of this anti-inflammatory action of testosterone. Caulin-Glaser *et al.* (1995), provide data supporting this mechanism, since they reported that 17β-estradiol also reduced IL-1-stimulated upregulation of ICAM-1, VCAM-1 and E-selectin in HUVEC. These two studies however used HUVEC from umbilical cord of female foetuses, and therefore may not be reflective of steroid actions in cells of male origin as used in the present study.

The lack of a significant modulation of CX$_3$CL1 and CCL2 at the mRNA level by testosterone may not be reflective of membrane protein expression and function. Lui *et al.* (2005) introduced the concept that CX$_3$CL1 can be stored in intracellular pools and demonstrated that the equilibrium of trafficking between subcellular compartments and the cell membrane adds an additional level of functional control to CX$_3$CL1 expression beyond genetic regulation (Huang *et al.* 2009). Additionally, it is considered that the functional adhesiveness of CX$_3$CL1 requires molecular aggregation at the cell surface, increasing its avidity for CX$_3$CR1 (Hermand *et al.* 2008). This may take place through oligomerisation during self-assembly leading to molecular clustering. Taken together, it is therefore possible that rather than influencing CX$_3$CL1 gene upregulation (as measured by qRT-PCR) or whole cell protein concentrations (as measured by ELISA of cell lysates), that testosterone may influence either cell surface abundance or functional adhesiveness of this chemokine through actions on endosomal storage or focal membrane distribution. Flow cytometry and confocal immunocytochemical analysis would provide further insight to this hypothesis and detailed investigations into the mechanisms and signalling pathways involved would be required for definitive conclusions.

Taken together, the slight modifications of cytokine-induced CX$_3$CL1 upregulation and AR antagonism suggest that testosterone may function through AR-dependent mechanisms in HAEC and AR-independent mechanisms in HASMC. This conclusion is tentative however, as DHT, which primarily signals only through AR and with a higher affinity than testosterone, had no effect on CX$_3$CL1 expression in the present study.

No effect of androgen treatment on BrdU incorporation and total protein, as measures of proliferation and cell death affecting final cell numbers at time of sample collection, was detected in the present study, suggesting that any effect or lack of effect in subsequent target expression was not due to these factors. Ma *et al.* (2005b) also reported that testosterone did not affect DNA synthesis and cell number. Contrary to this, testosterone has been found to increase proliferation in human umbilical cord smooth muscle cells and HASMC, by inducing a gene known to be involved in proliferation (Nakamura *et al.* 2006). This supports work by Fujimoto *et al.* (1994) who suggested that androgens may directly accelerate atherosclerosis by stimulation of vascular SMC proliferation. Alternatively, testosterone has been suggested to enhance apoptotic damage resulting from serum deprivation in HUVEC (Ling *et al.* 2002). Also, vascular SMC proliferation has been shown to be inhibited by 17β-estradiol (Morey *et al.* 1997) and dehydroepiandrosterone (Williams *et al.* 2002). Opposing findings of investigations of endothelial cells revealed that oestrogens protect from apoptotic damage (Alvarez *et al.* 1997, Spyridopoulos *et al.* 1997, Florian *et al.* 2007). Taken together, this data suggests that sex steroid hormones can influence proliferative and apoptotic mechanisms in vascular cells.

The lack of effect of androgen treatments on proliferation in the present study is potentially due to the serum-deprived culture conditions, whereby growth factors (that would be present in the serum) are absent. This is supported by the significant increase in BrdU incorporation seen with cells incubated with 10% serum as a positive control. However, when cell treatments were carried out in serum-containing medium, again no androgen modulation of CX_3CL1 or CCL2 expression was observed, although these conditions were not assessed for any effects on proliferation or protein synthesis. Therefore, it is possible that any down-regulatory effects of androgen treatment may be balanced by an increase in cell proliferation. This scenario is unlikely however, as reference gene expression in qRT-PCR analysis accounts for increases in overall synthesis and displays target expression data relative to this.

To investigate whether the presence of growth factors is necessary for androgens to exert a modulatory action on inflammation, as suggested by Orio *et al.* (2002) and Bakin *et al.* (2003), media containing serum was used in additional experiments. Blockade of the AR with flutamide ruled out any effect of low-dose androgens that may have been present in the serum in the medium, on CX_3CL1 and CCL2 expression. This did not, however, eliminate potential effects through the ER or of any oestrogens present in the serum. Comparison of mRNA data between serum-containing and serum-free media conditions revealed consistent cytokine expression levels, suggesting that the presence of serum in the media had no modulatory effect on chemokine expression. The removal of hormones from the serum by charcoal-stripping would allow for the benefits of serum factors present in the media while

eliminating potential steroid influence, and would therefore be useful in future work. The use of phenol red as a pH indicator in culture media is standard practice, but may attribute methodological limitations to the present study. At concentrations found in tissue culture media, phenol red is considered to possess significant oestrogenic activity due to its structural resemblance to certain non-steroidal oestrogens (Berthois *et al*. 1986). This creates unwanted ambiguity as to the stimulatory state of the cells studied and the potential to create misleading results. However, as the same lack of modulation of CX_3CL1 and CCL2 mRNA expression was observed in HAEC, where phenol red-free media was used, the potential influence of this chemical may be limited in the present study. To rule out any confounding factors, it would be beneficial to use phenol red-free media for any further work.

The lack of effect of testosterone or DHT on TNFα and IFNγ-induced CX_3CL1 or CCL2 mRNA expression in the current study could be due to its inability to affect the greatly elevated expression of these molecules caused by the combined cytokine stimulation used. At low cytokine concentrations (1ng/ml TNFα plus IFNγ) large increases in mRNA were detected (between 80 to >1000 fold change for CX_3CL1, and approximately 15-fold difference for CCL2). As STAT-1 and NFκB transcription factors are thought to bind DNA independently (Ohmori *et al*. 1997), and due to the bidirectional enhancement of these factors on gene expression (e.g. IFNγ enhances NFκB transcription, and TNFα enhances STAT-1 activation), greatly elevated transcription may occur. Additionally, the synergy of TNFα-induced NFκB and IFNγ-activated STAT-1 may be, at least in part, due to physical interactions forming a complex that binds with higher avidity to the recognition sites, than the transcription factors individually (Paludan 2000). In this particular cell model, with cytokine concentrations causing greatly elevated upregulatory activation, it may be possible that androgen effects may not be sufficient to modulate these synergistically-enhanced mechanisms. All previous investigations into steroid modulation of inflammatory molecules have utilised single cytokine stimulations (see Tables 2.1 and 2.2). Repeating the present study with IFNγ alone may unmask a detectable androgen modulation.

Although DHT was used to investigate the effects of AR activity on inflammatory mediators, as it is non-aromatable to 17β-estradiol, it has recently been suggested that some of the effects of testosterone and DHT may be attributed to alternate metabolites capable of activating the ER. Norata *et al*. (2010) demonstrated that 5α-androstane-3β,17β-diol (3β-adiol), a metabolite resulting from the catabolism of DHT by the enzyme 3-hydroxysteroid dehydrogenase, reduces TNFα- and LPS-induced inflammatory responses including expression of ICAM-1, VCAM-1 and CCL2. These effects were inhibited or abolished by blocking the ER, in particular ERβ. This suggests that testosterone metabolites, other than those generated through aromatisation,

could exert a series of biological effects, which mediate ER activation and potential anti-inflammatory effects. As the conversion between DHT and 3β-adiol occurs almost ubiquitously (Norata *et al.* 2010) it is reasonable to propose that any effects, or lack of effects, of testosterone or DHT may be influenced by activity of their metabolites, as the existence of ligand-selective pathways of ER and AR compensate and contribute to the cellular response. It would therefore be desirable in future investigations to inhibit both AR and ER activity, in addition to the inhibition of metabolic enzymes in the steroidogenesis pathway, in order to delineate the role of potential underlying mechanisms and influencing factors.

Several previous investigations of vascular cell cultures have also failed to demonstrate an effect of androgens on particular inflammatory adhesion molecules, such as ICAM-1 (McCrohon *et al.* 1999, Zhang *et al.* 2002), E-selectin (McCrohon *et al.* 1999, Norata *et al.* 2006), PECAM-1 (Norata *et al.* 2006) and VCAM-1 (Aziz and Wakefield 1995). Many other studies have reported conflicting results regarding androgen modulation, and the effect seems to be dependent upon the sex steroid used, the cell type studied, the inflammatory target measured, the pro-inflammatory stimulus, the duration of incubations and the method of analysis (see Table 2.1).

The anti-inflammatory actions of testosterone and its reported protective effect on atherogenesis demonstrated *in vivo*, may function through the modulation of leukocytes. Specifically, androgen modulation of macrophages has been shown *in vitro* with DHT reducing LOX-1 expression and subsequent foam cell formation (Qui *et al.* 2010). Additionally, the upregulation of SR-BI and consequential increase in cholesterol efflux (Langer *et al.* 2002) and the reduced expression pro-inflammatory cytokines TNFα and IL-1β (Corcoran et al. 2010) in cultured human monocyte-derived macrophages in response to testosterone treatment, suggests that androgens may act on plaque monocyte/macrophages rather than vascular cells to modulate athero-inflammation. Therefore, the lack of androgen modulation on the expression of pro-inflammatory mediators observed in the present study may disprove the current hypothesis, yet does not discount the role of potential anti-inflammatory actions of testosterone in atheroma formation.

2.4.7 General considerations

The implications of the results from cell culture studies, where investigators fail to identify the gender or hormonal status of the original donor studied, may be limited although it is accepted that this is often beyond the control of the investigator. The gender origin of cells used in such studies will influence hormone receptor expression and therefore the responsiveness of the

169

cells to particular steroid treatments. This, therefore, makes it difficult to compare data across different studies. As the donors of vascular cells in the present study were relatively young (15 and 16 years old) males, their prior hormone exposure may be variable, dependent upon the individual's rate of sexual maturation. With this consideration, it may be useful to establish a cell culture model of hypogonadism in which cells are propagated and maintained in DHT- or testosterone-containing media, with deprivation of the androgen prior to the experimental procedure. This would standardise prior exposure, and potentially the responsiveness of the cells, while creating a situation more closely paralleled with the age-related androgen decline observed in men.

Cell culture models use isolated components (cells) of relevant tissues to investigate specific mechanisms, limiting the relevance to the *in vivo* situation. In the present study, it may be possible that androgens exert their atheroprotective and anti-inflammatory effects through actions on vessel wall vasodilation and subsequent improvements in vascular dysfunction (See Channer *et al.* 2003 and Wever *et al.* 1998). Therefore, androgen actions may not be demonstrable in isolated cells. In addition, the multiple cytokines, chemokines and enzymes which make up the complex milieu at sites of atheroma formation seen *in vivo* are difficult to recreate in vitro. Although *in vitro* investigations do allow some insight into potential pathways and enables their manipulation to assess specific functioning, these may not be reflective of the *in vivo* inflammation associated with atherosclerosis.

Another consideration in the present study is that agents used in culture may be degraded over the duration of the experiment, particularly in lengthy incubations, resulting in a lower exposure of the cells over time than nominally proposed. It should also be acknowledged that inconsistencies exist between the concentrations of agents required to produce effects *in vitro* and *in vivo*, particularly with the difficulties in estimating local cytokine concentrations.

2.4.8 Summary

The present study was successful in establishing a cell culture model of pro-inflammatory cytokine upregulation of CX_3CL1 and $CCL2$. Androgens had no significant modulating effects on the expression of these molecules, and where slight trends were observed these effects were not consistent across cell type, androgen treatment and receptor function. Although this may be due to the limitations of the cell culture model and the greatly enhanced cell responsiveness to cytokine treatments masking any subtle androgen modulation, thorough investigation indicates that testosterone does not have anti-inflammatory actions on CX_3CL1

and CCL2 expression in vascular cells. It is considered that testosterones anti-inflammatory mechanisms may act on monocytes/macrophages to confer atheroprotection.

CHAPTER 3

In vivo investigation of the effects of testosterone in early atherosclerosis

3.1 Introduction

3.1.1 Animal models of atherosclerosis

Animal studies have become invaluable in atherosclerosis research due to the difficulties in obtaining human tissue samples, particularly in a sequential manner, which has restricted investigations to cross-sectional studies on tissues acquired from cadavers or end-point corrective surgery. The recent advancement in non-invasive imaging modalities has offered new possibilities to overcome such limitations, and as technology and techniques improve the value of these investigations may add clinical relevance and become more influential in research. However, as human lesions develop over years to decades, whereas small animal atherogenesis can be induced over much shorter periods, most existing evidence from atherosclerosis studies is derived from the use of animal models and currently this remains an important tool.

3.1.1.2 Mouse models of atherosclerosis

Many animal models have been used over the years, but due to handling difficulties, large animal breeding expenses, breeding time and rate of plaque development, murine models have become the *de facto* model for *in vivo* atherosclerosis studies (Catanozi *et al.* 2009). Much of the recent advancement in knowledge of atherogenesis has come from murine models in which atherosclerosis can be induced by genetic and/or dietary intervention over relatively short periods of time (Tannock *et al.* 2010). As a species, the mouse is markedly resistant to atherosclerosis, necessitating inducing susceptibility via genetic manipulation and dietary intervention. Amongst the inbred strains, C57BL/6 mice have been determined as the strain most susceptible to diet-induced atherosclerosis, although even this was limited to small lesions in the aortic root, and this strain is therefore the strain of choice for producing genetically manipulated models (Daugherty 2002). The relative ease in which the mouse

genome can be altered to over-express or delete specific genes of interest has allowed for the creation of atherosclerosis-susceptible strains of mice valuable in the investigation of the mechanisms of the stages of disease development (Daugherty 2002).

The most extensively characterised genetically-manipulated strains of mice used in atherosclerosis research are the apolipoprotein E (apoE) and LDL receptor (LDLr) deficient animals. ApoE plays a key protective role in atherosclerosis by facilitating hepatic uptake of lipoproteins and stimulating cholesterol efflux from macrophages, thus maintaining overall plasma cholesterol homeostasis (Greenow *et al.* 2005). In a similar way, the LDLr is essential for clearance of circulating lipoproteins in the liver and uptake into macrophages in peripheral tissue. Therefore, lesion development in animals that lack these regulatory protective molecules is accelerated and is further exacerbated by feeding on a high-cholesterol, high-fat diet (Daugherty and Ratteri 2005). By combining these manipulations with deletion or up-regulation of a gene of interest, the direct testing of the role of certain proteins in atherosclerosis can be investigated.

3.1.2 Testosterone therapy in animal models of atherosclerosis

Several studies have reported the beneficial effects of hormone supplementation on atherosclerotic parameters in animal models, often in relation to castration, orchidectomy and ovariectomy. One early report identified a reduction in cholesterol accumulation in the aorta of orchidectomised male rabbits fed a pro-atherogenic diet and administered bi-weekly intra-muscular injections of testosterone, compared to placebo treated animals (Larsen *et al.* 1993). Comparable to these findings, Bruck *et al.* (1997) demonstrated gender-specific anti-atherogenic effects of testosterone and estradiol in orchidectomised male and female rabbits fed a high fat, high cholesterol diet. Testosterone administration significantly attenuated atheroma formation in male rabbits but not females, in which an increase in plaque size was observed. Equally, no protective effect of estradiol was seen in male rabbits, although atheroma formation was significantly inhibited in females. Interestingly, this study also demonstrated that a simultaneous administration of both testosterone and estradiol to both sexes resulted in a reduction in atherosclerosis (Bruck *et al.* 1997).

Alexandersen *et al.* (1999) found that castration *per se* resulted in an increase of aortic atherosclerosis in male cholesterol-fed rabbits, with the increase markedly inhibited following TRT compared to placebo. Intra-muscular injection of testosterone showed the highest degree of atherosclerotic inhibition in this study, potentially due to increased circulating levels over

173

time when compared to oral administration. The mode of testosterone action was thought to be via its conversion to estradiol and subsequent ER activity, although this was extrapolated purely on the basis that lower ER expression was present in the aortas of treated animals, possibly due to down-regulation as a result of chronic oestrogen exposure from testosterone aromatisation (Alexandersen *et al.* 1999). In a recent model of balloon injury, whereby balloon catheter over-inflation induced moderate or severe vascular damage in the coronary artery of male swine, neointima plaque formation was increased in castrated animals compared to controls (Tharp *et al.* 2009). This effect was attenuated by testosterone replacement in castrated animals and neointima formation was seen to be inversely related to testosterone concentration.

Contrary to these results, Aydilek and Aksakal (2005) demonstrated that intramuscular injection of testosterone in male New Zealand white rabbits exacerbated atherogenic lipid profiles, increasing total cholesterol (TC):HDL-cholesterol (HDL-C) ratio and decreasing HDL-C:LDL-C. This may be due to elevated testosterone concentrations as a result of supplementing otherwise healthy males. Castrated males in this study, however, displayed mildly improved lipid profiles compared to controls and significantly favourable HDL-C:LDL-C and TC:HDL-C compared to testosterone-injected rabbits, although TC alone was greatly elevated. Testosterone treatment also lead to an increase in LDL-C and detrimental lipid ratios in rhesus monkeys (Tyagi *et al.* 1999).

3.1.2.1 *Testosterone therapy in mouse models of atherosclerosis*

Testosterone therapy has also been studied in mouse models of atherosclerosis, and sub-dermal testosterone administration to castrated male apoE deficient mice decreased total serum and LDL-cholesterol following high-fat, high-cholesterol feeding (Elhage *et al.* 1997). These lipid lowering effects were reflected in a decrease in fatty streak formation.

Male and female apoE-/- mice receiving either testosterone or DHT via subdermal implant demonstrated differential effects on lesion size depending on the vascular territory (McRobb *et al.* 2009). DHT significantly reduced plaque area in the innominate artery of males and females compared to same-gender controls, as did testosterone in females. Both testosterone and DHT, however, increased lesion calcification, as a feature of advanced arterial plaques, in both sexes in the same vascular location. Testosterone and DHT reduced aortic sinus lesion area in females, but had no effect in males, whereas testosterone elevated calcification in both genders in this vascular bed. Although these results may suggest that androgens are capable of

174

increasing lesion calcification, this may be due to the heightened dosage. Androgens appear to be generally protective of lesion growth even at supraphysiological concentrations, but because they are supraphysiological levels, they may also present some concurrent detrimental effects (i.e. the calcification) (McRobb *et al.* 2009). It is possible that physiological concentrations of testosterone supplementation may not have these additional detrimental actions and bestow a primarily protective action.

Nathan *et al.* (2001) suggest that testosterone inhibits atherogenesis via it's conversion to estradiol by aromatase. In this study, orchidectomised LDLr knockout male mice on a high cholesterol diet had a greater extent of early lesion formation compared to mice receiving testosterone supplementation. This inhibitory effect of testosterone on plaque development was similar to that seen with estradiol administration in the same model. It was demonstrated that mice supplemented with testosterone and an aromatase inhibitor simultaneously developed increased lesion formation compared to those administered testosterone alone, and to a similar degree as untreated high-cholesterol diet fed mice. Conversion to 17-β-estradiol was implicated as the sole mechanism of action of testosterone in reducing lesion formation, and interestingly, the extent of lesion development appeared to be inversely correlated with plasma oestrogen measurements, suggesting that the protective effects of testosterone are, at least in part, due to aromatisation of testosterone to estradiol and actions via the ER (Nathan *et al.* 2001).

The idea of oestrogenic protection is supported by the reduction in lesion area observed in both male and female apoE deficient mice receiving 17β-estradiol treatment (Bourassa *et al.* 1996), and also the suggestion that ERα may be a key target in the atheroprotective effect of oestrogens in LDLr knockout mice (Billon-Gales *et al.* 2009). Additionally, treatment of 17β-estradiol significantly reduces the incidence and severity of angiotensin II-induced atherosclerosis in male apoE -/- mice, an effect believed to be associated with the down-regulation of NFκB-related inflammatory mediators in the aorta (Martin-McNulty *et al.* 2003). 17β-estradiol replacement also attenuated the negative vascular remodelling observed in ovariectomised female lipoprotein-a (Lp-a) transgenic mice (Nakagami *et al.* 2010).

Contrary to these studies that attribute a beneficial effect of testosterone preventing atheroma formation, two reports demonstrate a negative action of androgens. Following suppression of testosterone by administration of gonadotropin releasing hormone (GnRH), aortic sinus and ascending aorta atheroma formation in male mice was decreased, whilst testosterone treatment led to an increase in lesion size (von Dehn *et al.* 2001). Also, despite not using TRT, Villablanca *et al.* (2004) conclude from their ERα knockout model that it is

specifically this receptor that mediates susceptibility to early atherosclerosis in a testosterone-dependent manner. ERα wild-type male mice developed increased lesion size, number of lesions, more advanced lesions, and at a faster rate than ERα knockout mice, an effect that was eliminated by castration. Thus the actual effects of the AR and TRT on atheroma requires further investigation.

3.1.2.1.1 The Testicular Feminised Mouse

The murine equivalent of human complete androgen insensitivity syndrome (cAIS) was first described in the 1970s and named the Tfm mouse (Lyon *et al.* 1970). The Tfm mouse has developed a mutation that results in affected animals exhibiting an X-linked, single base-pair deletion in the gene encoding the classical androgen receptor (Charest *et al.* 1991). A frameshift mutation in the mRNA encoding the AR occurs as result of this mutation, leading to a stop codon in the amino-terminal region. Therefore, upon translation premature termination of AR protein synthesis occurs and a truncated receptor is produced that lacks both DNA- and steroid-binding domains (He *et al.* 1991). As such, Tfm mice are rendered completely androgen insensitive and express a phenotype that is outwardly female. In addition, the Tfm mouse has a reduced level of circulating testosterone, due to a deficiency of the enzyme 17α hydroxylase in the Leydig cells of the testis, a key enzyme in steroidogenesis (Murphy *et al.* 1991, Le Goascogne *et al.* 1993). The reduced activity of 17α hydroxylase is thought to be due to the intra-abdominal location of the testes and the absence of androgen action *in utero* (Murphy and O'Shaughnessy 1991). This additionally leads to elevated luteinising hormone (LH) production, as the negative long loop feedback mechanism of testosterone in the activation of pituitary AR is absent, activating mechanisms for increased testosterone production. As this negative feedback cannot occur due to AR dysfunction and low testosterone levels, circulating levels of LH are elevated, however due to the lack of 17α hydroxylase, circulating testosterone remains reduced (Murphy and O'Shaughnessy 1991).

Nettleship *et al.* (2007a) investigated the influence of the AR in atheroprotection in Tfm mice. When fed a high-fat, high-cholesterol diet, Tfm mice display a significant increase in aortic root lipid deposition compared to littermates, suggesting that testosterone and/or AR has an atheroprotective effect. Physiological testosterone administration prevented fatty streak formation when compared to untreated Tfm's and castrated littermate controls. Aromatase inhibition and ERα antagonism only moderately, but not completely, attenuated this response, and therefore the beneficial effects of testosterone were concluded to be independent of the AR and only partly due to ER actions via aromatase conversion. The protective actions of testosterone were considered to act, at least in part, via non-classical receptor mechanisms.

The AR-independent component of these atheroprotective effects were suggested to be due to testosterone-mediated improvements in endothelial function and vascular reactivity previously suggested by Jones *et al.* (2003). The distinct underlying mechanisms were not fully elucidated. This study did not investigate the potential modulation of TRT on inflammation, and to the best of my knowledge, there are no mouse models of atherosclerosis which investigate the relationship of these parameters.

3.1.3 Summary

Testosterone therapy is implicated as beneficial in preventing the development of atherosclerosis in animal models, with the mouse being the preferred species of investigation. The underlying mechanisms of these actions of testosterone remain unclear, with the AR, ER and alternative pathways all potential pathways for athero-modulation. With treatment outcome being dependent upon dosage, formulation, route of administration, vascular territory, genotype and gender, the potential athero-protective effects of testosterone require further investigation and the Tfm mouse provides a suitable model for investigating the effects of AR and testosterone function in atherosclerosis.

3.1.4 Hypothesis and aims of the *in vivo* study

The aim of the in vivo study was to use a mouse model of androgen insensitivity to address the hypothesis that TRT reduces diet-induced early atheroma formation in the Tfm mouse through anti-inflammatory actions and via AR-independent mechanisms.

Aims

1. To investigate the effects of low endogenous testosterone and a non-functional AR on atherosclerotic and inflammatory parameters using the Tfm mouse model.

2. To investigate the effects of high-cholesterol diet on these atherosclerotic and inflammatory parameters and the role of low endogenous testosterone and non-functional AR on such effects.

3. To investigate the effect of testosterone replacement on atherosclerotic and inflammatory parameters in the Tfm mouse fed a high-cholesterol diet.

3.2 Methods

3.2.1 The Testicular Feminised Mouse

The Tfm mouse originates from the C57BL/6 strain which has developed a mutation in the gene encoding the classical androgen receptor and a deficiency of the enzyme 17α hydroxylase (Charest *et al.* 1991, Murphy and O'Shaughnessy 1991, Le Goascogne *et al.* 1993). As such, Tfm mice express a non-functional AR and reduced levels of circulating testosterone, and consequently are phenotypically female. Therefore, Tfm mouse is considered a suitable model for investigating the effects of AR in testosterone function.

3.2.2 Animal Husbandry

The inherited mutation in the AR of Tfm mice is X-linked, resulting in only one quarter of the progeny of a breeding pair being affected. Two breeding schemes were employed in the present study, using mice of specified genotype. The mice were identified by inherent coat colour markers and gender phenotype (Figure 3.1). Tfm mice ($X^{Tfm}Y$ males) exhibit a dark agouti coat colour and have a female phenotype. Unaffected littermate males ($X^{Blo}Y$ or $X^{Ta33H}Y$) have a male phenotype and have either light coloured coats ($X^{Blo}Y$) or dark agouti coats, with bald patches behind the ears and dark patches around the eyes ($X^{Ta33H}Y$). Carrier females ($X^{Tfm}X$) have light fur and exhibit prominent transverse stripes or have dark fur with irregular patches, whereas non-carrier females ($X^{Ta33H}X$ or $X^{Blo}X$) have both the stripes and the light coloured patches (see figure 3.1).

The breeding colony of Tfm mice (strain C57BL/6J-A) used in this study was derived from frozen embryos obtained from the Medical Research Council genome project (MRC Harwell, UK). Mice were bred in sterile barrier conditions at The University of Sheffield Field Laboratories and $X^{Tfm}Y$ and male littermate controls ($X^{Blo}Y$ or $X^{Ta33H}Y$) were transferred to the holding room upon weaning (6 weeks old), where they were maintained for the duration of the experiment. Non-carrier females and carrier females not required for breeding were sacrificed via a UK Home Office-approved schedule 1 method once weaned. All animals used for the experimental procedures were maintained in cages containing up to 3 animals, on a twelve-hour light/dark cycle in a temperature (between 19 and 23°C) and humidity controlled (55 ± 10%) environment. All procedures were carried out under the jurisdiction of UK Home Office personal and project licences (project licence number 40/3165, personal licence number 60/11754), governed by the Animals Scientific Procedures Act 1986.
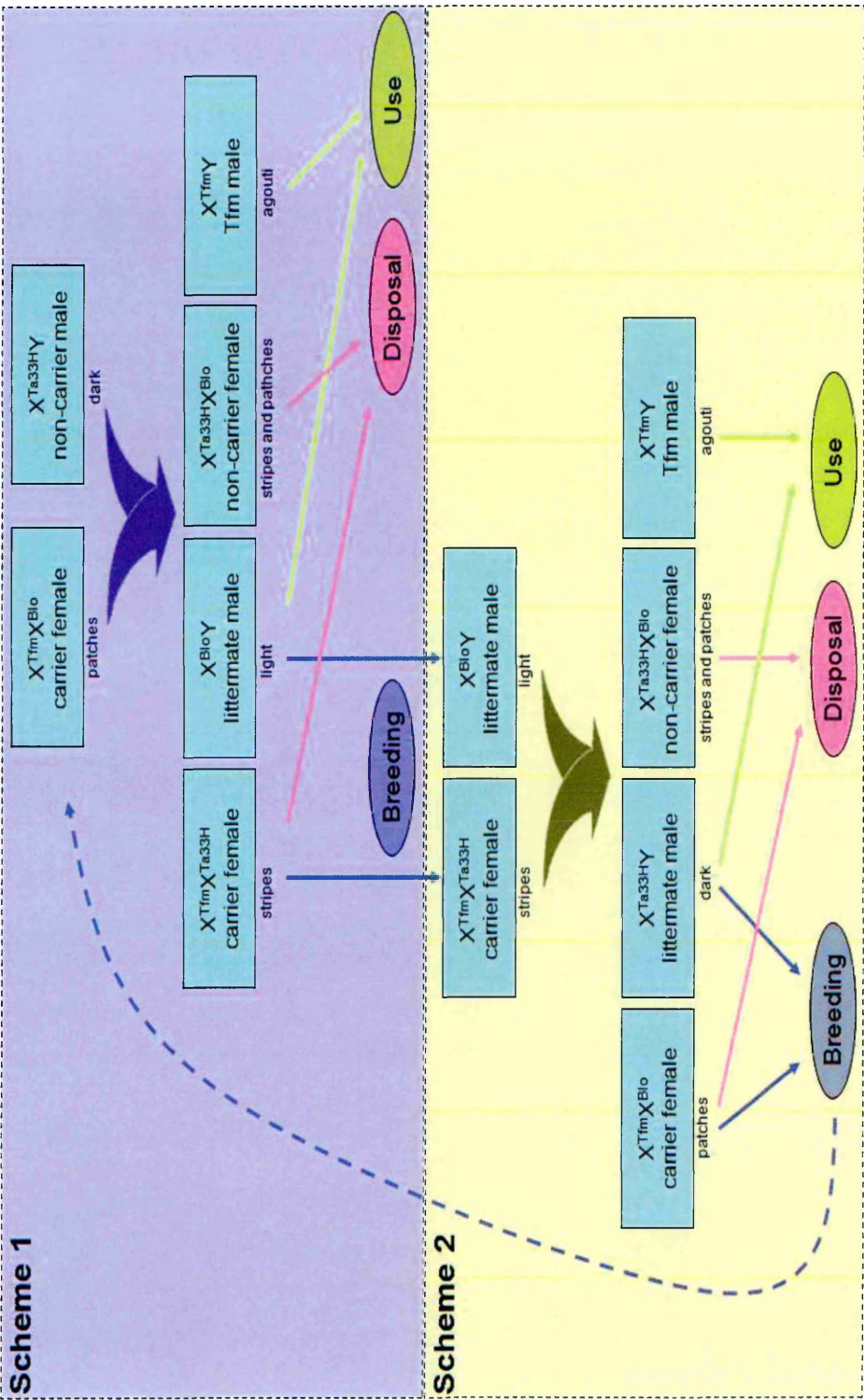
Figure 3.1: Schematic representation of the two breeding schemes used to generate Tfm mice. Carrier females ($X^{Tfm}X^{Blo}$ and $X^{Tfm}X^{Ta33H}$) and non-carrier males ($X^{Ta33H}Y$ and $X^{Blo}Y$) are bred producing a 1:4 ratio of affected offspring ($X^{Tfm}Y$), identified by coat-colour and markings. Adapted from Jones *et al.* (2003).

3.2.3 Experimental treatments

Animals were randomly assigned to specific diet and treatment groups after weaning until desired group numbers were reached.

Strain	Diet	Treatment	Abbreviation
XY Littermate	Normal chow diet	No treatment	XY ND
	High-cholesterol diet	No treatment	XY D
		10µl intra-muscular saline injection	XY S
Testicular feminised mouse	Normal chow diet	No treatment	Tfm ND
	High-cholesterol diet	No treatment	Tfm D
		10µl intra-muscular saline injection	Tfm S
		10µl intra-muscular sustanon100® injection	Tfm T

3.2.3.1   Promotion of atheroma formation

At age 8 weeks, Tfm and littermate controls were placed on a diet containing 42% butterfat and 1.25% cholesterol, along with 0.5% cholate, which is required for cholesterol absorption in the mouse (Special Diet Services, UK), for a period of 28 weeks, *ad libitum*. Prior to receiving this high-cholesterol diet, animals received a normal chow diet. Control mice received normal chow diet for the duration of the study.

3.2.3.2   Testosterone treatment

Mice that underwent testosterone or saline treatment received this via intramuscular injections. The hind leg of the mouse was held so to immobilise the quadriceps and the injection site shaved with a hair trimmer, previously cleaned with hibitane (SSL International Plc, UK). The shaven area was then gently wiped clean using a 1:200 dilution of hibitane. A sterile 0.3mL 30G needle (BD, UK) was introduced at a right angle to the skin surface into the centre of the muscle mass and 10µL of either Sustanon® 100 (20mg/mL testosterone propionate, 40mg/mL testosterone phenylpropionate, 40mg/mL testosterone isocaproate; equivalent to 74mg per mL testosterone) or physiological saline was injected. Animals were then returned to cages. Mice were injected once fortnightly, from 7 weeks of age, alternating the leg injected to minimise discomfort or irritation.

Animals were carefully monitored for the duration of the study and were weighed on a weekly basis.

3.2.4 Sry gender determination of animals

Sry (sex determining region Y) gene is a locus located on the Y chromosome. The Sry protein is a testis-specific transcription factor that promotes several genes leading to the formation of the testis and subsequent sexual differentiation and development in males (Sekido 2010). This phenotypic differentiation and male development is driven by the production and secretion of testosterone. Tfm mice are phenotypically female, as they possess a non-functional AR and express only low levels of testosterone, both elements necessary for male differentiation (Murphy *et al.* 1991), but they remain genetically male. Female mice lack the Sry gene, whereas males express the Sry gene regardless of their phenotype. Therefore, testing for the presence or absence of the Sry gene is very useful in the molecular assessment of mice with abnormal sexual differentiation.

The following methods were carried out in conjunction with BioServ UK Ltd, part of the University of Sheffield.

3.2.4.1   DNA isolation and collection

Ear clips were taken from Tfm mice and XY littermate controls and stored in autoclaved Eppendorf tubes overnight at 4°C, prior to analysis. 100μl of lysis buffer (10ng/ml Proteinase K, 1% sodium dodecyl sulphate (SDS), 50mM ethylenediaminetetraacetic acid (EDTA)) was added to the tube to cover the tissue, followed by a 30-60min incubation at 55°C, with repeated intermittent agitation, until the tissue was completely degraded. Phenol chloroform separation buffer (Sigma-Aldrich, UK) was added to the lysed tissue suspension at 2:1 volume:volume (200μl), briefly vortexed to mix, then centrifuged at 15.7 x g for 10mins at room temperature. After centrifugation, the suspension separated out into 3 layers; an upper aqueous layer containing DNA/RNA, a lower organic layer containing protein, and a small intermediate layer containing debris. The DNA-containing upper aqueous layer was transferred to a fresh autoclaved tube and mixed with an equal volume (100μl) of phenol chloroform separation buffer and then vortexed and centrifuged as before. The upper aqueous layer was transferred to a fresh autoclaved Eppendorf tube. To precipitate and clean the DNA, two volumes (approx 110μl) of 100% ethanol was added to the tube and mixed by gentle inversion, so as to not shear the DNA. Samples were centrifuged at 15.7 x g for 5mins. The DNA formed a small, not always visible, pellet on the bottom and side of the tube. The supernatant was carefully removed and the pellet was allowed to air dry for 3-5mins. The DNA was resuspended in 30μl of ultrapure diethylpyrocarbonate (DEPC)-treated water (Sigma-Aldrich, UK) with repeat

pipetting to mix. Samples were heated to 65°C for 10mins to denature any remaining remnants of proteinase K. Finally sample temperature was reduced to 4°C by storage at -20°C for 5 mins.

3.2.4.2   PCR gene amplification

A PCR buffer containing 10x master mix (2μl), 2mM MgCl$_2$ (0.8μl of 50mM), 200μM dNTPs (0.16μl of 100mM dNTPs mix containing 25mM of each dNTP), 1.5 units Taq polymerase (0.3μl of 5 unit/μl), forward and reverse primers for Sry and a reference gene TagE (0.4μl), was made up to 15μl with ultrapure DEPC treated water (10.14μl). Primer sequences and the selection of the reference gene were pre-designed and optimised by BioServ UK, Ltd.

Primer	Sequence
Sry (forward)	TGTTCAGCCCTACAGCCACATG
Sry (reverse)	CCACTCCTCTGTGACACTTTAGCC
TagE (forward)	GGAGGAGAGAGACCCCGTGAAA
TagE (reverse)	ACACGAAGTGACGCCCATCCGT

1μl of mouse ear clip extracted DNA was mixed with 4μl of ultrapure DEPC treated water and added to the PCR buffer mix to give a final volume of 20μl. The samples, along with a negative control (containing no DNA) and a positive control (a previously run sample expressing the Sry gene) were amplified in a Techne Touchgene Gradient thermocycler (Krackeler Scientific Inc., USA) under the following reaction conditions; 30 cycles at 94°C for 30s, 60°C for 30s and 72°C for 1min, and 1 cycle at 72°C for 5mins and 4°C hold.

To determine PCR products, the amplified DNA was run on a 2% agarose gel containing ethidium bromide. 5μl of 2x loading dye (bromophenol blue) was added to 5μl of the amplified DNA and 10μl of this mixture was loaded into individual wells of the agarose gel along with a 100bp DNA ladder (Sigma-Aldrich, UK) and the gel run at 150v for 1h. Amplification products were visualised under UV light to ascertain the presence or absence of the Sry gene product at 340bp. The housekeeping gene product at 450bp indicated a successful PCR amplification and acted as an internal control for the method.

3.2.5 Collection of animal tissues

At the end of the treatment period (36 weeks old) mice were killed by cervical dislocation, a Home Office approved Schedule 1 technique.

All samples collected from the mice after this point were labelled numerically, corresponding to the individual animals. Details of the experimental procedures that each animal underwent

were not revealed until all sample analysis was complete, so that the investigator was blind to the test groups throughout sample processing.

3.2.5.1   Serum Collection

Following cervical dislocation, a mid-line sternotomy was performed, the diaphragm was slit open and the thoracic aorta severed. Whole blood for serum measurements was collected from the chest cavity using a 2ml syringe (BD, UK), collected into 1.5ml Eppendorf tubes and allowed to clot for a minimum of 30 minutes at room temperature. Whole blood was then centrifuged at 0.8 x g for 10 minutes at room temperature and the serum removed and frozen in 60µl aliquots at -80°C, until analysis. All analyses were carried out on non-pooled serum, and samples underwent only one freeze-thaw cycle to maintain sample integrity.

3.2.5.2   Tissue collection

Following mid-line sternotomy and removal of whole blood from the chest cavity, the rib cage was opened and the lungs dissected clear. The heart, with the thoracic aorta attached, was carefully dissected free from the adventitia. The basal half of the ventricles was cut on a plane parallel with a plane formed by drawing a line between the tips of the atria, and the tissue removed. Dissection at this angle resulted in a final tissue orientation that allowed true cross-sections of the aortic root to be obtained, by compensating for the angle at which the aorta leaves the heart. The ascending aorta was then removed and any extraneous tissue was trimmed, taking care not to remove any tissue from the heart or aorta. The heart was perfused with PBS to remove any blood clots. The upper half of the heart, with the aortic root and initial section of the aortic arch still attached, was placed in a PVC cryogenic tissue mould measuring 13mm x 5mm (Fisher Scientific, UK) and embedded in optimum cutting temperature (OCT) compound (Bright Cryo-M-Bed; Bright Instrument Company Ltd., UK), with the aorta centred and facing upwards. Hearts were then frozen in liquid nitrogen cooled isopentane (Sigma-Aldrich, UK) and stored at -80°C until cryosectioning (Figure 3.2).

3.2.5.3   Cryosectioning

The aortic sinus was used to assess atherosclerotic plaque development as it has characteristic landmarks enabling reproducible location and identification of the aorta between animals (Paigen et al. 1987). In addition, the aortic sinus is the site most prone to atherosclerosis development in C57BL/6J mice (Paigen et al. 1987), and fatty streak formation has been previously demonstrated in the aortic root of Tfm mice fed on a high cholesterol diet (Nettleship et al. 2007a). Furthermore, lesions in this area have been shown to correlate with

later development of more advanced atherosclerotic lesions in the entire aorta, thus making it a good model of early atherosclerosis (Tangirala *et al*. 1995).

Method

OCT embedded mouse hearts were removed from -80°C storage and left at -20°C for 30 minutes to equilibrate to this temperature. Starting at the apex and moving towards the base of the heart, transverse sections were taken through the tissue using a Leica CM1850 UV cryostat at -16 to -18°C. Unstained sections were examined on an Olympus CH2 microscope to check for aortic positioning and sections were discarded until the valve leaflets became visible in the aorta. Once the appropriate region was located, 8μm sections through the aortic sinus (approximately 50 per mouse) were collected onto polysine charged slides (Thermo Scientific, UK) until the 3-valve cusps or the characteristic architecture of the aortic wall disappeared. Slides were stored at -80°C for later lipid and immunohistochemical analysis.

3.2.6 Measurement of serum testosterone via ELISA

In order to measure serum total testosterone levels in the mice a solid-phase competitive ELISA was used. In this assay microtitre wells were pre-coated with an antibody directed against a unique antigenic site on the testosterone molecule. The principle of the assay is that endogenous testosterone in the serum samples competed with a testosterone-horseradish peroxidase enzyme conjugate for binding to the antibody-coated well. After washing off unbound testosterone, the addition of a substrate solution resulted in a colour change that is inversely proportional to the amount of testosterone in the sample.

All reagents and multiwell plates contained in the testosterone ELISA kit (DRG Diagnostics, Germany) were allowed to equilibrate to room temperature, following 4°C storage. 25μl of testosterone standards (0, 0.2, 0.5, 1, 2, 6, and 16 ng/ml) and test serum were dispensed into the appropriate wells in duplicate, followed by the addition of 200μl of enzyme conjugate to each well. The plate was mixed for 10 seconds on a plate shaker and allowed to incubate at room temperature for 60 minutes. Following incubation, the wells were emptied by inversion and 400μl/well of wash solution was added. The wash solution was emptied from all wells and the plate was blotted onto clean absorbent paper to ensure complete removal of residual droplets. This wash procedure was repeated 3 times. The substrate solution (200μl) was then added to each well and the plate incubated at room temperature for 15 minutes before the addition of 100μl of stop solution (0.5M H_2SO_4) to terminate the enzymatic reaction. The absorbance of the well contents was determined using a Wallac multiscan plate reader (Perkin Elmer, UK) at 450±10nm within 5 minutes of stop solution addition. Serum testosterone
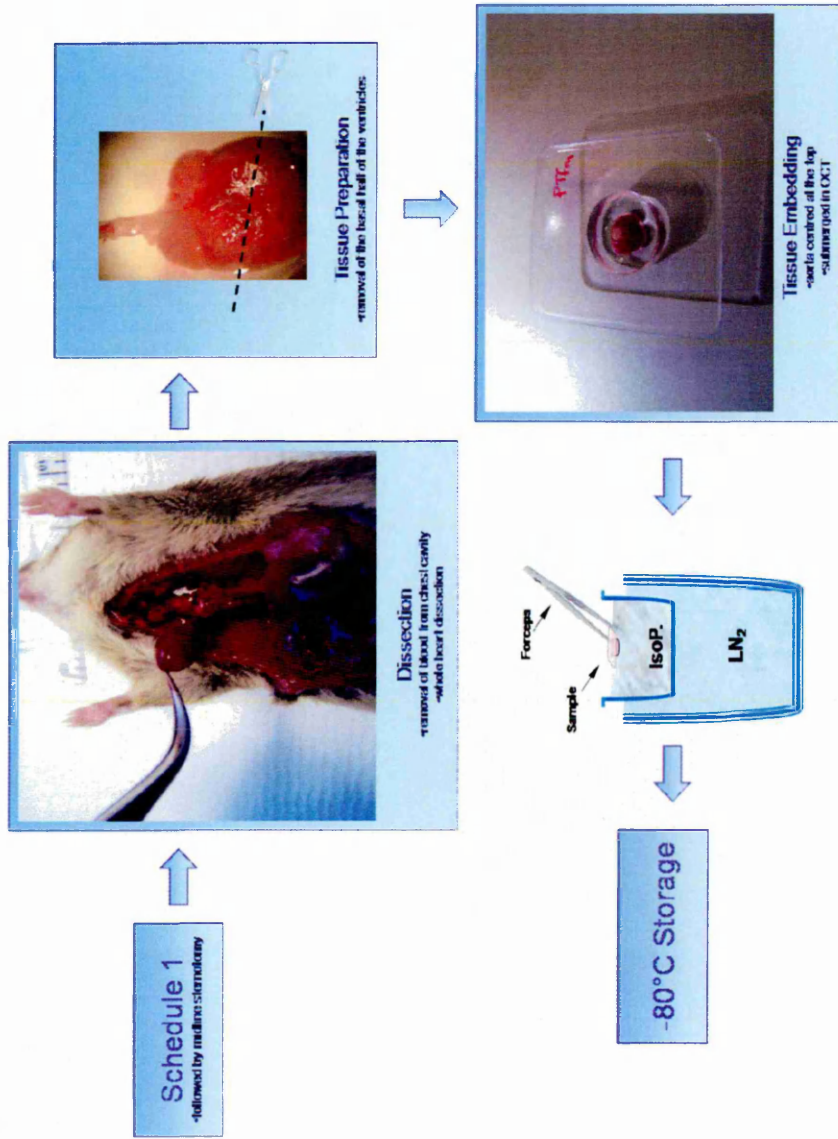
Figure 3.2; Collection and preparation of animal tissue. Following mid-line sternotomy and removal of whole blood from the chest cavity, the rib cage was opened and the heart with the thoracic aorta attached was carefully dissected free from the adventitia. The basal half of the ventricles was cut on a plane parallel with a plane formed by drawing a line between the tips of the atria and removed. The upper half of the heart was placed in a cryomould and embedded in OCT compound, with the aorta centred at the top. Hearts were then frozen in liquid nitrogen cooled isopentane and stored at -80°C. *LN$_2$, Liquid nitrogen; IsoP, Isopentane.*

185

concentrations were calculated from the standard curve in ng/ml using Microsoft Excel (Microsoft, USA) and converted into the more widely applied SI units (nmol/L) via multiplication by the known testosterone conversion factor 3.467 (http://www.soc-bdr.org/rds/authors/unit_tables_conversions_and_genetic_dictionaries_e5196/index_en.html).

3.2.7 Measurement of serum estradiol via ELISA

Estradiol (17β-estradiol) is the most potent naturally occurring oestrogen and is primarily produced by the female ovaries and the placenta, and to a lesser extent by the adrenals and testes in males (Hess *et al.* 1997). A solid-phase competitive ELISA was used to measure estradiol levels in mouse serum. Microtitre wells were pre-coated with a polyclonal antibody directed against an antigenic site on the estradiol molecule. Endogenous estradiol in the serum samples competed with an estradiol-horseradish peroxidase enzyme conjugate for binding to the antibody coated well. The addition of a substrate solution resulted in a colour change inversely proportional to the amount of estradiol in the sample.

All reagents and multiwell plates contained in the estradiol ELISA kit (Demeditec Diagnostics, Germany) were allowed to equilibrate to room temperature, following 4°C storage. 100μl of estradiol standards (0, 3, 10, 50, and 200pg/ml) and serum samples were dispensed into the duplicate wells, followed by the addition of 200μl of enzyme conjugate to each well. The plate was mixed for 10 seconds on a plate shaker and incubated at room temperature for 4h. Following incubation, the wells were emptied by inversion and 400μl of wash solution was added to each well. The wash solution was emptied from all wells and the plate was blotted onto clean absorbent paper to ensure complete removal of residual droplets. This wash procedure was repeated 3 times. The substrate solution (200μl) was then added to each well and the plate incubated at room temperature for 30 minutes before addition of 100μl of stop solution (0.5M H_2SO_4) to terminate the enzymatic reaction. The absorbance was determined using a multiscan plate reader as for testosterone ELISA. Serum concentrations of estradiol were converted to SI units (nmol/L) via multiplication by the known estradiol conversion factor 3.671 (http://www.soc-bdr.org/rds/authors/unit_tables_conversions_and_genetic_diction aries /e5196/index_en.html).

3.2.8 Measurement of serum lipids

Total cholesterol (TC), high-density lipoprotein-cholesterol (HDL-C) and triglycerides (TRIG) were measured using a VITROS®5, 1 FS high capacity chemistry system (Orthoclinical

Diagnostics, UK) with parallel processing at the Department of Clinical Chemistry, Sheffield Children's Hospital. The VITROS® chemistry technology is performed on the MicroSlide, an entire integrated test environment on a thin piece of layered film.

Mouse serum was thawed at 4°C and diluted two-fold with 7% BSA (VITROS®). A minimum of 70μl of sample was transferred to a loading cup and placed in a rack in the VITROS®5, 1 FS analyser. All three lipid measurements were obtained from each sample and values were adjusted for dilution factors. The principles underlying the three measurements are outlined below.

3.2.8.1   *Cholesterol*

5.5μl of sample was automatically transferred to the microslide for the enzymatic reaction to occur. The sample is evenly distributed on the MicroSlide due to the spreading layer containing Triton X-100, which aids the dissociation of the cholesterol and cholesterol esters from lipoprotein complexes. Cholesterol ester hydrolase, in the underlying layer, catalyses the hydrolysis of cholesterol esters to form cholesterol and fatty acids. Free cholesterol is then oxidised, forming cholestenone and hydrogen peroxide. Hydrogen peroxide can finally oxidise a leuco dye in the presence of peroxidase, also present in the reagent layer, to generate a coloured dye (Allain *et al.* 1974). The colorimetric density of the dye that is formed is measured by reflectance spectrophotometry and is proportional to the cholesterol concentration (figure 3.3).

3.2.8.2   *Triglyceride*

5.5μl of sample was automatically transferred to the microslide and is evenly distributed due to the spreading layer containing Triton X-100, which aids in the dissociation of triglycerides from the lipoprotein complexes. The triglyceride molecules are hydrolysed by lipase in the spreading layer to generate glycerol and fatty acids. Glycerol diffuses into the underlying reagent layer where it is phosphorylated by glycerol kinase, to L-α-glycerophosphate, in the presence of ATP and MgCl$_2$. L-α-glycerophosphate is then oxidised to dihydroxyacetone phosphate and hydrogen peroxide by L-α-glycerophosphate oxidase, present in the reagent layer. Hydrogen peroxide can finally oxidise a leuco dye in the presence of peroxidase, to generate a coloured dye (Spayd *et al.* 1978). The colorimetric density of the dye that is formed is measured by reflectance spectrophotometry and is proportional to the starting triglyceride concentration (figure 3.4).

187

A
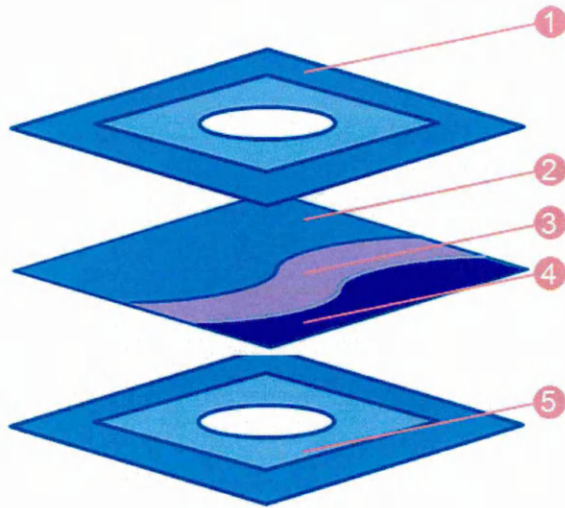
Cholesterol

1. **Upper slide mount**
2. **Spreading layer (BaSO$_4$)**
   - Triton X-100
3. **Reagent layer**
   - buffer, pH 6.25
   - cholesterol ester hydrolase
   - cholesterol oxidase
   - peroxidase
   - leuco dye
4. **Support layer**
5. **Lower slide mount**

B

Sample

lipoprotein $\xrightarrow{\text{TX100}}$ cholesterol + cholesterol esters + proteins

cholesterol esters + H$_2$O $\xrightarrow{\text{Cholesterol ester hydrolase}}$ cholesterol + fatty acids

cholesterol + O$_2$ $\xrightarrow{\text{Cholesterol oxidase}}$ cholestenone + H$_2$O$_2$

H$_2$O$_2$ + leuco dye $\xrightarrow{\text{Peroxidase}}$ dye + 2H$_2$O
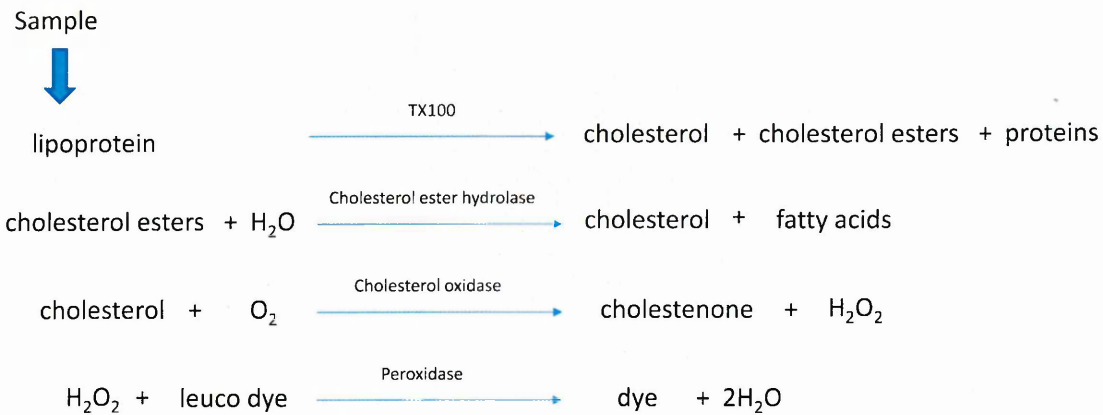
Figure 3.3; Total cholesterol measurement by the VITROS® chemistry system. The VITROS CHOL slide is a multilayered, analytical element coated on a polyester support. The entire integrated test environment, with specific test reagents, is contained on a thin piece of layered film (A), where all reactions take place (B). The final measurable colour change is proportional to the amount of cholesterol in the sample and is detected by reflectance spectrophotometry.

A
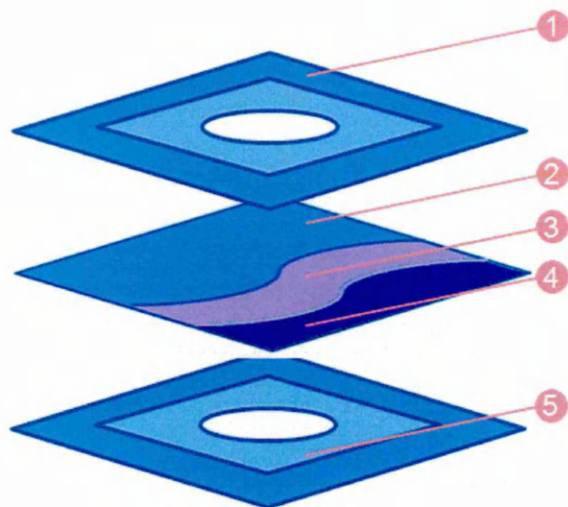
Triglyceride

1. Upper slide mount
2. Spreading layer (TIO_2)
   - Triton X-100
   - Lipase
3. Reagent layer
   - buffer, pH 8.0
   - glycerol kinase
   - ATP
   - L-α-glycerophosphate oxidase
   - peroxidase
   - leuco dye
4. Support layer
5. Lower slide mount

B

Sample

$$lipoprotein \xrightarrow{TX100} triglycerides + proteins$$

$$triglycerides + H_2O \xrightarrow{Lipase} glycerol + fatty\ acids$$

$$glycerol + ATP \xrightarrow{Glycerol\ Kinase + MgCl_2} L\text{-}\alpha\text{-glycerophosphate} + ADP$$

$$L\text{-}\alpha\text{-glycerophosphate} + O_2 \xrightarrow{L\text{-}\alpha\text{-glycerol-phosphate oxidase}} dihydroxyacetone\ phosphate + H_2O_2$$

$$H_2O_2 + leuco\ dye \xrightarrow{Peroxidase} dye + 2H_2O$$
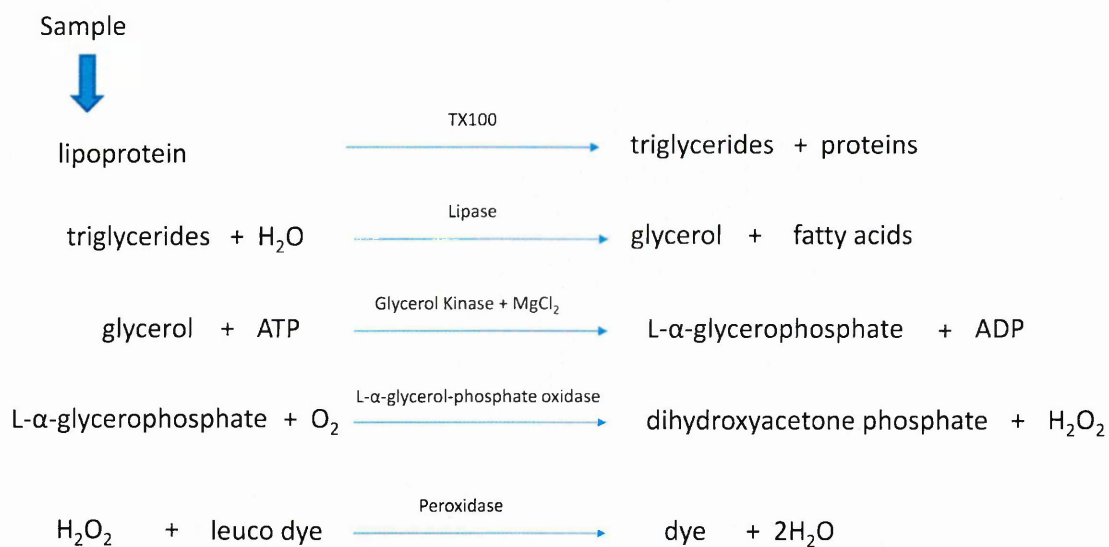
Figure 3.4; Triglyceride measurement by the VITROS® chemistry system. The VITROS TRIG slide is a multilayered, analytical element coated on a polyester support. The entire integrated test environment, with specific test reagents, is contained on a thin piece of layered film (A), where all reactions take place (B). The final measurable colour change is proportional to the amount of triglyceride in the sample and is detected by reflectance spectrophotometry.

189

3.2.8.3   High density lipoprotein cholesterol (HDL-C)

10μl of sample was automatically transferred to the microslide to measure serum HDL-C. The sample is evenly distributed by the spreading layer and non-HDL is precipitated using phosphotungstic acid (PTA) and magnesium chloride contained in this layer. Emulgen B-66 is a surfactant in the spreading layer that aids the selective dissociation of cholesterol and cholesterol ester from the HDL lipoprotein complexes in the sample. Cholesterol ester hydrolase in the underlying layer catalyses the hydrolysis of HDL-derived cholesterol esters to cholesterol and fatty acids. Free cholesterol is then oxidised forming cholestenone and hydrogen peroxide which can finally oxidise a leuco dye in the presence of peroxidase, to generate a coloured dye (Burstein *et al.* 1970, Allain *et al.* 1974). The colourmetric density of the dye that is formed is measured by reflectance spectrophotometry and is proportional to the HDL concentration of the sample (figure 3.5).

3.2.8.4   Low density lipoprotein cholesterol (LDL-C)

The concentration of serum LDL-C was calculated from the total cholesterol, HDL-C and Triglyceride measurements using the Friedewald equation (Friedewald *et al.* 1972). As very low density lipoprotein (VLDL) carries the majority of the circulating triglycerides, VLDL-C can be estimated from the measured total triglycerides divided by 2.2 (See Warnick *et al.* 1990, Obineche *et al.* 2001). LDL-C is then calculated as:

$$LDL\text{-}C = TC - (measured\ HDLC + estimated\ VLDLC).$$

3.2.9 Quantification of fatty streak formation using oil red O staining

Oil red O (ORO) staining is a histological technique utilised for the detection and localisation of lipids in pathological tissue. ORO is a lysochrome (fat soluble dye) capable of staining unsaturated hydrophobic lipids, such as cholesterol and triglycerides. It can be solubilised in solvent to produce a histological stain. Since lysochromes stain by preferential solubility, lipids will take up the dye and appear deep red, whilst phospholipids appear pink. By counterstaining with haematoxylin, lipids can be assessed at a cytological and structural level within the tissue. Haematoxylin is a commonly used stain to demonstrate general tissue architecture. Preferentially colouring acidic components of the cell blue, haematoxylin is a base that stains the nucleus and regions of the cytoplasm containing DNA or RNA. In the present study ORO was used for the detection and measurement of lipid deposition within the aortic root of previously frozen heart sections.

190

A
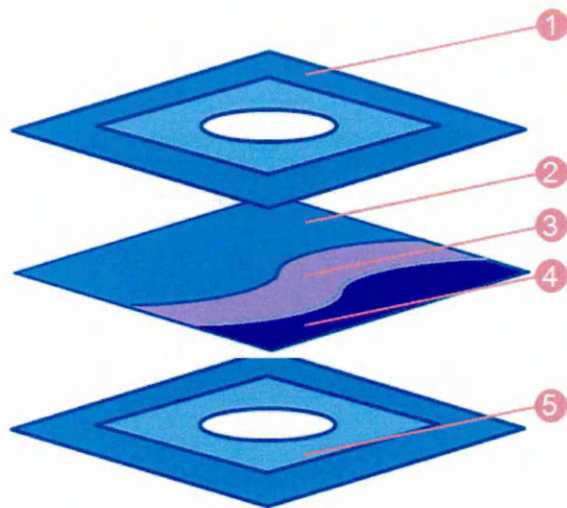
dHDL

1. Upper slide mount
2. Spreading layer (BaSO$_4$)
   - Emulgen B-66
   - Phosphotungstic acid
   - Magnesium chloride
3. Reagent layer
   - buffer, pH 7.0
   - cholesterol ester hydrolase
   - cholesterol oxidase
   - peroxidase
   - leuco dye
4. Support layer
5. Lower slide mount

B

Sample

⬇

HDL + non-HDL $\xrightarrow{\text{PTA/MgCl}_2}$ HDL

HDL $\xrightarrow{\text{Emulgen B-66}}$ cholesterol + HDL cholesterol esters + proteins

HDL cholesterol esters + H$_2$O $\xrightarrow{\text{Cholesterol ester hydrolase}}$ cholesterol + fatty acids

cholesterol + O$_2$ $\xrightarrow{\text{Cholesterol oxidase}}$ cholestenone + H$_2$O$_2$

H$_2$O$_2$ + leuco dye $\xrightarrow{\text{Peroxidase}}$ dye + 2H$_2$O
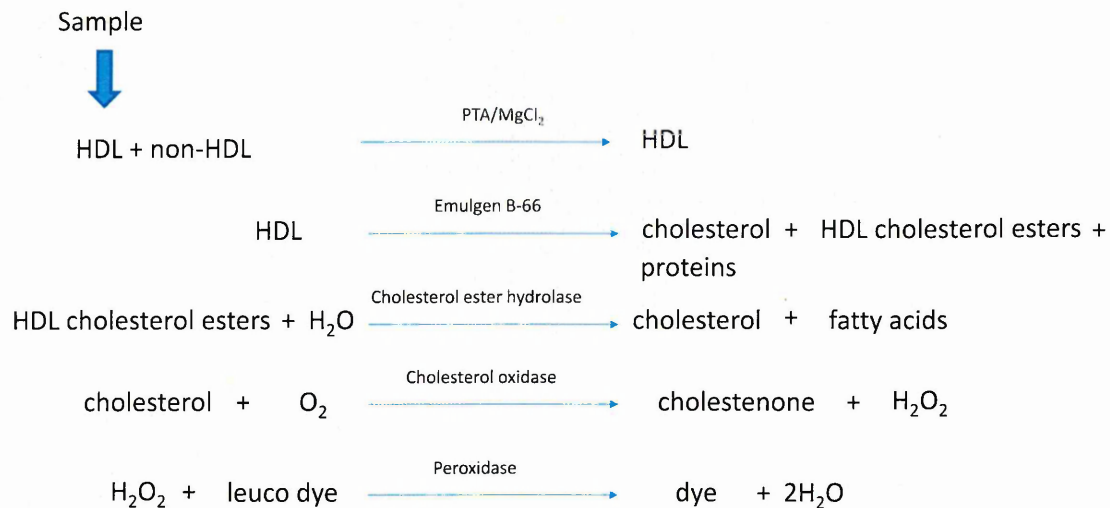
Figure 3.5; Direct HDL cholesterol measurement by the VITROS® chemistry system. The VITROS dHDL slide is a multilayered, analytical element coated on a polyester support. The entire integrated test environment, with specific test reagents, is contained on a thin piece of layered film (A), where all reactions take place (B). The final measurable colour change is proportional to the starting amount of HDL in the sample and is detected by reflectance spectrophotometry.

Method

A 1% ORO solution was prepared fresh before each use by dissolving 500mg Oil Red O (Sigma-Aldrich, UK) in 50ml of 60% triethyl phosphate (TEP) (Sigma-Aldrich, UK) and heating to 95-100°C for 5 minutes with constant stirring. The resulting solution was filtered, whilst still warm, through student grade filter paper (Whatman, UK) then left to settle and cool for a minimum of 1h at room temperature. The ORO solution was filtered a second time before use.

Frozen sections, 5 per animal distributed evenly throughout the aortic root (approximately every 10th serial section) were air dried for 30 minutes at room temperature. The sections were fixed in cold 4% PFA for 45 minutes on the bench then rinsed with tap water. Sections were then rinsed in 60% TEP for 5 minutes and stained for 30 minutes with ORO. Slides were then briefly rinsed in 60% TEP until the non-lipid areas of the sections appeared colourless (approximately 5-10 seconds), and further washed in tap water. Slides were then slowly dipped 5 times in Harris's haematoxylin (20% v/v) (Sigma-Aldrich, UK) to counterstain the nuclei, and then washed well in tap water to blue the counterstain and remove any excess stain. Finally, slides were mounted using 60°C -heated glycerol gelatin (Sigma-Aldrich, UK).

Following ORO staining, the sections of aortic root were digitally photographed using an Olympus BX60 microscope with a CoolSNAP-Pro (Media Cybernetics) imaging system. Quantification of the lipid stained areas was performed with computer-assisted morphometry, using Image J software (National Institute of Health, USA). Analysis was performed by manually outlining the outer and inner medial areas of the aortic root, followed by outlining the lesions from the internal elastic lamina to the luminal edge. The lipid-stained areas were expressed as a percentage of the medial area (figure 3.6).

Measurements were taken from 5 sections per mouse and mean values calculated. Randomly selected annotated photographs were examined by a second investigator to confirm acceptable accuracy of area selection. As with the original analysis, both procedures were carried out with investigators blinded to the animal group.

3.2.10 Measurement of serum cytokines by Multiplex Bead Array Assay

Multiple soluble proteins in samples such as serum, plasma, other body fluids and cell culture supernatants can be measured simultaneously using multiplex bead array assay (MBAA) technology. MBAA combines the principles of ELISA and flow cytometry. Different intensities of dyes are loaded into specific beads to create a range of spectrally distinct bead populations,

192
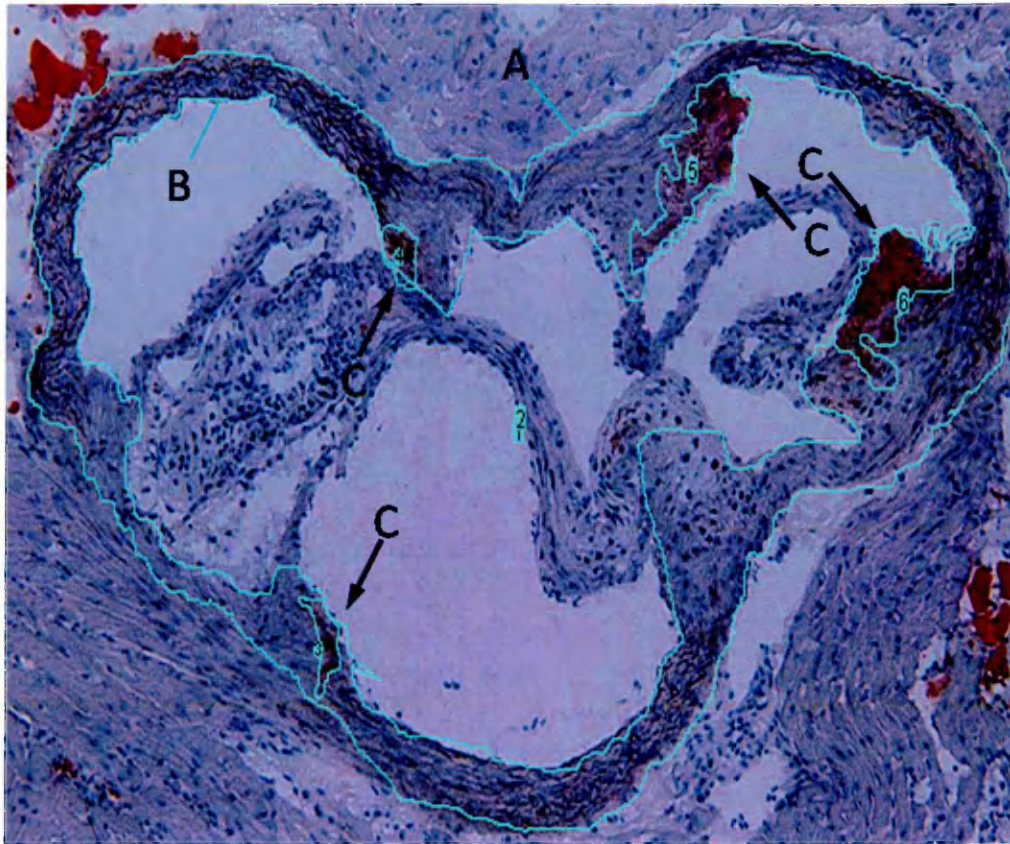
$$\frac{\text{ORO stained area (C)}}{\text{Outer medial area (A)} - \text{Inner medial area (B)}} \quad \text{X 100\%}$$

Figure 3.6; Quantification of atheroma formation in aortic root using oil red O staining and Image J analysis software. By manually outlining the outer medial area (B) and subtracting the inner medial area (C) of the aortic root a total area of the vascular wall of the aortic root was obtained. The Oil red O stained areas (A) within the vessel wall were also outlined (3-6), from the internal elastic lamina to the luminal edge, and used to calculate the percentage of the medial area stained, as shown.

distinguishable by flow cytometric analysis (figure 3.7a&b) (Khan *et al.* 2004). These distinct bead populations can then be coated with antibodies directed against a particular soluble protein or target. The targets are captured to the beads and detected with a secondary fluorescent antibody against the analyte of interest, which forms a sandwich complex (figure 3.7c). Using flow cytometry for excitation and subsequent detection of emission of the fluorochromes conjugated to the detection antibody, which is different to the emission wavelength of the bead dye, analytes can be measured quantitatively against a range of standards with known concentration. Multiple distinct bead sets can be added to an individual sample to detect multiple targets simultaneously, allowing for small sample volumes to be analysed for multiple analytes.

In the present study the Becton Dickinson cytometric bead array (CBA) flex set kits, targeted against IL-1β, IL-6, IL-10, CCL2 and TNFα, were used. These provide individual bead sets distinguishable on the red and near infrared (NIR) spectra that can be used in multiplex to measure serum concentrations of the cytokines (figure 3.2.8b).

Method

All reagents and 96-well assay plates were supplied by Becton Dickinson (BD, UK). All sample preparation and analysis was performed at the University of Sheffield core research facilities by Susan Newton.

The capture bead stock solutions provided were vortexed to resuspend the beads thoroughly. 1µl of each of the different analyte-specific capture bead suspensions were pipetted into a tube for each sample or standard to be run (i.e. 1µl per 20 samples and 8 standards would equal 28µl of bead suspension A, and 28µl of bead suspension B etc., added to the tube) followed by 0.5ml of wash buffer. The multi-bead suspension was centrifuged at 200 x g for 5 minutes. The supernatant was carefully aspirated and discarded and the bead pellet was resuspended in capture bead diluent equal to 50µl per test (sample and standard). The bead suspension was incubated at room temperature for 15 minutes to block for non-specific binding.

A phycoerytherin (PE) detection reagent was made up with 1µl of each analyte-specific detection reagent provided and detection reagent diluent added to create a final volume of 25µl per well, or sample (i.e. 4 targets would equal 4µl of combined detection reagents and 21µl of diluent). These volumes were multiplied by the number of samples and standards (i.e. the number of separate assay wells) to generate one PE detection reagent working solution with the multiple PE-conjugated detection antibodies specific to the different analytes. All

A

Different Dye Intensities

B

NIR-A

Red-A

C

Bead   Capture antibody

Capture bead

Bead antibody 'sandwich' complex

Target analyte   Fluorescent detection antibody
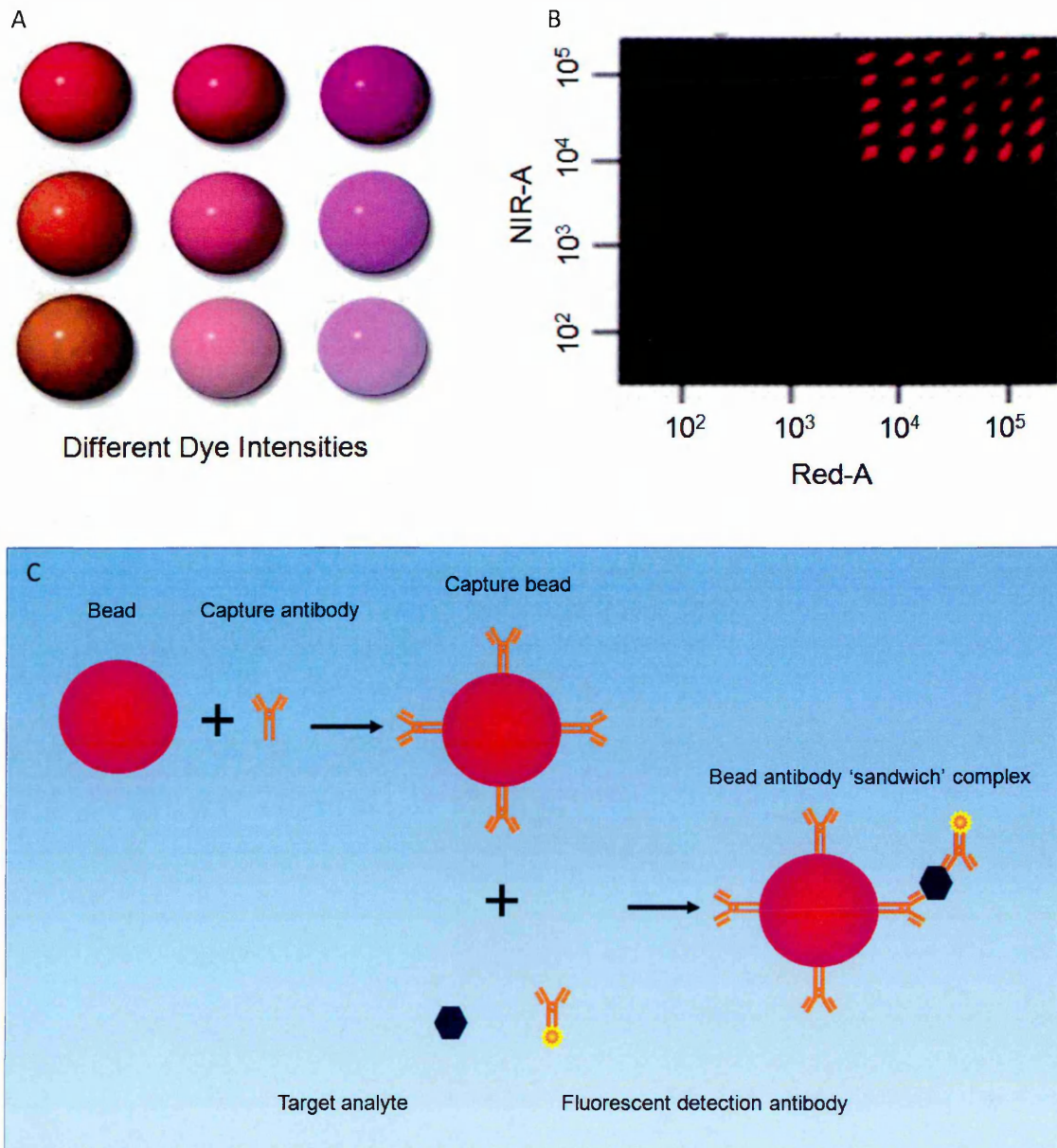
Figure 3.7; Multiplex bead analysis array. Beads are loaded with different intensities of dyes (A) to create spectrally distinct bead populations, distinguishable by flow cytometric analysis. As varying intensities of near infra-red (NIR) and red fluorescent dye in a bead create a grouping of particular bead populations by dot plot analysis, separate targets can be investigated (B). Each spectrally different bead population is coated with specific capture antibodies against a target analyte. When the sample and the fluorescent detection antibody is added, a sandwich complex forms (C). By gating around a specific population on the dot plot separated by the different bead dye properties (B), a specific analyte can be analysed for fluorescence intensity, which is proportional to the amount of antibody bound, and therefore analyte, in a sample. Multiple analytes can be analysed in a single sample by this separation of distinct bead populations with distinct antibody.

reagent working solutions were made up fresh on the day and were stored at 4°C until use. The serum samples were thawed at 4°C. A standard curve of known concentrations of each cytokine target was produced by serially diluting the standards provided in the flex set kit. 96 well reaction plates were pre-wet by addition of 100µl of wash buffer to each well, followed by immediate removal of this volume. Capture bead working solution was vortexed directly before use and 50µl was added to each assay well. 50µl of sample or standard was added to each assay well. The plate was then mixed for 5 minutes on a shaker at 500rpm and then incubated at room temperature for 1h. 50µl of PE detection reagent working solution was added to each assay well. The plates were then mixed on a shaker as before and incubated at room temperature for 2h. Assay wells were drained by vacuum and the beads were resuspended in 150µl of wash buffer per well, followed by shaking for 5 minutes. The assay plate was measured on the BD FACS Array™ flow cytometer and analysed using FCAP Array™ software.

3.2.11 Measurement of CX$_3$CL1 in mouse serum via ELISA

To measure the concentration of CX$_3$CL1 in mouse serum the mouse CX$_3$CL1 ELISA development kit (R&D Systems, UK) was used, which employs the same methods and principles as the human CX$_3$CL1 ELISA used in section 2.2.9.2. However, in this assay a rat anti-mouse CX$_3$CL1 antibody and a biotinylated goat anti-mouse CX$_3$CL1 antibody were used as the capture and detection antibody pair respectively.

3.2.12 Analysis of plaque composition by immunohistochemistry

Aortic root samples identified as containing atherosclerotic plaques from ORO lipid deposition analysis were further investigated by immunohistochemistry for a visual indication of lesion composition. Sections adjacent to, and as close as possible to, ORO stained sections were selected, single stained for targets, and plaque areas matched for comparison. Antibodies targeting vWF were used to identify the endothelial lining of the aorta and anti-MOMA2, a mouse-specific monocyte/macrophage marker, used to identify cells in the vessel wall. Antibodies for CX$_3$CL1 and CX$_3$CR1 were additionally used to investigate their presence in the lesions. Isotype controls directed against non-relevant targets were included where possible following the same procedure as target antibodies. A peptide block for CX$_3$CR1 (AbCam, UK) was used as an additional control by incubating the primary antibody with peptide for 30 minutes in an Eppendorf tube prior to tissue staining procedure. This would specifically block the antigenic sites of the primary antibody. All steps subsequent to the block were as with target antibodies. The fixation method, blocking, antibody dilution, and incubation period was

optimised to give the strongest specific antigen staining with the lowest non-specific binding for each antibody. Once this was established, the same procedure was repeatedly utilised for immunostaining (See Table 3.1).

Method

Sections were removed from -80°C storage and allowed to air dry for 30 min. During this time, sections were encircled with a wax hydrophobic pen (Vector Labs Inc, UK) to form a barrier around the sample. Sections were then fixed by submerging in ice-cold acetone for 5 min followed by 10 min air drying. Blocking with 5% serum of the secondary antibody host species for 30 min at room temperature in a humidified chamber was followed by incubation with 75μl (enough to completely cover the section) of pre-optimised concentrations of primary antibodies for 1h at humidified room temperature in the dark. Unbound antibody was then removed by 3 x 5 min washes in PBS. 75μl of pre-optimised concentrations of appropriate secondary antibody was applied to the sections and incubated for 1h at room temperature in the dark and in a humidified chamber. The wash procedure was repeated and sections were completely covered with Sudan black solution for 10 min at room temperature. To make the Sudan black solution, 0.3g of Sudan black B powder was dissolved in 100ml of 70% ethanol with continuous stirring at room temperature in the dark for 2h. The resulting solution was filtered through student grade filter paper (Whatman, UK), and stored at 4°C until use.

Following Sudan black staining, sections were then washed briefly with PBS, 8 times in succession to remove excess Sudan black stain, and mounted in Vectashield mounting medium for fluorescence (Vector Labs Inc, UK) containing DAPI to stain the nuclei. Sections were covered with coverslips and were sealed at the edges with nail varnish to prevent tissue drying. Negative controls omitting the primary antibody were included to determine non-specific binding of the secondary antibodies. Cells were examined and images captured using a Zeiss 510 laser scanning confocal microscope (Carl Zeiss Ltd, UK).

3.2.13 Statistical Analysis

Data is presented as mean ± SEM unless otherwise stated. Experimental groups were assessed for normality and equal variance as previously described (see section 2.2.12). Appropriate statistical analyses were selected to establish significant differences between groups as detailed previously. Significance was accepted at $P \leq 0.05$.

Antibody	Company	Isotype	Dilution	Secondary
CX$_3$CL1	Abcam (ab25088)	IgG (rb, polyclonal)	**1:100** (1:50-1:800)	**Gt x Rb 568** (1:400-1:800) **1:400**
CX$_3$CR1	Abcam (ab8021)	IgG (rb, polyclonal)	**1:400** (1:50-1:500)	**Gt x Rb 568** (1:400-1:800) **1:800**
MOMA2	Abcam (ab33451)	IgG$_{2b}$ (rt, monoclonal)	**1:50** (1:25-1:200)	**Rb x Rt FITC** 1:400-1:800 **1:400**
vWF	Abcam (ab6994)	IgG (rb, polyclonal)	**1:800** (1:500-1:1000)	**Gt x Rb 568** (1:400-1:1000) **1:1000**
Isotype	Abcam (ab7260)	IgG (rb, polyclonal)	**1:100**	**Gt x Rb 568** (1:400-1:800) **1:400**
Isotype	R&D (MAB0061)	IgG$_{2b}$ (rt, monoclonal)	**1:50**	**Rb x Rt FITC** **1:400**
Peptide Block	Abcam (ab8125)	CX$_3$CR1 (C-term) peptide (ms)	**1:100**	**Gt x Rb 568** **1:400**

Table 3.1; Antibodies used for immunohistochemistry. Summary of the antibodies used for target protein detection in mouse aortic root sections following optimisation of methods. The block step and dilutions of primary and secondary antibodies were selected to produce the highest amount of specific staining whilst reducing, or preferentially eliminating, non-specific binding and background fluorescence. The range of antibody dilutions tested is shown, with the selected optimum dilution in bold. *vWF, von Willebrand Factor; FITC, fluorescein isothiocyanate; ms, mouse; rb, rabbit; rt, rat; gt, goat.*

3.3 Results

3.3.1   Gender Determination

PCR confirmed the expression of the Sry gene in all ear clip samples from Tfm mice at the expected product size of 340bp, indicating that all animals were genotypically males (figure 3.8). The expression of the reference gene was also confirmed in the extracted DNA, by observation of a band at 450bp. Two female samples utilised as negative controls showed no PCR product band at 340bp, but did display a band for the housekeeping gene (figure 3.8).

3.3.2   The effect of testicular feminization on atherosclerotic parameters

Tfm mice and XY littermates fed on a normal chow diet were compared across a range of parameters related to atherosclerosis.

3.3.2.1   Animal Body Weights

Animal body weights were compared over the treatment period between 8 weeks and 36 weeks old. XY littermates were significantly heavier than Tfm mice at the beginning of the study (8 weeks old), and this pattern was observed up to week 12 (figure 3.9A). Beyond week 12 body weights were similar between the two groups of animals, and by week 20 the Tfm mice were consistently heavier than XY littermates up to the end of the experimental period, although only significantly so at week 27.

The amount of weight gain over the experimental period was also calculated, in relation to starting weight (Figure 3.9B). Tfm mice demonstrated a significantly greater increase in weight from week 15 to the end of the study when compared to XY littermates (P<0.05, t test, n=16 and n=10 respectively). The total weight gain over the experimental period was 12.85g for Tfm and 8.4g for XY littermates (P<0.05, t test).

3.3.2.2   Serum hormone measurements

Serum hormone measurements were taken at the end of the experimental period and compared between Tfm and XY littermates. Mean serum testosterone concentration in XY littermates was within the expected physiological range of (10-30nM), although variability, demonstrated by the error bars, was large within this group. Serum testosterone was
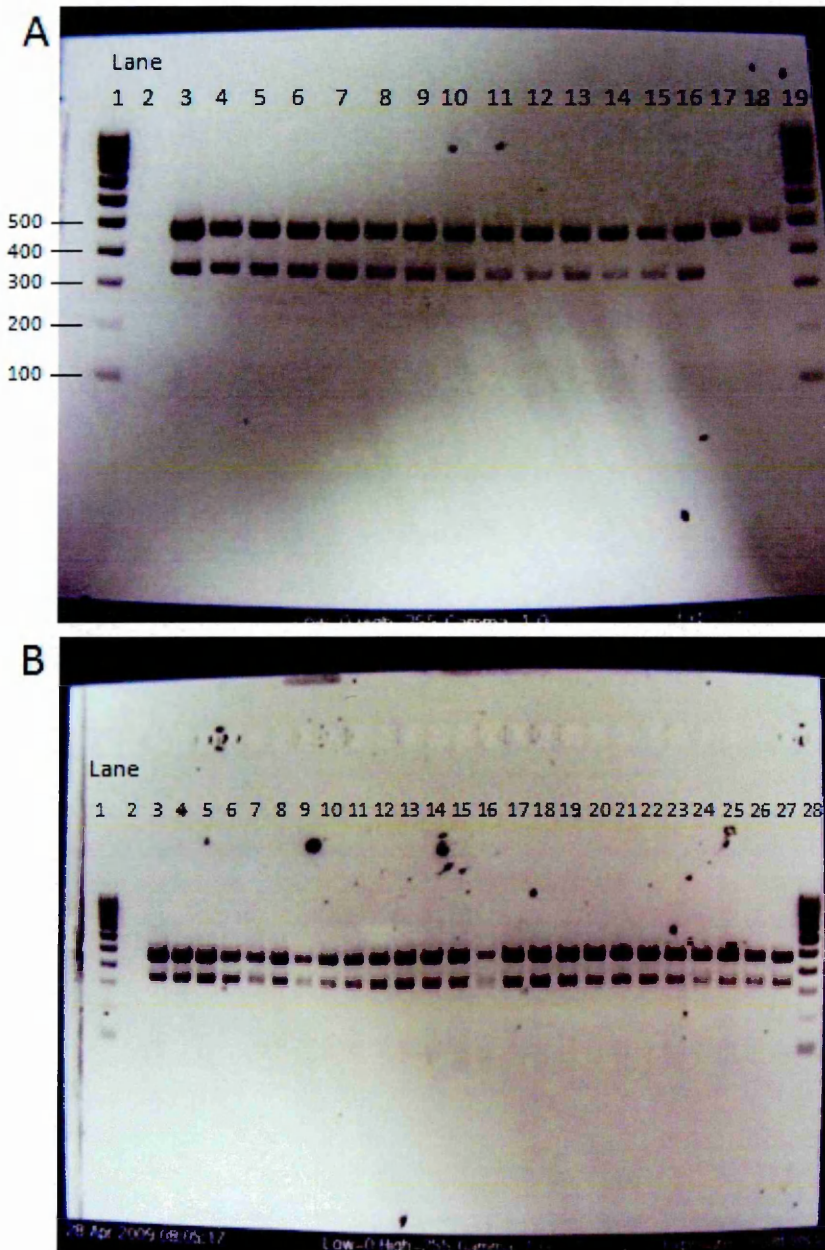
Figure 3.8; Agarose gel electrophoresis showing DNA samples from ear clips of Tfm mice amplified with Sry gene primers. A) The gel shows amplified products for Sry and the reference gene. Lane 1 and 19 show the DNA base pair (bp) marker ladders. Lane 2 is the negative control with no DNA, and lane 3 is a positive control containing sample known to express the Sry gene. Lanes 4-16 are samples from Tfm mice, showing expression of Sry and the reference gene. Lane 17-18 show samples from female mice amplified with the same primers, and showing expression of only the reference gene. B) The second gel was run in parallel to the previous gel. Lanes 1 and 28 contain DNA bp marker ladders. Lane 2 is the negative control with no DNA, and lanes 3-27 are further samples from Tfm mice.

A
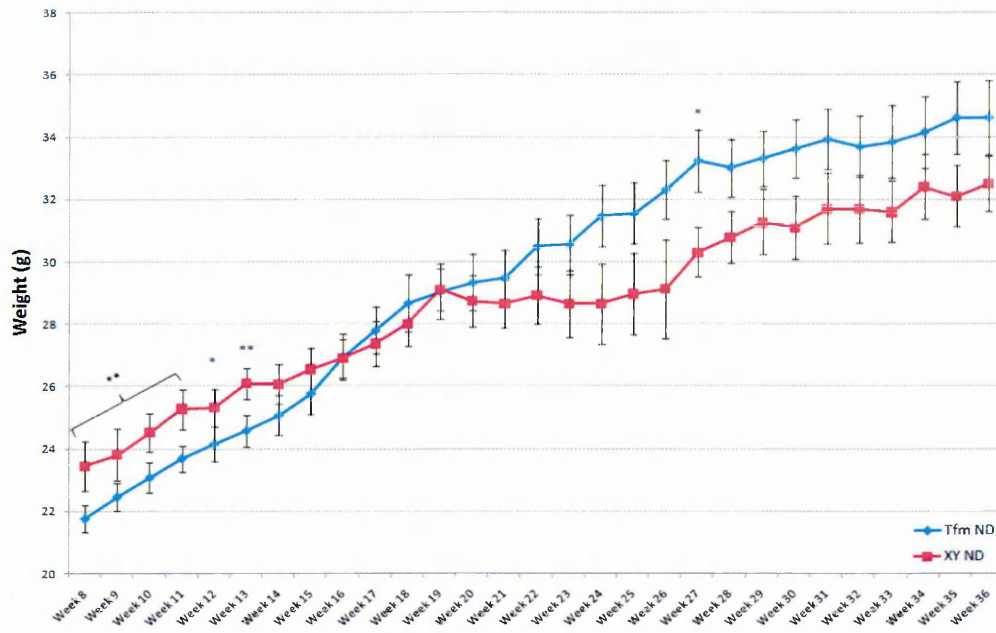
B
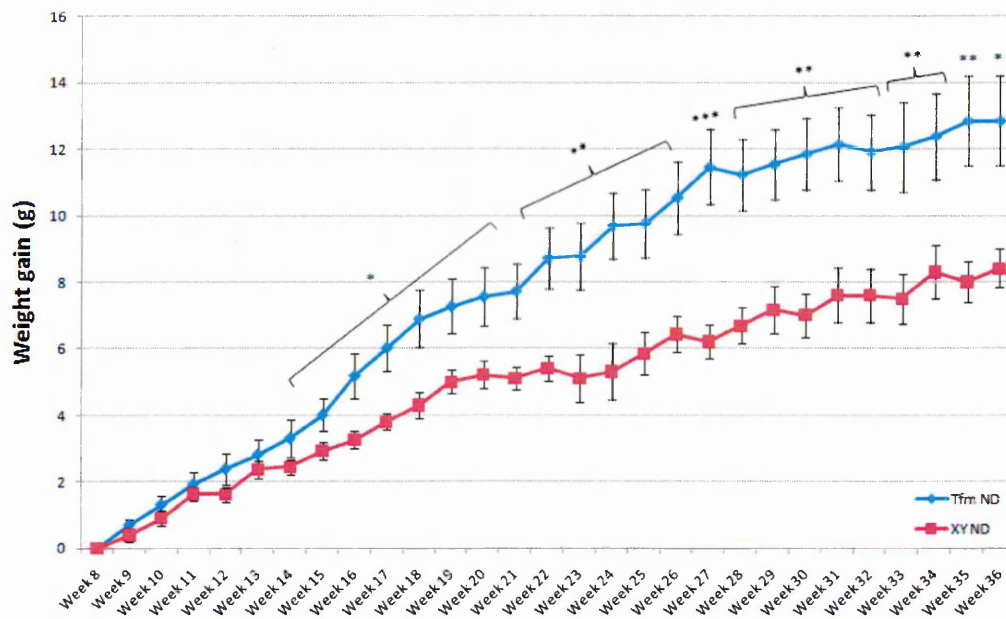
Figure 3.9; Total body weight and weight gain of Tfm mice and XY littermates on a normal chow diet (ND). Weekly weight measurements taken from week 8 onwards were compared between Tfm (n=16) and XY littermates (n=10) for the 28 week study period. A) Mean weekly weights and B) mean weight gains relative to week 8. Data is mean ± SEM (*P<0.05; **P<0.01; ***P<0.001 versus XY ND.).

significantly reduced in Tfm mice compared to XY littermates (P<0.05, n=12 and n=10 respectively) (figure 3.13). Serum estradiol concentrations in XY littermates were in the normal physiological range for male animals (figure 3.14). In comparison, serum estradiol concentration was significantly elevated in Tfm mice compared to littermate controls (P<0.01, Kruskal-Wallis, n=6).

3.3.2.3 Serum lipid measurements

Total cholesterol, HDL-C and LDL-C were all significantly elevated in the serum of Tfm mice fed a normal chow diet for 28 weeks (n=12) compared to XY littermate controls (n=10) (P<0.001, P<0.01, P<0.001 respectively; unpaired t test) (figure 3.15). Triglyceride levels were also raised in the serum of Tfm mice, but not significantly so. As serum LDL concentration was calculated from the total cholesterol, HDL and triglyceride measurements, inaccuracies may occur in samples with low total cholesterol and high HDL levels resulting in anomalous negative LDL values, as seen in XY mice. Statistical analyses were still performed on these negative values to accommodate group variability as opposed to zeroing the negatives.

3.3.2.4 Lipid deposition in the aortic root

ORO staining was distinguished from non-specific accumulation of the stain due to its cellular location identified by haemotoxylin counterstain compared to large droplets of red dye, respectively. Very low levels of ORO staining were detectable in the aortic root of Tfm mice fed a normal chow diet, when compared with XY littermate controls (figure 3.16a & c). Semi-quantification of ORO staining revealed that lipid deposition was marginally increased in Tfm mice compared to littermates (figure 3.14), in which no staining was detected (n=6).

3.3.2.5 Serum cytokine measurements

All serum cytokines (IL-1β, IL-6, IL-10, CCL2 and TNFα) were elevated in Tfm mice compared to XY littermates on normal chow diets (figure 3.17). IL-6 and TNFα were both significantly elevated in Tfm mice relative to controls (P<0.05, unpaired t test, n=6), whereas the differences for the other cytokines were not significant due to reduced power of low sample numbers and variability of the data.

3.3.2.6 Summary

In summary, testicular feminised mice demonstrated increased weight gain, elevated serum total cholesterol, HDL and LDL, occasional lipid deposition in the aortic root and elevated

serum cytokines, in particular IL-6 and TNFα, compared to XY littermate controls. In addition serum testosterone and estradiol concentrations were decreased and increased relative to XY littermate controls respectively.

3.3.3 The effect of high-cholesterol diet on atherosclerotic parameters

To investigate the effect of diet on atherosclerotic parameters, Tfm mice and XY littermate controls were fed a high cholesterol diet *ad libitum* for 28 weeks.

3.3.3.1 *Animal body weights*

Initially the body weights of Tfm mice fed a high-cholesterol diet (n=23) were similar to those on normal chow diet (n=13) (figure 3.10A). However, from week 8 of cholesterol feeding Tfm mice had consistently lower body weights than those on normal chow diet, significantly so from 14 weeks onwards (P<0.05-0.001, Mann Whitney). A similar pattern was seen when weight gain was calculated. Tfm mice on high cholesterol diet gained significantly less weight than those on normal chow diet (P<0.05-0.001, Mann Whitney) (figure 3.10B). Final weight gain over the 28 week feeding period was 8.06g for Tfm on high cholesterol diet, and 12.85g for Tfm on normal diet (P<0.01).

In XY littermates, a similar phenomenon was observed, with those on a high cholesterol diet (n=13) showing significantly lower body weights than XY littermates on normal diet (n=10), from week 9 of the regime onwards (figure 3.11A). Weight gain over the 28 week feeding period was significantly less in the XY littermates on high cholesterol diet than the XY littermates on normal diet (P<0.05-0.01, unpaired t test, n=13 and n=10 respectively) (figure 3.11B).

When comparing the total body weights and weight gain of high-cholesterol fed Tfm mice (n=23) with high-cholesterol fed XY littermates (n=13), Tfm mice tended to show higher body weights and a greater weight gain over the 28 week feeding period (figure 3.12), however these differences reached significance only at limited time points.

3.3.3.2 *Serum hormone measurements*

Serum testosterone levels appeared reduced following feeding on a high cholesterol diet for both Tfm mice (n=12) and XY littermates (n=12) compared to normal diet controls (n=12 and n=10 respectively) (figure 3.13). However, this reduction was only significant in XY littermates

203

A
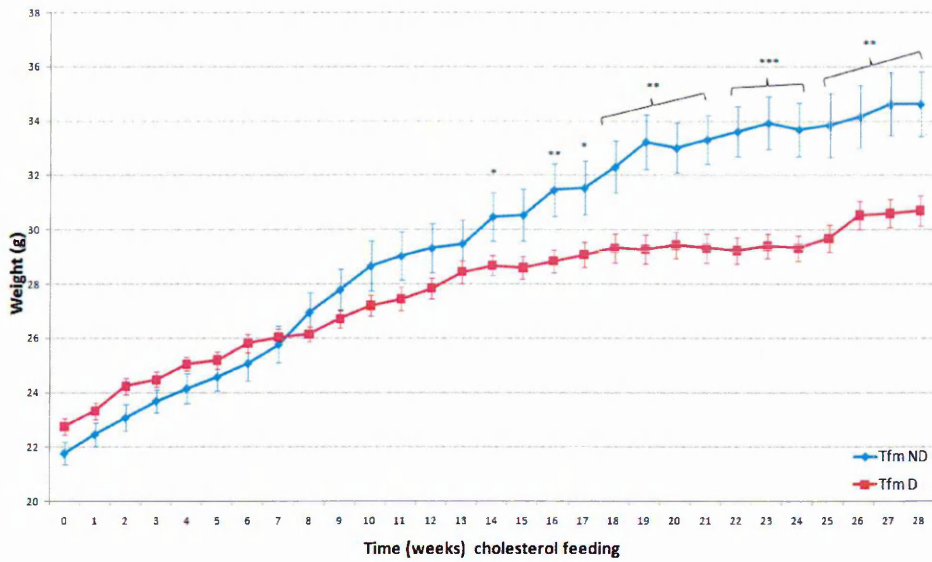
B
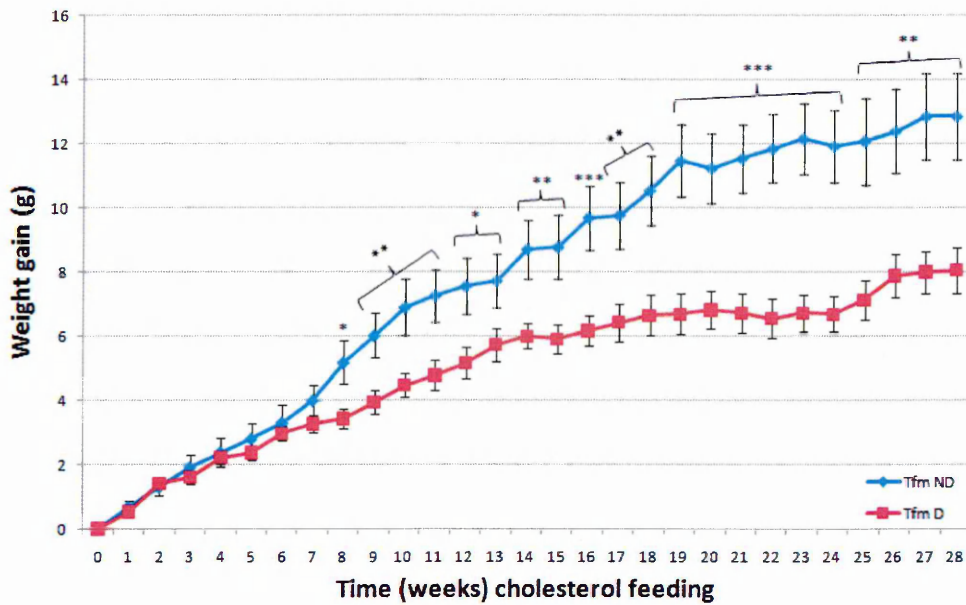
Figure 3.10; Total body weight and weight gain of Tfm mice fed a normal (ND) or high cholesterol diet (D). Weekly weight measurements were compared between Tfm mice on normal diet (n=13) and Tfm mice on high-cholesterol diet (n=23) for the 28 week study period. A) mean weekly weights and B) mean weight gains relative to week 8 start weights (*P<0.05; **P<0.01; ***P<0.001 vs Tfm ND; Mann Whitney test).

A
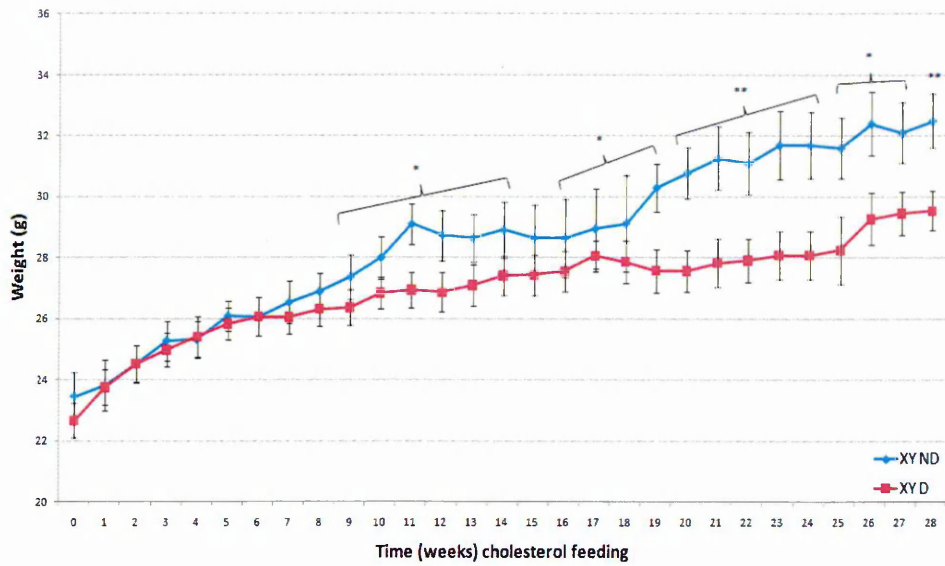
B
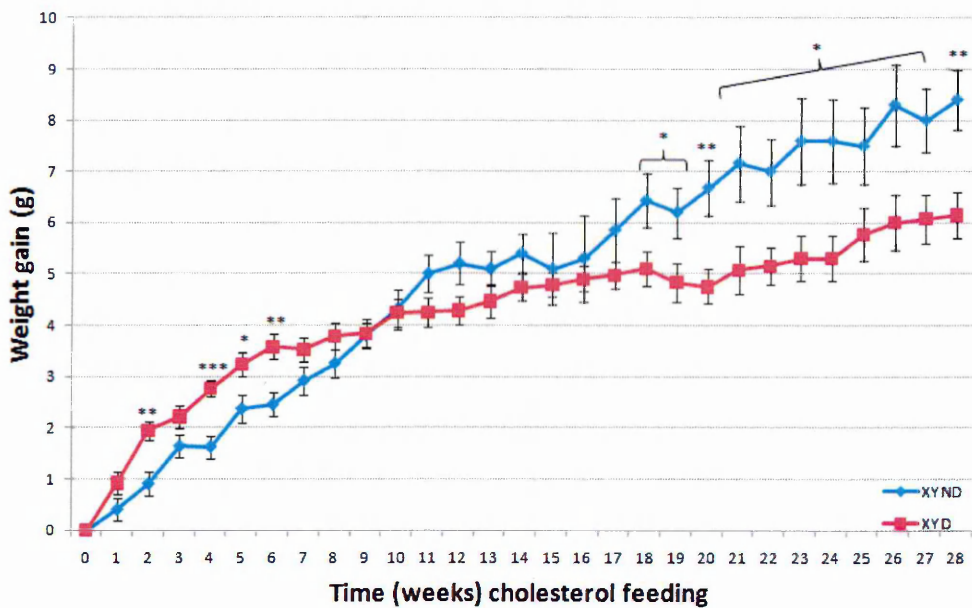
Figure 3.11; Total body weight and weight gain of XY littermate mice fed a normal (ND) or high cholesterol diet (D). Weekly weight measurements were compared between littermate mice on normal diet (n=10) and littermates on high-cholesterol diet (n=13) for the 28 week study period. A) Mean weekly weights and B) mean weight gains relative to week 8 start weights (*P<0.05; **P<0.01; ***P<0.001 vs XY ND; Mann Whitney test).

A
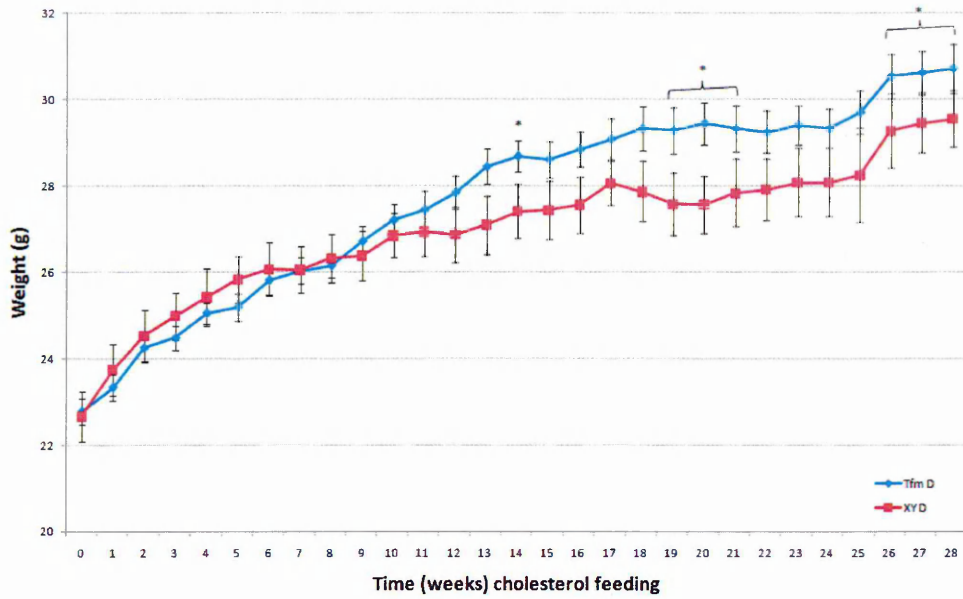
B
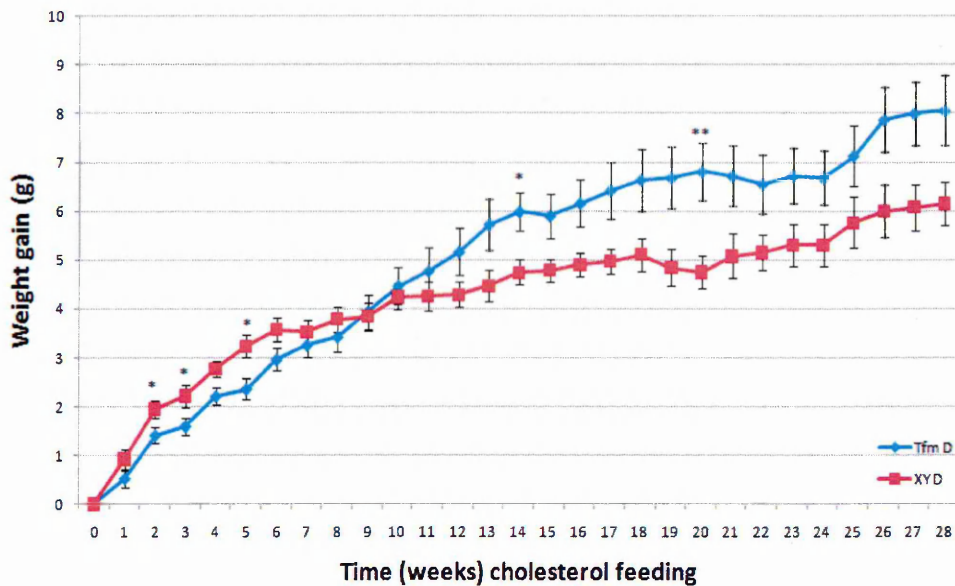
Figure 3.12; Total body weight and weight gain of Tfm mice and XY littermate mice fed a high cholesterol diet (D). Weekly weight measurements were compared between Tfm mice (n=23) and littermate mice (n=13) on high-cholesterol diet for the 28 week study period. A) Mean weekly weights and B) mean weight gains relative to week 8 starting weights (*$P<0.05$; **$P<0.01$; ***$P<0.001$ vs XY D; Mann Whitney test).

(P<0.01, Mann Whitney test). Although reduced compared to normal diet controls, serum testosterone levels of XY littermates on high-cholesterol diet remained higher than their Tfm counterparts.

28 weeks on a high cholesterol diet significantly reduced serum estradiol in Tfm mice compared to Tfm mice on normal diet (P<0.01, Mann-Whitney test, n=6) (figure 3.14). The high cholesterol diet did not affect serum estradiol concentrations in XY littermates compared to XY littermates on normal diet.

Thus, Tfm mice on high-cholesterol diet had similar serum estradiol concentrations to XY littermates on high cholesterol diet.

3.3.3.3   Serum lipid measurements

Total serum cholesterol was significantly elevated (P<0.001, unpaired t test) as an effect of feeding on a high cholesterol diet in both Tfm mice (n=14) and XY littermates (n=11) compared to normal diet controls (n=12 and n=10 respectively) (figure 3.15A). Additionally, Tfm mice on high-cholesterol diet displayed significantly higher serum cholesterol levels than XY littermates on high-cholesterol diet (P<0.001, unpaired t test). High cholesterol feeding reduced serum HDL concentrations in Tfm mice and XY littermates relative to their normal diets controls (figure 3.15B), although this was significant only in Tfm mice (P<0.001, unpaired t test). Serum HDL concentrations were similar in high cholesterol fed Tfm mice and high cholesterol fed XY littermates. High cholesterol feeding appeared to reduce serum triglyceride concentrations in Tfm mice relative to Tfm mice on normal diet (figure 3.15C), however this was not statistically significant. Serum triglyceride levels were similar between Tfm and XY littermates on high cholesterol diet. The high cholesterol diet significantly elevated serum LDLs in both Tfm and XY littermate mice (P<0.001, unpaired t test) (figure 3.15D). The difference was more pronounced in Tfm mice, which had significantly higher serum LDL levels than XY littermate controls on high-cholesterol diet (P<0.001, unpaired t test).

3.3.3.4   Lipid deposition in the aortic root

ORO staining of aortic root sections revealed increased lipid deposition in both Tfm mice and XY littermates following high-cholesterol diet, with multiple lesions observed (figure 3.16). Lesions occurred primarily at the shoulders of the valve cusps in both Tfm and XY mice. Consistent with serum lipid measurements, semi-quantification showed this increase in lipid deposition to be significant for Tfm mice when compared to normal diet Tfm controls (P<0.01
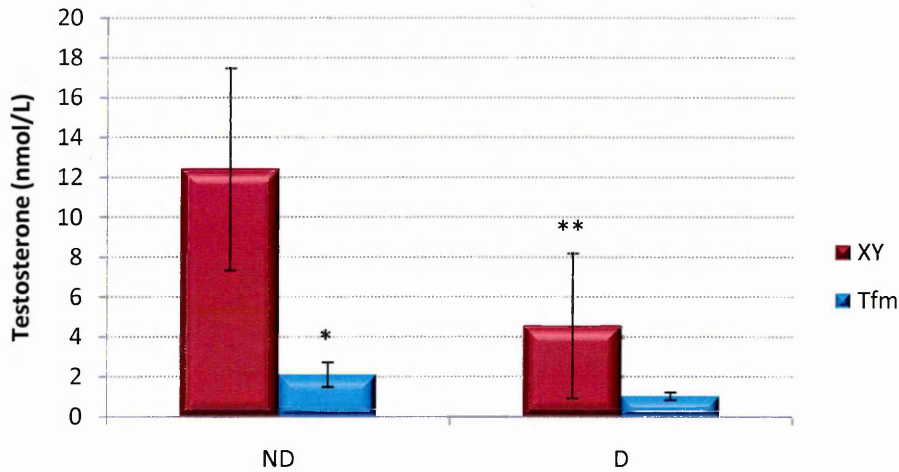
Figure 3.13; Serum testosterone concentration of Tfm mice and XY littermates fed a normal (ND) or high-cholesterol diet (D). Tfm mice on high cholesterol (n=12); Tfm mice on normal diet (n=12). XY littermates on high cholesterol (n=12), and XY littermates on normal diet (n=10) were compared for serum testosterone levels at the end of the 28 week experimental period. (*P<0.05, **P<0.01 vs XY littermates on normal diet, Mann Whitney test).
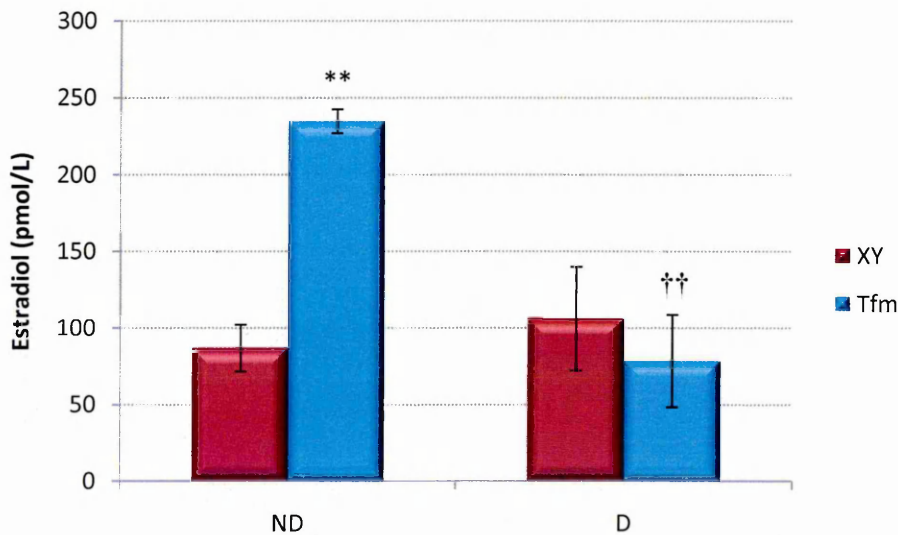
Figure 3.14; Serum estradiol concentration of Tfm mice and XY littermates fed a normal (ND) or high-cholesterol diet (D). Tfm mice on high cholesterol (n=6); Tfm mice on normal diet (n=6); XY on high cholesterol diet (n=6); and XY on normal diet (n=6) were compared for serum estradiol levels at the end of the 28 weeks experimental period (**P<0.01 vs XY on normal diet [††]P<0.01 vs Tfm on normal diet, Mann Whitney test).
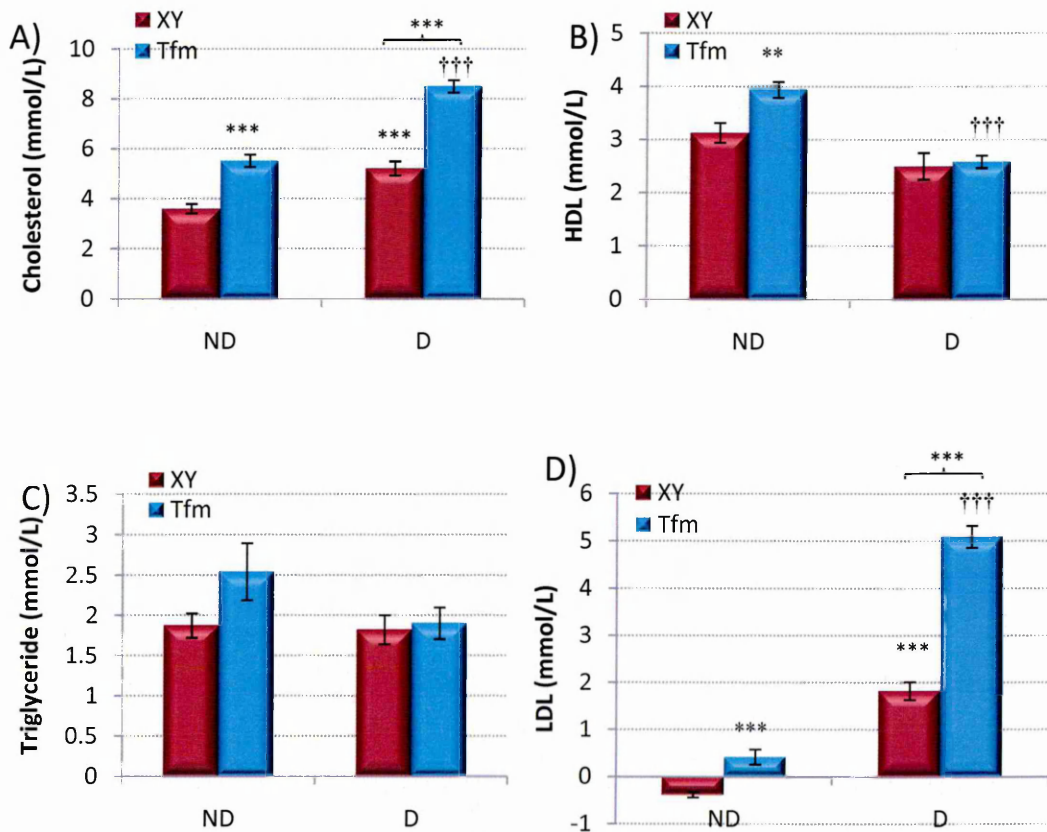
Figure 3.15; Serum lipid concentrations of Tfm mice and XY littermates fed a normal (ND) or high-cholesterol diet (D). Data is mean ± SEM. Tfm mice on normal diet (n=12), XY littermate controls on normal diet (n=10), Tfm mice on high-cholesterol diet (n=14), XY littermate controls on high-cholesterol diet (n=12) were compared for serum lipid levels at the end of the 28 week experimental period. **P<0.01, ***P<0.001 vs XY littermate control on normal diet, †††P<0.001 vs Tfm on normal diet; unpaired t test.
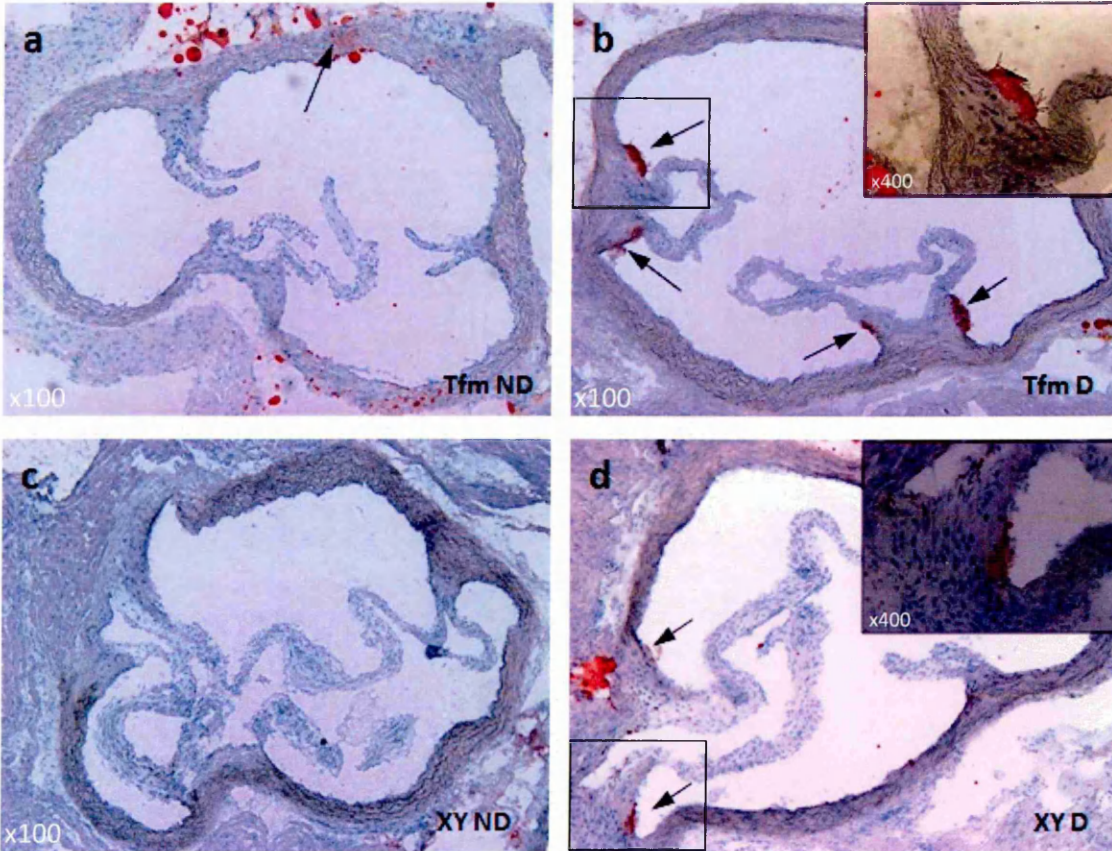
Figure 3.16; Representative oil red O staining of aortic root sections from Tfm mice and XY littermate controls on a normal chow diet (ND) and high-cholesterol diet (D). ORO stain was evident at low levels in the aortae of Tfm mice, but absent from XY littermates fed normal diet (a and c respectively). Staining was apparent in the vascular wall of aortae of both Tfm and XY littermate mice fed high-cholesterol diet (b and d respectively). Lesions developed primarily at the shoulders of the aortic valve cusps. Sections were counterstained with haemotoxylin.

In addition, lipid deposition was significantly greater in Tfm on high cholesterol diet than XY littermates on high cholesterol diet (figure 3.17).

3.3.3.5 Serum cytokine measurements

Serum CCL2 concentration was significantly elevated in Tfm mice fed high-cholesterol diet compared to Tfm mice on normal diet ($P<0.05$, unpaired t test, n=6) (figure 3.18D). All other serum cytokine concentrations were similar between Tfm mice on high cholesterol diet compared with Tfm on normal diet. However, although not statistically significant, IL-10 was reduced by high cholesterol diet in Tfm mice (figure 3.18C). In XY littermates high cholesterol feeding appeared to slightly elevate all serum cytokines, although only significantly so for CCL2 (figure 3.18D) and TNFα (figure 3.18E). No significant differences in serum cytokine measurements were observed between Tfm mice and XY littermates fed high-cholesterol diet (figure 3.18).

3.3.3.6 Summary

In summary, the administration of a high cholesterol diet caused an elevation of total serum cholesterol and serum LDL concentrations, increased lipid deposition in the aortic root, increased serum CCL2 concentrations, and a reduction in testosterone and weight gain in both Tfm and XY littermate mice. Differences were generally more pronounced in Tfm mice, with total cholesterol, LDL and lipid deposition being significantly greater than in XY littermates. In addition, Tfm mice displayed reduced estradiol levels following high-cholesterol diet.

3.3.4 The effect of testosterone replacement on atherosclerotic parameters

To investigate the role of testosterone and AR on atherosclerotic parameters, Tfm mice on a high-cholesterol diet were supplemented with fortnightly injections of Sustanon® 100, in order to restore testosterone to physiological levels. Atherosclerotic parameters were compared in placebo (saline)-injected Tfm and XY littermate mice also on high-cholesterol diet.

3.3.4.1 Animal body weights

No significant differences in total body weight or weight gain were seen between saline-injected Tfm mice (n=15), testosterone-injected Tfm mice (n=14) and saline injected littermate
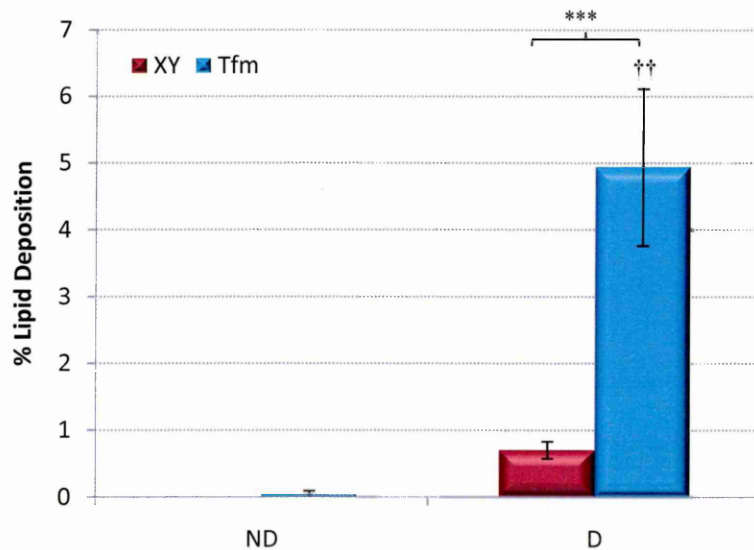
Figure 3.17; Percentage lipid deposition in aortic root sections from Tfm mice and XY littermate controls on a normal chow diet (ND) and high-cholesterol diet (D). Semi-quantification of lipid deposition in the aortic root (expressed as percentage of medial area) was elevated in Tfm mice and XY littermates following feeding on high cholesterol diet. Tfm mice on high-cholesterol diet displayed significantly elevated lipid deposition compared to normal diet controls ([††]P<0.01, Mann Whitney test, n=6) and XY littermates on high-cholesterol diet (***P<0.001, t test, n=6).
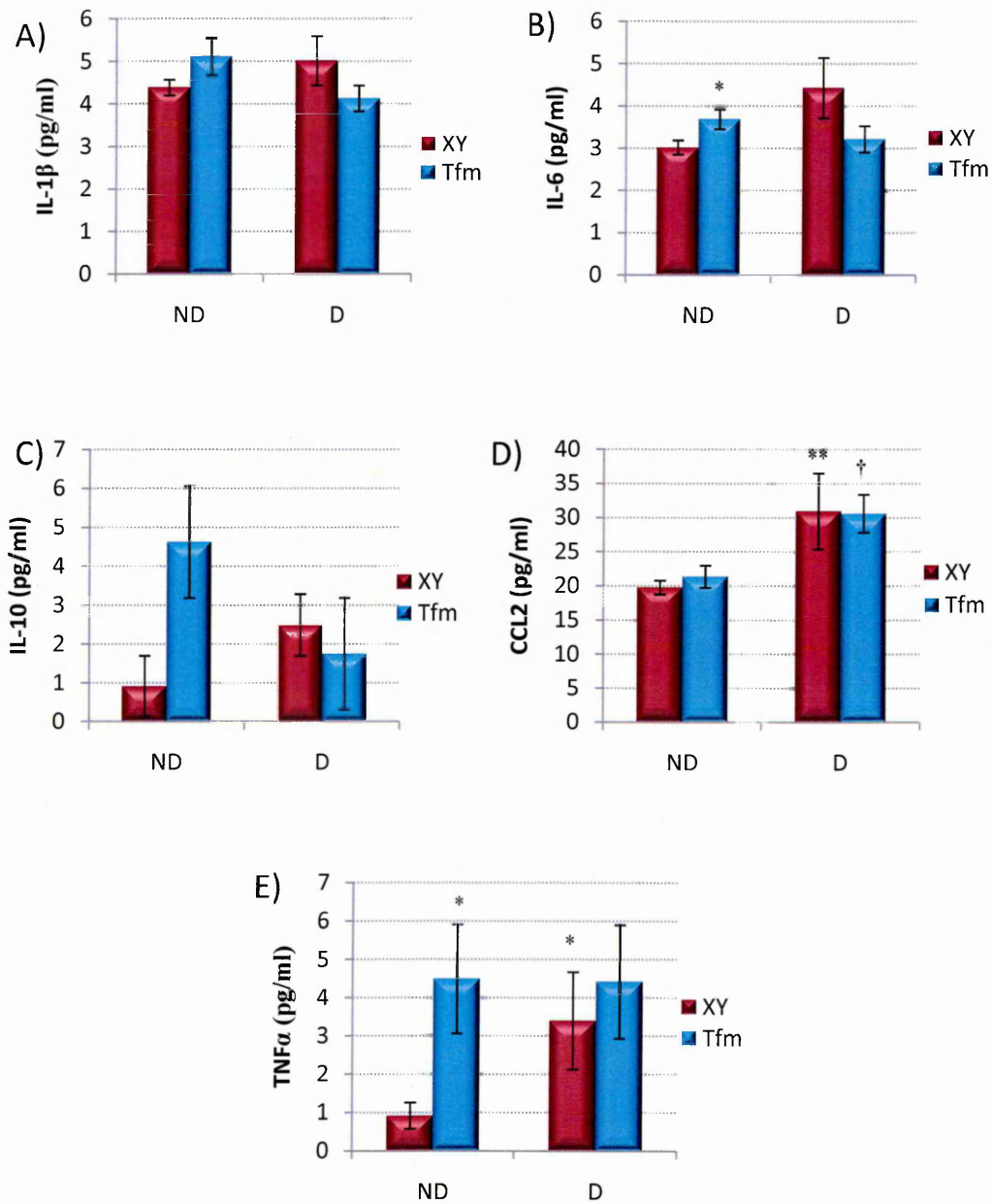
Figure 3.18; Serum cytokine concentrations of Tfm mice and XY littermates fed a normal chow diet (ND) and high-cholesterol diet (D). Tfm mice on normal (n=6) and high-cholesterol diet (n=6) and XY littermates on normal (n=6) and high-cholesterol diet (n=6) were compared for serum cytokine concentrations. *P<0.05, **P<0.01, vs XY littermate control on normal diet. [†]P<0.05, vs Tfm on normal diet; Mann-Whitney test, n=6.

controls (n=14) (figure 3.19). Although not statistically significant, Tfm mice receiving testosterone replacement were heavier and gained more weight over the 28 week experimental period than saline-injected Tfm mice and XY littermates (figure 3.19).

3.3.4.2   Serum hormone measurements

Fortnightly testosterone replacement was seen to be effective in elevating serum testosterone in Tfm mice on high-cholesterol diet (n=13) compared to saline-injected Tfm control mice on high-cholesterol diet (n=12) (P<0.01, Kruskal-Wallis) (figure 3.20). Testosterone replacement in this group increased serum Tfm levels to within the expected physiological range (10-30nM). However, surprisingly, when compared to saline-injected XY littermates (n=14), the testosterone-injected Tfm mice had significantly higher serum testosterone levels (P<0.01, Kruskal-Wallis) (figure 3.20). Serum testosterone concentrations in XY littermates were lower than physiologically predicted levels from previous investigations (Nettleship 2006), although still higher than saline-injected Tfm mice (figure 3.20). This was not statistically significant due to high levels of variability.

Serum estradiol concentrations were slightly, but non-significantly, raised in testosterone-injected Tfm mice compared to saline injected Tfm mice (figure 3.21), and although greater than saline-injected XY littermates, again this was not statistically significant (Kruskal-Wallis, n=6).

3.3.4.3   Serum lipid measurements

Total serum cholesterol and LDL concentrations were similar in Tfm mice receiving testosterone replacement (n=13) compared to saline-injected Tfm controls (n=14), and both were still significantly higher than seen in XY littermates (n=12, P<0.001, ANOVA) (figure 3.22a & d). Serum HDL concentrations were similar in testosterone-injected Tfm mice, saline-injected Tfm mice and saline-injected XY littermates (figure 3.22b). Serum triglyceride levels were also similar in Tfm mice injected with testosterone compared to saline-injected Tfm mice, and higher in saline-injected XY littermate controls compared to both groups of Tfm mice, although not significantly so (figure 3.22c).

3.3.4.4   Lipid deposition in the aortic root

Testosterone replacement in Tfm mice partially prevented the increase in lipid deposition in the aortic roots caused by high cholesterol feeding. Although ORO staining was detected in aortic root sections from Tfm mice injected with testosterone (figure 3.23), the degree of

A
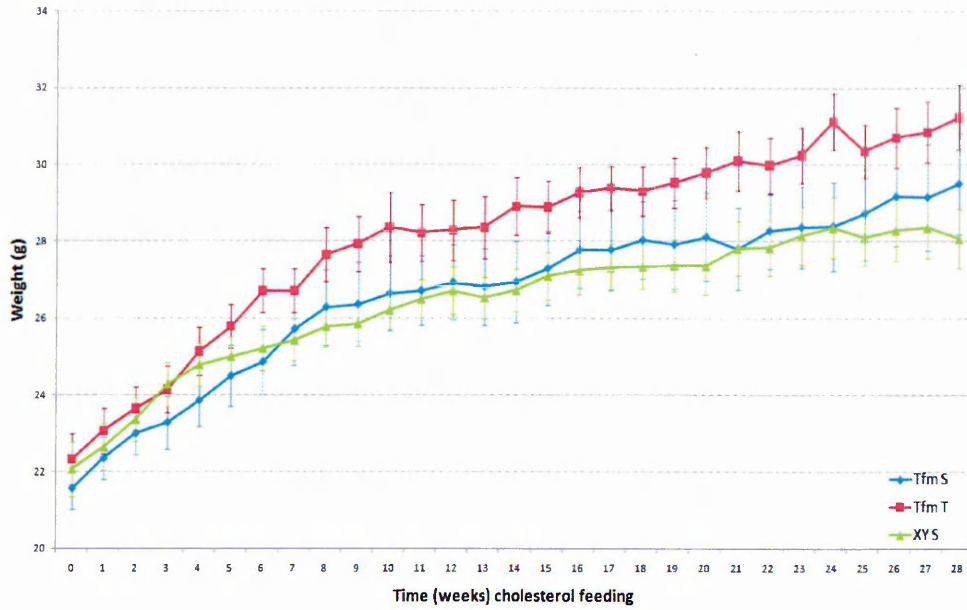
B
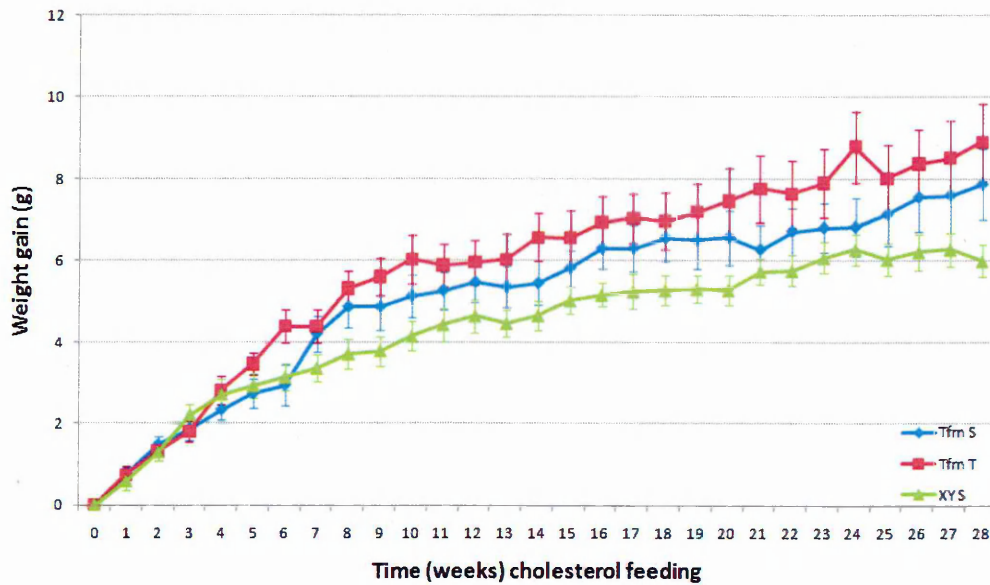
***Figure 3.19; Total body weight and weight gain of Tfm mice and XY littermate
mice fed a high cholesterol diet receiving testosterone (T) or saline (S) injections.***
Weekly weight measurements were compared between Tfm mice receiving
testosterone replacement (n=14), Tfm mice receiving saline (n=15) and littermate
mice receiving saline (n=14) all on high-cholesterol diet for the 28 week study
period. A) Mean weekly weights and B) mean weight gains relative to week 8
starting weights.

215
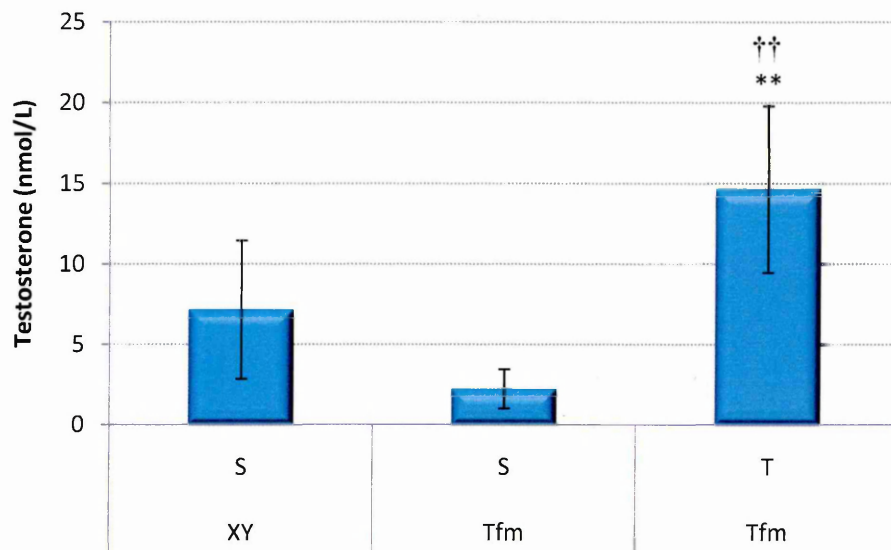
Figure 3.20; Serum testosterone concentration of Tfm mice and XY littermates fed a high-cholesterol diet and receiving either testosterone (T) or saline (S) injections. Testosterone concentrations compared between Tfm mice receiving saline injections (n=12); Tfm mice receiving testosterone injections (n=13), XY littermates receiving saline injections (n=14) all on high-cholesterol diet for the 28 week study period. (**P<0.01 vs XY S, and [††]P<0.01 vs Tfm S, Mann Whitney).
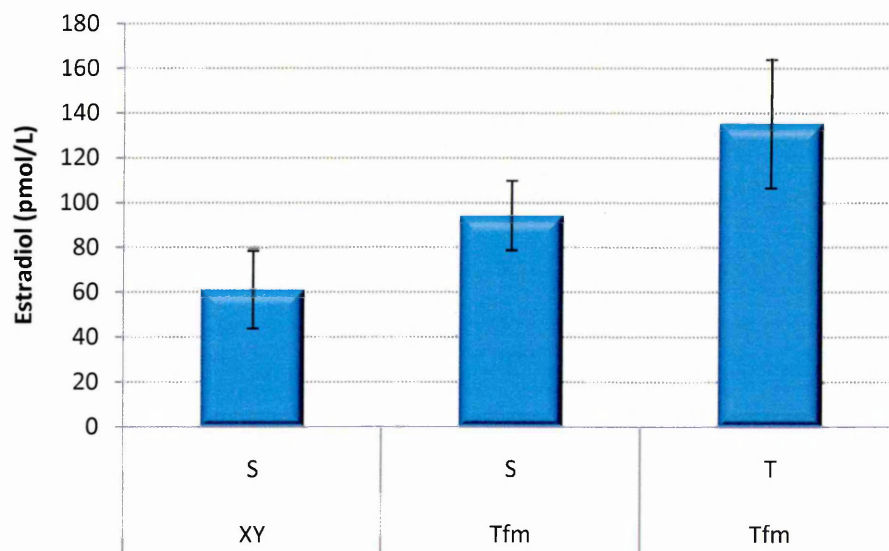
Figure 3.21; Serum estradiol concentration of Tfm mice and XY littermates fed a high-cholesterol diet and receiving either testosterone (T) or saline (S) injections. Estradiol concentrations compared between Tfm mice receiving saline injections (n=6); Tfm mice receiving testosterone injections (n=6), XY littermates receiving saline injections (n=6) all on high-cholesterol diet for the 28 week study period.
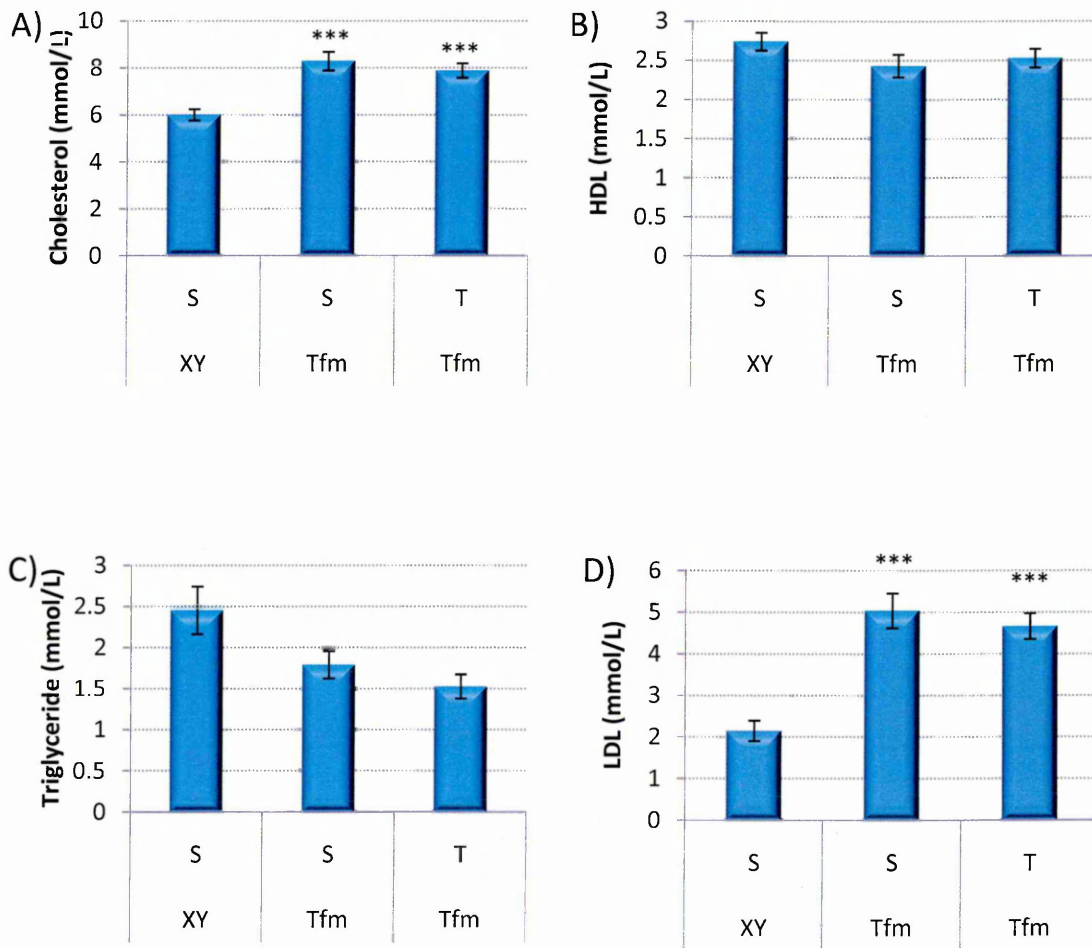
Figure 3.22; Serum lipid concentrations of Tfm mice and XY littermates fed a high-cholesterol diet and receiving either testosterone (T) or saline (S) injections. Lipid concentrations compared between Tfm mice receiving testosterone replacement (n=13), Tfm mice receiving saline (n=14) and littermate mice receiving saline (n=12) all on high-cholesterol diet for the 28 week study period. *P<0.05, **P<0.01, ***P<0.001 vs XY littermates receiving saline, Mann Whitney test.
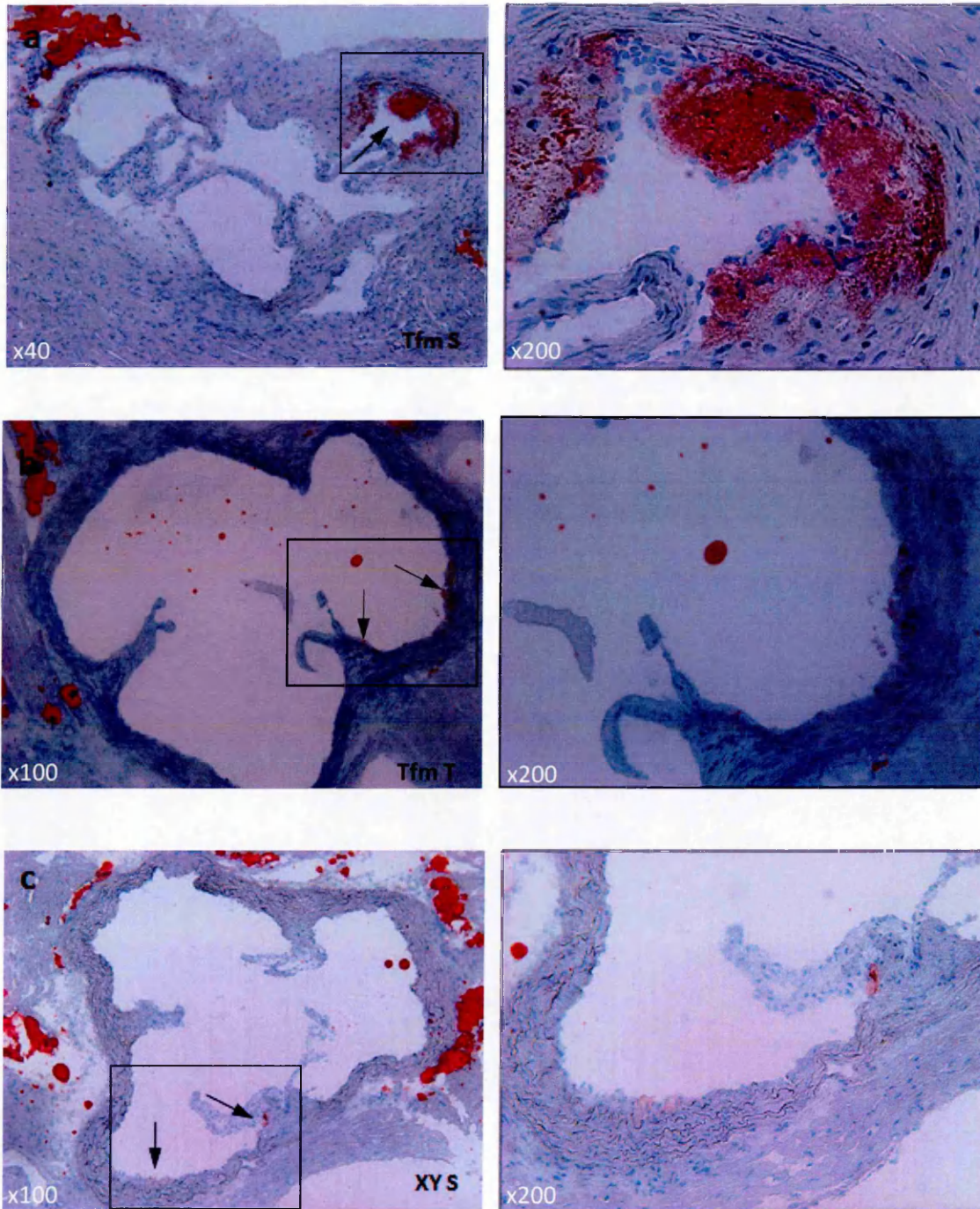
Figure 3.23; Representative oil red O staining of aortic root sections from Tfm mice and XY littermate controls on a high-cholesterol diet receiving either testosterone (T) or saline (S) injections. Staining was apparent in the vascular wall of aortae of both Tfm and XY littermate mice fed high-cholesterol diet and receiving saline injections and testosterone. Tfm mice receiving saline injections demonstrated much larger lesions (a). Lesions developed primarily at the shoulders of the aortic valve cusps in Tfm mice receiving testosterone (b) and XY littermates receiving saline (c). Sections were counterstained with haemotoxylin.

staining was decreased significantly when measured semi-quantitatively compared to saline-injected Tfm mice (P<0.05, ANOVA, n=6) (figure 3.24). ORO staining in the aortic root of testosterone-injected Tfm mice was still greater than saline-injected XY littermates, although not significantly.

3.3.4.5   *Serum cytokine measurements*

Concentrations of all serum cytokine (IL-1β, IL-6, IL-10, CCL2 and TNFα) appeared marginally, but non-significantly reduced by testosterone replacement in Tfm mice compared to saline-injected Tfm mice (figure 3.25). The previously observed increase in serum CCL2 levels in Tfm mice on high cholesterol diet was partially, but not significantly prevented by testosterone replacement. Serum levels of IL-6 and TNFα appeared to be reduced more markedly in Tfm mice injected with testosterone, although again not statistically so (n=6).

3.3.4.6   *Immunohistochemistry*

Aortic root sections known to contain lipid streaks from ORO staining were selected in sequence, where possible, or in the closest proximity to the detected lesion, for immunohistochemical analysis. Macrophage infiltration, detected by MOMA2 immunofluorescence staining, was observed in all sections adjacent to lipid streaks and directly below the endothelial layer, identified by von Willebrand staining. CX_3CR1 staining was present in the plaque regions of the Tfm placebo-treated mouse and to a lesser extent in the XY littermate placebo-treated mouse aortic roots. No CX_3CR1 was detected in the aortic root of the Tfm mouse receiving testosterone replacement. CX_3CL1 staining was only detected at low levels in the aortic root lipid streak region of the Tfm mouse on placebo. No CX_3CL1 was detected in the Tfm mouse receiving testosterone replacement or the littermate placebo control (figure 3.26).

No staining was detected in negative controls, with the omission of the primary antibodies, for both secondary antibodies, Alexafluor 488 (green) and Alexfluor 568 (red), indicating no non-specific binding of the secondary antibodies at the optimised conditions (figure 3.26). The positive control for the CX_3CR1 antibody was the cardiac tissue from a Tfm mouse which demonstrated specific staining throughout the myocardium. When this antibody was pre-incubated with a specific peptide block, no staining occurred. Isotype controls for VWF, CX_3CL1 and CX_3CR1 (which shared the same isotype) and MOMA2 demonstrated no staining following the same procedure as target antibodies, suggesting no non-specific binding of the primary antibodies (figure 3.27).
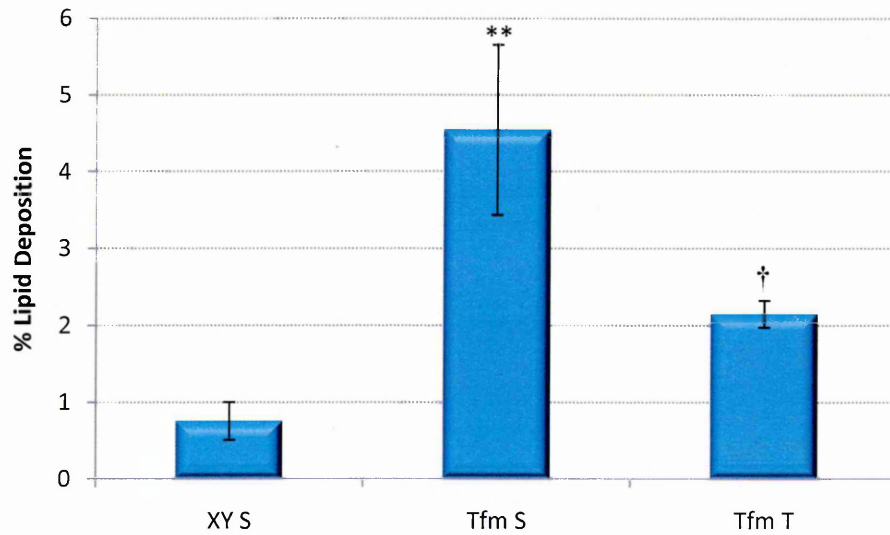
Figure 3.24; Percentage lipid deposition in aortic root sections from Tfm mice and XY littermates fed a high-cholesterol diet and receiving either testosterone (T) or saline (S) injections. Semi-quantification of lipid deposition in the aortic root (expressed as percentage of medial area) was elevated in Tfm mice compared to XY littermates receiving saline. Lipid deposition was also reduced in Tfm mice receiving testosterone injections compared to saline-injected Tfm mice, though not to levels seen in XY littermates (**P<0.01, vs XY littermates receiving saline; †P<0.05, vs Tfm mice receiving saline; Kruskal-Wallis, n=6).
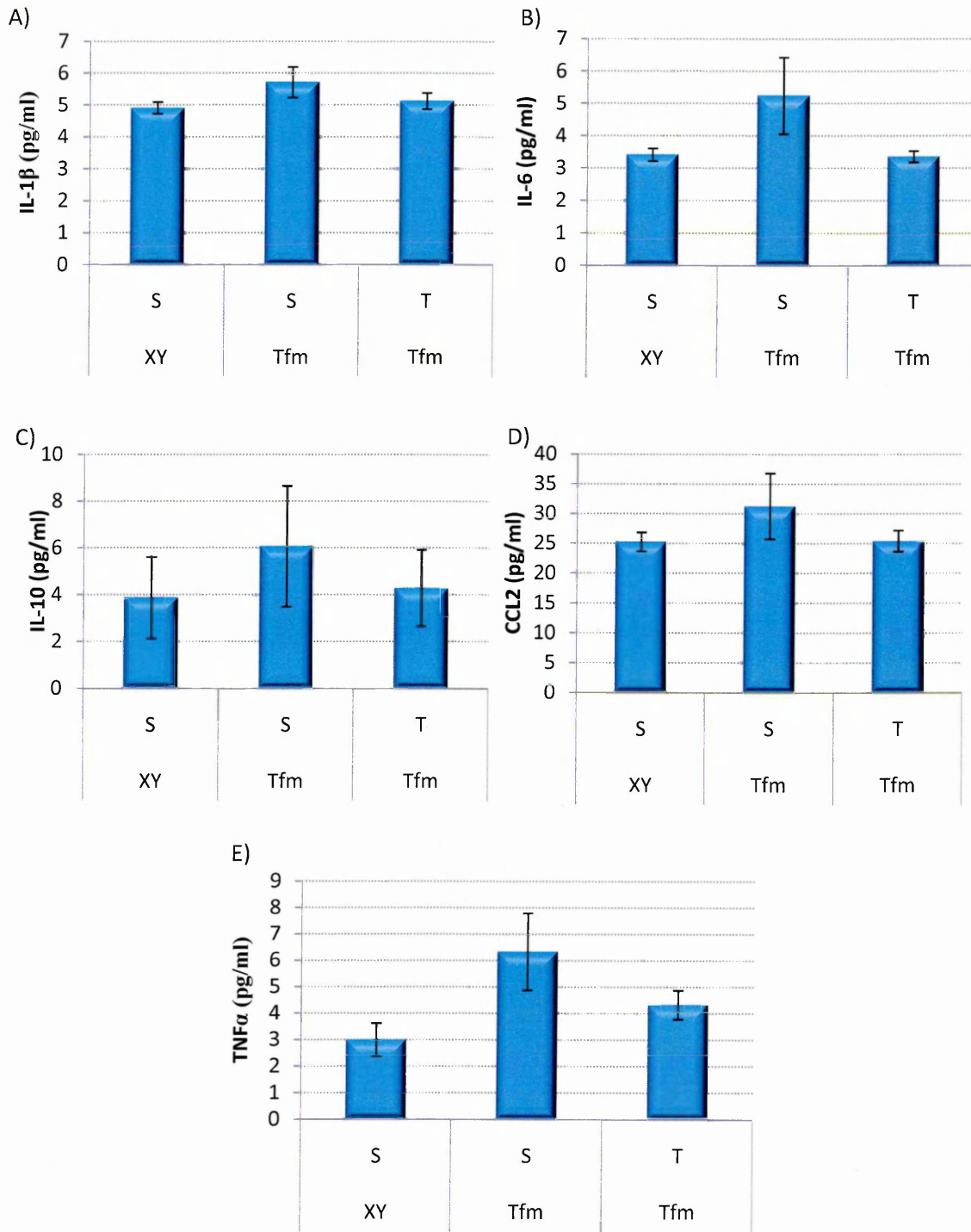
Figure 3.25; Serum cytokine concentrations of Tfm mice and XY littermates fed a high-cholesterol diet and receiving either testosterone (T) or saline (S) injections. XY littermates receiving fortnightly saline injections (n=6), Tfm mice receiving fortnightly saline injections (n=6) and Tfm mice receiving fortnightly testosterone injections (n=6) all on high-cholesterol diet were compared for serum cytokine concentrations. (unpaired t test).

	XY Placebo	Tfm Placebo	Tfm Testosterone
ORO			
VWF			
MOMA2			
CX3CR1			
CX3CL1			
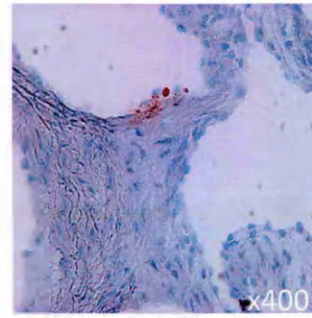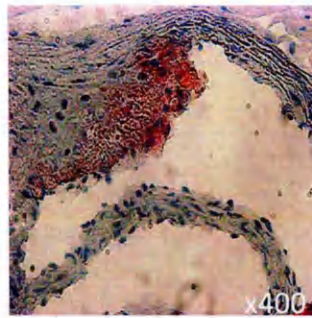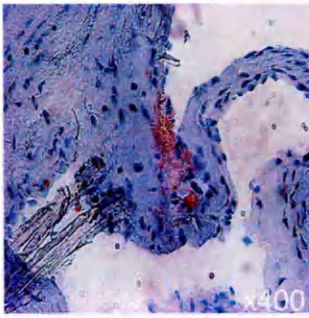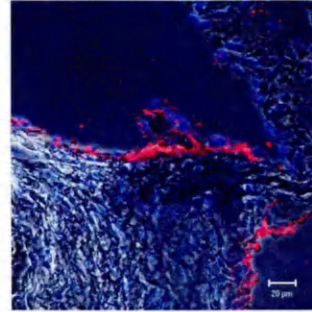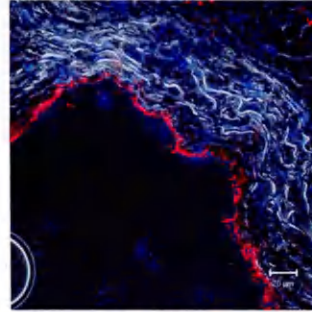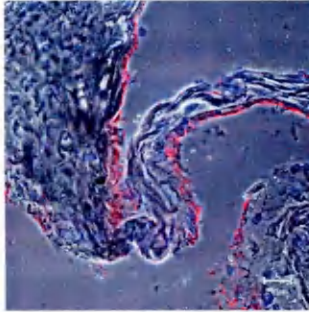
222
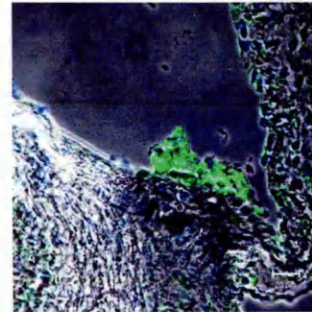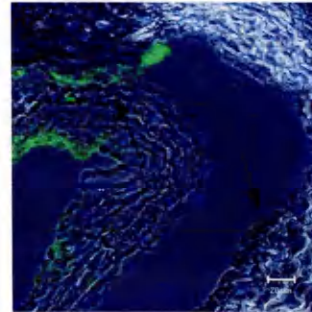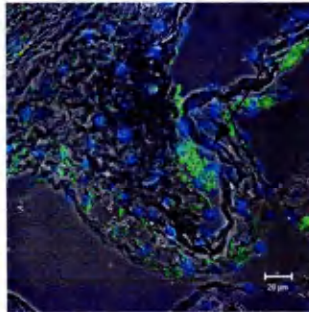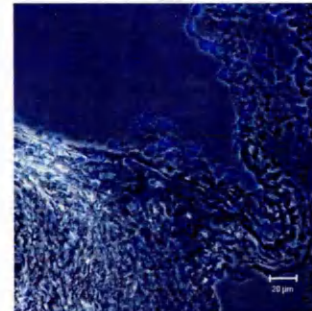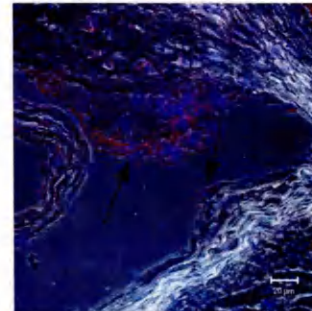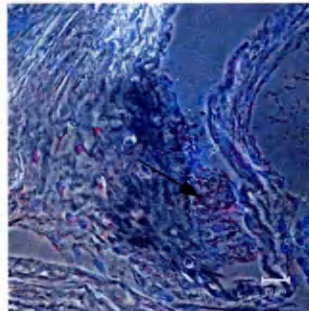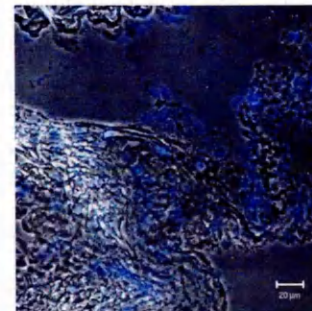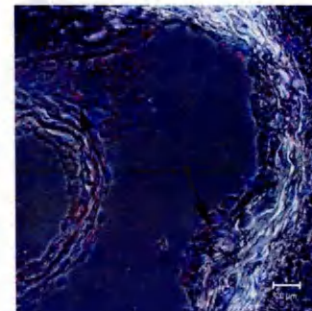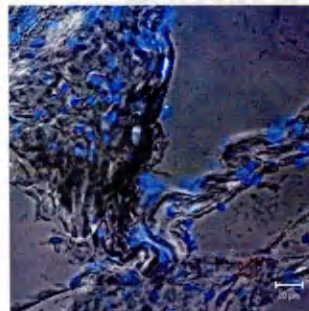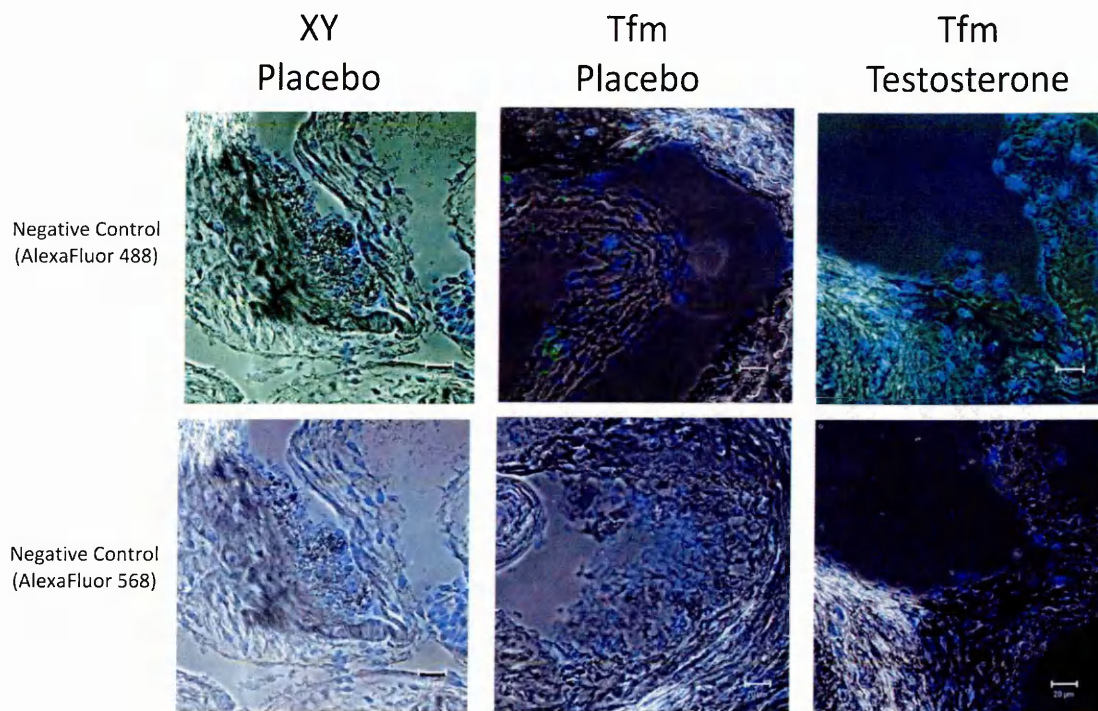
Figure 3.26; Immunohistochemical analysis of lipid streak composition in the aortic root of Tfm mice and XY littermates fed a high-cholesterol diet and receiving either testosterone or placebo treatment. Aortic root samples, identified as containing atherosclerotic plaques from oil red O (ORO) lipid deposition analysis, were selected. The endothelial layer was marked by von Willebrand factor (VWF, red) staining. Monocyte infiltration was detected locally adjacent to lipid streak areas (MOMA2, green). CX_3CR1 (red) was detected in the lipid streak areas of Tfm and littermate mice on placebo treatment, but not in Tfm mice receiving testosterone injections. Low level CX_3CL1 staining (red) was observed adjacent to lipid streaks in Tfm mice on placebo compared to littermates and Tfm mice on testosterone where no staining was seen. Negative controls with the omission of primary antibodies revealed no staining for both secondary antibodies labelled with AlexaFluor 488 (green) or AlexaFluor 568 (red). Cell nuclei were stained with DAPI (blue) and fluorescent images overlaid onto confocal images of the same area. Scale bar is 20μm
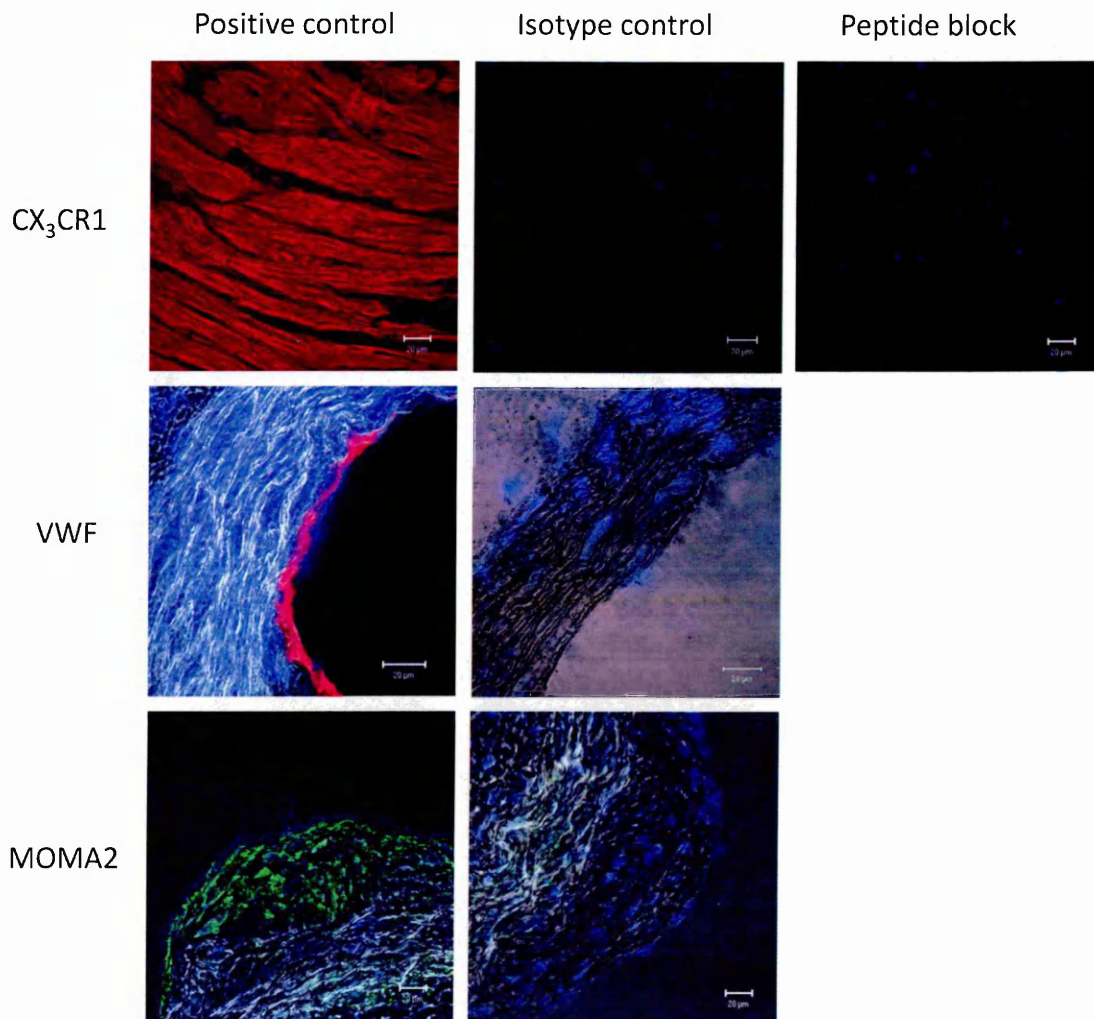
Figure 3.27; Immunohistochemistry controls for testing the specificity of primary antibodies and validity of immunostaining. Positive control tissues demonstrated clear staining for the target antigen with little non-specific staining following optimisation of the methods. Positive control tissues were; mouse cardiac tissue for CX_3CR1, mouse aorta for vWF, and mouse aortic root atherosclerotic plaque for MOMA2. Isotype controls showed no staining in serial sections of the same control tissue with antibodies directed against non-relevant antigens. Peptide blockade of CX_3CR1 primary antibody additionally revealed no staining.

3.3.4.7 Serum CX₃CL1 measurements

CX$_3$CL1 concentrations in the serum of animals from all experimental groups were below the detection limit of the ELISA.

3.3.4.8 Summary

In summary, fortnightly testosterone injection significantly increased serum testosterone levels in Tfm mice, but did not significantly affect estradiol levels when compared to Tfm placebo controls. A significant reduction in the amount of lipid deposition in the aortic root was demonstrated following testosterone replacement in Tfm mice fed a high-cholesterol diet. Additionally, testosterone-injected Tfm mice displayed marginally reduced serum cytokines, total cholesterol and LDL compared to placebo-injected Tfm controls, though these changes did not return parameters to the same level as XY littermate mice or normal diet-fed Tfms.

3.4 Discussion

3.4.1 Gender Determination

PCR confirmed the expression of the Sry gene in all ear clip samples from Tfm mice at the expected product size of 340bp, indicating that all animals were genotypically males. Thus it is possible to conclude that the breeding scheme was successful and that the Tfm strain was maintained throughout the process, based on the phenotypic expression of female characteristics by male mice. The conservation of the specific genetic manipulations of the Tfm strain was not investigated, but assumed to be maintained within the colony along with the inherent consequential symptoms of low endogenous testosterone and a non-functional androgen receptor. The low serum concentrations of testosterone observed in Tfm mice in this study further validate this assumption.

3.4.2 The effect of testicular feminization on atherosclerotic parameters

Tfm mice were shown to exhibit low endogenous serum testosterone levels compared to XY littermates. Serum levels of testosterone were approximately six-fold lower than that of XY littermates, and thus Tfm mice were overtly testosterone deficient, in addition to being unable to respond via the classical genomic signalling pathways mediated via AR activation. In a previous study using this mouse model, testosterone levels were found to be ten-fold lower than XY littermates (Nettleship *et al.* 2007a). The difference in magnitude of serum testosterone reduction between this and the present study may be explained by the timing of serum collection. Due to logistics and time limitations, all serum samples in the present study were collected mid-afternoon, when the diurnal rhythm of testosterone is declining toward the nadir of the cycle (Faiman and Winter 1971, Brambilla *et al.* 2009). In the previous study serum samples were taken closer to the morning peak in the cycle, when serum testosterone concentrations are considered more reliable and representative of the overall androgen status (Brambilla *et al.* 2009). Thus in future investigations samples would preferably be taken in the morning to investigate peak serum testosterone concentrations.

The low endogenous serum testosterone, along with a non-functional AR, were associated with a significant increase in weight gain over the course of the investigation in Tfm mice. Decreased levels of testosterone have been found in obese men, linking low levels of androgens with weight gain and fat accumulation (Zumoff *et al.* 1990, Derby *et al.* 2006,

Goncharov *et al.* 2009). In the present study Tfm mice had inherent low serum testosterone and a non-functional AR, which would suggest that the increased weight gain was a consequence of androgen insensitivity rather than increased weight leading to low testosterone levels.

In contrast, serum estradiol levels in Tfm mice were unexpectedly and significantly elevated by almost three-fold compared to XY littermates. Although this was not observed by Nettleship *et al.* (2007a), this may be due to the use of different methods of analysis, with potential disparities in the sensitivity of the assays. The present study used an ELISA to directly detect hormone levels in serum samples, whereas Nettleship *et al.* (2007a) applied an extraction procedure to the samples prior to assaying. The elevated oestrogen levels in the Tfm group could also be related to increased adipose tissue, as this group also demonstrated the greatest weight gains, significantly greater than XY littermates. Adipose tissue contains a high concentration of aromatase, which is capable of converting testosterone to estradiol and/or androstenedione to oesterone, thus creating a more oestrogenic profile in males (Hammoud *et al.* 2006). In addition, adipose tissue has been shown to express several steroidogenic and steroid-inactivating enzymes (Blouin and Tchernof 2008). Although adipose tissue was not directly measured in this study, weight gain may be indicative of visceral fat accumulation. The elevated lipid status of Tfm mice compared to littermates in this study lends support to this theory. A low testosterone/high 17β-estradiol serum profile has also previously been demonstrated in a male mouse model that has a partial deletion in the long arm of the Y chromosome, which contains a region of genes related to spermatogenesis and development of male characteristics (Kotula-Balak *et al.* 2004).

Several cross-sectional studies have reported that low endogenous serum testosterone is associated with high serum levels of either total and/or LDL-cholesterol in humans (Barrett-Conner *et al.* 1988, Barrett-Conner *et al.* 1992, Haffner *et al.* 1993, Simon *et al.* 1997, Barud *et al.* 2002) and animals (Jones *et al.* 2002). The present study supports this as total serum cholesterol and LDL cholesterol were shown to be significantly increased in Tfm mice compared to XY littermates. Elevated total cholesterol in the Tfm mice is consistent with previous reports (Nettleship *et al.* 2007a, Jones *et al.* 2003). As serum LDL concentration was calculated from the total cholesterol, HDL and triglyceride measurements, inaccuracies may occur in samples with low total cholesterol and high HDL levels, resulting in anomalous negative LDL values, as was seen in XY mice. Statistical analyses were still performed on these negative values to accommodate group variability as opposed to zeroing the negatives. However, the significance between the differences observed should be regarded with caution. Although higher than XY controls, the levels of serum LDL measured in the Tfm group were low

and therefore may not be significantly different from the XY littermate concentrations if the negative values were not included in analyses. Serum HDL was also elevated in Tfm mice, which would potentially counteract the negative effects associated with elevated LDL-cholesterol. On the other hand, due to the reported atheroprotective effects of HDLs (Reviewed in Murphy *et al.* 2009) and the multiple negative effects of non-HDL lipoproteins, it is often more pertinent to consider lipid profiles rather than individual lipid fractions (Tarchalski *et al.* 2003, Penalva *et al.* 2008, Okamura *et al.* 2009, Tamada *et al.* 2010). It is becoming more apparent, that HDL levels *per se* may not represent the whole story, as clinical studies have identified individuals with a significant atherosclerotic burden despite normal or elevated HDL cholesterol (reviewed in Ragbir and Farmer 2010). It has recently been proposed that the mechanism by which HDL-C levels are raised may influence their pro- or anti-atherogenic effects (Leite and Fernandez 2010). Increased HDL as a result of increased synthesis appears to be protective against cardiovascular diseases, whereas an increase due to decreased catabolism has been associated with a greater number of cardiovascular-related deaths (reviewed in Leite and Fernandez 2010). In addition, the heightened oxidative status associated with vascular dysfunction and atherosclerosis is capable of oxidatively modifying HDL, generating dysfunctional HDL which is often incapable of reverse cholesterol transport (Heinecke *et al.* 2008, Li *et al.* 2009). Therefore, the functionality of HDL may be more indicative of negative cardiovascular outcomes.

The minimal lipid deposition found in the aortic root of Tfm mice in the present study however, would suggest that although these mice have elevated serum lipids and low endogenous testosterone, they remain relatively resistant to early atherosclerosis. It remains unknown from this investigation whether this is due to the elevated serum oestrogen, the moderately raised HDL levels or simply due to the fact that C57BL/6 mice are relatively resistant to spontaneous atheroma formation and require a high fat diet to induce atherosclerosis (Daugherty *et al.* 2002).

Serum IL-6 and TNFα were significantly elevated in Tfm mice compared to XY littermates, suggesting that low endogenous testosterone and non-functional ARs may influence selective cytokines and, therefore, inflammatory status. As elevated IL-6 levels have been shown to predict cardiovascular events in healthy men, and survival amongst patients with acute coronary syndromes, and TNFα has been associated with an elevated risk of MI and cardiovascular death (Ridker *et al.* 2000a), it may be postulated that elevated levels in the current model are predictive or indicative of early athero-inflammatory events. It has been suggested that plasma cytokine levels correlate negatively with androgen levels in men (Yesilova *et al.* 2000;) and women (Christodoulakos *et al.* 2007). Yang *et al.* (2005) confirmed a

significant inverse correlation between serum testosterone levels and IL-6, sICAM-1 and C-reactive protein (CRP) in elderly males. An inverse relationship was seen between serum IL-1β and endogenous testosterone in 69 male CAD patients diagnosed with ischaemic heart disease (Nettleship *et al.* 2007b). The increase in IL-1β was significantly related to disease severity in a stepwise manner, yet no association was observed for TNFα, IL-6 and IL-10 (Nettleship *et al.* 2007b). Although IL-6 and TNFα were elevated in Tfm mice on normal chow diet in the present study, no association with lipid deposition in the aortic root was observed. This was due to a lack of lesion development, in line with previous suggestions in C57BL/6 mice on normal diet (Paigen *et al.* 1987). As this is a model of early atherogenesis, the elevated lipid and cytokine parameters observed in Tfm mice may be indicative of a pre-atherosclerotic state, preceding the development of lesions at an older age. Investigating lipid deposition in the aortic root of these animals on normal diet beyond the 36 weeks of age could help elucidate this.

3.4.3   The effect of high-cholesterol diet on atherosclerotic parameters

Animals were fed a diet containing 42% butterfat, 1.25% cholesterol and 0.5% cholate, a diet previously reported to induce atheroma formation in mice following feeding between 5 and 26 weeks (Abramovitz *et al.* 1999, Calleja *et al.* 1999, Lichtman *et al.* 1999, Merat *et al.* 1999, Murakami *et al.* 1999, Tangirala *et al.* 1999, Tribble *et al.* 1999 Nathan *et al.* 2001). In these previous studies the animals had increased susceptibility to atherosclerosis through knockout of the LDLr. In addition to this, 28 weeks of feeding on this high-cholesterol diet has been previously shown to be sufficient to establish lipid streak formation in the Tfm mouse model (Nettleship *et al.* 2007a). This previous study reported a weight gain in Tfm mice compared to XY littermates over the feeding period, whereas the present study demonstrated inconsistent and only slightly elevated weights in Tfm mice, although they were significantly elevated by the end of the study period. When body weights were converted to weight gain, to account for variations in starting weights of animals, the differences were not statistically significant, although Tfm mice maintained the highest weight gains. Surprisingly, a decline in both body weight and weight gain following high-fat diet feeding compared to normal chow fed mice was seen in the current investigation in Tfm mice. The decrease in weight gain following high-fat diet consumption is inconsistent with previous studies using animal models, which report either weight gains (Nettleship *et al.* 2007a, Bourassa *et al.* 1999) or no change in body weight (Alexandersen *et al.* 1999). As XY littermates demonstrated similar decreases in total body weight and weight gain, it may be proposed that the palatability of the diet affected the amount of food consumed. Food intake was not monitored in the present study, but could be

a useful additional parameter to monitor in future studies, to evaluate dietary habits in relation to weight.

The apparent decline in serum testosterone observed in XY littermates following 28 weeks high-cholesterol diet may be due to feedback mechanisms on steroidogenesis. Several enzymatic steps are involved in the biosynthesis of steroid hormones from cholesterol, the first one of which is the conversion of cholesterol to pregnenolone (see figure 1.9) in the mitochondria of steroid hormone producing cells (Stocco and Clark 1996). Sugawara *et al* (2007) demonstrated that human adrenal carcinoma H295R cells displayed significantly decreased pregnenolone production when cultured with varying amounts of cholesterol sulphate. In addition, specific transport proteins are necessary to deliver cholesterol to the mitochondria for this enzymatic conversion (Strauss *et al*. 1999). Increased levels of cholesterol sulphate have been reported to inhibit cholesterol movement in the mitochondria from isolated rat adrenal cells, and thus decrease steroidogenesis (Lambeth *et al*. 1987). While this implicates a mechanism by which increased dietary cholesterol can result in reduced testosterone production, the effect of cholesterol on steroidogenesis remains unclear (Clemens *et al*. 2000).

Additionally, the concept of bioavailable testosterone, which comprises free testosterone and that loosely bound to albumin, may be considered a more accurate assessment of androgen status and may be of more use than total testosterone measures in future studies. In a report by Muller *et al*. (2004), free testosterone but not total testosterone, was associated with the progression of atherosclerosis in elderly men, although opposing results have also been shown (Svartberg *et al*. 2006). These conflicting results encourage the measurement of total and free testosterone in addition to SHBG and albumin levels as more encompassing parameters of testosterone assessment in future investigations.

17β-estradiol was significantly reduced by high-cholesterol diet in Tfm mice, again potentially due to cholesterol feedback mechanisms acting upon the regulation of steroidogenesis. Estradiol levels were comparable between Tfm mice and XY littermates on high-cholesterol diet. This is important in the context of this investigation as it ensures that any differences in the atherosclerotic parameters may be attributable to the low testosterone concentrations and non-functional AR associated with the Tfm mouse, rather than any estradiol-mediated events.

As previously demonstrated (Barrett-Conner *et al*. 1988, Barrett-Conner *et al*. 1992, Haffner *et al*. 1993, Simon *et al*. 1997, Barud *et al*. 2002), serum lipid measurements significantly favour an atherogenic profile, following high-cholesterol diet feeding. Both Tfm mice and XY

230

littermates displayed elevated total cholesterol and LDL-cholesterol after high-cholesterol feeding compared to normal diet. Additionally, HDL was decreased in Tfm mice, potentiating the atherogenic lipid balance. Despite the diet-induced increase in total cholesterol and LDL in XY littermates, Tfm mice displayed significantly higher concentrations of both, indicating that low testosterone and a non-functional AR negatively influence circulating lipids to favour dyslipidaemia. Simon et al. (1997) conducted a case-controlled study of 25 age- and ethnicity-matched males and demonstrated that low testosterone was significantly associated with higher total cholesterol, LDL cholesterol and lower HDL cholesterol. Laughlin et al. (2008) also reported an inverse relationship between endogenous testosterone and serum triglyceride, and a positive association with HDL cholesterol in a prospective population-based study of 794 elderly men. Thus, the animal model demonstrated similar lipid profiles to patients with low testosterone, indicating that it is a good model in which to study atherosclerosis.

In agreement with these circulating serum lipid levels, significant fatty streak formation was detected within the aortic root of Tfm mice following 28 weeks feeding on the high-cholesterol diet. XY littermates also demonstrated increased lipid deposition compared to XY littermates on normal diet, though the lesions were fewer and significantly smaller than those in Tfm mice, when quantified. Comparable with these observations, several animal studies have reported a negative association between low endogenous testosterone levels in male animals and aortic atherosclerosis. Indeed, Alexandersen et al. (1999) examined the effects of natural androgen on lipids in sexually mature male rabbits. Following either bilateral castration or sham operation, 20 male rabbits per group were fed an atherogenic diet for 30 weeks to induce aortic atheroma formation. It was reported that aortic plaque formation was doubled in castrated rabbits compared to sham-operated controls (Alexandersen et al. 1999). Moreover, Nathan et al. (2001) demonstrated that sub-physiological testosterone levels in orchidectomised male LDL-receptor KO mice exacerbated aortic lesion formation compared to testes-intact controls, following 8 weeks cholesterol feeding. Such data provides further evidence that low serum testosterone is linked to atherosclerosis.

Many studies have investigated the association between serum levels of testosterone and CAD in men (Philips et al. 1994, Kabakci et al. 1999, English et al. 2000c, Pugh et al. 2004, Van den Beld et al. 2003, Rosano et al. 2007). Though these studies differ in the parameters used to measure atherosclerosis, consistent conclusions are reported that serum testosterone levels are not raised in men with CAD. Moreover, the majority of these studies conclude that serum testosterone is reduced in male CAD patients. Phillips et al. (1994) related the extent of CAD with declining levels of serum testosterone in men aged 39-89, and Van den Beld et al. (2003) similarly reported an inverse relationship between testosterone and carotid atherosclerosis. In

addition, Pugh *et al.* (2004) reported a 24% prevalence of hypogonadism in a cohort of 831 male subjects exhibiting >75% stenosis of at least one major coronary artery. In a study by Rosano *et al.* (2007), 129 male angina patients with symptoms suggestive of CAD were evaluated for plasma hormone levels. An inverse relationship between the degree of CAD and plasma testosterone levels was found. Premature CAD in men below the age of 45 was associated with lower concentrations of total and free testosterone compared to age matched controls (Turhan *et al.* 2007). In addition to CAD studies, Akishita *et al.* (2009) have recently reported that low testosterone is predictive of cardiovascular events in a Japanese population of 171 middle-aged male outpatients who initially had any coronary risk factor (hypertension, diabetes, dyslipidemia, smoking, and obesity) without a previous history of CV disease. IMT, as an indicator of general atherosclerosis, was also found to be associated with low total testosterone measures in a large male population-based study (Svartberg *et al.* 2006). Such studies provide strong evidence that negative cardiovascular events are associated with low testosterone, and the present study supports this.

Serum CCL2 levels were elevated in both Tfm mice and XY littermates following high-cholesterol diet feeding, suggesting that this diet influences inflammatory status regardless of serum androgen levels or AR functioning. Raised CCL2 levels have been associated with CVD. Elevated plasma CCL2 has been reported in patients with severe acute MI (Parissis *et al.* 2002, Kobusiak-Prokopowicz *et al.* 2007). PBMCs from patients with CAD spontaneously secrete more CCL2 than PBMCs from healthy controls, and release greater amounts when stimulated with oxLDL (Breland *et al.* 2008, Oliveira *et al.* 2009). Additionally, increased serum CCL2 has been reported in rodent obesity as a direct result of high-fat diet feeding (Takahashi *et al.* 2003). Although CCL2 was not related to body mass in the present study, body composition may have been a more relevant parameter to measure as adipose tissue may increase without altering total body weight or weight gain, as fat distribution shifts. Increased circulating CCL2 may be linked to monocytosis and a heightened inflammatory state associated with elevated monocytes in the blood. High-cholesterol diet feeding was additionally seen to significantly increase circulating TNFα concentrations in XY littermates. Adipocytes express TNFα (Fain *et al.* 2004) and, although circulating levels are low in comparison with local tissue concentrations, serum levels have been correlated with obesity (Fernandez-Real *et al.* 2003), an elevated risk of MI and cardiovascular death (Ridker *et al.* 2000b), severity of PAD (Tedgui and Mallat 2006) and burden of atherosclerosis (Skoog *et al.* 2002). The lack of increase in serum TNFα in Tfm mice on high-cholesterol diet in the present study may be due to the high baseline levels observed compared to XY littermates.

No significant differences were observed between Tfm mice and XY littermates on high-cholesterol diet for all serum cytokines measured, whereas earlier observations of mice on normal diet revealed differences between these groups for TNFα and IL-6, potentially due to low testosterone and non-functional AR. This suggests that high-cholesterol diet may have a greater effect on cardiovascular-related systemic markers of inflammation than androgen status, masking any effects of testosterone in these groups. Measurement of circulating cytokines, however, may not be indicative of the local inflammatory state at the site of lipid streak formation observed in the animal groups. Following secretion from activated cells, cytokines are often rapidly bound to high affinity receptors on neighbouring cells. As the lipid streaks, which developed as a result of high-cholesterol diet feeding, were localised to the aortic root, any associated inflammation may have been insufficient to produce a systemic inflammatory response. Therefore, measuring circulating levels is not necessarily indicative of cytokine activity relevant to aortic atherosclerosis. Many cytokines, such as IL-1β, IL-6, IL-10, IFNγ and TNFα are highly expressed in atherosclerotic regions at multiple stages of disease progression (Tedgui and Mallat 2006), but may not reach detectable circulating levels, particularly in models of early atherogenesis, where lesions are local to specific areas of the vasculature. In addition, the use of cholate in the high-fat diet, to facilitate cholesterol absorption and promote the development of atherosclerosis in this murine model, could have influenced inflammatory processes through the induction of inflammatory response genes, as suggested by Vergnes *et al.* (2003).

Clearly the data presented in this section show that low endogenous testosterone leads to aortic fatty streak formation and a pro-atherogenic lipid profile following cholesterol feeding. However, whether it is the testosterone deficiency, or the effects of non-functional ARs, that cause fatty streak formation cannot be concluded from these data alone. Further experiments employing TRT were undertaken to investigate this.

3.4.4   The effect of testosterone replacement on atherosclerotic parameters

The present study confirmed previous findings that fortnightly injections of testosterone (Sustanon 100® (100mg/ml)) were capable of returning serum testosterone concentrations to within the physiological (10-30nmol/L) range in Tfm mice (Nettleship 2006). It has been shown previously that the fortnightly serum testosterone levels in Tfm mice following intramuscular injection of Sustanon 100® fluctuated from supraphysiological directly after injections, to subphysiological by day 14, due to metabolism and excretion. For the duration of this cycle, circulating testosterone levels mostly remained within the physiological range. In the present

study, serum samples were collected at day 7 post-injection and correspond with the lower end of physiological (14.65±5.15 nmol/L) levels seen at this time point in the previous investigation. This highlights the robustness of the testosterone replacement protocol.

Serum testosterone levels in XY littermates were lower than previously described (Nettleship 2006), potentially due to the time of sample collection corresponding with the afternoon nadir of the diurnal testosterone cycle. Thus serum testosterone levels were significantly higher in Tfm mice receiving Sustanon 100® as supplemented testosterone does not display diurnal patterns. Tfm mice receiving placebo injections of saline demonstrated low endogenous testosterone levels, at levels similar to those of Tfm mice on high-cholesterol diet alone or normal chow diet. This further confirms that the Tfm mutation generates a phenotype with low circulating testosterone.

No significant differences were observed between the 17β-estradiol levels of XY littermates on placebo injections, Tfm mice on placebo injections and Tfm mice receiving testosterone replacement and were comparable to mice on high-cholesterol diet alone. Although not significant, estradiol levels appeared elevated in Tfm mice receiving TRT. This increase may be due to increased expression of aromatase, as similarly noted in mice with partial deletion of the Y chromosome (Kotula-Balak et al. 2004;), or increased aromatase in adipose tissue resulting from high-cholesterol diet feeding (Hammoud et al. 2006). As testosterone is increased from TRT, amplified enzyme expression would therefore increase conversion to estradiol compared to Tfm placebo mice, where the substrate hormone is reduced.

No significant differences in body weight were observed between Tfm mice and XY littermates on high-cholesterol diet and receiving either testosterone or placebo. This observation demonstrates that changes in serum lipid parameters were independent of change in weight and suggests that they may arise from a direct modulation of metabolic processes by testosterone rather than a reduction in weight. TRT investigations have revealed that testosterone treatment can alter body composition (Snyder et al. 1999, Isidori et al. 2005, Allan et al. 2008). Snyder et al (1999) reported a decrease in fat mass and an increase of lean mass in testosterone treated elderly (>65 years) men compared to placebo-treated controls. Comparable to the present study, no significant differences were observed in overall body mass (Snyder et al. 1999). Similarly, transdermal testosterone therapy was shown to inhibit visceral fat accumulation and improve fat-free mass and muscle mass compared to placebo-treated controls in a population of men aged 55 years or older with low-normal testosterone (Allan et al. 2008). These studies suggest that body composition rather than body weight, may

be influenced by testosterone, which may in turn be more relevant to metabolic syndrome and atherosclerosis.

Tfm mice on high-cholesterol diet had significantly higher total cholesterol and LDL serum concentrations compared to XY littermates. TRT in Tfm mice had no further modulatory effects on any of the lipid fractions measured. The lack of effect on the pro-atherogenic LDL and triglyceride fractions is in agreement with the study by Nettleship *et al* (2007a). Nettleship *et al.* (2007a) reported that physiological testosterone therapy had no lowering effect upon non-HDL-C in the Tfm mouse. These authors did show, however, an improvement in the serum concentrations of atheroprotective HDL-C in testosterone-treated Tfm mice compared to placebo-treated controls. These improvements brought HDL-C concentrations to levels comparable with XY littermates, suggesting that the beneficial effect of testosterone was not via AR activation. Moreover, blockade of ERα or aromatase inhibition abolished this increase in HDL-C, indicating that the effect of testosterone is dependent upon ERα activation and conversion of testosterone to estradiol (Nettleship *et al.* 2007a). Returning testosterone levels to low-normal by intramuscular injection in elderly men with subnormal levels was demonstrated to have no effect on circulating total cholesterol, LDL, HDL and triglyceride levels (Agledahl *et al.* 2008). Additionally, and similar to the present investigation, Allan *et al.* (2008) concluded that transdermal testosterone treatment did not alter serum lipid measurements (total cholesterol, HDL-C, LDL-C and triglycerides) in a cohort of healthy but symptomatic, elderly men. Favourable body composition changes were observed in the testosterone-treated group compared to placebo-treated controls (Allan *et al.* 2008). In contrast, several other studies have reported beneficial modulatory effects of TRT on lipid profiles as shown in chapter one table 1.2 (See Jones and Saad 2009 for review).

Although serum LDL measurements remain an important predictor of atherosclerosis, evidence is emerging that the subclass of LDL may provide greater insight into cardiovascular risk. LDLs are heterogeneous particles and comprise at least four major subspecies that differ in size, density, physicochemical composition, metabolic and oxidative behaviour (Griffin *et al.* 1990;). In particular, small dense LDLs express greater atherogenicity due to their increased long residence in the circulation, oxidative susceptibility, decreased receptor mediated uptake and increased endothelial penetration (Rizzo *et al.* 2009). In the present study, it is plausible that TRT may reduce the atherogenicity of the lipids by altering subclass, whilst not affecting the collective measurements of serum LDL and total cholesterol. This is supported by the protective effect of fortnightly sustanon 100® injections on lipid streak development in the aortic root of Tfm mice, in the absence of gross lipid changes, observed in the present study.

The present study supports the findings of numerous animal studies that have shown beneficial effects of androgen supplementation in atherogenesis, as lipid deposition in the aortic root was significantly inhibited by testosterone therapy in Tfm mice on high-cholesterol diet. Larsen *et al*. (1993) showed a significant reduction in aortic cholesterol accumulation following testosterone supplementation in orchidectomised male rabbits fed a pro-atherogenic diet. Alexanderssen *et al*. (1999) published similar results. Castrated male rabbits and sham-operated controls were fed an atherogenic diet for 35 weeks to induce aortic atherosclerosis and additionally received either daily oral testosterone, twice weekly intramuscular injection or placebo. Both oral and intramuscular testosterone were associated with a reduction in plaque formation (Alexanderssen *et al*. 1999). Similar findings were reported by Bruck *et al* (1997). Moreover, a reduction in plaque development was also demonstrated in orchidectomised male LDLr KO mice receiving testosterone supplementation compared to controls (Nathan *et al*. 2001). Most pertinently, Nettleship *et al*. (2007a) revealed that physiological testosterone therapy virtually abolished the increased aortic root lipid deposition seen in Tfm mice fed a pro-atherogenic diet. As the present study showed that aortic root lipid streak formation was only partially retarded by testosterone therapy in Tfm mice, and not reduced to the level of deposition seen in XY littermates, it may be concluded that the protective effects of testosterone act via both AR-dependent and independent pathways. Interestingly, and contradictory to the majority of studies, Villablanca *et al*. (2004) reported the potentiating effects of testosterone on fatty streak development in high-fat, high cholesterol fed male mice. Castration of ERα knock-out mice and wild-type controls almost prevented lesion formation in the aorta. Compared to wild-type controls, intact ERα-deficient mice displayed reduced atherosclerosis leading the authors to conclude that the negative effects of testosterone act via local conversion to 17β-estradiol and subsequent ERα activation (Villablanca *et al*. 2004).

The role of the AR has previously been implicated in CAD. Naturally occurring truncations in the polymorphic CAG repeats, that encode a varying number of polyglutamine residues in the AR molecular structure, have been associated with CAD (Zitzmann *et al*. 2001, Alevizaki *et al*. 2003). Shorter CAG repeats were associated with severity of CAD (Alevizaki *et al*. 2003). This may be, at least partly, due to effects on lipids, as lower HDL-C was reported in men with truncated CAG repeats (Zitzmann *et al*. 2001). The AR-independent mechanisms of testosterone's reported athero-protection are often considered to be mediated via a conversion to estradiol and subsequent activation of the ER. Nathan *et al*. (2001 described how the attenuating effects of testosterone on early atherogenesis, measured by aortic root lipid deposition in male LDLr KO mice, were not observed with simultaneous aromatase inhibition.

Also, the treatment of male ApoE KO mice with 17β-estradiol significantly reduced angiotensin II-induced suprarenal aortic lesion formation by 75% compared to controls (Martin-McNulty *et al.* 2003). These findings reflect those observed in apoE mouse models of diet-induced fatty streak formation (Bourassa *et al.* 1996) and spontaneous lesion development (Elhage *et al.* 1997), implicating a protective role for oestrogens. In contrast to these studies, Nettleship *et al.* (2007a) eloquently demonstrated that inhibition of aromatase and blockade of the ER only partially attenuated the protective effects of testosterone therapy in Tfm mice. This would suggest that testosterone additionally imparts beneficial effects on athero-development via non-classical non-genomic AR- and ER-independent mechanisms. The present study indicates both AR-dependent and independent protective functions of testosterone in athero-protection, although further investigation is required to elucidate the specific mechanisms involved.

No significant differences in serum cytokines were observed following testosterone treatment in Tfm mice on high-fat diet compared to littermates and placebo controls in the present study. Slight reductions in the diet-induced increases of IL-6, CCL2 and TNFα as a result of TRT were noted. The lack of significance may be due to the variability of the data, compounded by the small sample size, thus reducing the power of the investigation. Beneficial effects of testosterone supplementation in reducing pro-inflammatory cytokine concentrations have been previously reported (Hatakeyama *et al.* 2002, Malkin *et al.* 2004a, Malkin *et al.* 2004b, Corrales *et al.* 2006, Zitzmann *et al.* 2005). TRT reduced circulating levels of TNFα and IL-1β in a cohort of 27 hypogonadal men of whom 80% had CHD (Malkin *et al.* 2004b). Similarly, male hypogonadal patients with ischaemic heart disease who received testosterone treatment for 1 month demonstrated a significant decrease in serum TNFα (Malkin *et al.* 2004a). Interestingly, IL-6 was significantly reduced in healthy male volunteers following 16 weeks of testosterone supplementation (Zitzmann *et al.* 2005).

Studies investigating the effects of androgen therapy on cytokine levels in animal models are limited. Testosterone replacement in castrated mice reduced the heightened TNFα respone to lipopolysaccharide (Spinedi *et al.* 1992). In addition, DHT treatment of mice with experimental autoimmune encephalomyelitis decreased IFNγ concentrations, whilst elevating IL-10 (Dalal *et al.* 1997). Also, DHEA treatment reduced TNFα (Kimura *et al.* 1998) and IL-1 and LPS-induced TNFα (Ben-Nathan *et al.* 1999) in obese rats and mice respectively. These data implicate that androgens can modulate inflammation, potentially conferring beneficial effects against the development of inflammatory diseases such as atherosclerosis.

In the present study serum CX_3CL1 levels were below the detection range of the ELISA, potentially highlighting the local actions of these chemokines and indicating that localised inflammation may not be reflected in circulating markers. Similarly, Dougherty *et al.* (2005) found no change in serum levels of soluble ICAM-1 or VCAM-1 in 37 elderly hypogonadal men after normalising their testosterone levels, noting that circulating levels may not be indicative of local production. The circulating levels of both CCL2 and CX_3CL1 are associated with circulating monocyte number and subsequent accumulation in atherosclerotic plaques of ApoE-/- mice fed a high-fat diet (Combadiere *et al.* 2008). This may be partly due to chemokine control of monocyte emigration from the bone marrow to the circulation leading to a heightened immune response to local inflammatory stimuli. However, a reduction in atherosclerosis may not be indicative of a reduction in circulating monocytes or chemokines, as associations are not always observed (Rajavashisth *et al.* 1998;), and local cytokine activity may be more relevant to plaque progression.

To investigate local inflammatory activity, preliminary immunohistochemical staining of the fatty streak lesions in the aortic root of animals in the present study was undertaken, although due to the limited number of animals analysed, conclusions are tentative. As demonstrated in several other studies (Teupser *et al.* 2004), monocytes/macrophages were detected locally, adjacent to lipid streaks, indicating the presence of inflammatory leukocyte infiltration in atherosclerotic plaques. MOMA2 staining was consistent in the plaque areas of the different animal groups suggesting that monocytes and macrophages are present in the vessel wall at sites of atheroma, regardless of androgen influence. Monocyte/macrophages were located directly below the VWF-positive endothelial surface. As the size of the lipid streaks, analysed by ORO, were smaller and fewer in the aortic root of TRT treated Tfm mice and XY littermates, testosterone may not influence the proportion of monocytes/macrophages relative to lesion size, but may reduce overall immune reactivity and leukocyte entry to inhibit plaque formation. CX_3CR1 staining was present in the plaques of XY littermates and Tfm placebo mice, adjacent to ORO and MOMA2 staining. As dual staining was not carried out as part of this investigation, the localisation of CX_3CR1 could not be specifically designated to cell type. It's clear presence in the lipid streak area does, however, indicate a role for CX_3CL1 in early atherogenesis. Wong *et al.* (2002) reported CX_3CR1 staining in human atherosclerotic coronary arteries in the endothelium and immediate subendothelial cells. The authors localised the receptor to numerous infiltrating T cell and mononuclear cells seen within the adventitia. CX_3CR1 positive cells in human atherosclerotic plaques were demonstrated to be SMCs in intimal regions of coronary artery segments from heart transplant recipients (Lucas *et al.*

2003), suggesting a role for CX_3CL1 in vascular remodelling. A high amount of CX_3CR1 staining was present in the adventitia of AAA tissue (Patel *et al.* 2008).

CX_3CR1 staining in Tfm mice receiving TRT was not apparent in the lipid lesion. As XY littermates displayed lower levels of testosterone than anticipated and reduced concentrations compared to testosterone-treated Tfm mice, CX_3CR1 detection may be influenced by circulating testosterone levels. The staining apparent in XY littermates was of a relatively lower level than Tfm placebo, potentially supporting this idea, although this may have been simply reflective of lesion size. Reduced CX_3CR1 staining may be reflective of altered inflammatory cell phenotypes present in the fatty streak. Inflammatory monocytes are CX_3CR1^{lo}, and monocytes that express high CX_3CR1 are non-classical monocytes destined to become resident macrophages (Geissmann *et al.* 2003). Although it is not known at which stages in atheroma formation these subsets predominate and the actions they elicit, it may be postulated that testosterone influences specific recruitment or subset switching, thus altering relative CX_3CR1 abundance in the lesion without affecting monocyte/macrophage numbers. This may ultimately affect the nature and progression of the plaque. However, this is purely speculative and, as previously suggested, the predominant cell type expressing CX_3CR1 in human plaques has been demonstrated to be SMC (Lucas *et al.* 2003). Again, this may be indicative of altered lesion composition.

CX_3CL1 staining was only detected in Tfm placebo animals, and therefore corresponded with the severity of lipid streak formation. A protective effect of testosterone was apparent through the lack of CX_3CL1 staining in XY littermates, an effect that was independent of the AR, as TRT in Tfm mice appeared to abolish CX_3CL1 expression in aortic root plaques. CX_3CL1 expression appeared to be within the lesion area rather than on the luminal endothelial surface. This is in support of previous studies investigating CX_3CL1 expression in human coronary artery plaques (Lucas *et al.* 2003) and carotid and femoral arteries (Bazan *et al.* 1997). Lucas *et al.* (2003) provided evidence for CX_3CL1 positive cells just below the luminal endothelium of coronary artery lesions and through colocalistion of immune cell markers, and suggested that these cells were recently transmigrated monocytes. The authors reported that SMCs also expressed CX_3CL1 in the plaque regions, but the most substantial staining was localised to macrophages.

This may be explained by an effect of testosterone in inhibiting atherogenesis and therefore altering the expression and activity of chemokines at distinct phases of plaque progression. Cheng and colleagues (2007) report that CX_3CL1 is highly expressed only in advanced lesions of apoE-/- mice fed a high-fat high-cholesterol diet, where carotid arteries were subjected to low or oscillatory shear stress to induce plaque progression. However, Lesnik *et al* (2003)

239

demonstrate that CX$_3$CL1 is highly expressed in early aortic lesions of apoE-/- mice and plays an important role in atherogenesis. This, again, highlights the complexity of dissecting the role of a specific mediator in the multifaceted, dynamic and complex process of atherogenesis, which may be influenced by many other factors such as vascular territory and the initiating stimulus.

The direct mapping of multiple targets within the same lesion is difficult to achieve in the present study due to limitations in the sequential nature of the aortic root sections. Also, as sections are taken from different stages throughout the length of the lesion, plaque composition may alter. The upstream shoulder regions, or outer edges, of atherosclerotic lesions are considered to be subjected to increased shear stress and, although not sufficient to physically cause mechanical destruction of the plaque, rupture may be provoked via altered cellular and structural composition (Fukumoto et al. 2008). Macrophage-rich areas are more likely to form in these upstream shoulder regions than in downstream shoulders of the same lesion (Dirksen et al. 1998). As macrophages are the most abundant source of MMP production in lesions, it follows that these leukocytes accumulate at vulnerable regions (Galis et al. 1994a) and that plaque rupture is always colocalised with inflammatory cells (Pasterkamp et al. 1999). Therefore, it is possible that plaque composition may alter throughout the length of the lesion, potentially influencing cellular content and the expression of inflammatory markers, dependent upon the location of the section analysed. Therefore, a single section through a lesion at a particular point may not be representative of the entire fatty streak and its severity in terms of clinical consequence, and this highlights the importance of analysing multiple sections from an area of lesion and comparing representative data between different animals.

The major limitation of the immunohistochemical analysis in the present study is the lack of repetition. Only a single animal from each group was analysed due to time constraints, meaning no definitive conclusions can be drawn and suppositions are tentative. Additionally, the lack of complete sets of isotype controls and peptide blockade for all primary antibodies tested, brings into question the specificity of the staining and limits the reliability of the procedure. These limitations could be overcome in a continuation of the present investigation.

3.4.5 General considerations

As with all animal models of disease, the relevance to the pathophysiology of the human condition is always a consideration. In humans, the location and composition of the lesions are critical parameters that determine the severity and complication of the disease (Catanozi et al. 2009). The mechanisms and location of atherosclerosis that are responsible for overt clinical

symptoms in humans are often not those measured in mice, as it is often different areas that are prone to disease in animal models (Daugherty and Ratteri 2005). Although the lesions do not evolve into advanced fibrous plaques, this murine model mimics many of the features found in early lipid streak formation in humans. Feeding animals a high-cholesterol diet is a well established model for atheroma formation, although the dyslipidaemia induced differs compared to native human atherosclerosis. High LDL seen in humans and the associated mature plaques are replaced by high VLDL and cholesterol ester-enriched fatty streaks (Arad *et al.* 1989). These subtle differences may affect the delicate interplay between sex hormones and CVD, although fatty streaks as precursors of mature plaques appear to maintain similar morphology and cell behaviour in animal models as with human atheroma (Gordon *et al.* 1988).

It has been noted that the high degree of variation inherent with animal models and the frequent lack of Gaussian distribution often requires reasonably large group sizes for robust statistical analysis (suggested as 20 per group) (Daugherty and Ratteri 2005). Due to practical limitations, respect for the reduction element in ethical considerations of animal work design, and based on power calculations from the previous study (Nettleship *et al.* 2007a), the present study utilised much lower group numbers than Daugherty and Rateri (2005) suggest. The variation within and between groups in the current study make it difficult to draw definitive conclusions from the data. It is possible that due to this variance, apparent patterns in the data of the present investigation are assessed to be non-significant with poor statistical value. A repeat of the present study may elucidate some of the smaller differences that may be important underlying mechanisms of lesion formation. However, as the present investigation repeated several parameters of an earlier study (Nettleship *et al.* 2007a), with inconsistencies in the some of the findings, the variability of animal experimentation is highlighted. Daugherty and Rateri (2005) also recognised considerable variance in the extent of atherosclerosis and parameters measured for the same model in different laboratories.

Measurement of circulating total testosterone and estradiol may not be reflective of their local tissue-specific actions and would therefore be imperfect parameters for extrapolating information regarding the hormonal influence on atherogenesis. In addition, a single point measurement of androgen/oestrogen status may be limited in its ability to indicate the preceding conditions as a determinant of the prevailing manifestations at the time of investigation. However, with the limited amount of collectable blood and the sample volume requirements for analysis, this issue was unavoidable in this study.

Oil red O histological staining does not appear uniformly across the entire lesion, potentially due to regions of extracellular matrix and unesterified cholesterol that do not take up the neutral lipid stain (Daugherty and Ratteri 2005). This compromises the ability of image analysis software to quantitate lesion size and leads to potential investigator inaccuracies during manual assessment of area. This error should be consistent between samples however, and therefore can be accounted for when comparing groups. Although similar lipid staining may be seen in some animals from different groups, it is possible that differences in fatty acid composition may be present, and may result in different severity of lesion development in terms of clinical outcomes. In addition, Paigen *et al.* (1987) highlighted differences in plaques in the aortic wall and those on the valve cusps in C57BL/6 mice, and suggested that due to inconsistencies in reproducibility of each of these lesions, separate scoring or measurement of the different lesions should occur. The differences may be due to genetic factors, but it is considered that valve cusp lesions may not be as relevant to the human pathology, which involves arterial wall plaque formation. Due to the limited areas of ORO staining and taking into account details of previous studies (Nettleship *et al.* 2007a), all lesions were consistently quantified together in the present study. This may result in compositional variations being included. These factors may explain some of the within-group and between-experiment variance observed.

3.4.6   Summary

The data presented in this chapter demonstrate that testosterone has protective effects against diet-induced fatty streak development in early atherosclerosis. Decreased lipid deposition in aortic roots of Tfm mice following TRT suggest that these protective effects may be, at least in part, via mechanisms other than the AR. Both AR-dependent and independent actions appeared to offer atheroprotection. Slight beneficial actions of testosterone on inflammatory markers were apparent and these may translate locally to the lesion, where anti-inflammatory functioning could be more pronounced and result in a reduced plaque. However, due to the variable nature of the data definitive conclusions cannot be drawn and therefore, further investigations are required to confirm these mechanisms.

CHAPTER 4

General Discussion

4.1 General discussion

The main aim of this study was to investigate the potential anti-inflammatory actions of testosterone, in order to explain its proposed anti-atherogenic effects. The study design was two-pronged, and used both *in vitro* and *in vivo* approaches. In the first part of the study an *in vitro* cell culture model of vascular inflammation was investigated, in order to specifically determine the effect of androgens on key regulators of the athero-inflammatory process, and to determine whether any such effects were mediated via the classical AR. In the second part of the study, an *in vivo* mouse model of early atherogenesis, combined with complete androgen insensitivity, was used to investigate the effects of TRT on atheroma formation. More specifically this model was used to determine whether the known beneficial effects of testosterone upon fatty streak formation in cholesterol-fed mice are due to anti-inflammatory actions, and if so, whether such effects occur independently of the classical signalling pathway mediated by the nuclear AR.

Early suggestions in the literature, based upon the higher male-to-female incidence of CAD mortality, proposed that testosterone exerts a detrimental influence on the cardiovascular system. However, there is now convincing evidence that testosterone deficiency is a marker for early death in men and is closely associated with cardiovascular risk factors and degree of atherosclerosis (Jones 2010). Furthermore, the fact that testosterone levels decline with age, whilst atherosclerosis increases, suggests that testosterone does not promote atheroma formation, but may protect against its development (English *et al.* 2000c, Channer and Jones 2003). The aging male is characterised by a gradual reduction in total and free testosterone levels, the so called "andropause" (Vermeulen *et al.* 1999) and also decreased circulating levels of DHEA, the so called "adrenopause" (Herbert 1995). These low levels of testosterone are associated with multiple health consequences, and in particular, cardiovascular pathologies. Specifically, low serum levels of testosterone in elderly men are associated with aortic and carotid atherosclerosis (Hak *et al.* 2002, van den Beld *et al.* 2003) and also with CAD risk factors such as hypertension, obesity, hyperinsulinaemia and diabetes, and an adverse thrombotic profile (Malkin *et al.* 2003, Jones 2010). Although complicated by many conflicting

reports, the majority of the evidence investigating hormone intervention in these patients suggests that TRT may be beneficial, exerting positive effects on several of the contributory factors that shape the pathophysiology of atherosclerosis (Lesser *et al.* 1946, Rosano *et al.* 1999, Webb *et al.* 1999, English *et al.* 2000b, Pugh *et al.* 2004, Malkin *et al.* 2004a, Malkin *et al.* 2006b, Zitzmann *et al.* 2008). Androgenic immunomodulation may be one such mechanism, although the evidence to support this is relatively scarce and findings have been conflicting. In addition, an anti-atherogenic action of testosterone has been previously shown in cholesterol-fed animal models (Bruck *et al.* 1997, Alexandersen *et al.* 1999, Jones *et al.* 2003, Nettleship *et al.* 2007). The exact mechanisms by which these anti-atherogenic actions take place remain controversial, with genomic and non-genomic actions, AR, ER, and non-classical receptor activation all attributed to the beneficial effects, dependent upon vascular territory and stage of disease progression.

The findings reported in this thesis suggest that inflammatory cytokines are certainly involved in vascular inflammation and a role for the novel chemokine CX_3CL1 is evident, although such pro-atherogenic mediators were not always seen to be modulated systemically. CX_3CL1 was found to be both dose- and time-dependently upregulated by pro-inflammatory cytokines in smooth muscle and endothelial cells of the aorta and was present, in addition to its cognate receptor, within the aortic lipid streaks of some, but not all, experimental mice in the present study, indicating its potential role in atherogenesis. However, the effects of testosterone on CX_3CL1 expression remain unclear. The pro-inflammatory cytokines, TNFα and IL-6, were significantly elevated in the serum of Tfm mice on normal diet compared to XY littermates on normal diet, suggesting a heightened inflammatory state as a result of low testosterone levels and a non-functional AR. Although a measure at the systemic level, this may in itself represent susceptibility to inflammatory actions locally in the aorta, particularly since stimulation of HASMC and HAEC with TNFα in combination with IFNγ induced an upregulation of CX_3CL1 and CCL2 *in vitro*. Previous studies have demonstrated similar actions of local cytokine levels on vascular chemokine and/or adhesion molecule expression in cultured cells (Rollins *et al.* 1990, Sica *et al.* 1990, Cybulsky *et al.* 1991, Taubman *et al.* 1992, Shyy *et al.* 1994, Bazan *et al.* 1997, Gimbrone *et al.* 1997, Imaizumi *et al.* 2000, Garcia *et al.* 2000, Ollivier *et al.* 2003, Ahn *et al.* 2004, Lim *et al.* 2009). In the present study there was a lack of androgen modulation on this *in vitro* upregulation of cytokines. This may be due to testosterone having its effect upstream from CX_3CL1 expression. This is supported by the *in vivo* data, since TRT in the Tfm mouse marginally, but not significantly, reduced serum TNFα levels, and may potentially alter local concentrations at the aorta. Indeed, it has been noted in cell culture studies that testosterone reduced the expression of pro-inflammatory cytokines such as TNFα, IL-1 and IL-6 (See Malkin

et al. 2004a). TRT has also been previously shown to reduce circulating levels of TNFα in hypogonadal men, an effect that was concurrent with decreased myocardial ischaemia and favourable lipid profiles (Malkin *et al.* 2004a, Malkin *et al.* 2004b). In addition, in the present study there was an apparent reduction of CX$_3$CL1 expression in aortic lipid streaks of Tfm mice receiving TRT and littermates on placebo, which may indicate that the protective effect of testosterone in atherogenesis is via local anti-inflammatory actions and at least partially via AR-independent mechanisms. This is also, weakly, supported by the *in vitro* cell culture data in this thesis, as testosterone treatment reduced cytokine-induced expression of CX$_3$CL1 at the molecular level in HASMC, an effect not prevented by blockade of the AR. Definite conclusions cannot be drawn, however, due to the limited power of the data and lack of statistical significance.

Serum CCL2 also appeared slightly, although not significantly, reduced in Tfm mice following TRT, an effect that could not be robustly demonstrated in cultured vascular cells. CCL2 mRNA in HAEC did appear physiologically, although not statistically, down-regulated by testosterone, potentially supporting the data from the animal model. This *in vitro* effect however, was prevented by AR blockade, contradicting the data from the mouse model, where the AR is non-functional and therefore not involved in the observed effects. Monocyte infiltration in areas adjacent to lipid streak was consistent between the experimental animal groups, indicating that testosterone does not influence the extravasation of monocytes at the plaque site. Since the mean area of fatty streak was reduced by testosterone it may be that androgens reduce general aortic atherogenesis through mechanisms other than specifically influencing a particular local inflammatory process such as CCL2 or CX$_3$CL1 expression and subsequent leukocyte migration.

The work in this thesis demonstrates that the driving force behind atherosclerosis is a cholesterol-enriched diet, since both Tfm mice and littermates displayed increased lipid deposition in the aortic root following a period of high cholesterol feeding. This appears to be mediated through induction of a pro-atherogenic lipid profile, in particular, elevated circulating LDL and total cholesterol, although this was not related to obesity (body weight and weight gain) in this model. Although this has not been previously demonstrated in this Tfm mouse model, the concept of dietary influence on atherosclerosis is not novel (See Glueck 1979, Kromhout 2001). Of particular interest, the INCAP study of atherosclerosis and CHD investigated 22,516 aortae and coronary vessels from a mainly Latin American population and demonstrated that the strongest correlation for the severity of lesions was the fat content of the diet (Guzman 2010).

The present study has clearly reproduced previous findings that low endogenous testosterone is associated with fatty streak formation in the aortic root and a proatherogenic circulating lipid profile, after feeding on a cholesterol-enriched diet (Nettleship *et al.* 2007a). In fact, the elevated atherosclerotic parameters induced by high-cholesterol diet were significantly amplified as a result of low testosterone levels and a non-functional AR (Tfm mouse). The beneficial effects of testosterone on serum lipid concentrations appear to function through the AR, since TRT in Tfm mice did not significantly modulate lipid profiles, whereas LDL and total cholesterol were markedly lower in XY littermates. These findings are consistent with observations previously reported in this model, with no effect of TRT on total cholesterol and LDL-C in Tfm mice (Nettleship *et al.* 2007a). Clinical studies may indirectly support this idea as hypogonadal patients, with low serum testosterone and a functional AR, respond favourably to TRT. TRT is reported to induce significant reductions in total cholesterol and LDL-C in hypogonadal men (Tenover 1992, Zgliczynski *et al.* 1996, Tripathy *et al.* 1998, Howell *et al.* 2001, Ly *et al.* 2001). Furthermore, total cholesterol levels are shown to fall following physiological testosterone replacement in hypogonadal men with CAD (Malkin *et al.* 2004b). No clinical data exists for AR-deficient males or co-administration of AR antagonists with TRT to establish modes of action in men.

Although TRT had no effect on circulating lipids in the present study, it did decrease lipid deposition in the aortic root. This may result from a specific local effect of testosterone at the vessel wall, with testosterone protecting against the detrimental effects of pro-atherogenic lipids on lesion-associated vascular and immune cells. Indeed, previous research has shown an *in vitro* upregulation of CX$_3$CL1 and CCL2 in response to oxLDL exposure in vascular cells (Cushing *et al.* 1990, Yu *et al.* 1998, Dwivedi *et al.* 2001, Mackness *et al.* 2004, Barlic *et al.* 2007) and monocytes (Zhang *et al.* 2006). Therefore, it is reasonable to suggest that testosterone may be more likely to have an effect on oxLDL-induced CX$_3$CL1 or CCL2 upregulation in HASMC and HAEC in the present *in vitro* model (See future work). Additionally, testosterone may not exert anti-inflammatory effects on vascular cells, but may confer athero-protection within the plaque region through actions on immune cells. In particular, decreased cholesterol accumulation has been reported in cultured monocyte-derived macrphages through the reduction of LOX-1 expression and the upregulation of SR-BI following androgen treatment (Langer *et al.* 2002, Orekhov *et al.* 2009, Qui *et al.* 2010). Through these mechanisms of reduced foam cell formation and enhanced reverse cholesterol transport, testosterone may allow a protective effect on the inflammatory mechanisms of atheroma formation without influencing the immune recruitment directed by vascular cells, often considered a protective mechanism in early atherogenesis.

From the combined findings that TRT had no significant effects on circulating lipids or cytokines *in vivo*, and that testosterone treatment did not significantly modulate the expression of chemokines *in vitro*, although lipid streaks were reduced in Tfm mice following TRT, it may be possible that the athero-protective effects of androgens are via a local action in the vessel. Testosterone is known to have beneficial effects on vascular tone, which may protect from shear stress-related vascular dysfunction and subsequent inflammation and lipid entry, thus reducing early atheroma formation (Webb *et al.* 1999, Kang *et al.* 2002, Jones *et al.* 2003, Manolakou *et al.* 2009). Therefore, it is possible that the beneficial effects of TRT may not be seen systemically or in isolated cells.

The lack of convincing results regarding the effect of TRT on inflammatory mediators and circulating lipid profiles in this study, and the often contradictory reports from previous research, highlights the complexity of the relationship between testosterone and atherosclerosis and the difficulties in studying such mechanisms. Differences in study design, doses and formulations of androgens used, route of administration, animals or cell types used, vascular location studied, and/or methods of analysis may all influence the outcome of the experiments.

In addition, evidence suggests that the beneficial effects of testosterone may be gender-specific and may indicate a protective role of sex hormones in both genders, with regard to maintaining an anti-atherogenic gender-specific homeostasis. Potential opposing actions of sex hormones in men and women relating to atherosclerotic CVD and its risk factors have been noted previously (Phillips 2005;). Tomaszewski *et al.* (2009) repeated the findings of an earlier study implicating an association between increased oestrogen levels and unfavourable lipid profiles in young men (Wranicz *et al.* 2005). It is possible that the ratio between testosterone and oestrogen may prove to have a greater influence in athero-protection. However, these previous studies found no effect of TRT on lipid measurements. One cross-sectional study did demonstrate the link between low serum testosterone combined with elevated serum estradiol and peripheral arterial disease in elderly men (Tivesten *et al.* 2007;). The administration of anastrozole, an oral aromatase inhibitor, was able to normalise testosterone levels in hypogonadal men and reduce estradiol levels, thereby improving the sex hormone balance (Dougherty *et al.* 2005;). This however resulted in no significant changes to lipid profiles or markers of inflammation, contradicting previous work, although the study size was small and no direct measure of vessel atherosclerosis was investigated.

In support of a gender-specific hormone balance as an indicator of CV risk rather than simply androgen concentrations, post-menopausal women, whose oestrogen levels have declined,

demonstrate an increased risk similar to that of age-related males, after a post-menopausal catch-up time of around 10 years (Malkin *et al.* 2003b). These data would therefore suggest that oestrogen replacement therapy may have beneficial cardiovascular effects in post-menopausal women. However, this could not be confirmed by large randomised trials (Ouyang *et al.* 2006). This may in part be due to the timing of hormone therapy, as findings from the Women's Health Initiative trial suggest that hormone therapy should be initiated within six years of the menopause transition to achieve beneficial outcomes (Banks *et al.* 2009). Furthermore, the adverse effects of androgens in women is evident, with a correlation between both bioavailable and total testosterone levels and the degree of aortic atherosclerosis (Hak *et al.* 2002). These findings are strengthened by clinical case reports of female-to-male transsexuals who experience negative cardiovascular outcomes as a result of cross-gender hormone therapy (McCredie *et al.* 1998, Inoue *et al.* 2007). Inoue *et al.* (2007) described the sudden death of a female-to-male transsexual patient receiving cross-sex hormonal treatment. In this report the cause of death was concluded to be ischemic heart disease, influenced by high blood testosterone levels, as a result of bi-monthly intramuscular injections of testosterone for two years prior to death. Such reports are interesting, but may be limited in their clinical value as cardiovascular examination to determine systemic atherosclerotic state before hormone supplementation was not performed, and although elevated testosterone may have contributed to cause of death, a direct causality is difficult to delineate. Bruck *et al* (1997) eloquently demonstrated gender-specific effects of testosterone and oestrogen in castrated male and ovariectomised female cholesterol fed rabbits. IMT in the aortic arch was significantly reduced in castrated males receiving TRT, and reduced in ovariectomised females receiving oestrogen treatment. The reported differences were independent of changes in plasma lipid measurements. TRT in ovariectomised females resulted in a detrimental increase in IMT, whereas oestrogen treatment in males produced no significant effects. Interestingly, a combination of both testosterone and oestrogen treatment showed the greatest inhibition of intimal thickening in both genders.

To further complicate the androgen-oestrogen paradox, evidence exists for direct AR and ER interactions (Panet-Raymond *et al.* 2000), and the potential for androgens to interact with ER and oestrogens with AR reveals a complex interplay between sex hormone function (Kreitmann and Bayard 1979, Yeh *et al.* 1998). Additionally each hormone may affect the expression of the receptor for the other hormone (See Philips *et al.* 2005), leading to a complex level of control over local hormone-specific responses that may be atherogenic or atheroprotective depending upon cross-talk, receptor interactions and multiple other, largely as yet unknown, factors. Therefore, in depth molecular investigations, along with long-term

248

prospective studies, are needed to provide further insight into the gender-specific role of androgens and oestrogens in the development of atherosclerosis.

4.1.1 Future work

Although conflicting reports exist, accumulating evidence strongly supports a role for testosterone as an immunomodulatory and atheroprotective hormone in men, and certainly warrants further scientific and clinical research. It is important that future research focuses on delineating the physiological and biochemical mechanisms underlying the protective role of testosterone in the development and progression of atherosclerosis.

4.1.1.1 In vitro investigations

Since the cell culture model used in this thesis demonstrated greatly elevated upregulation of CX_3CL1 and CCL2 expression upon stimulation of cells with cytokines, and the fact that previous investigations into steroid modulation of inflammatory molecules utilised single cytokine stimulations (see tables 2.1.1 and 2.1.2), repeating the present study with IFNγ and TNFα alone may allow detection of androgen modulation of these chemokines. However, another possibility is that, as the *in vitro* work in this thesis was unable to demonstrate reproducible androgen modulation of cytokine-induced CX_3CL1 and CCL2 expression, this may indicate that these chemokines are in fact not modulated by testosterone. Thus a focussed gene expression profiling PCR array analysis of multiple inflammatory targets, simultaneously assessed for modulation by androgens under the same experimental conditions as in the present study, may be useful to highlight other potential inflammatory mediators to pursue.

The *in vitro* cell culture studies in this thesis were an attempt to simulate the vascular inflammation that would be associated with atherosclerosis via cytokine stimulation of cells, with subsequent investigation of the potential influences of androgens on this. The *in vivo* studies revealed a protective effect of TRT on lipid deposition in the aortic root and demonstrated a negative influence of low endogenous testosterone and a non-functional AR on lipid profiles and deposition in the context of high-cholesterol feeding. Thus, the *in vitro* actions of androgens on lipid actions are of interest. Studying the effects of native LDL and oxLDL on CX_3CL1 expression in HASMC and HAEC, and the potential protective effects of androgens, may highlight a link between the beneficial effects of testosterone on lipids within local aortic inflammation.

Implications from the present study and findings from recent reports suggesting that androgens influence macrophage behaviour in relation to atherosclerosis (Langer *et al.* 2002,

Ng et al. 2003, Orekhov et al. 2009, Corcoran et al. 2010, Qui et al. 2010) direct future studies towards investigating the effects of testosterone on monocyte/macrophage expression of CX_3CL1, CCL2 and their cognate receptors under pro-inflammatory conditions.

4.1.1.2 In vivo investigation

From the preliminary findings of this thesis, it cannot be definitely concluded that TRT has a protective effect on inflammatory mediators associated with atherosclerosis. This may be due to the variability associated with animal work, and the low power of small sample numbers. Repeating the present study to increase sample numbers may address the lack of significance observed in many of the parameters measured. Particularly, reproduction of the immunostaining seems essential for conclusive comparisons between the different experimental groups and for validating the staining observed. Additionally, dual staining of the current targets along with additional targets (such as T cell, macrophage, NK cell, dendritic cell markers) would enable co-localisation of CX_3CL1 and CX_3CR1 with specific cell types in the plaque region, thus providing further insight into the role of this chemokine in early atherogenesis.

4.1.1.3 New concepts

As the most pronounced effects of testosterone treatment observed in this thesis were the effects on lipids, be it circulating profiles or aortic deposition, further investigation into the potential protective effects of androgens on metabolic factors of lipidomics may reveal important mechanisms of atheroprotection. Lipases, the enzymes that hydrolyse ester bonds of triglycerides, phospholipids and cholesterol esters, offer an interesting mechanism by which lipids are regulated (Wong and Scholtz 2002). In atherosclerotic lesions, lipoprotein lipase (LPL) is expressed by macrophages and SMC, and is involved in the lipolysis of circulating VLDL and chylomicron remnants, leading to the accumulation of cholesterol esters (Hasham and Pillarisetti 2006). Elevated expression of this enzyme is associated with susceptibility to atherosclerosis in experimental mouse models (Babaev et al. 2000), and macrophage-derived foam cells were found to be the major source of LPL in human lesions (O'Brien et al. 1992), suggesting that LPL may be involved in focal lipid activity and fatty streak development. In addition, endothelial lipase (EL) is considered to have pro-atherogenic properties through indirectly modifying circulating HDL concentrations via its catalytic effects facilitating clearance and therefore reducing antioxidant and reverse cholesterol transport activities of HDL (Huang et al. 2010). EL can be synthesised by endothelial cells with expression highly regulated by cytokines and physical forces such as shear stress (Choi et al. 2002), and has been shown in

infiltrating SMC and macrophages of human coronary artery plaques (Azumi *et al.* 2003). Therefore, a role for EL in plaque lipidomics may be apparent. Hepatic lipase (HP) is synthesised in hepatocytes and remains in the liver where it additionally influences circulating lipid profiles via metabolic activities (Hasham and Pillarisetti 2006), although the role of HP in modulating atherogenic risk remains controversial. Therefore, the potential modulation of lipase expression and activity may elucidate some of the local and systemic athero-protective effects of testosterone, and would represent an interesting focus of research.

Recent evidence, that adipose tissue acts as an endocrine secretory organ, releasing numerous inflammatory factors, adipokines, highlights the importance of investigating the role of androgens in the regulation of lipid metabolism and adipose tissue formation. This may lead to more definite conclusions on the influence of androgens on inflammation and obesity as major contributors to distal atherosclerosis.

In addition to the potential influence of oestrogens on the modulatory actions of androgens in atherosclerosis, the contribution of other steroids may also need to be investigated further. In particular, DHEA (the most abundant circulating adrenal steroid) levels in men have an inverse relationship with cardiovascular mortality (Alexandersen *et al.* 1996, Beer *et al.* 1996). While these findings may be due to a direct action of DHEA, the presence of the enzymes responsible for the conversion of DHEA to androstenedione and subsequent reduction to testosterone, in addition to the previously mentioned aromatase, in peripheral tissues and perhaps the vasculature, implicate another potential source of androgen and oestrogen involvement (Ebeling and Koivisto 1994, Labrie *et al.* 1995). Additionally, the anti-inflammatory actions of glucocorticoids are well known, although their mechanisms are not fully understood. With the potential to reduce vascular inflammation, glucocorticoids may confer beneficial actions on specific mediators of atheroma formation. In particular, CX_3CL1 expression has been shown to be suppressed by glucocorticoid treatment in lung epithelial cells via reduction in gene promoter recruitment of NFκB (Bhavsar *et al.* 2008). Therefore, AR and glucocorticoid receptor actions may be coregulatory and influence inflammatory responses in conditions such as atherosclerosis. Furthermore, a high cortisol/testosterone ratio has been associated with incident ischemic heart disease (Araujo *et al.* 2007). When investigating androgenic parameters it may be necessary to include measures of additional steroids, co-related enzymes and metabolites, and their signalling pathways, to dissect the specific role of testosterone in cardiovascular function.

4.1.2   Conclusion

This thesis has investigated in detail the potentially beneficial effects of androgens in the male cardiovascular system with particular focus on anti-inflammatory mechanisms. Evidence has been presented here which demonstrates that testosterone treatment, at physiological levels, does not have a detrimental effect on the cardiovascular system, but in fact may confer beneficial effects. Part of these effects may be via anti-inflammatory actions, shown by small physiological, but not statistically significant, modulations to inflammatory markers, whether detected locally or systemically. In addition, work in this thesis has confirmed that TRT can significantly inhibit fatty streak formation, a process known to involve immune interactions, and shown that this effect is only partially mediated through the AR. However, androgens exert a vast array of effects *in vivo* such that it may be misleading to extrapolate isolated experimental findings to the wider clinical setting and generalise population specifics, or individual differences, to all. The complexities of androgen interactions and the often conflicting results in the research do not allow unequivocal conclusions to be made, and consequently, much remains unknown in the effort to delineate the actions of testosterone for improved treatment of the aging male.

References

Abi-Younes, S., Sauty, A., Mach, F., Sukhova, G.K., Libby, P., and Luster, A.D. *2000*. The stromal cell-derived factor-1 chemokine is a potent platelet agonist highly expressed in atherosclerotic plaques. *Circ.Res.* 86:131-138.

Abramovitz, D., Gavri, S., Harats, D., Levkovitz, H., Mirelman, D., Miron, T., Eilat-Adar, S., Rabinkov, A., Wilchek, M., Eldar, M., and Vered, Z. *1999*. Allicin-induced decrease in formation of fatty streaks (atherosclerosis) in mice fed a cholesterol-rich diet. *Coron Artery Dis. 10(7):515-9.*

Adachi, O., Kawai, T., Takeda, K., Matsumoto, M., Tsutsui, H., Sakagami, M., Nakanishi, K., and Akira, S. *1998*. Targeted disruption of the MyD88 gene results in loss of IL-1- and IL-18-mediated function. - *Immunity. 9(1):143-50.*

Agledahl, I., Hansen, J.B., and Svartberg, J. *2008*. Impact of testosterone treatment on postprandial triglyceride metabolism in elderly men with subnormal testosterone levels. - *Scand J Clin Lab Invest.;68(7):641-8.*

Ahn, S.Y., Cho, C.H., Park, K.G., Lee, H.J., Lee, S., Park, S.K., Lee, I.K., and Koh, G.Y. *2004*. Tumor necrosis factor-alpha induces fractalkine expression preferentially in arterial endothelial cells and mithramycin A suppresses TNF-alpha-induced fractalkine expression. *Am.J.Pathol.* 164:1663-1672.

Aiello, R.J., Bourassa, P.A., Lindsey, S., Weng, W., Natoli, E., Rollins, B.J., and Milos, P.M. *1999*. Monocyte chemoattractant protein-1 accelerates atherosclerosis in apolipoprotein E-deficient mice. *Arterioscler.Thromb.Vasc.Biol.* 19:1518-1525.

Ait-Oufella, H., Taleb, S., Mallat, Z., and Tedgui, A. *2009*. Cytokine network and T cell immunity in atherosclerosis. - *Semin Immunopathol.31(1):23-33.*

Akashi, T., Koizumi, K., Nagakawa, O., Fuse, H., and Saiki, I. *2006*. Androgen receptor negatively influences the expression of chemokine receptors (CXCR4, CCR1) and ligand-mediated migration in prostate cancer DU-145. - *Oncol Rep. 16(4):831-6.*

Akishita, M., Hashimoto, M., Ohike, Y., Ogawa, S., Iijima, K., Eto, M., and Ouchi, Y. *2009*. Low testosterone level as a predictor of cardiovascular events in Japanese men with coronary risk factors. - *Atherosclerosis. 13.*

Alberts B., Bray, D., Lewis, J., Raff, M., Roberts, K., and Watson, J.D. *1994*. Molecular Biology of the Cell. Garland Publishing Inc. 1352 pp.

Alevizaki, M., Cimponeriu, A.T., Garofallaki, M., Sarika, H.L., Alevizaki, C.C., Papamichael, C., Philippou, G., Anastasiou, E.A., Lekakis, J.P., Mand Mavrikakis, M. *2003*. The androgen receptor gene CAG polymorphism is associated with the severity of coronary artery disease in men. - *Clin Endocrinol (Oxf). Dec;59(6):749-55.*

Alexandersen, P., Haarbo, J., Byrjalsen, I., Lawaetz, H., and Christiansen, C. *1999*. Natural androgens inhibit male atherosclerosis: a study in castrated, cholesterol-fed rabbits. *Circ.Res.* 84:813-819.

Alexandersen, P., Haarbo, J., and Christiansen, C. *1996*. The relationship of natural androgens to coronary heart disease in males: a review. *Atherosclerosis.* 125:1-13.

Alison, M.R. *1995.* Assessing cellular proliferation: what's worth measuring? - *Hum Exp Toxicol. 14(12):935-44.*

Allain, C.C., Poon, L.S., Chan, C.S., Richmond, W., and Fu, P.C. *1974.* Enzymatic determination of total serum cholesterol. - *Clin Chem. 20(4):470-5.*

Allan, C.A., Strauss, B.J., Burger, H.G., Forbes, E.A., and McLachlan, R.I. *2008.* Testosterone therapy prevents gain in visceral adipose tissue and loss of skeletal muscle in nonobese aging men. - *J Clin Endocrinol Metab. 93(1):139-46.*

Almeida, E.A., Ilic, D., Han, Q., Hauck, C.R., Jin, F., Kawakatsu, H., Schlaepfer, D.D., and Damsky, C.H. *2000.* Matrix survival signaling: from fibronectin via focal adhesion kinase to c-Jun NH(2)-terminal kinase. *J.Cell Biol.* 149:741-754.

Alvarez, R.J., Gips, S.J., Moldovan, N., Wilhide, C.C., Milliken, E.E., Hoang, A.T., Hruban, R.H., Silverman, H.S., Dang, C.V., and Goldschmidt-Clermont, P.J. *1997.* 17beta-Estradiol Inhibits Apoptosis of Endothelial Cells. - *Biochem Biophys Res Commun. 237(2):372-81.*

Amento, E.P., Ehsani, N., Palmer, H., and Libby, P. *1991.* Cytokines and growth factors positively and negatively regulate interstitial collagen gene expression in human vascular smooth muscle cells. - *Arterioscler Thromb. 11(5):1223-30.*

Amour, A., Knight, C.G., Webster, A., Slocombe, P.M., Stephens, P.E., Knäuper, V., Docherty, A.J.P., and Murphy, G. 2000. The in vitro activity of ADAM-10 is inhibited by TIMP-1 and TIMP-3. *FEBS Lett.* 473:275-279.

Amour, A., Slocombe, P.M., Webster, A., Butler, M., Knight, C.G., Smith, B.J., Stephens, P.E., Shelley, C., Hutton, M., Knäuper, V., Docherty, A.J.P., and Murphy, G.1998. TNF-α converting enzyme (TACE) is inhibited by TIMP-3. *FEBS Lett.* 435:39-44.

An, G., Wang, H., Tang, R., Yago, T., McDaniel, J.M., McGee, S., Huo, Y., and Xia, L. *2008.* P-selectin glycoprotein ligand-1 is highly expressed on Ly-6Chi monocytes and a major determinant for Ly-6Chi monocyte recruitment to sites of atherosclerosis in mice. - *Circulation. 117(25):3227-37.*

Andersson, J., Libby, P., and Hansson, G.K. *2010.* Adaptive immunity and atherosclerosis. *Clinical Immunology.* 134:33-46.

Apostolakis, S., Amanatidou, V., Papadakis, E.G., and Spandidos, D.A. *2009.* Genetic diversity of CX3CR1 gene and coronary artery disease: New insights through a meta-analysis. *Atherosclerosis.* 207:8-15.

Apostolakis, S., Baritaki, S., Kochiadakis, G.E., Igoumenidis, N.E., Panutsopulos, D., and Spandidos, D.A. *2007a.* Effects of polymorphisms in chemokine ligands and receptors on susceptibility to coronary artery disease. *Thrombosis Research.* 119:63-71.

Apostolakis, S., E. Krambovitis, Z. Vlata, G.E. Kochiadakis, S. Baritaki, and D.A. Spandidos. 2007b. CX3CR1 receptor is up-regulated in monocytes of coronary artery diseased patients: Impact of pre-inflammatory stimuli and renin–angiotensin system modulators. *Thrombosis Research,.* 121:387-395.

Arad, Y., Badimon, J.J., Badimon, L., Hembree, W.C., and Ginsberg, H.N. *1989.* Dehydroepiandrosterone feeding prevents aortic fatty streak formation and cholesterol accumulation in cholesterol-fed rabbit. — *Arteriosclerosis 9(2):159-66.*

Arakelyan, A., Petrkova, J., Hermanova, Z., Boyajyan, A., Lukl, J., and Petrek, M. *2005.* Serum levels of the MCP-1 chemokine in patients with ischemic stroke and myocardial infarction. - *Mediators Inflamm. 2005(3):175-9.*

Araujo, A.B., Kupelian, V., Page, S.T., Handelsman, D.J., Bremner, W.J., and McKinlay, J.B. *2007.* Sex steroids and all-cause and cause-specific mortality in men. - *Arch Intern Med. 167(12):1252-60.*

Arimura, K., Egashira, K., Nakamura, R., Ide, T., Tsutsui, H., Shimokawa, H., and Takeshita, A. *2001.* Increased inactivation of nitric oxide is involved in coronary endothelial dysfunction in heart failure. - *Am J Physiol Heart Circ Physiol. 280(1):H68-75.*

Aydilek, N., and Aksakal, M. *2005.* Effects of testosterone on lipid peroxidation, lipid profiles and some coagulation parameters in rabbits. - *J Vet Med A Physiol Pathol Clin Med. 52(9):436-9.*

Aziz, K.E., and Wakefield, D. 1996. Modulation of endothelial cell expression of ICAM-1, E-selectin, and VCAM-1 by beta-estradiol, progesterone, and dexamethasone. *Cell.Immunol.* 167:79-85.

Azumi, H., Hirata, K., Ishida, T., Kojima, Y., Rikitake, Y., Takeuchi, S., Inoue, N., Kawashima, S., Hayashi, Y., Itoh, H., Quertermous, T., and Yokoyama, M. *2003.* Immunohistochemical localization of endothelial cell-derived lipase in atherosclerotic human coronary arteries. - *Cardiovasc Res. 58(3):647-54.*

Babaev, V.R., Patel, M.B., Semenkovich, C.F., Fazio, S., and Linton, M.F. *2000.* Macrophage lipoprotein lipase promotes foam cell formation and atherosclerosis in low density lipoprotein receptor-deficient mice. - *J Biol Chem. 275(34):26293-9.*

Badimon, L., Vilahur, G., and Padro, T. *2009.* Lipoproteins, platelets and atherothrombosis. - *Rev Esp Cardiol. 62(10):1161-78.*

Bagatell, C.J., Heiman, J.R., Matsumoto, A.M., Rivier, J.E., and Bremner, W.J. *1994.* Metabolic and behavioral effects of high-dose, exogenous testosterone in healthy men. - *J Clin Endocrinol Metab. 79(2):561-7.*

Bai, Y., Ahmad, U., Wang, Y., Li, J.H., Choy, J.C., Kim, R.W., Kirkiles-Smith, N., Maher, S.E., Karras, J.G., Bennett, C.F., Bothwell, A.L., Pober, J.S., and Tellides, G. *2008.* Interferon-gamma induces X-linked inhibitor of apoptosis-associated factor-1 and Noxa expression and potentiates human vascular smooth muscle cell apoptosis by STAT3 activation. - *J Biol Chem. 283(11):6832-42.*

Bakin, R.E., Gioeli, D., Sikes, R.A., Bissonette, E.A., and Weber, M.J. *2003.* Constitutive activation of the Ras/mitogen-activated protein kinase signaling pathway promotes androgen hypersensitivity in LNCaP prostate cancer cells. - *Cancer Res. 63(8):1981-9.*

Banks, E., and Canfell, K. *2009.* Invited Commentary: Hormone therapy risks and benefits--The Women's Health Initiative findings and the postmenopausal estrogen timing hypothesis. - *Am J Epidemiol. 170(1):24-8.*

Barath, P., Fishbein, M.C., Cao, J., Berenson, J., Helfant, R.H., and Forrester, J.S. *1990.* Detection and localization of tumor necrosis factor in human atheroma. *Am.J.Cardiol.* 65:297-302.

Barber, R.D., Harmer, D.W., Coleman, R.A., and Clark, B.J. *2005.* GAPDH as a housekeeping gene: analysis of GAPDH mRNA expression in a panel of 72 human tissues. - *Physiol Genomics. 21(3):389-95.*

Barlic, J., Zhang, Y., Foley, J.F., and Murphy, P.M. *2006.* Oxidized lipid-driven chemokine receptor switch, CCR2 to CX3CR1, mediates adhesion of human macrophages to coronary artery smooth muscle cells through a peroxisome proliferator-activated receptor gamma-dependent pathway. *Circulation.* 114:807-819.

Barlic, J., Zhang, Y., and Murphy, P.M. *2007.* Atherogenic lipids induce adhesion of human coronary artery smooth muscle cells to macrophages by up-regulating chemokine CX3CL1 on smooth muscle cells in a TNFalpha-NFkappaB-dependent manner. *J.Biol.Chem.* 282:19167-19176.

Barrett-Connor, E. *1992.* Lower endogenous androgen levels and dyslipidemia in men with non-insulin-dependent diabetes mellitus. - *Ann Intern Med. 117(10):807-11.*

Barrett-Connor, E., and Khaw, K.T. *1988.* Endogenous sex hormones and cardiovascular disease in men. A prospective population-based study. - *Circulation. 78(3):539-45.*

Barter, P. 2005. The inflammation: Lipoprotein cycle. *Atherosclerosis Supplements.* 6:15-20.

Barud, W., Palusinski, R., Beltowski, J., and Wójcicka, G. *2002.* Inverse relationship between total testosterone and anti-oxidized low density lipoprotein antibody levels in ageing males. *Atherosclerosis.* 164:283-288.

Bazan, J.F., Bacon, K.B., Hardiman, G., Wang, W., Soo, K., Rossi, D., Greaves, D.R., Zlotnik, A., and Schall, T.J. *1997.* A new class of membrane-bound chemokine with a CX3C motif. *Nature.* 385:640-644.

Beer, N.A., Jakubowicz, D.J., Matt, D.W., Beer, R.M., and Nestler, J.E. *1996.* Dehydroepiandrosterone reduces plasma plasminogen activator inhibitor type 1 and tissue plasminogen activator antigen in men. - *Am J Med Sci. 311(5):205-10.*

Ben-Nathan, D., Padgett, D.A., and Loria, R.M. *1999.* Androstenediol and dehydroepiandrosterone protect mice against lethal bacterial infections and lipopolysaccharide toxicity. - *J Med Microbiol. 48(5):425-31.*

Bennett, M.R. *2001.* Reactive oxygen species and death: oxidative DNA damage in atherosclerosis. - *Circ Res. 88(7):648-50.*

Benten, W.P., Lieberherr, M., Stamm, O., Wrehlke, C., Guo, Z., and Wunderlich, F. *1999.* Testosterone signaling through internalizable surface receptors in androgen receptor-free macrophages. *Mol.Biol.Cell.* 10:3113-3123.

Berthois, Y., Katzenellenbogen, J.A., and Katzenellenbogen, B.S. *1986.* Phenol red in tissue culture media is a weak estrogen: implications concerning the study of estrogen-responsive cells in culture. - *Proc Natl Acad Sci U S A. 83(8):2496-500.*

256

Bettoun, D.J., Scafonas, A., Rutledge, S.J., Hodor, P., Chen, O., Gambone, C., Vogel, R., McElwee-Witmer, S., Bai, C., Freedman, L., and Schmidt, A. *2005.* Interaction between the androgen receptor and RNase L mediates a cross-talk between the interferon and androgen signaling pathways. *J.Biol.Chem.* 280:38898-38901.

Bhasin, S., Storer, T.W., Berman, N., Callegari, C., Clevenger, B., Phillips, J., Bunnell, T.J., Tricker, R., Shirazi, A., and Casaburi, R. *1996.* The effects of supraphysiologic doses of testosterone on muscle size and strength in normal men. - *N Engl J Med. 335(1):1-7.*

Bhavsar, P.K., Sukkar, M.B., Khorasani, N., Lee, K.Y., and Chung, K.F. *2008.* Glucocorticoid suppression of CX3CL1 (fractalkine) by reduced gene promoter recruitment of NF-kappaB. - *FASEB J. 22(6):1807-16.*

Billon-Gales, A., Fontaine, C., Douin-Echinard, V., Delpy, L., Berges, H., Calippe, B., Lenfant, F., Laurell, H., Guery, J.C., Gourdy, P., and Arnal, J.F. *2009.* Endothelial estrogen receptor-alpha plays a crucial role in the atheroprotective action of 17beta-estradiol in low-density lipoprotein receptor-deficient mice. - *Circulation. 120(25):2567-76.*

Blankenberg, S., Tiret, L., Bickel, C., Peetz, D., Cambien, F., Meyer, J., and Rupprecht, H.J. *2002.* Interleukin-18 is a strong predictor of cardiovascular death in stable and unstable angina. - *Circulation. 106(1):24-30.*

Blasi, C. *2008.* The autoimmune origin of atherosclerosis. *Atherosclerosis.* 201:17-32.

Blouin, K., Boivin, A., and Tchernof, A. *2008.* Androgens and body fat distribution. *J.Steroid Biochem.Mol.Biol.* 108:272-280.

Blouin, K., Després, J., Couillard, C., Tremblay, A., Prud'homme, D., Bouchard, C., and Tchernof, A. *2005.* Contribution of age and declining androgen levels to features of the metabolic syndrome in men. *Metab.Clin.Exp.* 54:1034-1040.

Boon, R.A., and Horrevoets, A.J. *2009.* Key transcriptional regulators of the vasoprotective effects of shear stress. - *Hamostaseologie. 29(1):39-40, 41-3.*

Boring, L., Gosling, J., Chensue, S.W., Kunkel, S.L., Farese, R.V. Jr., Broxmeyer, H.E., and Charo, I.F. *1997.* Impaired monocyte migration and reduced type 1 (Th1) cytokine responses in C-C chemokine receptor 2 knockout mice. - *J Clin Invest. 100(10):2552-61.*

Boring, L., Gosling, J., Cleary, M., and Charo, I.F. *1998.* Decreased lesion formation in CCR2-/- mice reveals a role for chemokines in the initiation of atherosclerosis. *Nature.* 394:894-897.

Bourassa, P.A., Milos, P.M., Gaynor, B.J., Breslow, J.L., and Aiello, R.J. *1996.* Estrogen reduces atherosclerotic lesion development in apolipoprotein E-deficient mice. - *Proc Natl Acad Sci U S A. 17;93(19):10022-7.*

Bourd-Boittin, K., Basset, L., Bonnier, D., L'helgoualc'h, A., Samson, M., and Theret, N. *2009.* CX3CL1/fractalkine shedding by human hepatic stellate cells: contribution to chronic inflammation in the liver. - *J Cell Mol Med. 13(8A):1526-35.*

Boyle, J.J., Weissberg, P.L., and Bennett, M.R. *2003.* Tumor necrosis factor-alpha promotes macrophage-induced vascular smooth muscle cell apoptosis by direct and autocrine mechanisms. - *Arterioscler Thromb Vasc Biol. 23(9):1553-8.*

Braga-Basaria, M., Muller, D.C., Carducci, M.A., Dobs, A.S., and Basaria, S. *2006.* Lipoprotein profile in men with prostate cancer undergoing androgen deprivation therapy. - *Int J Impot Res. 18(5):494-8.*

Brambilla, D.J., Matsumoto, A.M., Araujo, A.B., and McKinlay, J.B. *2009.* The effect of diurnal variation on clinical measurement of serum testosterone and other sex hormone levels in men. - *J Clin Endocrinol Metab. 94(3):907-13.*

Branen, L., Hovgaard, L., Nitulescu, M., Bengtsson, E., Nilsson, J., and Jovinge, S. 2004. Inhibition of tumor necrosis factor-alpha reduces atherosclerosis in apolipoprotein E knockout mice. *Arterioscler.Thromb.Vasc.Biol.* 24:2137-2142.

Breland, U.M., Halvorsen, B., Hol, J., Oie, E., Paulsson-Berne, G., Yndestad, A., Smith, C., Otterdal, K., Hedin, U., Waehre, T., Sandberg, W.J., Froland, S.S., Haraldsen, G., Gullestad, L., Damas, J.K., Hansson, G.K., and Aukrust, P. *2008.* A potential role of the CXC chemokine GROalpha in atherosclerosis and plaque destabilization: downregulatory effects of statins. - *Arterioscler Thromb Vasc Biol. 28(5):1005-11.*

Bruck, B., Brehme, U., Gugel, N., Hanke, S., Finking, G., Lutz, C., Benda, N., Schmahl, F.W., Haasis, R., and Hanke, H. *1997.* Gender-specific differences in the effects of testosterone and estrogen on the development of atherosclerosis in rabbits. - *Arterioscler Thromb Vasc Biol. 17(10):2192-9.*

Bugno, M., Witek, B., Bereta, J., Bereta, M., Edwards, D.R., and Kordula, T. *1999.* Reprogramming of TIMP-1 and TIMP-3 expression profiles in brain microvascular endothelial cells and astrocytes in response to proinflammatory cytokines. *FEBS Lett.* 448:9-14.

Bui, Q.T., Prempeh, M., and Wilensky, R.L. 2009. Atherosclerotic plaque development. *Int.J.Biochem.Cell Biol.* 41:2109-2113.

Buono, C., Come, C.E., Stavrakis, G., Maguire, G.F., Connelly, P.W., and Lichtman, A.H. *2003.* Influence of interferon-gamma on the extent and phenotype of diet-induced atherosclerosis in the LDLR-deficient mouse. - *Arterioscler Thromb Vasc Biol. 23(3):454-60.*

Burstein, M., Scholnick, H.R., and Morfin, R. *1970.* Rapid method for the isolation of lipoproteins from human serum by precipitation with polyanions. - *J Lipid Res. 11(6):583-95.*

Bustin, S.A., Benes, V., Garson, J.A., Hellemans, J., Huggett, J., Kubista, M., Mueller, R., Nolan, T., Pfaffl, M.W., Shipley, G.L., Vandesompele, J., and Wittwer, C.T. *2009.* The MIQE guidelines: minimum information for publication of quantitative real-time PCR experiments. - *Clin Chem. 55(4):611-22.*

Bustin, S.A., and Mueller, R. *2005.* Real-time reverse transcription PCR (qRT-PCR) and its potential use in clinical diagnosis. - *Clin Sci (Lond). 109(4):365-79.*

Bustin, S.A., Benes, V., Nolan, T., and Pfaffl, M.W. 2005. Quantitative real-time RT-PCR--a perspective. *J.Mol.Endocrinol.* 34:597-601.

Calleja, L., Paris, M.A., Paul, A., Vilella, E., Joven, J., Jimenez, A., Beltran, G., Uceda, M., Maeda, N., and Osada, J. *1999.* Low-cholesterol and high-fat diets reduce atherosclerotic lesion development in ApoE-knockout mice. - *Arterioscler Thromb Vasc Biol. 19(10):2368-75.*

Cambien, B., Pomeranz, M., Schmid-Antomarchi, H., Millet, M.A., Breittmayer, V., Rossi, B., and Schmid-Alliana, A. *2001*. Signal transduction pathways involved in soluble fractalkine-induced monocytic cell adhesion. *Blood*. 97:2031-2037.

Campbell, J.J., Hedrick, J., Zlotnik, A., Siani, M.A., Thompson, D.A., and Butcher, E.C. *1998*. Chemokines and the arrest of lymphocytes rolling under flow conditions. - *Science*. *279(5349):381-4*.

Cardona-Sanclemente, L.E., and Born, G.V. *1995*. Effect of inhibition of nitric oxide synthesis on the uptake of LDL and fibrinogen by arterial walls and other organs of the rat. - *Br J Pharmacol*. *114(7):1490-4*.

Casanueva, F.F., Moreno, B., Rodriguez-Azeredo, R., Massien, C., Conthe, P., Formiguera, X., Barrios, V., and Balkau, B. *2009*. Relationship of abdominal obesity with cardiovascular disease, diabetes and hyperlipidaemia in Spain. - *Clin Endocrinol (Oxf)*. *Oct 15*.

Catanozi, S., Rocha, J.C., Passarelli, M., Chiquito, F.C., Quintao, E.C., and Nakandakare, E.R. *2009*. Pitfalls in the assessment of murine atherosclerosis. - *Braz J Med Biol Res*. *42(6):471-5*.

Caulin-Glaser, T., Watson, C.A., Pardi, R., and Bender, J.R. *1996*. Effects of 17beta-estradiol on cytokine-induced endothelial cell adhesion molecule expression. - *J Clin Invest*. *98(1):36-42*.

Ceballos, G., Figueroa, L., Rubio, I., Gallo, G., Garcia, A., Martinez, A., Yanez, R., Perez, J., Morato, T., and Chamorro, G. *1999*. Acute and nongenomic effects of testosterone on isolated and perfused rat heart. - *J Cardiovasc Pharmacol*. *33(5):691-7*.

Chandra, D., Ramana, K.V., Friedrich, B., Srivastava, S., Bhatnagar, A., and Srivastava, S.K. 2003. Role of aldose reductase in TNF-α-induced apoptosis of vascular endothelial cells. *Chem.Biol.Interact*. 143-144:605-612.

Chandrasekar, B., Mummidi, S., Mahimainathan, L., Patel, D.N., Bailey, S.R., Imam, S.Z., Greene, W.C., and Valente, A.J. 2006. Interleukin-18-induced human coronary artery smooth muscle cell migration is dependent on NF-kappaB- and AP-1-mediated matrix metalloproteinase-9 expression and is inhibited by atorvastatin. *J.Biol.Chem*. 281:15099-15109.

Chandrasekar, B., Mummidi, S., Perla, R.P., Bysani, S., Dulin, N.O., Liu, F., and Melby, P.C. 2003. Fractalkine (CX3CL1) stimulated by nuclear factor kappaB (NF-kappaB)-dependent inflammatory signals induces aortic smooth muscle cell proliferation through an autocrine pathway. *Biochem.J*. 373:547-558.

Channer, K.S., and Jones, T.H. *2003*. Cardiovascular effects of testosterone: implications of the "male menopause" - *Heart*. *89(2):121-2*.

Chapman, G.A., Moores, K., Harrison, D., Campbell, C.A., Stewart, B.R., and Strijbos, P.J. *2000a*. Fractalkine cleavage from neuronal membranes represents an acute event in the inflammatory response to excitotoxic brain damage. - *J Neurosci*. *20(15):RC87*.

Chapman, G.A., Moores, K.E., Gohil, J., Berkhout, T.A., Patel, L., Green, P., Macphee, C.H. and Stewart, B.R. 2000b. The role of fractalkine in the recruitment of monocytes to the endothelium. *European Journal of Pharmacology*. 392:189-195.

Charest NJ, Zhou ZX, Lubahn DB, Olsen KL, Wilson EM, and French FS. *1991*. A frameshift mutation destabilizes androgen receptor messenger RNA in the Tfm mouse. - *Mol Endocrinol. 5(4):573-81.*

Charo IF, Myers SJ, Herman A, Franci C, Connolly AJ, and Coughlin SR. *1994*. Molecular cloning and functional expression of two monocyte chemoattractant protein 1 receptors reveals alternative splicing of the carboxyl-terminal tails. - *Proc Natl Acad Sci U S A. 91(7):2752-6.*

Charo, I.F., and M.B. Taubman. 2004. Chemokines in the pathogenesis of vascular disease. *Circ.Res.* 95:858-866.

Chen XL, Zhang Q, Zhao R, and Medford RM. *2004a*. Superoxide, H2O2, and iron are required for TNF-alpha-induced MCP-1 gene expression in endothelial cells: role of Rac1 and NADPH oxidase. - *Am J Physiol Heart Circ Physiol. 286(3):H1001-7.*

Chen YM, Chiang WC, Lin SL, Wu KD, Tsai TJ, and Hsieh BS. *2004b*. Dual regulation of tumor necrosis factor-alpha-induced CCL2/monocyte chemoattractant protein-1 expression in vascular smooth muscle cells by nuclear factor-kappaB and activator protein-1: modulation by type III phosphodiesterase inhibition. - *J Pharmacol Exp Ther. 309(3):978-86.*

Chen, J., Y. Chen, and S. Lin. 2006. Long-term exposure to oxidized low-density lipoprotein enhances tumor necrosis factor-α-stimulated endothelial adhesiveness of monocytes by activating superoxide generation and redox-sensitive pathways. *Free Radical Biology and Medicine.* 40:817-826.

Cheng C, Tempel D, van Haperen R, de Boer HC, Segers D, Huisman M, van Zonneveld AJ, Leenen PJ, van der Steen A, Serruys PW, de Crom R, and Krams R. *2007*. Shear stress-induced changes in atherosclerotic plaque composition are modulated by chemokines. - *J Clin Invest. 117(3):616-26.*

Cho A, and Reidy MA. *2002*. Matrix metalloproteinase-9 is necessary for the regulation of smooth muscle cell replication and migration after arterial injury. - *Circ Res. 91(9):845-51.*

Choi SY, Hirata K, Ishida T, Quertermous T, and Cooper AD. *2002*. Endothelial lipase: a new lipase on the block. - *J Lipid Res. 43(11):1763-9.*

Choy, J.C., D.J. Granville, D.W.C. Hunt, and B.M. McManus. 2001. Endothelial Cell Apoptosis: Biochemical Characteristics and Potential Implications for Atherosclerosis. *J.Mol.Cell.Cardiol.* 33:1673-1690.

Christodoulakos, G.E., I.V. Lambrinoudaki, E.V. Economou, C. Papadias, N. Vitoratos, C.P. Panoulis, E.E. Kouskouni, S.A. Vlachou, and G.C. Creatsas. 2007. Circulating chemoattractants RANTES, negatively related to endogenous androgens, and MCP-1 are differentially suppressed by hormone therapy and raloxifene. *Atherosclerosis.* 193:142-150.

Cid MC, Kleinman HK, Grant DS, Schnaper HW, Fauci AS, and Hoffman GS. *1994*. Estradiol enhances leukocyte binding to tumor necrosis factor (TNF)-stimulated endothelial cells via an increase in TNF-induced adhesion molecules E-selectin, intercellular adhesion molecule type 1, and vascular cell adhesion molecule type 1. - *J Clin Invest. 93(1):17-25.*

Clark AK, Yip PK, Grist J, Gentry C, Staniland AA, Marchand F, Dehvari M, Wotherspoon G, Winter J, Ullah J, Bevan Sand Malcangio M. *2007*. Inhibition of spinal microglial cathepsin S for the reversal of neuropathic pain. - *Proc Natl Acad Sci U S A.104(25):10655-60.*

Claxton, N.S., T.J. Fellers, and M.W. Davidson. 2005. Laser scanning confocal microscopy. *Http://www.Olympusconfocal.com/theory/LSCMIntro.Pdf.* Last visited on June 2010:1-37.

Clemens JW, Kabler HL, Sarap JL, Beyer AR, Li PK, and Selcer KW. *2000.* Steroid sulfatase activity in the rat ovary, cultured granulosa cells, and a granulosa cell line. - *J Steroid Biochem Mol Biol.75(4-5):245-52.*

Clinton SK, Underwood R, Hayes L, Sherman ML, Kufe DW, and Libby P. *1992.* Macrophage colony-stimulating factor gene expression in vascular cells and in experimental and human atherosclerosis. - *Am J Pathol. 140(2):301-16.*

Coll, B., C. Alonso-Villaverde, and J. Joven. 2007. Monocyte chemoattractant protein-1 and atherosclerosis: Is there room for an additional biomarker? *Clinica Chimica Acta.* 383:21-29.

Combadiere C, Potteaux S, Rodero M, Simon T, Pezard A, Esposito B, Merval R, Proudfoot A, Tedgui A, and Mallat Z. *2008.* Combined inhibition of CCL2, CX3CR1, and CCR5 abrogates Ly6C(hi) and Ly6C(lo) monocytosis and almost abolishes atherosclerosis in hypercholesterolemic mice. - *Circulation. 117(13):1649-57.*

Combadiere, C., S. Potteaux, J.L. Gao, B. Esposito, S. Casanova, E.J. Lee, P. Debre, A. Tedgui, P.M. Murphy, and Z. Mallat. 2003. Decreased atherosclerotic lesion formation in CX3CR1/apolipoprotein E double knockout mice. *Circulation.* 107:1009-1016.

Combadiere, C., J. Gao, H.L. Tiffany, and P.M. Murphy. 1998. Gene Cloning, RNA Distribution, and Functional Expression of mCX3CR1,a Mouse Chemotactic Receptor for the CX3C Chemokine Fractalkine, *Biochem.Biophys.Res.Commun.* 253:728-732.

Corcoran MP, Meydani M, Lichtenstein AH, Schaefer EJ, Dillard A, and Lamon-Flava S. *2010.* Sex hormone modulation of proinflammatory cytokine and C-reactive protein expression in macrphages from older men and postmenopausal women. *J Endocrinology. 206(2):217-24.*

Corona G, Mannucci E, Fisher AD, Lotti F, Petrone L, Balercia G, Bandini E, Forti G, and Maggi M. *2008.* Low levels of androgens in men with erectile dysfunction and obesity. - *J Sex Med. 5(10):2454-63.*

Corona G, Mannucci E, Lotti F, Fisher AD, Bandini E, Balercia G, Forti G, and Maggi M. *2009.* Pulse pressure, an index of arterial stiffness, is associated with androgen deficiency and impaired penile blood flow in men with ED. - *J Sex Med. 6(1):285-93.*

Corrales JJ, Almeida M, Burgo R, Mories MT, Miralles JM, and Orfao A. *2006.* Androgen-replacement therapy depresses the ex vivo production of inflammatory cytokines by circulating antigen-presenting cells in aging type-2 diabetic men with partial androgen deficiency. - *J Endocrinol. 189(3):595-604.*

Couffinhal, T., C. Duplaa, C. Moreau, J.M. Lamaziere, and J. Bonnet. 1994. Regulation of vascular cell adhesion molecule-1 and intercellular adhesion molecule-1 in human vascular smooth muscle cells. *Circ.Res.* 74:225-234.

Crocker SJ, Pagenstecher A, and Campbell IL. *2004.* The TIMPs tango with MMPs and more in the central nervous system. - *J Neurosci Res.75(1):1-11.*

Crola Da Silva C, Lamerant-Fayel N, Paprocka M, Mitterrand M, Gosset D, Dus D, and Kieda C. *2009*. Selective human endothelial cell activation by chemokines as a guide to cell homing. - *Immunology. 126(3):394-404.*

Cushing SD, Berliner JA, Valente AJ, Territo MC, Navab M, Parhami F, Gerrity R, C.J. Schwartz CJ, and Fogelman AM. *1990*. Minimally modified low density lipoprotein induces monocyte chemotactic protein 1 in human endothelial cells and smooth muscle cells. - *Proc Natl Acad Sci U S A. 87(13):5134-8.*

Cybulsky MI, and Gimbrone MA Jr. *1991*. Endothelial expression of a mononuclear leukocyte adhesion molecule during atherogenesis. - *Science. 251(4995):788-91.*

Dabagh M, Jalali P, and Tarbell JM. *2009*. The transport of LDL across the deformable arterial wall: the effect of endothelial cell turnover and intimal deformation under hypertension. - *Am J Physiol Heart Circ Physiol. 297(3):H983-96.*

D'Agostino P, Milano S, Barbera C, Di Bella G, La Rosa M, Ferlazzo V, Farruggio R, Miceli DM, Miele M, Castagnetta L, and Cillari E. *1999*. Sex hormones modulate inflammatory mediators produced by macrophages. - *Ann N Y Acad Sci. 876:426-9.*

Dai G, Kaazempur-Mofrad MR, Natarajan S, Zhang Y, Vaughn S, Blackman BR, Kamm RD, Garcia-Cardena G, and Gimbrone MA Jr. *2004*. Distinct endothelial phenotypes evoked by arterial waveforms derived from atherosclerosis-susceptible and -resistant regions of human vasculature. - *Proc Natl Acad Sci U S A. 101(41):14871-6.*

Dalal M, Kim S, and Voskuhl RR. *1997*. Testosterone therapy ameliorates experimental autoimmune encephalomyelitis and induces a T helper 2 bias in the autoantigen-specific T lymphocyte response. - *J Immunol. 159(1):3-6.*

D'Amico AV, Denham JW, Crook J, Chen MH, Goldhaber SZ, Lamb DS, Joseph D, Tai KH, Malone S, Ludgate C, Steigler A, and Kantoff PW. *2007*. Influence of androgen suppression therapy for prostate cancer on the frequency and timing of fatal myocardial infarctions. - *J Clin Oncol. 25(17):2420-5.*

Daniels TF, Killinger KM, Michal JJ, Wright RW Jr, and Jiang Z. *2009*. Lipoproteins, cholesterol homeostasis and cardiac health. - *Int J Biol Sci. 5(5):474-88.*

Daoudi M, Lavergne E, Garin A, Tarantino N, Debre P, Pincet F, Combadiere C, and Deterre P. *2004*. Enhanced adhesive capacities of the naturally occurring Ile249-Met280 variant of the chemokine receptor CX3CR1. - *J Biol Chem. 279(19):19649-57.*

Daugherty A. *2002*. Mouse models of atherosclerosis. - *Am J Med Sci. 323(1):3-10.*

Daugherty, A., and D.L. Rateri. 2005. Development of experimental designs for atherosclerosis studies in mice. *Methods. 36:129-138.*

Davies PF. *2009*. Hemodynamic shear stress and the endothelium in cardiovascular pathophysiology. - *Nat Clin Pract Cardiovasc Med. 6(1):16-26.*

Dawson, T.C., W.A. Kuziel, T.A. Osahar, and N. Maeda. 1999. Absence of CC chemokine receptor-2 reduces atherosclerosis in apolipoprotein E-deficient mice. *Atherosclerosis. 143:205-211.*

de Boer OJ, van der Meer JJ, Teeling P, Chris M, van der Loos CM, and van der Wal AC. *2007.* Low numbers of FOXP3 positive regulatory T cells are present in all developmental stages of human atherosclerotic lesions. - *PLoS One. 2(1):E779.*

De Caterina, R., P. Libby, H.B. Peng, V.J. Thannickal, T.B. Rajavashisth, M.A. Gimbrone Jr, W.S. Shin, and J.K. Liao. 1995. Nitric oxide decreases cytokine-induced endothelial activation. Nitric oxide selectively reduces endothelial expression of adhesion molecules and proinflammatory cytokines. *J.Clin.Invest.* 96:60-68.

de Lemos, J.A., D.A. Morrow, M.A. Blazing, P. Jarolim, S.D. Wiviott, M.S. Sabatine, R.M. Califf, and E. Braunwald. 2007. Serial Measurement of Monocyte Chemoattractant Protein-1 After Acute Coronary Syndromes: Results From the A to Z Trial. *J.Am.Coll.Cardiol.* 50:2117-2124.

de Nigris F, Lerman LO, Ignarro SW, Sica G, Lerman A, Palinski W, Ignarro LJ, and Napoli C. *2003.* Beneficial effects of antioxidants and L-arginine on oxidation-sensitive gene expression and endothelial NO synthase activity at sites of disturbed shear stress. - *Proc Natl Acad Sci U S A. 100(3):1420-5.*

De Pergola, G., N. Pannacciulli, M. Ciccone, M. Tartagni, P. Rizzon, and R. Giorgino. 2003. Free testosterone plasma levels are negatively associated with the intima-media thickness of the common carotid artery in overweight and obese glucose-tolerant young adult men. *Int.J.Obes.Relat.Metab.Disord.* 27:803-807.

Dean RA, C.M. and Overall CM. *2007.* Proteomics discovery of metalloproteinase substrates in the cellular context by iTRAQ labeling reveals a diverse MMP-2 substrate degradome. - *Mol Cell Proteomics. 6(4):611-23.*

Death, A.K., K.C. McGrath, M.A. Sader, S. Nakhla, W. Jessup, D.J. Handelsman, and D.S. Celermajer. 2004. Dihydrotestosterone promotes vascular cell adhesion molecule-1 expression in male human endothelial cells via a nuclear factor-kappaB-dependent pathway. *Endocrinology.* 145:1889-1897.

Debette S, Bevan S, Dartigues JF, Sitzer M, Lorenz M, Ducimetiere P, Amouyel P, and Markus HS. *2009.* Fractalkine receptor/ligand genetic variants and carotid intima-media thickness. - *Stroke. 40(6):2212-4.*

Defranco DB. *2000.* Role of molecular chaperones in subnuclear trafficking of glucocorticoid receptors. - *Kidney Int. 57(4):1241-9.*

Denti, L., G. Pasolini, P. Cortellini, L. Sanfelici, R. Benedetti, A. Cecchetti, S. Ferretti, L. Bruschieri, F. Ablondi, and G. Valenti. 2000. Changes in HDL-cholesterol and lipoprotein Lp(a) after 6-month treatment with finasteride in males affected by benign prostatic hyperplasia (BPH). *Atherosclerosis.* 152:159-166.

Deo, R., A. Khera, D.K. McGuire, S.A. Murphy, J. de P. Meo Neto, D.A. Morrow, and J.A. de Lemos. 2004. Association among plasma levels of monocyte chemoattractant protein-1, traditional cardiovascular risk factors, and subclinical atherosclerosis. *J.Am.Coll.Cardiol.* 44:1812-1818.

Derby CA, Zilber S, Brambilla D, Morales KH, and McKinlay JB. *2006.* Body mass index, waist circumference and waist to hip ratio and change in sex steroid hormones: the Massachusetts Male Ageing Study. - *Clin Endocrinol (Oxf). 65(1):125-31.*

Despres JP. *2009.* Targeting abdominal obesity and the metabolic syndrome to manage cardiovascular disease risk. - *Heart. 95(13):1118-24.*

Dimmeler S, Breitschopf K, Haendeler J, and Zeiher AM. *1999.* Dephosphorylation targets Bcl-2 for ubiquitin-dependent degradation: a link between the apoptosome and the proteasome pathway. - *J Exp Med. 189(11):1815-22.*

Ding, A.Q., and J.N. Stallone. 2001. Testosterone-induced relaxation of rat aorta is androgen structure specific and involves K+ channel activation. *J.Appl.Physiol.* 91:2742-2750.

Dirksen MT, van der Wal AC, van den Berg FM, van der Loos CM, and Becker AE. *1998.* Distribution of inflammatory cells in atherosclerotic plaques relates to the direction of flow. - *Circulation. 98(19):2000-3.*

Dobs AS, Bachorik PS, Arver S, Meikle AW, Sanders SW, Caramelli KE, and Mazer NA. *2001.* Interrelationships among lipoprotein levels, sex hormones, anthropometric parameters, and age in hypogonadal men treated for 1 year with a permeation-enhanced testosterone transdermal system. - *J Clin Endocrinol Metab. 86(3):1026-33.*

Dockery F, Bulpitt CJ, Agarwal S, Donaldson M, and Rajkumar C. *2003.* Testosterone suppression in men with prostate cancer leads to an increase in arterial stiffness and hyperinsulinaemia. - *Clin Sci (Lond). 104(2):195-201.*

Doedens JR, and Black RA. *2000.* Stimulation-induced down-regulation of tumor necrosis factor-alpha converting enzyme. - *J Biol Chem. 275(19):14598-607.*

Dollery, C.M., J.R. McEwan, and A.M. Henney. 1995. Matrix metalloproteinases and cardiovascular disease. *Circ.Res.* 77:863-868.

Doran AC, Meller N, and McNamara CA. *2008.* Role of smooth muscle cells in the initiation and early progression of atherosclerosis. - *Arterioscler Thromb Vasc Biol. 28(5):812-9.*

Dougherty RH, Rohrer JL, Hayden D, Rubin SD, and Leder BZ. *2005.* Effect of aromatase inhibition on lipids and inflammatory markers of cardiovascular disease in elderly men with low testosterone levels. - *Clin Endocrinol (Oxf). 62(2):228-35.*

Dunn JF, Nisula BC, and Rodbard D. *1981.* Transport of steroid hormones: binding of 21 endogenous steroids to both testosterone-binding globulin and corticosteroid-binding globulin in human plasma. - *J Clin Endocrinol Metab. 53(1):58-68.*

Durand E, Scoazec A, Lafont A, Boddaert J, Al Hajzen A, Addad F, Mirshahi M, Desnos M, Tedgui A, and Mallat Z. *2004.* In vivo induction of endothelial apoptosis leads to vessel thrombosis and endothelial denudation: a clue to the understanding of the mechanisms of thrombotic plaque erosion. - *Circulation. 109(21):2503-6.*

Dwivedi, A., E.E. Änggård, and M.J. Carrier. 2001. Oxidized LDL-Mediated Monocyte Adhesion to Endothelial Cells Does Not Involve NFκB. *Biochem.Biophys.Res.Commun.* 284:239-244.

Ebeling P, V.A. FAU - Koivisto, and Koivisto VA. *1994.* Physiological importance of dehydroepiandrosterone. - *Lancet. 343(8911):1479-81.*

Eicheler, W., P. Tuohimaa, P. Vilja, K. Adermann, W.G. Forssmann, and G. Aumuller. 1994. Immunocytochemical localization of human 5 alpha-reductase 2 with polyclonal antibodies in androgen target and non-target human tissues. *J.Histochem.Cytochem.* 42:667-675.

Elhage R, Arnal JF, Pieraggi MT, Duverger N, Fievet C, Faye JC, and Bayard F. *1997.* 17 beta-estradiol prevents fatty streak formation in apolipoprotein E-deficient mice. - *Arterioscler Thromb Vasc Biol. 17(11):2679-84.*

Elisaf M, Karabina SA, Bairaktari E, Goudevenos JA, Siamopoulos KC, and Tselepis AD. *1999.* Increased platelet reactivity to the aggregatory effect of platelet activating factor, in vitro, in patients with heterozygous familial hypercholesterolaemia. - *Platelets.;10(2-3):124-31.*

Emmelot-Vonk MH, Verhaar HJ, Nakhai Pour HR, Aleman A, Lock TM, Bosch JL, Grobbee DE, and van der Schouw YT. *2008.* Effect of testosterone supplementation on functional mobility, cognition, and other parameters in older men: a randomized controlled trial. - *JAMA. 299(1):39-52.*

English KM, Jones RD, Jones TH, Morice AH, and Channer KS. *2000a.* Aging reduces the responsiveness of coronary arteries from male Wistar rats to the vasodilatory action of testosterone. - *Clin Sci (Lond). 99(1):77-82.*

English KM, Steeds RP, Jones TH, Diver MJ, and Channer KS. *2000b.* Low-dose transdermal testosterone therapy improves angina threshold in men with chronic stable angina: A randomized, double-blind, placebo-controlled study. - *Circulation. 102(16):1906-11.*

English, K.M., O. Mandour, R.P. Steeds, M.J. Diver, T.H. Jones, and K.S. Channer. 2000c. Men with coronary artery disease have lower levels of androgens than men with normal coronary angiograms. *Eur.Heart J.* 21:890-894.

Faiman C, and Winter JS. *1971.* Diurnal cycles in plasma FSH, testosterone and cortisol in men. - *J Clin Endocrinol Metab. 33(2):186-92.*

Fain JN, Madan AK, Hiler ML, Cheema P, and Bahouth SW. *2004.* Comparison of the release of adipokines by adipose tissue, adipose tissue matrix, and adipocytes from visceral and subcutaneous abdominal adipose tissues of obese humans. - *Endocrinology. 145(5):2273-82.*

Falk, E., P.K. Shah, and V. Fuster. 1995. Coronary plaque disruption. *Circulation.* 92:657-671.

Fassina G, Ferrari N, Brigati C, Benelli R, Santi L, Noonan DM, and Albini A. *2000.* Tissue inhibitors of metalloproteases: regulation and biological activities. - *Clin Exp Metastasis.;18(2):111-20.*

Faure S, Meyer L, Costagliola D, Vaneensberghe C, Genin E, Autran B, Delfraissy JF, McDermott DH, Murphy PM, Debre P, Theodorou I, and Combadiere C. *2000.* Rapid progression to AIDS in HIV+ individuals with a structural variant of the chemokine receptor CX3CR1. - *Science. 287(5461):2274-7.*

Fernandez-Real JM, W. FAU - Ricart, and Ricart W. *2003.* Insulin resistance and chronic cardiovascular inflammatory syndrome. - *Endocr Rev. 24(3):278-301.*

Fleige, S., and M.W. Pfaffl. 2006. RNA integrity and the effect on the real-time qRT-PCR performance. *Mol.Aspects Med.* 27:126-139.

Florian, M., and S. Magder. 2008. Estrogen decreases TNF-α and oxidized LDL induced apoptosis in endothelial cells. *Steroids.* 73:47-58.

Fong AM, Erickson HP, Zachariah JP, Poon S, Schamberg NJ, Imai T, and Patel DD. *2000.* Ultrastructure and function of the fractalkine mucin domain in CX(3)C chemokine domain presentation. - *J Biol Chem. 275(6):3781-6.*

Fong, A.M., L.A. Robinson, D.A. Steeber, T.F. Tedder, O. Yoshie, T. Imai, and D.D. Patel. 1998. Fractalkine and CX3CR1 mediate a novel mechanism of leukocyte capture, firm adhesion, and activation under physiologic flow. *J.Exp.Med.* 188:1413-1419.

Forstermann U. *2010.* Nitric oxide and oxidative stress in vascular disease. - *Pflugers Arch. 459(6):923-39.*

Foussat A, Coulomb-L'Hermine A, Gosling J, Krzysiek R, Durand-Gasselin I, Schall T, Balian A, Richard Y, Galanaud P, and Emilie D. *2000.* Fractalkine receptor expression by T lymphocyte subpopulations and in vivo production of fractalkine in human. - *Eur J Immunol. 30(1):87-97.*

Fraticelli, P., M. Sironi, G. Bianchi, D. D'Ambrosio, C. Albanesi, A. Stoppacciaro, M. Chieppa, P. Allavena, L. Ruco, G. Girolomoni, F. Sinigaglia, A. Vecchi, and A. Mantovani. 2001. Fractalkine (CX3CL1) as an amplification circuit of polarized Th1 responses. *J.Clin.Invest.* 107:1173-1181.

Friedewald WT, Levy RI, and Fredrickson DS. *1972.* Estimation of the concentration of low-density lipoprotein cholesterol in plasma, without use of the preparative ultracentrifuge. - *Clin Chem. 18(6):499-502.*

Fritschy JM. *2008.* Is my antibody-staining specific? How to deal with pitfalls of immunohistochemistry. - *Eur J Neurosci. 28(12):2365-70.*

Fujimoto, R., I. Morimoto, E. Morita, H. Sugimoto, Y. Ito, and S. Eto. 1994. Androgen receptors, 5 alpha-reductase activity and androgen-dependent proliferation of vascular smooth muscle cells. *J.Steroid Biochem.Mol.Biol.* 50:169-174.

Fukui M, Kitagawa Y, Nakamura N, Kadono M, Mogami S, Hirata C, Ichio N, Wada K, Hasegawa G, and Yoshikawa T. *2003.* Association between serum testosterone concentration and carotid atherosclerosis in men with type 2 diabetes. - *Diabetes Care. 26(6):1869-73.*

Fukumoto Y, Hiro T, Fujii T, Hashimoto G, Fujimura T, Yamada J, Okamura T, and Matsuzaki M. *2008.* Localized elevation of shear stress is related to coronary plaque rupture: a 3-dimensional intravascular ultrasound study with in-vivo color mapping of shear stress distribution. - *J Am Coll Cardiol. 51(6):645-50.*

Galis ZS, Sukhova GK, Kranzhofer R, Clark S, and Libby P. *1995.* Macrophage foam cells from experimental atheroma constitutively produce matrix-degrading proteinases. - *Proc Natl Acad Sci U S A. 92(2):402-6.*

Galis ZS, Sukhova GK, Lark MW, and Libby P. *1994a.* Increased expression of matrix metalloproteinases and matrix degrading activity in vulnerable regions of human atherosclerotic plaques. - *J Clin Invest. 94(6):2493-503.*

Galis, Z.S., and J.J. Khatri. 2002. Matrix metalloproteinases in vascular remodeling and atherogenesis: the good, the bad, and the ugly. *Circ.Res.* 90:251-262.

Galis, Z.S., M. Muszynski, G.K. Sukhova, E. Simon-Morrissey, E.N. Unemori, M.W. Lark, E. Amento, and P. Libby. 1994b. Cytokine-stimulated human vascular smooth muscle cells synthesize a complement of enzymes required for extracellular matrix digestion. *Circ.Res.* 75:181-189.

Galkina E, K. and Ley K. *2007.* Vascular adhesion molecules in atherosclerosis. - *Arterioscler Thromb Vasc Biol. 27(11):2292-301.*

Gallagher SR, and Desjardins PR. *2008.* Quantitation of DNA and RNA with absorption and fluorescence spectroscopy. - *Curr Protoc Protein Sci. Appendix 3:Appendix 4K.*

Garcia, G.E., Y. Xia, S. Chen, Y. Wang, R.D. Ye, J.K. Harrison, K.B. Bacon, H.G. Zerwes, and L. Feng. 2000. NF-kappaB-dependent fractalkine induction in rat aortic endothelial cells stimulated by IL-1beta, TNF-alpha, and LPS. *J.Leukoc.Biol.* 67:577-584.

Garton, K.J., P.J. Gough, C.P. Blobel, G. Murphy, D.R. Greaves, P.J. Dempsey, and E.W. Raines. 2001. Tumor necrosis factor-alpha-converting enzyme (ADAM17) mediates the cleavage and shedding of fractalkine (CX3CL1). *J.Biol.Chem.* 276:37993-38001.

Geissmann F, Jung S, and Littman DR. *2003.* Blood monocytes consist of two principal subsets with distinct migratory properties. - *Immunity. 19(1):71-82.*

George, S.J. 2000. Therapeutic potential of matrix metalloproteinase inhibitors in atherosclerosis. *Expert Opin.Investig.Drugs.* 9:993-1007.

Gerdes, N., G.K. Sukhova, P. Libby, R.S. Reynolds, J.L. Young, and U. Schonbeck. 2002. Expression of interleukin (IL)-18 and functional IL-18 receptor on human vascular endothelial cells, smooth muscle cells, and macrophages: implications for atherogenesis. *J.Exp.Med.* 195:245-257.

Gerszten RE, Garcia-Zepeda EA, Lim YC, Yoshida M, Ding HA, Gimbrone MA Jr, Luster AD, Luscinskas FW, and Rosenzweig A. *1999.* MCP-1 and IL-8 trigger firm adhesion of monocytes to vascular endothelium under flow conditions. - *Nature. 398(6729):718-23.*

Ghosh S, and Baltimore D. *1990.* Activation in vitro of NF-kappa B by phosphorylation of its inhibitor I kappa B. - *Nature. 344(6267):678-82.*

Gimbrone MA Jr, Resnick N, Nagel T, Khachigian LM, Collins T, and Topper JN. *1997.* Hemodynamics, endothelial gene expression, and atherogenesis. - *Ann N Y Acad Sci. 811:1-10; Discussion 10-1.*

Glaudemans AW, Slart RH, Bozzao A, Bonanno E, Arca M, Dierckx RA, and Signore A. *2010.* Molecular imaging in atherosclerosis. - *Eur J Nucl Med Mol Imaging. Mar 20.*

Glueck CJ. *1979.* Dietary fat and atherosclerosis. - *Am J Clin Nutr. 32(12 Suppl):2703-11.*

Goda, S., T. Imai, O. Yoshie, O. Yoneda, H. Inoue, Y. Nagano, T. Okazaki, H. Imai, E.T. Bloom, N. Domae, and H. Umehara. 2000. CX3C-chemokine, fractalkine-enhanced adhesion of THP-1 cells to endothelial cells through integrin-dependent and -independent mechanisms. *J.Immunol.* 164:4313-4320.

Goldstein JL, and Brown MS. *1977.* The low-density lipoprotein pathway and its relation to atherosclerosis. - *Annu Rev Biochem.;46:897-930.*

Gomis-Ruth FX, Maskos K, Betz M, Bergner A, Huber R, Suzuki K, Yoshida N, Nagase H, Brew K, Bourenkov GP, Bartunik H, and Bode W. *1997.* Mechanism of inhibition of the human matrix metalloproteinase stromelysin-1 by TIMP-1. - *Nature. 389(6646):77-81.*

Goncharov NP, Katsya GV, Chagina NA, and Gooren LJ. *2009.* Testosterone and obesity in men under the age of 40 years. - *Andrologia. 41(2):76-83.*

Gordon GB, Bush DE, and Weisman HF. *1988.* Reduction of atherosclerosis by administration of dehydroepiandrosterone. A study in the hypercholesterolemic New Zealand white rabbit with aortic intimal injury. - *J Clin Invest. 82(2):712-20.*

Gordon S. *2003.* Alternative activation of macrophages. - *Nat Rev Immunol. 3(1):23-35.*

Gornstein RA, Lapp CA, Bustos-Valdes SM, and Zamorano P. *1999.* Androgens modulate interleukin-6 production by gingival fibroblasts in vitro. - *J Periodontol. 70(6):604-9.*

Gosling, J., S. Slaymaker, L. Gu, S. Tseng, C.H. Zlot, S.G. Young, B.J. Rollins, and I.F. Charo. 1999. MCP-1 deficiency reduces susceptibility to atherosclerosis in mice that overexpress human apolipoprotein B. *J.Clin.Invest.* 103:773-778.

Gracie JA, Robertson SE, I.B. and McInnes IB. *2003.* Interleukin-18. - *J Leukoc Biol. 73(2):213-24.*

Gratzner HG. *1982.* Monoclonal antibody to 5-bromo- and 5-iododeoxyuridine: A new reagent for detection of DNA replication. - *Science. 218(4571):474-5.*

Greaves, D.R., and S. Gordon. 2001. Immunity, atherosclerosis and cardiovascular disease. *Trends in Immunology.* 22:180-181.

Green SR, Han KH, Chen Y, Almazan F, Charo IF, Miller YI, and Quehenberger O. *2006.* The CC chemokine MCP-1 stimulates surface expression of CX3CR1 and enhances the adhesion of monocytes to fractalkine/CX3CL1 via p38 MAPK. - *J Immunol. 176(12):7412-20.*

Greenow K, Pearce NJ, and Ramji DP. *2005.* The key role of apolipoprotein E in atherosclerosis. - *J Mol Med. 83(5):329-42.*

Grewal T, Priceputu E, Davignon J, and Bernier L. *2001.* Identification of a gamma-interferon-responsive element in the promoter of the human macrophage scavenger receptor A gene. - *Arterioscler Thromb Vasc Biol. 21(5):825-31.*

Griffin, B.A., M.J. Caslake, B. Yip, G.W. Tait, C.J. Packard, and J. Shepherd. 1990. Rapid isolation of low density lipoprotein (LDL) subfractions from plasma by density gradient ultracentrifugation. *Atherosclerosis.* 83:59-67.

Grover-Páez, F., and A.B. Zavalza-Gómez. 2009. Endothelial dysfunction and cardiovascular risk factors. *Diabetes Res.Clin.Pract.* 84:1-10.

Gu, L., Y. Okada, S.K. Clinton, C. Gerard, G.K. Sukhova, P. Libby, and B.J. Rollins. 1998. Absence of monocyte chemoattractant protein-1 reduces atherosclerosis in low density lipoprotein receptor-deficient mice. *Mol.Cell.* 2:275-281.

Guerini V, Sau D, Scaccianoce E, Rusmini P, Ciana P, Maggi A, Martini PG, Katzenellenbogen BS, Martini L, Motta M, and Poletti A. *2005.* The androgen derivative 5alpha-androstane-

3beta,17beta-diol inhibits prostate cancer cell migration through activation of the estrogen receptor beta subtype. - *Cancer Res. 65(12):5445-53.*

Gunston, F.D., J.L. Harwood, and A.J. Dijkstra. 2007. The Lipid Handbook. CRC Press, United States of America.

Guo, J., T. Chen, B. Wang, M. Zhang, H. An, Z. Guo, Y. Yu, Z. Qin, and X. Cao. 2003. Chemoattraction, adhesion and activation of natural killer cells are involved in the antitumor immune response induced by fractalkine/CX3CL1. *Immunol.Lett.* 89:1-7.

Gupta S, Pablo AM, Jiang X, Wang N, Tall AR, and Schindler C. *1997.* IFN-gamma potentiates atherosclerosis in ApoE knock-out mice. - *J Clin Invest. 99(11):2752-61.*

Guzman MA. *2010.* Diet and chronic diseases: INCAP studies of atherosclerosis and coronary heart disease. - *Food Nutr Bull. 31(1):141-51.*

Gygi SP, Y. Rochon Y, BFranza BR, R. and Aebersold R. *1999.* Correlation between protein and mRNA abundance in yeast. - *Mol Cell Biol. 19(3):1720-30.*

Haffner SM, Mykkanen L, Valdez RA, and Katz MS. *1993.* Relationship of sex hormones to lipids and lipoproteins in nondiabetic men. - *J Clin Endocrinol Metab. 77(6):1610-5.*

Haidar A, Yassin A, Saad F, and Shabsigh R. *2007.* Effects of androgen deprivation on glycaemic control and on cardiovascular biochemical risk factors in men with advanced prostate cancer with diabetes. - *Aging Male. 10(4):189-96.*

Hak AE, Witteman JC, de Jong FH, Geerlings MI, Hofman A, and Pols HA. *2002.* Low levels of endogenous androgens increase the risk of atherosclerosis in elderly men: the Rotterdam study. - *J Clin Endocrinol Metab. 87(8):3632-9.*

Hammoud AO, Gibson M, Peterson CM, Hamilton BD, and Carrell DT. *2006.* Obesity and male reproductive potential. - *J Androl. 27(5):619-26.*

Han KH, Tangirala RK, Green SR, and Quehenberger O. *1998.* Chemokine receptor CCR2 expression and monocyte chemoattractant protein-1-mediated chemotaxis in human monocytes. A regulatory role for plasma LDL. - *Arterioscler Thromb Vasc Biol. 18(12):1983-91.*

Hansson GK. *2005.* Inflammation, atherosclerosis, and coronary artery disease. - *N Engl J Med. 352(16):1685-95.*

Hansson GK, Hellstrand M, Rymo L, Rubbia L, and Gabbiani G. *1989a.* Interferon gamma inhibits both proliferation and expression of differentiation-specific alpha-smooth muscle actin in arterial smooth muscle cells. - *J Exp Med. 170(5):1595-608.*

Hansson GK, Holm J, and Jonasson L. *1989b.* Detection of activated T lymphocytes in the human atherosclerotic plaque. - *Am J Pathol. 135(1):169-75.*

Hansson GK, Zhou X, Tornquist E, and Paulsson G. *2000.* The role of adaptive immunity in atherosclerosis. - *Ann N Y Acad Sci. 902:53-62; Discussion 62-4.*

Hansson, G.K., and P. Libby. 2006. The immune response in atherosclerosis: a double-edged sword. *Nat.Rev.Immunol.* 6:508-519.

Harada, N., H. Sasano, H. Murakami, T. Ohkuma, H. Nagura, and Y. Takagi. 1999. Localized expression of aromatase in human vascular tissues. *Circ.Res.* 84:1285-1291.

Haring R, Volzke H, Steveling A, Krebs A, Felix SB, Schofl C, Dorr M, Nauck M, and Wallaschofski H. *2010.* Low serum testosterone levels are associated with increased risk of mortality in a population-based cohort of men aged 20-79. - *Eur Heart J. Feb 17.*

Harrison, J.K., A.M. Fong, P.A. Swain, S. Chen, Y.R. Yu, M.N. Salafranca, W.B. Greenleaf, T. Imai, and D.D. Patel. 2001. Mutational analysis of the fractalkine chemokine domain. Basic amino acid residues differentially contribute to CX3CR1 binding, signaling, and cell adhesion. *J.Biol.Chem.* 276:21632-21641.

Hasham SN, and Pillarisetti S. *2006.* Vascular lipases, inflammation and atherosclerosis. - *Clin Chim Acta. 372(1-2):179-83.*

Haskell CA, Cleary MD, and Charo IF. *1999.* Molecular uncoupling of fractalkine-mediated cell adhesion and signal transduction. Rapid flow arrest of CX3CR1-expressing cells is independent of G-protein activation. - *J Biol Chem. 274(15):10053-8.*

Hastings NE, Simmers MB, McDonald OG, Wamhoff BR, B.R. and Blackman BR. *2007.* Atherosclerosis-prone hemodynamics differentially regulates endothelial and smooth muscle cell phenotypes and promotes pro-inflammatory priming. - *Am J Physiol Cell Physiol. 293(6):C1824-33.*

Hatakeyama, H., M. Nishizawa, A. Nakagawa, S. Nakano, T. Kigoshi, and K. Uchida. 2002. Testosterone inhibits tumor necrosis factor-α-induced vascular cell adhesion molecule-1 expression in human aortic endothelial cells. *FEBS Letters.* 530:129-132.

Hattori, H., D. Ito, N. Tanahashi, M. Murata, I. Saito, K. Watanabe, and N. Suzuki. 2005. T280M and V249I polymorphisms of fractalkine receptor CX3CR1 and ischemic cerebrovascular disease. *Neuroscience Letters.* 374:132-135.

Hauer, J., S. Puschner, P. Ramakrishnan, U. Simon, M. Bongers, C. Federle, and H. Engelmann. 2005. TNF receptor (TNFR)-associated factor (TRAF) 3 serves as an inhibitor of TRAF2/5-mediated activation of the noncanonical NF-kappaB pathway by TRAF-binding TNFRs. *Proc.Natl.Acad.Sci.U.S.A.* 102:2874-2879.

Hay RJ, Macy ML, and Chen TR. *1989.* Mycoplasma infection of cultured cells. - *Nature. 339(6224):487-8.*

Hayes, I.M., N.J. Jordan, S. Towers, G. Smith, J.R. Paterson, J.J. Earnshaw, A.G. Roach, J. Westwick, and R.J. Williams. 1998. Human vascular smooth muscle cells express receptors for CC chemokines. *Arterioscler.Thromb.Vasc.Biol.* 18:397-403.

He WW, M.V. Kumar MV, and Tindall DJ. *1991.* A frame-shift mutation in the androgen receptor gene causes complete androgen insensitivity in the testicular-feminized mouse. - *Nucleic Acids Res. 19(9):2373-8.*

Heinlein, C.A., and C. Chang. 2002. The roles of androgen receptors and androgen-binding proteins in nongenomic androgen actions. *Mol.Endocrinol.* 16:2181-2187.

Heistad DD, Wakisaka Y, Miller J, Chu Y, and Pena-Silva R. *2009.* Novel aspects of oxidative stress in cardiovascular diseases. - *Circ J. 73(2):201-7.*

Henn V, Slupsky JR, Grafe M, Anagnostopoulos I, Forster R, Muller-Berghaus G, and Kroczek RA. *1998.* CD40 ligand on activated platelets triggers an inflammatory reaction of endothelial cells. - *Nature. 391(6667):591-4.*

Herbert J. *1995.* The age of dehydroepiandrosterone. - *Lancet. 345(8959):1193-4.*

Herder C, Baumert J, Thorand B, Martin S, Lowel H, Kolb H, and Koenig W. *2006.* Chemokines and incident coronary heart disease: results from the MONICA/KORA Augsburg case-cohort study, 1984-2002. - *Arterioscler Thromb Vasc Biol. 26(9):2147-52.*

Hermand P, Pincet F, Carvalho S, Ansanay H, Trinquet E, Daoudi M, Combadiere C, and Deterre P. *2008.* Functional adhesiveness of the CX3CL1 chemokine requires its aggregation. Role of the transmembrane domain. - *J Biol Chem. 283(44):30225-34.*

Herzenberg LA, Tung J, Moore WA, Herzenberg LA, and Parks DR. *2006.* Interpreting flow cytometry data: a guide for the perplexed. - *Nat Immunol. 7(7):681-5.*

Hess RA, Bunick D, Lee KH, Bahr J, Taylor JA, Korach KS, and Lubahn DB. *1997.* A role for oestrogens in the male reproductive system. - *Nature. 390(6659):509-12.*

Hofbauer LC, Ten RM, and Khosla S. *1999.* The anti-androgen hydroxyflutamide and androgens inhibit interleukin-6 production by an androgen-responsive human osteoblastic cell line. - *J Bone Miner Res. 14(8):1330-7.*

Hong YM. *2010.* Atherosclerotic cardiovascular disease beginning in childhood. - *Korean Circ J. 40(1):1-9.*

Hoogeveen, R.C., A. Morrison, E. Boerwinkle, J.S. Miles, C.E. Rhodes, A.R. Sharrett, and C.M. Ballantyne. 2005. Plasma MCP-1 level and risk for peripheral arterial disease and incident coronary heart disease: Atherosclerosis Risk in Communities study. *Atherosclerosis.* 183:301-307.

Hörkkö, S., C.J. Binder, P.X. Shaw, M. Chang, G. Silverman, W. Palinski, and J.L. Witztum. 2000. Immunological responses to oxidized LDL. *Free Radical Biology and Medicine.* 28:1771-1779.

Hosono, M., O.J. de Boer, A.C. van der Wal, C.M. van der Loos, P. Teeling, J.J. Piek, M. Ueda, and A.E. Becker. 2003. Increased expression of T cell activation markers (CD25, CD26, CD40L and CD69) in atherectomy specimens of patients with unstable angina and acute myocardial infarction. *Atherosclerosis.* 168:73-80.

Hou J, V. Baichwal V, and Cao Z. *1994.* Regulatory elements and transcription factors controlling basal and cytokine-induced expression of the gene encoding intercellular adhesion molecule 1. - *Proc Natl Acad Sci U S A. 91(24):11641-5.*

Howell SJ, Radford JA, Adams JE, Smets EM, Warburton R, and Shalet SM. *2001.* Randomized placebo-controlled trial of testosterone replacement in men with mild Leydig cell insufficiency following cytotoxic chemotherapy. - *Clin Endocrinol (Oxf). 55(3):315-24.*

Huang YW, Su P, Liu GY, Crow MR, Chaukos D, Yan H, and Robinson LA. *2009.* Constitutive endocytosis of the chemokine CX3CL1 prevents its degradation by cell surface metalloproteases. - *J Biol Chem. 284(43):29644-53.*

Huang, J., H. Qian, Z. Li, J. Zhang, S. Wang, Y. Tao, Y. Gao, C. Yin, B. Que, T. Sun, Z. Zhao, and Z. Li. 2010. Role of endothelial lipase in atherosclerosis. *Translational Research.* 156:1-6.

Huber SA, Sakkinen P, David C, Newell MK, and Tracy RP. *2001.* T helper-cell phenotype regulates atherosclerosis in mice under conditions of mild hypercholesterolemia. - *Circulation. 103(21):2610-6.*

Hundhausen, C., D. Misztela, T.A. Berkhout, N. Broadway, P. Saftig, K. Reiss, D. Hartmann, F. Fahrenholz, R. Postina, V. Matthews, K.J. Kallen, S. Rose-John, and A. Ludwig. 2003. The disintegrin-like metalloproteinase ADAM10 is involved in constitutive cleavage of CX3CL1 (fractalkine) and regulates CX3CL1-mediated cell-cell adhesion. *Blood.* 102:1186-1195.

Hurley BF, Seals DR, Hagberg JM, Goldberg AC, Ostrove SM, Holloszy JO, Wiest WG, and Goldberg AP. *1984.* High-density-lipoprotein cholesterol in bodybuilders v powerlifters. Negative effects of androgen use. - *JAMA. 252(4):507-13.*

Ikeda, U., and K. Shimada. 2003. Matrix metalloproteinases and coronary artery diseases. *Clin.Cardiol.* 26:55-59.

Imai, T., K. Hieshima, C. Haskell, M. Baba, M. Nagira, M. Nishimura, M. Kakizaki, S. Takagi, H. Nomiyama, T.J. Schall, and O. Yoshie. 1997. Identification and Molecular Characterization of Fractalkine Receptor CX3CR1, which Mediates Both Leukocyte Migration and Adhesion. *Cell.* 91:521-530.

Imaizumi, T., T. Matsumiya, K. Fujimoto, K. Okamoto, X. Cui, U. Ohtaki, Hidemi, Yoshida, and K. Satoh. 2000. Interferon-gamma stimulates the expression of CX3CL1/fractalkine in cultured human endothelial cells. *Tohoku J.Exp.Med.* 192:127-139.

Imaizumi, T., H. Yoshida, and K. Satoh. 2004. Regulation of CX3CL1/fractalkine expression in endothelial cells. *J.Atheroscler.Thromb.* 11:15-21.

Inoue, H., N. Nishida, N. Ikeda, A. Tsuji, K. Kudo, M. Hanagama, and M. Nata. 2007. The sudden and unexpected death of a female-to-male transsexual patient. *Journal of Forensic and Legal Medicine,.* 14:382-386.

Isidori AM, Giannetta E, Greco EA, Gianfrilli D, Bonifacio V, Isidori A, Lenzi A, and Fabbri A. *2005.* Effects of testosterone on body composition, bone metabolism and serum lipid profile in middle-aged men: a meta-analysis. - *Clin Endocrinol (Oxf). 63(3):280-93.*

Itabe H. *2009.* Oxidative modification of LDL: its pathological role in atherosclerosis. - *Clin Rev Allergy Immunol. 37(1):4-11.*

Itai T, Tanaka M, and Nagata S. *2001.* Processing of tumor necrosis factor by the membrane-bound TNF-alpha-converting enzyme, but not its truncated soluble form. - *Eur J Biochem. 268(7):2074-82.*

Iwai N, Kajimoto K, Kokubo Y, Okayama A, Miyazaki S, Nonogi H, Goto Y, and Tomoike H. *2006.* Assessment of genetic effects of polymorphisms in the MCP-1 gene on serum MCP-1 levels and myocardial infarction in Japanese. - *Circ J. 70(7):805-9.*

Jaffe, M.D. 1977. Effect of testosterone cypionate on postexercise ST segment depression. *Br.Heart J.* 39:1217-1222.

Jaffer, F.A., P. Libby, and R. Weissleder. 2006. Molecular and Cellular Imaging of Atherosclerosis: Emerging Applications. *J.Am.Coll.Cardiol.* 47:1328-1338.

Jagnandan D, Sessa WC, and Fulton D. *2005.* Intracellular location regulates calcium-calmodulin-dependent activation of organelle-restricted eNOS. - *Am J Physiol Cell Physiol.* *289(4):C1024-33.*

Jaroszeski MJ, and Radcliff G. *1999.* Fundamentals of flow cytometry. - *Mol Biotechnol.* *11(1):37-53.*

Jessup W. *1996.* Oxidized lipoproteins and nitric oxide. - *Curr Opin Lipidol.* *7(5):274-80.*

Jiang P, Xu J, Zheng S, Huang J, Xiang Q, Fu X, and Wang T. *2010.* 17beta-estradiol down-regulates lipopolysaccharide-induced MCP-1 production and cell migration in vascular smooth muscle cells. - *J Mol Endocrinol.* *45(2):87-97.*

Johnson, J.L. 2007. Matrix metalloproteinases: influence on smooth muscle cells and atherosclerotic plaque stability. *Expert Rev.Cardiovasc.Ther.* 5:265-282.

Johnson, J.L., S.J. George, A.C. Newby, and C.L. Jackson. 2005. Divergent effects of matrix metalloproteinases 3, 7, 9, and 12 on atherosclerotic plaque stability in mouse brachiocephalic arteries. *Proc.Natl.Acad.Sci.U.S.A.* 102:15575-15580.

Johnson, J.L., R. Fritsche-Danielson, M. Behrendt, A. Westin-Eriksson, H. Wennbo, M. Herslof, M. Elebring, S.J. George, W.L. McPheat, and C.L. Jackson. 2006. Effect of broad-spectrum matrix metalloproteinase inhibition on atherosclerotic plaque stability. *Cardiovascular Research.* 71:586-595.

Jones PJ. *1997.* Regulation of cholesterol biosynthesis by diet in humans. - *Am J Clin Nutr.* *66(2):438-46.*

Jones RD, Pugh PJ, Hall J, Channer KS, and Jones TH. *2003.* Altered circulating hormone levels, endothelial function and vascular reactivity in the testicular feminised mouse. - *Eur J Endocrinol.* *148(1):111-20.*

Jones, R.D., K.M. English, T.H. Jones, and K.S. Channer. 2004. Testosterone-induced coronary vasodilatation occurs via a non-genomic mechanism: evidence of a direct calcium antagonism action. *Clin.Sci.(Lond).* 107:149-158.

Jones, R.D., K.M. English, P.J. Pugh, A.H. Morice, T.H. Jones, and K.S. Channer. 2002. Pulmonary vasodilatory action of testosterone: evidence of a calcium antagonistic action. *J.Cardiovasc.Pharmacol.* 39:814-823.

Jones, T.H. 2010. Testosterone deficiency: a risk factor for cardiovascular disease? *Trends in Endocrinology & Metabolism.* 21:496-503.

Jones, T.H., and F. Saad. 2009. The effects of testosterone on risk factors for, and the mediators of, the atherosclerotic process. *Atherosclerosis.* 207:318-327.

Kabakci G, Yildirir A, Can I, Unsal I, and Erbas B. *1999.* Relationship between endogenous sex hormone levels, lipoproteins and coronary atherosclerosis in men undergoing coronary angiography. - *Cardiology.;92(4):221-5.*

Kalaitzidis, D., and T.D. Gilmore. 2005. Transcription factor cross-talk: the estrogen receptor and NF-κB. *Trends in Endocrinology and Metabolism.* 16:46-52.

Kanakaraj P, Ngo K, Wu Y, Angulo A, Ghazal P, Harris CA, Siekierka JJ, Peterson PA, and Fung-Leung WP. *1999.* Defective interleukin (IL)-18-mediated natural killer and T helper cell type 1 responses in IL-1 receptor-associated kinase (IRAK)-deficient mice. - *J Exp Med. 189(7):1129-38.*

Kanda N, Tsuchida T, and Tamaki K. *1996.* Testosterone inhibits immunoglobulin production by human peripheral blood mononuclear cells. - *Clin Exp Immunol. 106(2):410-5.*

Kang, S., Y. Jang, J.i. Kim, N. Chung, S. Cho, J.S. Chae, and J.o. Lee. 2002. Effect of oral administration of testosterone on brachial arterial vasoreactivity in men with coronary artery disease. *Am.J.Cardiol.* 89:862-864.

Kapoor D, Goodwin E, Channer KS, and Jones TH. *2006.* Testosterone replacement therapy improves insulin resistance, glycaemic control, visceral adiposity and hypercholesterolaemia in hypogonadal men with type 2 diabetes. - *Eur J Endocrinol. 154(6):899-906.*

Karsdal MA, Larsen L, Engsig MT, Lou H, Ferreras M, Lochter A, Delaisse JM, and Foged NT. *2002.* Matrix metalloproteinase-dependent activation of latent transforming growth factor-beta controls the conversion of osteoblasts into osteocytes by blocking osteoblast apoptosis. - *J Biol Chem. 277(46):44061-7.*

Kaszubska W, Hooft van Huijsduijnen R, Ghersa P, DeRaemy-Schenk AM, Chen BP, Hai T, DeLamarter JF, and Whelan J. *1993.* Cyclic AMP-independent ATF family members interact with NF-kappa B and function in the activation of the E-selectin promoter in response to cytokines. - *Mol Cell Biol. 13(11):7180-90.*

Keating NL, O'Malley AJ, and Smith MR. *2006.* Diabetes and cardiovascular disease during androgen deprivation therapy for prostate cancer. - *J Clin Oncol. 24(27):4448-56.*

Keller ET, Ershler WB, and Chang C. *1996.* The androgen receptor: a mediator of diverse responses. - *Front Biosci. Mar 1;1:D59-71.*

Kervinen, H., M. Mänttäri, M. Kaartinen, H. Mäkynen, T. Palosuo, K. Pulkki, and P.T. Kovanen. 2004. Prognostic usefulness of plasma monocyte/macrophage and T-lymphocyte activation markers in patients with acute coronary syndromes. *Am.J.Cardiol.* 94:993-996.

Khaw KT, Dowsett M, Folkerd E, Bingham S, Wareham N, Luben R,Welch A, and Day N. *2007.* Endogenous testosterone and mortality due to all causes, cardiovascular disease, and cancer in men: European prospective investigation into cancer in Norfolk (EPIC-Norfolk) Prospective Population Study. - *Circulation. 116(23):2694-701.*

Khosla S, Atkinson EJ, Dunstan CR, and O'Fallon WM. *2002.* Effect of estrogen versus testosterone on circulating osteoprotegerin and other cytokine levels in normal elderly men. - *J Clin Endocrinol Metab. 87(4):1550-4.*

Kiel, D.P., J.A. Baron, S.R. Plymate, and C.G. Chute. 1989. Sex hormones and lipoproteins in men. *Am.J.Med.* 87:35-39.

Kienitz, T., and M. Quinkler. 2008. Testosterone and blood pressure regulation. *Kidney Blood Press.Res.* 31:71-79.

Kim CS, Park HS, Kawada T, Kim JH, Lim D, Hubbard NE, Kwon BS, Erickson KL, and Yu R. *2006.* Circulating levels of MCP-1 and IL-8 are elevated in human obese subjects and associated with obesity-related parameters. - *Int J Obes (Lond). 30(9):1347-55.*

Kim-Schulze, S., K.A. McGowan, S.C. Hubchak, M.C. Cid, M.B. Martin, H.K. Kleinman, G.L. Greene, and H.W. Schnaper. 1996. Expression of an estrogen receptor by human coronary artery and umbilical vein endothelial cells. *Circulation.* 94:1402-1407.

Kimura M, Tanaka S, Yamada Y, Kiuchi Y, Yamakawa T, and Sekihara H. *1998.* Dehydroepiandrosterone decreases serum tumor necrosis factor-alpha and restores insulin sensitivity: independent effect from secondary weight reduction in genetically obese Zucker fatty rats. - *Endocrinology. 139(7):3249-53.*

Kinlay S, Grewal J, Manuelin D, Fang JC, Selwyn AP, Bittl JA, and Ganz P. *2002.* Coronary flow velocity and disturbed flow predict adverse clinical outcome after coronary angioplasty. - *Arterioscler Thromb Vasc Biol.;22(8):1334-40.*

Knopp RH. *1999.* Drug treatment of lipid disorders. - *N Engl J Med. 341(7):498-511.*

Kobusiak-Prokopowicz, M., J. Orzeszko, G. Mazur, A. Mysiak, A. Orda, R. Poreba, and W. Mazurek. 2007. Chemokines and left ventricular function in patients with acute myocardial infarction. *Eur.J.Intern.Med.* 18:288-294.

Kohlhuber, F., N.C. Rogers, D. Watling, J. Feng, D. Guschin, J. Briscoe, B.A. Witthuhn, S.V. Kotenko, S. Pestka, G.R. Stark, J.N. Ihle, and I.M. Kerr. 1997. A JAK1/JAK2 chimera can sustain alpha and gamma interferon responses. *Mol.Cell.Biol.* 17:695-706.

Kojda G, and Harrison D. *1999.* Interactions between NO and reactive oxygen species: pathophysiological importance in atherosclerosis, hypertension, diabetes and heart failure. - *Cardiovasc Res. 43(3):562-71.*

Kol A, Bourcier T, Lichtman AH, and Libby P. *1999.* Chlamydial and human heat shock protein 60s activate human vascular endothelium, smooth muscle cells, and macrophages. - *J Clin Invest. 103(4):571-7.*

Korybalska K, Pyda M, Grajek S, Lanocha M, Breborowicz A, and Witowski J. *2010.* Serum profiles of monocyte chemoattractant protein-1 as a biomarker for patients recovering from myocardial infarction. - *Clin Res Cardiol. Feb 7.*

Kota, R.S., C.V. Ramana, F.A. Tenorio, R.I. Enelow, and J.C. Rutledge. 2005. Differential effects of lipoprotein lipase on tumor necrosis factor-alpha and interferon-gamma-mediated gene expression in human endothelial cells. *J.Biol.Chem.* 280:31076-31084.

Kotenko, S.V., and S. Pestka. 2000. Jak-Stat signal transduction pathway through the eyes of cytokine class II receptor complexes. *Oncogene.* 19:2557-2565.

Kotula-Balak M, Grzmil P, Styrna J, and Bilinska B. *2004.* Immunodetection of aromatase in mice with a partial deletion in the long arm of the Y chromosome. - *Acta Histochem. 106(1):55-64.*

Kovacs EJ, Faunce DE, Ramer-Quinn DS, Mott FJ, Dy PW, and Frazier-Jessen MR. *1996.* Estrogen regulation of JE/MCP-1 mRNA expression in fibroblasts. - *J Leukoc Biol. 59(4):562-8.*

Kreitmann B, and Bayard F. *1979.* Androgen interaction with the oestrogen receptor in human tissues. - *J Steroid Biochem. 11(5-6):1589-95.*

Kromhout D. *2001.* Diet and cardiovascular diseases. - *J Nutr Health Aging.;5(3):144-9.*

Krutzik SR, Tan B, Li H, Ochoa MT, Liu PT, Sharfstein SE, Graeber TG, Sieling PA, Liu YJ, Rea TH, Bloom BR, and Modlin RL. *2005.* TLR activation triggers the rapid differentiation of monocytes into macrophages and dendritic cells. - *Nat Med. 11(6):653-60.*

Kukreti S, K. Konstantopoulos K, Smith CW, and McIntire LV. *1997.* Molecular mechanisms of monocyte adhesion to interleukin-1beta-stimulated endothelial cells under physiologic flow conditions. - *Blood. 89(11):4104-11.*

Kumai T, Tanaka M, Watanabe M, Nakura H, and Kobayashi S. *1995.* Influence of androgen on tyrosine hydroxylase mRNA in adrenal medulla of spontaneously hypertensive rats. - *Hypertension. 26(1):208-12.*

Kurihara T, Warr G, Loy J, and Bravo R. *1997.* Defects in macrophage recruitment and host defense in mice lacking the CCR2 chemokine receptor. - *J Exp Med. 186(10):1757-62.*

Kuschert GS, Coulin F, Power CA, Proudfoot AE, Hubbard RE, Hoogewerf AJ, and Wells TN. *1999.* Glycosaminoglycans interact selectively with chemokines and modulate receptor binding and cellular responses. - *Biochemistry. 38(39):12959-68.*

Kuziel WA, Morgan SJ, Dawson TC, Griffin S, Smithies O, Ley K, and Maeda N. *1997.* Severe reduction in leukocyte adhesion and monocyte extravasation in mice deficient in CC chemokine receptor 2. - *Proc Natl Acad Sci U S A. 94(22):12053-8.*

Labrie F, Belanger A, Simard J, Van Luu-The, and Labrie C. *1995.* DHEA and peripheral androgen and estrogen formation: intracinology. - *Ann N Y Acad Sci. 774:16-28.*

Lai JJ, Lai KP, Chuang KH, Chang P, Yu IC, Lin WJ, and Chang C. 2009. Monocyte/macrophage androgen receptor suppresses cutaneous wound healing in mice by enhancing local TNF-alpha expression. J Clin Invest. 119(12):3739-51.

Laman, J.D., E. Claassen, and R.J. Noelle. 1996. Functions of CD40 and its ligand, gp39 (CD40L). *Crit.Rev.Immunol.* 16:59-108.

Lambeth JD, Xu XX, and Glover M. *1987.* Cholesterol sulfate inhibits adrenal mitochondrial cholesterol side chain cleavage at a site distinct from cytochrome P-450scc. Evidence for an intramitochondrial cholesterol translocator. - *J Biol Chem. 262(19):9181-8.*

Landsman L, Bar-On L, Zernecke A, Kim KW, Krauthgamer R, Shagdarsuren E, Lira SA, Weissman IL, Weber C, and Jung S. *2009.* CX3CR1 is required for monocyte homeostasis and atherogenesis by promoting cell survival. - *Blood. 113(4):963-72.*

Langer C, Gansz B, Goepfert C, Engel T, Uehara Y, von Dehn G, Jansen H, Assmann G, and von Eckardstein A. *2002.* Testosterone up-regulates scavenger receptor BI and stimulates cholesterol efflux from macrophages. *Biochemical and Biophysical Research Communications. 296: 1051-1057.*

Larsen, B.A., B.G. Nordestgaard, S. Stender, and K. Kjeldsen. 1993. Effect of testosterone on atherogenesis in cholesterol-fed rabbits with similar plasma cholesterol levels. *Atherosclerosis.* 99:79-86.

Laughlin GA, Barrett-Connor E, Jand Bergstrom J. *2008.* Low serum testosterone and mortality in older men. - *J Clin Endocrinol Metab. 93(1):68-75.*

Le Goascogne C, Sannanes N, Gouezou M, Baulieu EE, and Robel P. *1993.* Suppressed expression of the cytochrome P45017 alpha protein in the testicular feminized (Tfm) mouse testes. - *J Endocrinol. 139(1):127-30.*

Lee B, and Moon SK. *2005.* Resveratrol inhibits TNF-alpha-induced proliferation and matrix metalloproteinase expression in human vascular smooth muscle cells. - *J Nutr. 135(12):2767-73.*

Lee YG, S. FAU - Korenchuk, Korenchuk S, J. FAU - Lehr, Lehr J, S. FAU - Whitney, Whitney S, R. FAU - Vessela, Vessela R, K.J. FAU - Pienta, and Pienta KJ. Establishment and characterization of a new human prostatic cancer cell line: DuCaP. - *in Vivo.2001 Mar-Apr;15(2):157-62.*

Leite JO, and Fernandez ML. *2010.* Should we take high-density lipoprotein cholesterol levels at face value? - *Am J Cardiovasc Drugs.;10(1):1-3.*

Leon ML, and Zuckerman SH. *2005.* Gamma interferon: a central mediator in atherosclerosis. - *Inflamm Res. 54(10):395-411.*

Lerner DJ, and Kannel WB. *1986.* Patterns of coronary heart disease morbidity and mortality in the sexes: a 26-year follow-up of the Framingham population. - *Am Heart J. 111(2):383-90.*

Lesnik, P., C.A. Haskell, and I.F. Charo. 2003. Decreased atherosclerosis in CX3CR1-/- mice reveals a role for fractalkine in atherogenesis. *J.Clin.Invest.* 111:333-340.

Lesser, M.A. 1946. Testosterone propionate therapy in one hundred cases of angina pectoris. *The Journal of Clinical Endocrinology and Metabolism.* 6:549-557.

Ley K, Laudanna C, Cybulsky MI, and Nourshargh S. *2007.* Getting to the site of inflammation: the leukocyte adhesion cascade updated. - *Nat Rev Immunol. 7(9):678-89.*

Li GX, Liu P, Xu L, Miao F, Liu YF, Zhao H, and Zhang ZW. *2009.* [Effects of high-density lipoprotein on the cholesterol efflux from endothelial cells.]. - *Nan Fang Yi Ke Da Xue Xue Bao. 29(11):2191-3.*

Li H, Freeman MW, and Libby P. *1995.* Regulation of smooth muscle cell scavenger receptor expression in vivo by atherogenic diets and in vitro by cytokines. - *J Clin Invest. Jan;95(1):122-33.*

Li PF, Dietz R, and von Harsdorf R. *1997.* Differential effect of hydrogen peroxide and superoxide anion on apoptosis and proliferation of vascular smooth muscle cells. - *Circulation. 96(10):3602-9.*

Li X, and Fan H. *2004.* Loss of ectodomain shedding due to mutations in the metalloprotease and cysteine-rich/disintegrin domains of the tumor necrosis factor-alpha converting enzyme (TACE). - *J Biol Chem. 279(26):27365-75.*

Li ZG, Danis VA, and Brooks PM. *1993.* Effect of gonadal steroids on the production of IL-1 and IL-6 by blood mononuclear cells in vitro. - *Clin Exp Rheumatol11(2):157-62.*

Libby P, Nahrendorf M, Pittet MJ, and Swirski FK. *2008.* Diversity of denizens of the atherosclerotic plaque: not all monocytes are created equal. - *Circulation. 117(25):3168-70.*

Libby P, and Theroux P. *2005.* Pathophysiology of coronary artery disease. - *Circulation. 111(25):3481-8.*

Libby, P. 2006. Inflammation and cardiovascular disease mechanisms. *Am.J.Clin.Nutr.* 83:456S-460S.

Libby, P., and M. Aikawa. 2002b. Vitamin C, collagen, and cracks in the plaque. *Circulation.* 105:1396-1398.

Libby, P., P.M. Ridker, and A. Maseri. 2002a. Inflammation and atherosclerosis. *Circulation.* 105:1135-1143.

Libby, P. 2005. Act Local, Act Global: Inflammation and the Multiplicity of "Vulnerable" Coronary Plaques. *Journal of the American College of Cardiology.* 45:1600-1602.

Libby, P. 2001a. What have we learned about the biology of atherosclerosis? The role of inflammation. *The American Journal of Cardiology.* 88:3-6.

Libby, P., P.M. Ridker, and G.K. Hansson. 2009. Inflammation in Atherosclerosis: From Pathophysiology to Practice. *J.Am.Coll.Cardiol.* 54:2129-2138.

Lichtman AH, Clinton SK, Iiyama K, Connelly PW, Libby P, and Cybulsky MI. *1999.* Hyperlipidemia and atherosclerotic lesion development in LDL receptor-deficient mice fed defined semipurified diets with and without cholate. - *Arterioscler Thromb Vasc Biol. 19(8):1938-44.*

Lim JH, Um HJ, Park JW, Lee IK, and Kwon TK. *2009.* Interleukin-1b promotes the expression of monocyte chemoattractant protein-1 (MCP1) in human aorta smooth muscle cells via multiple signaling pathways. - *Exp Mol Med. Jun 29.*

Lindemann S, Kramer B, Seizer P, and Gawaz M. *2007.* Platelets, inflammation and atherosclerosis. - *J Thromb Haemost. 5 Suppl 1:203-11.*

Ling S, Dai A, Williams MR, Myles K, Dilley RJ, Komesaroff PA, and Sudhir K. *2002.* Testosterone (T) enhances apoptosis-related damage in human vascular endothelial cells. - *Endocrinology. 143(3):1119-25.*

Liu GY, Kulasingam V, Alexander RT, Touret N, Fong AM, Patel DD, and Robinson LA. *2005.* Recycling of the membrane-anchored chemokine, CX3CL1. - *J Biol Chem. 280(20):19858-66.*

Liu, P.Y., A.K. Death, and D.J. Handelsman. 2003. Androgens and cardiovascular disease. *Endocr.Rev.* 24:313-340.

Liva, S.M., and R.R. Voskuhl. 2001. Testosterone acts directly on CD4+ T lymphocytes to increase IL-10 production. *J.Immunol.* 167:2060-2067.

Livak KJ, Flood SJ, Marmaro J, Giusti W, and Deetz K. *1995.* Oligonucleotides with fluorescent dyes at opposite ends provide a quenched probe system useful for detecting PCR product and nucleic acid hybridization. - *PCR Methods Appl. 4(6):357-62.*

Livak, K.J., and T.D. Schmittgen. 2001. Analysis of Relative Gene Expression Data Using Real-Time Quantitative PCR and the 2–ΔΔCT Method. *Methods.* 25:402-408.

Lorincz A, and Nusser Z. *2008.* Specificity of immunoreactions: the importance of testing specificity in each method. - *J Neurosci. 28(37):9083-6.*

Lucas, A.D., C. Bursill, T.J. Guzik, J. Sadowski, K.M. Channon, and D.R. Greaves. 2003. Smooth muscle cells in human atherosclerotic plaques express the fractalkine receptor CX3CR1 and undergo chemotaxis to the CX3C chemokine fractalkine (CX3CL1). *Circulation.* 108:2498-2504.

Ludwig, A., T. Berkhout, K. Moores, P. Groot, and G. Chapman. 2002. Fractalkine is expressed by smooth muscle cells in response to IFN-gamma and TNF-alpha and is modulated by metalloproteinase activity. *J.Immunol.* 168:604-612.

Luscinskas FW, Gerszten RE, Garcia-Zepeda EA, Lim YC, Yoshida M, Ding HA, Gimbrone MA Jr, Luster AD, and Rosenzweig A. *2000.* C-C and C-X-C chemokines trigger firm adhesion of monocytes to vascular endothelium under flow conditions. - *Ann N Y Acad Sci. 902:288-93.*

Ly LP, Jimenez M, Zhuang TN, Celermajer DS, Conway AJ, and Handelsman DJ. *2001.* A double-blind, placebo-controlled, randomized clinical trial of transdermal dihydrotestosterone gel on muscular strength, mobility, and quality of life in older men with partial androgen deficiency. - *J Clin Endocrinol Metab. 86(9):4078-88.*

Lyon MF, and Hawkes SG. *1970.* X-linked gene for testicular feminization in the mouse. - *Nature. 227(5264):1217-9.*

Ma R, Wu S, and Lin Q. *2005a.* Homologous up-regulation of androgen receptor expression by androgen in vascular smooth muscle cells. - *Horm Res.;63(1):6-14.*

Ma R, Wu SZ, Lin QS, and Jiang SS. *2005b.* [Regulation of androgen receptor mRNA expression by testosterone in cultured vascular smooth muscle cells]. - *Di Yi Jun Yi Da Xue Xue Bao. 25(3):298-300.*

Mach F, Sauty A, Iarossi AS, Sukhova GK, Neote K, Libby P, and Luster AD. *1999.* Differential expression of three T lymphocyte-activating CXC chemokines by human atheroma-associated cells. - *J Clin Invest. 104(8):1041-50.*

Mackay CR. *1996.* Chemokine receptors and T cell chemotaxis. - *J Exp Med. 184(3):799-802.*

Mackness, B., D. Hine, Y. Liu, M. Mastorikou, and M. Mackness. 2004. Paraoxonase-1 inhibits oxidised LDL-induced MCP-1 production by endothelial cells. *Biochem.Biophys.Res.Commun.* 318:680-683.

Madamanchi NR, Vendrov A, and Runge MS. *2005.* Oxidative stress and vascular disease. - *Arterioscler Thromb Vasc Biol. 25(1):29-38.*

Maeda S, Dean DD, Gomez R, Schwartz Z, and Boyan BD. *2002.* The first stage of transforming growth factor beta1 activation is release of the large latent complex from the extracellular

matrix of growth plate chondrocytes by matrix vesicle stromelysin-1 (MMP-3). - *Calcif Tissue Int. 70(1):54-65.*

Maggio M, and Basaria S. *2009.* Welcoming low testosterone as a cardiovascular risk factor. - *Int J Impot Res. 21(4):261-4.*

Maggio M, Basaria S, Ceda GP, Ble A, Ling SM, Bandinelli S, Valenti G, and Ferrucci L. *2005.* The relationship between testosterone and molecular markers of inflammation in older men. - *J Endocrinol Invest.;28(11 Suppl Proceedings):116-9.*

Mahboubi, K., and J.S. Pober. 2002. Activation of signal transducer and activator of transcription 1 (STAT1) is not sufficient for the induction of STAT1-dependent genes in endothelial cells. Comparison of interferon-gamma and oncostatin M. *J.Biol.Chem.* 277:8012-8021.

Maison P, Byrne CD, Hales CN, Day NE, and Wareham NJ. *2001.* Do different dimensions of the metabolic syndrome change together over time? Evidence supporting obesity as the central feature. - *Diabetes Care. 24(10):1758-63.*

Makinen, J., M.J. Jarvisalo, P. Pollanen, A. Perheentupa, K. Irjala, M. Koskenvuo, J. Makinen, I. Huhtaniemi, and O.T. Raitakari. 2005. Increased carotid atherosclerosis in andropausal middle-aged men. *J.Am.Coll.Cardiol.* 45:1603-1608.

Malkin CJ, Pugh PJ, Jones TH, and Channer KS. *2003a.* Testosterone for secondary prevention in men with ischaemic heart disease? - *QJM. 96(7):521-9.*

Malkin CJ, Pugh PJ, Morris PD, Kerry KE, Jones RD, Jones TH, and Channer KS. *2004a* . Testosterone replacement in hypogonadal men with angina improves ischaemic threshold and quality of life*. - Heart. 90(8):871-6.*

Malkin, C.J., P.J. Pugh, R.D. Jones, T.H. Jones, and K.S. Channer. 2003b. Testosterone as a protective factor against atherosclerosis--immunomodulation and influence upon plaque development and stability. *J.Endocrinol.* 178:373-380.

Malkin, C.J., P.J. Pugh, R.D. Jones, D. Kapoor, K.S. Channer, and T.H. Jones. 2004b. The effect of testosterone replacement on endogenous inflammatory cytokines and lipid profiles in hypogonadal men. *J.Clin.Endocrinol.Metab.* 89:3313-3318.

Malkin, C.J., P.J. Pugh, J.N. West, E.J. van Beek, T.H. Jones, and K.S. Channer. 2006. Testosterone therapy in men with moderate severity heart failure: a double-blind randomized placebo controlled trial. *Eur.Heart J.* 27:57-64.

Mallat Z, Corbaz A, Scoazec A, Graber P, Alouani S, Esposito B, Humbert Y, Chvatchko Y, and Tedgui A. *2001a.* Interleukin-18/interleukin-18 binding protein signaling modulates atherosclerotic lesion development and stability. - *Circ Res. 89(7):E41-5.*

Mallat Z, Gojova A, Marchiol-Fournigault C, Esposito B, Kamate C, Merval R, Fradelizi D, and Tedgui A. *2001b.* Inhibition of transforming growth factor-beta signaling accelerates atherosclerosis and induces an unstable plaque phenotype in mice. - *Circ Res. 89(10):930-4.*

Mallat Z, Henry P, Fressonnet R, Alouani S, Scoazec A, Beaufils P, Chvatchko Y, and Tedgui A. *2002.* Increased plasma concentrations of interleukin-18 in acute coronary syndromes. - *Heart. 88(5):467-9.*

Mallat Z, Taleb S, Ait-Oufella H, and Tedgui A. *2009*. The role of adaptive T cell immunity in atherosclerosis. - *J Lipid Res. 50 Suppl:S364-9.*

Mallat, Z., A. Corbaz, A. Scoazec, S. Besnard, G. Leseche, Y. Chvatchko, and A. Tedgui. 2001c. Expression of interleukin-18 in human atherosclerotic plaques and relation to plaque instability. *Circulation.* 104:1598-1603.

Mancini A, Leone E, Festa R, Grande G, Silvestrini A, de Marinis L, Pontecorvi A, Maira G, Littarru GP, and Meucci E. *2008*. Effects of testosterone on antioxidant systems in male secondary hypogonadism. - *J Androl. 29(6):622-9.*

Mandal K, Jahangiri M, and Xu Q. *2005*. Autoimmune mechanisms of atherosclerosis. - *Handb Exp Pharmacol.;(170):723-43.*

Manolakou P, Angelopoulou R, Bakoyiannis C, and Bastounis E. *2009*. The effects of endogenous and exogenous androgens on cardiovascular disease risk factors and progression. - *Reprod Biol Endocrinol. 7:44.*

Mantovani A, Bonecchi R, and Locati M. *2006*. Tuning inflammation and immunity by chemokine sequestration: decoys and more. - *Nat Rev Immunol. 6(12):907-18.*

Martinet W, Knaapen MW, De Meyer GR, Herman AG, and Kockx MM. *2001*. Oxidative DNA damage and repair in experimental atherosclerosis are reversed by dietary lipid lowering. - *Circ Res. 88(7):733-9.*

Martinez FO, Helming L, and Gordon S. *2009*. Alternative activation of macrophages: an immunologic functional perspective. - *Annu Rev Immunol. 27:451-83.*

Martin-McNulty B, Tham DM, da Cunha V, Ho JJ, Wilson DW, Rutledge JC, Deng GG, Vergona R, Sullivan ME, and Wang YX. 17 *2003*. Beta-estradiol attenuates development of angiotensin II-induced aortic abdominal aneurysm in apolipoprotein E-deficient mice. - *Arterioscler Thromb Vasc Biol. 23(9):1627-32.*

Martinovic I, Abegunewardene N, Seul M, Vosseler M, Horstick G, Buerke M, Darius H, and Lindemann S. *2005*. Elevated monocyte chemoattractant protein-1 serum levels in patients at risk for coronary artery disease. - *Circ J. 69(12):1484-9.*

Massafra C, Gioia D, De Felice C, Picciolini E, De Leo V, Bonifazi M, and Bernabei A. *2000*. Effects of estrogens and androgens on erythrocyte antioxidant superoxide dismutase, catalase and glutathione peroxidase activities during the menstrual cycle. - *J Endocrinol. 167(3):447-52.*

Masuda A, Mathur R, and Halushka PV. *1991*. Testosterone increases thromboxane A2 receptors in cultured rat aortic smooth muscle cells. - *Circ Res. 69(3):638-43.*

Matsumiya T, Ota K, Imaizumi T, Yoshida H, Kimura H, and Satoh K. *2010*. Characterization of synergistic induction of CX3CL1/Fractalkine by TNF-alpha and IFN-gamma in vascular endothelial cells: an essential role for TNF-alpha in post-transcriptional regulation of CX3CL1. - *J Immunol. 184(8):4205-14.*

Maus U, Henning S, Wenschuh H, Mayer K, Seeger W, and Lohmeyer J. *2002*. Role of endothelial MCP-1 in monocyte adhesion to inflamed human endothelium under physiological flow. - *Am J Physiol Heart Circ Physiol. 283(6):H2584-91.*

McCredie, R.J., J.A. McCrohon, L. Turner, K.A. Griffiths, D.J. Handelsman, and D.S. Celermajer. 1998. Vascular reactivity is impaired in genetic females taking high-dose androgens. *J.Am.Coll.Cardiol.* 32:1331-1335.

McCrohon, J.A., W. Jessup, D.J. Handelsman, and D.S. Celermajer. 1999. Androgen exposure increases human monocyte adhesion to vascular endothelium and endothelial cell expression of vascular cell adhesion molecule-1. *Circulation.* 99:2317-2322.

McDermott DH, Yang Q, Kathiresan S, Cupples LA, Massaro JM, Keaney JF Jr, Larson MG, Vasan RS, Hirschhorn JN, O'Donnell CJ, Murphy PM, and Benjamin EJ. *2005.* CCL2 polymorphisms are associated with serum monocyte chemoattractant protein-1 levels and myocardial infarction in the Framingham Heart Study. - *Circulation. 112(8):1113-20.*

McDermott, D.H., A.M. Fong, Q. Yang, J.M. Sechler, L.A. Cupples, M.N. Merrell, P.W. Wilson, R.B. D'Agostino, C.J. O'Donnell, D.D. Patel, and P.M. Murphy. 2003. Chemokine receptor mutant CX3CR1-M280 has impaired adhesive function and correlates with protection from cardiovascular disease in humans. *J.Clin.Invest.* 111:1241-1250.

McDermott, D.H., J.P. Halcox, W.H. Schenke, M.A. Waclawiw, M.N. Merrell, N. Epstein, A.A. Quyyumi, and P.M. Murphy. 2001. Association between polymorphism in the chemokine receptor CX3CR1 and coronary vascular endothelial dysfunction and atherosclerosis. *Circ.Res.* 89:401-407.

McKay, L.I., and J.A. Cidlowski. 1999. Molecular control of immune/inflammatory responses: interactions between nuclear factor-kappa B and steroid receptor-signaling pathways. *Endocr.Rev.* 20:435-459.

McRobb L, Handelsman DJ, and Heather AK. *2009.* Androgen-induced progression of arterial calcification in apolipoprotein E-null mice is uncoupled from plaque growth and lipid levels. - *Endocrinology. 150(2):841-8.*

Merat S, Casanada F, Sutphin M, Palinski W, and Reaven PD. *1999.* Western-type diets induce insulin resistance and hyperinsulinemia in LDL receptor-deficient mice but do not increase aortic atherosclerosis compared with normoinsulinemic mice in which similar plasma cholesterol levels are achieved by a fructose-rich diet. - *Arterioscler Thromb Vasc Biol. 19(5):1223-30.*

Michos, E.D., D. Vaidya, S.M. Gapstur, P.J. Schreiner, S.H. Golden, N.D. Wong, M.H. Criqui, and P. Ouyang. 2008. Sex hormones, sex hormone binding globulin, and abdominal aortic calcification in women and men in the multi-ethnic study of atherosclerosis (MESA). *Atherosclerosis.* 200:432-438.

Midzak, A.S., H. Chen, V. Papadopoulos, and B.R. Zirkin. 2009. Leydig cell aging and the mechanisms of reduced testosterone synthesis. *Mol.Cell.Endocrinol.* 299:23-31.

Miller, V.M., and S.L. Mulvagh. 2007. Sex steroids and endothelial function: translating basic science to clinical practice. *Trends Pharmacol.Sci.* 28:263-270.

Mizutani N, Sakurai T, Shibata T, Uchida K, Fujita J, Kawashima R, Kawamura YI, Toyama-Sorimachi N, Imai T, and Dohi T. *2007.* Dose-dependent differential regulation of cytokine secretion from macrophages by fractalkine. - *J Immunol. 179(11):7478-87.*

Moatti, D., S. Faure, F. Fumeron, M. Amara, P. Seknadji, D.H. McDermott, P. Debre, M.C. Aumont, P.M. Murphy, D. de Prost, and C. Combadiere. 2001. Polymorphism in the fractalkine receptor CX3CR1 as a genetic risk factor for coronary artery disease. *Blood.* 97:1925-1928.

Montecucco F, and Mach F. *2009.* Atherosclerosis is an inflammatory disease. - *Semin Immunopathol. 31(1):1-3.*

Morey AK, Pedram A, Razandi M, Prins BA, Hu RM, Biesiada E, and Levin ER. *1997.* Estrogen and progesterone inhibit vascular smooth muscle proliferation. - *Endocrinology. 138(8):3330-9.*

Mosedale, D.E., D.J. Smith, S. Aitken, P.M. Schofield, S.C. Clarke, D. McNab, H. Goddard, C.R. Gale, C.N. Martyn, H.W.L. Bethell, C. Barnard, S. Hayns, C. Nugent, A. Panicker, and D.J. Grainger. 2005. Circulating levels of MCP-1 and eotaxin are not associated with presence of atherosclerosis or previous myocardial infarction. *Atherosclerosis.* 183:268-274.

Moss, M.L., S.-.C. Jin, J.D. Becherer, D.M. Bickett, W. Burkhart, W.-. Chen, D. Hassler, M.T. Leesnitzer, G. McGeehan, M. Milla, M. Moyer, W. Rocque, T. Seaton, F. Schoenen, J. Warner, and D. Willard. 1997. Structural features and biochemical properties of TNF-α converting enzyme (TACE). *J.Neuroimmunol.* 72:127-129.

Mourão, P.A.S., and C.A. Bracamonte. 1984. The binding of human aortic glycosaminoglycans and proteoglycans to plasma low density lipoproteins. *Atherosclerosis.* 50:133-146.

Mukherjee, T.K., H. Dinh, G. Chaudhuri, and L. Nathan. 2002. Testosterone attenuates expression of vascular cell adhesion molecule-1 by conversion to estradiol by aromatase in endothelial cells: implications in atherosclerosis. *Proc.Natl.Acad.Sci.U.S.A.* 99:4055-4060.

Muller, M., A.W. van den Beld, M.L. Bots, D.E. Grobbee, S.W. Lamberts, and Y.T. van der Schouw. 2004. Endogenous sex hormones and progression of carotid atherosclerosis in elderly men. *Circulation.* 109:2074-2079.

Murakami S, Kondo Y, Tomisawa K, and Nagate T. *1999.* Prevention of atherosclerotic lesion development in mice by taurine. - *Drugs Exp Clin Res.;25(5):227-34.*

Murakami, H., N. Harada, and H. Sasano. 2001. Aromatase in atherosclerotic lesions of human aorta. *J.Steroid Biochem.Mol.Biol.* 79:67-74.

Murphy AJ, and Woollard KJ. *2009.* High Density Lipoprotein - a Potent Inhibitor of Inflammation. - *Clin Exp Pharmacol Physiol. Nov 23.*

Murphy L, and O'Shaughnessy PJ. *1991.* Testicular steroidogenesis in the testicular feminized (Tfm) mouse: loss of 17 alpha-hydroxylase activity. - *J Endocrinol. 131(3):443-9.*

Musunuru K. *2010.* Atherogenic Dyslipidemia: Cardiovascular Risk and Dietary Intervention. - *Lipids. Jun 4.*

Naito Y, Tsujino T, Fujioka Y, Ohyanagi M, Okamura H, and Iwasaki T. *2002.* Increased circulating interleukin-18 in patients with congestive heart failure. - *Heart. 88(3):296-7.*

Nakagami, F., H. Nakagami, M.K. Osako, M. Iwabayashi, Y. Taniyama, T. Doi, H. Shimizu, M. Shimamura, H. Rakugi, and R. Morishita. 2010. Estrogen attenuates vascular remodeling in Lp(a) transgenic mice. *Atherosclerosis.* 211:41-47.

Nakamura, Y., T. Suzuki, K. Igarashi, J. Kanno, T. Furukawa, C. Tazawa, F. Fujishima, I. Miura, T. Ando, N. Moriyama, T. Moriya, H. Saito, S. Yamada, and H. Sasano. 2006. PTOV1: a novel testosterone-induced atherogenic gene in human aorta. *J.Pathol.* 209:522-531.

Napoli, C., F. de Nigris, S. Williams-Ignarro, O. Pignalosa, V. Sica, and L.J. Ignarro. 2006. Nitric oxide and atherosclerosis: An update. *Nitric Oxide.* 15:265-279.

Napoli, C., and L.J. Ignarro. 2001. Nitric Oxide and Atherosclerosis. *Nitric Oxide.* 5:88-97.

Narins, C.R., D.A. Lin, P.B. Burton, Z. Jin, and B.C. Berk. 2004. Interleukin-18 and interleukin-18 binding protein levels before and after percutaneous coronary intervention in patients with and without recent myocardial infarction. *Am.J.Cardiol.* 94:1285-1287.

Nathan, L., W. Shi, H. Dinh, T.K. Mukherjee, X. Wang, A.J. Lusis, and G. Chaudhuri. 2001. Testosterone inhibits early atherogenesis by conversion to estradiol: critical role of aromatase. *Proc.Natl.Acad.Sci.U.S.A.* 98:3589-3593.

Neish AS, Williams AJ, Palmer HJ, Whitley MZ, and Collins T. *1992.* Functional analysis of the human vascular cell adhesion molecule 1 promoter. - *J Exp Med. 176(6):1583-93.*

Nelken NA, Coughlin SR, Gordon D, and Wilcox JN. *1991.* Monocyte chemoattractant protein-1 in human atheromatous plaques. - *J Clin Invest. 88(4):1121-7.*

Neote K, DiGregorio D, Mak JY, Horuk R, and Schall TJ. *1993.* Molecular cloning, functional expression, and signaling characteristics of a C-C chemokine receptor. - *Cell. 72(3):415-25.*

Nettleship, J.E. 2006. The Effect of Testosterone Upon Fatty Streak Formation in the Testicular Feminised Mouse. PhD Biomedical Sciences, The University of Sheffield.

Nettleship, J.E., T.H. Jones, K.S. Channer, and R.D. Jones. 2007a. Physiological Testosterone Replacement Therapy Attenuates Fatty Streak Formation and Improves High-Density Lipoprotein Cholesterol in the Tfm Mouse. An Effect That Is Independent of the Classic Androgen Receptor. *Circulation.* 116(21):2427-34.

Nettleship, J.E., P.J. Pugh, K.S. Channer, T. Jones, and R.D. Jones. 2007b. Inverse relationship between serum levels of interleukin-1beta and testosterone in men with stable coronary artery disease. *Horm.Metab.Res.* 39:366-371.

Ng, M.K.C., C.M. Quinn, J.A. McCrohon, S. Nakhla, W. Jessup, D.J. Handelsman, D.S. Celermajer, and A.K. Death. 2003. Androgens Up-Regulate Atherosclerosis-Related Genes in Macrophages From Males But Not Females: Molecular Insights Into Gender Differences in Atherosclerosis. *Journal of the American College of Cardiology.* 42:1306-1313.

Nibbs RJ, Wylie SM, Pragnell IB, and Graham GJ. *1997.* Cloning and characterization of a novel murine beta chemokine receptor, D6. Comparison to three other related macrophage inflammatory protein-1alpha receptors, CCR-1, CCR-3, and CCR-5. - *J Biol Chem. 272(19):12495-504.*

Niessner A, Marculescu R, Haschemi A, Endler G, Zorn G, Weyand CM, Maurer G, Mannhalter C, Wojta J, Wagner O, and Huber K. *2005.* Opposite effects of CX3CR1 receptor polymorphisms V249I and T280M on the development of acute coronary syndrome. A possible implication of fractalkine in inflammatory activation. - *Thromb Haemost. 93(5):949-54.*

Nieto M, Navarro F, Perez-Villar JJ, del Pozo MA, Gonzalez-Amaro R, Mellado M, Frade JM, Martinez-A C, Lopez-Botet M, and Sanchez-Madrid F. *1998.* Roles of chemokines and receptor polarization in NK-target cell interactions. - *J Immunol. 161(7):3330-9.*

Nikkari ST, O'Brien KD, Ferguson M, Hatsukami T, Welgus HG, Alpers CE, and Clowes AW. *1995.* Interstitial collagenase (MMP-1) expression in human carotid atherosclerosis. - *Circulation. 92(6):1393-8.*

Nishiyama T, Ishizaki F, Anraku T, Shimura H, and Takahashi K. *2005.* The influence of androgen deprivation therapy on metabolism in patients with prostate cancer. - *J Clin Endocrinol Metab. 90(2):657-60.*

Nolan JP, and Yang L. *2007.* The flow of cytometry into systems biology. - *Brief Funct Genomic Proteomic. 6(2):81-90.*

Nomiyama, H., T. Imai, J. Kusuda, R. Miura, D.F. Callen, and O. Yoshie. 1998. Human chemokines fractalkine (SCYD1), MDC (SCYA22) and TARC (SCYA17) are clustered on chromosome 16q13. *Cytogenet.Cell Genet.* 81:10-11.

Norata, G.D., G. Tibolla, P.M. Seccomandi, A. Poletti, and A.L. Catapano. 2006. Dihydrotestosterone decreases tumor necrosis factor-alpha and lipopolysaccharide-induced inflammatory response in human endothelial cells. *J.Clin.Endocrinol.Metab.* 91:546-554.

Norata, G.D., P. Cattaneo, A. Poletti, and A.L. Catapano. 2010. The androgen derivative 5α-androstane-3β,17β-diol inhibits tumor necrosis factor α and lipopolysaccharide induced inflammatory response in human endothelial cells and in mice aorta. *Atherosclerosis.* 212(1):100-6.

O'Brien KD, Gordon D, Deeb S, Ferguson M, and Chait A. *1992.* Lipoprotein lipase is synthesized by macrophage-derived foam cells in human coronary atherosclerotic plaques. - *J Clin Invest. 89(5):1544-50.*

Ochensberger B, Tassera L, Bifrare D, Rihs S, and Dahinden CA. *1999.* Regulation of cytokine expression and leukotriene formation in human basophils by growth factors, chemokines and chemotactic agonists. - *Eur J Immunol. 29(1):11-22.*

Oemar BS, Tschudi MR, Godoy N, Brovkovich V, Malinski T, and Luscher TF. *1998.* Reduced endothelial nitric oxide synthase expression and production in human atherosclerosis. - *Circulation. 97(25):2494-8.*

Ogunrinade O, Kameya GT, and Truskey GA. *2002.* Effect of fluid shear stress on the permeability of the arterial endothelium. - *Ann Biomed Eng. 30(4):430-46.*

Ohman MK, and Eitzman DT. *2009.* Targeting MCP-1 to reduce vascular complications of obesity. - *Recent Pat Cardiovasc Drug Discov. 4(3):164-76.*

Ohmori Y, Schreiber RD, and Hamilton TA. *1997.* Synergy between interferon-gamma and tumor necrosis factor-alpha in transcriptional activation is mediated by cooperation between signal transducer and activator of transcription 1 and nuclear factor kappaB. - *J Biol Chem. 272(23):14899-907.*

Okamura, T., Y. Kokubo, M. Watanabe, A. Higashiyama, Y. Miyamoto, Y. Yoshimasa, and A. Okayama. 2009. Low-density lipoprotein cholesterol and non-high-density lipoprotein

cholesterol and the incidence of cardiovascular disease in an urban Japanese cohort study: The Suita study. *Atherosclerosis.* 203:587-592.

Okumoto S, Taniguchi Y, Nakashima A, Masaki T, Ito T, Ogawa T, Takasugi N, Kohno N, and Yorioka N. *2009.* C-C chemokine receptor 2 expression by circulating monocytes influences atherosclerosis in patients on chronic hemodialysis. - *Ther Apher Dial. 13(3):205-12.*

Oliveira, R.T.D.d., R.L. Mamoni, J.R.M. Souza, J.L. Fernandes, F.J.O. Rios, M. Gidlund, O.R. Coelho, and M.H.S.L. Blotta. 2009. Differential expression of cytokines, chemokines and chemokine receptors in patients with coronary artery disease. *Int.J.Cardiol.* 136:17-26.

Ollivier, V., S. Faure, N. Tarantino, S. Chollet-Martin, P. Deterre, C. Combadière, and D. de Prost. 2003. Fractalkine/CX3CL1 production by human aortic smooth muscle cells impairs monocyte procoagulant and inflammatory responses. *Cytokine.* 21:303-311.

Orekhov A, Sobenin I, and Smirnov. 2009. Sex hormones decrease intracellular cholesterol accumulation caused by modified lipoprotein. Atherosclerosis Supplement. 10(2):P1136. Boston MA, USA.

Orio, F., B. Térouanne, V. Georget, S. Lumbroso, C. Avances, C. Siatka, and C. Sultan. 2002. Potential action of IGF-1 and EGF on androgen receptor nuclear transfer and transactivation in normal and cancer human prostate cell lines. *Mol.Cell.Endocrinol.* 198:105-114.

OuYang P, Peng LS, Yang H, Wu WY, and Xu AL. *2002.* [Recombinant human interleukin-10 inhibits vascular smooth muscle cell proliferation induced by TNF-alpha]. - *Sheng Li Xue Bao. 54(1):79-82.*

Ouyang, P., E.D. Michos, and R.H. Karas. 2006. Hormone Replacement Therapy and the Cardiovascular System: Lessons Learned and Unanswered Questions. *J.Am.Coll.Cardiol.* 47:1741-1753.

Packard RR, Lichtman AH, and Libby P. *2009.* Innate and adaptive immunity in atherosclerosis. - *Semin Immunopathol. 31(1):5-22.*

Paddock SW. *2000.* Principles and practices of laser scanning confocal microscopy. - *Mol Biotechnol. 16(2):127-49.*

Page ST, Amory JK, Bowman FD, Anawalt BD, Matsumoto AM, Bremner WJ, and Tenover JL. *2005.* Exogenous testosterone (T) alone or with finasteride increases physical performance, grip strength, and lean body mass in older men with low serum T. - *J Clin Endocrinol Metab. 90(3):1502-10.*

Paigen B, Morrow A, Holmes PA, Mitchell D, and Williams RA. *1987.* Quantitative assessment of atherosclerotic lesions in mice. - *Atherosclerosis. 68(3):231-40.*

Paigen, B., A. Morrow, C. Brandon, D. Mitchell, and P. Holmes. 1985. Variation in susceptibility to atherosclerosis among inbred strains of mice. *Atherosclerosis.* 57:65-73.

Paludan SR. *2000.* Synergistic action of pro-inflammatory agents: cellular and molecular aspects. - *J Leukoc Biol. 67(1):18-25.*

Pan S. *2009.* Molecular mechanisms responsible for the atheroprotective effects of laminar shear stress. - *Antioxid Redox Signal. 11(7):1669-82.*

Panet-Raymond, V., B. Gottlieb, L.K. Beitel, L. Pinsky, and M.A. Trifiro. 2000. Interactions between androgen and estrogen receptors and the effects on their transactivational properties. *Mol.Cell.Endocrinol.* 167:139-150.

Papadopoulos EJ, Sassetti C, Saeki H, Yamada N, Kawamura T, Fitzhugh DJ, Saraf MA, Schall T, Blauvelt A, Rosen SD, and Hwang ST. *1999.* Fractalkine, a CX3C chemokine, is expressed by dendritic cells and is up-regulated upon dendritic cell maturation. - *Eur J Immunol. 29(8):2551-9.*

Parissis JT, Adamopoulos S, Venetsanou KF, Mentzikof DG, Karas SM, and Kremastinos DT. *2002.* Serum profiles of C-C chemokines in acute myocardial infarction: possible implication in postinfarction left ventricular remodeling. - *J Interferon Cytokine Res. 22(2):223-9.*

Pasterkamp G, Schoneveld AH, van der Wal AC, Hijnen DJ, van Wolveren WJ, Plomp S, Teepen HL, and Borst C. *1999.* Inflammation of the atherosclerotic cap and shoulder of the plaque is a common and locally observed feature in unruptured plaques of femoral and coronary arteries. - *Arterioscler Thromb Vasc Biol. 19(1):54-8.*

Patel, A., V.P. Jagadesham, K.E. Porter, D.J.A. Scott, and S.R. Carding. 2008. Characterisation of Fractalkine/CX3CL1 and Fractalkine Receptor (CX3CR1) Expression in Abdominal Aortic Aneurysm Disease. *European Journal of Vascular and Endovascular Surgery.* 36:20-27.

Patel, R.P., D. Moellering, J. Murphy-Ullrich, H. Jo, J.S. Beckman, and V.M. Darley-Usmar. 2000. Cell signaling by reactive nitrogen and oxygen species in atherosclerosis. *Free Radical Biology and Medicine.* 28:1780-1794.

Paulsson G, Zhou X, Tornquist E, and Hansson GK. *2000.* Oligoclonal T cell expansions in atherosclerotic lesions of apolipoprotein E-deficient mice. - *Arterioscler Thromb Vasc Biol. 20(1):10-7.*

Pawlak, K., D. Pawlak, S. Brzosko, and M. Mysliwiec. 2006. Carotid atherosclerosis is associated with enhanced β-chemokine levels in patients on continuous ambulatory peritoneal dialysis. *Atherosclerosis.* 186:146-151.

Penalva RA, Huoya Mde O, Correia LC, Feitosa GS, and Ladeia AM. *2008.* Lipid profile and intensity of atherosclerosis disease in acute coronary syndrome. - *Arq Bras Cardiol. 90(1):24-30.*

Perros, F., P. Dorfmuller, R. Souza, I. Durand-Gasselin, V. Godot, F. Capel, S. Adnot, S. Eddahibi, M. Mazmanian, E. Fadel, P. Herve, G. Simonneau, D. Emilie, and M. Humbert. 2007. Fractalkine-induced smooth muscle cell proliferation in pulmonary hypertension. *Eur.Respir.J.* 29:937-943.

Pfeiffer, M.J., and J.A. Schalken. 2010. Stem Cell Characteristics in Prostate Cancer Cell Lines. *Eur.Urol.* 57:246-255.

Phillips GB. Is atherosclerotic cardiovascular disease an endocrinological disorder? The estrogen-androgen paradox. - *J Clin Endocrinol Metab.2005 may;90(5):2708-11.*

Phillips GB, Jing TY, Resnick LM, Barbagallo M, Laragh JH, and Sealey JE. *1993.* Sex hormones and hemostatic risk factors for coronary heart disease in men with hypertension. - *J Hypertens. 11(7):699-702.*

Phillips GB, Pinkernell BH, T.Y. and Jing TY. *1994.* The association of hypotestosteronemia with coronary artery disease in men. - *Arterioscler Thromb. 14(5):701-6.*

Phipps, R.P. 2000. Atherosclerosis: the emerging role of inflammation and the CD40-CD40 ligand system. *Proc.Natl.Acad.Sci.U.S.A.* 97:6930-6932. .

Ping D, Jones PL, and Boss JM. *1996.* TNF regulates the in vivo occupancy of both distal and proximal regulatory regions of the MCP-1/JE gene. - *Immunity. 4(5):455-69.*

Post W, Bielak LF, Ryan KA, Cheng YC, Shen H, Rumberger JA, Sheedy PF 2nd, Shuldiner AR, Peyser PA, and Mitchell BD. *2007.* Determinants of coronary artery and aortic calcification in the Old Order Amish. - *Circulation. 115(6):717-24.*

Pratt WB, and Toft DO. *1997.* Steroid receptor interactions with heat shock protein and immunophilin chaperones. - *Endocr Rev. 18(3):306-60.*

Pritchard KA Jr, Groszek L, Smalley DM, Sessa WC, Wu M, Villalon P, Wolin MS, and Stemerman MB. *1995.* Native low-density lipoprotein increases endothelial cell nitric oxide synthase generation of superoxide anion. - *Circ Res. 77(3):510-8.*

Pugh P.J., English K.M., Jones T.H.and K.S. Channer. *2000.* Testosterone: a natural tonic for the failing heart? *QJM.* 93:689-694.

Pugh PJ, Jones RD, Jones TH, and Channer KS. *2002.* Heart failure as an inflammatory condition: potential role for androgens as immune modulators. *Eur J Heart Failure. 4:673-680.*

Pugh P.J., Jones R.D., Malkin C.J., Hall J., Nettleship J.E., Kerry K.E., Jones T.H., and Channer K.S. 2005. Physiologic testosterone therapy has no effect on serum levels of tumour necrosis factor-alpha in men with chronic heart failure. *Endocr.Res.* 31:271-283.

Pugh P.J., Jones R.D., West, J.N. Jones T.H., and Channer K.S. *2004.* Testosterone treatment for men with chronic heart failure. *Heart.* 90:446-447.

Pugh PJ, Jones TH, and Channer KS. *2003* Acute haemodynamic effects of testosterone in men with chronic heart failure. - *Eur Heart J. 24(10):909-15.*

Puren AJ, Fantuzzi G, Gu Y, Su MS, and Dinarello CA. *1998.* Interleukin-18 (IFNgamma-inducing factor) induces IL-8 and IL-1beta via TNFalpha production from non-CD14+ human blood mononuclear cells. - *J Clin Invest. 101(3):711-21.*

Qui Y, Yanase T, Hu H, Tanaka T, Nishi Y, Liu M, Sueishi K, Sawamura T, and Nawata H. *2010.* Dihydrotestosterone suppresses foam cell formation and attenuates atherosclerosis development. *Endocrinology. 151(7):3307-3316.*

Radcliff G, and Jaroszeski MJ. *1998.* Basics of flow cytometry. - *Methods Mol Biol.;91:1-24.*

Ragbir S, and Farmer JA. *2010.* Dysfunctional High-Density Lipoprotein and Atherosclerosis. - *Curr Atheroscler Rep. may 27.*

Rajagopalan, S., X.P. Meng, S. Ramasamy, D.G. Harrison, and Z.S. Galis. 1996. Reactive oxygen species produced by macrophage-derived foam cells regulate the activity of vascular matrix metalloproteinases in vitro. Implications for atherosclerotic plaque stability. *J.Clin.Invest.* 98:2572-2579.

Rajavashisth T, Qiao JH, Tripathi S, Tripathi J, Mishra N, Hua M, Wang XP, Loussararian A, Clinton S, Libby P, and Lusis A. *1998.* Heterozygous osteopetrotic (op) mutation reduces atherosclerosis in LDL receptor- deficient mice. - *J Clin Invest. 101(12):2702-10.*

Rajavashisth, T.B., A. Andalibi, M.C. Territo, J.A. Berliner, M. Navab, A.M. Fogelman, and A.J. Lusis. 1990. Induction of endothelial cell expression of granulocyte and macrophage colony-stimulating factors by modified low-density lipoproteins. *Nature.* 344:254-257.

Rajesh M, Mukhopadhyay P, Hasko G, Huffman JW, K. Mackie K, and Pacher P. *2008.* CB2 cannabinoid receptor agonists attenuate TNF-alpha-induced human vascular smooth muscle cell proliferation and migration. - *Br J Pharmacol. 153(2):347-57.*

Ramana, K.V., A. Bhatnagar, and S.K. Srivastava. 2004. Aldose reductase regulates TNF-α-induced cell signaling and apoptosis in vascular endothelial cells. *FEBS Lett.* 570:189-194.

Randolph GJ, and Furie MB. *1996.* Mononuclear phagocytes egress from an in vitro model of the vascular wall by migrating across endothelium in the basal to apical direction: role of intercellular adhesion molecule 1 and the CD11/CD18 integrins. - *J Exp Med. 183(2):451-62.*

Rang, H.P., M. Dale, and J.M. Ritter. 1999. Pharmacology. Churchill Livingston.

Ranjbaran, H., S.I. Sokol, A. Gallo, R.E. Eid, A.O. Iakimov, A. D'Alessio, J.R. Kapoor, S. Akhtar, C.J. Howes, M. Aslan, S. Pfau, J.S. Pober, and G. Tellides. 2007. An inflammatory pathway of IFN-gamma production in coronary atherosclerosis. *J.Immunol.* 178:592-604.

Rayner M, Allender S, and Scarborough P. *2009.* Cardiovascular disease in Europe. - *Eur J Cardiovasc Prev Rehabil. 16 Suppl 2:S43-7.*

Rayner, M., C. Mockford, and A. Boaz. 1998. Coronary heart disease statistics. In: British heart foundation statistics database. .

Read MA, Whitley MZ, Williams AJ, and Collins T. *1994.* NF-kappa B and I kappa B alpha: an inducible regulatory system in endothelial activation. - *J Exp Med. 179(2):503-12.*

Reape, T.J., and P.H. Groot. 1999. Chemokines and atherosclerosis. *Atherosclerosis.* 147:213-225.

Reckelhoff JF, Zhang H, and Srivastava K. *2000.* Gender differences in development of hypertension in spontaneously hypertensive rats: role of the renin-angiotensin system. - *Hypertension. 35(1 Pt 2):480-3.*

Reiss AB, Patel CA, Rahman MM, Chan ES, Hasneen K, Montesinos MC, Trachman JD, and Cronstein BN. *2004.* Interferon-gamma impedes reverse cholesterol transport and promotes foam cell transformation in THP-1 human monocytes/macrophages. - *Med Sci Monit. 10(11):BR420-5.*

Ridker PM, Rifai N, Pfeffer M, Sacks F, Lepage S, and Braunwald E. *2000a* . Elevation of tumor necrosis factor-alpha and increased risk of recurrent coronary events after myocardial infarction. - *Circulation. 101(18):2149-53.*

Ridker PM, Rifai N, Stampfer MJ, and Hennekens CH. *2000b.* Plasma concentration of interleukin-6 and the risk of future myocardial infarction among apparently healthy men. - *Circulation. 101(15):1767-72.*

Rizzo, M., J. Kotur-Stevuljevic, K. Berneis, G. Spinas, G.B. Rini, Z. Jelic-Ivanovic, V. Spasojevic-Kalimanovska, and J. Vekic. 2009. Atherogenic dyslipidemia and oxidative stress: a new look. *Translational Research.* 153:217-223.

Roden AC, Moser MT, Tri SD, Mercader M, Kuntz SM, Dong H, Hurwitz AA, McKean DJ, Celis E, Leibovich BC, Allison JP, and Kwon ED. *2004.* Augmentation of T cell levels and responses induced by androgen deprivation. *J Immunol. 15;173(10):6098-108.*

Rollins BJ, Yoshimura T, Leonard EJ, and Pober JS. *1990.* Cytokine-activated human endothelial cells synthesize and secrete a monocyte chemoattractant, MCP-1/JE. - *Am J Pathol. 136(6):1229-33.*

Rollins, B.J. 1997. Chemokines. *Blood.* 90:909-928.

Rommerts, F.F.G. 2004. Testosterone: an overview of biosynthesis, transport, metabolism and non-genomic actions. *In* Testosterone: Actions, Deficiency, Substitution. E. Nieschlag and H.M. Behre, editors. Cambridge University, UK.

Rosano GM, Sheiban I, Massaro R, Pagnotta P, Marazzi G, Vitale C, Mercuro G, Volterrani M, Aversa A, and Fini M. *2007.* Low testosterone levels are associated with coronary artery disease in male patients with angina. - *Int J Impot Res. 19(2):176-82.*

Rosano, G.M., F. Leonardo, P. Pagnotta, F. Pelliccia, G. Panina, E. Cerquetani, P.L. della Monica, B. Bonfigli, M. Volpe, and S.L. Chierchia. 1999. Acute anti-ischemic effect of testosterone in men with coronary artery disease. *Circulation.* 99:1666-1670.

Rosner D, Stoneman V, Littlewood T, McCarthy N, Figg N, Wang Y, Tellides G, and Bennett M. *2006* . Interferon-gamma induces Fas trafficking and sensitization to apoptosis in vascular smooth muscle cells via a PI3K- and Akt-dependent mechanism. - *Am J Pathol. 168(6):2054-63.*

Rosner W, Hryb DJ, Khan MS, Nakhla AM, and Romas NA. *1992.* Sex hormone-binding globulin. Binding to cell membranes and generation of a second messenger. - *J Androl. 13(2):101-6.*

Rottem S, and Yogev D. *2000.* Mycoplasma interaction with eukaryotic cells. - *Subcell Biochem.;33:199-227.*

Ruan, H., and H.F. Lodish. 2003. Insulin resistance in adipose tissue: direct and indirect effects of tumor necrosis factor-α. *Cytokine Growth Factor Rev.* 14:447-455.

Rus HG, Niculescu F, and Vlaicu R. *1991.* Tumor necrosis factor-alpha in human arterial wall with atherosclerosis. - *Atherosclerosis. 89(2-3):247-54.*

Ruth JH, Volin MV, Haines GK 3rd, Woodruff DC, Katschke KJ Jr, Woods JM, Park CC, Morel JC, and Koch AE. *2001.* Fractalkine, a novel chemokine in rheumatoid arthritis and in rat adjuvant-induced arthritis. - *Arthritis Rheum. 44(7):1568-81.*

Ryu J, Lee CW, Hong KH, Shin JA, Lim SH, Park CS, Shim J, Nam KB, Choi KJ, Kim YH, and Han KH. *2008.* Activation of fractalkine/CX3CR1 by vascular endothelial cells induces angiogenesis through VEGF-A/KDR and reverses hindlimb ischaemia. - *Cardiovasc Res. 78(2):333-40.*

Saad F, Gooren L, Haider A, A. and Yassin A. *2008.* Effects of testosterone gel followed by parenteral testosterone undecanoate on sexual dysfunction and on features of the metabolic syndrome. - *Andrologia. 40(1):44-8.*

Saad F, Gooren LJ, Haider A, and Yassin A. *2008.* A dose-response study of testosterone on sexual dysfunction and features of the metabolic syndrome using testosterone gel and parenteral testosterone undecanoate. - *J Androl. 29(1):102-5.*

Saad F, Gooren L, Haider A, and Yassin A. *2007b.* An exploratory study of the effects of 12 month administration of the novel long-acting testosterone undecanoate on measures of sexual function and the metabolic syndrome. - *Arch Androl. 53(6):353-7.*

Saederup N, Chan L, Lira SA, and Charo IF. *2008.* Fractalkine deficiency markedly reduces macrophage accumulation and atherosclerotic lesion formation in CCR2-/- mice: evidence for independent chemokine functions in atherogenesis. - *Circulation. 117(13):1642-8.*

Sahar, S., R.S. Dwarakanath, M.A. Reddy, L. Lanting, I. Todorov, and R. Natarajan. 2005. Angiotensin II enhances interleukin-18 mediated inflammatory gene expression in vascular smooth muscle cells: a novel cross-talk in the pathogenesis of atherosclerosis. *Circ.Res.* 96:1064-1071.

Saigal CS, Gore JL, Krupski TL, Hanley J, Schonlau M, and Litwin MS. *2007.* Androgen deprivation therapy increases cardiovascular morbidity in men with prostate cancer. - *Cancer. 110(7):1493-500.*

Salcedo, R., M.L. Ponce, H.A. Young, K. Wasserman, J.M. Ward, H.K. Kleinman, J.J. Oppenheim, and W.J. Murphy. 2000. Human endothelial cells express CCR2 and respond to MCP-1: direct role of MCP-1 in angiogenesis and tumor progression. *Blood.* 96:34-40.

Sambrook, J., and D.W. Russel. 2001. Molecular Cloning: A Laboratory Manual. CSH Laboratory Press, Cold Spring Harbour, NY.

Sandhu KS, and Acharya KK. *2005.* ExPrimer: to design primers from exon--exon junctions. - *Bioinformatics. 21(9):2091-2.*

Sandison, D.R., and W.W. Webb. 1994. Background rejection and signal-to-noise optimization in confocal and alternative fluorescence microscopes. *Appl. Opt.* 33:603-615.

Schafer A, Schulz C, Eigenthaler M, Fraccarollo D, Kobsar A, Gawaz M, Ertl G, Walter U, and Bauersachs J. *2004.* Novel role of the membrane-bound chemokine fractalkine in platelet activation and adhesion. - *Blood. 103(2):407-12.*

Schecter AD, Berman AB, Yi L, Ma H, Daly CM, Soejima K, Rollins BJ, Charo IF, and Taubman MB. *2004.* MCP-1-dependent signaling in CCR2(-/-) aortic smooth muscle cells. - *J Leukoc Biol. 75(6):1079-85.*

Schlitt A, Heine GH, Blankenberg S, Espinola-Klein C, Dopheide JF, Bickel C, Lackner KJ, Iz M, Meyer J, Darius H, and Rupprecht HJ. *2004.* CD14+CD16+ monocytes in coronary artery disease and their relationship to serum TNF-alpha levels. - *Thromb Haemost. 92(2):419-24.*

Schlondorff J, Becherer JD, and Blobel CP. *2000.* Intracellular maturation and localization of the tumour necrosis factor alpha convertase (TACE). - *Biochem J. 347 Pt 1:131-8.*

Schneider G, Kirschner MA, Berkowitz R, and Ertel NH. *1979.* Increased estrogen production in obese men. - *J Clin Endocrinol Metab. 48(4):633-8.*

Schonbeck, U., F. Mach, G.K. Sukhova, C. Murphy, J.Y. Bonnefoy, R.P. Fabunmi, and P. Libby. 1997. Regulation of matrix metalloproteinase expression in human vascular smooth muscle cells by T lymphocytes: a role for CD40 signaling in plaque rupture? *Circ.Res.* 81:448-454.

Schulte, A., B. Schulz, M.G. Andrzejewski, C. Hundhausen, S. Mletzko, J. Achilles, K. Reiss, K. Paliga, C. Weber, S. Rose John, and A. Ludwig. 2007. Sequential processing of the transmembrane chemokines CX3CL1 and CXCL16 by α- and γ-secretases. *Biochem.Biophys.Res.Commun.* 358:233-240.

Schulz, C., A. Schafer, M. Stolla, S. Kerstan, M. Lorenz, M.L. von Bruhl, M. Schiemann, J. Bauersachs, T. Gloe, D.H. Busch, M. Gawaz, and S. Massberg. 2007. Chemokine fractalkine mediates leukocyte recruitment to inflammatory endothelial cells in flowing whole blood: a critical role for P-selectin expressed on activated platelets. *Circulation.* 116:764-773.

Schwarz N, Pruessmeyer J, Hess FM, Dreymueller D, Pantaler E, Koelsch A, Windoffer R, Voss M, Sarabi A, Weber C, Sechi AS, Uhlig S, and Ludwig A. *2010.* Requirements for leukocyte transmigration via the transmembrane chemokine CX3CL1. - *Cell Mol Life Sci. Jun 18.*

Seimon T, I. FAU - Tabas, and Tabas I. *2009.* Mechanisms and consequences of macrophage apoptosis in atherosclerosis. - *J Lipid Res. 50 Suppl:S382-7.*

Sekido, R. 2010. SRY: A transcriptional activator of mammalian testis determination. *Int.J.Biochem.Cell Biol.* 42:417-420.

Seta Y, Kanda T, Tanaka T, Arai M, Sekiguchi K, Yokoyama T, Kurimoto M, Tamura J, and Kurabayashi M. *2000.* Interleukin 18 in acute myocardial infarction. - *Heart. 84(6):668.*

Shahani S, Braga-Basaria M, and Basaria S. *2008.* Androgen deprivation therapy in prostate cancer and metabolic risk for atherosclerosis. - *J Clin Endocrinol Metab. 93(6):2042-9.*

Shimada K. *2009.* Immune system and atherosclerotic disease. - *Circ J. 73(6):994-1001.*

Shin WS, Hong YH, Peng HB, De Caterina R, Libby P, and Liao JK. *1996.* Nitric oxide attenuates vascular smooth muscle cell activation by interferon-gamma. The role of constitutive NF-kappa B activity. - *J Biol Chem. 271(19):11317-24.*

Shyy YJ, Hsieh HJ, Usami S, and Chien S. *1994.* Fluid shear stress induces a biphasic response of human monocyte chemotactic protein 1 gene expression in vascular endothelium. - *Proc Natl Acad Sci U S A. 91(11):4678-82.*

Sica A, Wang JM, Colotta F, Dejana E, Mantovani A, Oppenheim JJ, Larsen CG, Zachariae CO, and Matsushima K. *1990.* Monocyte chemotactic and activating factor gene expression induced in endothelial cells by IL-1 and tumor necrosis factor. - *J Immunol. 144(8):3034-8.*

Siegel-Axel D, Daub K, Seizer P, Lindemann S, and Gawaz M. *2008.* Platelet lipoprotein interplay: trigger of foam cell formation and driver of atherosclerosis. - *Cardiovasc Res. 78(1):8-17.*

Silverthorn, D.U. 1997. Human Physiology: An Intergrated Approach. Benjamin Cummings. 783 pp.

Sima AV, Stancu CS, and Simionescu M. *2009.* Vascular endothelium in atherosclerosis. - *Cell Tissue Res. 335(1):191-203.*

Simon D, Charles MA, Nahoul K, Orssaud G, Kremski J, Hully V, Joubert E, Papoz L, and Eschwege E. *1997*. Association between plasma total testosterone and cardiovascular risk factors in healthy adult men: The Telecom Study. - *J Clin Endocrinol Metab. 82(2):682-5.*

Simoncini, T., S. Maffei, G. Basta, G. Barsacchi, A.R. Genazzani, J.K. Liao, and R. De Caterina. 2000. Estrogens and glucocorticoids inhibit endothelial vascular cell adhesion molecule-1 expression by different transcriptional mechanisms. *Circ.Res.* 87:19-25.

Singh R, Artaza JN, Taylor WE, Gonzalez-Cadavid NF, and Bhasin S. *2003*. Androgens stimulate myogenic differentiation and inhibit adipogenesis in C3H 10T1/2 pluripotent cells through an androgen receptor-mediated pathway. - *Endocrinology. 144(11):5081-8.*

Singh, R.J.R., J.C. Mason, E.A. Lidington, D.R. Edwards, R.K. Nuttall, R. Khokha, V. Knauper, G. Murphy, and J. Gavrilovic. 2005. Cytokine stimulated vascular cell adhesion molecule-1 (VCAM-1) ectodomain release is regulated by TIMP-3. *Cardiovascular Research.* 67:39-49.

Skalen K, Gustafsson M, Rydberg EK, Hulten LM, Wiklund O, Innerarity TL, and Boren J. *2002*. Subendothelial retention of atherogenic lipoproteins in early atherosclerosis. - *Nature. 417(6890):750-4.*

Skalli O, Ropraz P, Trzeciak A, Benzonana G, Gillessen D, and Gabbiani G. *1986*. A monoclonal antibody against alpha-smooth muscle actin: a new probe for smooth muscle differentiation. - *J Cell Biol. 103(6 Pt 2):2787-96.*

Skoog T, Dichtl W, Boquist S, Skoglund-Andersson C, Karpe F, Tang R, Bond MG, de Faire U, Nilsson J, Eriksson P, and Hamsten A. *2002*. Plasma tumour necrosis factor-alpha and early carotid atherosclerosis in healthy middle-aged men. - *Eur Heart J. 23(5):376-83.*

Smith JC, Bennett S, Evans LM, Kynaston HG, Parmar M, Mason MD, J.R. Cockcroft JR, Scanlon MF, and Davies JS. *2001*. The effects of induced hypogonadism on arterial stiffness, body composition, and metabolic parameters in males with prostate cancer. - *J Clin Endocrinol Metab. 86(9):4261-7.*

Smith MR. *2008*. Androgen deprivation therapy and risk for diabetes and cardiovascular disease in prostate cancer survivors. - *Curr Urol Rep. 9(3):197-202.*

Snapp KR, Craig R, Herron M, Nelson RD, Stoolman LM, and Kansas GS. *1998*. Dimerization of P-selectin glycoprotein ligand-1 (PSGL-1) required for optimal recognition of P-selectin. - *J Cell Biol. 142(1):263-70.*

Snyder PJ, Peachey H, Hannoush P, Berlin JA, Loh L, Lenrow DA, Holmes JH, Dlewati A, Santanna J, Rosen CJ, and Strom BL. *1999*. Effect of testosterone treatment on body composition and muscle strength in men over 65 years of age. - *J Clin Endocrinol Metab. 84(8):2647-53.*

Sozzani S, Luini W, Borsatti A, Polentarutti N, Zhou D, Piemonti L, D'Amico G, Power CA, Wells TN, Gobbi M, Allavena P, and Mantovani A. *1997*. Receptor expression and responsiveness of human dendritic cells to a defined set of CC and CXC chemokines. - *J Immunol. 159(4):1993-2000.*

Spayd RW, Bruschi B, Burdick BA, Dappen GM, Eikenberry JN, Esders TW, Figueras J, Goodhue CT, LaRossa DD, Nelson RW, Rand RN, and Wu TW. *1978*. Multilayer film elements for clinical analysis: applications to representative chemical determinations. - *Clin Chem. 24(8):1343-50.*

Spinedi E, Suescun MO, Hadid R, Daneva T, and Gaillard RC. *1992.* Effects of gonadectomy and sex hormone therapy on the endotoxin-stimulated hypothalamo-pituitary-adrenal axis: evidence for a neuroendocrine-immunological sexual dimorphism. - *Endocrinology. 131(5):2430-6.*

Spyridopoulos I, Sullivan AB, Kearney M, Isner JM, and Losordo DW. *1997.* Estrogen-receptor-mediated inhibition of human endothelial cell apoptosis. Estradiol as a survival factor. - *Circulation. 95(6):1505-14.*

Stanworth RD, Tand Jones TH. *2009.* Testosterone in obesity, metabolic syndrome and type 2 diabetes. - *Front Horm Res.;37:74-90.*

Stein, B., and M.X. Yang. 1995. Repression of the interleukin-6 promoter by estrogen receptor is mediated by NF-kappa B and C/EBP beta. *Mol.Cell.Biol.* 15:4971-4979.

Stemme S, Faber B, Holm J, Wiklund O, Witztum JL, and Hansson GK. *1995.* T lymphocytes from human atherosclerotic plaques recognize oxidized low density lipoprotein. - *Proc Natl Acad Sci U S A. 92(9):3893-7.*

Stetler-Stevenson WG, Krutzsch HC, and Liotta LA. *1989.* Tissue inhibitor of metalloproteinase (TIMP-2). A new member of the metalloproteinase inhibitor family. - *J Biol Chem. 264(29):17374-8.*

Stocco DM, and Clark BJ. *1996.* Regulation of the acute production of steroids in steroidogenic cells. - *Endocr Rev. 17(3):221-44.*

Stoneman VE, and Bennett MR. *2004.* Role of apoptosis in atherosclerosis and its therapeutic implications. - *Clin Sci (Lond). 107(4):343-54.*

Strauss JF 3rd, Kallen CB, Christenson LK, Watari H, Devoto L, Arakane F, Kiriakidou M, and Sugawara T. *1999.* The steroidogenic acute regulatory protein (StAR): a window into the complexities of intracellular cholesterol trafficking. - *Recent Prog Horm Res.;54:369-94; Discussion 394-5.*

Strieter RM, Kunkel SL, Showell HJ, Remick DG, Phan SH, Ward PA, and Marks RM. *1989a* . Endothelial cell gene expression of a neutrophil chemotactic factor by TNF-alpha, LPS, and IL-1 beta. - *Science. 243(4897):1467-9.*

Strieter, R.M., R. Wiggins, S.H. Phan, B.L. Wharram, H.J. Showell, D.G. Remick, S.W. Chensue, and S.L. Kunkel. 1989b. Monocyte chemotactic protein gene expression by cytokine-treated human fibroblasts and endothelial cells. *Biochem.Biophys.Res.Commun.* 162:694-700.

Sugawara T, Nomura E, and Hoshi N. *2007.* Cholesterol sulphate affects production of steroid hormones by reducing steroidogenic acute regulatory protein level in adrenocortical cells. - *J Endocrinol. 195(3):451-8.*

Supakar, P.C., M.H. Jung, C.S. Song, B. Chatterjee, and A.K. Roy. 1995. Nuclear factor kappa B functions as a negative regulator for the rat androgen receptor gene and NF-kappa B activity increases during the age-dependent desensitization of the liver. *J.Biol.Chem.* 270:837-842.

Surmi, B.K., and A.H. Hasty. 2010. The role of chemokines in recruitment of immune cells to the artery wall and adipose tissue. *Vascular Pharmacology.* 52:27-36.

Surya II, J.W. and Akkerman JW. *1993.* The influence of lipoproteins on blood platelets. - *Am Heart J. 125(1):272-5.*

Svartberg J, von Muhlen D, Mathiesen E, Joakimsen O, Bonaa KH, and Stensland-Bugge E. *2006.* Low testosterone levels are associated with carotid atherosclerosis in men. - *J Intern Med. 259(6):576-82.*

Swirski FK, Libby P, Aikawa E, Alcaide P, Luscinskas FW, Weissleder R, and Pittet MJ. *2007.* Ly-6Chi monocytes dominate hypercholesterolemia-associated monocytosis and give rise to macrophages in atheromata. - *J Clin Invest. 117(1):195-205.*

Tabas I. *2005.* Consequences and therapeutic implications of macrophage apoptosis in atherosclerosis: the importance of lesion stage and phagocytic efficiency. - *Arterioscler Thromb Vasc Biol. 25(11):2255-64.*

Tabas I. *2009a.* Macrophage Apoptosis in Atherosclerosis: Consequences on Plaque Progression and the Role of Endoplasmic Reticulum Stress. - *Antioxid Redox Signal. Feb 25.*

Tabas I. *2009b.* Macrophage death and defective inflammation resolution in atherosclerosis. - *Nat Rev Immunol. Dec 4.*

Tacke F, D. Alvarez D, Kaplan TJ, Jakubzick C, Spanbroek R, Llodra J, Garin A, Liu J, Mack M, van Rooijen N, Lira SA, Habenicht AJ, and Randolph GJ. *2007.* Monocyte subsets differentially employ CCR2, CCR5, and CX3CR1 to accumulate within atherosclerotic plaques. - *J Clin Invest. 117(1):185-94.*

Takahashi K, Mizuarai S, Araki H, Mashiko S, Ishihara AKanatani A, Itadani H, and Kotani H. *2003.* Adiposity elevates plasma MCP-1 levels leading to the increased CD11b-positive monocytes in mice. - *J Biol Chem. 278(47):46654-60.*

Tamada, M., S. Makita, A. Abiko, Y. Naganuma, M. Nagai, and M. Nakamura. 2010. Low-density lipoprotein cholesterol to high-density lipoprotein cholesterol ratio as a useful marker for early-stage carotid atherosclerosis. *Metab.Clin.Exp.* 59:653-657.

Tandon NN, Kralisz U, and Jamieson GA. *1989.* Identification of glycoprotein IV (CD36) as a primary receptor for platelet-collagen adhesion. - *J Biol Chem. 264(13):7576-83.*

Tangirala RK, Murao K, and Quehenberger O. *1997.* Regulation of expression of the human monocyte chemotactic protein-1 receptor (hCCR2) by cytokines. - *J Biol Chem. 272(12):8050-6.*

Tangirala RK, Rubin EM, and Palinski W. *1995.* Quantitation of atherosclerosis in murine models: correlation between lesions in the aortic origin and in the entire aorta, and differences in the extent of lesions between sexes in LDL receptor-deficient and apolipoprotein E-deficient mice. - *J Lipid Res. 36(11):2320-8.*

Tannock, L.R., and V.L. King. 2010. Animal models of atherosclerosis: More than mice. *Atherosclerosis.* 212(1):32-3.

Tao J, Yang Z, Wang JM, Tu C, and Pan SR. *2006.* Effects of fluid shear stress on eNOS mRNA expression and NO production in human endothelial progenitor cells. - *Cardiology.;106(2):82-8.*

Tarchalski J, Guzik P, and Wysocki H. *2003.* Correlation between the extent of coronary atherosclerosis and lipid profile. - *Mol Cell Biochem. 246(1-2):25-30.*

Taub, D.D., and J.J. Oppenheim. 1994. Chemokines, inflammation and the immune system. *Ther.Immunol.* 1:229-246.

Taubman MB, Rollins BJ, Poon M, J. Marmur J, Green RS, Berk BC, and Nadal-Ginard B. *1992.* JE mRNA accumulates rapidly in aortic injury and in platelet-derived growth factor-stimulated vascular smooth muscle cells. - *Circ Res. 70(2):314-25.*

Tedgui A. *2005.* The role of inflammation in atherothrombosis: implications for clinical practice. - *Vasc Med. 10(1):45-53.*

Tedgui, A., and Z. Mallat. 2006. Cytokines in atherosclerosis: pathogenic and regulatory pathways. *Physiol.Rev.* 86:515-581.

Tellier, E., M. Canault, L. Rebsomen, B. Bonardo, I. Juhan-Vague, G. Nalbone, and F. Peiretti. 2006. The shedding activity of ADAM17 is sequestered in lipid rafts. *Exp.Cell Res.* 312:3969-3980.

Templeton NS. *1992.* The polymerase chain reaction. History, methods, and applications. - *Diagn Mol Pathol. 1(1):58-72.*

Tenover JS. *1992.* Effects of testosterone supplementation in the aging male. - *J Clin Endocrinol Metab. 75(4):1092-8.*

Teupser, D., S. Pavlides, M. Tan, J.C. Gutierrez-Ramos, R. Kolbeck, and J.L. Breslow. 2004. Major reduction of atherosclerosis in fractalkine (CX3CL1)-deficient mice is at the brachiocephalic artery, not the aortic root. *Proc.Natl.Acad.Sci.U.S.A.* 101:17795-17800.

Tharp DL, Masseau I, Ivey J, Ganjam VK, and Bowles DK. *2009.* Endogenous testosterone attenuates neointima formation after moderate coronary balloon injury in male swine. - *Cardiovasc Res. 82(1):152-60.*

Thelen, M. 2001. Dancing to the tune of chemokines. *Nat.Immunol.* 2:129-134.

Thellin O, Zorzi W, Lakaye B, De Borman B, Coumans B, Hennen G, Grisar T, Igout A, and Heinen E. *1999.* Housekeeping genes as internal standards: use and limits. - *J Biotechnol. 75(2-3):291-5.*

Thompson PD, Cullinane EM, Sady SP, Chenevert C, Saritelli AL, Sady MA and Herbert PN. *1989.* Contrasting effects of testosterone and stanozolol on serum lipoprotein levels. - *JAMA. 261(8):1165-8.*

Tipping PG, and Hancock WW. *1993.* Production of tumor necrosis factor and interleukin-1 by macrophages from human atheromatous plaques. - *Am J Pathol. 142(6):1721-8.*

Tivesten, Å., D. Mellström, H. Jutberger, B. Fagerberg, B. Lernfelt, E. Orwoll, M.K. Karlsson, Ö. Ljunggren, and C. Ohlsson. 2007. Low Serum Testosterone and High Serum Estradiol Associate With Lower Extremity Peripheral Arterial Disease in Elderly Men: The MrOS Study in Sweden. *J.Am.Coll.Cardiol.* 50:1070-1076.

Tomaszewski, M., F.J. Charchar, C. Maric, R. Kuzniewicz, M. Gola, W. Grzeszczak, N.J. Samani, and E. Zukowska-Szczechowska. 2009. Association between lipid profile and circulating concentrations of estrogens in young men. *Atherosclerosis.* 203:257-262.

Traish, A.M., R. Abdou, and K.E. Kypreos. 2009. Androgen deficiency and atherosclerosis: The lipid link. *Vascular Pharmacology.* 51:303-313.

Tribble DL, Barcellos-Hoff MH, Chu BM, and Gong EL. *1999.* Ionizing radiation accelerates aortic lesion formation in fat-fed mice via SOD-inhibitable processes. - *Arterioscler Thromb Vasc Biol. 19(6):1387-92.*

Tripathy D, Shah P, Lakshmy R, and Reddy KS. *1998.* Effect of testosterone replacement on whole body glucose utilisation and other cardiovascular risk factors in males with idiopathic hypogonadotrophic hypogonadism. - *Horm Metab Res. 30(10):642-5.*

Truman LA, Ford CA, Pasikowska M, Pound JD, Wilkinson SJ, Dumitriu IE, Melville L, Melrose LA, Ogden CA, Nibbs R, Graham G, Combadiere C, and Gregory CD. *2008.* CX3CL1/fractalkine is released from apoptotic lymphocytes to stimulate macrophage chemotaxis. - *Blood. 112(13):5026-36.*

Tsai HK, D'Amico AV, Sadetsky N, Chen MH, and Carroll PR. *2007.* Androgen deprivation therapy for localized prostate cancer and the risk of cardiovascular mortality. - *J Natl Cancer Inst. 99(20):1516-24.*

Tsou, C.L., C.A. Haskell, and I.F. Charo. 2001. Tumor necrosis factor-alpha-converting enzyme mediates the inducible cleavage of fractalkine. *J.Biol.Chem.* 276:44622-44626.

Tsuchiya S, Yamabe M, Yamaguchi Y, Kobayashi Y, Konno T, and Tada K. *1980.* Establishment and characterization of a human acute monocytic leukemia cell line (THP-1). - *Int J Cancer. 26(2):171-6.*

Turhan S, Tulunay C, Gulec S, Ozdol C, Kilickap M, Altin T, Gerede M, and Erol C. *2007.* The association between androgen levels and premature coronary artery disease in men. - *Coron Artery Dis. 18(3):159-62.*

Tyagi A, Rajalakshmi M, Jeyaraj DA, Sharma RS, and Bajaj JS. *1999.* Effects of long-term use of testosterone enanthate. II. Effects on lipids, high and low density lipoprotein cholesterol and liver function parameters. - *Int J Androl. 22(6):347-55.*

Ueda A, Ishigatsubo Y, Okubo T, and Yoshimura T. *1997.* Transcriptional regulation of the human monocyte chemoattractant protein-1 gene. Cooperation of two NF-kappaB sites and NF-kappaB/Rel subunit specificity. - *J Biol Chem. 272(49):31092-9.*

Ueda A, Okuda K, Ohno S, Shirai A, Igarashi T, Matsunaga K, Fukushima J, Kawamoto S, Ishigatsubo Y, and Okubo T. *1994.* NF-kappa B and Sp1 regulate transcription of the human monocyte chemoattractant protein-1 gene. - *J Immunol. 153(5):2052-63.*

Umehara, H., E.T. Bloom, T. Okazaki, Y. Nagano, O. Yoshie, and T. Imai. 2004. Fractalkine in vascular biology: from basic research to clinical disease. *Arterioscler.Thromb.Vasc.Biol.* 24:34-40.

Umehara, H., S. Goda, T. Imai, Y. Nagano, Y. Minami, Y. Tanaka, T. Okazaki, E.T. Bloom, and N. Domae. 2001. Fractalkine, a CX3C-chemokine, functions predominantly as an adhesion molecule in monocytic cell line THP-1. *Immunol.Cell Biol.* 79:298-302.

Uyanik BS, Ari Z, Gumus B, Yigitoglu MR, and Arslan T. *1997*. Beneficial effects of testosterone undecanoate on the lipoprotein profiles in healthy elderly men. A placebo controlled study. - *Jpn Heart J. 38(1):73-82.*

Valente AJ, Graves DT, Vialle-Valentin CE, Delgado R, and Schwartz CJ. *1988*. Purification of a monocyte chemotactic factor secreted by nonhuman primate vascular cells in culture. - *Biochemistry. 27(11):4162-8.*

Valente AJ, Xie JF, Abramova MA, Wenzel UO, Abboud HE, and Graves DT. *1998*. A complex element regulates IFN-gamma-stimulated monocyte chemoattractant protein-1 gene transcription. - *J Immunol. 161(7):3719-28.*

van Amsterdam, J., A. Opperhuizen, and F. Hartgens. *2010* Adverse health effects of anabolic–androgenic steroids. *Regulatory Toxicology and Pharmacology.* 57(1):117-23.

van den Beld AW, Bots ML, Janssen JA, Pols HA, Lamberts SW, and Grobbee DE. *2003*. Endogenous hormones and carotid atherosclerosis in elderly men. - *Am J Epidemiol. 157(1):25-31.*

Van der Heiden K, Cuhlmann S, Luong le A, Zakkar M, and Evans PC. *2010*. Role of nuclear factor kappaB in cardiovascular health and disease. - *Clin Sci (Lond). 118(10):593-605.*

Van Herreweghe F, Festjens N, Declercq W, and Vandenabeele P. *2010*. Tumor necrosis factor-mediated cell death: to break or to burst, that's the question. - *Cell Mol Life Sci. 67(10):1567-79.*

Van Pottelbergh, I., L. Braeckman, D. De Bacquer, G. De Backer, and J.M. Kaufman. 2003. Differential contribution of testosterone and estradiol in the determination of cholesterol and lipoprotein profile in healthy middle-aged men. *Atherosclerosis.* 166:95-102.

van Puijvelde, G.H., A.D. Hauer, P. de Vos, R. van den Heuvel, M.J. van Herwijnen, R. van der Zee, W. van Eden, T.J. van Berkel, and J. Kuiper. 2006. Induction of oral tolerance to oxidized low-density lipoprotein ameliorates atherosclerosis. *Circulation.* 114:1968-1976.

Vandesompele J, De Preter K, Pattyn F, Poppe B, Van Roy N, De Paepe A, and Speleman F. *2002*. Accurate normalization of real-time quantitative RT-PCR data by geometric averaging of multiple internal control genes. - *Genome Biol. 3(7):RESEARCH0034.*

Vergnani L, Hatrik S, Ricci F, Passaro A, Manzoli N, Zuliani G, Brovkovych V, Fellin R, and Malinski T. *2000*. Effect of native and oxidized low-density lipoprotein on endothelial nitric oxide and superoxide production : key role of L-arginine availability. - *Circulation. 101(11):1261-6.*

Vergnes L, Phan J, Strauss M, Tafuri S, and Reue K. *2003*. Cholesterol and cholate components of an atherogenic diet induce distinct stages of hepatic inflammatory gene expression. - *J Biol Chem. 278(44):42774-84.*

Vermeulen A, Goemaere S, and Kaufman JM. *1999*. Testosterone, body composition and aging. - *J Endocrinol Invest.;22(5 Suppl):110-6.*

Vermeulen A, Kaufman JM, Deslypere JP, and Thomas G. *1993*. Attenuated luteinizing hormone (LH) pulse amplitude but normal LH pulse frequency, and its relation to plasma androgens in hypogonadism of obese men. - *J Clin Endocrinol Metab. 76(5):1140-6.*

Vermeulen, A., and L. Verdonck. 1968. Studies on the binding of testosterone to human plasma. *Steroids*. 11:609-635.

Vidal-Vanaclocha F, Fantuzzi G, Mendoza L, Fuentes AM, Anasagasti MJ, Martin J, Carrascal T, Walsh P, Reznikov LL, Kim SH, Novick D, Rubinstein M, and Dinarello CA. *2000*. IL-18 regulates IL-1beta-dependent hepatic melanoma metastasis via vascular cell adhesion molecule-1. - *Proc Natl Acad Sci U S A. 97(2):734-9*.

Viedt, C., J. Vogel, T. Athanasiou, W. Shen, S.R. Orth, W. Kubler, and J. Kreuzer. 2002. Monocyte chemoattractant protein-1 induces proliferation and interleukin-6 production in human smooth muscle cells by differential activation of nuclear factor-kappaB and activator protein-1. *Arterioscler.Thromb.Vasc.Biol.* 22:914-920.

Vikan T, Johnsen SH, Schirmer H, Njolstad I, and Svartberg J. *2009*. Endogenous testosterone and the prospective association with carotid atherosclerosis in men: the Tromso study. - *Eur J Epidemiol.;24(6):289-95*.

Villablanca A, Lubahn D, Shelby L, Lloyd K, and Barthold S. *2004*. Susceptibility to early atherosclerosis in male mice is mediated by estrogen receptor alpha. - *Arterioscler Thromb Vasc Biol. 24(6):1055-61*.

Vitale, C., M.E. Mendelsohn, and G.M. Rosano. 2009. Gender differences in the cardiovascular effect of sex hormones. *Nat.Rev.Cardiol.*

Vitale, S., A. Schmid-Alliana, V. Breuil, M. Pomeranz, M.A. Millet, B. Rossi, and H. Schmid-Antomarchi. 2004. Soluble fractalkine prevents monocyte chemoattractant protein-1-induced monocyte migration via inhibition of stress-activated protein kinase 2/p38 and matrix metalloproteinase activities. *J.Immunol.* 172:585-592.

Volin MV, Woods JM, Amin MA, Connors MA, Harlow LA, and Koch AE. *2001*. Fractalkine: a novel angiogenic chemokine in rheumatoid arthritis. - *Am J Pathol. 159(4):1521-30*.

von Dehn, G., O. von Dehn, W. Volker, C. Langer, G.F. Weinbauer, H.M. Behre, E. Nieschlag, G. Assmann, and A. von Eckardstein. 2001. Atherosclerosis in apolipoprotein E-deficient mice is decreased by the suppression of endogenous sex hormones. *Horm.Metab.Res.* 33:110-114.

Wågsäter, D., P.S. Olofsson, L. Norgren, B. Stenberg, and A. Sirsjö. 2004. The chemokine and scavenger receptor CXCL16/SR-PSOX is expressed in human vascular smooth muscle cells and is induced by interferon γ. *Biochem.Biophys.Res.Commun.* 325:1187-1193.

Walch, L., L. Massade, M. Dufilho, A. Brunet, and F. Rendu. 2006. Pro-atherogenic effect of interleukin-4 in endothelial cells: Modulation of oxidative stress, nitric oxide and monocyte chemoattractant protein-1 expression. *Atherosclerosis*. 187:285-291.

Walcheck B, Herrera AH, St Hill C, Mattila PE, Whitney AR, and Deleo FR. *2006*. ADAM17 activity during human neutrophil activation and apoptosis. - *Eur J Immunol. 36(4):968-76*.

Walker JM. *1994*. The bicinchoninic acid (BCA) assay for protein quantitation. - *Methods Mol Biol.;32:5-8*.

Webb, C.M., D.L. Adamson, D. de Zeigler, and P. Collins. 1999. Effect of acute testosterone on myocardial ischemia in men with coronary artery disease. *Am.J.Cardiol.* 83:437-439.

299

Weber C. *2003.* Novel mechanistic concepts for the control of leukocyte transmigration: specialization of integrins, chemokines, and junctional molecules. - *J Mol Med. 81(1):4-19.*

Weber C, Zernecke A, and Libby P. *2008.* The multifaceted contributions of leukocyte subsets to atherosclerosis: lessons from mouse models. - *Nat Rev Immunol. 8(10):802-15.*

Weber KS, Nelson PJ, Grone HJ, and Weber C. *1999a.* Expression of CCR2 by endothelial cells : implications for MCP-1 mediated wound injury repair and In vivo inflammatory activation of endothelium. - *Arterioscler Thromb Vasc Biol. 19(9):2085-93.*

Weber, C., G. Draude, K.S.C. Weber, J. Wübert, R.L. Lorenz, and P.C. Weber. 1999b. Downregulation by tumor necrosis factor-α of monocyte CCR2 expression and monocyte chemotactic protein-1-induced transendothelial migration is antagonized by oxidized low-density lipoprotein: A potential mechanism of monocyte retention in atherosclerotic lesions. *Atherosclerosis.* 145:115-123.

Wehrle-Haller B, and Imhof BA. *2003.* Integrin-dependent pathologies. - *J Pathol. 200(4):481-7.*

Weihua Z, Lathe R, Warner M, and Gustafsson JA. *2002.* An endocrine pathway in the prostate, ERbeta, AR, 5alpha-androstane-3beta,17beta-diol, and CYP7B1, regulates prostate growth. - *Proc Natl Acad Sci U S A. 99(21):13589-94.*

Wever RM, Luscher TF, Cosentino F, and Rabelink TJ. *1998.* Atherosclerosis and the two faces of endothelial nitric oxide synthase. - *Circulation. 97(1):108-12.*

White GE, Tan TC, John AE, Whatling C, McPheat WL, and Greaves DR. *2010.* Fractalkine has anti-apoptotic and proliferative effects on human vascular smooth muscle cells via epidermal growth factor receptor signalling. - *Cardiovasc Res. 85(4):825-35.*

Wierda RJ, Geutskens SB, Jukema JW, Quax PH, and van den Elsen PJ. *2010.* Epigenetics in atherosclerosis and inflammation. - *J Cell Mol Med. Jan 30.*

Williams, M.R., S. Ling, T. Dawood, K. Hashimura, A. Dai, H. Li, J.P. Liu, J.W. Funder, K. Sudhir, and P.A. Komesaroff. 2002. Dehydroepiandrosterone inhibits human vascular smooth muscle cell proliferation independent of ARs and ERs. *J.Clin.Endocrinol.Metab.* 87:176-181.

Wojciak-Stothard B, Entwistle A, Garg R, and Ridley AJ. *1998.* Regulation of TNF-alpha-induced reorganization of the actin cytoskeleton and cell-cell junctions by Rho, Rac, and Cdc42 in human endothelial cells. - *J Cell Physiol. 176(1):150-65.*

Wong ML, J. and Medrano JF. *2005.* Real-time PCR for mRNA quantitation. - *Biotechniques. Jul;39(1):75-85.*

Wong H, and Schotz MC. *2002.* The lipase gene family. - *J Lipid Res. 43(7):993-9.*

Wong LM, Myers SJ, Tsou CL, Gosling J, Arai H, and Charo IF. *1997.* Organization and differential expression of the human monocyte chemoattractant protein 1 receptor gene. Evidence for the role of the carboxyl-terminal tail in receptor trafficking. - *J Biol Chem. 272(2):1038-45.*

Wong, B.W., D. Wong, and B.M. McManus. 2002. Characterization of fractalkine (CX3CL1) and CX3CR1 in human coronary arteries with native atherosclerosis, diabetes mellitus, and transplant vascular disease. *Cardiovasc.Pathol.* 11:332-338.

Woollard KJ, and Geissmann F. *2010.* Monocytes in atherosclerosis: subsets and functions. - *Nat Rev Cardiol. 7(2):77-86.*

Wranicz, J.K., I. Cygankiewicz, M. Rosiak, P. Kula, K. Kula, and W. Zareba. 2005. The relationship between sex hormones and lipid profile in men with coronary artery disease. *Int.J.Cardiol.* 101:105-110.

Wu, F.C., and A. von Eckardstein. 2003. Androgens and coronary artery disease. *Endocr.Rev.* 24:183-217.

Wuttge DM, Zhou X, Sheikine Y, Wagsater D, Stemme V, Hedin U, Stemme S, Hansson GK, and Sirsjo A. *2004.* CXCL16/SR-PSOX is an interferon-gamma-regulated chemokine and scavenger receptor expressed in atherosclerotic lesions. - *Arterioscler Thromb Vasc Biol. 24(4):750-5.*

Xing D, Feng W, Miller AP, Weathington NM, Chen YF, Novak L, Blalock JE, and Oparil S. *2007.* Estrogen modulates TNF-alpha-induced inflammatory responses in rat aortic smooth muscle cells through estrogen receptor-beta activation. - *Am J Physiol Heart Circ Physiol. 292(6):H2607-12.*

Yamada K, Hayashi T, Kuzuya M, Naito M, Asai K, and Iguchi A. *1996.* Physiological concentration of 17 beta-estradiol inhibits chemotaxis of human monocytes in response to monocyte chemotactic protein 1. - *Artery.;22(1):24-35.*

Yang XP, Mattagajasingh S, Su S, Chen G, Cai Z, Fox-Talbot K, Irani K, and Becker LC. *2007.* Fractalkine upregulates intercellular adhesion molecule-1 in endothelial cells through CX3CR1 and the Jak Stat5 pathway. - *Circ Res. 101(10):1001-8.*

Yang YM, Lv XY, Huang WD, Xu ZR, and Wu LJ. *2005.* Study of androgen and atherosclerosis in old-age male. - *J Zhejiang Univ Sci B. 6(9):931-5.*

Yannucci, J., J. Manola, M.B. Garnick, G. Bhat, and G.J. Bubley. 2006. The Effect of Androgen Deprivation Therapy on Fasting Serum Lipid and Glucose Parameters. *J.Urol.* 176:520-525.

Yassin AA, Saad F, and Gooren LJ. *2008.* Metabolic syndrome, testosterone deficiency and erectile dysfunction never come alone. - *Andrologia. 40(4):259-64.*

Yeh S, Miyamoto H, Shima H, and Chang C. *1998.* From estrogen to androgen receptor: a new pathway for sex hormones in prostate. - *Proc Natl Acad Sci U S A. ;95(10):5527-32.*

Yesilova Z, Ozata M, Kocar IH, Turan M, Pekel A, Sengul A, and Ozdemir IC. *2000.* The effects of gonadotropin treatment on the immunological features of male patients with idiopathic hypogonadotropic hypogonadism. - *J Clin Endocrinol Metab. 85(1):66-70.*

Yilmaz A, Lipfert B, Cicha I, Schubert K, Klein M, Raithel D, Daniel WG, and Garlichs CD. *2007.* Accumulation of immune cells and high expression of chemokines/chemokine receptors in the upstream shoulder of atherosclerotic carotid plaques. - *Exp Mol Pathol. 82(3):245-55.*

Yla-Herttuala S, Lipton BA, Rosenfeld ME, Sarkioja T, Yoshimura T, Leonard EJ, Witztum JL, and Steinberg D. *1991.* Expression of monocyte chemoattractant protein 1 in macrophage-rich areas of human and rabbit atherosclerotic lesions. - *Proc Natl Acad Sci U S A. 88(12):5252-6.*

Yoneda O, Imai T, Goda S, Inoue H, Yamauchi A, Okazaki T, Imai H, Yoshie O, Bloom ET, Domae N, and Umehara H. *2000.* Fractalkine-mediated endothelial cell injury by NK cells. - *J Immunol. 164(8):4055-62.*

Yoshida, H., T. Imaizumi, K. Fujimoto, N. Matsuo, K. Kimura, X. Cui, T. Matsumiya, K. Tanji, T. Shibata, W. Tamo, M. Kumagai, and K. Satoh. 2001. Synergistic stimulation, by tumor necrosis factor-α and interferon-γ, of fractalkine expression in human astrocytes. *Neuroscience Letters.* 303:132-136.

Yoshimura T, Robinson EA, Tanaka S, Appella E, and Leonard EJ. *1989.* Purification and amino acid analysis of two human monocyte chemoattractants produced by phytohemagglutinin-stimulated human blood mononuclear leukocytes. - *J Immunol. 142(6):1956-62.*

Yu G, Deng Z, and Qu Z. *1998.* [Effects of oxidatively modified lipoproteins on the expression of monocyte chemoattractant protein-1 in endothelial cells]. - *Zhonghua Bing Li Xue Za Zhi. 27(3):174-6.*

Yu Q, and Stamenkovic I. *2000.* Cell surface-localized matrix metalloproteinase-9 proteolytically activates TGF-beta and promotes tumor invasion and angiogenesis. - *Genes Dev. 14(2):163-76.*

Yu, J., M. Eto, M. Akishita, T. Okabe, and Y. Ouchi. 2009. A selective estrogen receptor modulator inhibits TNF-α-induced apoptosis by activating ERK1/2 signaling pathway in vascular endothelial cells. *Vascular Pharmacology.* 51:21-28.

Zar, J.H. 2010. Biostatistical Analysis. Pearson Prentice Hall, Inc., United States of America. 944 pp.

Zgliczynski, S., M. Ossowski, J. Slowinska-Srzednicka, A. Brzezinska, W. Zgliczynski, P. Soszynski, E. Chotkowska, M. Srzednicki, and Z. Sadowski. 1996. Effect of testosterone replacement therapy on lipids and lipoproteins in hypogonadal and elderly men. *Atherosclerosis.* 121:35-43.

Zhang Y, and Wahl LM. *2006.* Synergistic enhancement of cytokine-induced human monocyte matrix metalloproteinase-1 by C-reactive protein and oxidized LDL through differential regulation of monocyte chemotactic protein-1 and prostaglandin E2. - *J Leukoc Biol. 79(1):105-13.*

Zhang, X., L. Wang, T. Jiang, H. Zhang, Y. Dou, J. Zhao, H. Zhao, Z. Qiao, and J. Qiao. 2002. Effects of testosterone and 17-β-estradiol on TNF-α-induced E-selectin and VCAM-1 expression in endothelial cells: Analysis of the underlying receptor pathways. *Life Sciences.* 71:15-29.

Zhao R, Wang Y, Shen R, and Sun Y. *2010.* Relationship between CX3CR1 genetic polymorphism and carotid atherosclerosis. - *Artif Cells Blood Substit Immobil Biotechnol.;38(1):19-23.*

Zhou X, Caligiuri G, Hamsten A, Lefvert AK, and Hansson GK. *2001.* LDL immunization induces T-cell-dependent antibody formation and protection against atherosclerosis. - *Arterioscler Thromb Vasc Biol. 21(1):108-14.*

Zhu JP, Su CL, Chen M, and Lin JF. *2009.* [Role of testosterone in tumor necrosis factor-alpha and monocyte chemotactic protein-1 expression in mouse macrophage RAW264.7 and its molecular mechanism]. - *Zhonghua Yi Xue Za Zhi. 89(35):2500-3.*

Zitzmann M, Brune M, Kornmann B, Gromoll J, von Eckardstein S, von Eckardstein A, and Nieschlag E. *2001*. The CAG repeat polymorphism in the AR gene affects high density lipoprotein cholesterol and arterial vasoreactivity. - *J Clin Endocrinol Metab. 86(10):4867-73.*

Zitzmann M, Erren M, Kamischke A, Simoni M, and Nieschlag E. *2005*. Endogenous progesterone and the exogenous progestin norethisterone enanthate are associated with a proinflammatory profile in healthy men. - *J Clin Endocrinol Metab. 90(12):6603-8.*

Zitzmann M, and Nieschlag E. *2007*. Androgen receptor gene CAG repeat length and body mass index modulate the safety of long-term intramuscular testosterone undecanoate therapy in hypogonadal men. - *J Clin Endocrinol Metab. 92(10):3844-53.*

Zitzmann, M., E. Verona, M. Wenk, F. Saad, and E. Nieschlag. 2008. Testosterone administration decreases carotiod artery intima media thickness as indicator of vascular damage in middle-aged overweight men. *J Androl.* 29:54-5.

Zlotnik, A., and O. Yoshie. 2000. Chemokines: a new classification system and their role in immunity. *Immunity.* 12:121-127.

Zumoff B, Strain GW, Miller LK, Rosner W, Senie R, Seres DS, and Rosenfeld RS. *1990*. Plasma free and non-sex-hormone-binding-globulin-bound testosterone are decreased in obese men in proportion to their degree of obesity. - *J Clin Endocrinol Metab. 71(4):929-31.*

303

	Gene Name	Assay ID	Category	Gene Group
BACTIN	actin, beta	Hs99999903_m1	Cytoskeletal protein	Actin family cytoskeletal protein
ADAM17	ADAM metallopeptidase domain 10	Hs00153853_m1	Protease	Metalloprotease
ADAM10	ADAM metallopeptidase domain 17	Hs01041915_m1	Protease	Metalloprotease
AR	androgen receptor	Hs00171172_m1	Transcription factor	Nuclear hormone receptor
B2M	beta-2-microglobulin	Hs00187842_m1	Defense/immunity protein	Major histocompatibility complex antigen
CX3CL1	chemokine (C-X3-C motif) ligand 1	Hs00171086_m1	Signaling molecule	Chemokine
CX3CR1	chemokine (C-X3-C motif) receptor 1	Hs00365842_m1	Receptor	G-protein coupled receptor
GAPDH	glyceraldehyde-3-phosphate dehydrogenase	Hs99999905_m1	Oxidoreductase	Dehydrogenase
HPRT	hypoxanthine phosphoribosyltransferase 1	Hs01003267_m1	Transferase	Glycosyltransferase
RPL13A	ribosomal protein L13a;ribosomal protein L13a pseudogene 5	Hs03043885_g1	Nucleic acid binding	Ribosomal protein
SDHA	succinate dehydrogenase complex, subunit A, flavoprotein (Fp)	Hs00188166_m1	Oxidoreductase	Dehydrogenase
TIMP1	TIMP metallopeptidase inhibitor 1	Hs99999139_m1	Select regulatory molecule	Protease inhibitor
TIMP3	TIMP metallopeptidase inhibitor 3	Hs00165949_m1	Select regulatory molecule	Protease inhibitor

Appendix 1; Taqman® qRT-PCR primer probe assays purchased from Applied Biosystems